



UNIVERSITY OF LEEDS

Literature and experimental  
reactivity data: a case study with  
*N*-nitrosamines

George Hodgin

Submitted in accordance with the requirements for the degree  
of PhD. Chemistry

The University of Leeds

Faculty of Engineering and Physical Sciences

School of Chemistry

Feb 2024

# Abstract

*N*-nitrosamines (nitrosamines) are highly potent carcinogens that have been an industry wide problem since 2018 when *N*-nitrosodimethylamine (NDMA) was discovered at above acceptable levels in the block-buster blood pressure regulator drug Valsartan. This finding led to the recall of a number of structurally similar drug products from the market. The regulatory bodies demanded that costly and time consuming batch testing of all Active Pharmaceutical Ingredients (API), intermediates, and materials of drug products must be carried out to rule out *N*-nitrosamine contamination. Estimations about the associated risk of contamination in the API can, however, be made in-silico, and these estimations are largely based on the physicochemical properties of the nitrosamine impurity and how these properties influence its removal or “purge” during the API synthesis. Reactivity data on *N*-nitrosamines will greatly improve knowledge about their purge during a drug manufacturing process. Current reviews of *N*-nitrosamine reactivity focus on dialkyl and aryl nitrosamines, due to their prevalence in early discoveries of *N*-nitrosamine contamination in drug products. Although, recent research has discovered that many more structural classes of *N*-nitrosamine may be of concern to human health, with the API’s themselves being potential *N*-nitrosamine precursors. This renders the current knowledge base of *N*-nitrosamine reactivity insufficient, and calls for a more comprehensive investigation. Furthermore, the current reported reaction conditions to destroy *N*-nitrosamines are often harsh or with limited substrate scope. This prompts the discovery of milder reaction conditions which are applicable to a diverse range of structural classes of *N*-nitrosamine which can be applied during high-value chemical manufacture.

The following work details a data-driven review of *N*-nitrosamine reactivity, incorporating cheminformatics processes to condense data to retrieve reactions on *N*-nitrosamines. The curated dataset includes reactivity examples for multiple structural classes of *N*-nitrosamines. The findings indicate that the reactivity of *N*-nitrosamines is highly dependent on the surrounding

---

structural environment, particularly the  $\alpha$  and  $\beta$  positions relative to the N-N=O substructure shared by all *N*-nitrosamines, as structural modifications at these positions can open the door to otherwise unaccessible reactivity. The summarised reactivity table generated is significant in the advancement of purge assessment tools, as it can be applied to a broad range of structural classes of *N*-nitrosamine to estimate their reactivity, and possibly negate the requirement for costly and time consuming empirical analysis.

Following this, a reactivity screen is performed on eight relevant *N*-nitrosamines, whose reactivity is expected to be representative of all structural classes of *N*-nitrosamine. Four broad spectrum methods of destroying *N*-nitrosamines are found, that are milder reaction conditions than previously reported. Namely, these reaction conditions are as follows: 1. Ethanolic hydrochloride (HCl) at 50°C for 16 hours at 20 molar equivalents of HCl, 2. Diisobutylaluminium hydride (DiBAL-H) (5 molar equivalents) in tetrahydrofuran (THF) at room temperature for 1 hour, 3. Sodium dithionite (20 molar equivalents) in 20% w/v sodium hydroxide (NaOH) at 50°C for 16 hours, 4. Sodium dithionite (20 molar equivalents) in 1 M NaOH at 50°C for 16 hours. These findings, particularly reaction condition 4, have a significant purpose in the late stage removal of *N*-nitrosamines during API manufacture, as the nitrosamines can be removed with confidence without modifications to the API itself.

# Intellectual Property

The candidate confirms that the work submitted is his own and that appropriate credit has been given where reference has been made to the work of others.

This copy has been supplied on the understanding that it is copyright material and that no quotation from the thesis may be published without proper acknowledgement.

© 2024 The University of Leeds, George Hodgkin

# Acknowledgements

I would firstly like to thank my supervisor, Professor Bao Nguyen, for all of his patience and guidance throughout the project. Specifically, for allowing me to pursue my own interests, and allow them to contribute to the main body of work I have produced during my PhD, and for giving me the chance to begin a PhD in the first place.

Additionally, I would not have made it through this journey without some people I hold very dearly to my heart. Matthew, for all the good work he has done in day to day aspects of life; ensuring that I was always able to focus my attention on my work and also allowing me to vent my frustrations and problems. I couldn't have done it without you mate! To Holly, who has made me smile even through the most stressful times, thank you for believing in me always. To Mum, Dad, and Ruari, thank you for your continued support over these past three and a half years, it's nice to know I always have a place to go to take it easy for a little while.

A big thank you to those who took the time to proof read my work: Rachel, Andy and Sam. Your helpful comments have made a valuable contribution to this work, and I also thank you all for being a pleasure to work with.

A special thanks to Stuart Warriner, for all the advice during my annual progress reviews, for the help with the mass-spec and for being a great laugh! Also to Chris and Ben from the ROAR team at ICL, I learned so much on these visits that I was able to apply to my work. Finally thanks to the sponsors, LHASA Ltd. and specifically to Mike and Sam, for their thoughtful discussions and contributions throughout the project.

# Contents

<b>1</b>	<b>Introduction</b>	<b>1</b>
1.1	Scope of this chapter . . . . .	1
1.2	<i>N</i> -nitrosamines . . . . .	2
1.3	Carcinogenicity . . . . .	3
1.4	The nitrosamine crisis . . . . .	3
1.5	Controlling risk . . . . .	6
1.6	Known reactivity . . . . .	8
1.6.1	Reduction . . . . .	8
1.6.2	Electrophilic and nucleophilic reactions . . . . .	12
1.6.3	Oxidation . . . . .	15
1.6.4	Photochemistry . . . . .	16
1.7	Other sources of <i>N</i> -nitrosamine . . . . .	16
1.8	Automatic reaction classification . . . . .	18
1.9	Conclusions . . . . .	25
<b>2</b>	<b>Analysis of literature <i>N</i>-nitrosamine reactions</b>	<b>28</b>
2.1	Scope of the chapter . . . . .	28
2.2	Introduction . . . . .	28
2.3	Methods . . . . .	30
2.3.1	Data extraction and refinement . . . . .	30
2.3.2	Manual classification . . . . .	33
2.4	Results and Discussion . . . . .	39
2.4.1	UMAP plot of nitrosamine structural classes . . . . .	39
2.4.2	Examples of reactivity . . . . .	40

2.4.3	Structure-reactivity relationships . . . . .	59
2.4.4	Promising reaction conditions . . . . .	60
2.5	Conclusions . . . . .	61
<b>3</b>	<b>Reactivity Screen on <i>N</i>-nitrosamines</b>	<b>63</b>
3.1	Scope of chapter . . . . .	63
3.2	Introduction . . . . .	63
3.3	Safety . . . . .	67
3.4	Initial investigations in Flow . . . . .	67
3.4.1	Flow reaction protocol . . . . .	69
3.4.2	Flow reaction analysis workflow . . . . .	70
3.4.3	Results for N6 with NaBH <sub>4</sub> . . . . .	71
3.4.4	Autosampler issues . . . . .	72
3.5	General experimental procedure . . . . .	74
3.6	Experimental protocols . . . . .	78
3.7	Calibrations for conversion analysis . . . . .	88
3.7.1	HPLC Calibrations . . . . .	90
3.7.2	GC-MS/MS Calibrations . . . . .	91
3.7.3	Conversion calculation . . . . .	92
3.8	GC-MS/MS peak identification . . . . .	94
3.8.1	LC-MS/MS peak identification . . . . .	96
3.9	Results and Discussion . . . . .	97
3.10	Conclusions . . . . .	130
<b>4</b>	<b>Final Conclusions and Future Work</b>	<b>133</b>
	<b>References</b>	<b>138</b>
<b>A</b>	<b>Code listings</b>	<b>155</b>
A.1	XML parse . . . . .	155
A.2	AAM and ReactionCodes . . . . .	162
<b>B</b>	<b>Classification heirarchies</b>	<b>172</b>
<b>C</b>	<b>Stock solution preparation</b>	<b>178</b>

---

<b>D HPLC Calibrations</b>	<b>181</b>
<b>E GC-MS/MS Calibrations</b>	<b>191</b>
<b>F GC-MS/MS References</b>	<b>195</b>
<b>G GC-MS/MS Experiment plots</b>	<b>216</b>
<b>H LC-MS/MS References</b>	<b>242</b>
<b>I LC-MS/MS Experiment chromatograms</b>	<b>255</b>
<b>J NMR Analysis</b>	<b>281</b>
J.1 N4 Condition 1 . . . . .	281
J.2 N5 Condition 5 . . . . .	285



# List of Figures

1.1	Calculation of purge factors for mutagenic impurities. [2]	7
1.2	<i>N</i> -nitrosamine purge prediction by Mirabilis in the synthetic route to Candesar-tan. Figure taken from reference [2] (Figure 6).	7
1.3	Comparison of the pseudo-first order rate coefficient of various hydrogenation catalysts applied to NDMA.	11
1.4	An example of Morgan fingerprint generation to store molecular information.	21
1.5	Breakdown of a simple ReactionCode.	24
2.1	The reaxys search criteria for reactions on <i>N</i> -nitrosamines.	30
2.2	Loss of data with processing steps.	31
2.3	The lack of yield, temperature and reaction time data in the dataset of <i>N</i> -nitrosamine reactions.	33
2.4	The number of stoichiometrically balanced reactions in the dataset.	34
2.5	Counts of the 15 structural classes of <i>N</i> -nitrosamine in the dataset.	35
2.6	Counts of the grouped structural classes of <i>N</i> -nitrosamine in the dataset.	37
2.7	UMAP plot of the nitrosamine classes.	40
2.8	Reagents that affect more than one class of nitrosamine.	61
3.1	The eight nitrosamines used in this study.	66
3.2	Flow reaction setup (general). Showing both manual loading using syringes with luer-lock, and automated loading using the autosampler. The online analysis IR traces are shown on the laptop screen.	68
3.3	Flow reaction setup for the reaction of N6 with sodium borohydride.	69
3.4	Area under the curve (AUC) plots for the reaction between <i>N</i> -methyl- <i>N</i> -nitrosourethane (N6) and NaBH <sub>4</sub> . Showing consumption of both the N=O and C=O bonds.	71

3.5	Graphs of the peak shapes for three separate reference runs for the eight nitrosamines studied. . . . .	73
3.6	Graph to show the deviation in peak areas of the AUC plots across three reference runs. . . . .	74
3.7	Images of reaction setup. . . . .	76
3.8	HPLC Calibration curve for <i>N</i> -nitrosodiethylamine (N1) at 210nm. . . . .	77
3.9	Overlap of nitrosamine and amine peaks in GC-MS/MS with <i>N</i> -nitrosodiphenylamine (N4). . . . .	78
3.10	The workflow used to calculate the conversions with respect to the nitrosamine in the reactivity screen. . . . .	89
3.11	An example HPLC chromatogram with applied processing method. . . . .	90
3.12	The eight nitrosamines used in this study, repeated for readability. . . . .	98
3.13	Summary tables for the results of the reactivity screen showing a) The conversions with respect to the <i>N</i> -nitrosamine and b) The products of the reactions determined by GC-MS/MS and LC-MS/MS. . . . .	99
3.14	Summary tables for the results of the reactivity screen for conditions 1 and 2 showing a) The conversions with respect to the <i>N</i> -nitrosamine and b) The products of the reactions determined by GC-MS/MS and LC-MS/MS. . . . .	100
3.15	LC-MS/MS results for N4 in condition 1. . . . .	101
3.16	<sup>1</sup> H and <sup>13</sup> C NMR for the reaction of N4 in H <sub>2</sub> O <sub>2</sub> producing diphenylamine. . . . .	102
3.17	GC-MSMS plots for N1, N2, N3 and N5 condition 2. . . . .	103
3.18	LC-MS/MS results for N4 in condition 2. . . . .	104
3.19	HPLC results for N4 in condition 2. . . . .	104
3.20	LC-MS/MS results for N7 reactivity under condition 2. . . . .	105
3.21	LC-MS/MS results for N8 reactivity under condition 2. . . . .	106
3.22	Reactivity of <i>N</i> -nitrosamines under acidic conditions 3-7. a) Conversions with respect to the <i>N</i> -nitrosamine and b) Products of the reactions determined by GC-MS/MS and LC-MS/MS. . . . .	109
3.23	The Nitroso-N NBO charges for the eight nitrosamines in the study. . . . .	110
3.24	GC-MS/MS Chromatogram for N6 in condition 3 showing the denitrosation product methylethylcarbamate . . . . .	110
3.25	HPLC Chromatograms for N4 under acidic conditions. . . . .	112

3.26	LC-MS/MS results for N4 reactivity under conditions 4 and 5. . . . .	113
3.27	LC-MS/MS results for N4 reactivity under condition 3. . . . .	114
3.28	LC-MS/MS results for N4 reactivity under conditions 6 and 7. . . . .	115
3.29	<sup>1</sup> H NMR of the crude reaction mixture for N5 in condition 6. . . . .	116
3.30	LC-MS/MS results for N8 reactivity under condition 3. . . . .	117
3.31	GC-MS/MS chromatogram for N3 in condition 7 showing the amine product. . .	118
3.32	LC-MS/MS chromatogram for N7 in condition 7 showing the amine product. . .	118
3.33	Reactivity of <i>N</i> -nitrosamines with hydride reductants in conditions 8-10. a) Conversions with respect to the nitrosamine and b) Products of the reactions determined by GC-MS/MS and LC-MS/MS. . . . .	120
3.34	LC-MS/MS chromatogram for <i>N</i> -nitrosodiphenylamine (N4) in reaction condi- tion 8. . . . .	120
3.35	GC-MS/MS chromatogram for N6 in condition 8 showing the complete reduction of the nitrosamine. . . . .	121
3.36	LC-MS/MS summary for N4 in conditions 9 and 10. . . . .	122
3.37	GC-MSMS plots for N1, N2, N3 and N5-7 for condition 9. . . . .	123
3.38	LC-MS/MS experiment chromatogram for ethyl- <i>N</i> -(2-hydroxyethyl)nitrosamine (N8) in reaction condition 9. . . . .	124
3.39	Reactivity of <i>N</i> -nitrosamines with sulfur-based reductants in conditions 11-19. a) Conversions with respect to the nitrosamine and b) Products of the reactions determined by GC-MS/MS and LC-MS/MS. . . . .	125
3.40	LC-MSMS chromatogram for <i>N</i> -nitrosodiphenylamine (N4) in reaction condition 14. . . . .	127
3.41	GC-MSMS plots for N1, N2, N3 and N5 condition 14. Jump back to experimental procedure 3.6 . . . . .	128
3.42	GC-MSMS plots for N6-N8 for condition 14. . . . .	129
3.43	LC-MS/MS experiment chromatogram for <i>N</i> -nitrosodiphenylamine (N4) in re- action condition 19. . . . .	130
D.1	HPLC Calibration curves for <i>N</i> -nitrosodiethylamine (N1) at 210nm. Referenced in Chapter 3, general experimental procedure Section 3.5 and in Table 3.5. . . .	182

D.2	HPLC Calibration curves for N-nitrosodiethylamine (N1) at 220nm. Referenced in Chapter 3, general experimental procedure Section 3.5 and in Table 3.5. . . . .	183
D.3	HPLC Calibration curves for N-nitrosodipropylamine (N2). Referenced in Chapter 3, general experimental procedure Section 3.5 and in Table 3.5. . . . .	184
D.4	HPLC Calibration curves for N-nitrosodibutylamine (N3). Referenced in Chapter 3, general experimental procedure Section 3.5 and in Table 3.5. . . . .	185
D.5	HPLC Calibration curves for N-nitrosodiphenylamine (N4). Referenced in Chapter 3, general experimental procedure Section 3.5 and in Table 3.4. . . . .	186
D.6	HPLC Calibration curves for N-nitrosomorpholine (N5). Referenced in Chapter 3, general experimental procedure Section 3.5 and in Table 3.5. . . . .	187
D.7	HPLC Calibration curves for N-methyl-N-nitrosourethane (N6). Referenced in Chapter 3, general experimental procedure Section 3.5 and in Table 3.5. . . . .	188
D.8	HPLC Calibration curves for N-butyl-N-(4-hydroxybutyl)nitrosamine (N7). Referenced in Chapter 3, general experimental procedure Section 3.5 and in Table 3.5.	189
D.9	HPLC Calibration curves for N-ethyl-N-(2-hydroxyethyl)nitrosamine (N8). Referenced in Chapter 3, general experimental procedure Section 3.5 and in Table 3.5.	190
E.1	GC-MSMS Calibration curve for N-nitrosodiethylamine (N1). Referenced in Chapter 3, general experimental procedure Section 3.5 and in Table 3.7. . . . .	191
E.2	GC-MSMS Calibration curve for N-nitrosodipropylamine (N2). Referenced in Chapter 3, general experimental procedure Section 3.5 and in Table 3.7. . . . .	192
E.3	GC-MSMS Calibration curve for N-nitrosodibutylamine (N3). Referenced in Chapter 3, general experimental procedure Section 3.5 and in Table 3.7. . . . .	192
E.4	GC-MSMS Calibration curve for N-nitrosomorpholine (N5). Referenced in Chapter 3, general experimental procedure Section 3.5 and in Table 3.7. . . . .	193
E.5	GC-MSMS Calibration curve for N-methyl-N-nitrosourethane (N6). Referenced in Chapter 3, general experimental procedure Section 3.5 and in Table 3.7. . . . .	193
E.6	GC-MSMS Calibration curve for N-butyl-N-(4-hydroxybutyl)nitrosamine (N7). Referenced in Chapter 3, general experimental procedure Section 3.5 and in Table 3.7. . . . .	194

E.7	GC-MSMS Calibration curve for N-ethyl-N-(2-hydroxyethyl)nitrosamine (N7). Referenced in Chapter 3, general experimental procedure Section 3.5 and in Table 3.7. . . . .	194
F.1	GC-MSMS reference for N-nitrosodiethylamine. Referenced in Table 3.8 . . . . .	195
F.2	GC-MSMS reference for N-nitrosodipropylamine. Referenced in Table 3.8 . . . . .	196
F.3	GC-MSMS reference for N-nitrosodibutylamine. Referenced in Table 3.8 . . . . .	197
F.4	GC-MSMS reference for N-nitrosomorpholine. Referenced in Table 3.8 . . . . .	198
F.5	GC-MSMS reference for N-methyl-N-nitrosourethane. Referenced in Table 3.8 . . . . .	199
F.6	GC-MSMS reference for N-butyl-N-(4-hydroxybutyl)-nitrosamine. Referenced in Table 3.8 . . . . .	200
F.7	GC-MSMS reference for N-ethyl-N-(2-hydroxyethyl)-nitrosamine. Referenced in Table 3.8 . . . . .	201
F.8	GC-MSMS reference for dibutylamine. Referenced in Table 3.8 . . . . .	202
F.9	GC-MSMS reference for dipropylamine and dipropylhydrazine, from reaction of N2 with DiBAL-H. Referenced in Table 3.8 . . . . .	203
F.10	GC-MSMS reference for dibutylamine and dibutylhydrazine, from reaction of N3 with DiBAL-H. Referenced in Table 3.8 . . . . .	204
F.11	GC-MSMS reference for morpholine and 4-aminomorpholine, from reaction of N5 with DiBAL-H. Referenced in Table 3.8 . . . . .	205
F.12	GC-MSMS reference for 4-(butylamino)-1-butanol and N-butyl-N-(4-hydroxybutyl)hydrazine, from reaction of N7 with DiBAL-H. Referenced in Table 3.8 . . . . .	206
F.13	GC-MSMS reference for 2-(ethylamino)ethanol and 2-(1-ethylhydrazino) ethanol, and possible cyclisation product from reaction of N8 with DiBAL-H. Referenced in Table 3.8 . . . . .	207
F.14	GC-MSMS reference for N-nitrodiethylamine from reaction of N1 with $\text{CH}_3\text{CO}_3\text{H}$ . Referenced in Table 3.8 . . . . .	208
F.15	GC-MSMS reference for N-nitrodipropylamine from reaction of N2 with $\text{CH}_3\text{CO}_3\text{H}$ . Referenced in Table 3.8 . . . . .	209
F.16	GC-MSMS reference for 2-Chloro-1,3,5-trimethoxybenzene from reaction of N6 with $\text{H}_2\text{O}_2$ . Referenced in Table 3.9 . . . . .	210

F.17 GC-MSMS reference for 2-Chloro-1,3,5-trimethoxybenzene (M+EtOH adduct) from reaction of N1 with CH <sub>3</sub> CO <sub>3</sub> H. Referenced in Table 3.9 . . . . .	211
F.18 GC-MSMS reference for 2,4-dichloro-1,3,5-trimethoxybenzene from reaction of N3 with CH <sub>3</sub> CO <sub>3</sub> H. Referenced in Table 3.9 . . . . .	212
F.19 GC-MSMS reference for 2,4-dichloro-1,3,5-trimethoxybenzene (M+EtOH adduct) from reaction of N5 with CH <sub>3</sub> CO <sub>3</sub> H. Referenced in Table 3.9 . . . . .	213
F.20 GC-MSMS reference for 2,6-di-tert-butyl-4-methylphenol (BHT) from reaction of N1 with NaBH <sub>4</sub> . Referenced in Table 3.8 . . . . .	214
F.21 GC-MSMS reference for 2-Bromo-4-chloro-1,3,5-trimethoxybenzene M+EtOH adduct from reaction of N7 with HBr. Referenced in Table 3.9 . . . . .	215
G.1 GC-MSMS plots for N1, N2, N3 and N5 condition 1. As referenced in Section 3.6	217
G.2 GC-MSMS plots for N6-8 for condition 1. As referenced in Section 3.6 . . . . .	218
G.3 GC-MSMS plots for N1, N2, N3 and N5 condition 2. As referenced in Section 3.6	219
G.4 GC-MSMS plots for N6-8 for condition 2. As referenced in Section 3.6 . . . . .	220
G.5 GC-MSMS plots for N1, N2, N3, and N5-7 for condition 3. As referenced in Section 3.6 . . . . .	221
G.6 GC-MSMS plots for N1, N2, N3 and N5 condition 5. As referenced in Section 3.6	222
G.7 GC-MSMS plots for N6-8 for condition 5. As referenced in Section 3.6 . . . . .	223
G.8 GC-MSMS plots for N1, N2, N3, N5 and N6 for condition 7. As referenced in Section 3.6 . . . . .	224
G.9 GC-MSMS plots for N1, N2, N3, N5 and N6 for condition 8. As referenced in Section 3.6 . . . . .	225
G.10 GC-MSMS plots for N1, N2, N3 and N5-7 for condition 9. As referenced in Section 3.6 . . . . .	226
G.11 GC-MSMS plots for N1, N2, N3 and N5-7 for condition 10. As referenced in Section 3.6 . . . . .	227
G.12 GC-MSMS plots for N1, N2, N3 and N5 condition 11. As referenced in Section 3.6	228
G.13 GC-MSMS plots for N6-8 for condition 11. As referenced in Section 3.6 . . . . .	229
G.14 GC-MSMS plots for N1-3, N5, N7 and N8 for condition 12. As referenced in Section 3.6 . . . . .	230
G.15 GC-MSMS plots for N1, N2, N3 and N5 condition 13. As referenced in Section 3.6	231

G.16 GC-MSMS plots for N6-N8 for condition 13. As referenced in Section 3.6 . . . .	232
G.17 GC-MSMS plots for N1, N2, N3 and N5 condition 14. As referenced in Section 3.6.233	
G.18 GC-MSMS plots for N6-N8 for condition 14. As referenced in Section 3.6 . . . .	234
G.19 GC-MSMS plots for N1, N2, N3 and N5 condition 15. As referenced in Section 3.6.235	
G.20 GC-MSMS plots for N6-N8 for condition 15. As referenced in Section 3.6 . . . .	236
G.21 GC-MSMS plots for N1-3, N5, N7 and N8 for condition 17. As referenced in Section 3.6 . . . . .	237
G.22 GC-MSMS plots for N1, N2, N3 and N5 condition 19. As referenced in Section 3.6.238	
G.23 GC-MSMS plots for N6-N8 for condition 19. As referenced in Section 3.6 . . . .	239
G.24 GC-MSMS plots for N1, N2, N3 and N5 condition 21. As referenced in Section 3.6.240	
G.25 GC-MSMS plots for N6-N8 for condition 21. As referenced in Section 3.6 . . . .	241
H.1 LC-MSMS reference chromatogram for N-nitrosodiphenylamine (N4). As refer- enced in Table 3.11. . . . .	242
H.2 LC-MSMS reference mass peaks for N-nitrosodiphenylamine (N4). As referenced in Table 3.11. . . . .	243
H.3 LC-MSMS reference chromatogram for diphenylamine. As referenced in Table 3.11.	244
H.4 LC-MSMS reference reference mass peaks for diphenylamine. As referenced in Table 3.11. . . . .	245
H.5 LC-MSMS reference chromatogram for N,N'-diphenylhydrazine. As referenced in Table 3.11. . . . .	246
H.6 LC-MSMS reference mass peaks for N,N'-diphenylhydrazine. As referenced in Table 3.11. . . . .	247
H.7 LC-MSMS reference chromatogram for <i>p</i> -nitrosodiphenylamine from reaction condition 4. As referenced in Table 3.11. . . . .	248
H.8 LC-MSMS reference mass peaks for <i>p</i> -nitrosodiphenylamine from reaction con- dition 4. As referenced in Table 3.11. . . . .	249
H.9 LC-MSMS reference chromatogram for N-butyl-N(4-hydroxybutyl)nitrosamine N7. As referenced in Table 3.11. . . . .	250
H.10 LC-MSMS reference mass peaks for N-butyl-N(4-hydroxybutyl)nitrosamine N7. As referenced in Table 3.11. . . . .	251

H.11 LC-MSMS reference chromatogram for N-ethyl-N(2-hydroxyethyl)nitrosamine N8. As referenced in Table 3.11. . . . .	251
H.12 LC-MSMS reference mass peaks for N-ethyl-N(2-hydroxyethyl)nitrosamine N8. As referenced in Table 3.11. . . . .	252
H.13 LC-MSMS reference chromatogram for 4-(butylamino)-1-butanol from condition 7. As referenced in Table 3.11. . . . .	253
H.14 LC-MSMS reference mass peaks for 4-(butylamino)-1-butanol from condition 7. As referenced in Table 3.11. . . . .	254
I.1 LC-MSMS experiment chromatogram for N-nitrosodiphenylamine (N4) in reac- tion condition 1. Referenced in Section 3.6. . . . .	256
I.2 LC-MSMS experiment chromatogram for N-nitrosodiphenylamine (N4) in reac- tion condition 2. Referenced in Section 3.6. . . . .	257
I.3 LC-MSMS experiment chromatogram for N-nitrosodiphenylamine (N4) in reac- tion condition 3. Referenced in Section 3.6. . . . .	258
I.4 LC-MSMS experiment chromatogram for N-ethyl-N-(2-hydroxyethyl)nitrosamine (N8) in reaction condition 3. Referenced in Section 3.6. . . . .	259
I.5 LC-MSMS experiment chromatogram for N-nitrosodiphenylamine (N4) in reac- tion condition 4. Referenced in Section 3.6. . . . .	260
I.6 LC-MSMS experiment chromatogram for N-nitrosodiphenylamine (N4) in reac- tion condition 5. Referenced in Section 3.6. . . . .	261
I.7 LC-MSMS experiment chromatogram for N-nitrosodiphenylamine (N4) in reac- tion condition 6. Referenced in Section 3.6. . . . .	262
I.8 LC-MSMS experiment chromatogram for N-nitrosodiphenylamine (N4) in reac- tion condition 7. Referenced in Section 3.6. . . . .	263
I.9 LC-MSMS experiment chromatogram for N-butyl-N-(4-hydroxybutyl)nitrosamine (N7) in reaction condition 7. Referenced in Section 3.6. . . . .	264
I.10 LC-MSMS experiment chromatogram for N-ethyl-N-(2-hydroxyethyl)nitrosamine (N8) in reaction condition 7. Referenced in Section 3.6. . . . .	265
I.11 LC-MSMS experiment chromatogram for N-nitrosodiphenylamine (N4) in reac- tion condition 8. Referenced in Section 3.6. . . . .	266



I.12	LC-MSMS experiment chromatogram for N-butyl-N-(4-hydroxybutyl)nitrosamine (N7) in reaction condition 8. Referenced in Section 3.6. . . . .	267
I.13	LC-MSMS experiment chromatogram for N-ethyl-N-(2-hydroxyethyl)nitrosamine (N8) in reaction condition 8. Referenced in Section 3.6. . . . .	268
I.14	LC-MSMS experiment chromatogram for N-nitrosodiphenylamine (N4) in reaction condition 9. Referenced in Section 3.6. . . . .	269
I.15	LC-MSMS experiment chromatogram for ethyl-N-(2-hydroxyethyl)nitrosamine (N8) in reaction condition 9. Referenced in Section 3.6. . . . .	270
I.16	LC-MSMS experiment chromatogram for N-nitrosodiphenylamine (N4) in reaction condition 10. Referenced in Section 3.6. . . . .	271
I.17	LC-MSMS experiment chromatogram for ethyl-N-(2-hydroxyethyl)nitrosamine (N8) in reaction condition 10. Referenced in Section 3.6. . . . .	272
I.18	LC-MSMS experiment chromatogram for N-nitrosodiphenylamine (N4) in reaction condition 11. Referenced in Section 3.6. . . . .	273
I.19	LC-MSMS experiment chromatogram for N-nitrosodiphenylamine (N4) in reaction condition 12. Referenced in Section 3.6. . . . .	274
I.20	LC-MSMS experiment chromatogram for N-nitrosodiphenylamine (N4) in reaction condition 13. Referenced in Section 3.6. . . . .	275
I.21	LC-MSMS experiment chromatogram for N-nitrosodiphenylamine (N4) in reaction condition 14. Referenced in Section 3.6. . . . .	276
I.22	LC-MSMS experiment chromatogram for N-nitrosodiphenylamine (N4) in reaction condition 15. Referenced in Section 3.6. . . . .	277
I.23	LC-MSMS experiment chromatogram for N-nitrosodiphenylamine (N4) in reaction condition 17. Referenced in Section 3.6. . . . .	278
I.24	LC-MSMS experiment chromatogram for N-nitrosodiphenylamine (N4) in reaction condition 19. Referenced in Section 3.6. . . . .	279
I.25	LC-MSMS experiment chromatogram for N-nitrosodiphenylamine (N4) in reaction condition 21. Referenced in Section 3.6. . . . .	280
J.1	$^1\text{H}$ NMR analysis of crude reaction mixture for N4 in condition 1. . . . .	282
J.2	$^{13}\text{C}$ NMR analysis of crude reaction mixture for N4 in condition 1. . . . .	283
J.3	$^1\text{H}$ NMR analysis of crude reaction mixture for N5 in condition 6. . . . .	285

# List of Tables

1.1	EMA potency categories for <i>N</i> -nitrosamines. . . . .	17
2.1	Class hierarchy for the structural classes of <i>N</i> -nitrosamines. . . . .	37
2.2	Classification summary table . . . . .	39
2.3	De/transnitrosation reactions summary table. . . . .	42
2.4	Diazonium formation reactions summary table. . . . .	47
2.5	<i>N</i> -alkylation reactions summary table. . . . .	50
2.6	Azo formation reactions summary table. . . . .	52
2.7	N <sub>3</sub> formation with amine reactions summary table . . . . .	53
2.8	O-Si/C/S bond formation summary table. . . . .	55
2.9	Reduction reactions summary table. . . . .	58
3.1	Reaction conditions based on Mirabilis tool for reactivity screening against common <i>N</i> -nitrosamines. . . . .	64
3.2	The reagents to be tested in the reactivity screen. . . . .	66
3.3	Summary of the reaction conditions for the batch HPLC reactivity screen. . . . .	79
3.4	HPLC calibration curve equations with line equation form: $y = y_0 + A \cdot \exp(R_0 \cdot x)$ . . . . .	90
3.5	HPLC calibration curve equations with line equation form: $y = a + b \cdot x$ . . . . .	91
3.6	Gas chromatography settings. . . . .	92
3.7	The determined calibration curve equations for the nitrosamines analysed by GC for conditions 9 and 10. . . . .	92
3.8	GC-MS/MS peak data for known products. . . . .	95
3.9	GC-MS/MS peak data for side products. . . . .	96
3.10	LC-MS/MS method settings. . . . .	97
3.11	LC-MS/MS reference mass peaks and retention times. . . . .	97

---

B.1	Transformation classification class hierarchy. . . . .	173
B.2	Reagent classification class hierarchy. . . . .	174
C.1	N-nitrosamine stock solution preparation as referenced in Chapter 3, general experimental procedure Section 3.5. . . . .	178

# List of Schemes

1.1	Zwitterionic behaviour of <i>N</i> -nitrosamines. . . . .	2
1.2	Protonated forms of NDMA. . . . .	3
1.3	Metabolism of NDMA by cytochrome enzymes in the liver. . . . .	3
1.4	The change in manufacturing process leading to nitrosamine impurities in Val- sartan. . . . .	4
1.5	NDMA formation from nitrous acid. . . . .	4
1.6	NDEA formation from nitrous acid <i>via</i> tertiary amine precursor (TEA). . . . .	5
1.7	Primary and aromatic amines are not precursors for <i>N</i> -nitrosamines. . . . .	5
1.8	NDMA formation from Ranitidine. . . . .	6
1.9	Reduction of nitrosamines to amines and hydrazines. . . . .	8
1.10	Reduction of nitrosamines with zinc under acidic conditions. . . . .	9
1.11	Reduction of nitrosamines with lithium aluminium hydride. . . . .	10
1.12	Metal-free conditions to reduce <i>N</i> -nitrosamines by Chaudhary and coworkers. [33, 32]. . . . .	12
1.13	Na <sub>2</sub> S <sub>2</sub> O <sub>4</sub> in basic media used to reduce a cyclic nitrosamine . . . . .	12
1.14	Reactions of nitrosamines with electrophilic reagents. . . . .	13
1.15	Deprotonation-cyclisation with nitriles. . . . .	13
1.16	Reaction of nitrosamines with lithium amide. . . . .	13
1.17	<i>N</i> -alkylation reactions of <i>N</i> -nitrosamines. . . . .	14
1.18	Reactions of aryl nitrosamines in acid. . . . .	15
1.19	Oxidation of <i>N</i> -nitrosamines to <i>N</i> -nitramines. . . . .	16
1.20	Photolytic cleavage of N-N followed by addition to unsaturated C=C bonds. . . .	16
1.21	High-risk <i>N</i> -nitroso API impurities. Figure adapted from [54]. . . . .	17
1.22	The SMILES language for molecular structure representation. . . . .	19

1.23	Workflow for AAM in the RDT . . . . .	23
2.1	Selecting depth one cores to incorporate the N–N=O substructure. . . . .	32
2.2	Examples of the structural classes of <i>N</i> -nitrosamine with count > 10 in the dataset. . . . .	35
2.3	Example structures of the grouped <i>N</i> -nitrosamine classes. . . . .	36
2.4	Numbered grouped <i>N</i> -nitrosamine classes. . . . .	38
2.5	Deprotonation-cyclisation with CN transformation example reaction. . . . .	41
2.6	General reaction scheme for denitrosation reactions with acid. . . . .	42
2.7	Reaction of an alkyl; amide <i>N</i> -nitrosamine under photochemical and acidic conditions. . . . .	43
2.8	Denitrosation by strong <i>N</i> -nucleophile. . . . .	43
2.9	Denitrosation by stabilised carbanion. . . . .	44
2.10	Examples of transnitrosation reactions. . . . .	44
2.11	Examples of denitrosation reactions under basic conditions. . . . .	45
2.12	Denitrosation reaction with transition metal (TM) catalyst. . . . .	46
2.13	Diazonium formation under basic and thermal conditions. . . . .	48
2.14	Diazonium formation under thermal conditions. . . . .	49
2.15	diazonium formation reaction with a sulfonium bromide. . . . .	49
2.16	diazonium formation reaction with a dialkyl nitrosamine. . . . .	49
2.17	Intramolecular cyclisations forming new C=N bonds, classified as <i>N</i> -alkylation reactions in the dataset. . . . .	51
2.18	<i>N</i> -alkylation reaction with a rhodium (III) catalyst. . . . .	51
2.19	Azo formation from an electrophilic nitrosamine and an arene in basic conditions. . . . .	52
2.20	Azo formation from an aryl nitrosamine after Fischer-Hepp rearrangement. . . . .	53
2.21	Triazene formation with electrophilic nitrosamines. . . . .	53
2.22	Triazene resonance structures. . . . .	54
2.23	Triazene formation with dialkyl nitrosamines. . . . .	54
2.24	Cyclisation of a $\beta$ - cyano nitrosamine to form a sydnone imine. . . . .	56
2.25	Cyclisation of a $\beta$ - carboxylic acid nitrosamine to form a sydnone. . . . .	56
2.26	O-alkylation reaction with an $\alpha$ -hydroxyl nitrosamine. . . . .	57
2.27	Reduction of an imino nitrosamine by lithium aluminium hydride to form the diazo compound. . . . .	58

---

2.28	Reduction of an electrophilic nitrosamine by zinc in acetic acid. . . . .	58
2.29	$\text{Na}_2\text{S}_2\text{O}_4$ in basic media used to reduce a cyclic nitrosamine . . . . .	59
3.1	Metal-free conditions to reduce <i>N</i> -nitrosamines by Chaudhary and coworkers. [33, 32] . . . . .	65
3.2	$\text{Na}_2\text{S}_2\text{O}_4$ in basic media used to reduce a cyclic nitrosamine . . . . .	65
3.3	Reactivity of <i>N</i> -nitrosamines under acidic conditions for a) aryl <i>N</i> -nitrosamines and b) dialkyl <i>N</i> -nitrosamines. . . . .	107
3.4	Comparison of the acid-base chemistry for conditions 3, 4 and 6. . . . .	108
3.5	Redox reaction and cell potential for $\text{Na}_2\text{S}_2\text{O}_4$ and $\text{Na}_2\text{SO}_3$ in basic media.[133] .	126
B.1	Examples of denitrosation reactions under basic conditions. . . . .	177

# Chapter 1

## Introduction

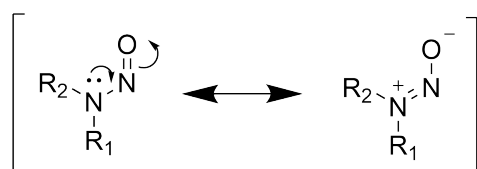
### 1.1 Scope of this chapter

This chapter introduces a case-study into *N*-nitrosamines, which are an important class of genotoxin whose relevance and importance to high-value chemical manufacture became paramount in 2018 upon the discovery of *N*-nitrosodimethylamine (NDMA) in the blockbuster angiotensin II receptor blocker (ARB) drug Valsartan. [1] These findings prompted an industry-wide effort to risk assess all commercial synthetic routes to a number of ARB's. This chapter details the *in-silico* tool, Mirabilis, developed by this project's sponsor, LHASA Ltd., which is able to report the risk of *N*-nitrosamine contamination in a given Active Pharmaceutical Ingredient (API), through the use of physicochemical parameters to determine the degree to which *N*-nitrosamines are removed during a given synthetic step. [2] With these points considered, this chapter then identifies the need for reactivity data on *N*-nitrosamines, which can be used to supplement the risk assessment process for API syntheses. The reported reactivity of *N*-nitrosamines published in two leading reviews is summarised [3, 4], highlighting that the reactivity described covers a narrow range of structural classes of *N*-nitrosamine, namely dialkyl and aryl *N*-nitrosamines due to their significance in high-value chemical manufacture, and their potency as DNA mutagens. Furthermore, it is indicated that the known reaction conditions which transform *N*-nitrosamines into safer moieties are harsh and thus they are of little use as methods of de-risking *N*-nitrosamine formation in high-value chemical manufacture due to inevitable adverse reactions with the API. This then prompts the description of the data-driven analysis and classification of existing *N*-nitrosamine reactivity data and subsequent batch reactivity screen performed in

this project.

## 1.2 *N*-nitrosamines

*N*-nitrosamines (interchangeably called nitrosamines throughout this text) can be characterised by the substructure N–N=O. That is, a nitroso group (N=O) attached to the nitrogen atom of a secondary amine (*N*-nitrosamine), amide (*N*-nitrosamide), carbamate (*N*-nitrosocarbamate), sulfonamide (*N*-nitrososulfonamide) etc. Two key resonance structures arise from the donation of the nitrogen lone pair into the  $\pi$  system of the adjacent nitroso group (Scheme 1.1). [5] The increased  $\pi$  character of the N-N bond causes the R<sub>1</sub>N(R<sub>2</sub>)NO moiety to be planar, with restricted rotation around N-N, which gives rise to a magnetic non-equivalence of R<sub>1</sub> and R<sub>2</sub> due to the orientation of the nitroso oxygen, which provides shielding to the syn oriented R-group (R<sub>2</sub> in Scheme 1.1). [6]

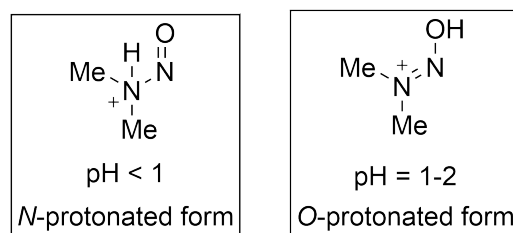


Scheme 1.1: Zwitterionic behaviour of *N*-nitrosamines.

The significance of this is the splitting of the NMR signals of the protons around N–N=O, with *N*-nitrosodimethylamine (NDMA) showing two signals in both <sup>1</sup>H and <sup>13</sup>C NMR instead of the expected one. [7] This leads to overlapping signals in the NMR spectra when dealing with some of the nitrosamines with longer alkyl chains (e.g. *N*-nitrosodibutylamine) and complicates the analysis by this method. The commonly used methods for *N*-nitrosamine detection are high performance liquid chromatography with tandem mass-spectrometry (LC-MS/MS) and gas chromatography tandem mass spectrometry (GC-MS/MS). [8, 9]

The resonance structures shown in Scheme 1.1 indicate that nitrosamines are most basic at the nitroso oxygen, with the amine nitrogen lone pair being unavailable, as the zwitterionic species is the favoured resonance form. [5] The O-protonated species is the predominant form of the nitrosamine in acidic conditions up until a pH of 1-2. Below this, the *N*-protonated species can exist (Scheme 1.2) and this is significant in the acid catalysed denitrosation reaction pathway which will be explained in Section 1.6. [10]

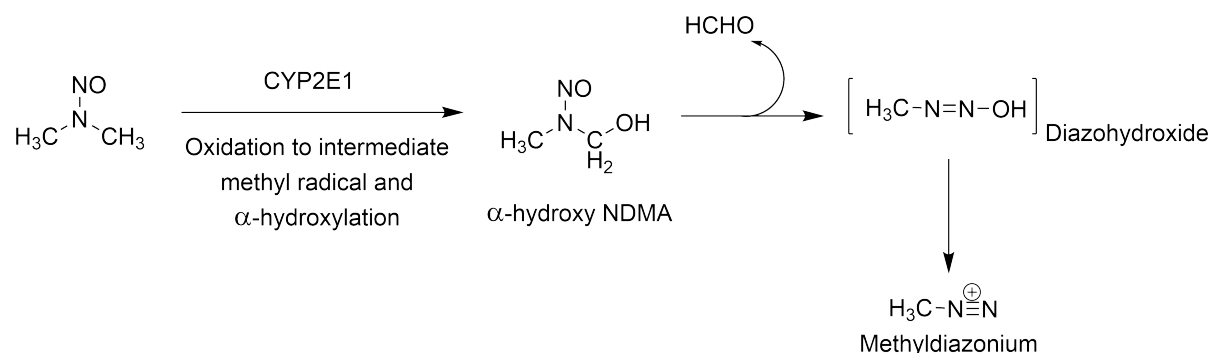




Scheme 1.2: Protonated forms of NDMA.

### 1.3 Carcinogenicity

It has long been known that *N*-nitrosamines are carcinogenic to humans. [11] The pathway to the mutagenic species with NDMA occurs in the liver (Scheme 1.3), through  $\alpha$ -hydroxylation by cytochrome P2E1, which causes the loss of an aldehyde and the production of an unstable primary nitrosamine which rearranges and subsequently loses water to form a diazonium ion, which can alkylate DNA. [12]



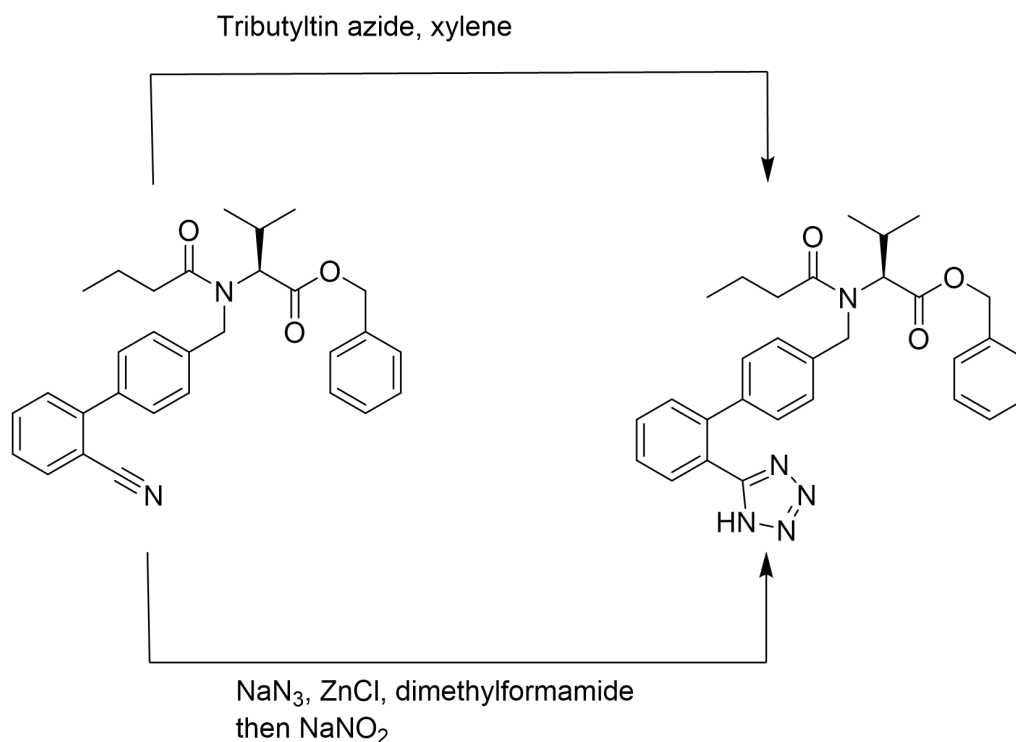
Scheme 1.3: Metabolism of NDMA by cytochrome enzymes in the liver.

There are multiple pathways to mutagenic activity, and this depends on the structure of the nitrosamine. Dialkyl nitrosamines require metabolic activation, while other nitrosamines such as *N*-nitrosamides and *N*-nitrosoureas do not. The effect is that the site of tumour formation can vary between different nitrosamines. [13]

### 1.4 The nitrosamine crisis

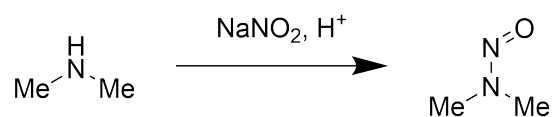
*N*-nitrosamines became a relevant industry-wide problem in 2018 with the discovery of NDMA in the blockbuster blood pressure regulator drug Valsartan. [14] The level of contamination was found to be above the regulatory limit for NDMA of 96 ng/day for a person weighing 50 kg; this precipitated blanket recalls of a number of similar Sartan APIs. [1] The root cause of the

introduction of the nitrosamine impurity was traced back to a change in the manufacture of the tetrazole ring (Scheme 1.4). The change saw the introduction of sodium nitrite ( $\text{NaNO}_2$ ) which was used to quench any unreacted azide, producing nitrogen monoxide ( $\text{NO}$ ) gas, nitrogen ( $\text{N}_2$ ) gas and sodium hydroxide ( $\text{NaOH}$ ). A pH correction was then performed, introducing acid into the reaction mixture which is thought to have reacted with excess sodium nitrite to produce nitrous acid ( $\text{HNO}_2$ ). [15]



Scheme 1.4: The change in manufacturing process leading to nitrosamine impurities in Valsartan.

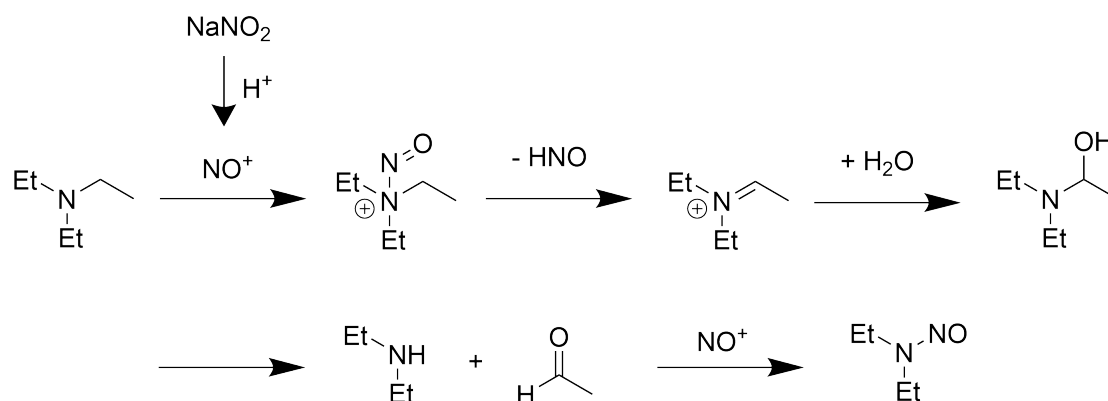
The presence of nitrous acid, along with dimethylamine, a trace impurity/decomposition product of the solvent, dimethylformamide (DMF) led to the production of NDMA in the reaction mixture (Scheme 1.5). [1]



Scheme 1.5: NDMA formation from nitrous acid.

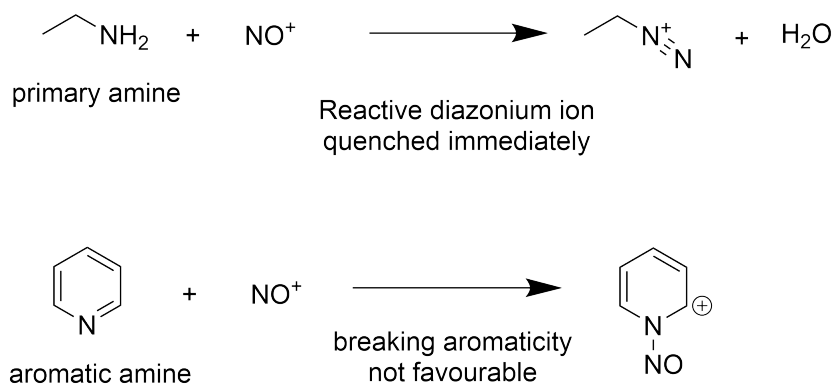
Formation of *N*-nitrosamines can also occur *via* tertiary amine precursors. This is particularly important because of the ubiquitous use of triethylamine (TEA) in industrial syntheses.

The formation pathway for TEA is suggested to occur *via* loss of an aldehyde, producing diethylamine, which is then nitrosated to produce *N*-nitrosodiethylamine (NDEA) (Scheme 1.6). [1]



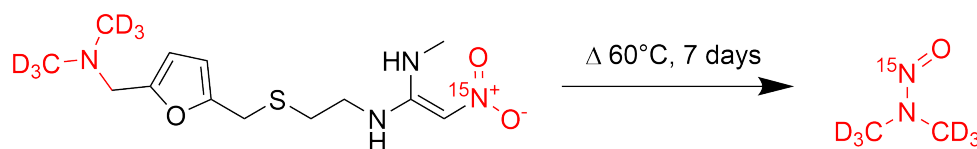
Scheme 1.6: NDEA formation from nitrous acid *via* tertiary amine precursor (TEA).

New studies on the generation of *N*-nitrosamines indicates that primary amine precursors may pose a lower risk. This is attributed to the formation of diazonium ions as a result of their reaction with nitrosonium, and these ions are highly reactive, and are thus quenched upon their formation. Additionally, aromatic amines are also of a weaker concern, as the disruption of aromaticity necessary for N-N bond formation is disfavoured (Scheme 1.7). [16]



Scheme 1.7: Primary and aromatic amines are not precursors for *N*-nitrosamines.

Worryingly, nitrosamine formation is not confined to reactions with trace impurities. NDMA contamination was also found in Ranitidine, a drug used to treat stomach ulcers. After extensive elimination of possible nitrite sources from both the precursor syntheses and from known impurities, isotopic labelling studies discovered that NDMA was formed during decomposition of the API itself (Scheme 1.8). Use of Ranitidine has been suspended since 2020. [17]



Scheme 1.8: NDMA formation from Ranitidine.

## 1.5 Controlling risk

The risk of formation of *N*-nitrosamines is of great concern to regulatory bodies. The International Council for Harmonisation of Technical Requirements for Pharmaceuticals for Human Use (ICH) has four options for the control of such mutagenic impurities, based on the associated risk of contamination. [18] The first three options involve the analytical testing of each batch of the final API, intermediate, or materials to ensure the impurity in question is not present at above acceptable levels. Batch analytical testing is time consuming and costly. However, option four permits the use of an assessment based on theoretical calculations of the degree to which a given impurity is removed as part of the manufacturing process. With option four, satisfactory assessments are based on the theoretical assessments alone. [18] The assessment of the removal of a given impurity during a process has been given the term “purge factor”, which is calculated based on physicochemical parameters of the impurity, and is used to estimate the fate of the impurity at each synthetic step during an API synthesis. A higher purge factor is associated with a lower risk of contamination. [19] Purge ratios are calculated from the ratio between the calculated overall purge factor for a process and the required purge factor for the impurity to fall within acceptable limits (Figure 1.1). [2] The sponsor company of this project, LHASA Ltd., developed the Mirabilis software to predict purge ratios based on empirical data and physicochemical parameters using *in-silico* methods. [2]

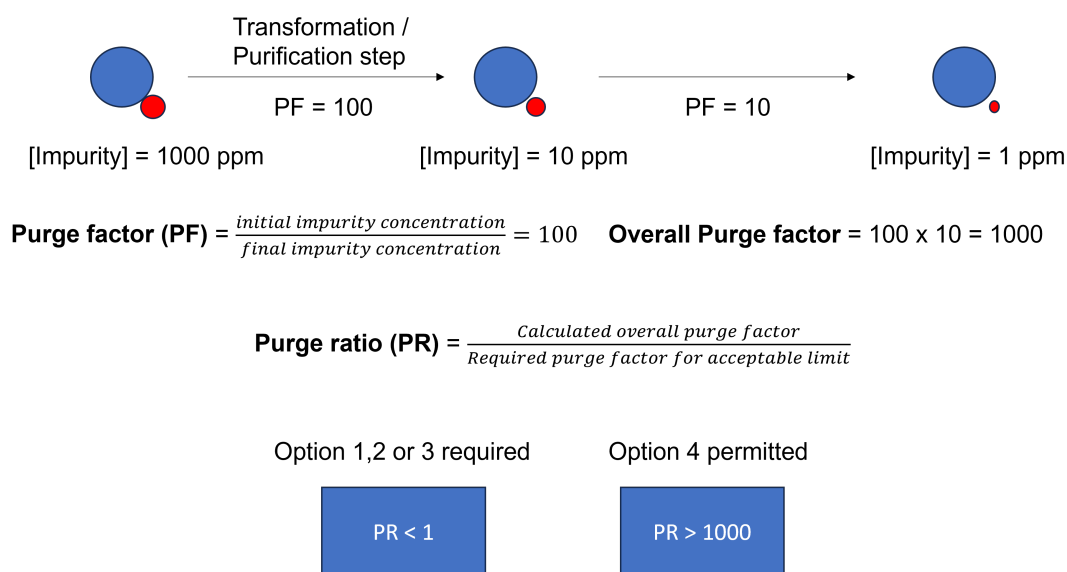
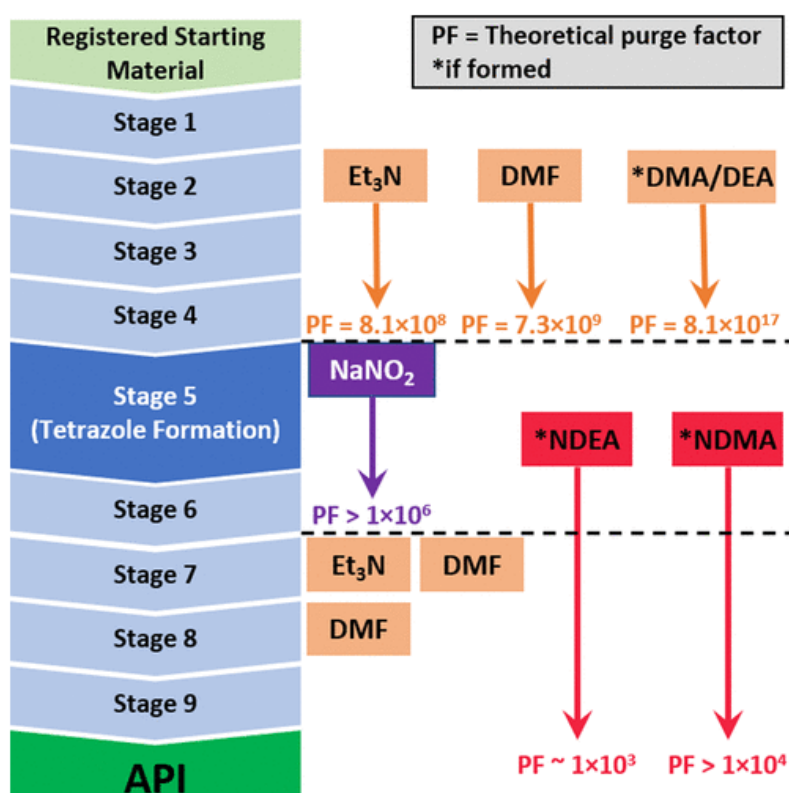


Figure 1.1: Calculation of purge factors for mutagenic impurities. [2]

The significance of purge factor calculations was demonstrated by Mirabilis when the software was applied to the synthesis of Candesartan, another tetrazole containing drug similar to Valsartan, but with a slightly different synthetic roadmap (Figure 1.2).

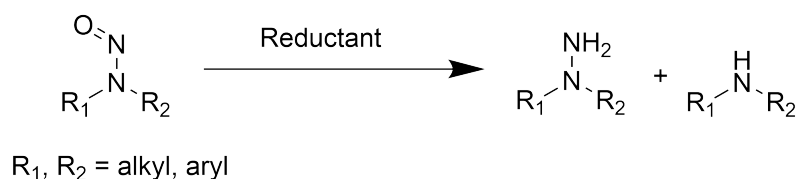
Figure 1.2: *N*-nitrosamine purge prediction by Mirabilis in the synthetic route to Candesartan. Figure taken from reference [2] (Figure 6).

Mirabilis was able to prove that the risk of NDMA and NDEA contamination was negligible ( $PF > 1000$ ) for this particular API, and hence the drug could be removed from the recall list and put back on the market. [2] This indicates that the better our understanding of the behaviour of *N*-nitrosamines during industrial process chemistry, the better the impurities can be controlled.

## 1.6 Known reactivity

The current assessment of safety with respect to *N*-nitrosamine contamination was based predominantly on physicochemical parameters until two reviews summarising *N*-nitrosamine reactivity were published in 2021. [3, 4] Both reviews focus on dialkyl and aryl nitrosamine chemistry as these classes of *N*-nitrosamine were prevalent at the time. This section is dedicated to summarising the reported methods to destroy these nitrosamines, with an emphasis on the difference the structure of the nitrosamine starting material has on its reactivity.

### 1.6.1 Reduction

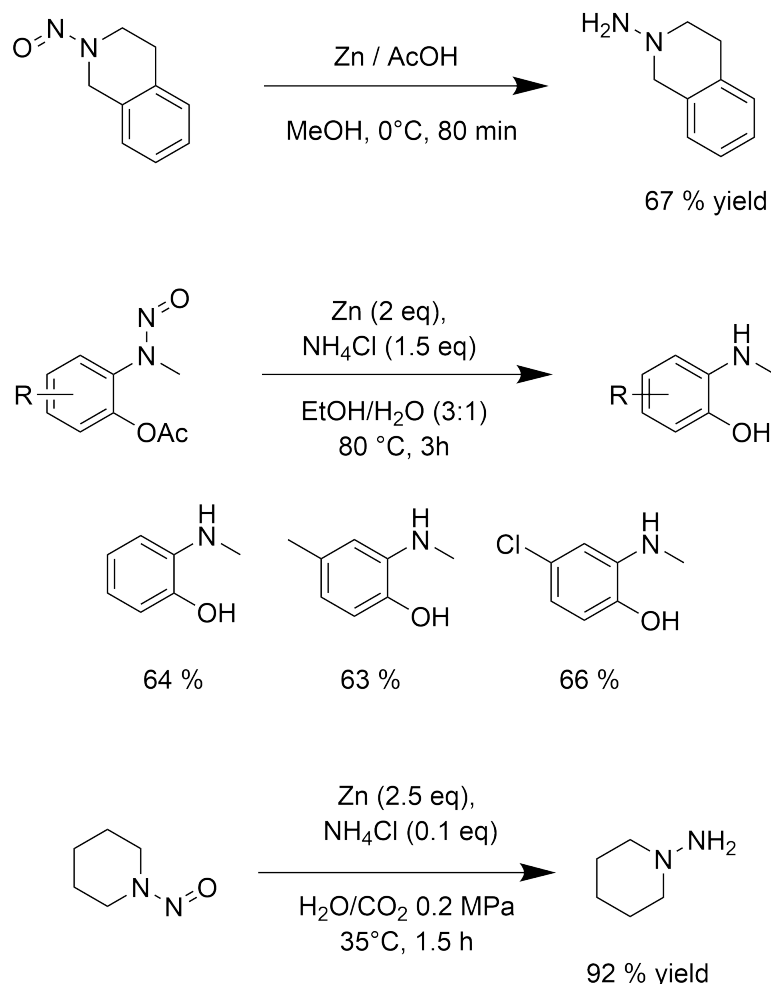


Scheme 1.9: Reduction of nitrosamines to amines and hydrazines.

*N*-nitrosamines can be reduced to their parent amines and hydrazines by numerous methods (Scheme 1.9). The more electron deficient aryl nitrosamines are more prone to reduction than dialkyl nitrosamines, as will be proved by the examples of reagents that are shown in this section. The conditions that apply to both dialkyl and aryl nitrosamines are often metals and hydride reductants and a number of reactions of these types have been reported.

Zinc dust under acidic conditions has long been used to reduce NDMA to its parent hydrazine in the production of rocket fuel. [20] More recent examples show that over reduction of other nitrosamines to the amine can be controlled by maintaining the reaction temperature at 0°C (Scheme 1.10), and while increased temperatures can lead to the amine product exclusively, the functional group tolerance under these conditions is low. [21, 22] An example where high selectivity (confirmed by GC-MS) towards the hydrazine product is achieved under mild conditions

uses an autoclave and pressurised CO<sub>2</sub> in a water solvent to provide a weakly acidic reaction medium, though the pH had to be further decreased with NH<sub>4</sub>Cl to achieve better conversions. [23]



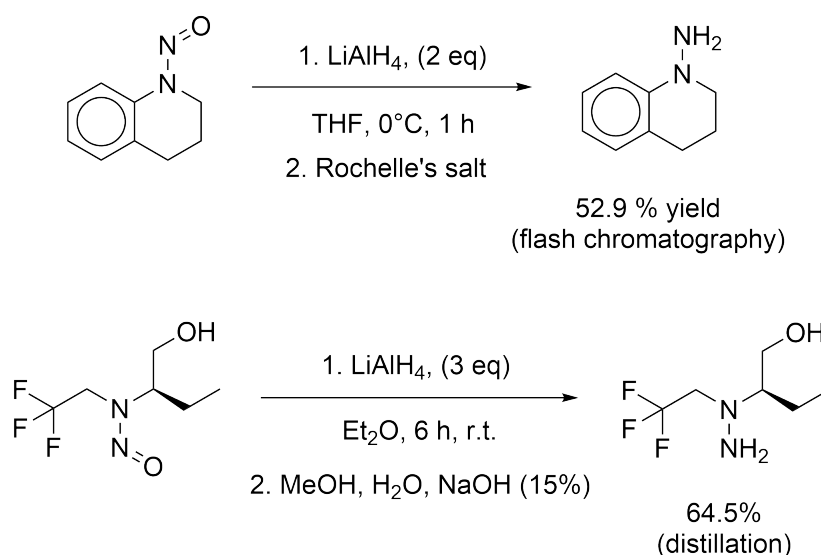
Scheme 1.10: Reduction of nitrosamines with zinc under acidic conditions.

Similar behaviour is observed with low-valent (Ti (II)) titanium reagents which are formed by the reduction of titanium tetrachloride TiCl<sub>4</sub> through various methods. While the reported methods offer some control over the selectivity between the amine and the hydrazine product for aryl nitrosamines, total control was not achieved. This study did not perform tests on dialkyl nitrosamines. [24]

Electrochemical conditions using a mercury cathode ( $E_{\text{cell}} = -0.9 \text{ V}$ ) have also been reported to reduce a range of alkyl and aryl nitrosamines to their corresponding hydrazines. The authors did however report amine products and other rearrangement products with aryl nitrosamines, and this is probably a result of the acid that is present in the electrolyte solution (see electrophilic

reactions). [25]

Reduction by lithium aluminium hydride (LAH) is also well known. Many examples on both alkyl and aryl nitrosamines indicate that the reaction produces the hydrazine with no mention of the amine product (Scheme 1.11). [26, 27] However, the majority of workup conditions do not apply a base wash, meaning that the amine products could be lost to the aqueous layer, with the less basic hydrazines remaining in the organic layer which is concentrated under vacuo for purification. Furthermore, purification techniques used to isolate the hydrazines such as flash chromatography or distillation seem to be focused only on achieving the hydrazine product. The moderate yields achieved in both examples shown in Scheme 1.11 could be a reflection of the over reduction product being present in the reaction mixture.



Scheme 1.11: Reduction of nitrosamines with lithium aluminium hydride.

Many hydrogenation catalysts have been investigated. [28, 29, 30, 31] The reactivity review by Borths and coworkers provided a summary of the normalised pseudo first order rate coefficients for the hydrogenation of NDMA which is displayed in Figure 1.3. [3] Ruthenium and palladium-nickel couples were found to be the most effective catalysts. The major product of the hydrogenation reactions is the parent amine compound, though there are different routes to achieve this. With the palladium-nickel couple it is thought that the nitrosamine initially binds to nickel, and then spillover activated hydrogen from palladium reduces the nitrosamine *via* reductive cleavage of the N-N bond. [28] With the ruthenium catalyst, the detection of small amounts of hydrazine product suggest that the nitroso-group is first reduced, followed by cleavage of the N-N bond to achieve the amine product. [29]



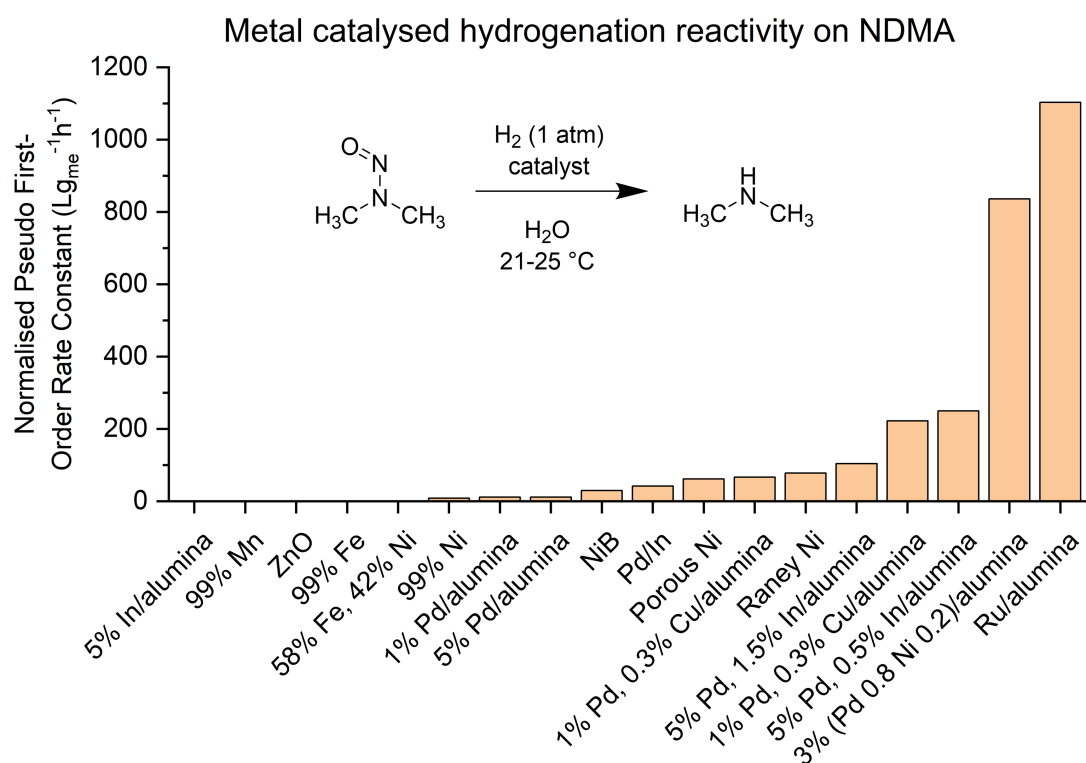
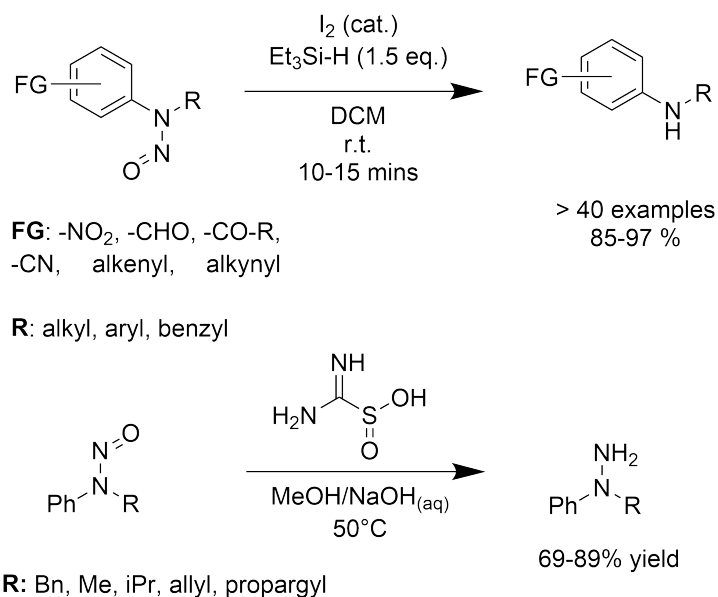


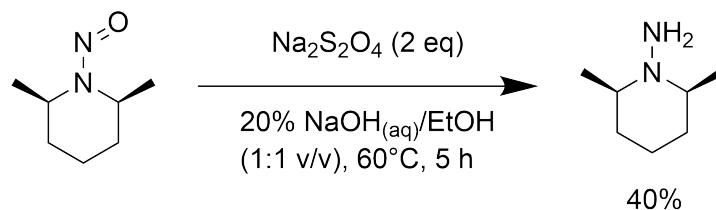
Figure 1.3: Comparison of the pseudo-first order rate coefficient of various hydrogenation catalysts applied to NDMA.

Metal free reaction conditions to reduce aryl nitrosamines to their parent and hydrazines have also been discovered. Chaudhary *et al.* introduced two metal-free methods to reduce aryl nitrosamines to the corresponding amines and hydrazines. The first uses thiourea dioxide in basic media at 50°C [32], and the second uses combination of triethylsilane and iodine [33], with the latter having the advantage that it can be performed at room temperature. The issue with the two methods is that no evidence is given of their effectiveness on a wider substrate scope and it is assumed that these conditions are only applicable to secondary aryl nitrosamines. (Scheme 1.12).



Scheme 1.12: Metal-free conditions to reduce *N*-nitrosamines by Chaudhary and coworkers. [33, 32]

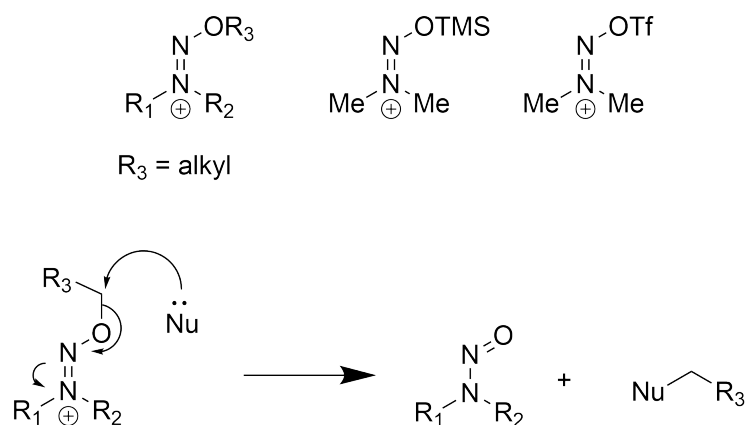
Another metal-free method by Overberger used sodium dithionite (Na<sub>2</sub>S<sub>2</sub>O<sub>4</sub>) in basic media to reduce a range of aryl *N*-nitrosamines and one cyclic dialkyl *N*-nitrosamine (Scheme 1.13). Although, the strongly basic solution does pose a safety risk. [34]



Scheme 1.13: Na<sub>2</sub>S<sub>2</sub>O<sub>4</sub> in basic media used to reduce a cyclic nitrosamine

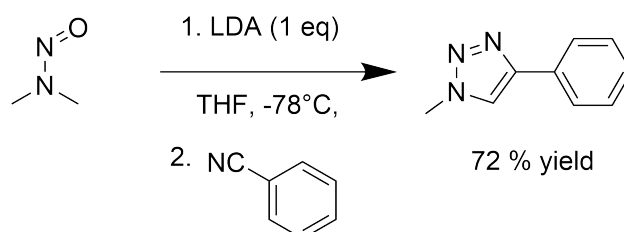
## 1.6.2 Electrophilic and nucleophilic reactions

As mentioned, *N*-nitrosamines are most basic at their nitroso-oxygen, and a number of reactions with electrophiles are known. Studied reagents include alkylating agents, producing alkoxydiazonium salts [35, 36], with *O*-trimethylsilyl and *O*-triflyl derivatives of NDMA also having been prepared (Scheme 1.14). The formed diazenium salts are unstable to nucleophiles, and the nitrosamine is quickly reformed if a nucleophile is present. [37]



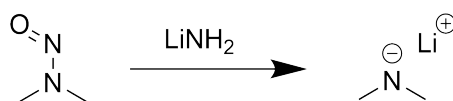
Scheme 1.14: Reactions of nitrosamines with electrophilic reagents.

Lithiation at the  $\alpha$  carbon can be achieved with strong bases such as lithium diisopropylamide (LDA). The resulting lithiated species can act as a nucleophile in [3+2] cycloaddition reactions with nitrile functional groups (Scheme 1.15) leading to 1,2,3-triazoles. [38]



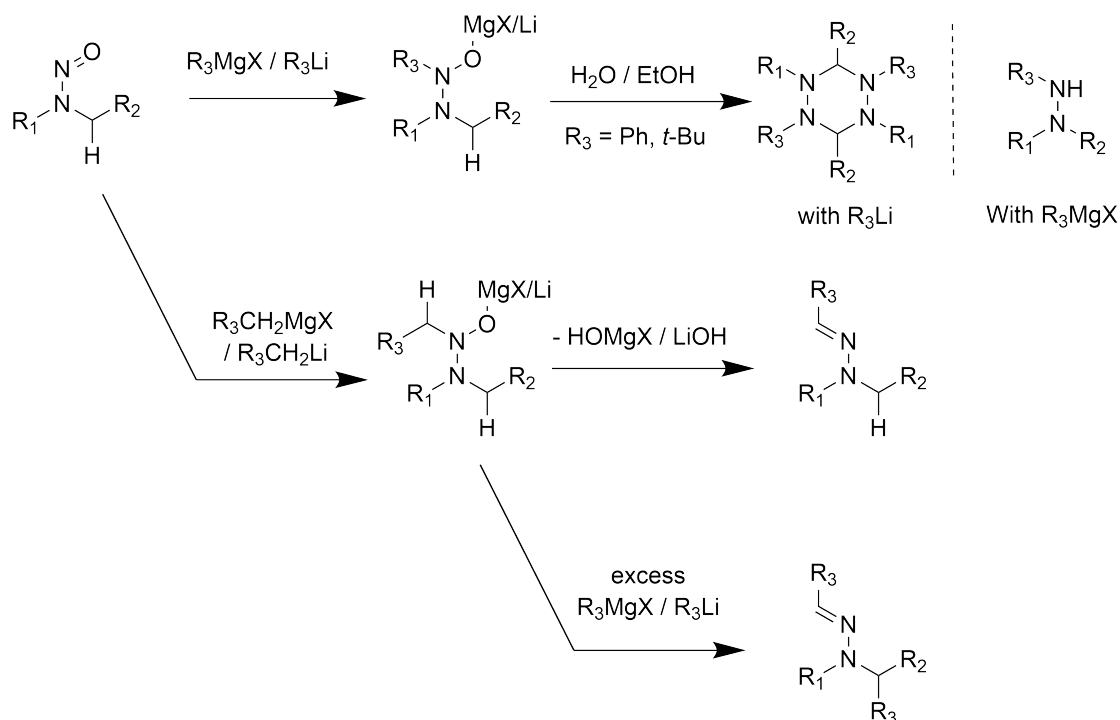
Scheme 1.15: Deprotonation-cyclisation with nitriles.

Reaction with lithium amides occurs by direct nucleophilic attack at the nitroso nitrogen, furnishing the lithiated amine product (Scheme 1.16). [39]



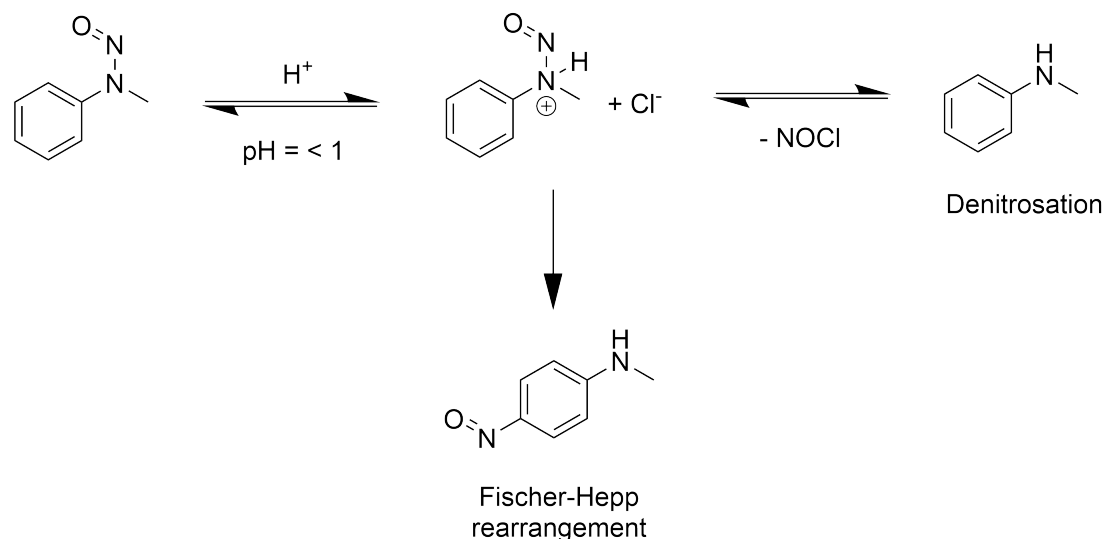
Scheme 1.16: Reaction of nitrosamines with lithium amide.

*N*-alkylation reactions with alkyl lithium and Grignard reagents are known to produce trisubstituted alkyl hydrazines. [40, 41] If there is an  $\alpha$ -hydrogen present on the reagent, then elimination of LiOH or HOMgX can occur, yielding the hydrazone product (Scheme 1.17). [42] Further substitutions can occur in an excess of the reagent, leading to alkylation at the  $\alpha$ -carbon. [43] If no  $\alpha$ -hydrogen is present on the reagent, dimerisation can occur in the case of alkyl lithium reagents, whereas the trisubstituted hydrazine is the product in the case of Grignard reagents. [44]

Scheme 1.17: *N*-alkylation reactions of *N*-nitrosamines.

Aryl nitrosamines are particularly sensitive to reactions with acid. [45] The presence of the phenyl ring has the effect of making the nitroso nitrogen more electron deficient, and therefore more susceptible to nucleophilic attack. [46] It is known that the *N*-protonated nitrosamine becomes kinetically relevant at a pH of  $< 1$  [10], and when added nucleophiles are present. Nucleophilic attack at the nitroso nitrogen of the *N*-protonated form yields the parent amine (Scheme 1.18). This reaction is reversible and depends on the concentration of the acid. [47] The rate of the denitrosation reaction has a high dependency on the strength of the nucleophile added ( $Cl^-$ ,  $Br^-$ ,  $SCN^-$ ,  $I^-$  ; 1 : 54 : 5300 : 15,000). [45] The denitrosation reaction is in competition with the Fischer-Hepp rearrangement (forming the *p*-nitroso compound), which is irreversible, and can be promoted by adding electron donating substituents to the phenyl ring of the nitrosamine. [48] Interestingly, if nitrite traps (e.g. hydrazoic acid, hydrazine, and sulphamic acid) are added, the yield of the denitrosation product drops, and the product of rearrangement increases, pointing towards an intramolecular reaction mechanism for the Fischer-Hepp rearrangement. [48] Furthermore, the reaction solvent has a marked effect on reactivity, with reactions in ethanol solvent proceeding at a higher rate than in water solvent with the product of denitrosation being favoured in ethanol. [47] It is thought that with acids that have nucleophilic conjugate bases (e.g.  $HCl$ ), the decrease in solvation of the nucleophile

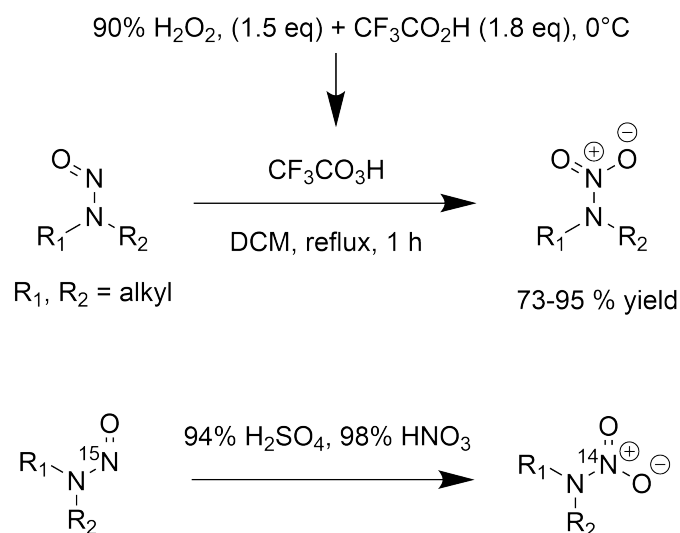
in ethanol solvent increases the rate of the nucleophilic attack at the nitroso nitrogen, making the protonation step of the nitrosamine rate limiting in this case. [47] The evidence for the denitrosation reactions of dialkyl nitrosamines is lacking, and one study found no reaction with NDMA in a number of reaction media with varying acidity and nucleophilic strength at room temperature. [47]



Scheme 1.18: Reactions of aryl nitrosamines in acid.

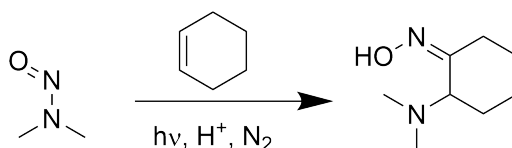
### 1.6.3 Oxidation

Oxidation of *N*-nitrosamines to *N*-nitramines has been achieved with nitric acid (HNO<sub>3</sub>) and peroxytrifluoroacetic acid (CF<sub>3</sub>CO<sub>3</sub>H) at elevated temperatures (Scheme 1.19). The two reagents have different mechanisms, with nitric acid substituting NO for NO<sub>2</sub> and peroxytrifluoroacetic acid oxidising the existing NO moiety. With peroxytrifluoroacetic acid, increase in the electron donating ability of the substituents led to an improved yield. [49, 50] Again these are extremely harsh reaction conditions which would likely interfere with API's in process chemistry.

Scheme 1.19: Oxidation of *N*-nitrosamines to *N*-nitramines.

### 1.6.4 Photochemistry

UV irradiation of nitrosamines causes cleavage of the N-N bond. The products of the reactions are highly dependent on the reaction conditions, with the reaction solvent playing an important part in the N-N bond homolysis efficiency. [51] The mechanisms of photolytic cleavage are poorly understood, but in all studied cases of NDMA photolysis, the first step is cleavage of the N-N bond. The radical species produced then go on to combine to form various oxides of NO (nitrite and nitrate included), formic acid, formaldehyde, dimethylamine, and methylamine; the literature is well covered in the review by Beard *et al.* [52, 4] Most importantly, in the presence of unsaturated C=C bonds the nitrosamine adds across C=C, yielding oxime products (Scheme 1.20). This reaction is dependent on the aminium radical, and so acidic conditions are required. [53]



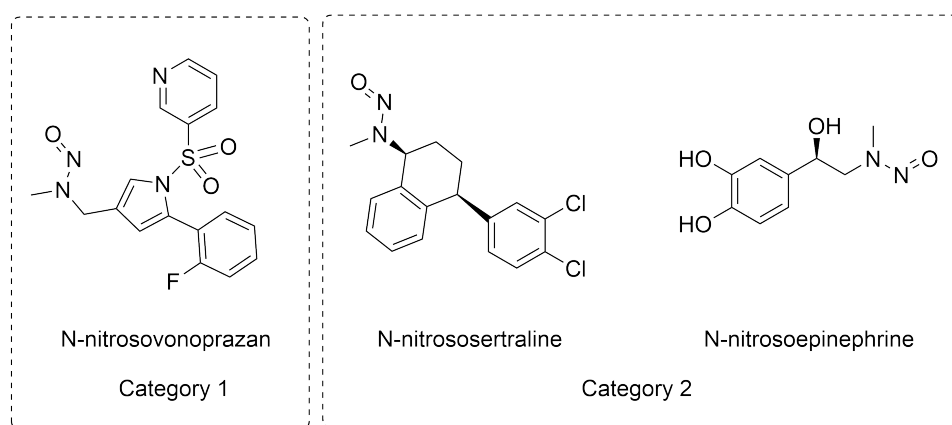
Scheme 1.20: Photolytic cleavage of N-N followed by addition to unsaturated C=C bonds.

## 1.7 Other sources of *N*-nitrosamine

Recent work has brought attention to other sources of *N*-nitrosamine, mainly the API's themselves, demonstrating that these too are a cause for concern. Burns and coworkers surveyed over

12K API small molecule drugs and impurities extracted from the Global Substance Registration System (GSRS) database and found that 40.4% of the API's and 29.6% of the impurities screened have the required secondary or tertiary amine moieties to produce *N*-nitrosamines. [16] However soon after, the European Medicine Agency (EMA) announced five new potency categories for carcinogens, based on Structure-Activity Relationships (SAR) of *N*-nitrosamines with known carcinogenicity data. The five categories are related to their acceptable daily limit (Table 1.1). This led to revised work to show that only a small number of these potential *N*-nitrosamines would require strict control measures (examples in Scheme 1.21) and that *ca.* 2/3 of the structures occupy categories four and five. [54] Nonetheless, the work by Burns and coworkers is purely academic and unforeseen high levels of carcinogenicity could arise with a given *N*-nitrosamine impurity because of the lack of empirical carcinogenicity data.

Category	Acceptable intake (ng/day)
1	18
2	100
3	400
4	1500
5	1500

Table 1.1: EMA potency categories for *N*-nitrosamines.Scheme 1.21: High-risk *N*-nitroso API impurities. Figure adapted from [54].

Having considered that more classes of *N*-nitrosamine may become important carcinogens in the future, the current level of easily accessible knowledge on *N*-nitrosamine reactivity becomes insufficient and a more comprehensive analysis is required. Specifically, it is important to understand those reaction conditions that are specific to a single structural class of *N*-nitrosamine, and which apply to multiple classes. This information is vital to *in-silico* purge predictions for

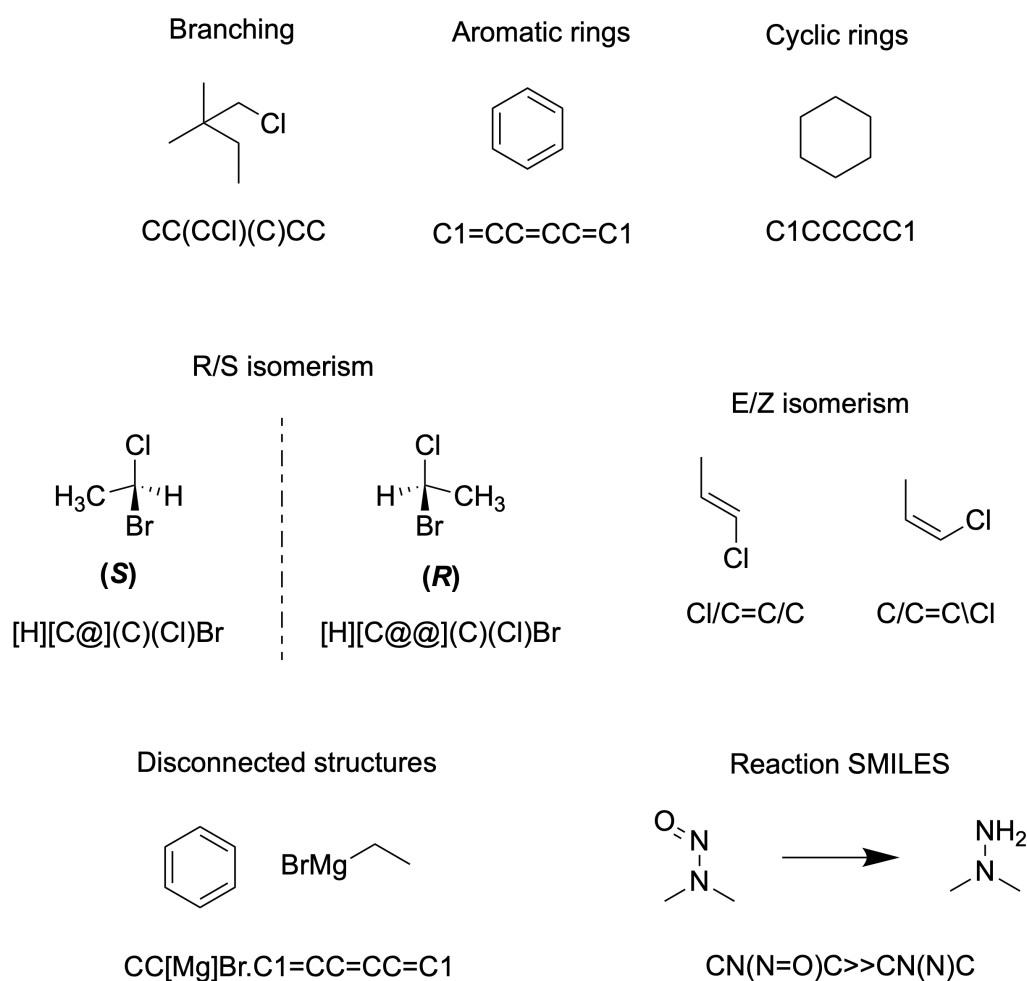
*N*-nitrosamines in high-value chemical manufacture. By increasing the knowledge of their reactivity, a better assessment of the purge can be performed. Furthermore, the reported reaction conditions that destroy nitrosamines are typically harsh, with low functional group tolerance, and the milder conditions seem to be limited to electron deficient aryl nitrosamines. Therefore, the discovery of milder reaction conditions that affect a broad range of structural classes of nitrosamines becomes important, with a view to their use in high-value chemical manufacture.

## 1.8 Automatic reaction classification

Having noted that the current knowledge base on *N*-nitrosamine reactivity is insufficient to cover all the classes of nitrosamine which may be of concern to human health, a more comprehensive study of the literature reactions on *N*-nitrosamines is required. Many advancements have been made in *in-silico* methods to predict chemical properties such as reaction yields [55], nucleophilicities [56] and even reaction outcomes [57] over the past decade, and the availability of reaction data through databases such as Reaxys [58], and the dataset of patent reactions from the USPTO mined by Daniel Lowe and subsequently classified by NextMove [59] have made it possible to obtain datasets of specific reactions to make informed decisions about particular chemistry. Taking a data-driven approach to gain a deeper understanding of *N*-nitrosamine reactivity is appealing as it allows for a larger dataset of reactions to be gathered and processed, and thus better insights can be made on the reactivity from the published literature. There exists no dataset of classified reactions on *N*-nitrosamines, and this work is dedicated to producing such a dataset.

Importantly, chemical structures in reaction databases can be represented in machine-readable text strings, named SMILES (Simplified Molecular Line Input System). [60] The advantage of SMILES codes are that they have a low memory requirement, yet carry all the structural information required to describe the atoms and bonds that make up a molecule (Scheme 1.22).





Scheme 1.22: The SMILES language for molecular structure representation.

SMILES codes for chemical reactions can be built with the separator “>>” to divide reactants and products, and reaction SMILES strings are often present in reaction databases, making the information accessible and processable. SMILES codes can be used to generate vector representations of molecules and reactions which can then be used in reaction classification. [55, 61, 62, 63] The vector representations of molecules and reactions are called fingerprints, and many methods have been developed to generate them [55, 63, 62]. Fingerprints store representations of substructures of molecules in vectors, often with one and zero representing the presence or absence of a structural unit respectively. The structural features can be predetermined from a list of common structural features [64] or generated on-the-fly *via* a hashing function which generates unique number codes for the structures which are then assigned an index in the vector by a folding function. [65]

To provide more context, an example of one of the most commonly used hash-based fingerprint, the Morgan fingerprint, is given. This fingerprint uses the Morgan algorithm to generate circular

substructures at various depths from the atoms in a molecule, and then stores each unique structure as an index in a binary vector. [65] Morgan fingerprints are generated with two parameters, the length of the final binary vector, and the radius of the circular substructures generated (Figure 1.4). [65] These two parameters control the amount of detail which is stored in the fingerprint, with longer length fingerprints capturing more structural features without substructures being assigned the same index, and a larger radius giving more structural features to take into consideration, but with fewer unique substructures to consider (Figure 1.4 (step two)). The problem with the use of such fingerprints with previously unclassified reaction data is that the hashes of substructures can be folded into the same index depending on the folding function used, the length of the fingerprint and the radius selected by the user. This introduces the problem that key structural features for reaction classification may be replaced by noise from the surrounding structural features which are not involved in the reaction. This problem is not unique to Morgan fingerprints. Other difference fingerprints generated by different methods also share the same problem of so called “collisions” during the folding process. [55, 63]

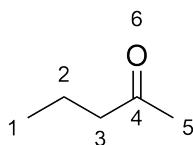
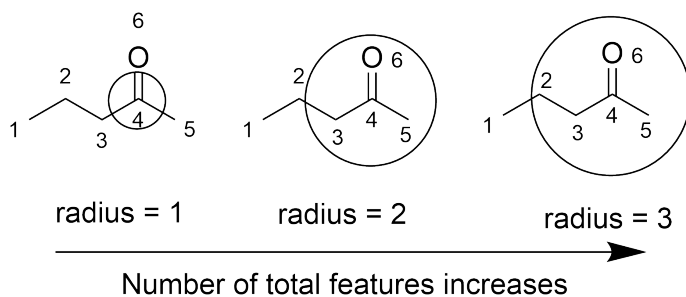
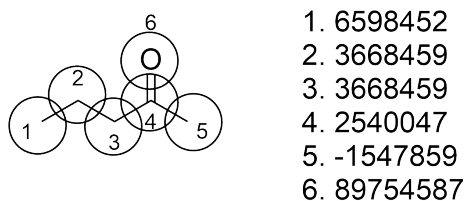
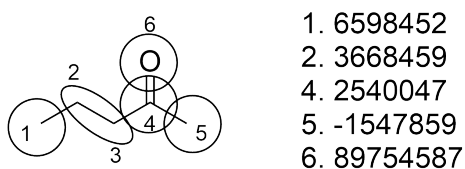
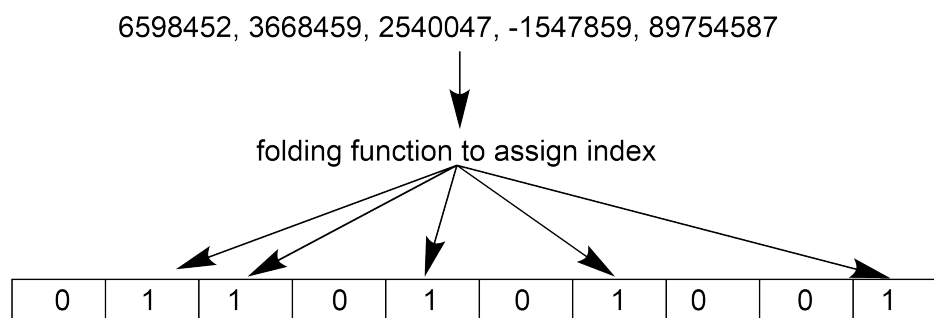
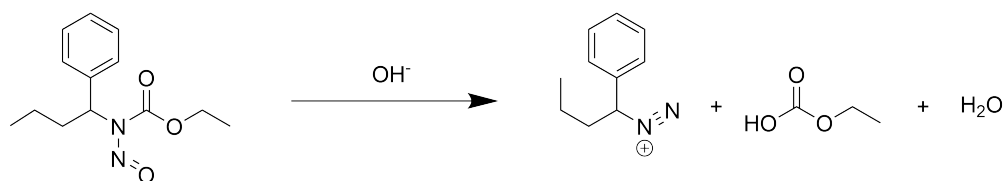
**1. Input molecule:****2. Generate hash codes at selected radius:****3. Hash codes for substructures at radius = 1:****4. Remove duplicate hashes:****5. Fold the hash codes into a binary fingerprint of predetermined length:**

Figure 1.4: An example of Morgan fingerprint generation to store molecular information.

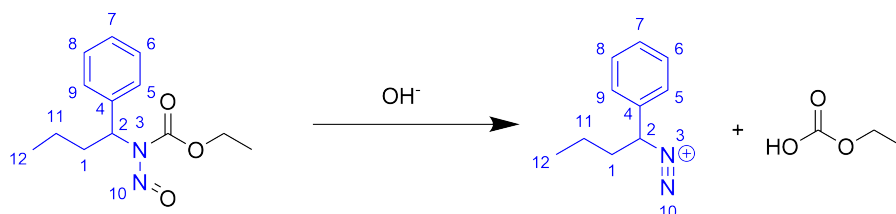
Other fingerprint techniques attempt to avoid this problem, Gillet *et al.* used set-specific atom pairs fingerprints to represent chemical reactions, and generated fingerprints in which the indices stored the count of the unique atom pairs for the entire dataset of chemical reactions. This representation was found to be successful when a machine learning model was trained to predict the reaction class from a dataset consisting of 336 reaction classes. [61] The problem with all reaction fingerprint based methods of reaction classification is data quality. If reactions have missing entities e.g. reactants, products and reagents, the fingerprints cannot pick up on important chemical features and misclassifications can occur.

One method which avoids the inclusion of noise generated by extraneous features to the reaction is classification by reaction centres. Reaction centres are defined as the atoms and bonds which change during a reaction. [66] This method requires that the atoms in the reactant are mapped into the products, in a process called Atom-Atom Mapping (AAM). If the atoms in the starting materials are numbered, and then traced through to the products, the atoms and bonds which change in a reaction can be extracted. Automated atom-atom mapping algorithms have been developed, and there are various ways in which the mapping is achieved. [67, 68, 69] A comparison study of a number of leading automated AAM models found that the best performing model was the Reaction Decoder Tool (RDT) [70], which achieved 76% accuracy in mapping reactions in a curated dataset containing a mixture of balanced and unbalanced reactions. [71] The RDT operates based on a maximum common substructure algorithm (MCS), which, using graph isomorphism, finds the largest common substructure between the reactants and products and maps these atoms first (Scheme 1.23). The MCS is then removed and further MCS operations are performed until no more atoms can be mapped. The best scoring method out of four algorithms which define the maximum common substructure differently is selected as the mapping result (Scheme 1.23). The score of the mapping is based on the the number of mapped atoms, the number of bond changes, the total bond-energy change and the number of subgraph fragments determined for a reaction. [72]

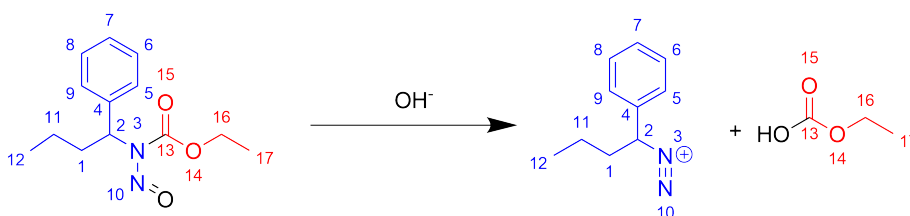
Input reaction



1. Find MCS and map it

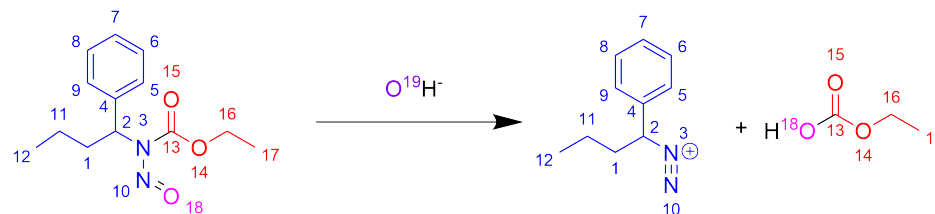


2. Find next MCS and map it

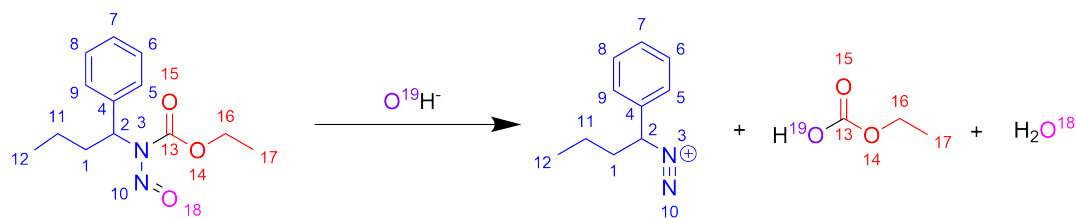


3. Assign remaining atoms based on scoring system:

mapping 1: unmapped atoms in reaction - disregard

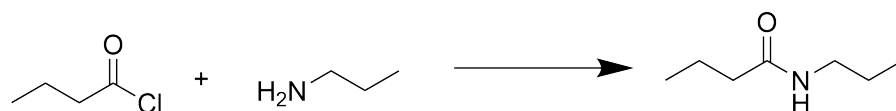


mapping 2: all atoms mapped - select

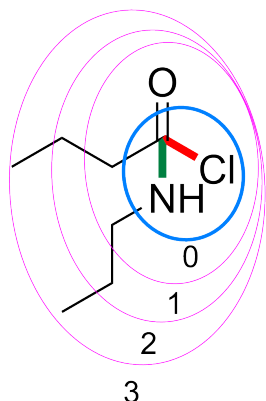


Scheme 1.23: Workflow for AAM in the RDT

With atom mapped reactions, classification of large datasets of reaction data by reaction centre extraction becomes possible. [73, 74] A number of methods have been developed to extract reaction centres [57, 75, 73] but the most versatile model is ReactionCode. [76]



Condensed Graph:



ReactionCode:

```

0:907()[1]906(01GG)[1]711(10GH)[1]
1:008(22GH)[1]006(11GG)[1]006(11GH)[1]
2:006(11GK)[1]006(11GL)[1]
3:006(11GM)[1]006(11GN)[1]

```

```

Reaction centre = 0:907 () [1] 906 (01GG) [1] 711 (10GH) [1] |
Atom index =      GG      GH      GI
Atomic symbol =   N       C       Cl
Atom codes =     907     906     711
Bond Codes =      ()      (01GG)  (10GH)
Stoichiometry =          [1]      [1]      [1]

```

Atom codes:

7 = A bond is broken and atom in reaction centre  
9 = A bond is formed and atom in reaction centre  
0 = unmarked (not part of reaction centre)

Atomic symbol:

07 = N  
06 = C  
08 = O  
11 = Cl

Bond codes:

(01)GG = a single bond is formed to atom GG  
(10)GH = a single bond is broken to atom GH  
(22)GH = a double bond remains to atom GH

Stoichiometry:

[1] : 1 bond of this type exists in the reaction

Figure 1.5: Breakdown of a simple ReactionCode.

ReactionCode relies on atom mapped reactions and works by first producing a condensed graph of the reactants and products so that the bond order changes can be extracted, thus defining the reaction centre with the accompanying atoms involved. After the atoms in the reaction centre and their bond order changes are labelled (Figure 1.5), a layered string based encoding of the

reaction can be built, starting with layer 0: the reaction centre, which defines the atoms and bonds directly involved in the reaction. Labelling of atoms is performed relative to the periodic table and the order in which the elements appear (C = 06, N = 07, O = 08, Cl = 11 etc.). If a bond is formed during the reaction, this has the highest priority in the ReactionCode string and is labelled with a nine if a bond is broken in the reaction it is labelled with a seven. Atoms are indexed by a two letter system, starting with the letters GH and moving through the alphabet (GG, GI, etc.). This allows the bond order changes to be captured by two numbers (e.g. (01) bond formed or (10) bond broken). The ReactionCode is built in layers, starting at the reaction centre (Depth = 0), and extending the radius outwards from the reaction centre by one atom per layer (e.g. layers zero and one combined give the reaction centre and its nearest neighbour atoms). Figure 1.5 provides a simple example of a reaction with no charge or stereochemistry components to consider, but these are also factored into ReactionCode with additional text before the terminating “|” for a given layer. Furthermore, if the reaction stoichiometry is not 1: 1, the stoichiometry parameter (in square brackets) can be updated to reflect the number of times the reaction centre repeats in the reaction. [76]

The advantage ReactionCodes give over other methods to extract reaction centres is that more structural features can be optionally included to describe reactions. This is important when considering multiple classes of reaction which may be dependent on the substructure surrounding the reaction centre. Furthermore, ReactionCodes are bidirectional, meaning that a ReactionCode can be transformed back into reaction SMILES, and by removing various layers, reaction SMILES for just the reaction centre can be obtained, allowing for parsing with cheminformatics software such as *rdkit* to extract information about the atoms and bonds involved in the reaction, and crucially, screen out undesired reactions that do not happen on the desired functional group.

These things considered, this work takes a dataset from Reaxys, applies AAM and subsequent ReactionCode encoding, followed by decoding into reaction centre SMILES which are then screened for reactions that destroy *N*-nitrosamines.

## 1.9 Conclusions

This section introduced the issues surrounding *N*-nitrosamines in high-value chemical manufacture. The structural nuances of the *N*-nitroso substructure were explained, and the issues

surrounding their analysis was presented. It was found that GC-MS/MS and LC-MS/MS have been used as appropriate methods to analyse nitrosamines, due to complications in their NMR spectra due to magnetic inequivalence around the N–N=O substructure. The methods by which the risk of contamination by *N*-nitrosamines in finished drug products is assessed was outlined, indicating that this assessment was based predominantly on physicochemical parameters. It was stated that knowledge about their reactivity could further estimations to support high purge factors, and thus less costly analytical batch testing. With that, the current knowledge base of *N*-nitrosamine reactivity was summarised, highlighting that the reaction conditions are often harsh with low functional group tolerance. Furthermore, the reported reactivity knowledge base is limited to aryl and dialkyl nitrosamines, which was deemed to be insufficient after research indicated that many API's and impurities have potential as *N*-nitrosamine precursors. It is reported that milder reaction conditions to destroy a broader range of structural classes of *N*-nitrosamine should be sought, with a view to using these conditions to destroy *N*-nitrosamines in high-value chemical manufacture.

The limited knowledge base on *N*-nitrosamine reactivity called for a more comprehensive review, incorporating more than just the two structural classes of *N*-nitrosamine that have already been covered. To achieve this, the literature on *in-silico* methods for mining reaction data and extracting useful information about reactions was reviewed. The use of reaction fingerprints to classify reactions on *N*-nitrosamines was ruled out due to expected noise from extraneous features in the reaction clouding the important chemistry that occurs. To overcome this, a reaction centres approach was selected, which incorporates atom-atom mapping to encode the changes between atoms and bonds in the reaction (the reaction centre), thus focusing directly on the important features of the reaction. ReactionCode software was selected to facilitate the extraction of the important features of the reaction centre, and specifically, to identify those reactions which destroy nitrosamines.

The following two chapters detail a data-driven search and subsequent classification of reactions that destroy *N*-nitrosamines, bringing attention to chemistry that applies to other structural classes of *N*-nitrosamines. Structure-reactivity relationships are discussed, and the reaction conditions most applicable to a diverse range of structural classes of *N*-nitrosamine are discussed. These findings then influenced a batch reactivity screen on eight commercially available *N*-nitrosamines, in an attempt to discover reaction conditions that are broadly applicable across



all structural classes of *N*-nitrosamine.

## Chapter 2

# Analysis of literature *N*-nitrosamine reactions

### 2.1 Scope of the chapter

This chapter extends the existing knowledge on *N*-nitrosamine reactivity by broadening the investigation to include a diverse array of structural classes of *N*-nitrosamines. Previous reviews primarily focused on dialkyl nitrosamines, given their significance in the industry due to the widespread use and necessity of secondary and tertiary amines in high-value chemical manufacturing. [4, 3] A cheminformatics workflow was employed to generate a dataset of reactions leading to the destruction of nitrosamines. Due to the suboptimal quality of the acquired data, manual classification of the reactions was carried out. The most frequent occurrences of reactivity were identified and discussed. Additionally, observations on structure-reactivity relationships were made, and the findings were utilized to propose reaction conditions capable of effectively eliminating nitrosamines across a diverse range of structural classes.

### 2.2 Introduction

With secondary and tertiary amines being ubiquitous in process chemistry due to their abundance in Active Pharmaceutical Ingredients (API's), and their use as organic bases, the current reviews on *N*-nitrosamines are unsurprisingly biased towards dialkyl *N*-nitrosamines. In addition, the first case of *N*-nitrosamine API contamination was *N*-nitrosodimethylamine (NDMA)

in Valsartan in 2018. [2]

The aforementioned study (Chapter one) into other possible sources of *N*-nitrosamines identified that more structurally diverse nitrosamines may be a cause for concern [16, 54], and having considered that more structural classes of *N*-nitrosamine may become important carcinogens in the future, the current level of easily accessible knowledge on *N*-nitrosamine reactivity becomes insufficient and a more comprehensive analysis is required. Specifically, it is important to differentiate reaction conditions that are generally reactive to all *N*-nitrosamine classes from those that are class-specific. This information is vital to *in-silico* purge predictions for *N*-nitrosamines in high-value chemical manufacture. By increasing the knowledge of their reactivity, a better assessment of the purge can be performed.

The need for a comprehensive review without human bias favours the use of an automated workflow to retrieve reactions on *N*-nitrosamines. An objective method ensures that as much information as possible is captured and processed. The most relevant work to this problem comes from Christ *et al.* who in 2012 developed a method to extract classified chemical reaction data from Electronic Laboratory Notebooks (ELNs). This involved computing reaction centres from atom-mapped reactions, grouping the unique reaction centres together to form classes, and assigning reaction classes based on a representative reaction in each group. [73] Further to this, a reaction classification method based on maximum common substructures between reactants and products was introduced in 2013 which also relies on atom-atom mapping, though this model was shown to fail when unmapped atoms were present in the reactants. [74]

The access to open source high quality reaction data was made available by Daniel Lowe in 2012 with his dataset of chemical reactions mined from patent literature, and the application of an expert rule-based reaction classification tool (NameRxn from NextMove) to this led to the foundation dataset for two important machine-learning models for reaction classification.[59, 77] Both models use vector fingerprints to represent chemical reactions but the method to achieve the fingerprint differs between the two models. Schneider *et al.* used the difference between the Morgan fingerprints of the reactants and products with the addition of the Morgan fingerprints of the agents at a reduced weight to achieve a final fingerprint representation of reactants. [62] In contrast, Gillet *et al.* used set specific atom-pairs at various depths to generate fingerprints for reactions by subtracting the reactant atom pairs vector from the product atom pairs vector. [61]

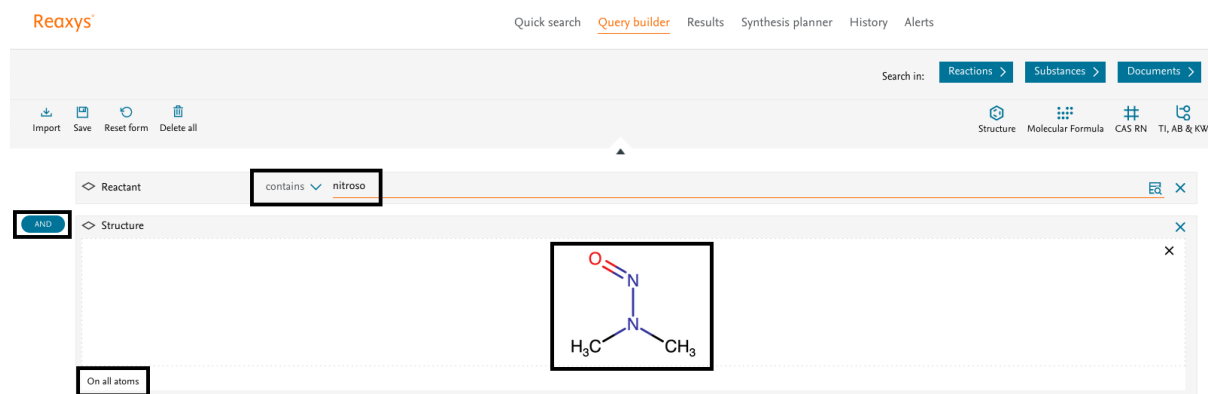
All of these classification tools require that the input data is of high quality. This means that the reactions are stoichiometrically balanced for accurate atom-atom mapping, reaction centre extraction and fingerprint generation. Also, it must be ensured that all the data for reaction conditions (*e.g.* reagents, photochemical conditions etc.) are present for each entry in the dataset so as to not lead to erroneous classifications. Unfortunately, as will be explained within, this was not the case for the extracted *N*-nitrosamine reactions dataset and instead, a manual classification was performed after refinement of the initial dataset to a small number of representative reactions.

The following chapter outlines the method by which the knowledge base of *N*-nitrosamine reactivity data was expanded *via* a cheminformatics based workflow. Initially, reactions capable of eliminating *N*-nitrosamines were retrieved from a dataset mined from the Reaxys database. Subsequently, these reactions underwent manual classification and analysis, aiming to offer a more inclusive perspective on *N*-nitrosamine reactivity, encompassing a variety of structural classes of *N*-nitrosamines.

## 2.3 Methods

### 2.3.1 Data extraction and refinement

A search of all reactions in Reaxys database containing NMDA as a sub-structure (including heteroatom substitutions at both carbons) of the starting material resulted in 15163 reactions, which was exported in XML format (Figure 2.1). The python code to extract and clean the reactions is listed in the Appendix Listing A.1.



The screenshot shows the Reaxys search interface. At the top, there is a navigation bar with 'Quick search', 'Query builder', 'Results', 'Synthesis planner', 'History', and 'Alerts'. Below this is a search bar with 'Search in:' and three tabs: 'Reactions', 'Substances', and 'Documents'. The 'Reactions' tab is selected. Below the search bar, there are icons for 'Import', 'Save', 'Reset form', and 'Delete all'. On the right, there are icons for 'Structure', 'Molecular Formula', 'CAS RN', and 'TI, AB & KW'. The main search area has a 'Reactant' field with a dropdown menu set to 'contains' and the text 'nitroso'. Below this is a 'Structure' field with a dropdown menu set to 'AND' and a chemical structure of N,N-dimethylnitrosamine (H<sub>3</sub>C-N(CH<sub>3</sub>)-NO) displayed. At the bottom left, there is a checkbox labeled 'On all atoms'.

Figure 2.1: The reaxys search criteria for reactions on *N*-nitrosamines.

For each reaction, SMILES strings for reactants and products, and text for reaction conditions, which included solvents, conditions (e.g. photochemical/electrochemical) and catalysts, were extracted with a Python script. The Python package *rdkit* was used to convert MDL Molfiles into SMILES strings. 3750 entries with erroneous SMILES strings either in the reactants or products were discarded. This resulted in 11413 reactions with extractable information. After this, multi-step reactions were removed as Reaxys does not provide intermediate structures, leaving 11087 single-step reactions. The Reaction Decoder Tool (RDT) [70] was employed to perform atom-atom mapping (AAM) based on the computed reaction SMILES strings, giving 11069 reactions (Figure 2.2).

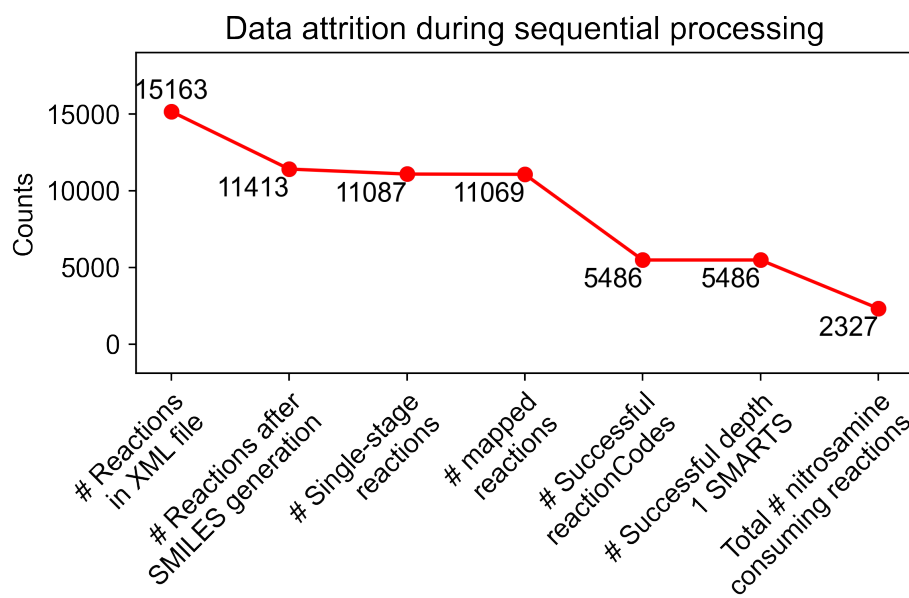
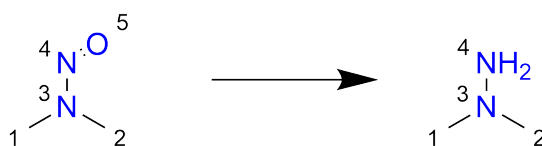


Figure 2.2: Loss of data with processing steps.

AAM is essential for reaction centre generation, [57, 75, 73] which will underpin automated processing of the collected reactions. The RDT was reported to achieve 76% accuracy in mapping reactions in a curated dataset containing a mixture of balanced and unbalanced reactions. [71] Against the unbalanced reactions from Reaxys, a 99.8% conversion rate was obtained due to the higher data quality of these curated reactions. This was followed by application of the ReactionCode software to encode the reactions into ReactionCodes. ReactionCodes are a layered string-based language which defines a reaction centre as the atoms and bonds which change in a reaction, and the reaction can be portrayed at various depths. [76] The depth was evaluated (Scheme 2.1) and a depth one core was found sufficient to capture the changes to the *N*-nitroso

substructure (N–N=O). A total of 5486 reactions successfully underwent these transformations.

N-nitroso substructure SMARTS: `[#7]-[#7]=[#8]`



Depth 0 Core: `[N]=[O]>>[N].[O]`

Depth 1 Core: `[N]-[N]=[O]>>[N]-[N].[O]`

Depth 2 Core: `[C][N]([C])-[N]=[O]>>[C][N]([C])-[N].[O]`

Scheme 2.1: Selecting depth one cores to incorporate the N–N=O substructure.

To ensure the dataset consisted only of reactions that destroyed *N*-nitrosamines i.e. did not have the *N*-nitrosamine as part of the leaving group, or if N–N=O was part of the reaction centre, the encoded ReactionCodes were then transformed into reaction SMARTS strings using the ReactionCode software. This transformation proceeded with no data loss. The transformation to SMARTS strings enabled parsing the resulting reaction centre SMARTS strings in python. Using rdkit again to loop through the atoms in the reactants, the atom map numbers of the N–N=O substructure were identified, and these atoms were searched for in the products. If the atom map numbers of N–N=O were found in the product SMARTS of the reaction centre, this indicated that the N–N=O groups was part of the reaction centre, and was transformed in some way during the reaction. After these filtering steps, 2327 reactions remained.

Finally, with a view to manually classifying the reactions, an attempt to standardise the reaction conditions was made in order to reduce the number of duplicate reactions. The Reaxys data was extremely inconsistent as to which columns solvents and reagents were assigned to. This made the number of unique values for the reaction conditions much higher than the true number of uniques due to the ordering of the reagents. To combat this, a list of common solvents was constructed, and solvents in this list were removed if they were present in the reagents column, and added to the solvents column. With the new list of solvents and reagents in hand, the set function in python was applied to each item in the new solvents and reagents list to reorder the items in the sub lists in a consistent manner. The ordered reagents and solvents lists were transformed into strings with the join function in python. To find unique entries,

the homogenised reagents and depth 0 transformation codes were considered. Duplicates were dropped based on these two columns leaving 1080 reactions which were then manually classified. The python code to achieve the final dataset can be found in the Appendix, Listing A.2.

### 2.3.2 Manual classification

The important features of reactions on *N*-nitrosamine are: the structural class of *N*-nitrosamine in the reaction, the type of transformation taking place, the reaction conditions and the rate constant for the reaction. Unfortunately, kinetic data for these reactions was unobtainable, and attempts to estimate rate constants from reaction time and yields were halted by the low number of entries that had yield or reaction time information (Figure 2.3).

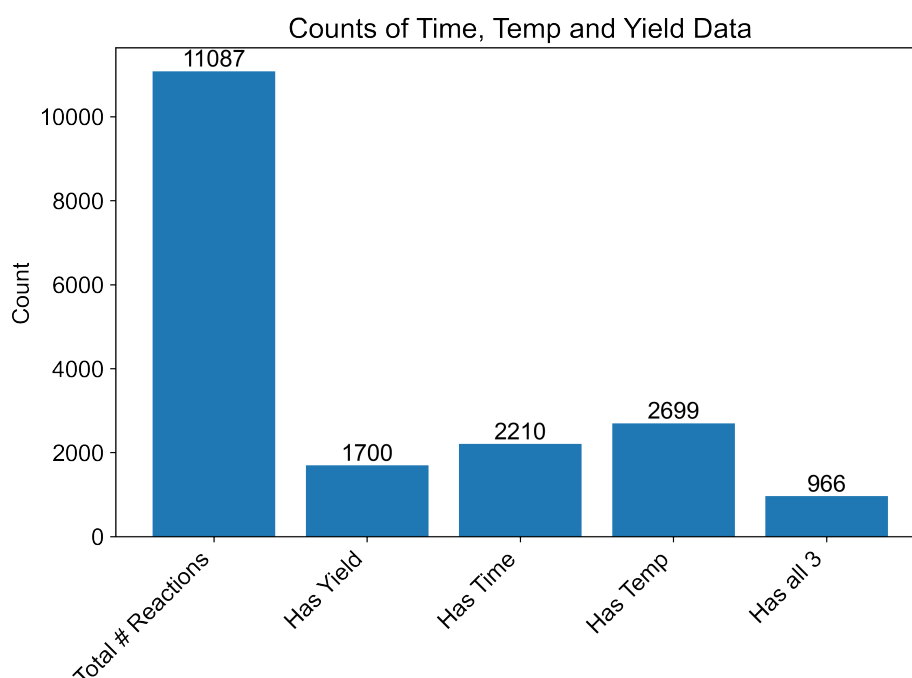


Figure 2.3: The lack of yield, temperature and reaction time data in the dataset of *N*-nitrosamine reactions.

This left the classification based on transformation, reaction conditions and the structural class of *N*-nitrosamine. Automated classification using reaction fingerprints was not trusted since there were many entries with unbalanced reactions. Figure 2.4 came from an analysis of the reactants and products of all the reactions in the dataset before and after processing. The unique set of atomic numbers from all the atoms on the reactants side was used to check if all the atoms in the products were accounted for in the reactants. This was true for 9562

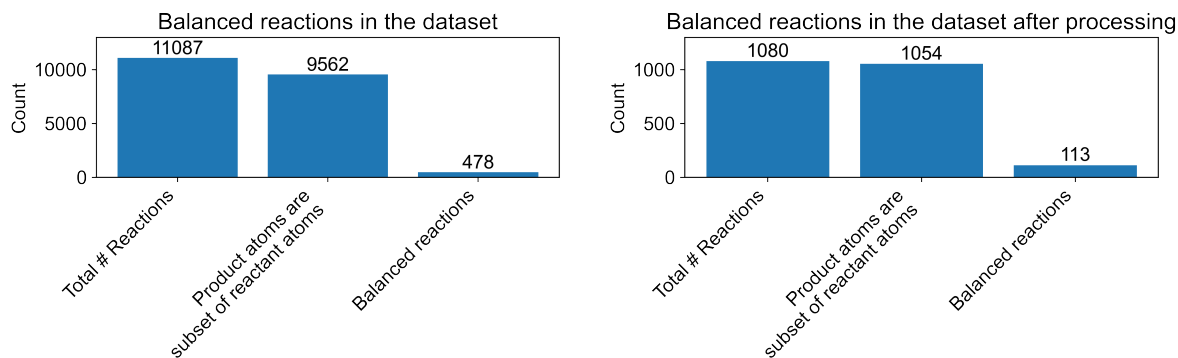


Figure 2.4: The number of stoichiometrically balanced reactions in the dataset.

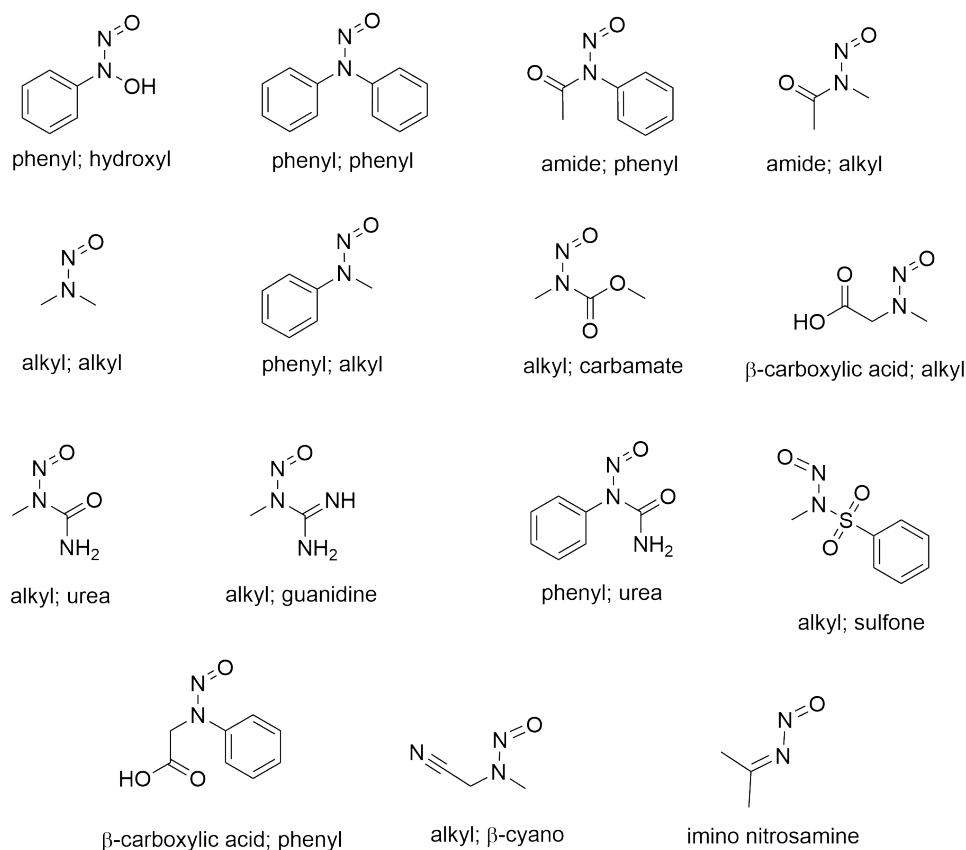
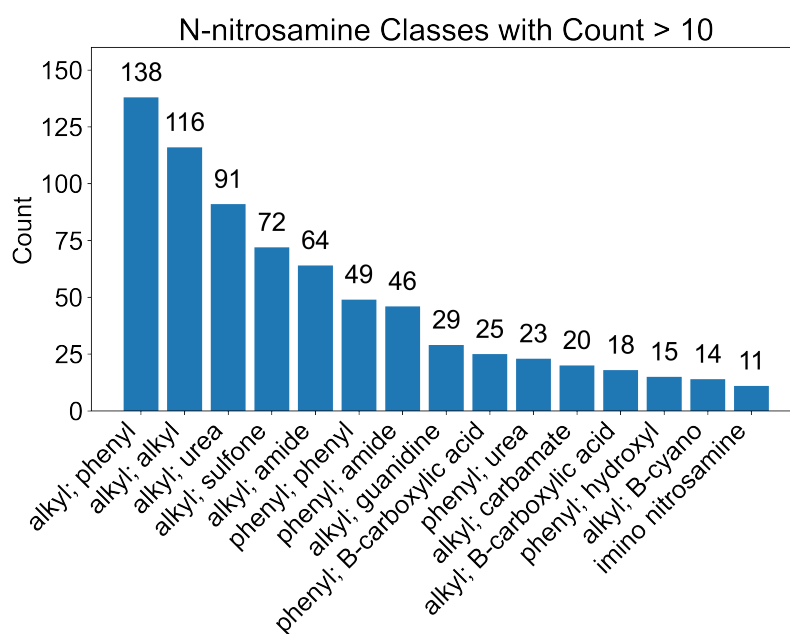
reactions. However, when the counts of the unique atoms were compared between the reactants and products, very few reactions were found to be fully balanced.

Because of this, and the fact that the data cleaning workflow left only 1080 representative reactions, the decision was made to manually classify the reactions in the dataset.

### Structural classes of *N*-nitrosamine

The first step in the manual classification workflow was to classify the *N*-nitrosamine involved in the reaction. The classification was based on the structure of the R-groups present either side of the N–N=O substructure. To increase confidence in the conclusions drawn from the analysis, only classes that had a count above ten were selected for further analysis. This count included examples from the same literature reference. Scheme 2.2 shows examples of the 15 structural classes of *N*-nitrosamine and Figure 2.5 shows their count in the dataset.

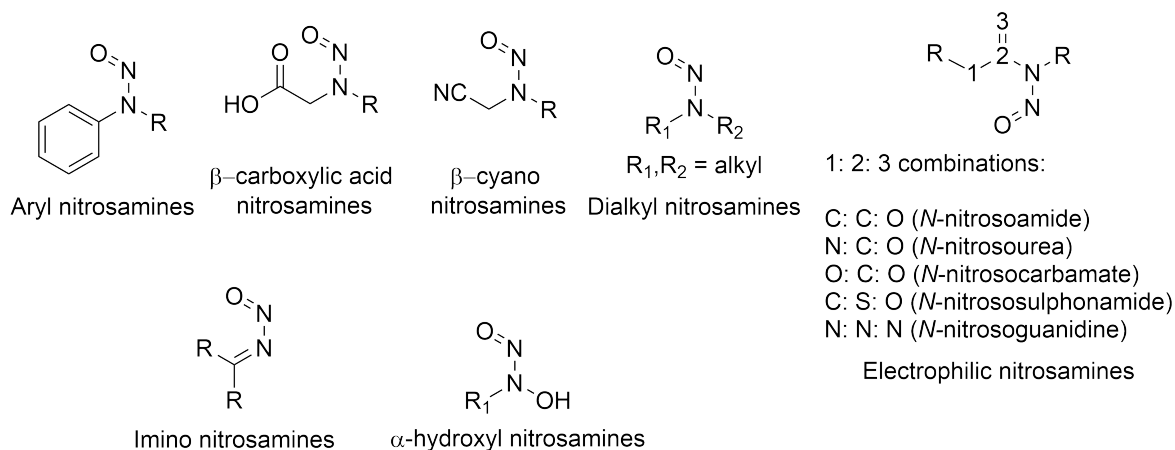


Scheme 2.2: Examples of the structural classes of *N*-nitrosamine with count > 10 in the dataset.Figure 2.5: Counts of the 15 structural classes of *N*-nitrosamine in the dataset.

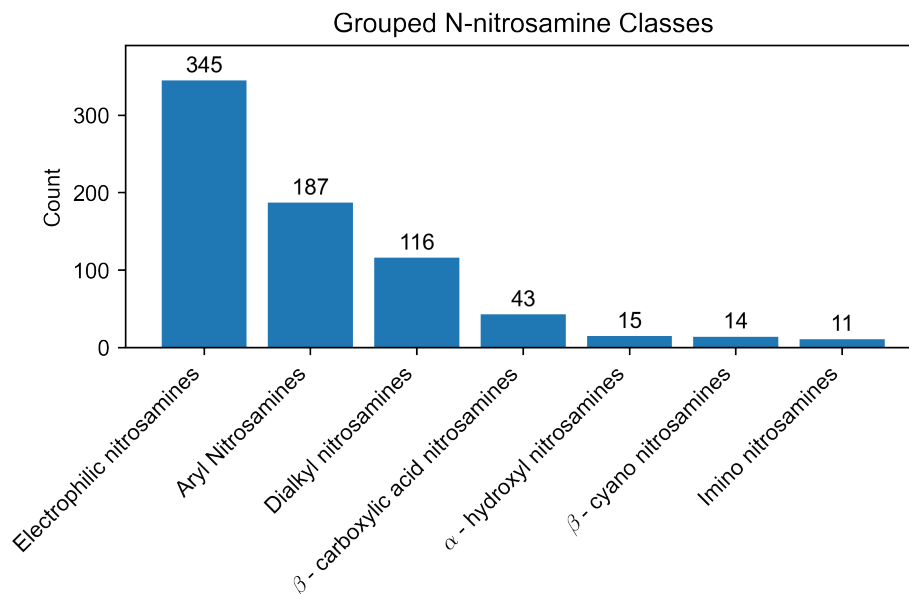
The 15 structural classes of *N*-nitrosamine that were selected for further analysis cover a much

broader chemical space than has previously been reviewed. And it is clear that alkyl; phenyl and alkyl; alkyl *N*-nitrosamines dominate in numbers, and much of their chemistry has been discussed previously, but they are included as there are examples of reactivity that were missed in the two previous reviews which are captured in this work. Interestingly, there are a number of structural classes that have an electrophilic centre  $\alpha$  to the N–N=O substructure, with the amine nitrogen of N–N=O forming part of commonly seen functional groups such as carbamates, ureas and sulphonamides etc. The structural classification in the first level of classification strays from conventional naming systems which might call an alkyl; carbamate *N*-nitrosamine an *N*-nitrosocarbamate. The reason for the difference in the naming system chosen in this work is that it incorporates a structure that is more easily read by a machine for potential machine learning models in the future, as well as providing more information about the atoms and bonds surrounding N–N=O which helps to explain the differences in reactivity.

The nitrosamine classes were further grouped into seven broader classes as shown in Scheme 2.3. The count of these structures in the filtered dataset is shown in Figure 2.6. This grouping was performed to combine classes which are likely to show similar reactivity. The hierarchical class system is detailed in Table 2.1.



Scheme 2.3: Example structures of the grouped *N*-nitrosamine classes.

Figure 2.6: Counts of the grouped structural classes of *N*-nitrosamine in the dataset.Table 2.1: Class hierarchy for the structural classes of *N*-nitrosamines.

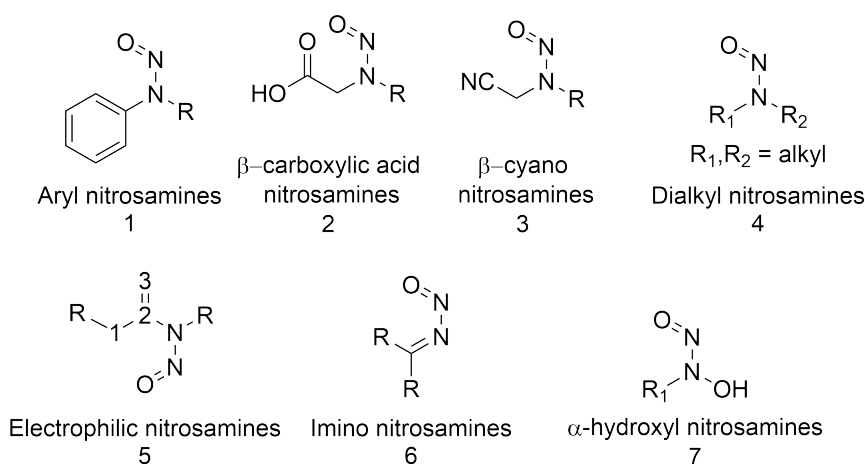
Nitrosamine Classification	Grouped Nitrosamine Classification
phenyl; hydroxyl	$\alpha$ - hydroxyl nitrosamines
alkyl; phenyl	Aryl nitrosamines
phenyl; phenyl	Aryl nitrosamines
phenyl; B-carboxylic acid	$\beta$ - carboxylic acid nitrosamines
alkyl; B-carboxylic acid	$\beta$ - carboxylic acid nitrosamines
alkyl; B-cyano	$\beta$ - cyano nitrosamines
alkyl; alkyl	Dialkyl nitrosamines
alkyl; guanidine	Electrophilic nitrosamines
phenyl; amide	Electrophilic nitrosamines
alkyl; carbamate	Electrophilic nitrosamines
alkyl; urea	Electrophilic nitrosamines
alkyl; amide	Electrophilic nitrosamines
phenyl; urea	Electrophilic nitrosamines
alkyl; sulfone	Electrophilic nitrosamines
imino nitrosamine	Imino nitrosamines

### *N*-nitrosamine transformations and reagents

With the most common nitrosamine classes in hand, the next step was to classify the reactions based on the reagents used and transformations that occurred. In each case a two stage classification was performed; initially assigning more detailed descriptions of the transformations and reagents which were present in each reaction. In the second stage, these were grouped together into more broad classes which allowed for better visual representation. The hierarchical classi-

fication tables for the detailed and grouped classifications of reagents and transformations can be found in the Appendix Tables B.1 and B.2. Only the second, broader classifications were discussed to keep the focus on the overall goal of finding methods to destroy multiple classes of nitrosamine.

The dataset of representative *N*-nitrosamine reactions was filtered to leave only the nitrosamines in Table 2.1. This decreased the number of reactions to 731 reactions. The resulting number of reagent classes was 32, and the number of transformation classes was 13. To ensure confidence in the data, only nitrosamine: reagent: transformation combinations with count higher than three were kept for analysis. This resulted in 652 total reactions, with ten transformation classes and 21 reagent classes. The results are summarised in Table 2.2, Scheme 2.4 shows the classes referenced by numbers 1-7 in the summary table. None of the ten transformation classes are applicable to every class of *N*-nitrosamine under study. At first glance, the most promising reaction conditions that are likely to apply to a wide range of *N*-nitrosamine structural classes are reductive conditions, which appear in four out of seven of the grouped structural classes. Some of the conditions e.g. “Diazonium formation” and “O-Si/C/S bond formation” appear to require that other functional groups are present in the nitrosamine; and some of the reaction conditions are only applicable to one class of *N*-nitrosamine: “Fischer-Hepp” and “Deprotonation cyclisation with CN”. The results of Table 2.2 will be discussed in the following section in terms of the grouped transformation classes, examples of reactivity will be given, and the usefulness of the reaction conditions with respect to industrial use will be commented on.



Scheme 2.4: Numbered grouped *N*-nitrosamine classes.

Table 2.2: Classification summary table

Grouped Transformation Classification	Grouped Reagent Classification	Grouped Nitrosamine Class						
		1	2	3	4	5	6	7
De/transnitrosation	Acid	6						
	Acid+hv				13			
	Amine					34		
	N-nucleophile	4						
	Stabilised carbanion	4						
	TM catalyst	9						
	Thiol					5		
	hv					11		
Deprotonation-cyclisation with CN	Base				4			
Diazonium formation	Amine					5		
	Base				10	179		
	Heating					5		
	N-nucleophile					4		
	Stabilised carbanion					16		
	Ambient temperature					6		
Fischer-Hepp	Acid	42						
<i>N</i> -alkylation	Heating					5		
	RMg/Li				10			
	TM catalyst	20						
N <sub>3</sub> formation with amine	Amine					5		
	Pb(OAc) <sub>4</sub> /Amine/base				4			
NO to NO <sub>2</sub>	HNO <sub>3</sub>	4						
O-Si/C/S bond formation	Acyating reagent		36					
	Alkylating reagent							14
	Heating			7				
Reduction	Electrochemical reduction	9						
	Hydride	10			22		7	
	Metal	39			34	10		
	S-based reductant	5						
	TM catalyst	15						
Azo formation	Arene	5				33		

## 2.4 Results and Discussion

### 2.4.1 UMAP plot of nitrosamine structural classes

The quality of the first level structural nitrosamine classification was assessed *via* a UMAP embedding of the Morgan fingerprints (radius=2, length=1024) of the 15 classes of *N*-nitrosamine which is plotted in Figure 2.7. [78, 65] Though there are clear discrete clusters, the reason

for the imperfect clustering is that some of the nitrosamines shared similar functional groups despite being members of different classes. The class was assigned relative to the chemistry that occurred on the nitrosamine in the reaction, so there may have been some conflicts in class selection if looking at just the nitrosamine structure alone.

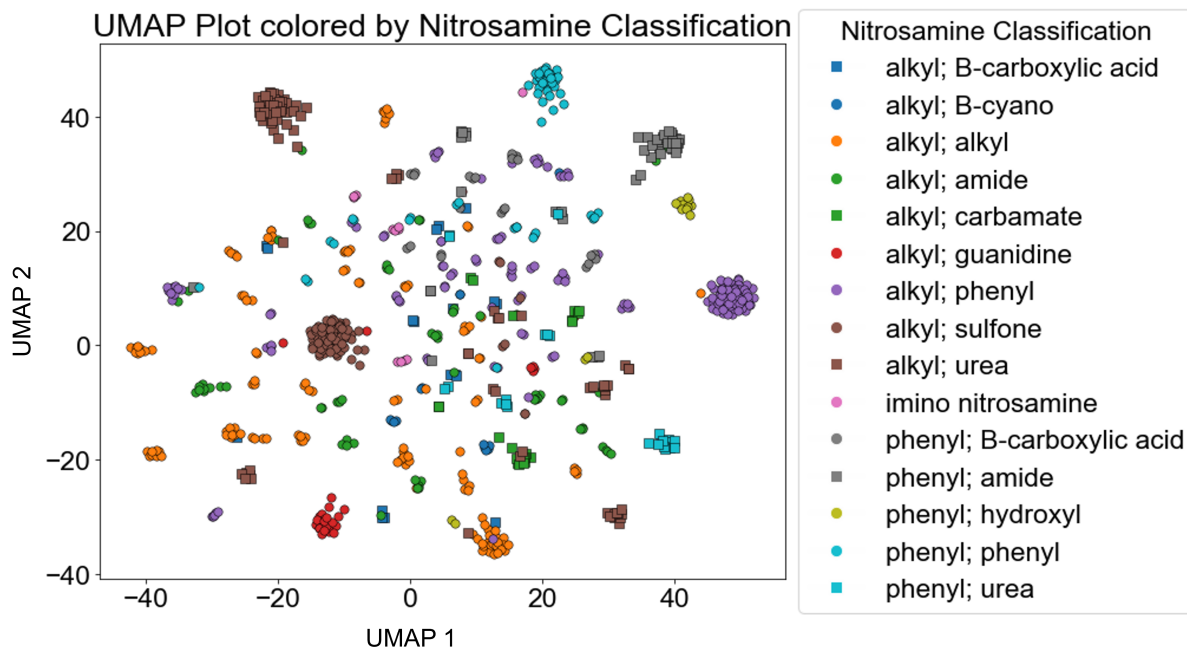


Figure 2.7: UMAP plot of the nitrosamine classes.

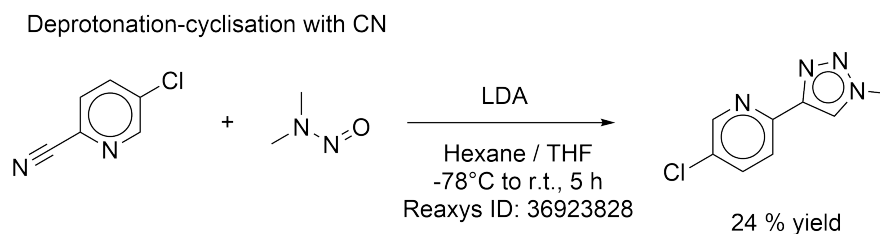
### 2.4.2 Examples of reactivity

While the summary table (Table 2.2) provides a global view of the transformations and reagents that can be used to destroy *N*-nitrosamines, specific examples of reactivity are necessary to fully understand the chemistry and the specific structural features that are required to observe a given reaction. As previously mentioned, some of the transformations in Table 2.2 already appear in the two reviews on *N*-nitrosamine reactivity, namely: Fischer-Hepp rearrangement reactions of aryl nitrosamines, Reduction reactions of alkyl; alkyl and alkyl; phenyl nitrosamines, NO to NO<sub>2</sub> and *N*-alkylation reactions. These transformations have been discussed in the introduction chapter and will only be discussed in the context of those cases that were missed in the two previous reviews.

#### Deprotonation-cyclisation with CN

This transformation was present in the review by Beard *et al.*, but it is highlighted here for it appears in the dataset of nitrosamine consuming reactions. The dataset contained examples

only with alkyl; alkyl (dialkyl) *N*-nitrosamines, and is specific enough to warrant its own class, separate from other methods of triazole formation in the dataset. Four examples exist which come from two separate sources [79, 80] and an example from reference [79] is shown in Scheme 2.5.



Scheme 2.5: Deprotonation-cyclisation with CN transformation example reaction.

The reaction proceeds by deprotonation of the carbon atom  $\alpha$  to the N–N=O substructure by the strong base lithium diisopropylamide (LDA). The resulting carbanion then serves as a nucleophile to attack the cyano carbon, breaking one of the CN  $\pi$  bonds and forming a new  $\sigma$  N–N bond between the cyano and nitroso nitrogens. Following an acidic workup, the triazole product is achieved in poor yield (24 %). The poor yield is probably due to the fact that the nitrosamine and the 5-chloro-2-cyanopyridine were added concurrently, as metallation with the aromatic substrate is likely to compete with the deprotonation of the nitrosamine. [79] Furthermore, *N*-alkylations of the nitrosamine in various forms are possible with organolithium compounds as was described in the introduction. There are a number of reasons to discount this transformation as a broad-spectrum method for destroying *N*-nitrosamines: it specific to one structural class of *N*-nitrosamine, it has clear issues with side reactions and low temperature conditions are required.

### De/Transnitrosation

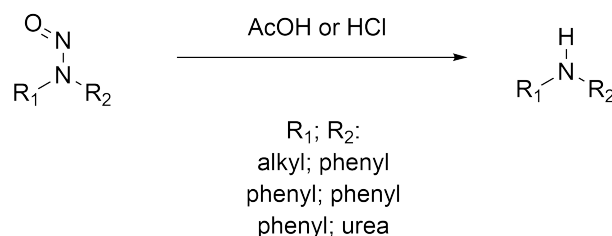
The “De/Transnitrosation” transformation class was much broader than the previous class. A summary table of the structural classes and reagents are displayed in Table 2.3. There are eight reagent classes that can be used, and some of those have already been discussed in the two reviews previously mentioned. Specifically, denitrosation under photochemical conditions, and denitrosation under acidic conditions, which is in competition with the Fischer-Hepp rearrangement in aryl nitrosamines. [45]

Table 2.3: De/transnitrosation reactions summary table.

De/transnitrosation Grouped Reagent Classification	Grouped Nitrosamine Class		
	Aryl nitrosamines	Dialkyl nitrosamines	Electrophilic nitrosamines
Acid	6		
Acid+hv		13	
Amine			34
N-nucleophile	4		
Stabilised carbanion	4		
TM catalyst	9		
Thiol			5
hv			11

Starting with the reactions that use acid as the reagent, all of the nitrosamines involved are aryl nitrosamines and this transformation is reported in the review by Borths *et al.* [3] Though these transformations are known, the fact that only aryl nitrosamines are present in the dataset supports the claims of Williams *et al.* who found that aryl nitrosamines showed higher reaction rates under acidic conditions than NDMA, which showed no reaction at all in aqueous HCl at ambient temperature. [46] A general reaction scheme for the denitrosation reactions by acids is shown in Scheme 2.6 though it is noted that this reaction is in competition with the Fischer-Hepp rearrangement reaction to give *p*-nitroso compounds. [45] Examples of two acids were found, hydrochloric acid and acetic acid. Notably, these acids have nucleophilic conjugate bases which are suggested to be important in the denitrosation mechanism. [47] Temperature and reaction time were not present in the data entries for any of the reactions, though Williams and coworkers reported the fast reaction of *N*-methyl-*N*-nitrosoaniline at room temperature in aqueous HCl. [45]

Acid (General reaction)



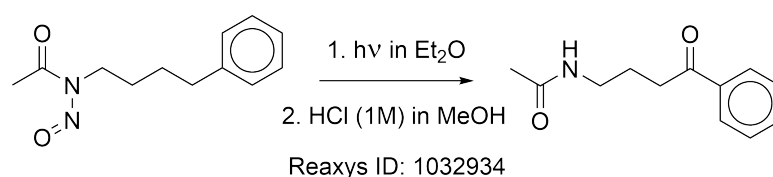
Scheme 2.6: General reaction scheme for denitrosation reactions with acid.

The photolysis reactions on *N*-nitrosodimethylamine were covered extensively in the review by Beard *et al.* [4] and the same literature was captured by the data processing workflow in



this work. In addition, this work also highlighted one further structural class of *N*-nitrosamine (alkyl; amide) that can also undergo cleavage of the N-N bond under the same photochemical conditions, initially producing the oximino compound, leading to the oxoacetamide product after addition of methanolic HCl (Scheme 2.7). [81] While these conditions are relatively mild, long irradiation times (31 h) are required and the reaction is plagued with many side products [4] making it not a viable option for broad-spectrum quenching of *N*-nitrosamines.

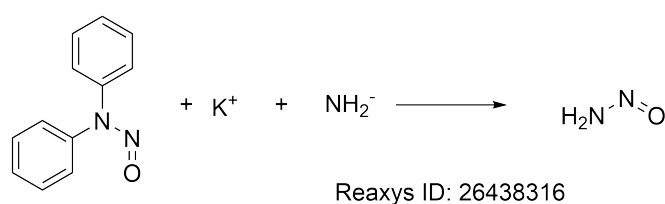
Acid + photochemical conditions



Scheme 2.7: Reaction of an alkyl; amide *N*-nitrosamine under photochemical and acidic conditions.

Another example of a denitrosation reaction is those where the reagent is a strong amine nucleophile ( $N^-$ ) e.g. potassium amide (Scheme 2.8).[82] This reaction involves the direct nucleophilic attack at the nitroso nitrogen, producing the salt of the parent amine. However, these conditions are not suitable for destroying nitrosamines as they are extremely harsh and would likely interfere with other functional groups present during API syntheses.

Denitrosation by potassium amide

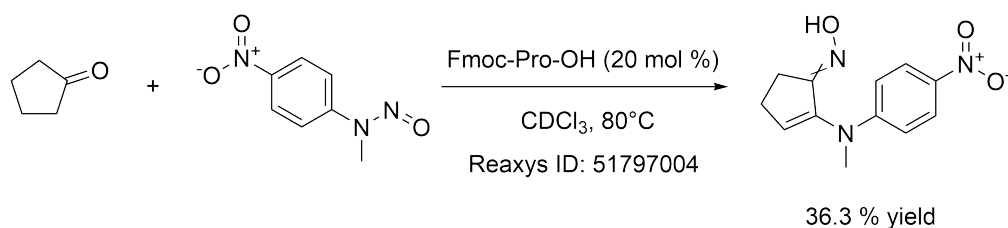


Scheme 2.8: Denitrosation by strong *N*-nucleophile.

One promising reaction condition uses an aldol type reaction, catalysed by a chiral alcohol, to form new C-N bonds with aryl nitrosamines using stabilised carbanions (Scheme 2.9). The reaction was performed at 80-90°C in refluxing chloroform. The role of the chiral alcohol is to promote the nucleophilic attack at the nitroso nitrogen as opposed to the nitroso oxygen. The reaction yield decreased for more electron dense nitrosamines (achieved by varying the substituents on the phenyl ring), indicating that this transformation only applies to aryl ni-

trosamines and is therefore not suitable for the purposes of this investigation . [83, 84]

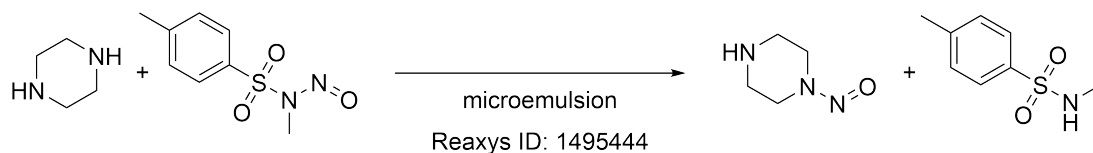
Denitrosation with stabilised carbanion



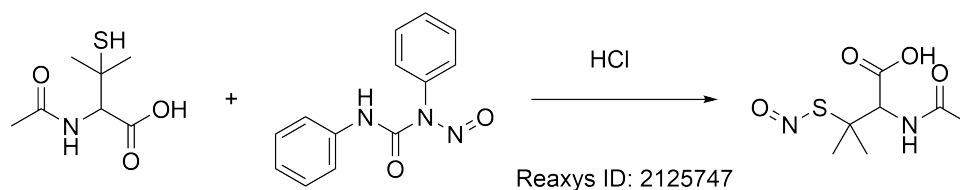
Scheme 2.9: Denitrosation by stabilised carbanion.

Transnitrosation reactions involve the transfer of nitrosonium cations ( $\text{NO}^+$ ) either inter- or intramolecularly. The most common type found in the classified dataset was the transfer from alkyl; sulfone nitrosamines to amines which had 30 examples (Scheme 2.10). These reactions came from a study by Garcia *et al.* who performed reactions in water/sodium bis(2-ethylhexyl)sulfosuccinate/alkane microemulsions. They discovered that the rate of the transnitrosation reaction was faster with more basic amines, and that smaller amines e.g. dimethylamine show faster rates than expected based on their  $\text{p}K_a$  due to their lack of steric hinderance. [85] Similarly, one example of transnitrosation from a phenyl; amide nitrosamine to a functionalised urea was reported, but under acidic conditions. [86] Transnitrosation to thiols is also present in the dataset, and these transformations were also performed under acidic conditions. [87] The acid is likely included to facilitate the denitrosation reaction by protonating the amine nitrogen, making it a good leaving group in subsequent nucleophilic attack by the thiol/amine.

Transnitrosation to amine



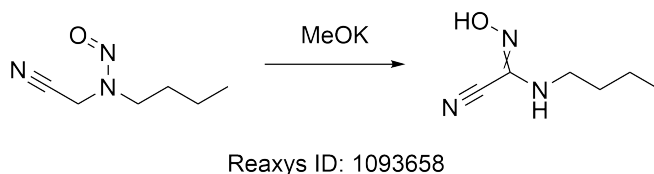
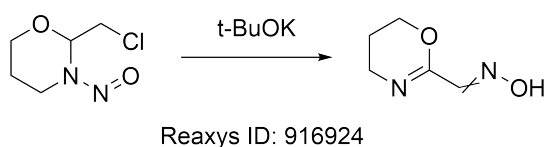
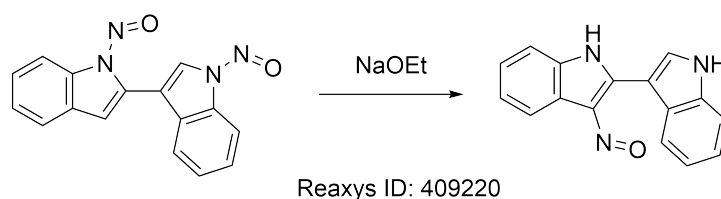
S-NO formation



Scheme 2.10: Examples of transnitrosation reactions.

Under certain circumstances, denitrosation can be achieved under basic conditions. The examples in the dataset all proceed *via* abstraction of a hydrogen  $\alpha$  to the N–N=O substructure *via* an alkoxide base, causing either a carbanion or an unsaturated C=C double bond. The nitroso group then migrates to this position, yielding C-nitroso amines and oximes as the products. [88, 89]

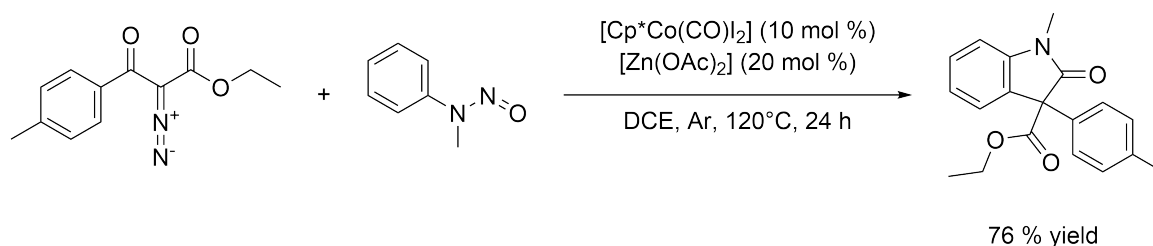
## Denitrosation reactions with base



Scheme 2.11: Examples of denitrosation reactions under basic conditions.

Finally, denitrosation on alkyl; phenyl nitrosamines has also been reported with transition metal (TM) catalysts (Scheme 2.12). Specifically with cobalt (III) complexes ( $[\text{Cp}^*\text{Co}(\text{CO})\text{I}_2]$  and  $[\text{Zn}(\text{OAc})_2]$  where the active species is  $[\text{Cp}^*\text{Co}(\text{OAc})_2]$ ). The mechanism for this reaction is well documented in the literature reference, and a copy of their Scheme four with a description of the mechanistic steps is included in the Appendix Scheme B.1. [90]

Denitrosation with transition metal catalyst



Scheme 2.12: Denitrosation reaction with transition metal (TM) catalyst.

This reaction is highly specific and the substrate scope is confined to aryl nitrosamines due to the key C-H activation step in the mechanism. Furthermore the reaction solvent is 1,2-dichloroethane whose use is discouraged in industry due to environmental concerns, and the reaction requires high temperatures and inert atmospheres which are costly.

In conclusion, while there exist many conditions for denitrosation which were not mentioned in the two previous reviews, they are quite specific to the nitrosamine involved, and often involve harsh or unsuitable reaction conditions for industrial use, combined with low functional group tolerance and a small substrate scope. Furthermore, if other nucleophilic species are present in the reaction mixture, transnitrosation becomes important, and other nitrosamines are produced which does not solve the problem. It appears from this data that the denitrosation under mild acidic conditions of more electron rich *N*-nitrosamines e.g. dialkyl nitrosamines is not possible, due to the absence of any reported reactivity on dialkyl nitrosamines except one special case which proceeds *via* an initial E2 elimination reaction in basic conditions. [89]

### Diazonium formation

Diazonium formation reactions from electrophilic nitrosamines make up a large proportion of reactions in the dataset (215 examples) (Table 2.4). This reaction is commonly used to produce diazoalkanes [91, 92] under basic conditions. There are a number of reagents which can be used to bring about this transformation but the end result is always the formation of diazonium ions which can go on to react in C-C bond formations or 3+2 cycloadditions. [93, 94]

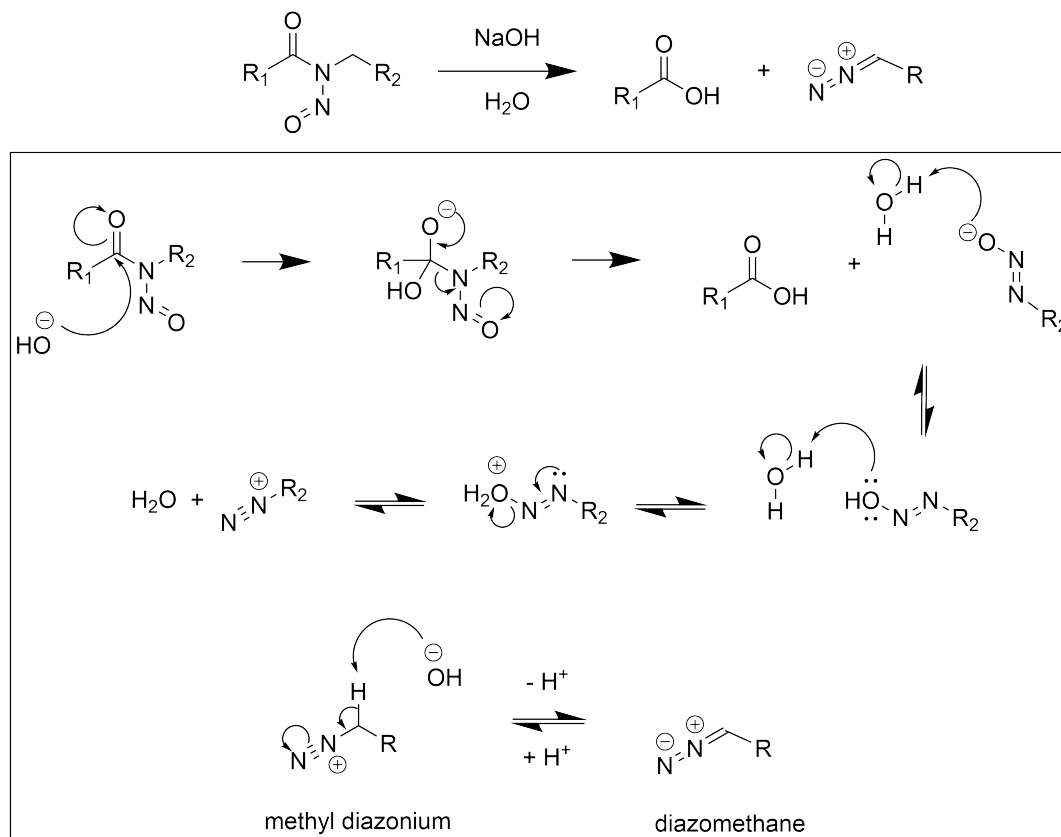
Table 2.4: Diazonium formation reactions summary table.

Diazonium formation Grouped Reagent Classification	Grouped Nitrosamine Classification	
	Dialkyl nitrosamines	Electrophilic nitrosamines
Amine		5
Base	10	179
Heating		5
<i>N</i> -nucleophile		4
Stabilised carbanion		16
Ambient temperature		6

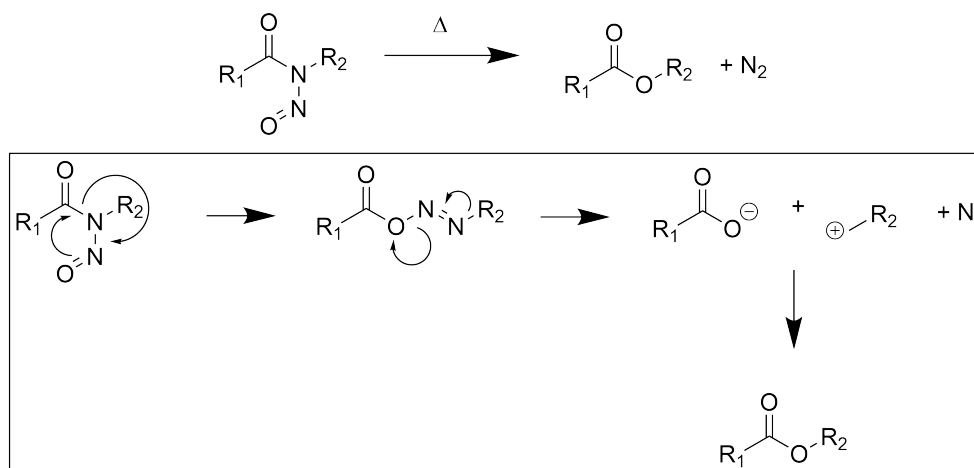
The mechanism by which this transformation occurs in all electrophilic nitrosamines is suggested in Scheme 2.13 (A) using the example of *N*-nitrosoamides in aqueous basic conditions. Nucleophilic attack at the electrophilic centre adjacent to the N–N=O amine and subsequent elimination yields an unstable deprotonated primary *N*-nitrosamine which loses water to form the diazonium compound. Alongside hydroxide and carbonates, multiple nucleophiles have been studied including aniline and substituted hydrazines (the “Amine” and “*N*-nucleophile” reagent classes in Table 2.4). [95, 96, 97] Furthermore, in some cases, simply heating the nitrosamine substrate is enough to initiate the transformation, [98] and with *N*-nitrosoamides the reaction is thought to produce a carboxylate anion and a carbocation which quickly recombine to give ester products (Scheme 2.13 (B)). [99] Furthermore, in the case of *N*-nitrosolactams with large ring size (>10), diazonium formation can occur spontaneously at ambient temperature. [100]

## Diazonium formation reaction mechanism

A) under basic conditions

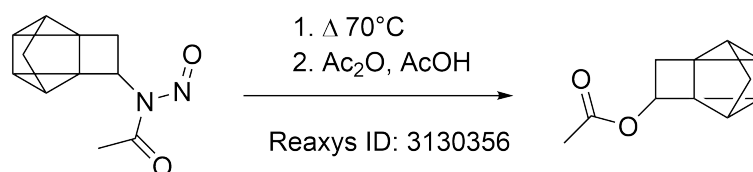


B) under thermal conditions



Scheme 2.13: Diazonium formation under basic and thermal conditions.

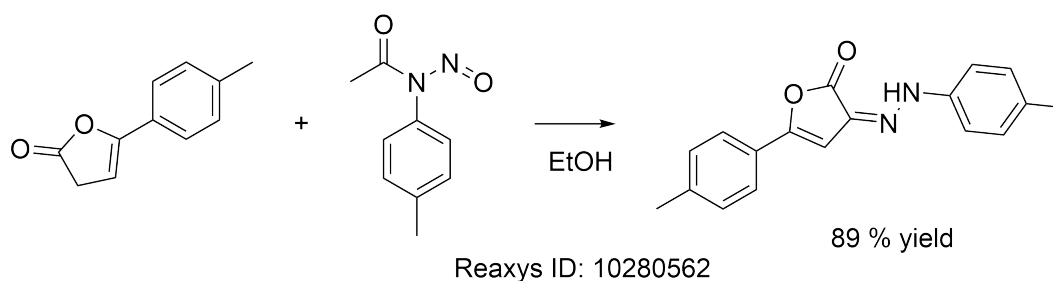
An example reaction which used heat to generate the diazonium species which was then acylated using acetic anhydride and acetic acid to produce the ester product is shown in Scheme 2.14 [101].



Scheme 2.14: Diazonium formation under thermal conditions.

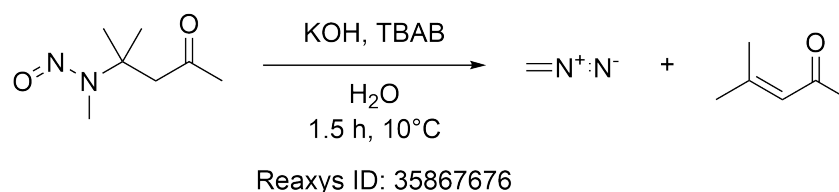
Further reactions of electrophilic *N*-nitrosamines occur with stabilised carbanions. The example in Scheme 2.15 involved the reaction of the diazonium salt of the aryl nitrosamine with the furanone, forming a new CN bond.

Stabilised carbanion



Scheme 2.15: diazonium formation reaction with a sulfonium bromide.

Diazonium formations are not specific to electrophilic nitrosamines, and examples were found with dialkyl nitrosamines (Scheme 2.16), though these compounds had removable protons at the  $\beta$  carbon which could facilitate diazonium formation *via* an E2 elimination mechanism. This reaction did require a 50% wt. solution of sodium hydroxide and therefore the required conditions are rather harsh. [102]



Scheme 2.16: diazonium formation reaction with a dialkyl nitrosamine.

In conclusion, diazonium formation reactions are a rather problematic method of destroying *N*-nitrosamines, since they produce alkylating diazonium ions which would lead to unwanted side reactions in industrial processes. While the example of a dialkyl nitrosamine forming

a diazonium salt is specific to those nitrosamines with a removable  $\beta$  protons, it should be recognised as a potential route for the purge of dialkyl nitrosamines.

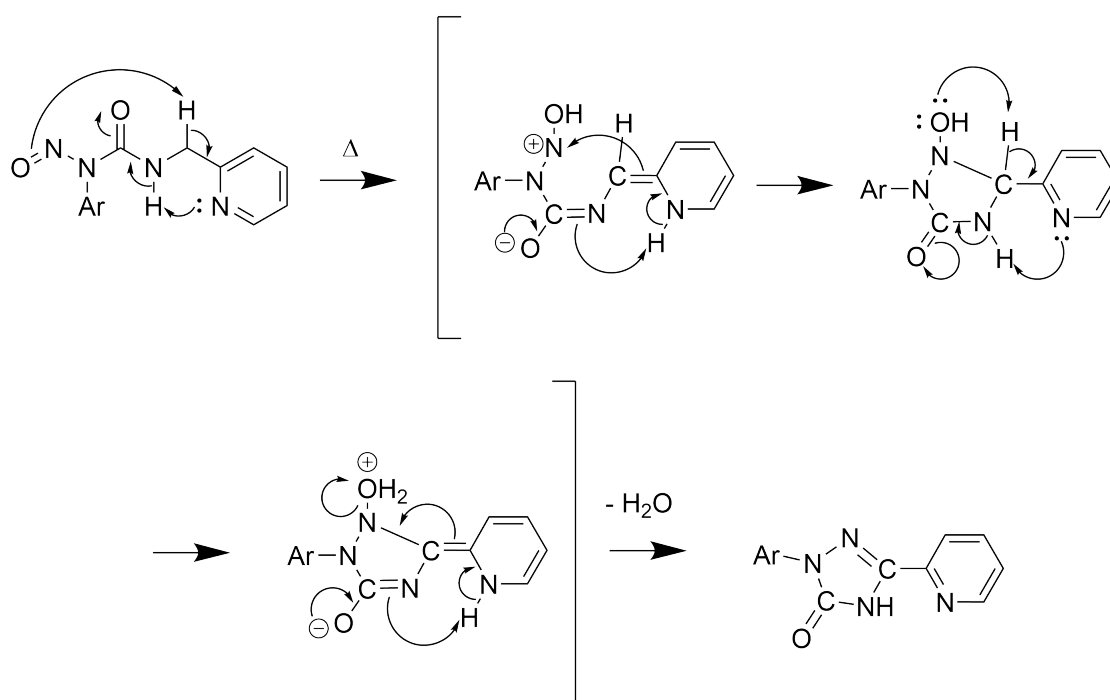
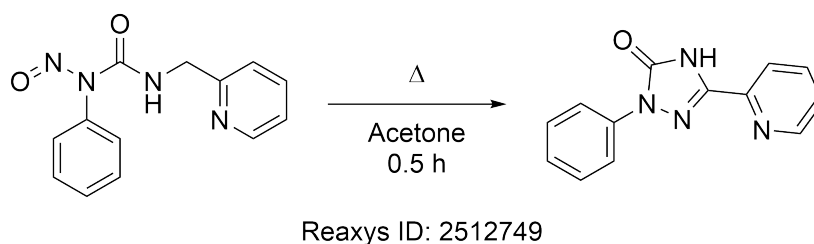
### *N*-alkylation

Table 2.5: *N*-alkylation reactions summary table.

<i>N</i> -alkylation Grouped Reagent Classification	Grouped Nitrosamine Class		
	Aryl nitrosamines	Dialkyl nitrosamines	Electrophilic nitrosamines
Heating			5
RMg/Li		10	
TM catalyst	20		

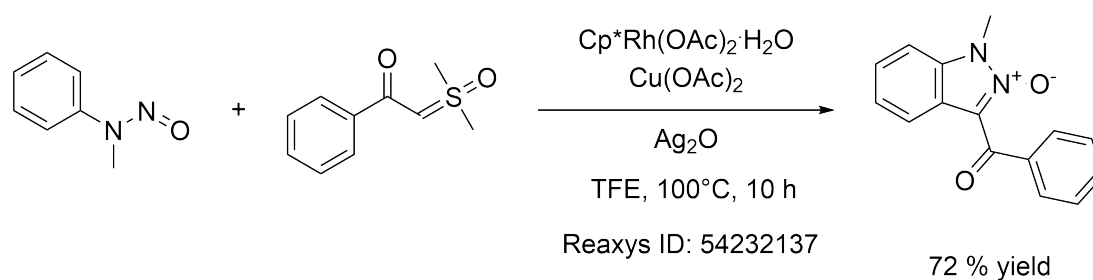
The reactions of dialkyl nitrosamines with alkyl lithium and alkyl Grignard reagents to produce hydrazines and hydrazones is well covered in the earlier reviews and will not be covered here. [4] The analysis in this work did, however, pick up other examples of *N*-alkylation reactions (Table 2.5). Among the new *N*-alkylations were examples of highly specific intramolecular cyclisations of electrophilic nitrosamines (Scheme 2.17) which occurred under thermal conditions in refluxing acetone. The authors noted that having electron donating groups attached to the aryl ring at the para position increased the yield of the cyclisation product, probably due to the enhanced ability to stabilise the positive charge which is formed on the nitroso nitrogen during the reaction mechanism (suggested in Scheme 2.17). [103] Because of the highly specific nature of the substrate this reaction is not of use as a method for destroying multiple classes of *N*-nitrosamine.





Scheme 2.17: Intramolecular cyclisations forming new C=N bonds, classified as *N*-alkylation reactions in the dataset.

The other type of *N*-alkylation reaction was also highly specific, and involved a transition metal catalyst ( $[\text{Cp}^*\text{Rh}(\text{OAc})_2 \cdot \text{H}_2\text{O}]$ ) with additional  $\text{Ag}_2\text{O}$  oxidant to form the *N*-oxide of the indazole product. This reaction is specific to aryl nitrosamines since the aromatic C-H activation is a key step in the mechanism. [104]



Scheme 2.18: *N*-alkylation reaction with a rhodium (III) catalyst.

These findings indicate that the harsh conditions to invoke *N*-alkylation reactions in dialkyl nitrosamines cannot be substituted for milder conditions, and that the *N*-alkylation pathway is not a facile method to destroying nitrosamines in an industrial setting.

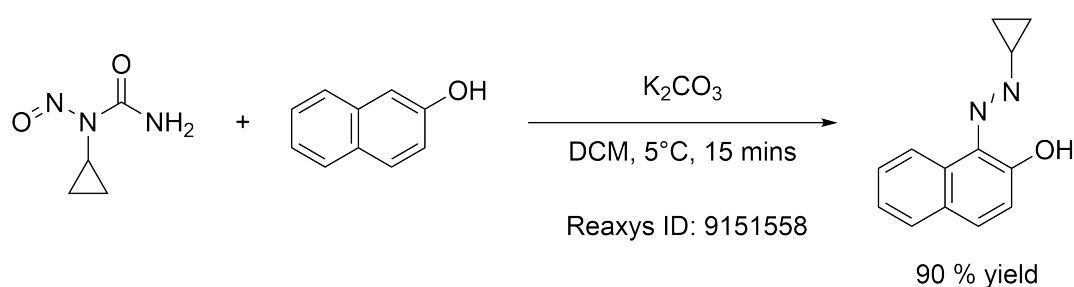
### N3 formation with amine and azo formation

These two classes of transformation were similar in that the mechanism of reaction has similarities, but the substrates are different for each class. Azo formations happen with arenes and the N3 formations occur when an amine is the substrate. Starting with azo formations, Table 2.6 shows that these transformations can occur on both aryl and electrophilic nitrosamines.

Table 2.6: Azo formation reactions summary table.

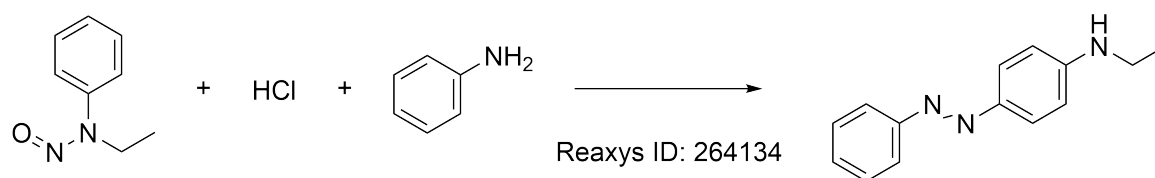
Azo formation	Grouped Nitrosamine Class	
Grouped Reagent Classification	Aryl nitrosamines	Electrophilic nitrosamines
Arene	5	33

The reaction of electrophilic nitrosamines proceeds *via* initial diazonium formation under basic conditions, and a subsequent electrophilic aromatic substitution reaction with the electron rich arene to afford the azo product. The authors in the example in Scheme 2.19 noted the propensity for di- and tri-azo products as well as alkylation reactions on the arene substrate. These findings are important to recognise if diazonium forming nitrosamines are present during API syntheses. [105]



Scheme 2.19: Azo formation from an electrophilic nitrosamine and an arene in basic conditions.

Azo formation reactions can also occur under acidic conditions with aryl nitrosamines. The reaction involves an initial Fischer-Hepp reaction which produces the para-substituted C-nitroso compound and subsequent reaction with an aromatic amine. The reference articles for these reactions are very old (1884) and the article could not be found. But the Reaxys ID's are given in Scheme 2.20.



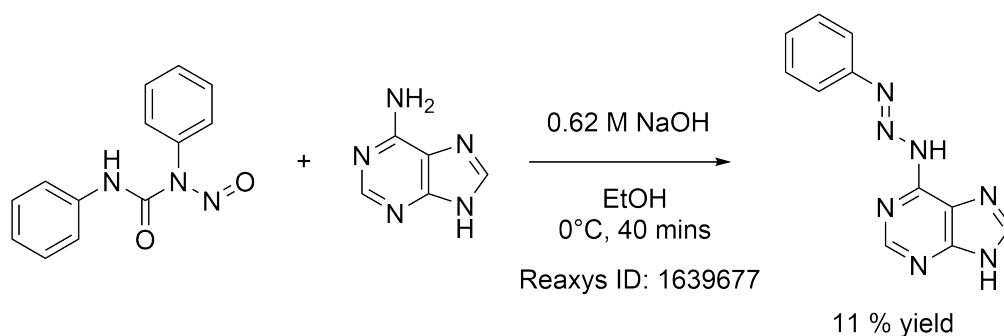
Scheme 2.20: Azo formation from an aryl nitrosamine after Fischer-Hepp rearrangement.

The N3 formation with amine class can be split into two types of reaction which both form triazene compounds (Table 2.7).

Table 2.7: N3 formation with amine reactions summary table

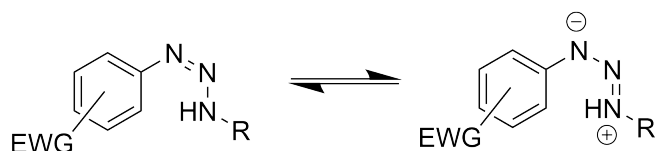
N3 formation with amine Grouped Reagent Classification	Nitrosamine class	
	Dialkyl nitrosamines	Electrophilic nitrosamines
Amine		5
Pb(OAc) <sub>4</sub> /Amine/base	4	

The first occurs *via* an initial diazonium formation with an electrophilic nitrosamine, and following this, nucleophilic attack on the diazonium species by an amine produces the triazene product (Scheme 2.21). [106] This reaction is similar to the azo formation reaction with electrophilic nitrosamines and hence the two classes were grouped together.



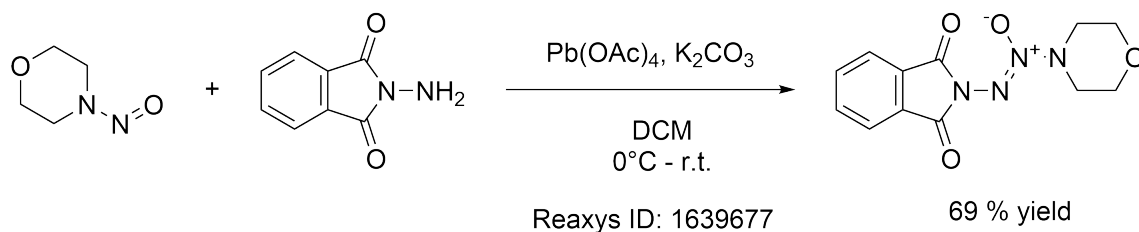
Scheme 2.21: Triazene formation with electrophilic nitrosamines.

A low yield was observed for the reaction of the aryl-nitrosourea with adenine, and this could be attributed to the lack of electron withdrawing substituents on the aryl ring of the nitrosamine substrate. The presence of electron withdrawing groups stabilise the triazene functional group by decreasing basicity of N1, decreasing its potential for protonation and subsequent breakdown of the triazene into the amine and diazonium species. [107, 108]



Scheme 2.22: Triazene resonance structures.

The other type of triazene forming reaction occurs with dialkyl nitrosamines. This reaction involves the use of a lead catalyst ( $\text{[Pb(OAc)}_4\text{]})$  to form the nitrene of the hydrazine substrate, which then undergoes nucleophilic attack by the nitrosamine to produce the triazene unit (Scheme 2.23). Evidence for the nitroso nitrogen bonding to the nitrene nitrogen came from mass spectrometry analysis which showed a fragmentation pattern indicative of loss of an oxygen atom from the product molecule. Lower yields were achieved with the electron deficient diphenylnitrosamine which also supports this claim. [109]



Scheme 2.23: Triazene formation with dialkyl nitrosamines.

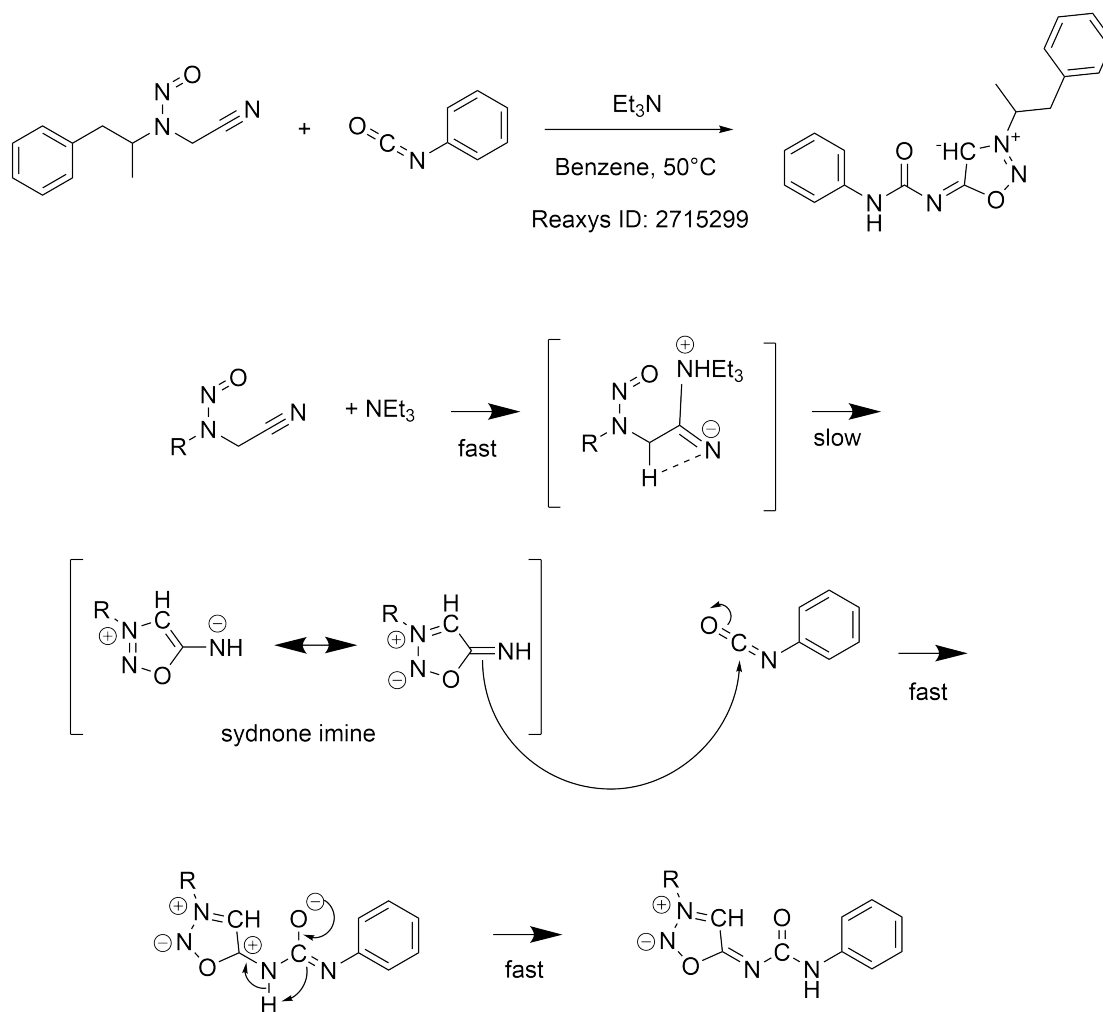
These findings indicate that further reactions can occur on the Fischer-Hepp reaction products of aryl nitrosamines if an aromatic amine is present, and should be considered in the denitrosation reactions of this class of nitrosamine. The triazene forming reactions with electrophilic nitrosamines appear to be less facile than the azo forming reactions, owing to the instability of the triazene unit, while azo formations with arenes tend to produce multiple products. Further, more specific triazene formations using lead catalysts are not of high importance in relation to industrial processes.

**O-Si/C/S bond formation**

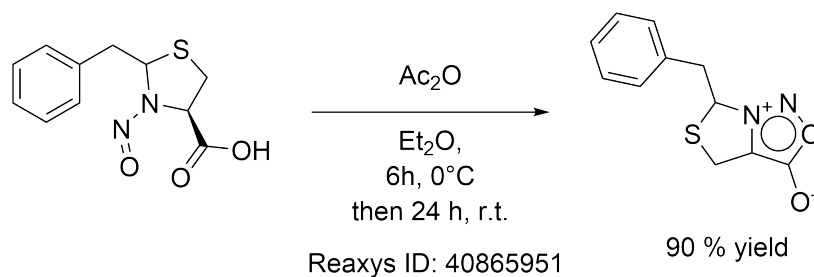
Table 2.8: O-Si/C/S bond formation summary table.

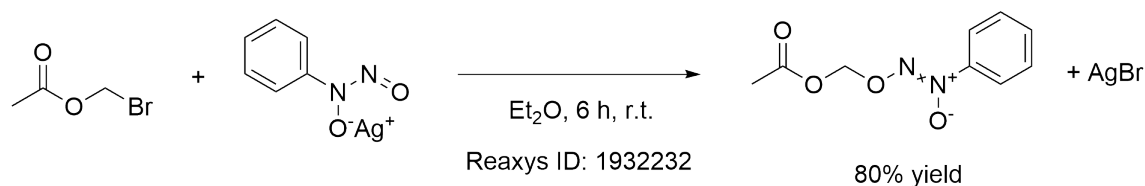
O-Si/C/S bond formation Grouped Reagent Classification	Grouped Nitrosamine Class		
	$\beta$ - carboxylic acid nitrosamines	$\beta$ - cyano nitrosamines	$\alpha$ - hydroxyl nitrosamines
Acylating reagent	36		
Alkylating reagent			14
Heating		7	

This class of transformation was defined by the formation of a new O-Si/C/S bond at the nitroso oxygen, the reactions forming O-Alkyl, O-Trimethylsilyl, and O-Triflyl compounds are covered well in the review by Beard *et al.*, and it is known that the cationic products easily fall apart to produce the parent nitrosamine after nucleophilic attack. [4] However, some special cases were found in this work, the first example (Scheme 2.24) being the reaction of  $\alpha$  - cyano nitrosamines under heat and basic conditions in apolar aprotic solvents. The mechanism is thought to proceed *via* addition of the amine base to the cyano carbon atom, and after rearrangement, a sydnone imine intermediate is formed which reacts quickly with the isocyanate to form the carbamoyl sydnone imine product. The authors noted that the reaction rate was dependent highly upon the concentration of the base, and therefore the rate determining step was thought to be the initial attack of the amine base at the cyano carbon. Electron withdrawing substituents on the nitrosamine led to an increase in reaction rate which further supports the suggested mechanism. [110]

Scheme 2.24: Cyclisation of a  $\beta$ -cyano nitrosamine to form a sydnone imine.

As well as sydnone imines, sydnone can be produced from  $\beta$ -carboxylic acid nitrosamines in the presence of an acylating reagent (e.g. acetic anhydride) (Scheme 2.25). This reaction appears to be more facile as lower temperatures were reported (*ca.*  $0$ - $20^\circ$ ). [111]

Scheme 2.25: Cyclisation of a  $\beta$ -carboxylic acid nitrosamine to form a sydnone.



Scheme 2.26: O-alkylation reaction with an  $\alpha$ -hydroxyl nitrosamine.

Additions to the nitroso oxygen atom in  $\alpha$ -hydroxyl nitrosamines have been achieved with many reagents including dimethyl sulfate [112], sulfonyl chlorides [113] and haloalkanes [114] (Scheme 2.26). The reactions typically involve either the salt of the starting  $\alpha$ -hydroxyl nitrosamine [115], or a base to deprotonate the hydroxyl group [112]. The reaction mechanism occurs by donation of the amine nitrogen lone pair into the N-N bond, forming a nitrogen cation. The  $\pi$  electrons in the N=O bond are then used to form the new bond to the reagent at the nitroso oxygen. The removal of the hydroxyl proton allows for a zwitterionic product which has greater stability over the cationic product produced in the absence of base. However, the zwitterionic products are known to be unstable, and in one study, yields rarely reached above 40% unless the alkylating agent was made more reactive by addition of an atom with a lone pair of electrons available at the  $\alpha$  position to the carbon with the leaving group. [115] For this reason, these reactions cannot be considered a robust method for removal of *N*-nitrosamines.

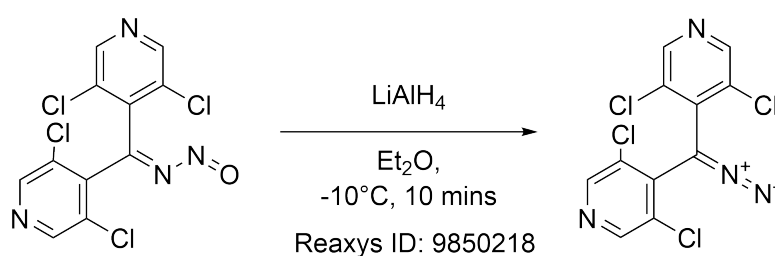
## Reduction

The reduction transformation class was dominated by reduction of aryl and dialkyl nitrosamines with hydride reductants and metal in acid. These reactions were well covered in the review by Borths *et al.* [3] and are known to produce mixtures of hydrazines and amines. The amine is the product of over-reduction after longer reaction times and higher temperatures. The review by Borths *et al.* also described the use of transition metal catalysts to reduce aryl nitrosamines across the N-N bond under hydrogenation conditions. [3] The cheminformatics workflow highlighted reductions on other classes of nitrosamine and examples of reagents not previously discussed (Table 2.9).

Table 2.9: Reduction reactions summary table.

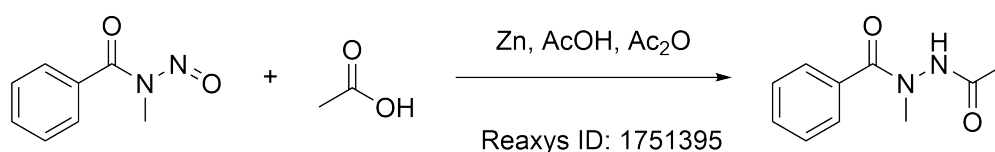
Reduction	Grouped Nitrosamine Class			
	Aryl nitrosamines	Dialkyl nitrosamines	Electrophilic nitrosamines	Imino nitrosamines
Electrochemical reduction	9			
Hydride	10	22		7
Metal	39	34	10	
S-based reductant	5			
TM catalyst	15			

Imino nitrosamines are reduced to the diazo compound and the reaction is extremely fast (Scheme 2.27), though low temperatures and anhydrous conditions are required. [116]



Scheme 2.27: Reduction of an imino nitrosamine by lithium aluminium hydride to form the diazo compound.

Furthermore, electrophilic nitrosamines can also be reduced to their corresponding hydrazines (Scheme 2.28). Again, this reaction was very fast and the authors removed the catalyst by filtering almost immediately after adding the Zn/AcOH suspension. [117]



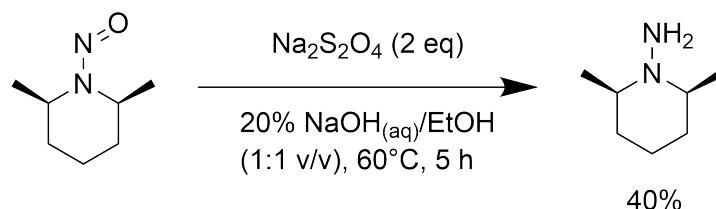
Scheme 2.28: Reduction of an electrophilic nitrosamine by zinc in acetic acid.

Overlooked in the previous reviews were electrochemical conditions that can be applied to aryl nitrosamines, though these reactions involve mercury cathodes which carry a high safety risk so discussion of these conditions is redundant. [118]

Finally, the sulfur based reductants in the dataset in this work were the same as those in the review by Borths *et al.*, using thiourea dioxide and sodium dithionite to reduce aryl nitrosamines with limited substrate scope. [32, 34] The cheminformatics workflow did not pick up on the one example of a cyclic dialkyl nitrosamine being reduced by sodium dithionite in strongly



basic media which was mentioned in the review by Borths *et al.*, and it was not present in the unfiltered dataset either. [3, 34] It is shown here for completeness (Scheme 2.29) as this is an important finding in the search for mild reaction conditions that can destroy a diverse range of structural classes of nitrosamine.



Scheme 2.29: Na<sub>2</sub>S<sub>2</sub>O<sub>4</sub> in basic media used to reduce a cyclic nitrosamine

The reductive conditions are the most promising in terms of broad spectrum destruction of nitrosamines, as the reactions destroy the nitrosamine substrate without the problem of potential transnitrosation to form other nitrosamines which plagues denitrosation reactions under acidic conditions. The majority of reductive conditions found in this work are harsh conditions with low functional group tolerance (LiAlH<sub>4</sub> and Zn/H<sup>+</sup>), and the more mild alternatives appear to be limited in their substrate scope to aryl nitrosamines. The example of a cyclic nitrosamine being reduced by sodium dithionite is promising, though the high sodium hydroxide concentration is problematic.

### 2.4.3 Structure-reactivity relationships

The newly reported literature in this text combined with the existing reviews on *N*-nitrosamine reactivity provided insights into how the structure surrounding the N–N=O substructure can influence its reactivity under certain reaction conditions. In the case of aryl nitrosamines, various instances of reactions involving aryl C–H activation at the ortho position relative to the N–N=O substructure resulted in the degradation of the nitrosamine through the use of transition metal catalysts, this reactivity is of course specific to aryl nitrosamines. Furthermore, the electron deficient aryl nitrosamines are more prone to denitrosation/ Fischer-Hepp reactions under acidic conditions, while dialkyl nitrosamines required photochemical conditions in the presence of acid to bring about the denitrosation reaction. This can be attributed to the mechanism of denitrosation outlined in the introduction, with more an electron deficient nitroso nitrogen being more susceptible to nucleophilic attack. This property of aryl nitrosamines also makes them susceptible to other nucleophiles such as stabilised carbanions (lactones). Denitro-

sations under acidic conditions should also be carefully monitored for possible transnitrosations to other nucleophilic molecules e.g. thiols and amines. Electrophilic nitrosamines primarily react *via* diazonium forming reactions, which can be achieved with a number of nucleophiles under mild conditions. The diazonium species itself is problematic due to the diverse reactivity it exhibits soon after it is generated, forming azo compounds in the presence of arenes and triazines in the presence of amines. When a removable proton is present at the  $\alpha$  position to the N–N=O substructure, a denitrosation pathway is opened that leads to the oxoimine product with alkoxide bases. This can be achieved with alkyl lithium reagents but there are associated side reactions.  $\beta$  - carboxylic acid and  $\beta$  - cyano nitrosamines are prone to the formation of sydnone (acylating reagents) and sydnone imines (with base) respectively. Reduction of a number of classes of nitrosamine is achievable with metal in acid and hydride reductant reagents, though these conditions have low functional group tolerance, milder - metal free reagents are available yet some are only effective on electron deficient aryl nitrosamines, though sodium dithionite in strongly basic media has been proven to work on a cyclic dialkyl nitrosamine.

#### 2.4.4 Promising reaction conditions

The primary objective of this chapter is to highlight the reaction conditions capable of eliminating nitrosamines across a diverse array of structural classes. Having illustrated all the examples of nitrosamine reactivity that were not previously discussed, the vast majority of the newly reported conditions discussed here can be ruled out on the basis of their small substrate scope and the low functional group tolerance of the reaction conditions. Denitrosation reactions may be a promising method, though there is a clear energy barrier that must be overcome to facilitate reaction with dialkyl nitrosamines. Reductive conditions seem to be the best method, with multiple classes of nitrosamine being reduced under more harsh reductive conditions. Interestingly, there is hope for the success of milder reductive conditions from the example of a cyclic dialkyl nitrosamine being reduced by sodium dithionite, but the high sodium hydroxide concentration is problematic. Further to these comments, an analysis was performed to attempt to find the most promising reaction conditions to apply ubiquitously to *N*-nitrosamines. Figure 2.8 shows the reaction conditions that apply to more than one of the *N*-nitrosamine classes.

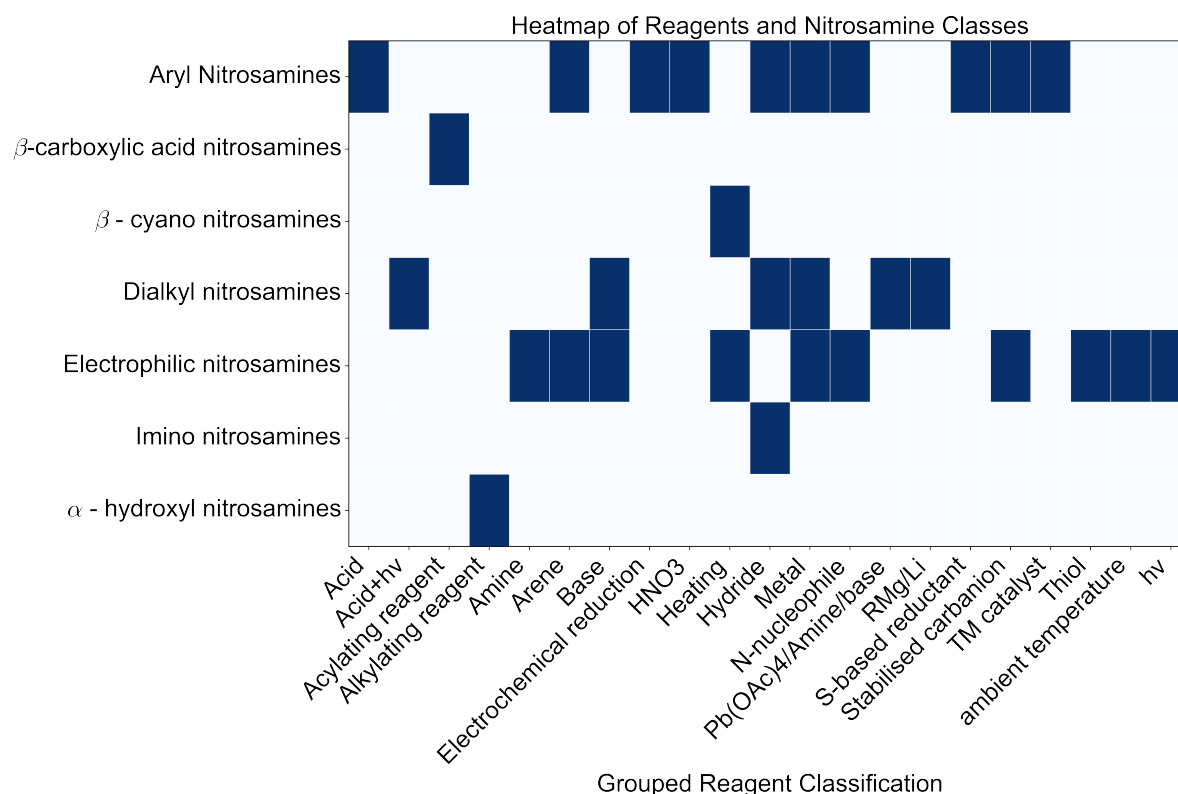


Figure 2.8: Reagents that affect more than one class of nitrosamine.

A key insight into whether or not a reagent will destroy multiple classes of nitrosamine is its ability to destroy dialkyl nitrosamines, with three out of the six reagent classes which affect multiple nitrosamine classes showing examples of reactivity on dialkyl nitrosamines. The point has been made that this class of nitrosamine is affected only by harsh reductants, organolithium/Grignard reagents, unusual metal catalysts, and acid under photochemical conditions. This finding suggests that screening reactions should first be performed on dialkyl nitrosamines to confirm reactivity on this chemically robust class before applying to other classes of *N*-nitrosamine.

## 2.5 Conclusions

This chapter improved on the two previous reviews on *N*-nitrosamine reactivity through a cheminformatics workflow to highlight reactions that destroyed a much broader range of structural classes of *N*-nitrosamine. The findings indicated that the previously unreported avenues of reactivity are specific to the nitrosamine structural class, and few are applicable across a diverse range of nitrosamines. This calls for an experimental regime to discover methods to destroy nitrosamines of multiple structural classes. The results from the classification highlighted that

reaction conditions that affect dialkyl nitrosamines often affect other classes of nitrosamine as well, and this class should be the first investigated by any experimental regime. The reaction conditions most likely to affect many classes of nitrosamine are acidic conditions, leading to denitrosation reactions, and amine products; and reductive conditions, leading to amine and hydrazine products.

## Chapter 3

# Reactivity Screen on *N*-nitrosamines

### 3.1 Scope of chapter

Building upon the knowledge obtained from the data analysis performed in Chapter two. This chapter details a reactivity screen that was performed on eight relevant commercially available *N*-nitrosamines, with the aim of discovering reaction conditions that can destroy a wide range of structural classes of *N*-nitrosamines. The reactivity screen was initially performed in flow, but after complications, the reactions were performed in a batch reaction regime. Conversions with respect to the nitrosamine were measured by HPLC, and the products of the reactions were determined by GC-MS/MS and LC-MS/MS. NMR analysis was performed in cases where unexpected results occurred to confirm the identity of the products.

### 3.2 Introduction

Chapter two provided information about the types of reaction conditions that transform *N*-nitrosamines in some way. In short, those conditions which appear most promising to work on numerous structural classes of *N*-nitrosamine are denitrosation reactions and reduction reactions since these conditions do not rely on functional groups other than the characteristic N-N=O substructure shared by all *N*-nitrosamines. Alongside the knowledge gained from chapter 2, a list was also provided by the sponsor company, LHASA Ltd., which contained some of the most common reaction conditions used in industrial processes sourced from the Mirabilis software. Table 3.1 shows the conditions on the list from LHASA and further shortlists them based on the harshness of the condition and whether it is likely to react with *N*-nitrosamines or not, and

also if there is literature data already confirming the reactivity.

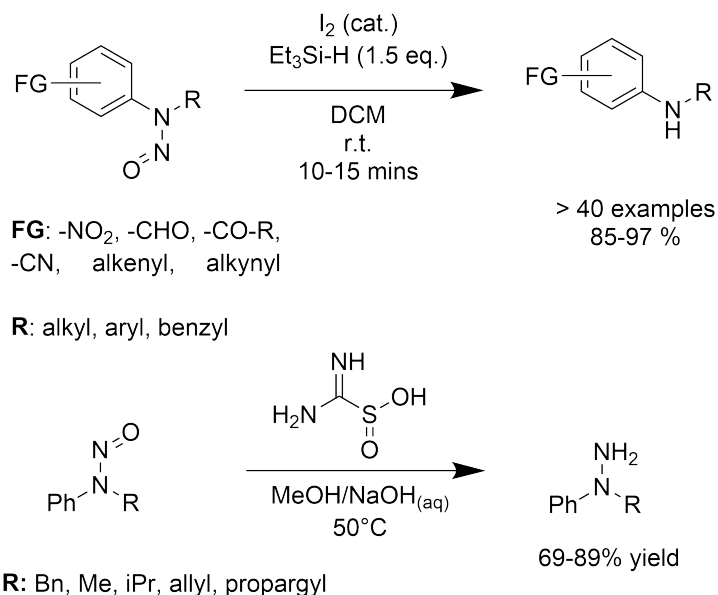
Table 3.1: Reaction conditions based on Mirabilis tool for reactivity screening against common *N*-nitrosamines.

No.	Reagents	Solvent	Reactivity screen	Reason
1	BnSH		No	Acute toxicity (inhalation)
2	BnNH <sub>2</sub>	isooctane	No	Literature data [119]
3	EtMgBr	diethyl ether	No	Literature data [120]
4	DBU	DCM/THF	No	Too mild to react
5	NaOH (2 M)	H <sub>2</sub> O	Yes	
6	NaHCO <sub>3</sub> sat.	H <sub>2</sub> O	No	Too mild to react
7	NaOEt (21%)	EtOH	Yes	
8	<i>n</i> BuLi	Hexane/THF	No	Literature data [121]
9	HCl 2M	H <sub>2</sub> O	Yes	Literature data, limited scope [122]
10	H <sub>2</sub> SO <sub>4</sub> 95%	None	No	Harsh conditions
11	H <sub>2</sub> SO <sub>4</sub> 2M	H <sub>2</sub> O	No	Literature data, too harsh [122]
12	HBr 33%	AcOH	Yes	
13	HCl	EtOH	Yes	Literature data, limited scope [47]
14	NaBH <sub>4</sub>	EtOH	Yes	
15	LiAlH <sub>4</sub>	THF	No	Literature data [123]
16	DIBAL-H	THF	Yes	
17	BH <sub>3</sub>		No	Harsh conditions
18	H <sub>2</sub> , 10% Pd/C	EtOH, <i>i</i> PrOH	No	Literature data [124, 125]
19	H <sub>2</sub> , 5% Pd/C	EtOH, <i>i</i> PrOH	No	Literature data [3]
20	H <sub>2</sub> , Raney Ni		No	Literature data [126]
21	NaClO <sub>4</sub>		No	Harsh conditions
22	H <sub>2</sub> O <sub>2</sub> 30%	H <sub>2</sub> O	Yes	Include at reduced concentration
23	AcOOH 40%	H <sub>2</sub> O	Yes	
24	KMnO <sub>4</sub>	DCM	No	Literature data [127]
25	IBX/DMP	DCE/MeCN	No	Too mild to react
26	TEMPO	MeCN	No	Too mild to react
27	<i>m</i> -CPBA	DCE/MeCN	No	Too mild to react
28	O <sub>3</sub>	THF	No	Harsh conditions

Since the majority of reported reaction conditions are harsh and have low functional group tolerance, harsh conditions such as NaClO<sub>4</sub> were eliminated and more mild conditions which showed promising results with harsher alternatives e.g. sodium borohydride NaBH<sub>4</sub> and diisobutylaluminium hydride (DiBAL-H) were kept. A common sense approach was used in deciding which conditions would be too mild to react with *N*-nitrosamines, for example the mild oxidising agents *m*-CPBA, IBX/DMP and TEMPO are excluded since extremely harsh conditions are required to oxidise *N*-nitrosamines to the *N*-nitro compound (CF<sub>3</sub>CO<sub>3</sub>H at high temperature). [49]

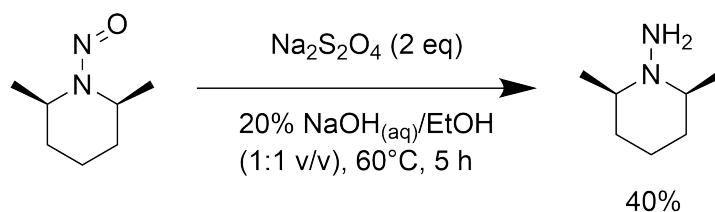
With a view to discovering mild reaction conditions to destroy *N*-nitrosamines, an attempt was

made to find a metal-free reaction condition that was effective across a wide range of structural classes of *N*-nitrosamine. As mentioned in the introductory chapter, Chaudhary *et al.* [32, 33] introduced two metal-free methods to reduce aryl nitrosamines to the corresponding amines and hydrazines, but no evidence is given of their effectiveness on a wider substrate scope and it is assumed that these are the limitations of the method (Scheme 3.1).



Scheme 3.1: Metal-free conditions to reduce *N*-nitrosamines by Chaudhary and coworkers. [33, 32]

The other previously reported metal-free method by Overberger used sodium dithionite (Na<sub>2</sub>S<sub>2</sub>O<sub>4</sub>) in basic media to reduce a wider range of *N*-nitrosamines including one cyclic *N*-nitrosamine (Scheme 3.2). This promising result led to the selection of Na<sub>2</sub>S<sub>2</sub>O<sub>4</sub> in basic media in the reactivity screen. A weaker sulfur-based reductant was selected (Na<sub>2</sub>SO<sub>3</sub>) in order to find the limit of the required conditions to reduce a broad range of *N*-nitrosamines. [34]



Scheme 3.2: Na<sub>2</sub>S<sub>2</sub>O<sub>4</sub> in basic media used to reduce a cyclic nitrosamine

The selected reagents to be included in the reactivity screen are listed in Table 3.2:

Table 3.2: The reagents to be tested in the reactivity screen.

#	Reagent	Supplier
1	H <sub>2</sub> O <sub>2</sub>	Fisher
2	CH <sub>3</sub> CO <sub>3</sub> H 40% wt.	Fisher
3	HBr 33% wt. in AcOH	Sigma
4	HCl 2M (aq)	Fisher
5	HCl 1.25M (EtOH)	Sigma
6	NaBH <sub>4</sub>	Fisher
7	DiBAL-H	Sigma
8	Na <sub>2</sub> S <sub>2</sub> O <sub>4</sub>	Fluorochem
9	Na <sub>2</sub> S <sub>2</sub> O <sub>4</sub> + NaOH 0.1M	Fluorochem
10	Na <sub>2</sub> S <sub>2</sub> O <sub>4</sub> + NaOH 1M	Fluorochem
11	Na <sub>2</sub> S <sub>2</sub> O <sub>4</sub> + 20% NaOH	Fluorochem
12	Na <sub>2</sub> SO <sub>3</sub>	Sigma
13	Na <sub>2</sub> SO <sub>3</sub> + 1M NaOH	Sigma

Eight *N*-nitrosamines were purchased from TCI chemicals and are shown in Figure 3.1. The majority of nitrosamines selected were dialkyl nitrosamines since Chapter two discovered that reaction conditions that destroy this class of nitrosamine are likely to affect other classes.

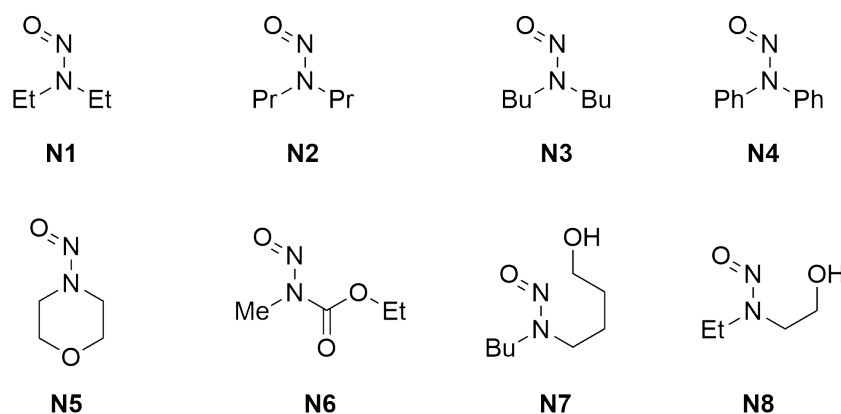


Figure 3.1: The eight nitrosamines used in this study.

This chapter goes on to detail flow and batch experimental protocols for *N*-nitrosamine stability under the above conditions, including safe quenching and disposal of *N*-nitrosamines, a conversion and reaction product analysis campaign using HPLC, GC-MS/MS and LC-MS/MS. Analysis of the conversions and reaction products will be discussed and conclusions will be made about the suitability of the reaction conditions for destroying *N*-nitrosamines in high-value chemical manufacture.



### 3.3 Safety

*N*-nitrosamines are potent carcinogens, and to ensure absolute safety with regards to handling them, a number of safety protocols were put in place before experimental work began. This started with the use of spill-trays which the screening reactions were performed inside to contain any spills. Blunt needles were also used when performing any transfers by needle and during reaction setup using inert atmospheres. Butyl-rubber gloves were worn during handling of the nitrosamine reagent bottles and when washing glassware. All HPLC and GC sample vials were kept after analysis and disposed of with the rest of the reaction waste to avoid exposing others. Reactions were also run at very small scale (0.1 mmol) to avoid producing large amounts of waste, and to minimise exposure.

In response to the success and cost effectiveness of  $\text{Na}_2\text{S}_2\text{O}_4$  in basic media as a reductant for *N*-nitrosamines, this was used as a final quench for all reaction conditions. After the screening reaction was completed, the quenched reaction mixture was washed (with ethanol and water) into a larger flask containing a basic aqueous solution (20 % NaOH) of  $\text{Na}_2\text{S}_2\text{O}_4$  which was then stirred and heated at 40°C overnight, the mixture was then cooled and poured into a hazardous waste container to be disposed of as hazardous waste.

The associated hazards of *N*-nitrosamines made flow chemistry an attractive approach to screening their reactivities. The use of a closed system in flow chemistry allows for minimum handling and exposure to *N*-nitrosamines, and quenching *in-line* means that the waste can be safely disposed of after a reactivity campaign.

### 3.4 Initial investigations in Flow

This section discusses the results of the flow reactions performed at the Rapid Online Analysis of Reactions (ROAR) facility at Imperial College London (ICL). The experimental campaign involved four, two week trips in which the experimental setup was constructed, and the reactions were ran and analysed. The data processing was performed afterwards, in Leeds, due to the time restrictions of each visit. Time restrictions also required that the results were generated as quickly as possible. This meant that initially, the flow apparatus (Vapourtec R-series) was used without all its requisite parts i.e. without the autosampler (Figure 3.2). In the first set of experiments, the injection loop was filled manually, *via* a syringe with luer-lock. The impact

of this is that only short reaction times could be measured due to the time cost of the manual loading aspect. The introduction of the autosampler in later trips allowed for longer reaction times to be measured, as the reactions could be started in the evening and ran overnight. The following sections detail the experimental setup, the reaction of N6 with sodium borohydride, and the issues surrounding the use of the autosampler for longer reaction times.

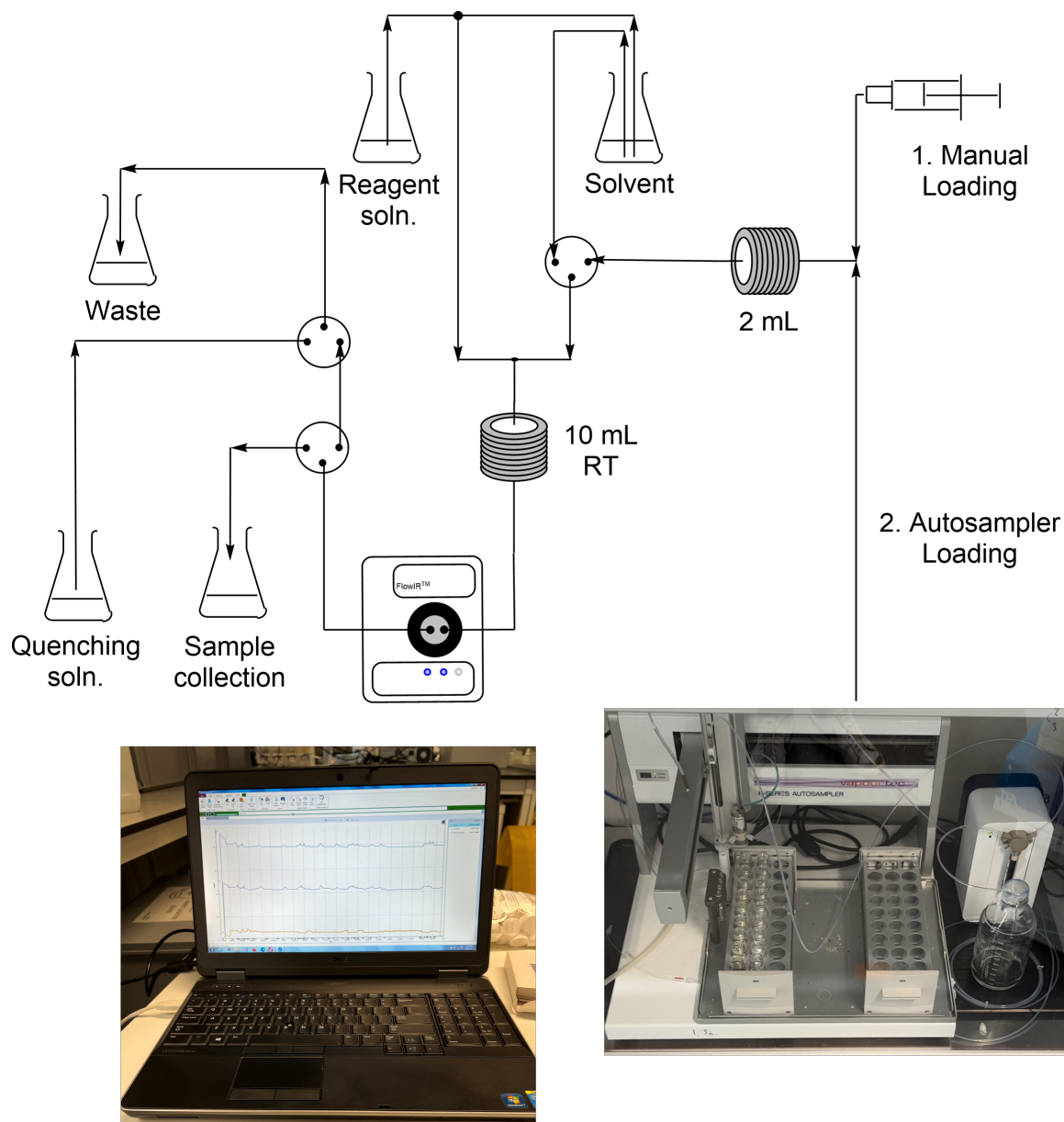


Figure 3.2: Flow reaction setup (general). Showing both manual loading using syringes with luer-lock, and automated loading using the autosampler. The online analysis IR traces are shown on the laptop screen.

### 3.4.1 Flow reaction protocol

A Vapourtec R-series was initially used without the autosampler, 0.5 M nitrosamine stock solutions were loaded into the injection loop manually, *via* a Luer-lock syringe, and the switching valve was triggered manually to introduce the nitrosamine into the system and begin the reaction (Figure 3.3).

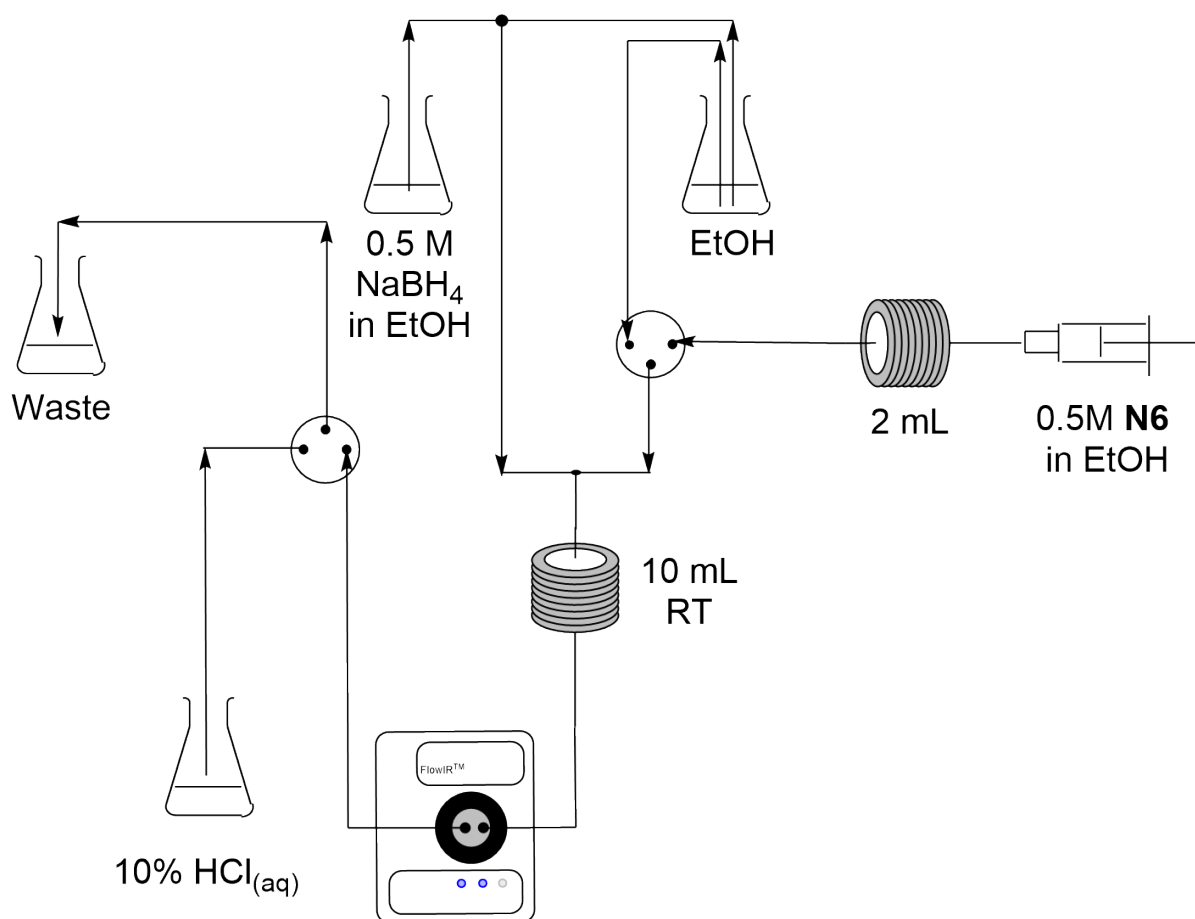


Figure 3.3: Flow reaction setup for the reaction of N6 with sodium borohydride.

The reactions were monitored by an in-line IR spectrometer (ReactIR) which was set up as per manufacturer instructions to measure between 0 and 3300  $\text{cm}^{-1}$ , the gain was modulated to within recommended limits (ca. 20000) and the instrument was cooled with liquid nitrogen before starting data collection. The scan rate was set to 15 seconds. The in-house software ICIR for data processing was unavailable, and a python script was written to extract the results from the raw data.

With reference to Figure 3.3, the procedure without the autosampler is as follows: a reference IR spectra for the nitrosamine in the reaction solvent is taken. This is achieved by pumping both

influx lines from the solvent reservoir (EtOH) at 5 mL/min (1 minute residence time). Next, the 2 mL injection loop is filled with a 0.5 M solution of nitrosamine in the reaction solvent. The switching valve is triggered, and the nitrosamine solution is injected into the system. At the point of injection, a note is made on the ICIR software, this reference point allows for the capture of the nitrosamine at the time it passes through the IR spectrometer during later processing. The time taken to reach the IR spectrometer was 61 seconds, this accounted for the 136 cm of 1 mm internal diameter tubing connecting the injection port to the 10 mL reactor coil and then from the reactor coil to the in-line IR probe. After the reference was taken, one of the influx lines was switched to pump from the 0.5 M NaBH<sub>4</sub> solution (the tubing from this line was shorter than that of the line used to inject the nitrosamine solution, to ensure that the reagent reached the reactor coil before the nitrosamine) and the injection loop was charged with a further 2 mL of the 0.5 M nitrosamine solution. The process described above was repeated with the reagent solution flowing through the system and the spectra were collected for analysis. This method allowed for qualitative analysis of the effect of the reagent on the nitroso group through comparison of the area under the curve of the nitroso stretch region (1499 - 1402 cm<sup>-1</sup>) for the reference and the reaction.

### 3.4.2 Flow reaction analysis workflow

The ICIR software which is provided with the ReactIR spectrometer was unavailable after data collection at the ROAR facility, and because of this analysis of the data was performed in python. The notes that were made about the time of injections for the reference and reaction spectra were exported as excel files, along with the raw IR data for the ReactIR run. The analysis workflow is as follows: The full IR traces for each time point were zoomed into the wavenumber region of interest (N=O 1499-1402 cm<sup>-1</sup>, and C=O 1752-1700 cm<sup>-1</sup>). The note for the injection time is entered and the average of three spectra surrounding this timepoint are taken as a reference spectra to which baseline correction is performed using asymmetric least squares (ALS) smoothing. This baseline is then subtracted from seven consecutive spectra, which start from 45 seconds after the injection note, to allow time for the reaction mixture to pass through the system. The area under the curve is calculated using Simpson's integrator from numpy. The area curve is then subjected to baseline correction by the ALS algorithm so that the change in areas can be compared, this is necessary due to the continuous shifting in baseline height during the data collection. The above procedure is performed for both the reference and

reaction injections, and the area under the curve (AUC) traces are plotted against each other using matplotlib.

### 3.4.3 Results for N6 with NaBH<sub>4</sub>

The reaction of N6 with NaBH<sub>4</sub> led to some obvious differences when comparing the AUC traces of the reference and the reaction. As shown in Figure 3.4, it is clear that both the N=O 1499-1402 cm<sup>-1</sup>, and C=O 1752-1700 cm<sup>-1</sup> bonds are consumed during the reaction.

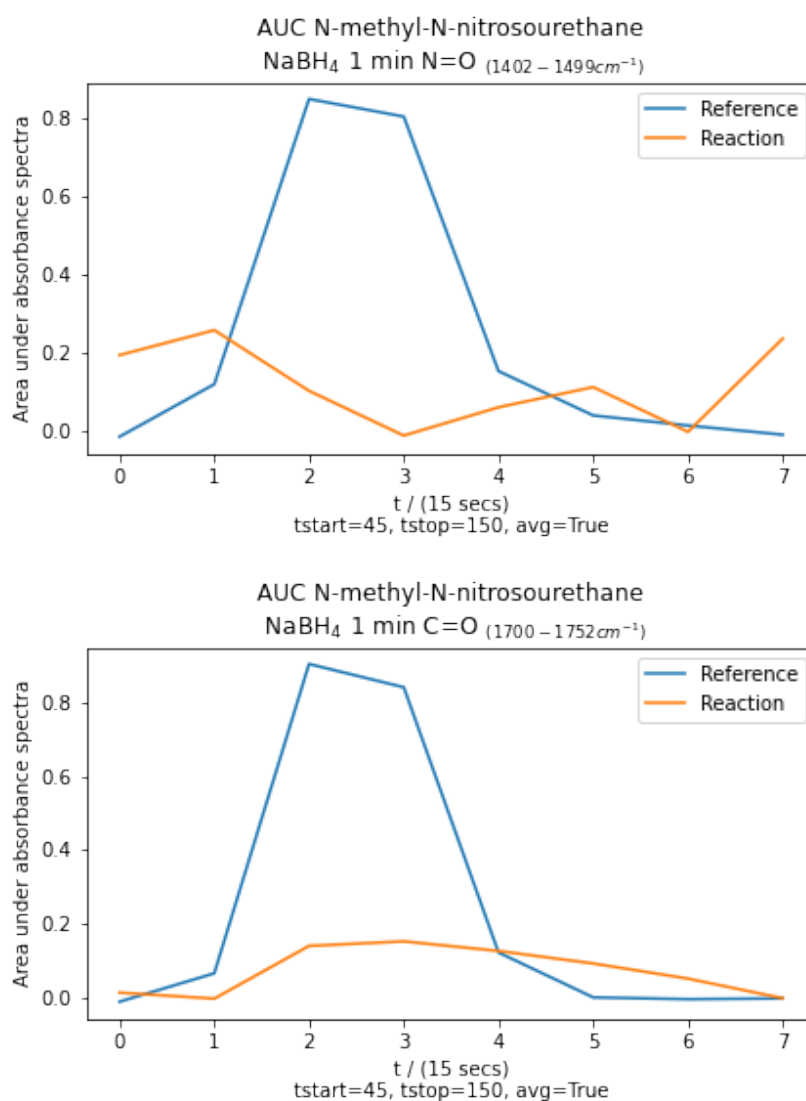


Figure 3.4: Area under the curve (AUC) plots for the reaction between *N*-methyl-*N*-nitrosourethane (N6) and NaBH<sub>4</sub>. Showing consumption of both the N=O and C=O bonds.

This result indicates that NaBH<sub>4</sub> is capable of reducing N6 which is unexpected due to the non-reactivity of BOC protected amines in the presence of one equivalent of sodium borohydride.

[128] It is hypothesised here that the electron withdrawing nature of the nitroso group facilitates hydride addition to the carbonyl carbon of N6, and formation of the unstable  $\alpha$ -hydroxy *N*-nitrosamine discussed in Chapter 1 (Scheme 1.3), leading ultimately to the complete degradation of N6.

#### 3.4.4 Autosampler issues

The introduction of the autosampler (Figure 3.2) allowed for longer reaction times to be measured. This was a necessary modification to the setup because the reaction rate of the applied conditions, if there was a reaction at all, was unknown. Because of this, longer reaction times were required to allow conversion to occur where possible.

The autosampler was set up to provide the nitrosamines with a 30 minute residence time. In this setup, to increase the mixing between reagent and nitrosamine solution, the 10 mL reactor coil was swapped for a 20 mL reactor coil with an internal static mixer. The flow rates were adjusted to 0.125 mL/min, and this led to a residence time of around 24 minutes due to the unknown internal volume of the new reactor coil.

The autosampler was set up to sequentially aspirate 2 mL of the nitrosamine solution from a sample vial in the rack and fill the injection loop for all the nitrosamines tested. This was problematic because the vials that fit into the rack were large, 20 mL sample vials (pictured in Figure 3.2) with a wide opening, allowing for evaporation of the solvent in the timeframe of running all of the injections. This meant that the stock solution became more concentrated and rendered the qualitative comparison of AUC curves unsuitable when using solvents with high vapour pressure. It was found that acetonitrile and ethanol were the best solvents due to their low vapour pressure at room temperature, miscibility with aqueous reagent solutions and ability to dissolve the nitrosamines at 0.1 M (minimum required concentration to visualise nitrosamines). The time taken to run one set of reference/reaction injections was around 8 hours, so the references were run first, with the run starting in the evening and running over night. The following morning the ReactIR was re-cooled with liquid nitrogen, and configured as necessary (gain adjustment if outside optimum). Unfortunately, this slight modification during setup led to variations in the peak areas of the nitrosamines. This, coupled with the inherent low intensity of the N=O stretching frequency meant that the references and reaction peaks could not be compared unless they were part of the same ReactIR experiment. Figures 3.5

and 3.6 show the inconsistencies in the peak shape and the deviation in peak areas respectively for three separate reference runs with acetonitrile and water solvent systems.

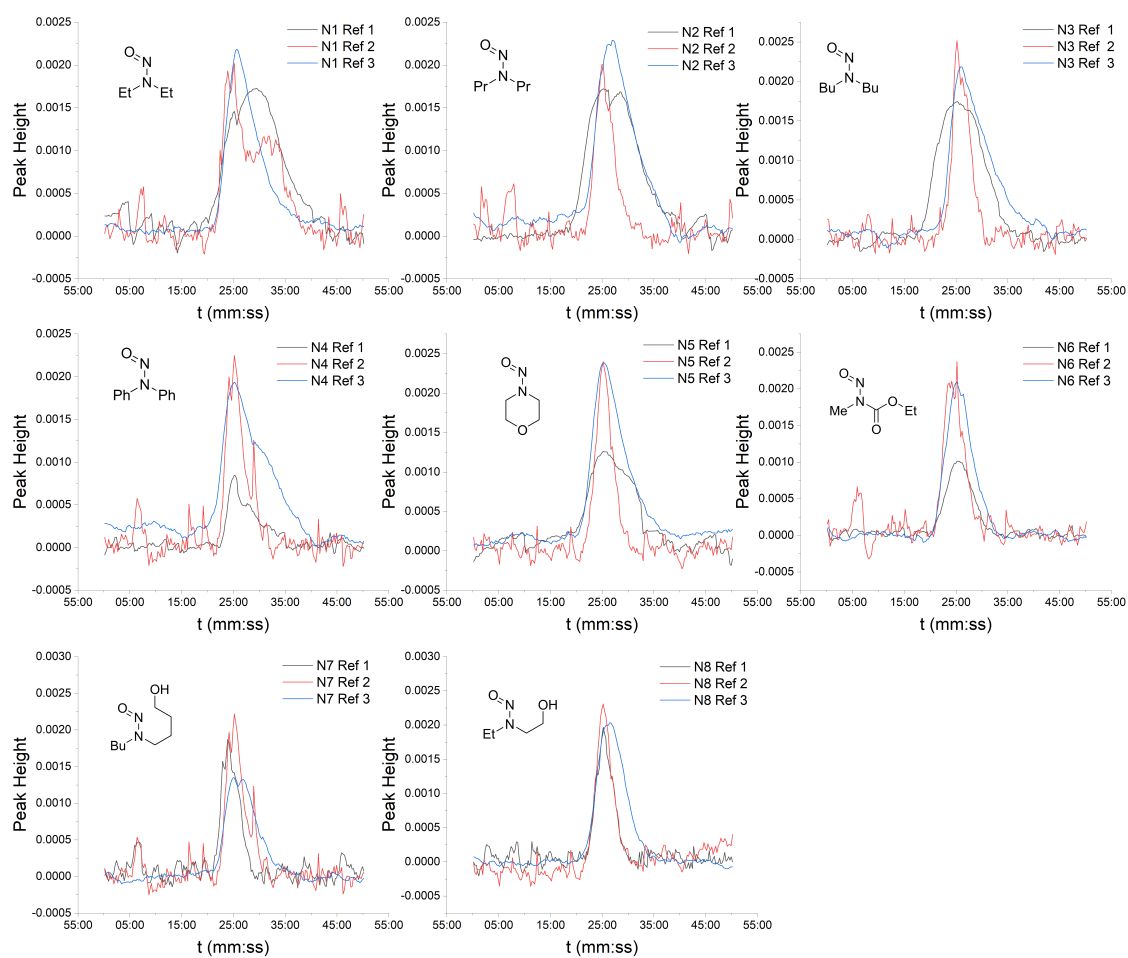


Figure 3.5: Graphs of the peak shapes for three separate reference runs for the eight nitrosamines studied.

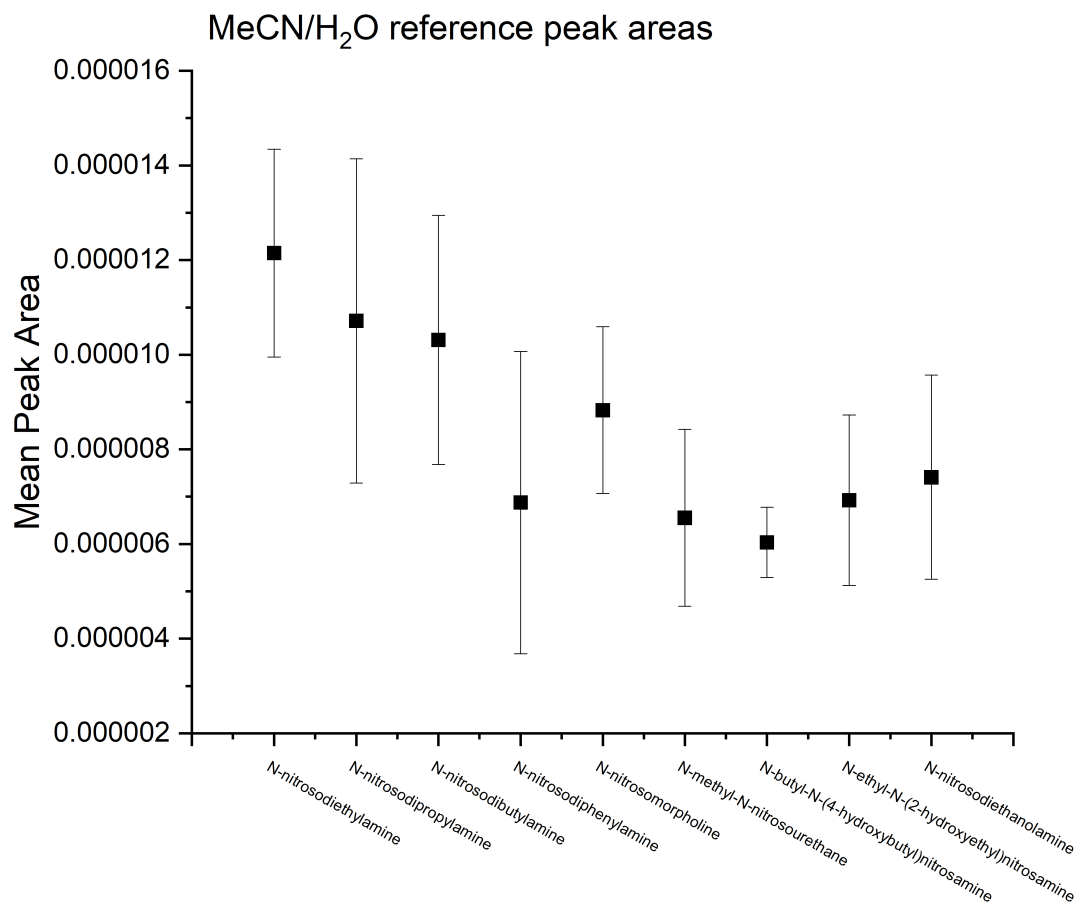


Figure 3.6: Graph to show the deviation in peak areas of the AUC plots across three reference runs.

Ultimately, this method was not viable for measuring reactions with low reaction rate, as it is required to include both reference and reaction injections in the same run. The limiting factors on the length of a run is the volume of solvent available, and the time which the ReactIR remains within the operational temperature range. These factors meant that an alternative approach had to be taken to build the best picture of *N*-nitrosamine reactivity, and the second approach took the form of a batch reaction campaign which was carried out at the University of Leeds.

### 3.5 General experimental procedure

For conducting batch reactions, a method was developed with minimal requirement for the handling of *N*-nitrosamines. This involved the preparation of stock solutions of the eight *N*-nitrosamines involved in an appropriate solvent. Simple solubility tests determined that ethanol was a suitable solvent for the dissolution of all *N*-nitrosamines tested in this study. The only deviation from this was for the reactions involving DiBAL-H and NaBH<sub>4</sub>, where tetrahydrofuan



(THF) was used. Appendix Table C.1 gives details on the preparation of all the stock solutions used in this study. Stock solutions were always made up to *ca.* 0.1 M (accurate millimolar initial nitrosamine concentrations are given in Table C.1). Stock solutions were cautiously given a month of use before being considered expired, and fresh solutions were prepared in place. All *N*-nitrosamines were treated as air-sensitive, with reagent bottles stored and handled under a nitrogen atmosphere during the preparation of stock solutions. All *N*-nitrosamines and stock solutions were stored in the refrigerator after use.

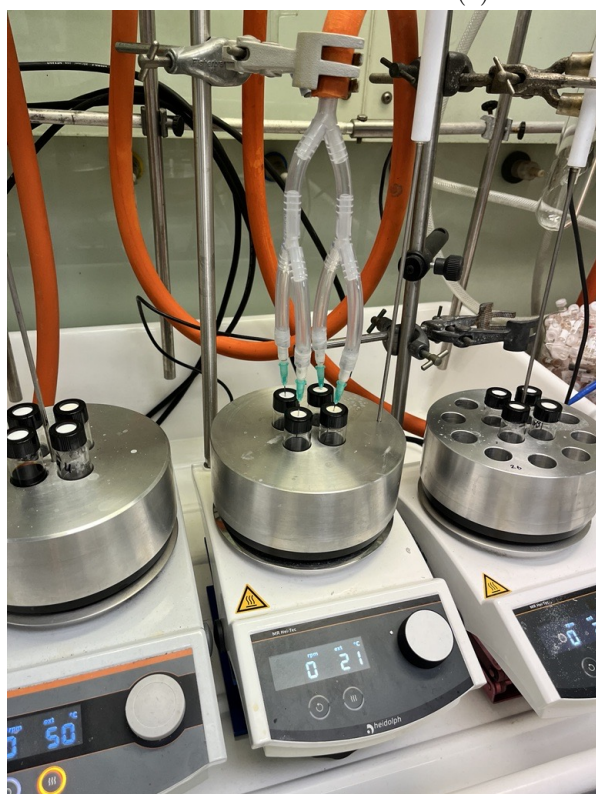
Reagent solutions were prepared such that reactions could be performed in high excess of the reagent; this was done intentionally to mimic the conditions of *N*-nitrosamine formation as trace impurities in process chemistry. For all the reactions, care was taken to ensure the solubility of both the *N*-nitrosamines and the reagents. Information about total reaction volume, reagent stock concentration, and added solvent volumes can be found in Table 3.3.

In performing the batch reactions, the required reagent volume was first added via 1000  $\mu$ L Gilson pipette (or 1 mL syringe in the case of DiBAL-H and HBr/AcOH) into a 15 mL vial in a custom-made aluminium block which ensured consistent heating and mixing when stirring at 400 rpm with a 20 mm magnetic stir bar (Figure 3.7). The required amount of solvent was next added to the reaction vial to ensure solubility. Heating was then applied *via* a stirrer hotplate to the reaction vial if required, and once at temperature, *N*-nitrosamine stock solution was added with stirring and the timer was started. Reactions were run at 24 hours if at room temperature, and 16 hours if run at 50°C.

An internal standard (IS) stock solution of 1,3,5-trimethoxybenzene (TMB) (1 mL, 0.3 M, 0.3 mmol) was also added to the reactions *via* Gilson pipette. The chosen internal standard is not stable to acid, and therefore in the reactions with acid, the internal standard solution was either omitted from the reaction, ignored during conversion calculation or added after the acid was quenched. Thus, HPLC calibrations with and without the internal standard are presented in Appendix Figures D.1 to D.9. For conditions nine and ten where the conversions and products were analysed by GC-MS/MS, the same internal standard amount was included, the calibration plots can be found in Appendix Figures E.1 to E.7. An example HPLC calibration for N1 is shown in Figure 3.8



(a) Batch reaction setup.



(b) Batch reaction setup for inert atmospheres.



(c) Blunt needles.

Figure 3.7: Images of reaction setup.

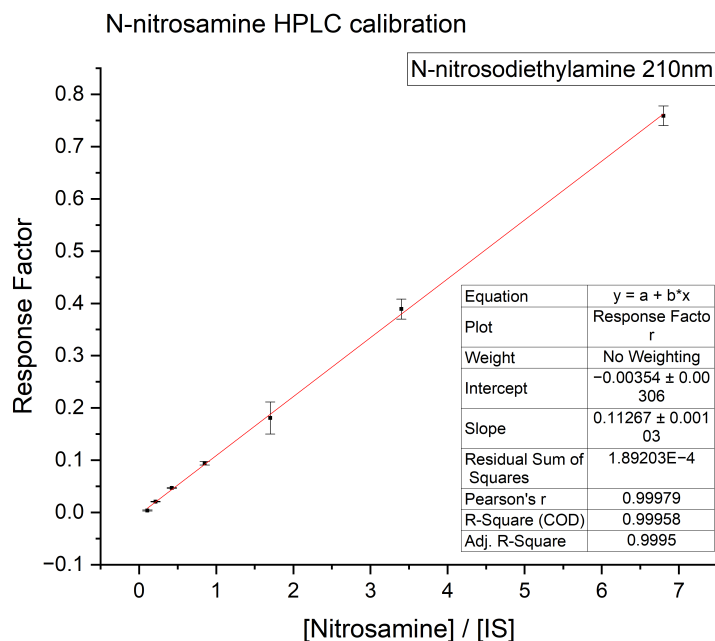


Figure 3.8: HPLC Calibration curve for *N*-nitrosodiethylamine (N1) at 210nm.

After the required reaction time, the quenching solution(s) was added to the reaction mixture, all quenches were performed at room temperature, and solutions were stirred for a further ten minutes before sampling directly from the reaction mixture into HPLC vials for conversion analysis by GC (DiBAL-H) or HPLC (all other reaction conditions).

Product identification was made difficult by the fact that the products (mainly amines and hydrazines) are HPLC silent as they do not possess a chromophore. This led to the development of a GC-MS/MS protocol to determine the products of the reactions (Section 3.7.2). This method was found to be unsuitable for N4, as authentic samples of the nitrosamine and the parent amine could not be separated. Furthermore, the electrospray ionisation used in the GC-MS/MS caused cleavage of the N-N bond which made determining which compound of the two was present very difficult (Figure 3.9). For determining the products of reactions on N4, an LC-MS/MS protocol was used (Section 3.8.1). The same protocol was also used in special cases where GC-MS/MS analysis needed further validation. These cases will be mentioned in Section 3.9.

LC-MS/MS samples were prepared directly from the reaction mixture post-quench at 10-50 ug/mL in methanol. GC-MS/MS sample preparation was performed after HPLC sample preparation. This involved adding 2.5 mL saturated NaCl solution to the quenched reaction mixture,

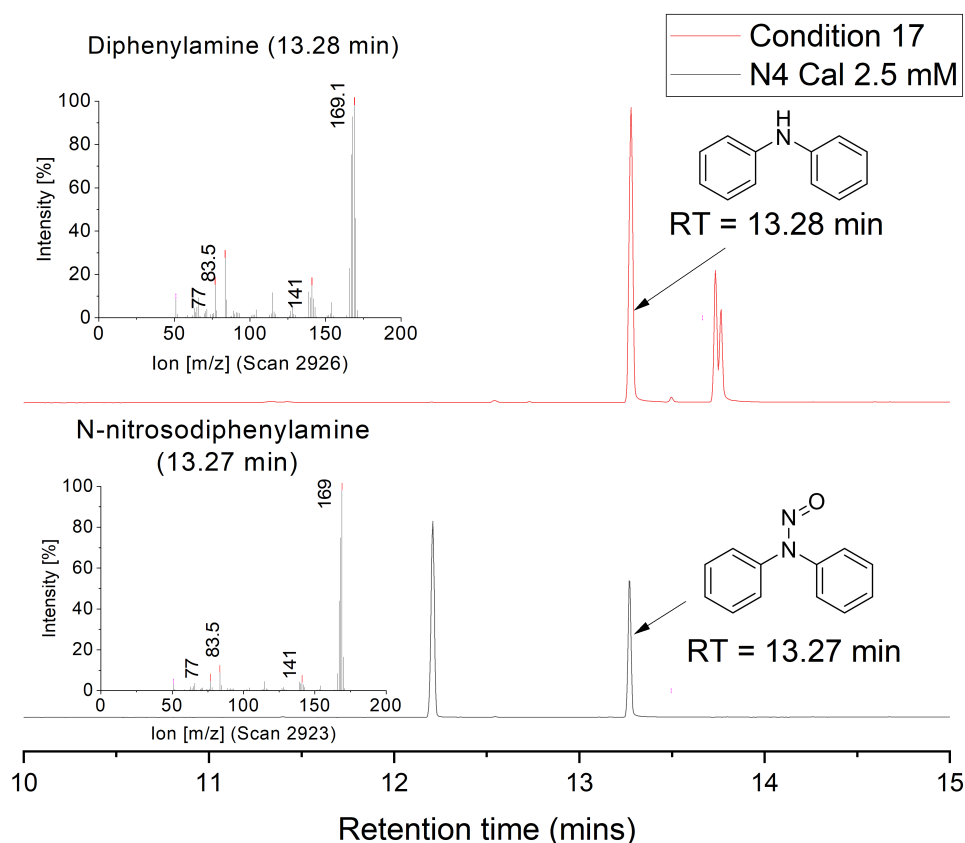


Figure 3.9: Overlap of nitrosamine and amine peaks in GC-MS/MS with *N*-nitrosodiphenylamine (N4).

followed by 2.5 mL of ethyl acetate or diethyl ether. The reaction vials were sealed with lids, and inverted to mix the biphasic system. After inversion, the mixture was allowed to settle, and a sample was taken from the organic layer and injected directly into the GC-MS/MS.

### 3.6 Experimental protocols

With reference to the general procedure given in Section 3.5 of this document, the detailed experimental protocols applied for each of the 21 screening reactions are summarised in Table 3.3 and are outlined below.

Table 3.3: Summary of the reaction conditions for the batch HPLC reactivity screen.

#	Reagent	t (h)	T (°C)	[Reagent] (M)	Vol Reagent (μL)	Vol Nitrosamine Stock (μL)	Vol H <sub>2</sub> O (μL)	Vol EtOH / THF(*) (μL)	Vol TMB Stock (μL)	Quench
1	H <sub>2</sub> O <sub>2</sub> (aq)	24	r.t.	2	1000	1000	0	0	1000	Catalase (1 mL, 1.3 mg/mL)
2	CH <sub>3</sub> CO <sub>3</sub> H	24	r.t.	5.33	375	1000	0	1000	1000	1. NaHCO <sub>3</sub> sat. (aq) 4 mL 2. Catalase (1 mL, 1.3 mg/mL)
3	HBr 33% wt. (in AcOH)	24	r.t.	5.5	300 +/- 10	1000	0	4000	1000	NaOH (aq) (1 mL, 2 M)
4	HCl (aq)	24	r.t.	2	1000	1000	0	0	1000	NaOH (aq) (1 mL, 2 M)
5	HCl (aq)	16	50	2	1000	1000	0	0	1000	NaOH (aq) (1 mL, 2 M)
6	HCl (EtOH)	24	r.t.	1.25	1600	1000	0	0	1000	NaOH (aq) (1 mL, 2 M)
7	HCl (EtOH)	16	50	1.25	1600	1000	0	0	1000	NaOH (aq) (1 mL, 2 M)
8	NaBH <sub>4</sub>	24	r.t.	0.40	4000	1000	0	0	1000	MeOH (1 mL)
9	DiBAL-H	0.5	r.t.	1.00	1000	2000	0	1000*	1000	1. EtOAc (1mL) 2. H <sub>2</sub> O (0.2 mL) 3. NaOH (0.4mL 2 M)
10	DiBAL-H	1	r.t.	1.00	1000	2000	0	1000*	1000	1. EtOAc (1mL) 2. H <sub>2</sub> O (0.2 mL)
11	Na <sub>2</sub> S <sub>2</sub> O <sub>4</sub>	24	r.t.	1.00	1000	500	2000	2000	1000	3. NaOH (0.4mL 2 M) H <sub>2</sub> O <sub>2</sub> (aq), (1 mL, 1 M)
12	Na <sub>2</sub> S <sub>2</sub> O <sub>4</sub> <sup>1</sup>	24	r.t.	1.00	1000	500	2000	2000	1000	H <sub>2</sub> O <sub>2</sub> (aq), (1 mL, 1 M)
13	Na <sub>2</sub> S <sub>2</sub> O <sub>4</sub> <sup>1</sup>	16	50	1.00	1000	500	3000	2000	1000	H <sub>2</sub> O <sub>2</sub> (aq), (1 mL, 1 M)
14	Na <sub>2</sub> S <sub>2</sub> O <sub>4</sub> <sup>2</sup>	16	50	0.25	4000	500	0	2000	1000	H <sub>2</sub> O <sub>2</sub> (aq), (1 mL, 1 M)
15	Na <sub>2</sub> S <sub>2</sub> O <sub>4</sub> <sup>2</sup>	3	50	0.25	4000	500	0	2000	1000	H <sub>2</sub> O <sub>2</sub> (aq), (1 mL, 1 M)
16	Na <sub>2</sub> S <sub>2</sub> O <sub>4</sub> <sup>2</sup>	1	50	0.25	4000	500	0	2000	1000	H <sub>2</sub> O <sub>2</sub> (aq), (1 mL, 1 M)
17	Na <sub>2</sub> S <sub>2</sub> O <sub>4</sub> <sup>3</sup>	16	50	0.25	4000	500	0	2000	1000	H <sub>2</sub> O <sub>2</sub> (aq), (1 mL, 1 M)
18	Na <sub>2</sub> SO <sub>3</sub>	24	r.t.	1.00	1000	500	1000	1000	1000	H <sub>2</sub> O <sub>2</sub> (aq), (1 mL, 1 M)
19	Na <sub>2</sub> SO <sub>3</sub> <sup>2</sup>	16	50	0.25	4000	500	0	2000	1000	H <sub>2</sub> O <sub>2</sub> (aq), (0.5 mL, 2 M)
20	NaOH	24	r.t.	2.00	1000	1000	0	0	1000	AcOH <sub>aq</sub> (1 mL, 2 M)
21	NaOEt 21% w/v	24	r.t.	2.55	1000	1000	0	1000	1000	H <sub>2</sub> O (5 mL)

<sup>1</sup>Reaction changed with additional NaOH (aq) (1 M, 1mL)<sup>2</sup>Stock solution prepared in NaOH (aq) (1 M)<sup>3</sup>Stock solution prepared in NaOH (aq) (20% w/v)

**Reaction condition 1: H<sub>2</sub>O<sub>2</sub>**

16 oven-dried 15 mL screw-top vials each equipped with a 20 mm magnetic flea were inserted into four aluminium heating blocks. To each of the vials was added H<sub>2</sub>O<sub>2</sub> (aq) (1 mL, 2 M, 2 mmol), internal standard stock solution (1 mL, 0.3 M, 0.3 mmol TMB in EtOH) and nitrosamine stock solution (1 mL, *ca.* 100 mM, 0.1 mmol in ethanol). Duplicate reactions were performed for each nitrosamine. The reaction vials were secured with lids with silicon septa and stirring was started. After the allotted reaction time (24 h), the reaction was quenched by addition of Catalase (aq) (1 mL, 1.3 mg/mL) with stirring for ten minutes. The quenched reaction mixture was filtered through 0.2 μm hydrophilic syringe filters and sampled into HPLC sample vials and subjected to analysis by HPLC. An LC-MS/MS sample for N4 was prepared from the filtered HPLC sample, diluted with methanol. The quenched reaction mixture was treated with brine (2.5 mL) and ethyl acetate (2.5 mL), the mixture was inverted and left until phase separation occurred. A sample from the organic layer was then analysed by GC-MS/MS. GC-MS/MS analysis can be found in Figures G.1 and G.2. LC-MS/MS analysis of N4 can be found in Figure I.1.

N4 was further analysed by <sup>1</sup>H and <sup>13</sup>C NMR. The screening reaction was repeated, with H<sub>2</sub>O<sub>2</sub> (aq) (1 mL, 2 M, 2 mmol) and nitrosamine stock solution (1 mL, *ca.* 100 mM, 0.1 mmol in ethanol). The TMB stock solution was substituted with 1 mL of ethanol. After 24 h, the reaction was suspended over equal portions of brine and ethyl acetate (*ca.* 15 mL). The aqueous layer was washed with a further two 15 mL portions of ethyl acetate, and the organic extracts were combined, dried over MgSO<sub>4</sub>, filtered and the solvent was removed by rotary evaporator. The crude reaction product was dissolved in deuterated methanol and analysed by <sup>1</sup>H and <sup>13</sup>C NMR.

**Reaction condition 2: CH<sub>3</sub>CO<sub>3</sub>H**

16 oven-dried 15 mL screw-top vials each equipped with a 20 mm magnetic flea were inserted into four aluminium heating blocks. To each of the vials was added CH<sub>3</sub>CO<sub>3</sub>H (38-40 % w/v, Fisher) (375 μL, 2 mmol), internal standard stock solution (1 mL, 0.3 M, 0.3 mmol TMB in EtOH) and nitrosamine stock solution (1 mL, *ca.* 100 mM, 0.1 mmol in ethanol). Duplicate reactions were performed for each nitrosamine. The reaction vials were secured with lids with silicon septa and stirring was started. After the allotted reaction time (24 h), the reaction

was quenched by addition of  $\text{NaHCO}_3$  (sat. (aq)) (4 mL) followed by Catalase (aq) (1 mL, 1.3 mg/mL) with stirring for ten minutes. The quenched reaction mixture was filtered through 0.2  $\mu\text{m}$  hydrophilic syringe filters and sampled into HPLC sample vials and subjected to analysis by HPLC. An LC-MS/MS sample for N4 was prepared from the filtered HPLC sample, diluted with methanol. The quenched reaction mixture was treated with brine (2.5 mL) and ethyl acetate (2.5 mL), the mixture was inverted and left until phase separation occurred. A sample from the organic layer was then analysed by GC-MS/MS. GC-MS/MS analysis can be found in Figures G.3 and G.4. LC-MS/MS analysis of N4 can be found in Figure I.2.

### Reaction Condition 3 : HBr 33% wt. in AcOH

8 oven-dried 15 mL screw-top vials each equipped with a 20 mm magnetic flea were inserted into two aluminium heating blocks. To each of the vials was added nitrosamine stock solution (1 mL, *ca.* 100 mM, 0.1 mmol in ethanol) and internal standard stock solution (1 mL, 0.3 M, 0.3 mmol TMB in EtOH) and ethanol (4 mL). The reaction vials were secured with lids with silicon septa and stirring was started. A nitrogen atmosphere was introduced via the septa and the reaction vials were purged in this state for ten minutes at medium nitrogen flow. After purging the  $\text{N}_2$  flow was reduced and HBr 33% wt. in acetic acid (0.3 mL  $\pm$  0.01 mL, 1.56-1.71 mmol, Sigma) was added *via* a 1 mL syringe at two minute intervals between reactions, removing the purge needle after the addition of acid. After the allotted reaction time (24 h), the reaction was quenched by addition of NaOH (1 mL, 2 M) with stirring for ten minutes. The quenched reaction mixture was filtered through 0.2  $\mu\text{m}$  hydrophilic syringe filters and sampled into HPLC sample vials and analysed by HPLC. An LC-MS/MS sample for N4 was prepared from the filtered HPLC sample, diluted with methanol. The quenched reaction mixture was treated with brine (2.5 mL) and ethyl acetate (2.5 mL), the mixture was inverted and left until phase separation occurred. A sample from the organic layer was then analysed by GC-MS/MS. GC-MS/MS analysis can be found in Figure G.5. LC-MS/MS analysis of N4 and N8 can be found in Figures I.3 and I.4.

### Reaction Conditions 4 & 5: HCl (aq)

16 oven-dried 15 mL screw-top vials each equipped with a 20 mm magnetic flea were inserted into four aluminium heating blocks either at room temperature (Condition 4) or heated to 50  $^\circ\text{C}$  (Condition 5). To each of the vials was added  $\text{HCl}_{(\text{aq})}$  (1 mL, 2 M, 2 mmol) followed by

nitrosamine stock solution (1 mL, *ca.* 100 mM, 0.1 mmol in ethanol). Duplicate reactions were performed for each nitrosamine. The reaction vials were secured with lids with silicon septa and stirring was started. After the allotted reaction time (Condition 4: 24 h, Condition 5: 16 h), the reaction was quenched by addition of NaOH<sub>(aq)</sub> (1 mL, 2 M) with stirring for ten minutes. Internal standard stock solution (1 mL, 0.3 M, 0.3 mmol TMB in EtOH) was added after quenching. The reaction mixture was filtered through 0.2  $\mu$ m hydrophilic syringe filters and sampled into HPLC sample vials and analysed by HPLC. An LC-MS/MS sample for N4 was prepared from the filtered HPLC sample, diluted with methanol. For condition 5, the quenched reaction mixture was treated with brine (2.5 mL) and ethyl acetate (2.5 mL), the mixture was inverted to mix and left until phase separation occurred. A sample from the organic layer was then analysed by GC-MS/MS. GC-MS/MS analysis for condition 5 can be found in figures G.6 and G.7. LC-MS/MS analysis of N4 for both conditions 4 and 5 can be found in figures I.5 and I.6.

#### Reaction Conditions 6 & 7: HCl<sub>(EtOH)</sub>

16 oven-dried 15 mL screw-top vials each equipped with a 20 mm magnetic flea were inserted into four aluminium heating blocks either at room temperature (Condition 6) or heated to 50 °C (Condition 7). To each of the vials was added HCl<sub>EtOH</sub> (1.6 mL, 1.25 M, 2 mmol) followed by nitrosamine stock solution (1 mL, *ca.* 100 mM, 0.1 mmol in ethanol) (1 nitrosamine per reaction vial) such that the reaction was performed in duplicate for each nitrosamine. The reaction vials were secured with lids with silicon septa and stirring was started. After the allotted reaction time (Condition 6: 24 h, Condition 7: 16 h), the reaction was quenched by addition of NaOH<sub>(aq)</sub> (1 mL, 2 M) with stirring. Internal standard stock solution (1 mL, 0.3 M, 0.3 mmol TMB in EtOH) was added after quenching. The reaction mixture was filtered through 0.2  $\mu$ m hydrophilic syringe filters and sampled into HPLC sample vials and subjected to analysis by HPLC. An LC-MS/MS sample for N4 was prepared from the filtered HPLC sample, diluted with methanol. For condition 7, the quenched reaction mixture was treated with brine (2.5 mL) and diethyl ether (2.5 mL), the mixture was inverted to mix and left until phase separation occurred. A sample from the organic layer was then subjected to analysis by GC-MS/MS. GC-MS/MS analysis for condition 7 can be found in Figure G.8. LC-MS/MS analysis of N4 for both conditions 6 and 7 can be found in Figures I.7 and I.8. LC-MS/MS analysis of N7 and N8 for condition 7 can be found in Figures I.9 and I.10.



In the case of N5 in condition 6, the analysis by GC-MS/MS showed no reaction product, while the conversion of the starting material by HPLC was 56%. The reaction was repeated so that NMR analysis could be performed. HCl<sub>EtOH</sub> (1.6 mL, 1.25 M, 2 mmol) followed by nitrosamine stock solution (1 mL, *ca.* 100 mM, 0.1 mmol in ethanol) were added to a 15 mL reaction vial, the reaction was stirred at 400 rpm for 24 h. The pH of the reaction mixture was adjusted to nine (measured by pH paper) using 1M NaOH and then the reaction mixture was suspended over equal portions of brine and dichloromethane (DCM) (*ca.* 15 mL), the organic layer was removed and the aqueous layer was washed a further two times with 15 mL DCM. The organic portions were combined and dried over MgSO<sub>4</sub> and the solvent was removed by rotary evaporator. The crude mixture was dissolved in deuterated chloroform and analysed by <sup>1</sup>H and <sup>13</sup>C NMR.

#### Reaction Condition 8: NaBH<sub>4</sub>

8 oven-dried 15 mL screw-top vials each equipped with a 20 mm magnetic flea were inserted into 2 aluminium heating blocks. To each of the vials was added nitrosamine stock solution (1 mL, *ca.* 100 mM, 0.1 mmol in THF) and internal standard stock solution (1 mL, 0.3 M, 0.3 mmol TMB in THF). The reaction vials were secured with lids with silicon septa and stirring was started. A nitrogen atmosphere was introduced via the septa and the reaction vials were purged in this state for ten minutes at medium nitrogen flow. After purging the N<sub>2</sub> flow was reduced and NaBH<sub>4</sub> (4 mL, 0.4 M, 1.6 mmol, Fisher) in ethanol was added *via* a 5 mL syringe at two minute interval between reactions, removing the purge needle after addition. After the allotted reaction time (24 h), the reaction was quenched by addition of MeOH (1 mL) with stirring for ten minutes. The quenched reaction mixture was filtered through 0.2 μm hydrophilic syringe filters and sampled into HPLC sample vials and subjected to analysis by HPLC. An LC-MS/MS sample for N4 was prepared from the filtered HPLC sample, diluted with methanol. The quenched reaction mixture was treated with brine (2.5 mL) and ethyl acetate (2.5 mL), the mixture was inverted to mix and left until phase separation occurred. A sample from the organic layer was then subjected to analysis by GC-MS/MS. GC-MS/MS analysis for condition 8 can be found in Figure G.9. LC-MS/MS analysis of N4, N7 and N8 can be found in Figures I.11 to I.13.

**Reaction Conditions 9 & 10: DiBAL-H**

8 oven-dried 15 mL screw-top vials each equipped with a 20 mm magnetic flea were inserted into two aluminium heating blocks as described in the general experimental procedure section of this document. To each of the vials was added THF (1 mL) and internal standard stock solution (1 mL, 0.3 M, 0.3 mmol TMB in THF). Nitrosamine stock solution (2 mL, *ca.* 100 mM in THF) was next added (1 nitrosamine per reaction vial). The reaction vials were secured with lids with silicon septa and stirring was started. A nitrogen atmosphere was introduced via the septa and the reaction vials were purged in this state for ten minutes at medium nitrogen flow. After purging the N<sub>2</sub> flow was reduced and DIBAL-H (1 mL, 1 M, 1 mmol in hexane, Sigma) was added *via* a 1 mL syringe at two minute intervals between reactions and the purge needle was removed after addition. Reactions were sampled at 0.5 and 1 hours by removing 0.5 mL of the reaction mixture with a 1 mL syringe and adding this to a sample vial containing ethyl acetate (1.6 mL) and NaOH (1M, 0.2 mL) the mixture was stirred at 300 rpm for *ca.* ten minutes. The now quenched reaction sample was filtered through a 0.2  $\mu$ m hydrophobic syringe filter into GC sample vials and analysed directly by HPLC (*N*-nitrosodiphenylamine) and GC-MS/MS (all other nitrosamines). An LC-MS/MS sample for N4 was prepared from the filtered HPLC sample, diluted with methanol. GC-MS/MS analysis can be found in Figures G.10 and G.11. LC-MS/MS analysis of N4 and N8 can be found in Figures I.14 to I.17.

**Reaction Condition 11: Na<sub>2</sub>S<sub>2</sub>O<sub>4</sub>**

16 oven-dried 15 mL screw-top vials each equipped with a 20 mm magnetic flea were inserted into four aluminium heating blocks either at room temperature as described in the general experimental procedure section of this document. To each of the vials was added Na<sub>2</sub>S<sub>2</sub>O<sub>4</sub> (aq) (1 mL, 1 M, 1 mmol) followed by deionised water (3 mL), absolute ethanol (2 mL), internal standard stock solution (1 mL, 0.3 M, 0.3 mmol TMB in ethanol) and nitrosamine stock solution (0.5 mL, *ca.* 100 mM, 0.05 mmol in ethanol) (1 nitrosamine per reaction vial) such that the reaction was performed in duplicate for each nitrosamine. The reaction vials were secured with lids with silicon septa and stirring was started. After the allotted reaction time (24 h), the reaction was quenched by addition of H<sub>2</sub>O<sub>2</sub> (aq) (1 mL, 1 M) with stirring for ten minutes. The reaction mixture was filtered through 0.2  $\mu$ m hydrophilic syringe filters and sampled into HPLC sample vials and subjected to analysis by HPLC. An LC-MS/MS sample for N4 was prepared from the filtered HPLC sample, diluted with methanol. The quenched reaction mixture was

treated with brine (2.5 mL) and ethyl acetate (2.5 mL), the mixture was inverted to mix and left until phase separation occurred. A sample from the organic layer was then subjected to analysis by GC-MS/MS. GC-MS/MS analysis can be found in Figures G.12 and G.13. LC-MS/MS analysis of N4 can be found in Figure I.18.

#### **Reaction Conditions 12 & 13: $\text{Na}_2\text{S}_2\text{O}_4$ (aq) in $\text{NaOH}$ (aq) (0.1 M)**

16 oven-dried 15 mL screw-top vials each equipped with a 20 mm magnetic flea were inserted into four aluminium heating blocks either at room temperature (Condition 12) or heated to 50 °C (Condition 13). To each of the vials was added  $\text{Na}_2\text{S}_2\text{O}_4$  (aq) (1 mL, 1 M, 1 mmol) followed by  $\text{NaOH}$  (aq) (1 mL, 1 M), deionised water (2 mL), absolute ethanol (2 mL), internal standard stock solution (1 mL, 0.3 M, 0.3 mmol TMB in ethanol) and nitrosamine stock solution (0.5 mL, *ca.* 100 mM, 0.05 mmol in ethanol) (1 nitrosamine per reaction vial) such that the reaction was performed in duplicate for each nitrosamine. The reaction vials were secured with lids with silicon septa and stirring was started. After the allotted reaction time (Condition 12: 24 h, Condition 13: 16 h), the reaction was quenched by addition of  $\text{H}_2\text{O}_2$  (aq) (1 mL, 1 M) with stirring for ten minutes. The reaction mixture was filtered through 0.2  $\mu\text{m}$  hydrophilic syringe filters and sampled into HPLC sample vials and subjected to analysis by HPLC. An LC-MS/MS sample for N4 was prepared from the filtered HPLC sample in methanol. The quenched reaction mixture was treated with brine (2.5 mL) and ethyl acetate (2.5 mL), the mixture was inverted to mix and left to settle. A sample from the organic layer was then subjected to analysis by GC-MS/MS. GC-MS/MS analysis can be found in figures G.14 to G.16. LC-MS/MS analysis of N4 in conditions 12 and 13 can be found in figures I.19 and I.20.

#### **Reaction Conditions 14, 15 & 16: $\text{Na}_2\text{S}_2\text{O}_4$ (aq) in $\text{NaOH}$ (aq) (1 M)**

16 oven-dried 15 mL screw-top vials each equipped with a 20 mm magnetic flea were inserted into four aluminium heating blocks heated to 50 °C as described in the general experimental procedure section of this document. To each of the vials was added  $\text{Na}_2\text{S}_2\text{O}_4$  (aq) in  $\text{NaOH}$  (aq) (1 M) (4 mL, 0.25 M, 1 mmol) followed by absolute ethanol (2 mL), internal standard stock solution (1 mL, 0.3 M, 0.3 mmol TMB in ethanol) and nitrosamine stock solution (0.5 mL, *ca.* 100 mM, 0.05 mmol in ethanol) (1 nitrosamine per reaction vial) such that the reaction was performed in duplicate for each nitrosamine. The reaction vials were secured with lids with silicon septa and stirring was started. After the allotted reaction time (Condition 14: 16 h,

Condition 15: 3 h, Condition 16: 1 h), the reaction was quenched by addition of  $\text{H}_2\text{O}_2$  (aq) (1 mL, 1 M) with stirring. The reaction mixture was filtered through 0.2  $\mu\text{m}$  hydrophilic syringe filters and sampled into HPLC sample vials and subjected to analysis by HPLC. An LC-MS/MS sample for N4 was prepared from the filtered HPLC sample in methanol. For conditions 14 and 15, the quenched reaction mixture was treated with brine (2.5 mL) and ethyl acetate (2.5 mL), the mixture was inverted to mix and left to settle. A sample from the organic layer was then subjected to analysis by GC-MS/MS. GC-MS/MS analysis was performed for conditions 14 and 15 and can be found in figures G.17 to G.20. LC-MS/MS analysis for N4 in conditions 14 and 15 can be found in figures I.21 and I.22.

**Reaction Condition 17:  $\text{Na}_2\text{S}_2\text{O}_4$  (aq) in  $\text{NaOH}$  (aq) (20 % w/v)**

16 oven-dried 15 mL screw-top vials each equipped with a 20 mm magnetic flea were inserted into four aluminium heating blocks heated to 50 °C. To each of the vials was added  $\text{Na}_2\text{S}_2\text{O}_4$  (aq) in  $\text{NaOH}$  (aq) (20 % w/v) (4 mL, 0.25 M, 1 mmol) followed by absolute ethanol (2 mL) and Nitrosamine stock solution (0.5 mL, *ca.* 100 mM, 0.05 mmol in ethanol) (1 nitrosamine per reaction vial) such that the reaction was performed in duplicate for each nitrosamine. The reaction vials were secured with lids with silicon septa and stirring was started. After the allotted reaction time (16 h), the reaction was quenched by addition of  $\text{H}_2\text{O}_2$  (aq) (1 mL, 1 M) with stirring. The reaction mixture was filtered through 0.2  $\mu\text{m}$  hydrophilic syringe filters and sampled into HPLC sample vials and subjected to analysis by HPLC. An LC-MS sample for N4 was prepared from the filtered HPLC sample, diluted in methanol. The quenched reaction mixture was treated with brine (2.5 mL) and ethyl acetate (2.5 mL), the mixture was inverted to mix and left until phase separation occurred. A sample from the organic layer was then subjected to analysis by GC-MS/MS. GC-MS/MS analysis can be found in figure G.21. LC-MS/MS analysis of N4 can be found in figure I.23.

**Reaction Condition 18:  $\text{Na}_2\text{SO}_3$  (aq)**

24 oven-dried 15 mL screw-top vials each equipped with a 20 mm magnetic flea were inserted into 6 aluminium heating blocks at room temperature. To each of the vials was added  $\text{Na}_2\text{SO}_3$  (aq) (1 mL, 1 M, 1 mmol) followed by deionised water (1 mL) absolute ethanol (1 mL), internal standard stock solution (1 mL, 0.3 M, 0.3 mmol TMB in ethanol) and Nitrosamine stock solution (0.5 mL, *ca.* 100 mM, 0.05 mmol in ethanol) (1 nitrosamine per reaction vial) such that the

reaction was performed in duplicate for each nitrosamine. The reaction vials were secured with lids with silicon septa and stirring was started. After the allotted reaction time (24 h), the reaction was quenched by addition of  $\text{H}_2\text{O}_2$  (aq) (1 mL, 1 M) with stirring. The reaction mixture was filtered through 0.2  $\mu\text{m}$  hydrophilic syringe filters and sampled into HPLC sample vials and subjected to analysis by HPLC.

**Reaction Condition 19:  $\text{Na}_2\text{SO}_3$  (aq) in  $\text{NaOH}$  (aq) (1 M)**

16 oven-dried 15 mL screw-top vials each equipped with a 20 mm magnetic flea were inserted into four aluminium heating blocks heated to 50 °C. To each of the vials was added  $\text{Na}_2\text{SO}_3$  (aq) in  $\text{NaOH}$  (aq) (1 M) (4 mL, 0.25 M, 1 mmol) followed by absolute ethanol (2 mL), internal standard stock solution (1 mL, 0.3 M, 0.3 mmol TMB in ethanol) and Nitrosamine stock solution (0.5 mL, *ca.* 100 mM, 0.05 mmol in ethanol) (1 nitrosamine per reaction vial) such that the reaction was performed in duplicate for each nitrosamine. The reaction vials were secured with lids with silicon septa and stirring was started. After the allotted reaction time (24 h), the reaction was quenched by addition of  $\text{H}_2\text{O}_2$  (aq) (0.5 mL, 2 M) with stirring. The reaction mixture was filtered through 0.2  $\mu\text{m}$  hydrophilic syringe filters and sampled into HPLC sample vials and subjected to analysis by HPLC. An LC-MS/MS sample for N4 was prepared from the filtered HPLC sample in methanol. The quenched reaction mixture was treated with brine (2.5 mL) and ethyl acetate (2.5 mL), the mixture was inverted to mix and until phase separation occurred. A sample from the organic layer was then subjected to analysis by GC-MS/MS. GC-MS/MS analysis can be found in Figures G.22 and G.23. LC-MS/MS analysis of N4 can be found in Figure I.24.

**Reaction Condition 20:  $\text{NaOH}$  (aq)**

16 oven-dried 15 mL screw-top vials each equipped with a 20 mm magnetic flea were inserted into four aluminium heating blocks as described in the general experimental procedure section of this document. To each of the vials was added  $\text{NaOH}$  (aq) (1 mL, 2 M, 2 mmol) followed by internal standard stock solution (1 mL, 0.3 M, 0.3 mmol TMB in ethanol) and Nitrosamine stock solution (1 mL, *ca.* 100 mM, 0.1 mmol in ethanol) (1 nitrosamine per reaction vial) such that the reaction was performed in duplicate for each nitrosamine. The reaction vials were secured with lids with silicon septa and stirring was started. After the allotted reaction time (24 h), the reaction was quenched by addition of acetic acid (aq) (1 mL, 2 M) with stirring.

The reaction mixture was filtered through 0.2  $\mu\text{m}$  hydrophilic syringe filters and sampled into HPLC sample vials and subjected to analysis by HPLC.

### Reaction Condition 21: NaOEt

16 oven-dried 15 mL screw-top vials each equipped with a 20 mm magnetic flea were inserted into four aluminium heating blocks at room temperature as described in the general experimental procedure section of this document. To each of the vials was added NaOEt (1 mL, 2.55 M, 2.55 mmol) followed by internal standard stock solution (1 mL, 0.3 M, 0.3 mmol TMB in ethanol) and Nitrosamine stock solution (1 mL, *ca.* 100 mM, 0.1 mmol in ethanol) (1 nitrosamine per reaction vial) such that the reaction was performed in duplicate for each nitrosamine. The reaction vials were secured with lids with silicon septa and stirring was started. After the allotted reaction time (24 h), the reaction was quenched by addition of deionised water (5 mL) with stirring. The reaction mixture was filtered through 0.2  $\mu\text{m}$  hydrophilic syringe filters and sampled into HPLC sample vials and subjected to analysis by HPLC. An LC-MS/MS sample for N4 was prepared from the filtered HPLC sample in methanol. The quenched reaction mixture was treated with brine (2.5 mL) and ethyl acetate (2.5 mL), the mixture was inverted to mix and left to settle. A sample from the organic layer was then subjected to analysis by GC-MS/MS. GC-MS/MS analysis can be found in figures G.24 and G.25. LC-MS/MS analysis of N4 can be found in figure I.25.

## 3.7 Calibrations for conversion analysis

The following section details the methods by which the conversion with respect to the nitrosamine starting materials was measured. The majority of reactions were performed in ethanol/water mixtures which made HPLC the obvious choice for analysis (see Section 3.7.1 for HPLC method details). All *N*-nitrosamines in this study could be visualised by diode array detector (DAD) at 220 nm. N1 had a stronger absorption at 210 nm and so a calibration was performed for both 210 and 220 nm in this case. The conversions for N1 were measured at 210 nm for all conditions except condition 3 (HBr in AcOH) and condition 2 ( $\text{CH}_3\text{COOH}$ ). This is because the acetic acid peak in both of these conditions overlapped with the peak for the nitrosamine and this was not the case in the 220 nm HPLC trace. For conditions 9 and 10 (DiBAL-H) the reaction samples were analysed using gas chromatography on an Agilent

8890 GC system with 7000E GC/TQ (triple quad mass spec) with hydroinert EI (Electrospray ionisation) 350 source using H<sub>2</sub> as a carrier gas and a DB-5MS UI, 20m x 0.180 mm, 0.18  $\mu$ m column. The analysis of the samples was performed on the Origin 2020 software after extraction of the CSV file for the chromatogram by either python script in the case of GC-MS/MS or through the open-source software OpenChrom for HPLC. After importing the csv files into Origin 2020, integrations of the peak areas for the analyte and internal standard were performed using the batch processing feature. A baseline was obtained by an asymmetric least-squares algorithm with default parameters. The baseline was then subtracted and the five largest peaks by peak height were picked and selected for integration which was performed automatically using the peaks and baseline tool in Origin 2020. This processing method was applied to both calibrations and reaction sample processing to ensure consistency. The retention times for the eight *N*-nitrosamines were found from the calibrations, and these were used to extract the integrations for the analyte and internal standard. The integrations were transferred to an excel spreadsheet where the line equations for the calibrations were used to calculate the conversions. Figure 3.10 outlines the workflow for conversion analysis.

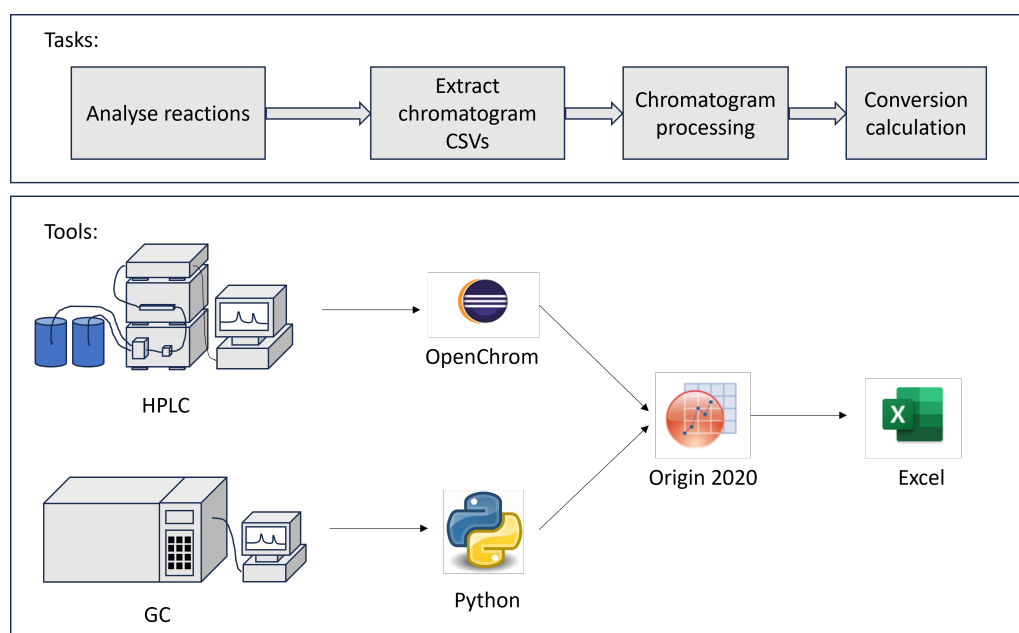


Figure 3.10: The workflow used to calculate the conversions with respect to the nitrosamine in the reactivity screen.

An example processed chromatogram is shown in Figure 3.11. All reactions were analysed within the calibration limits to avoid extrapolation. Both calibrations including and excluding the internal standard (IS) were performed for the reasons outlined in Section 3.5.

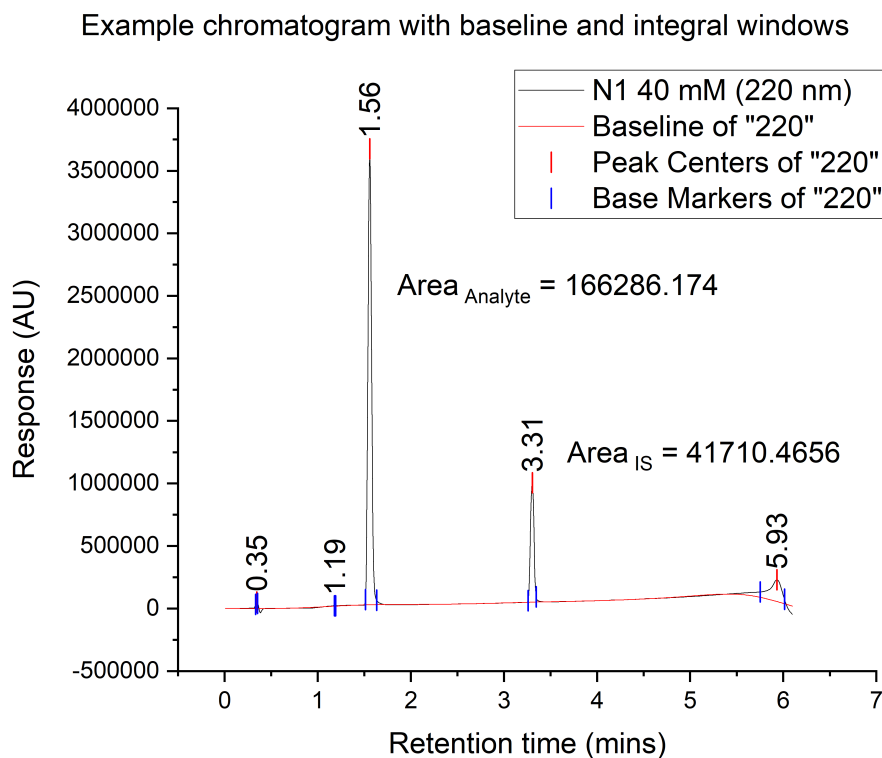


Figure 3.11: An example HPLC chromatogram with applied processing method.

### 3.7.1 HPLC Calibrations

The HPLC analysis of *N*-nitrosamine conversion was performed on an Agilent 1260 HPLC. The HPLC method used in all experiments is as follows: Solvents: A) MeCN 0.1% TFA, B) H<sub>2</sub>O 0.1% TFA. Flow rate = 1.5 mL/min. Polarity gradient: 0 mins; Solvent A 5%, Solvent B 95% 5 mins; Solvent A 95%, Solvent B 95%. Injection volume 1  $\mu$ L. Detector: DAD 210 nm & DAD 220 nm. Calibrations were performed for the eight *N*-nitrosamines in the concentration range of 40-0.625 mM. Summary tables for the determined line equations used to calculate conversions for each nitrosamine are provided in Tables 3.4 and 3.5. Links to the calibration curves are available from the summary tables.

Nitrosamine	$\lambda$ (nm)	IS (Y/N)	y0	A	R0	r <sup>2</sup>	ref
N4	220	Y	12.65281	-12.67495	-0.12402	0.9992	D.5
N4	220	N	496368.91381	-498165.74319	-0.02255	0.9993	D.5

Table 3.4: HPLC calibration curve equations with line equation form:  $y = y_0 + A \cdot \exp(R_0 \cdot x)$ .



Nitrosamine	$\lambda$ (nm)	IS (Y/N)	a	b	$r^2$	ref
N1	210	Y	-0.00354	0.11267	0.9996	D.1
N1	210	N	-355.84068	2269.40863	0.9997	D.1
N1	220	Y	0.03271	0.58155	0.9980	D.2
N1	220	N	1578.44055	4064.95359	0.9983	D.2
N2	220	Y	0.02893	0.49214	0.9984	D.3
N2	220	N	1019.94959	3522.83772	0.9989	D.3
N3	220	Y	-0.00385	0.53761	0.9991	D.4
N3	220	N	909.21290	3476.73713	0.9995	D.4
N5	220	Y	-0.01077	0.44284	0.9989	D.6
N5	220	N	-925.92477	3236.75029	0.9994	D.6
N6	220	Y	0.01140	0.42030	0.9998	D.7
N6	220	N	395.65576	2868.71231	0.9998	D.7
N7	220	Y	0.03870	0.44435	0.9993	D.8
N7	220	N	1361.67662	3193.89269	0.9996	D.8
N8	220	Y	-0.00759	0.59921	0.9996	D.9
N8	220	N	305.43737	4189.37773	0.9999	D.9

Table 3.5: HPLC calibration curve equations with line equation form:  $y = a + b \cdot x$ .

### 3.7.2 GC-MS/MS Calibrations

A GC-MS/MS method was used to measure conversions with respect to the nitrosamine in conditions 9 and 10 for all nitrosamines excluding N4 which was analysed by HPLC. This was because the starting material and authentic amine sample could not be separated with the method settings used. Furthermore, the major observed mass fragment with N4 in GC-MS/MS was 168 m/z, which is consistent with fragmentation at the N-N bond. This meant it was not possible to distinguish between the starting material and amine product. The GC-MS/MS method settings are listed in Table 3.6:

<b>Inlet</b>		
Mode	Split	
Split Ratio	25:1	
Septum Purge Flow	3 mL/min	
Heater	250 °C	
Pressure	7.9 psi	
Gas Saver	20 mL/min	
<b>Injector</b>		
Injection Volume	1 µL	
Solvent Washes	Acetone, MeOH	
<b>Oven Programme</b>		
t (mins)	T (°C) (rate °C/min)	Hold Time (mins)
0	50	3
3	80 (20°C/min)	2
6.5	100 (5°C/min)	2
12.5	280(35°C/min)	2.36
<b>Post Run</b>		
t (mins)	T (°C)	Hold Time (mins)
20	325	20

Table 3.6: Gas chromatography settings.

The line equations of the calibrations are summarised in Table 3.7. The GC-MS/MS calibrations were performed in the same manner as for the HPLC calibrations described in section 3.7.1, with TMB as an internal standard. The calibration plots can be found in Figures E.1 to E.7.

Table 3.7: The determined calibration curve equations for the nitrosamines analysed by GC for conditions 9 and 10.

Nitrosamine (ref)	fitting	a	b	y0	A	R0	r <sup>2</sup>
N1 (figure E.1)	$y = a + b*x$	0.00189	0.05604	-	-	-	0.99771
N2 (figure E.2)	$y = y0 + A*exp(R0*x)$	-	-	1.13987	-1.13919	-0.17267	0.99489
N3 (figure E.3)	$y = y0 + A*exp(R0*x)$	-	-	2.33399	-2.33784	-0.16082	0.99653
N5 (figure E.4)	$y = y0 + A*exp(R0*x)$	-	-	0.83249	-0.82662	-0.09051	0.99297
N6 (figure E.5)	$y = a + b*x$	-0.00172	0.01453	-	-	-	0.99691
N7 (figure E.6)	$y = a + b*x$	-0.00118	0.24806	-	-	-	0.99422
N8 (figure E.7)	$y = y0 + A*exp(R0*x)$	-	-	0.19386	-0.19154	-0.22543	0.97999

### 3.7.3 Conversion calculation

Conversion with respect to the nitrosamine was calculated in Excel using the calibration equations in Tables 3.4, 3.5 and 3.7. Due to the wide range of reaction conditions in the screen, calibrations with internal standard were plotted such that the internal standard concentration

could be varied within the reaction. Firstly, for those reactions using an internal standard the response factor was calculated from the ratio of the analyte peak area to the internal standard peak area (Equation (3.1)). If the internal standard was ignored or otherwise due to the presence of acid in the reaction mixture, the absolute integral was used in place of the response factor.

$$\frac{\text{Area}_{\text{Analyte}}}{\text{Area}_{\text{IS}}} = RF \quad (3.1)$$

For those calibrations plots with linear fit line equations, the equations take the forms in Equation (3.2) and Equation (3.3) for the calibrations including and excluding internal standard respectively.

$$RF = a + b \cdot \frac{[\text{Analyte}] \text{ (mM)}}{[\text{IS}] \text{ (mM)}} \quad (3.2)$$

$$\text{Area}_{\text{Analyte}} = a + b \cdot [\text{Analyte}] \text{ (mM)} \quad (3.3)$$

To find the concentration of the analyte, Equations (3.2) and (3.3) can be rearranged to give Equations (3.4) and (3.5) respectively:

$$[\text{Analyte}] \text{ (mM)} = \frac{RF - a}{b} \cdot [\text{IS}] \text{ (mM)} \quad (3.4)$$

$$[\text{Analyte}] \text{ (mM)} = \frac{\text{Area}_{\text{Analyte}} - a}{b} \quad (3.5)$$

Similarly, calibration graphs with an exponential fit line equation with forms Equations (3.6) and (3.7) can be rearranged for the analyte concentration to give Equations (3.8) and (3.9).

$$RF = y_0 + A \cdot e^{R_0 \cdot \frac{[\text{Analyte}] \text{ (mM)}}{[\text{IS}] \text{ (mM)}}} \quad (3.6)$$

$$\text{Area}_{\text{Analyte}} = y_0 + A \cdot \exp(R_0 \cdot [\text{Analyte}] \text{ (mM)}) \quad (3.7)$$

$$[\text{Analyte}] \text{ (mM)} = \frac{[\text{IS}] \text{ (mM)} \cdot \ln\left(\frac{RF-y_0}{A}\right)}{R_0} \quad (3.8)$$

$$[\text{Analyte}] \text{ (mM)} = \frac{\ln\left(\frac{\text{Area}_{\text{Analyte}}-y_0}{A}\right)}{R_0} \quad (3.9)$$

Equation 3.10 calculates the expected concentration of the analyte if no reaction were to occur ( $[\text{Analyte}]_0$ ) from the starting nitrosamine stock solution concentration and the total reaction volume at the time the HPLC sample is taken (Equation (3.10)). The conversion is then calculated as the average result over two or three repeat reactions of equation 3.11.

$$[\text{Analyte}]_0 \text{ (mM)} = \frac{[\text{Stock}]_{(\text{Analyte})} \cdot V_{\text{Stock}}}{V_{\text{Reaction}}} \quad (3.10)$$

$$\text{Conversion (\%)} = \frac{[\text{Analyte}] \text{ (mM)}}{[\text{Analyte}]_0 \text{ (mM)}} \cdot 100 \quad (3.11)$$

### 3.8 GC-MS/MS peak identification

The products of the screening reactions were determined by GC-MS/MS using the method settings listed in Table 3.6. The method was developed to ensure all *N*-nitrosamines could be captured by the same method. Table 3.8 summarises all the peaks detected for starting *N*-nitrosamines and the found products. Where possible, the reference peaks were from authentic reference samples or from the calibration solutions. The mass spectra and chromatograms can be found in the Appendix, at the reference listed in Table 3.8.

Table 3.8: GC-MS/MS peak data for known products.

Analyte	MW (g/mol)	RT (mins)	Mass peaks	Adduct	Source (ref)
N1	102.14	3.18	102; 85; 71; 57	M	Cal (Figure F.1)
<i>N</i> -nitrodiethylamine	118.14	5.31	118; 103.1; 91; 79	M	Condition 2 (Figure F.14)
N2	130.19	6.53	130; 113; 101; 70	M	Cal (figure F.2)
dipropylhydrazine	116.21	2.69	116.1; 87; 72; 59.1	M	Condition 9 (Figure F.9)
dipropylamine	101.19	5.05	142.1; 113.1; 85; 71	M+Na+H <sub>2</sub> O	Condition 9 (Figure F.9)
<i>N</i> -nitrodipropylamine	146.19	8.92	146; 117; 91; 79; 70	M	Condition 2 (Figure F.15)
N3	158.25	10.86	158; 141; 116; 99; 84	M	Cal (Figure F.3)
dibutylhydrazine	144.26	6.64	144.1; 101.1; 86.1; 59.1	M	Condition 9 (Figure F.10)
dibutylamine	129.15	4.48	129; 86	M	Authentic (Figure F.8)
dibutylamine	129.15	8.79	170.1; 127.1; 85; 71	M+Na+H <sub>2</sub> O	Condition 9 (Figure F.10)
N5	116.12	6.52	116; 86; 56	M	Cal (Figure F.4)
<i>N</i> -aminomorpholine	102.14	3.44	102; 86; 72; 57	M	Condition 9 (Figure F.11)
N6	132.12	3.89	132; 103; 58	M	Cal (Figure F.5)
<i>N</i> -methyl ethylcarbamate	103.12	2.57	103; 58	M	Cal (Figure F.5)
N7	174.24	12.91	157; 100; 84; 71	M	Cal (Figure F.6)
<i>N</i> -butyl- <i>N</i> - (4-hydroxybutyl) hydrazine	160.26	11.64	160.1; 117.1; 101.1	M	Condition 9 (Figure F.12)
4-(butylamino)-1- butanol	145.25	12.32	186.1; 143.1; 127.1	M+Na+H <sub>2</sub> O	Condition 9 (Figure F.12)
N8	118.14	8.02	87; 75; 57	M	Cal (Figure F.7)
2-(1-ethylhydrazino) ethanol	104.15	4.29	104; 73	M	Condition 9 (Figure F.13)
2-(ethylamino)ethanol	89.14	3.79	130.1; 115; 99; 73	M+Na+H <sub>2</sub> O	Condition 9 (Figure F.13)
N8 unexpected product	unknown	8.65	160.1; 129.1; 117.1; 103.1; 88; 73; 58.1	unknown	Condition 9 (Figure F.13)
TMB	168.19	12.10	168; 139; 25; 109	M	N1 Cal (Figure F.1)
2,6-di- <i>tert</i> -butyl-4- methylphenol	220.36	12.73	220.1; 205.1; 177; 145	M	N1 Condition 8 (Figure F.20)

Furthermore, side products associated with reaction of the internal standard in conditions 1 and 2 are also suggested. These peaks are not verified by authentic samples as they did not form part of the core objective of the project. Details of the retention times and mass peaks for the side products found are summarised in Table 3.9. Links to the reference plots are available by clicking the link in the “Source” column.

Table 3.9: GC-MS/MS peak data for side products.

Analyte	MW (g/mol)	RT (mins)	Mass peaks	Adduct	Source (ref)
2-Chloro-1,3,5-trimethoxybenzene	202.63	13.28	202; 173; 159; 138	M	N6 Condition 1 (Figure F.16)
2-Chloro-1,3,5-trimethoxybenzene	202.63	13.59	247.9; 245.9; 168; 138	M+EtOH	N1 Condition 2 (Figure F.17)
2,4-dichloro-1,3,5-trimethoxybenzene	202.63	13.64	237.9; 235.9; 192.9; 177.9	M	N3 Condition 2 (Figure F.18)
2,4-dichloro-1,3,5-trimethoxybenzene	202.63	13.95	283.9; 281.9; 238.9; 202	M+EtOH	N5 Condition 2 (Figure F.19)
2-bromo-4-chloro-1,3,5-trimethoxybenzene	281.53	14.26	327.9; 325.9; 324.0	M+EtOH	N7 Condition 3 (Figure F.21)

### 3.8.1 LC-MS/MS peak identification

In some cases the analysis by GC-MS/MS was insufficient to confirm the reaction products, either if no product was found by GC-MS/MS (e.g. N8 in condition 3) or if the GC-MS/MS method was insufficient to distinguish between reactants and products (N4 in all conditions). In these cases, a high sensitivity liquid chromatography tandem mass-spectrometry (LC-MS/MS) method was employed using a Bruker Impact II QqTOF system with Electrospray Ionisation (ESI). The LC-MS/MS method settings are listed in Table 3.10. Again, where possible, authentic reference chromatograms were obtained for each analyte, however some products were unavailable and hence their identification is determined through reaction conditions with known reactivity *i.e.* *p*-nitrosodiphenylamine. Table 3.11 details the retention time and mass peaks for the analytes determined by LC-MS/MS.

Table 3.10: LC-MS/MS method settings.

<b>Guard Column:</b>	
Waters Acquity Premier CSH C18 1.7 $\mu$ m VanGuard FIT 2.1mm x 5mm VanGuard FIT 2.1mm x 5mm	
<b>Column:</b>	
Waters Acquity Premier VanGuard FIT CSH C18 2.1mmx 1000mm	
<b>Method:</b>	
0.7ml/ min A: Water(0.1% formic acid) B: Acetonitrile (0.1% formic acid)	
<b>Gradient (linear interpolation):</b>	
t (mins)	% A
-1.2	99
2.5	95
4.0	70
6.0	5
7.5	99
7.9	99

Table 3.11: LC-MS/MS reference mass peaks and retention times.

Analyte	MW (g/mol)	RT (min)	Mass peaks	Adduct	Source	ref
N4	198.23	5.66	199.09; 184.07; 169.09	M+H	authentic	Figures H.1 and H.2
diphenylamine	169.23	5.75	170.10	M+H	authentic	Figures H.3 and H.4
N,N'-diphenylhydrazine	184.24	5.21	185.11; 168.08	M+H	authentic	Figures H.5 and H.6
<i>p</i> -nitrosodiphenylamine	198.23	5.42	199.08; 122.09	M+H	Condition 7	Figures H.7 and H.8
N7	174.24	4.62	175.14; 102.09	M+H	authentic	Figures H.9 and H.10
N8	118.14	1.42	119.08	M+H	authentic	Figures H.11 and H.12
4-(butylamino)-1-butanol	145.25	0.6	146.16	M+H	Condition 7	Figures H.13 and H.14

### 3.9 Results and Discussion

The conversions with respect to the nitrosamine from the 21 reaction conditions are presented in Figure 3.13 (a). The products found with reference to Tables 3.8 and 3.11 for each reaction by either LC-MS/MS or GC-MS/MS analysis are summarised in Figure 3.13 (b). Figure 3.1 is repeated here to refresh the reader on the eight nitrosamines used in the study. This section will, in turn, discuss the results of each reaction condition and draw conclusions about the reactivity of *N*-nitrosamines.

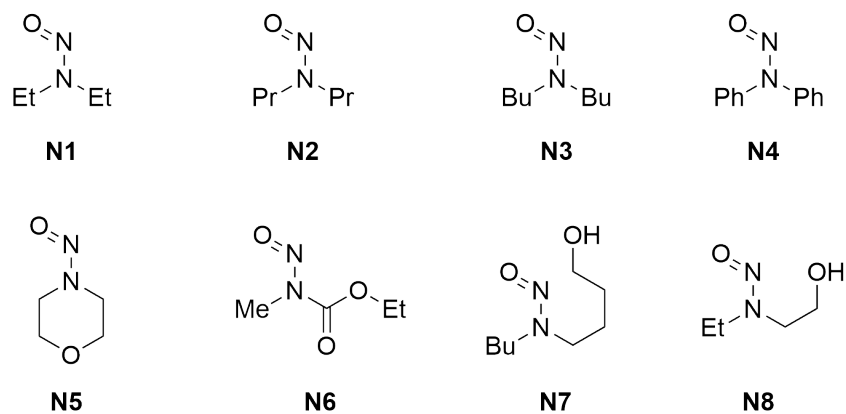


Figure 3.12: The eight nitrosamines used in this study, repeated for readability.



a)

Key:	0	50	100
conversion (%)			
No data			

No.	Class	Reagents	Solvent	Temp. (°C)	Reaction time (h)	N1	N2	N3	N4	N5	N6	N7	N8
1	Oxidant	H <sub>2</sub> O <sub>2</sub> 2M	H <sub>2</sub> O/EtOH	22	24	2	-3	4	17	0	2	2	5
2	Oxidant	CH <sub>3</sub> CO <sub>3</sub> H	EtOH	22	24	8	8	7	95	14	101	14	12
3	Acid	HBr	AcOH/EtOH	22	24	6	7	13	42	25	85	2	26
4	Acid	HCl 2M	H <sub>2</sub> O/EtOH	22	24	2	-5	6	37	-1	101	-12	6
5	Acid	HCl 2M	H <sub>2</sub> O/EtOH	50	16	1	-4	13	86	5	101	-14	6
6	Acid	HCl 2M	EtOH	22	24	-2	-2	3	100	56	101	-6	15
7	Acid	HCl 2M	EtOH	50	16	71	54	56	99	98	101	52	100
8	Reductant	NaBH <sub>4</sub> 16 eq	EtOH	22	24	3	0	3	23	-2	101	5	0
9	Reductant	DIBAL-H 5 eq.	THF/Hexane	22	0.5	72	66	61	76	101	100	51	69
10	Reductant	DIBAL-H 5 eq.	THF/Hexane	22	1	85	86	75	85	101	100	90	101
11	Reductant	Na <sub>2</sub> S <sub>2</sub> O <sub>4</sub>	H <sub>2</sub> O/EtOH	22	24	9	3	9	87	25	63	-5	5
12	Reductant	Na <sub>2</sub> S <sub>2</sub> O <sub>4</sub> + NaOH 0.1M	H <sub>2</sub> O/EtOH	22	24	-4	2	9	87	32		-9	2
13	Reductant	Na <sub>2</sub> S <sub>2</sub> O <sub>4</sub> + NaOH 0.1M	H <sub>2</sub> O/EtOH	50	16	18	7	11	99	67	101	6	40
14	Reductant	Na <sub>2</sub> S <sub>2</sub> O <sub>4</sub> + NaOH 1M	H <sub>2</sub> O/EtOH	50	16	78	57	56	99	99	101	87	99
15	Reductant	Na <sub>2</sub> S <sub>2</sub> O <sub>4</sub> + NaOH 1M	H <sub>2</sub> O/EtOH	50	3	18	1	11	99	75	101	14	32
16	Reductant	Na <sub>2</sub> S <sub>2</sub> O <sub>4</sub> + NaOH 1M	H <sub>2</sub> O/EtOH	50	1	18	2	12	97	44	101	-4	17
17	Reductant	Na <sub>2</sub> S <sub>2</sub> O <sub>4</sub> + 20% NaOH	H <sub>2</sub> O/EtOH	50	16	106	104	104	95	96		107	101
18	Reductant	Na <sub>2</sub> SO <sub>3</sub>	H <sub>2</sub> O/EtOH	22	24	4	-2	6	22	-2	102	-6	3
19	Reductant	Na <sub>2</sub> SO <sub>3</sub> + 1M NaOH	H <sub>2</sub> O/EtOH	50	16	2	1	7	75	1	101	-3	-1
20	Base	NaOH 2M	H <sub>2</sub> O/EtOH	22	24	0	-5	3	1	0	101	6	6
21	Base	NaOEt 21% w/v	EtOH	22	24	-7	1	6	-3	3	101	2	7

b)

Key:	Found	
	Absent	
	No Data	

R1-N(R2)-C(=O)OH  
 $n = 3$  (N7)  
 $n = 1$  (N8)  
**CA**

R1-NH2  
**H**

R1-NH-C6H4-N=O  
**P**

R1-N(R2)-NO2  
**O**

R1-NH-R2  
**A**

R1-N(R2)-NO  
**N**

No.	N1				N2				N3				N4				N5			N6			N7				N8			
	N	H	A	O	N	H	A	O	N	H	A	O	N	H	A	P	O	N	H	A	N	A	N	H	A	CA	N	H	A	CA
1																														
2																														
3																														
4																														
5																														
6																														
7																														
8																														
9																														
10																														
11																														
12																														
13																														
14																														
15																														
16																														
17																														
18																														
19																														
20																														
21																														

Figure 3.13: Summary tables for the results of the reactivity screen showing a) The conversions with respect to the *N*-nitrosamine and b) The products of the reactions determined by GC-MS/MS and LC-MS/MS.

### Basic conditions (20 and 21):

Since there is known reactivity under acidic conditions, and a basic quench would be required to investigate these conditions, the first reaction condition tested was NaOH<sub>aq</sub>, (condition 20). The results showed no conversions apart from the expected reactivity with N6 which undergoes

the well reported diazonium formation reaction as derived from the Chapter 2. Quenching with 2M acetic acid was chosen in response to the work done on the Fisher-Hepp reaction by Williams et al. [48] who reported that the nucleophilicity of the conjugate base of the acid is determinant in the denitrosation reaction, since acetate in acetic acid is more weakly nucleophilic than the chloride anion in HCl, it was considered to be a suitable acid to quench reactions with base without side reactions. Henceforth, it was deemed that the acetic acid which was a component of the peracetic acid and hydrogen bromide reagent solutions was less likely to be the active reagent in producing any conversion of the starting material in those cases. Switching to a stronger organic base in condition 21 with sodium ethoxide produced no further reactivity as expected. In the case of N6 in condition 21 the reaction produced total conversion of N6 and of *N*-methylethylcarbamate as neither were detected by GC (Appendix Figure G.24).

### Oxidative conditions (1 and 2):

Conditions 1 and 2 were performed in response to the known reactivity with trifluoroacetic acid and peracetic acid at elevated temperature producing *N*-nitramines. [49] These experiments sought to bring about the same transformations under milder reaction conditions.

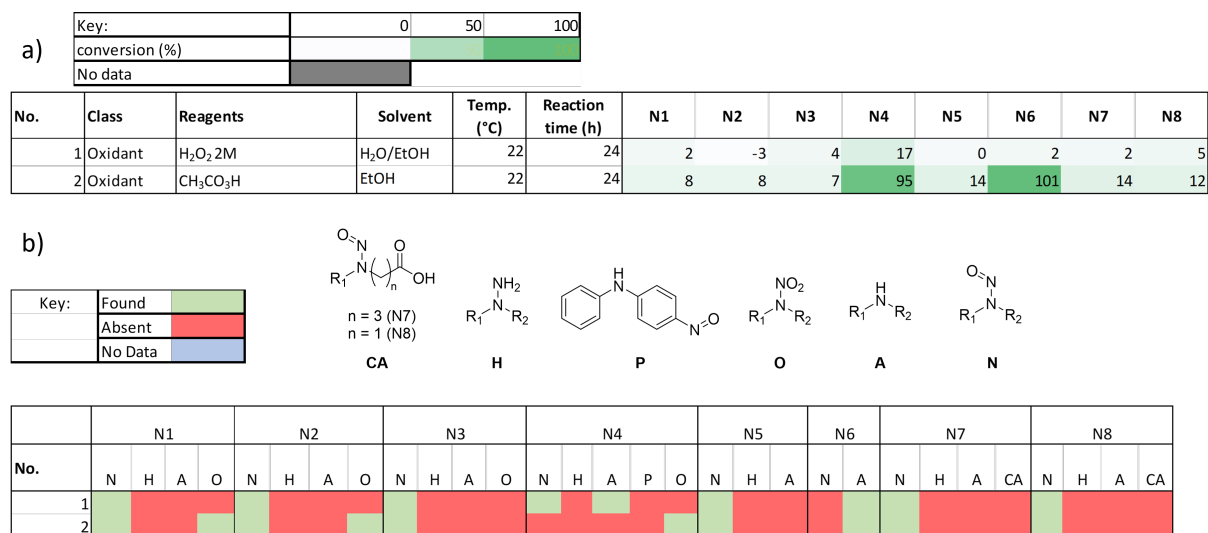
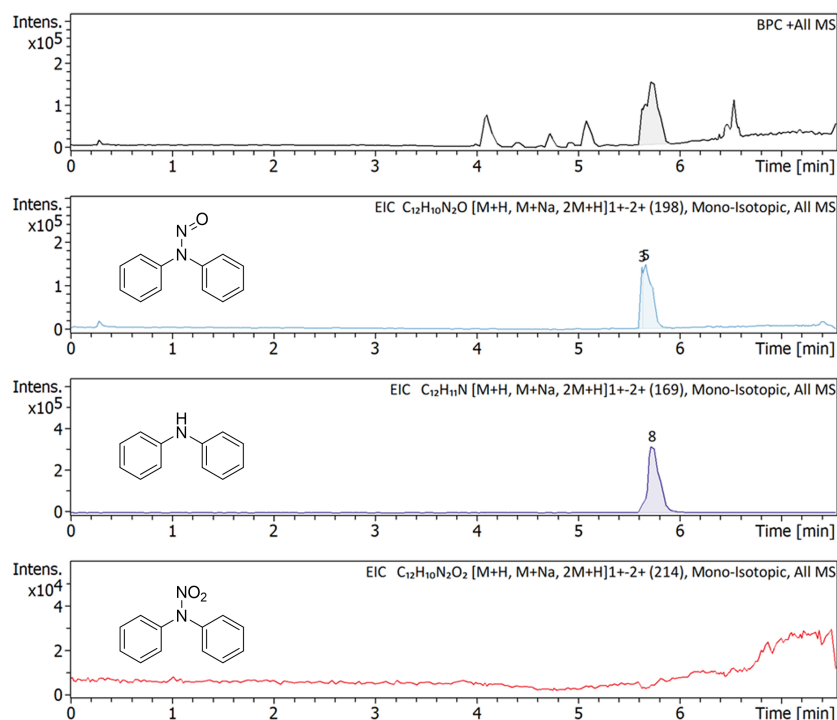


Figure 3.14: Summary tables for the results of the reactivity screen for conditions 1 and 2 showing a) The conversions with respect to the *N*-nitrosamine and b) The products of the reactions determined by GC-MS/MS and LC-MS/MS.

With H<sub>2</sub>O<sub>2</sub> in condition 1, reactivity was only seen with N4. Surprisingly, the observed product was not the *N*-nitramine ( $m/z = 214$ ) as expected, but diphenylamine ( $m/z = 169$ ), the corresponding amine (Figure I.1) (Figure 3.14). It is hypothesised that the acidity of the per-

oxide solution influences this transformation and the mechanism is that of the acid catalysed denitrosation pathway.



#### Summary of Results

Name	RT	BPC Area(%)	UV Area(%)	Confirm Formula Results
Cmpd 3, 5.6 min	5.63	no peak	27.9	C12H10N2O
Cmpd 5, 5.7 min	5.66	100.0	27.9	C12H10N2O,C12H11N
Cmpd 8, 5.7 min	5.72	100.0	15.9	C12H10N2O,C12H11N

Figure 3.15: LC-MS/MS results for N4 in condition 1.

The peaks in the LC-MS/MS are overlapping and it is difficult to know whether the amine is just picked from the fragmentation peak in the starting material. Therefore, the amine product was confirmed by  $^1\text{H}$  and  $^{13}\text{C}$  NMR (Figure 3.16). Full assignment can be found in Appendix Figures J.1 and J.2

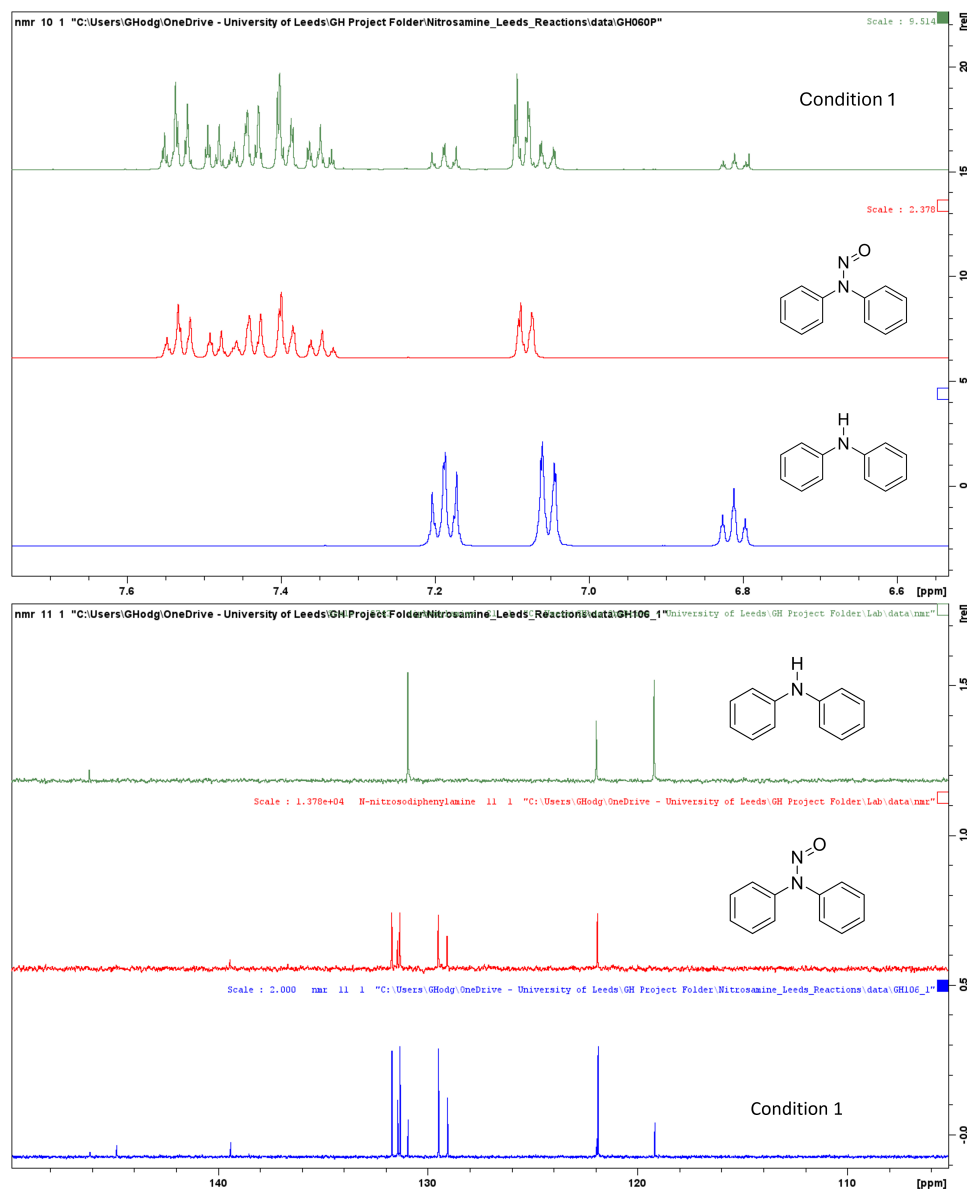


Figure 3.16:  $^1\text{H}$  and  $^{13}\text{C}$  NMR for the reaction of N4 in  $\text{H}_2\text{O}_2$  producing diphenylamine.

With N6 in condition 1, the corresponding amine product was seen in GC-MS/MS, in absence of the starting material. However, the conversion by HPLC was only 2%. This, coupled with the chlorination reaction on the internal standard observed post-quench (appendix Figure G.2) suggests other an unexpected side-reaction occurring post-quench, possibly initiated by the addition of NaCl in brine which may be oxidized to produce a chlorinating reagent and subsequently chlorinate the internal standard *via* and  $\text{S}_{\text{E}}\text{Ar}$  reaction.[129]

Condition 2 used a stronger oxidiser in peracetic acid which was bought from Fisher as a pre-prepared mixture of  $\text{H}_2\text{O}_2$ , AcOH and  $\text{CH}_3\text{CO}_3\text{H}$ . Under these conditions, low conversion (*ca.*) 10% was seen with N1-3 (dialkynitrosamines), N5 (cyclic nitrosamine) and N7 and N8

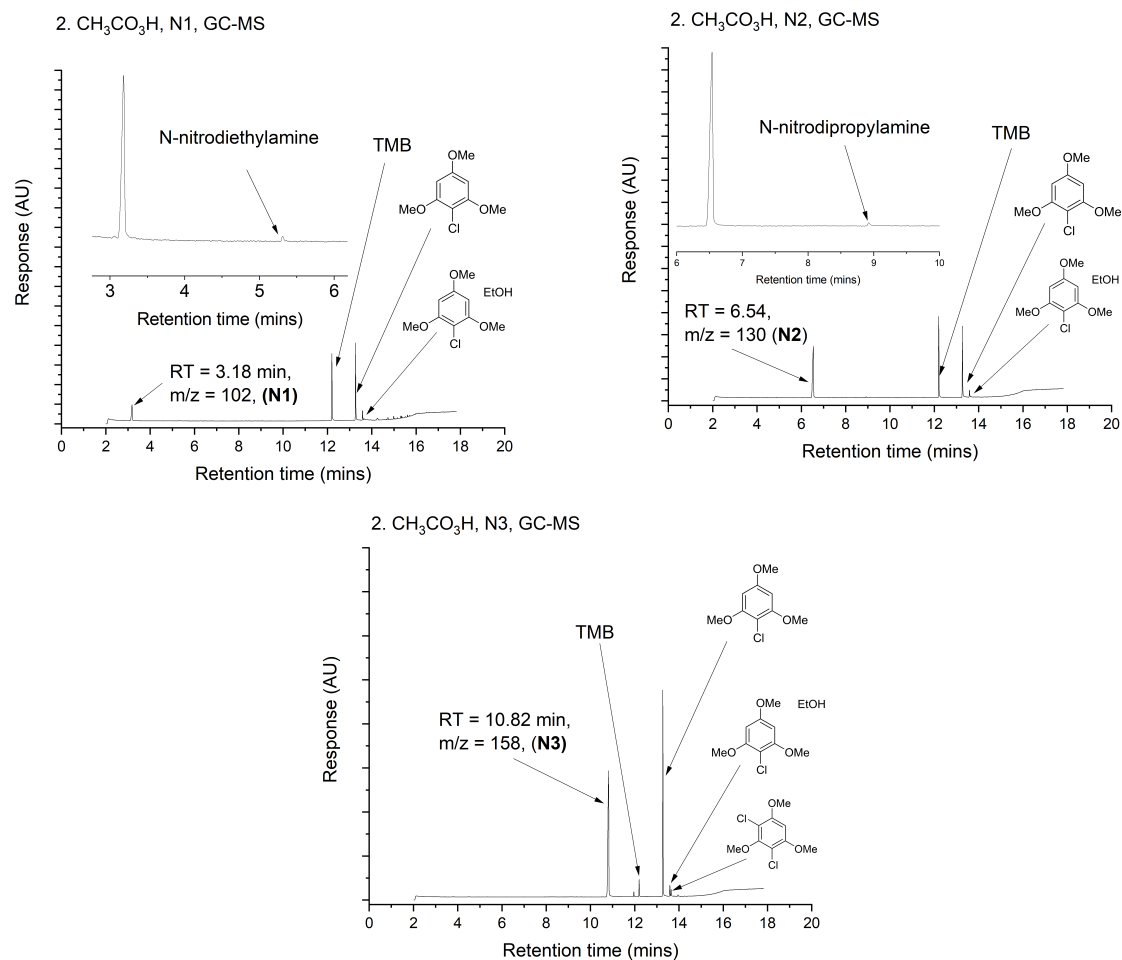


Figure 3.17: GC-MSMS plots for N1, N2, N3 and N5 condition 2.

( $\alpha$ -hydroxydialkyl nitrosamines). GC-MS/MS analysis showed that the *N*-nitramine product was present in the case of N1 and N2, but not N3 even though the conversions of the starting material were similar (Figure 3.17).

The reaction with N4 produced the amine and the *N*-nitramine (figure 3.18), however, this reaction was not clean and there were many side products visible by HPLC (Figure 3.19). The reaction mixture also went black suggesting tar production.

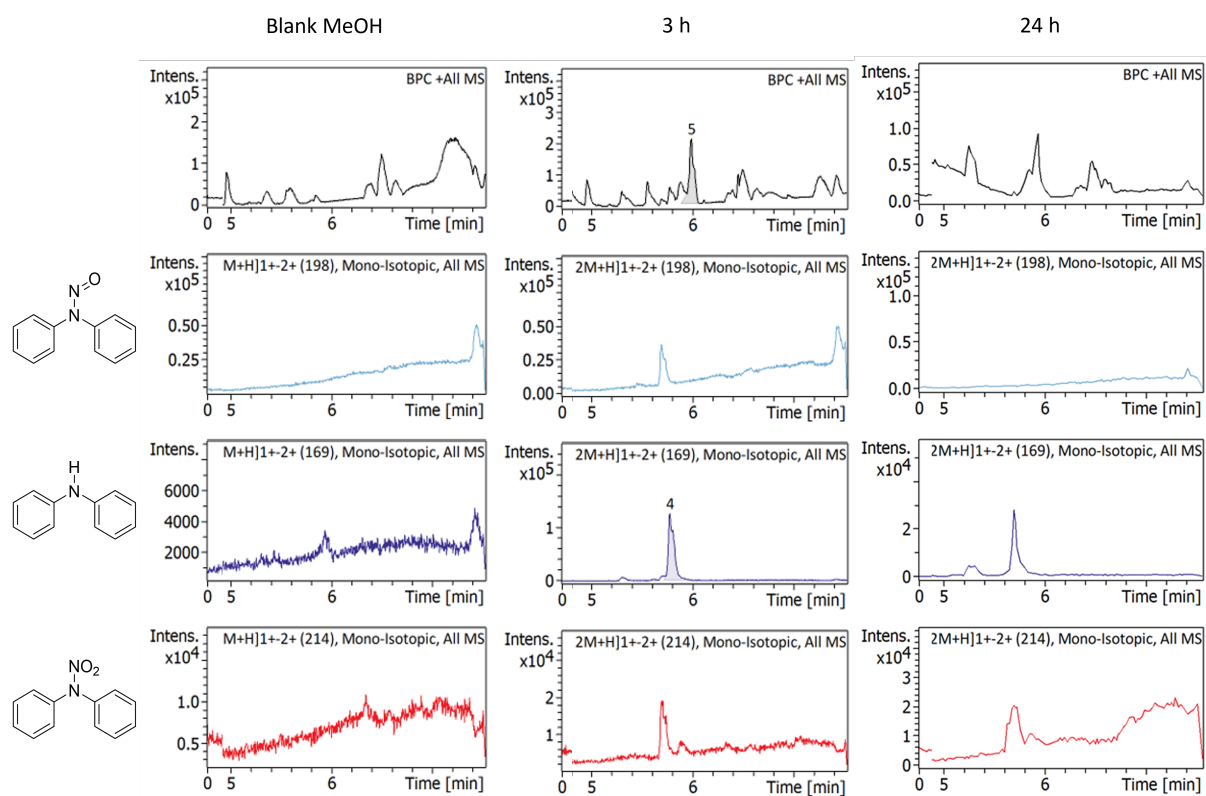


Figure 3.18: LC-MS/MS results for N4 in condition 2.

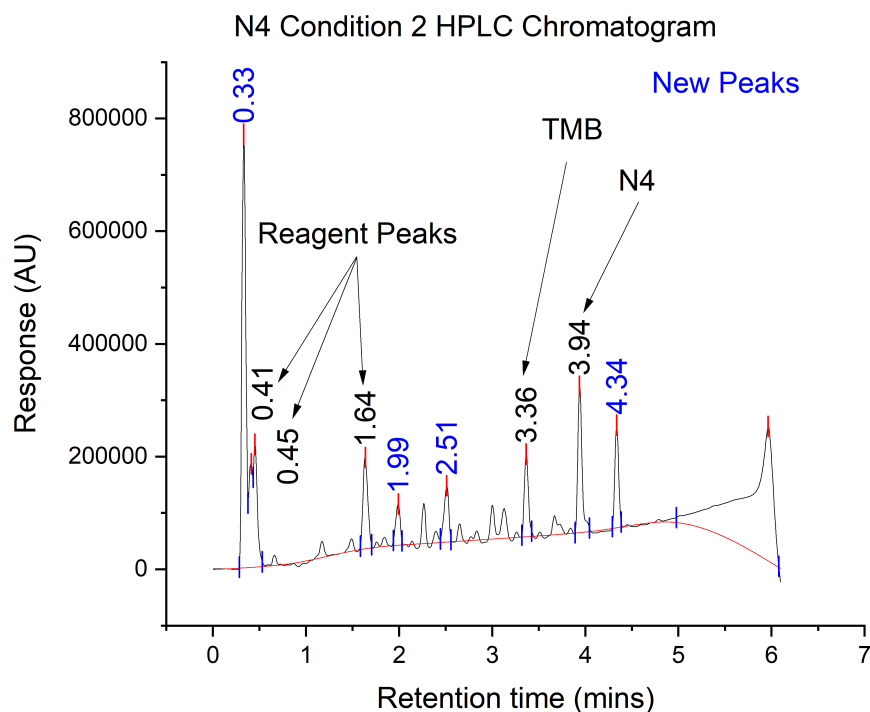


Figure 3.19: HPLC results for N4 in condition 2.

The products of the reactions of N7 and N8 in condition 2 were investigated by LC-MS/MS after no product was visible by GC-MS/MS. For N8, a broad peak with a retention time of 1.90 mins was found with 118  $m/z$  and a smaller peak barely visible at 132  $m/z$  (figure 3.21). Though this is evidence of the carboxylic acid product of the nitrosamine, the retention time being higher than that of the starting material goes against the presence of a more polar product. A more likely event is that the solvent system in the reaction sample being different by a small amount than in the reference sample has influenced the retention time of the starting material somewhat. This is supported by the fact that no carboxylic acid peak was seen in the case of N7 (Figure 3.20) and that the retention time of the starting material at 174  $m/z$  is also slightly shifted (4.75 min) compared to the reference nitrosamine injection (4.62 min).

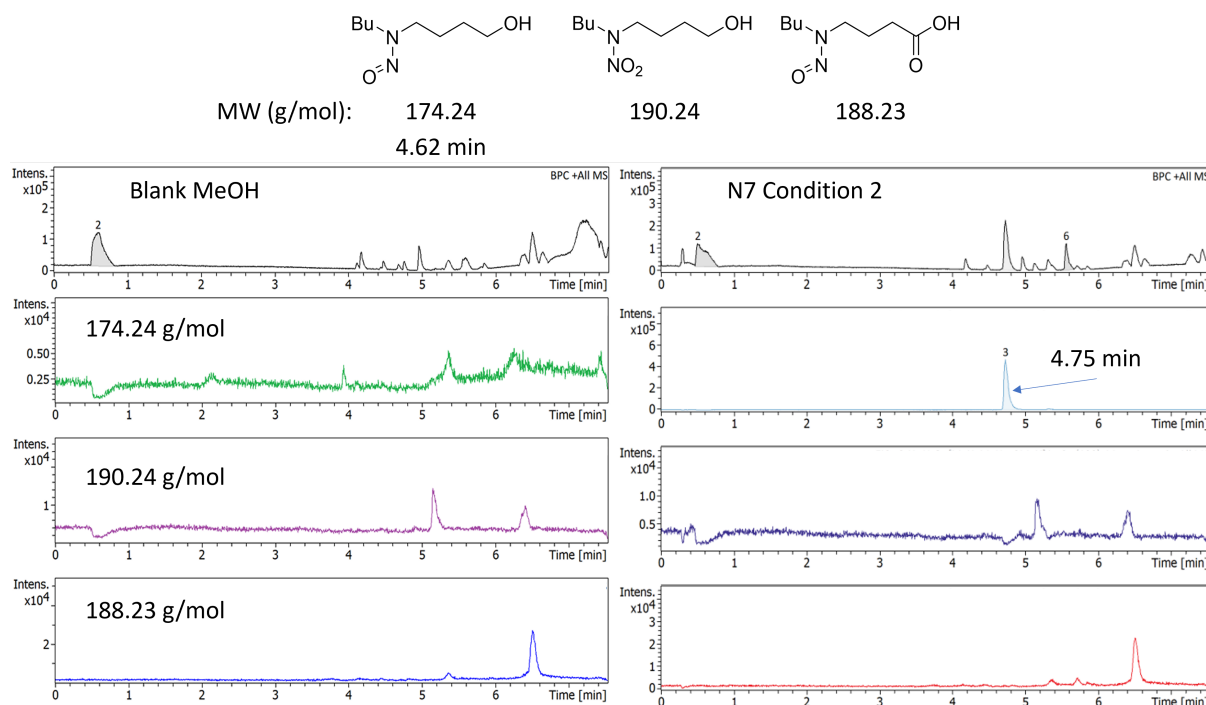


Figure 3.20: LC-MS/MS results for N7 reactivity under condition 2.

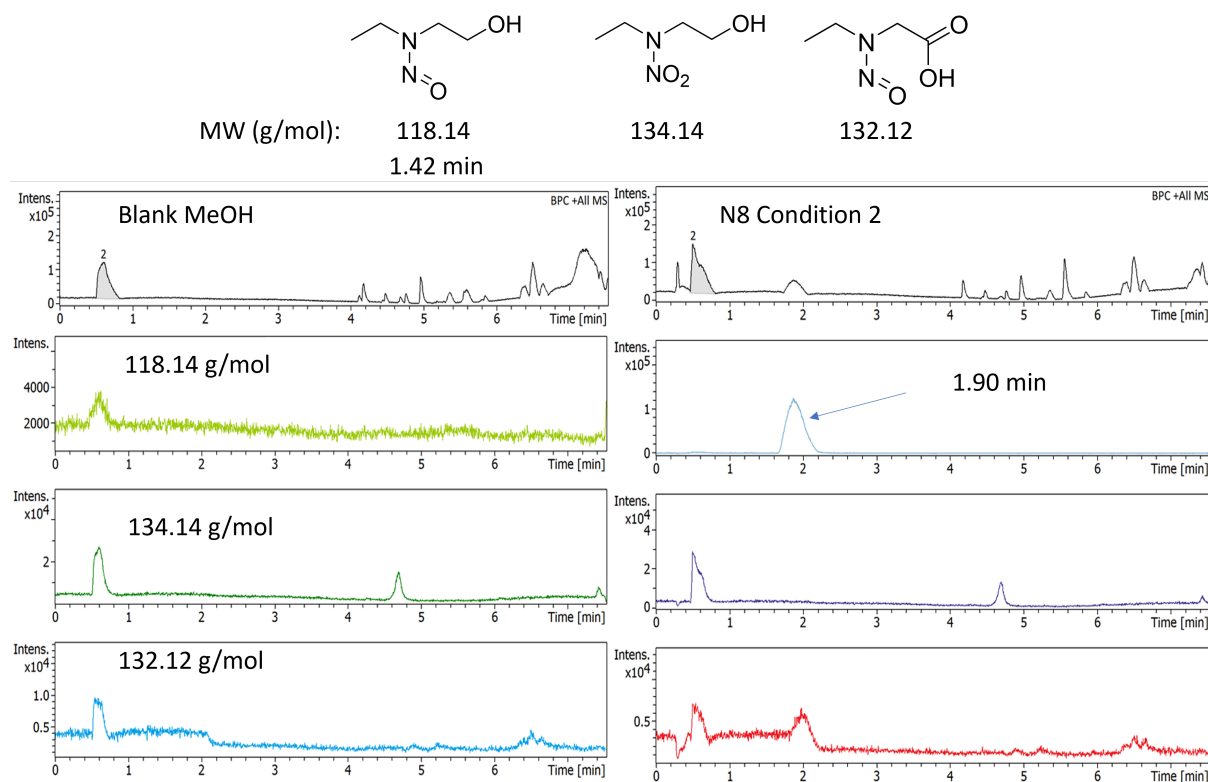
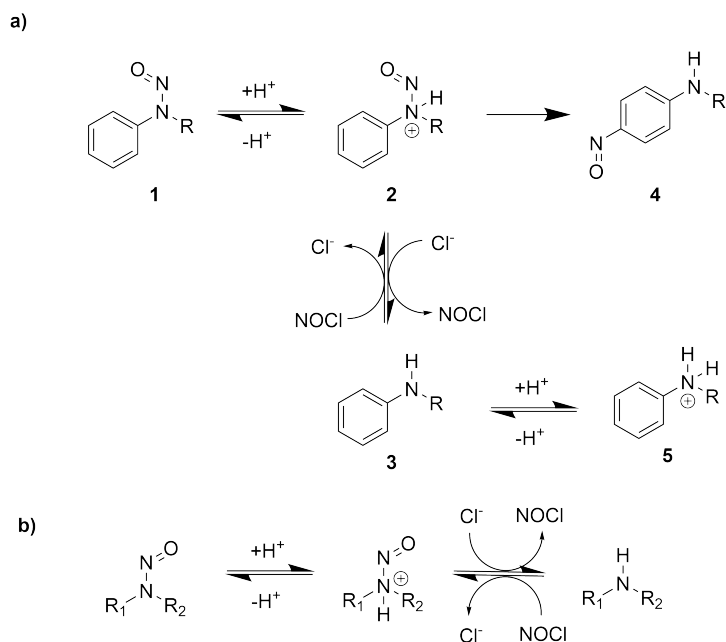


Figure 3.21: LC-MS/MS results for N8 reactivity under condition 2.

**Acidic conditions (3 - 7):**

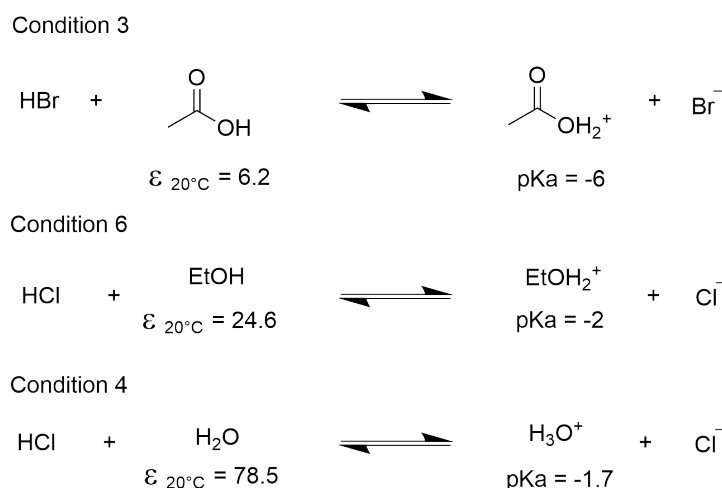
The reaction of aryl *N*-nitrosamines under acidic conditions is known to produce the *p*-nitroso compound *via* the Fischer-Hepp rearrangement in the presence of water. This reaction is in competition with the reversible denitrosation reaction brought about by nucleophilic attack of the protonated nitrosamine, usually by the conjugate base of the acid i.e.  $\text{Cl}^-$  in the case of HCl (Scheme 3.3 (a)). The route to the amine is hindered in the presence of water due to solvation of the nucleophile. Minimal evidence for reactivity exists on dialkyl *N*-nitrosamines, though it is expected that they would react *via* the denitrosation mechanism outlined by Williams *et al.* (Scheme 3.3 (b)). [46]





Scheme 3.3: Reactivity of *N*-nitrosamines under acidic conditions for a) aryl *N*-nitrosamines and b) dialkyl *N*-nitrosamines.

The chosen acidic reaction conditions differ in their composition, and this has a marked effect on the reactivity with respect to the *N*-nitrosamines used in this study. The best comparisons are made between the reactions performed at room temperature i.e. conditions 3, 4 and 6. Condition 3 used hydrogen bromide (HBr) at 33 % wt in acetic acid, Condition 4 used aqueous hydrochloric acid (HCl, 2 M) and condition 6 used an ethanolic solution of HCl at 1.25 M. In all of these conditions, the nitrosamine stock solution was prepared in ethanol, and the number of equivalents of acid was 20 in conditions 4 and 6, and 16.5 +/- 0.06 in condition 3. The differences in the composition of the three reaction conditions can be described by the strength of the acid in terms of the pKa or effective pKa of the solution, the polarity of the solvent mixture used and the strength of the nucleophile involved. Starting with the strength of the acid used, the acid-base reactions involved in each condition are shown in Scheme 3.4.



Scheme 3.4: Comparison of the acid-base chemistry for conditions 3, 4 and 6.

In condition 3, the strongest acid that can exist is the conjugate acid of acetic acid, which has a  $\text{pK}_a$  of around -6. [130] While in conditions 4 and 6 the strongest acids that can exist are the conjugate acids of water ( $\text{pK}_a = -1.7$ ) and ethanol ( $\text{pK}_a = -2$ ). This makes the HBr/AcOH system more acidic than the aqueous or ethanolic solutions of HCl. This has influence on the protonation step of the denitrosation mechanism outlined in Scheme 3.3 in that the less basic amine nitrogens among the nitrosamines in the reactivity screen are more likely to be protonated and thus go on to react in the denitrosation mechanism. The second component of difference between the solutions is the polarity of the solvent mixture used, with reference to Scheme 3.4 the dielectric constants show the order of polarity of the reaction mixtures to follow the order: Condition 4 > Condition 6 > Condition 3 [131], thus making the degree of solvation of the halide ion nucleophile follow the same order (4 > 6 > 3), making condition 3 the most reactive with respect to the polarity of the reaction mixture. Finally, with reference to Scheme 3.4 the halide anion is important in the denitrosation mechanism as it acts as the nucleophile which removes NO, yielding the parent amine. As the bromine anion ( $\text{Br}^-$ ) is a better nucleophile than the chloride anion ( $\text{Cl}^-$ ) it is expected that this step of the reaction will be faster in condition 3 than in conditions 4 and 6.

The results of the screening reactions under acidic conditions are outlined in Figure 3.22. Using 3.22 (a) to compare the conversions between conditions 3, 4 and 6 it is clear that condition 6 provided the highest conversions out of the three conditions. It must be noted that condition 3 used a higher dilution factor, as this reaction was run under a nitrogen atmosphere and there were concerns about solvent evaporation during the reaction. Though no conversion was seen

with the dialkyl nitrosamines under these conditions there was conversion with N4, N5, N6 and N8 in the case of condition 3. When the temperature is increased to 50 °C in ethanol solvent (Condition 7), conversion of the dialkyl nitrosamines is seen.

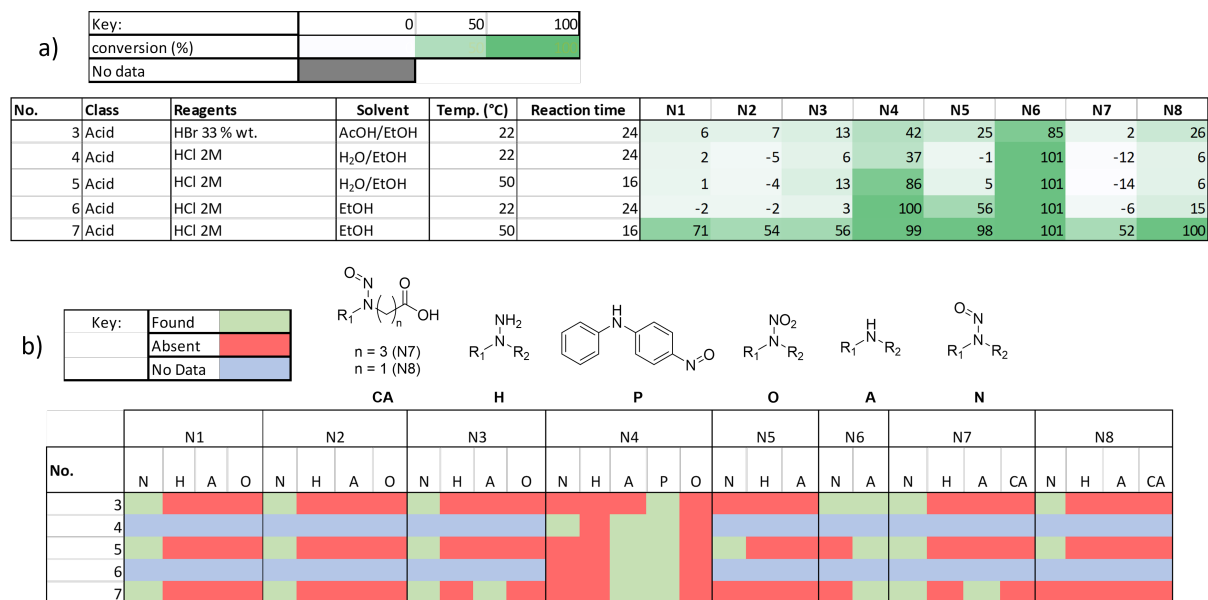


Figure 3.22: Reactivity of *N*-nitrosamines under acidic conditions 3-7. a) Conversions with respect to the *N*-nitrosamine and b) Products of the reactions determined by GC-MS/MS and LC-MS/MS.

### Acidic conditions applied to N6

In the case of N6 complete conversion of the starting material was seen in all acidic conditions except condition 3 where the conversion was 85 %. The lower conversion in condition 3 can be accounted for by the higher dilution factor. The reason that N6 is the most reactive towards acids can be explained by the natural-bond orbital (NBO) charges on the nitroso nitrogen which are shown for the eight nitrosamines in the study in Figure 3.23. The NBO charges were calculated on Gaussian 09 with the BL3YP/6-31G+(d) method. The higher partial positive charge on the nitroso nitrogen facilitates nucleophilic attack by the conjugate base of the acid, and this is reflected in the conversions. In all cases for N6, the product observed by GC-MS/MS was the parent amine (methylethylcarbamate) as shown for condition 3 in Figure 3.24. the remaining GC-MS/MS chromatograms can be found in appendix Figures G.7 and G.8.

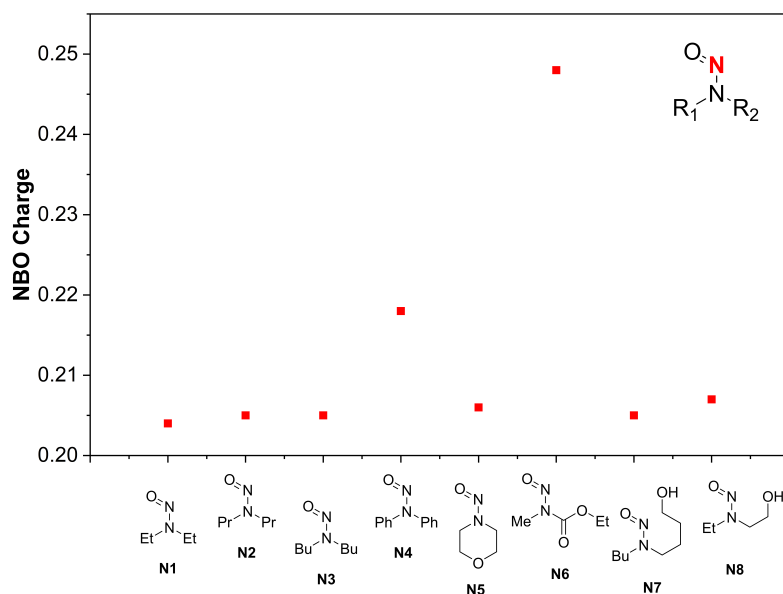


Figure 3.23: The Nitroso-N NBO charges for the eight nitrosamines in the study.

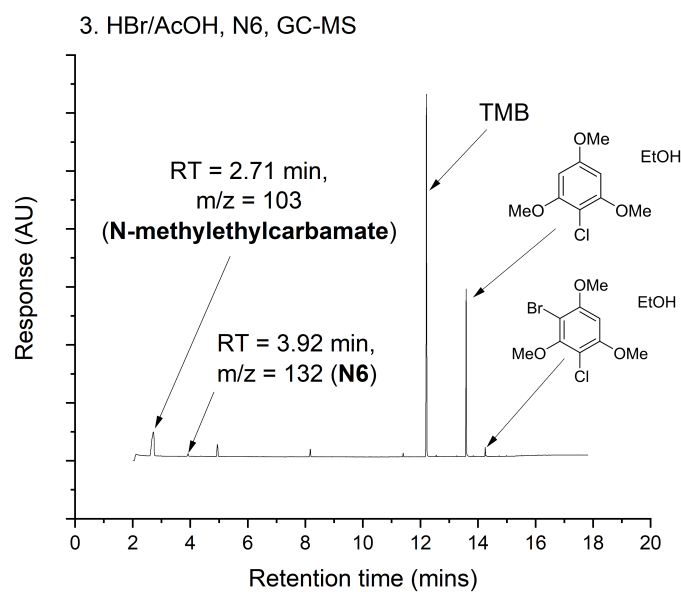


Figure 3.24: GC-MS/MS Chromatogram for N6 in condition 3 showing the denitrosation product methylethylcarbamate

#### Acidic conditions applied to N4

The second-most reactive nitrosamine to acid in the screen was N4 (*N*-nitrosodiphenylamine).

The first order rate coefficient of a structurally similar nitrosamine, *N*-methyl-*N*-nitrosoaniline,

reacting with aqueous HCl at 2.04 M was found to be  $437 \times 10^6 \text{ s}^{-1}$ . [45] A direct comparison between this reaction and to condition 4 with N4 cannot be made as the earlier study monitored the reaction in the presence of sulphamic acid, a nitrite trapping agent, which was used to study the mechanism of the reaction with regards to route to the amine and rearrangement products shown in Scheme 3.3. Nonetheless, it is not surprising that N4 showed the high conversions under acidic conditions. Reaction of N4 with all five acidic conditions produced multiple products, and in each case the reaction mixture darkened to an opaque black colour after the given reaction time. The HPLC chromatograms for N4 in all the acidic conditions are shown in Figure 3.25.

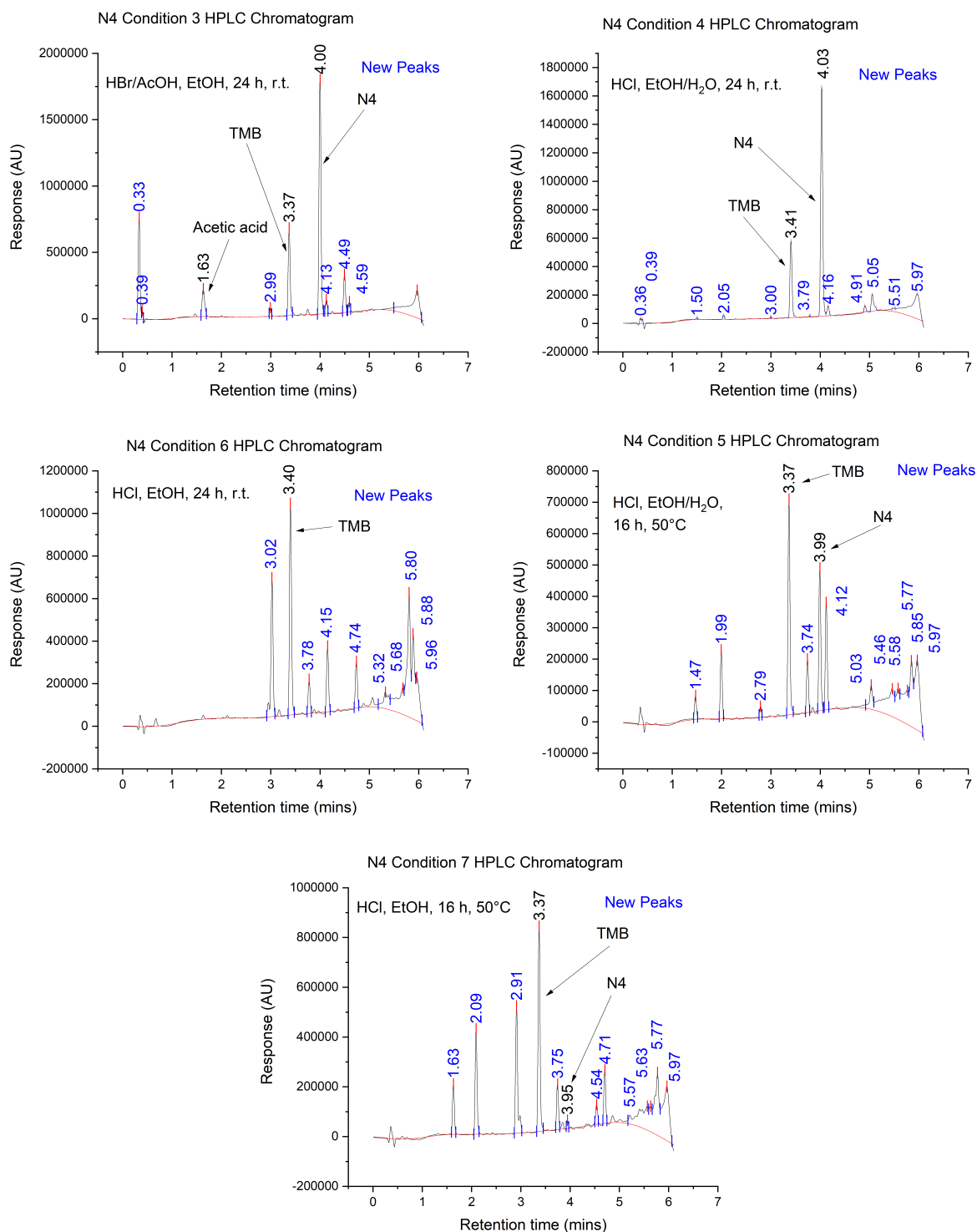


Figure 3.25: HPLC Chromatograms for N4 under acidic conditions.

Though these reactions were not clean and conditions 3-7 should be disregarded for the removal of aryl-nitrosamines, LC-MS/MS analysis was performed on these reactions in an attempt to elucidate the products. Starting with conditions 4 and 5 (Figure 3.26), the starting material N4 is seen in condition 4 (5.66 min with reference to Table 3.11). Also seen is a peak with  $m/z$

= 199.09, equal to that of N4, but with the lower retention time of 5.42 min. Based on the known reactivity of aryl nitrosamines as outlined in Scheme 3.3, and the fact that the retention time of the peak is lower than the starting material indicating a more polar product, this peak is assigned to the Fischer-Hepp rearrangement product. The parent amine is also seen at the same retention time as the reference injection (5.75 min). In condition 5 the starting material peak diminishes and the amine and rearrangement product are present. It is also noted that the base peak chromatogram (top row of plots for each injection) shows many more peaks in condition 5 than in condition 4. This shows that the increased temperature further increases the production of side products under acidic conditions.

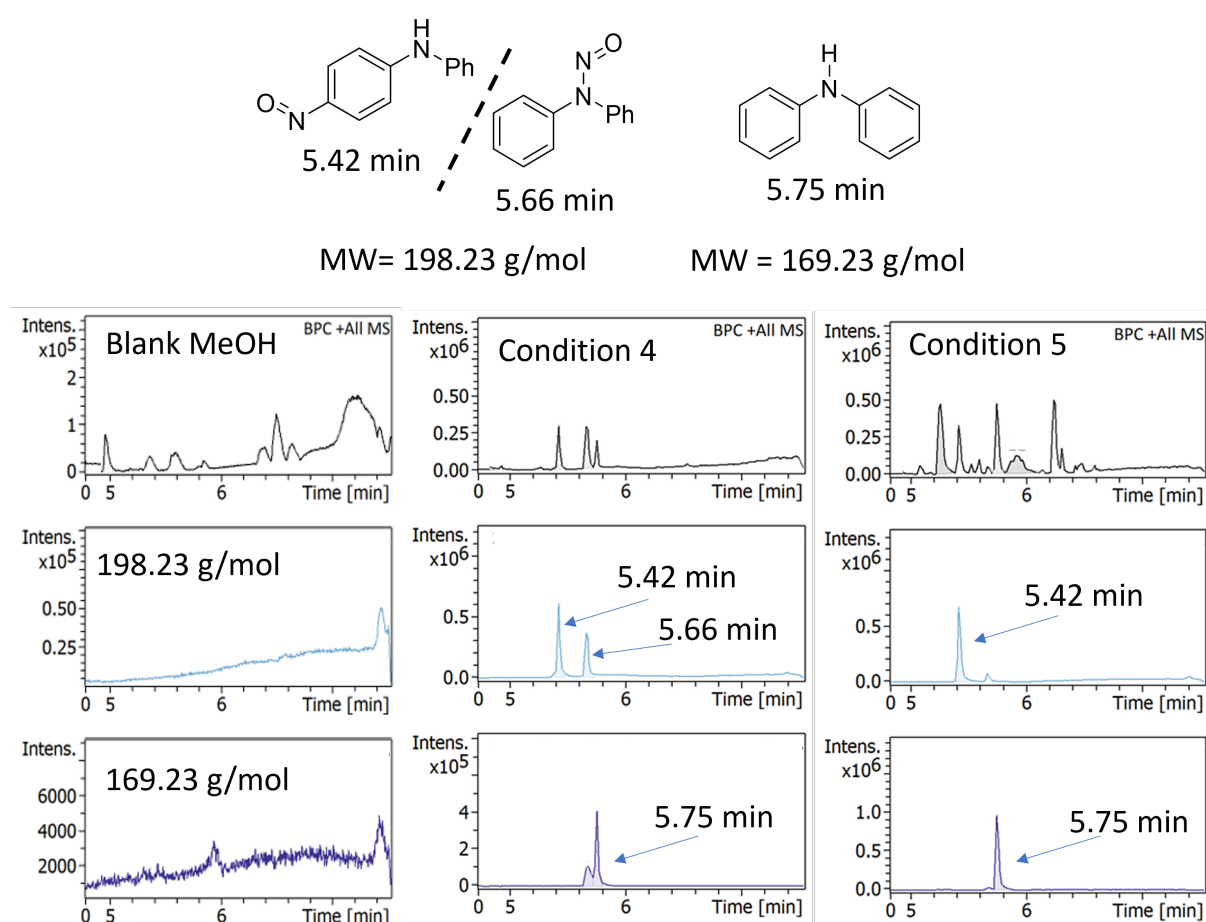


Figure 3.26: LC-MS/MS results for N4 reactivity under conditions 4 and 5.

The rearrangement product was also found in the reaction of N4 with HBr in acetic acid (condition 3), in absence of both the starting material and amine product (Figure 3.27). The fact that the starting material and amine are not present could be due to the fact that they are not present in high enough concentration in the LC-MS/MS sample to be seen. This is supported by the increased conversion of the starting material in condition 3.

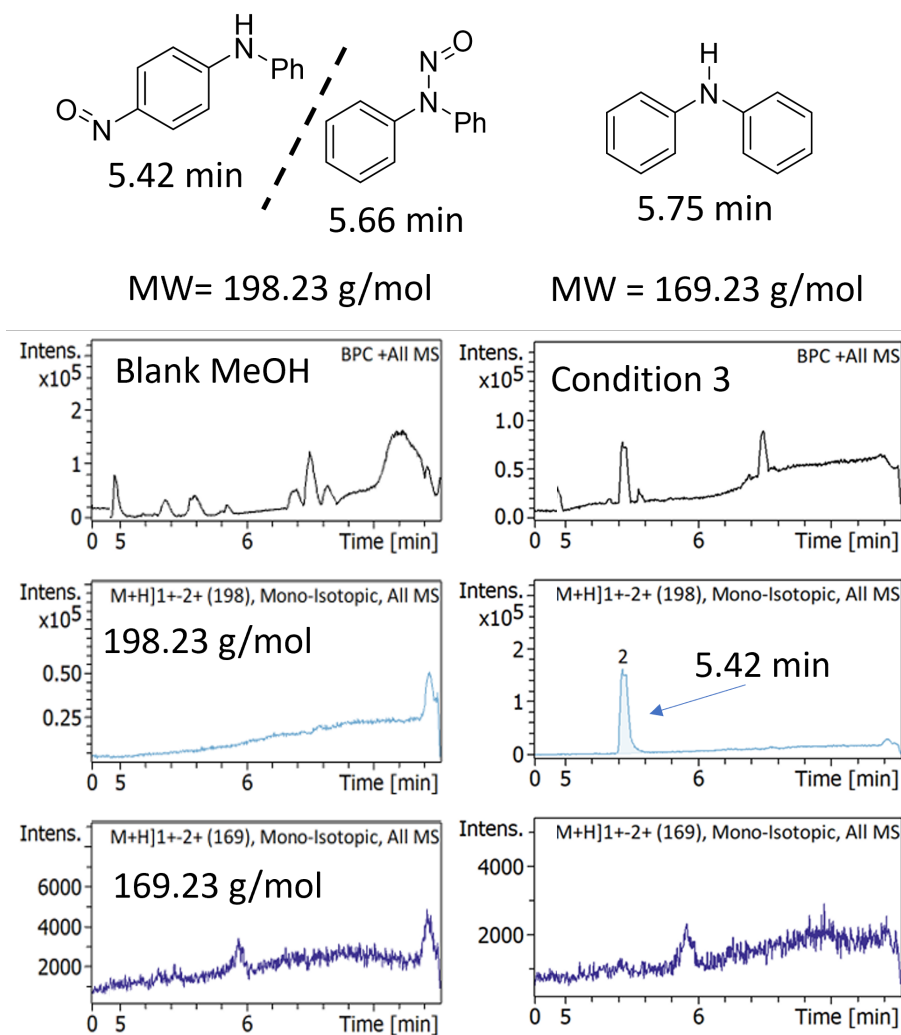


Figure 3.27: LC-MS/MS results for N4 reactivity under condition 3.

Finally, conditions 6 and 7 yielded the rearrangement product and the amine product in absence of the starting material (Figure 3.28).



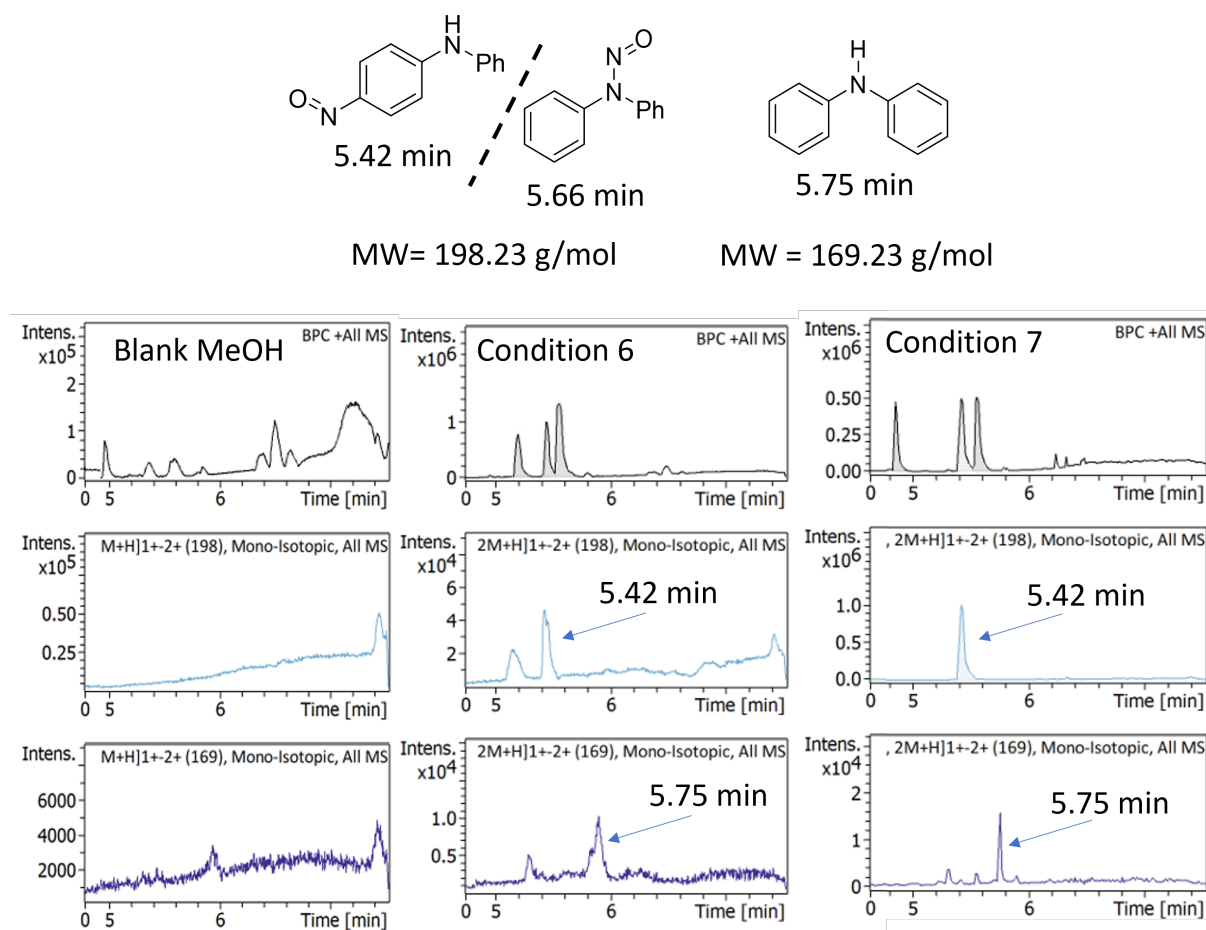


Figure 3.28: LC-MS/MS results for N4 reactivity under conditions 6 and 7.

The found products of N4 in condition 3 and condition 6 and 7 goes against the work of Williams *et al.*[45] who stated that the *p*-nitroso (Fischer-Hepp) product is the major product when water is present due to the solvation of the nucleophile, though the reaction times in this work are much longer. The fact that the Fischer-Hepp product is present in all of the acidic conditions after a longer reaction time than has been previously studied is not surprising as the Fischer-Hepp reaction is irreversible.

### N5 in conditions 3 and 6

Low conversion was seen with N5 in condition 3, and yet the GC-MSMS analysis method was unable to pick up the starting material or the reaction products. It was first thought that the aqueous sodium hydroxide used in the quench caused ring-opening at the ethereal oxygen, though no ring opening product peak was observed by GC-MS/MS, but this may have been too polar to be extracted into the ethyl acetate in the mini work-up.

To further these investigations, as reaction occurred with N5 in condition 6, the reaction was repeated and crude NMR analysis confirmed that the parent amine (morpholine) was the product of the reaction (Figure 3.29). Assignment of the NMR spectrum can be found in Appendix Figure J.3.

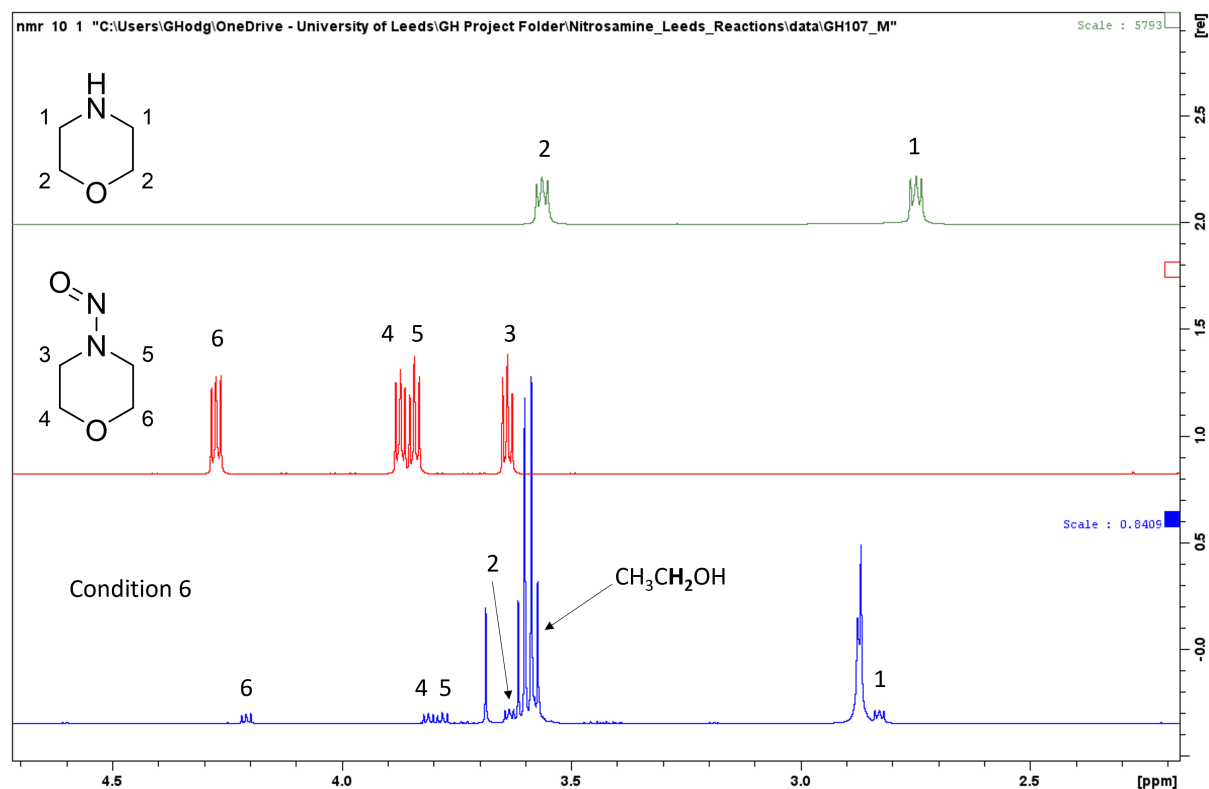


Figure 3.29:  $^1\text{H}$  NMR of the crude reaction mixture for N5 in condition 6.

### N8 in condition 3

26 % conversion was seen with N8 in condition 3, yet again no product was seen by GC-MS/MS or LC-MS/MS (Figure 3.30). The conversion was low in this case and the GC-FID response of the amine product 2-(ethylamino)ethanol is also low so it was assumed that the low concentration of product was undetectable using the GC-MS/MS regime. LC-MS/MS was therefore performed and again no product was seen. It is hypothesised that the retention time of the amine product would be very low due to the high polarity of the product and would therefore come off in the solvent front and be undetectable by LC-MS/MS.

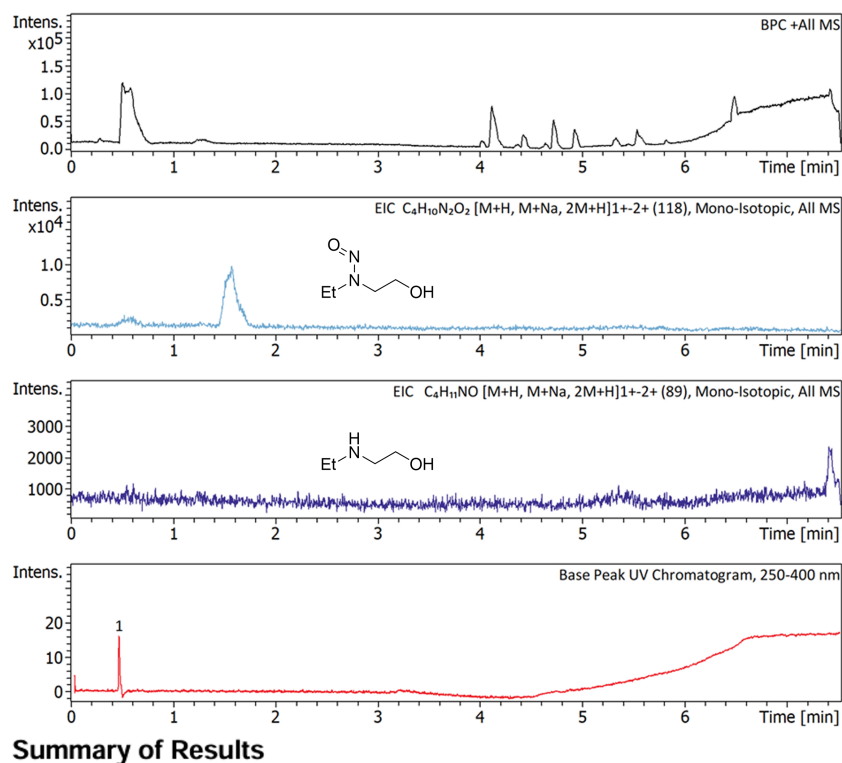


Figure 3.30: LC-MS/MS results for N8 reactivity under condition 3.

When the temperature was increased to 50 °C in condition 7 in with ethanol as the solvent, the dialkyl nitrosamines started to show conversion to their corresponding amines. This is exemplified by the GC-MS/MS chromatogram for N3 (*N*-nitrosodibutylamine) (Figure 3.31) and the LC-MS/MS chromatogram for N7 (*N*-butyl-*N*-(4-hydroxybutyl)nitrosamine) (Figure 3.32) which clearly show the amine product.

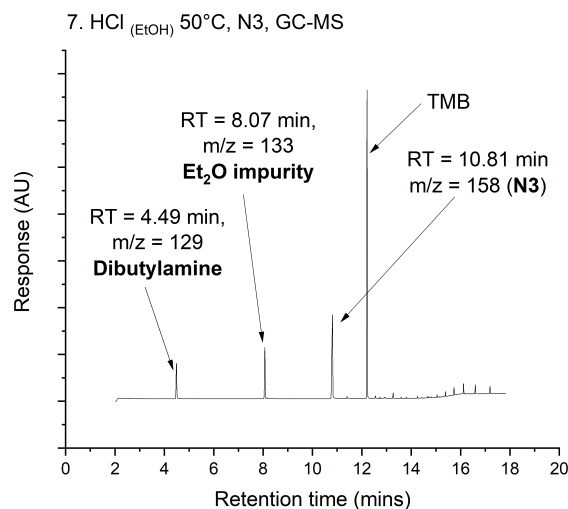
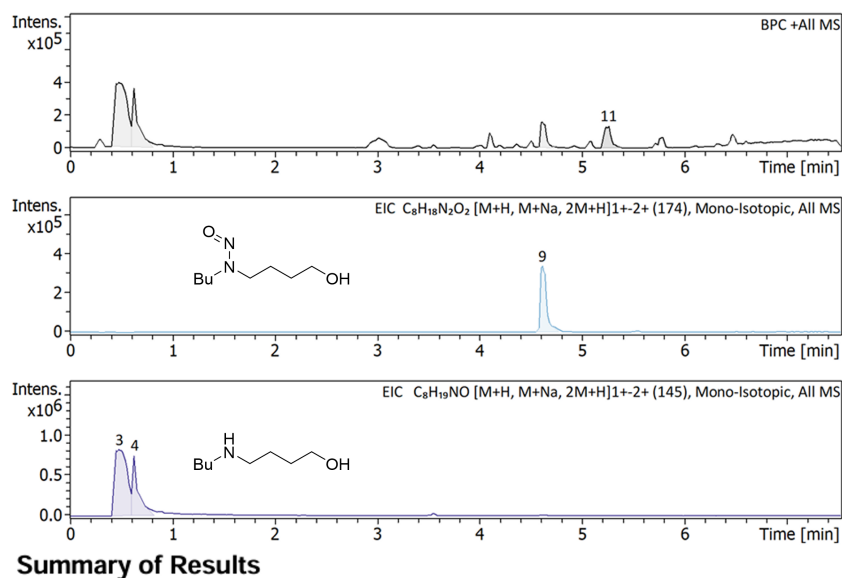


Figure 3.31: GC-MS/MS chromatogram for N3 in condition 7 showing the amine product.



#### Summary of Results

Name	RT	BPC Area(%)	UV Area(%)	Confirm Formula Results
Cmpd 3, 0.5 min	0.48	59.0	30.6	C8H19NO
Cmpd 4, 0.6 min	0.63	22.3	no peak	C8H19NO
Cmpd 9, 4.6 min	4.61	9.1	35.9	C8H18N2O2
Cmpd 11, 5.3 min	5.26	9.6	no peak	

Figure 3.32: LC-MS/MS chromatogram for N7 in condition 7 showing the amine product.

The improvement in reactivity from condition 5 to condition 7 supports the claim of Williams *et al.* [47] who stated that the solvation of the chloride anion was integral to the rate of reaction. [47] By removing the water in the system the chloride is free to attack at N=O and produce the amine products with reasonable conversion after 16 h. For condition 7, an attempt at determining the products in the cases of N1-3 and N5-N8 by GC-MSMS was successful in some

cases, with the amine products for N3, N6 and N7 being found. The reason for the other amines being absent from the GC-MS/MS analysis is a combination of two things; the first is that diethylamine has a low boiling point (55.5 °C) and likely evaporates after it is produced. The second thing is that while all the amines are likely protonated, for the smaller amines (N2, N3, N5, N8) it is likely that because these amines have a smaller hydrophobic portion, they are more soluble in the aqueous phase during sample preparation so they are not extracted into ethyl acetate and therefore are not seen on the GC chromatogram. For condition 7, N7 and N8 were analysed by LC-MS/MS as the GC-MS/MS analysis showed no products. The retention time of the parent amine of N7 was *ca.* 0.6 mins, it is assumed that the amine product of N8 has a shorter retention time and thus comes off the column with the solvent front and was therefore undetectable. Nonetheless, the conclusions from the amine products of N3 and N7 can be generalised and applied to N1,2,5 and 7, since these form a representative set for the dialky nitrosamines and for the  $\alpha$ -hydroxyalkyl; alkyl nitrosamines.

#### Hydride reductants (conditions 8 - 10):

The reaction with the highest count in the data analysis chapter of this work was the hydride reduction of *N*-nitrosamines by  $\text{LiAlH}_4$  to give hydrazines and amines. There is little literature representation of the other common hydride donor reductants diisobutylaluminium hydride (DiBAL-H) and sodium borohydride ( $\text{NaBH}_4$ ), though DiBAL-H has been proven to reduce benzylic *N*-nitrosamines to their corresponding hydrazines with reasonable yields (*ca.* 50%) after 2 h in dichloromethane, though the resulting hydrazines are prone to over reduction at extended reaction times (>2 h). [132]

No evidence of reactivity has been reported for  $\text{NaBH}_4$ , and the results of the reactivity screen show reaction with only N4 and N6 (Figure 3.33 (a)), producing the corresponding amine in the case of N4 (figure 3.34) with low conversion of the starting material (23 %).

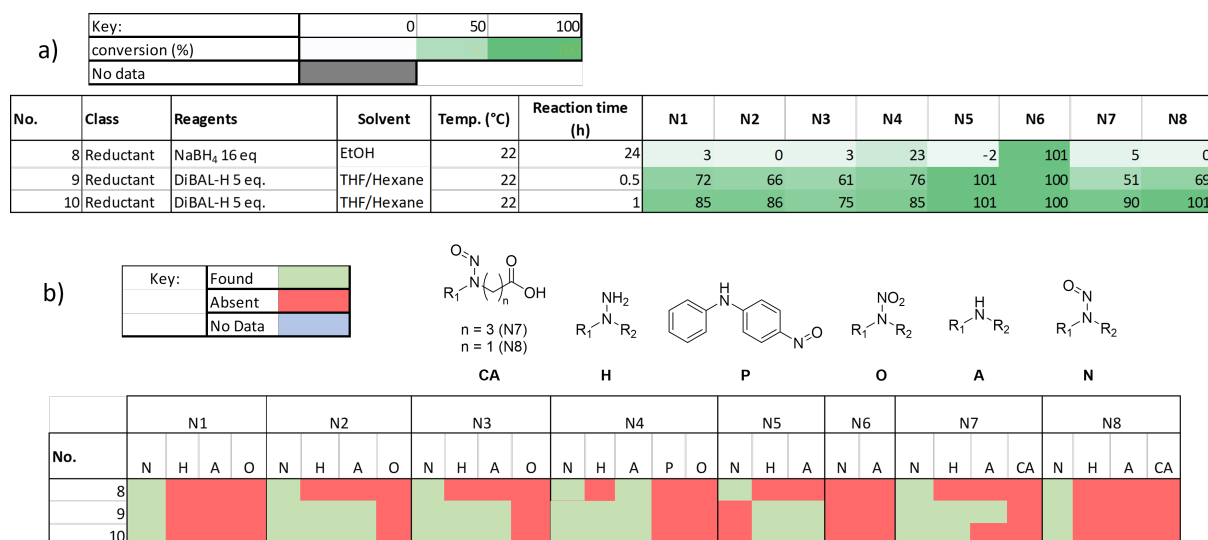
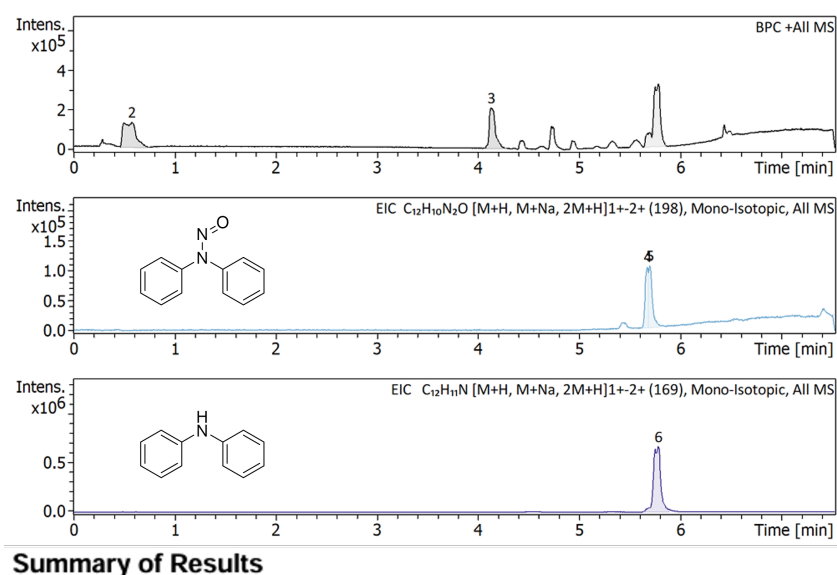


Figure 3.33: Reactivity of *N*-nitrosamines with hydride reductants in conditions 8-10. a) Conversions with respect to the nitrosamine and b) Products of the reactions determined by GC-MS/MS and LC-MS/MS.



#### Summary of Results

Name	RT	BPC Area(%)	UV Area(%)	Confirm Formula Results
Cmpd 2, 0.6 min	0.58	30.7	no peak	
Cmpd 3, 4.1 min	4.13	24.5	no peak	
Cmpd 4, 5.7 min	5.67	no peak	no peak	C12H10N2O
Cmpd 5, 5.7 min	5.70	no peak	no peak	C12H10N2O
Cmpd 6, 5.8 min	5.78	44.8	no peak	C12H11N

Figure 3.34: LC-MS/MS chromatogram for *N*-nitrosodiphenylamine (N4) in reaction condition 8.

With N6, the results of the flow reaction performed at the ROAR facility at ICL is confirmed, with complete conversion of the starting material. The *N*-methylethylcarbamate peak is absent from the GC-MS/MS chromatogram (Figure 3.35), indicating that it is also reduced by NaBH<sub>4</sub>.

As explained in Section 3.4, it is plausible that this reaction is facilitated by the presence of the electron withdrawing nitroso (N=O) group, which allows for reduction by NaBH<sub>4</sub> at the more electrophilic carbamate carbonyl carbon.

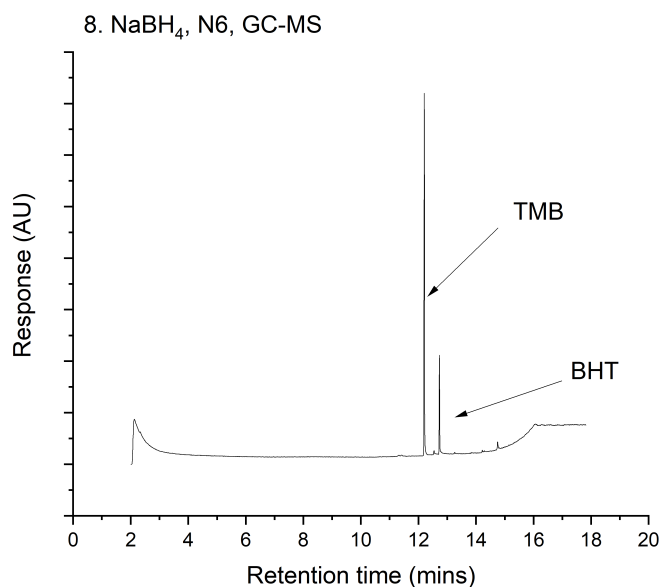


Figure 3.35: GC-MS/MS chromatogram for N6 in condition 8 showing the complete reduction of the nitrosamine.

Improved results were seen with DiBAL-H, and the amine and hydrazine products were found for N4 in both reactions with DiBAL-H (Figure 3.36).

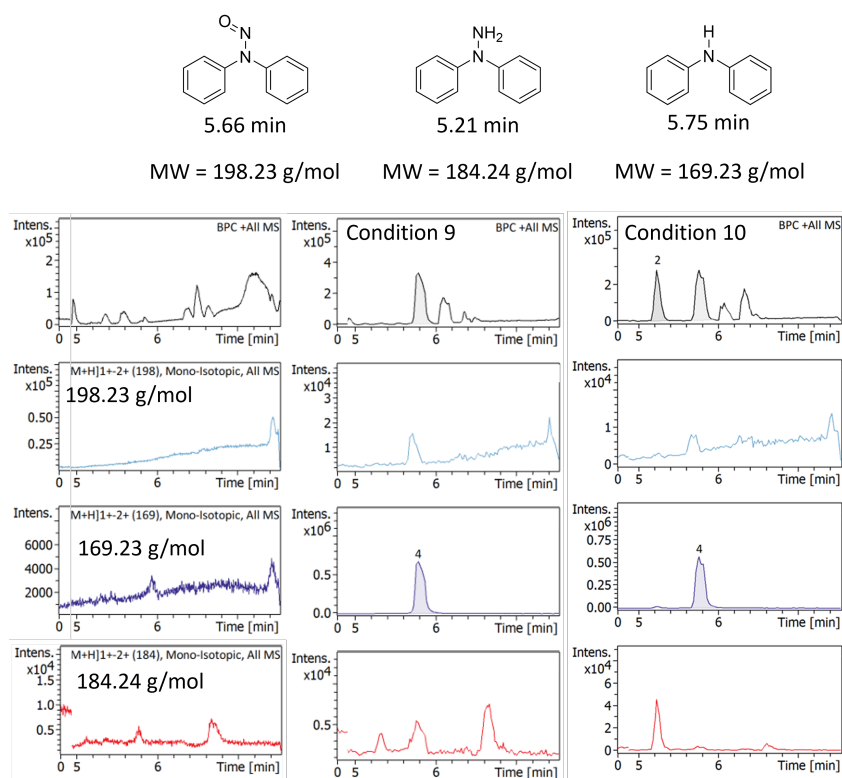


Figure 3.36: LC-MS/MS summary for N4 in conditions 9 and 10.

The dialkyl nitrosamines were also converted into their corresponding amines and hydrazines (Figure 3.37). The problem from condition 7 of not being able to observe the hydrazines or amine product in the case of N1 was still present, even though no heat was applied to the system and no mini work-up was performed. It is hypothesised that the amine and hydrazine products are volatile compounds that evaporate in the time frame between quenching the reaction and analysis by GC-MS/MS. N6 showed complete conversion of the starting material and N-methylethylcarbamate again, though this is not surprising considering the result from Condition 8.



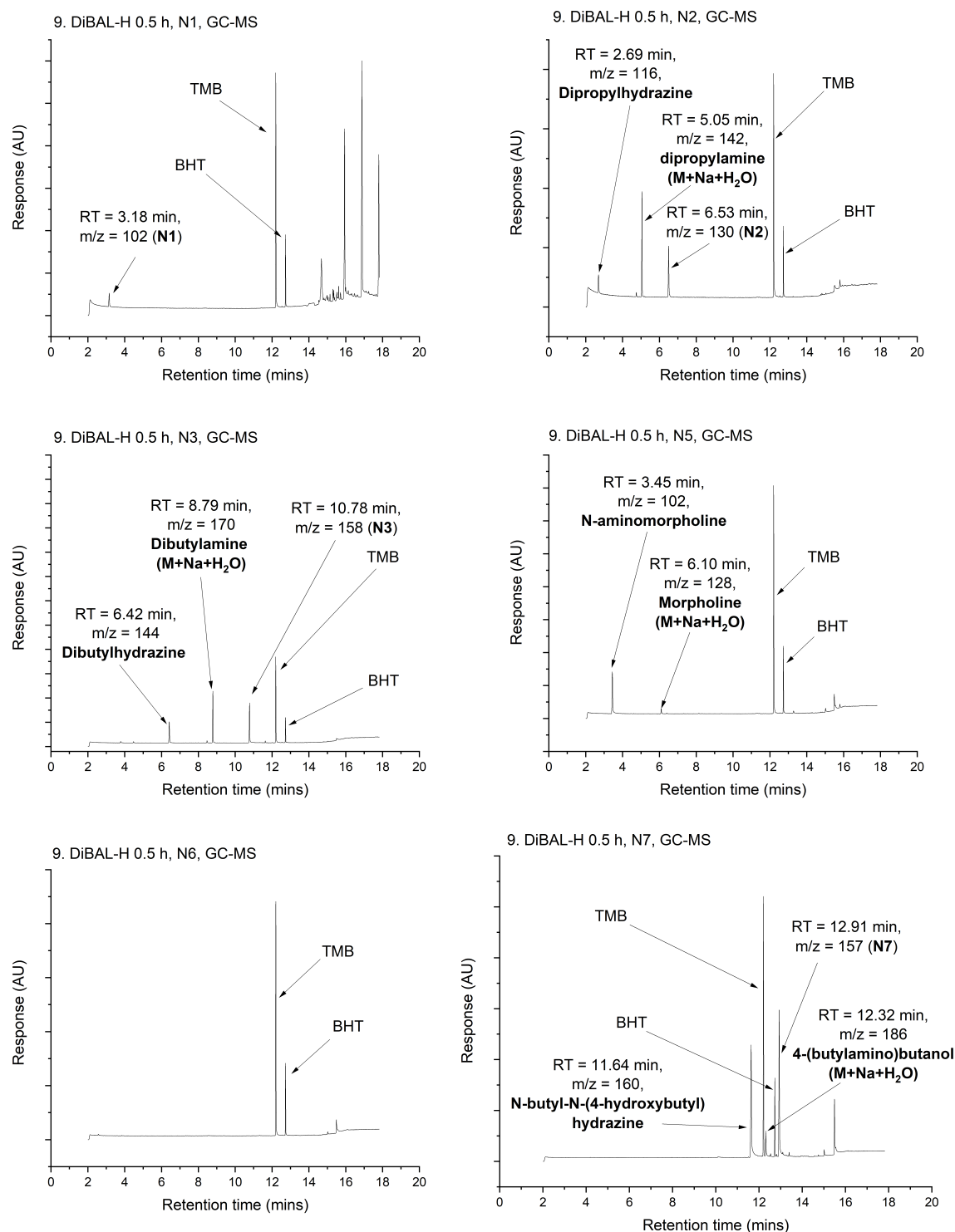
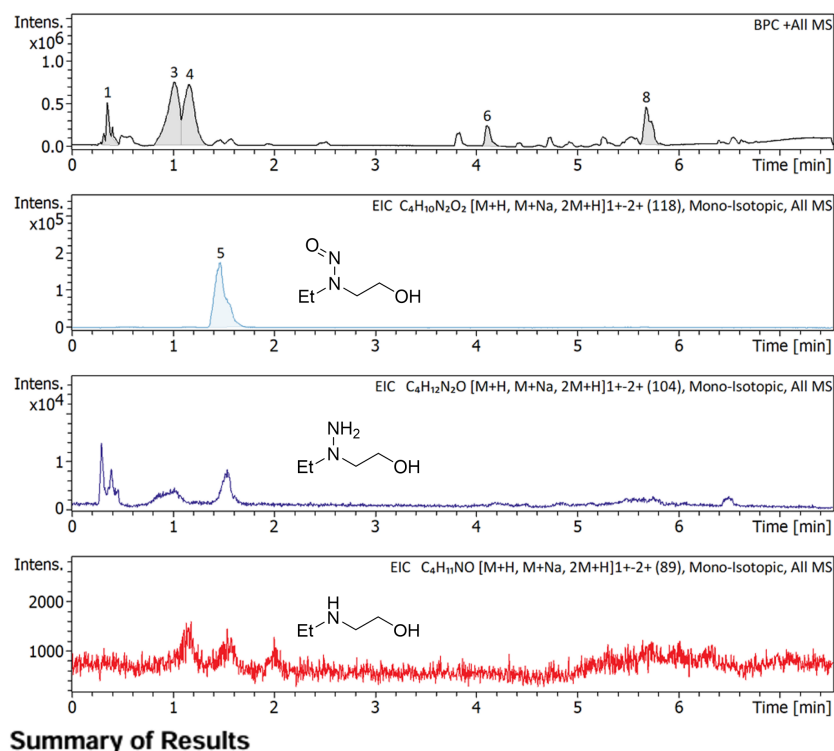


Figure 3.37: GC-MSMS plots for N1, N2, N3 and N5-7 for condition 9.

An unexpected product was seen in the case of N8. Upon further investigation by LC-MS/MS a peak with  $m/z = 160$  was found in the chromatogram (Peaks 3 and 4 in Figure 3.38). NMR of the crude reaction mixture was excessively complicated and purification by flash chromatography was made difficult by the lack of a chromophore in the amine product. The fact that this reaction

was not as clean as the others means it is not a suitable method to destroy this nitrosamine, and other alternatives should be sought in this case.



#### Summary of Results

Name	RT	BPC Area(%)	UV Area(%)	Confirm Formula Results
Cmpd 1, 0.4 min	0.36	7.9	no peak	
Cmpd 3, 1.0 min	1.01	37.9	no peak	
Cmpd 4, 1.2 min	1.17	34.3	no peak	
Cmpd 5, 1.5 min	1.47	no peak	no peak	C4H10N2O2, C4H10.5N2O2
Cmpd 6, 4.1 min	4.11	6.0	no peak	
Cmpd 8, 5.7 min	5.68	13.9	48.8	

Figure 3.38: LC-MS/MS experiment chromatogram for ethyl-*N*-(2-hydroxyethyl)nitrosamine (N8) in reaction condition 9.

#### Sulfur-based reductants (Conditions 11-19):

Though there were successes with DIBAL-H in conditions 9 and 10, this reductant isn't particularly tolerant to other functional groups. In fact, it is commonly known that DIBAL-H can reduce esters and amides to their corresponding aldehydes. As these functional groups are widely used in high-value chemical manufacture, it is important to seek alternatives to provide a milder, more selective route to reducing *N*-nitrosamines to less toxic products. Recent work by Chaudhary and coworkers discovered two metal-free routes to obtain hydrazines from aryl-*N*-nitrosamines, the first using thiourea dioxide in basic media at 50°C in methanol, and the second using triethylsilane and iodine at room temperature in dichloromethane. [33, 32] While their work is promising, the fact that they only showed successes on aryl nitrosamines

suggests that these conditions are too mild for dialkyl nitrosamines. Work from Overberger *et al.* showed, amongst other aryl and benzylic nitrosamines, one example of a cyclic nitrosamine being reduced to the hydrazine in moderate yield by sodium dithionite  $\text{Na}_2\text{S}_2\text{O}_4$  at  $60^\circ\text{C}$  with concentrated sodium hydroxide solution (20% wt. NaOH) and ethanol as a solvent. [34] This more promising result prompted an investigation into sodium dithionite as a broad-spectrum, mild reductant for *N*-nitrosamines. The conditions tested are summarised in Figure 3.39. In all cases 20 equivalents of the reductant was used.

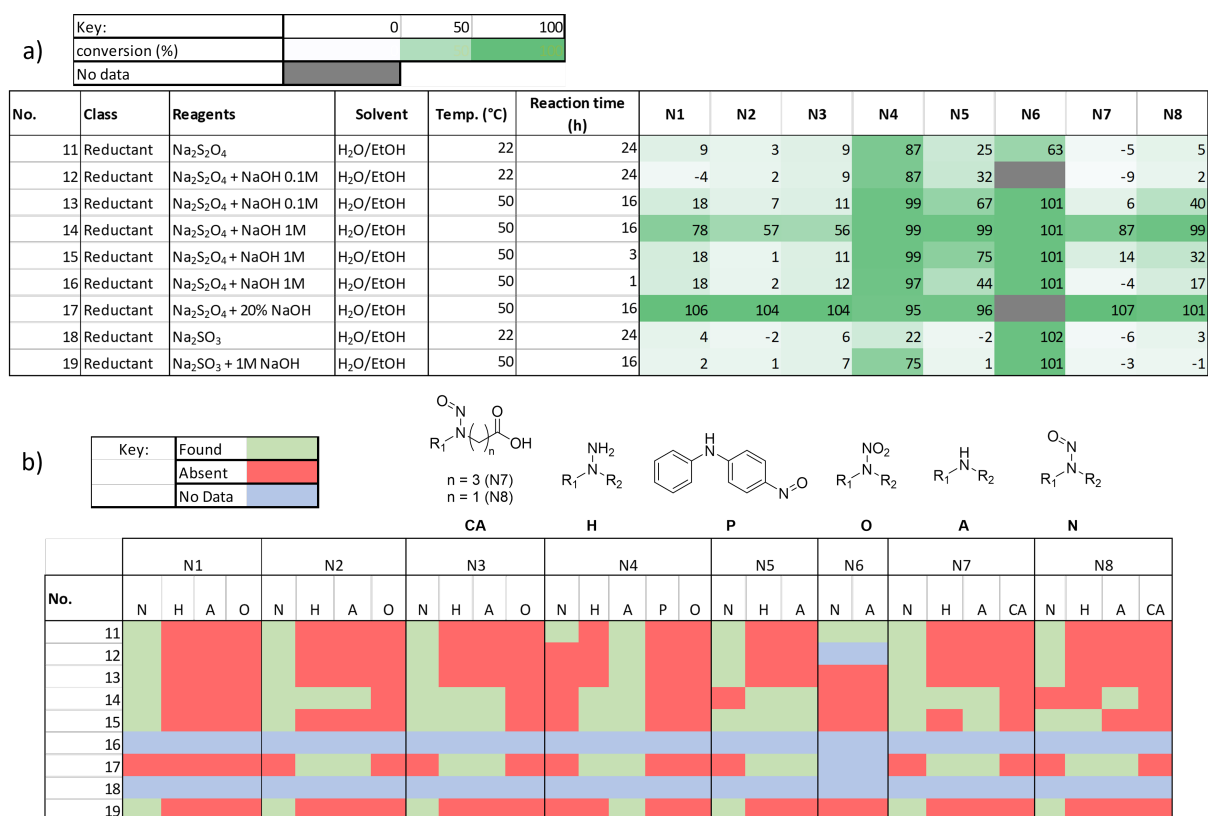
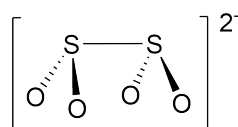
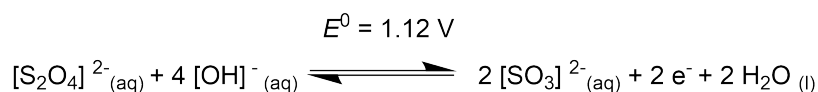


Figure 3.39: Reactivity of *N*-nitrosamines with sulfur-based reductants in conditions 11-19. a) Conversions with respect to the nitrosamine and b) Products of the reactions determined by GC-MS/MS and LC-MS/MS.

Starting with the conditions most similar to those used in Overberger's study (Condition 17),  $\text{Na}_2\text{S}_2\text{O}_4$  in aqueous NaOH (20% w/v) at  $50^\circ\text{C}$  showed complete conversion after 16 h. In each case the reaction produced both amines and hydrazines amines and hydrazines. LC-MS/MS analysis of N4 can be found in appendix Figure I.23 and GC-MS/MS analysis of the remaining nitrosamines can be found in appendix Figure G.21. While it is promising that the problematic dialkyl nitrosamines were converted under these conditions, the use of 20 % w/v NaOH (aq) is prohibitive in high-value chemical manufacture due to safety concerns and it being incompatible

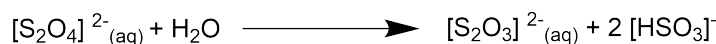
with many functional groups. The reason for the high sodium hydroxide concentration is that the redox potential of  $\text{Na}_2\text{S}_2\text{O}_4$  is increased in strongly basic media as per Scheme 3.5. The long S-S bond is weak and  $\text{Na}_2\text{S}_2\text{O}_4$  is oxidised to give  $\text{SO}_2$  in air, and reaction with water in neutral aqueous solutions destroys the reducing agent. [133]

a) Sodium dithionite redox reaction in basic media:

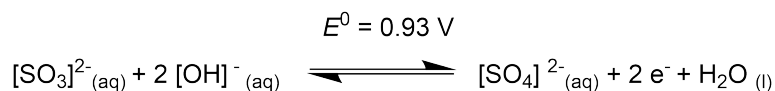


S-S = 239 pm  
S-O = 151 pm

b) Sodium dithionite reaction in water:



c) Sodium sulfite redox reaction in basic media:



Scheme 3.5: Redox reaction and cell potential for  $\text{Na}_2\text{S}_2\text{O}_4$  and  $\text{Na}_2\text{SO}_3$  in basic media.[133]

$\text{Na}_2\text{S}_2\text{O}_4$  in neutral media was tested in condition 11, though this only showed high conversion with N4 which produced the hydrazine product (Figure I.18). Increasing the pH of the solution with the addition of aqueous sodium hydroxide (1 mL, 1M) caused an improvement in conversion in the case of N5, but this coupled with additional heat in condition 13 started to show more promising results, with N8 showing 40 % and N1 showing 18% conversion. The best result was achieved when the  $\text{Na}_2\text{S}_2\text{O}_4$  solution was prepared in aqueous sodium hydroxide solution (1M), and the reaction was heated to 50°C (Condition 16). After 16 h, moderate conversion was seen with the dialkyl nitrosamines and the alkyl; hydroxyalkyl nitrosamines showed higher conversion. This result has introduced a more mild set of conditions that can be used to destroy *N*-nitrosamines, which can be tuned by altering the concentration of sodium hydroxide, to reduce a broad range of *N*-nitrosamines. The products of the reaction of N4 in condition 14 determined by LC-MS/MS are shown in Figure 3.40 and the GC-MS/MS results of the

remaining *N*-nitrosamines are shown in Figures 3.41 and 3.42

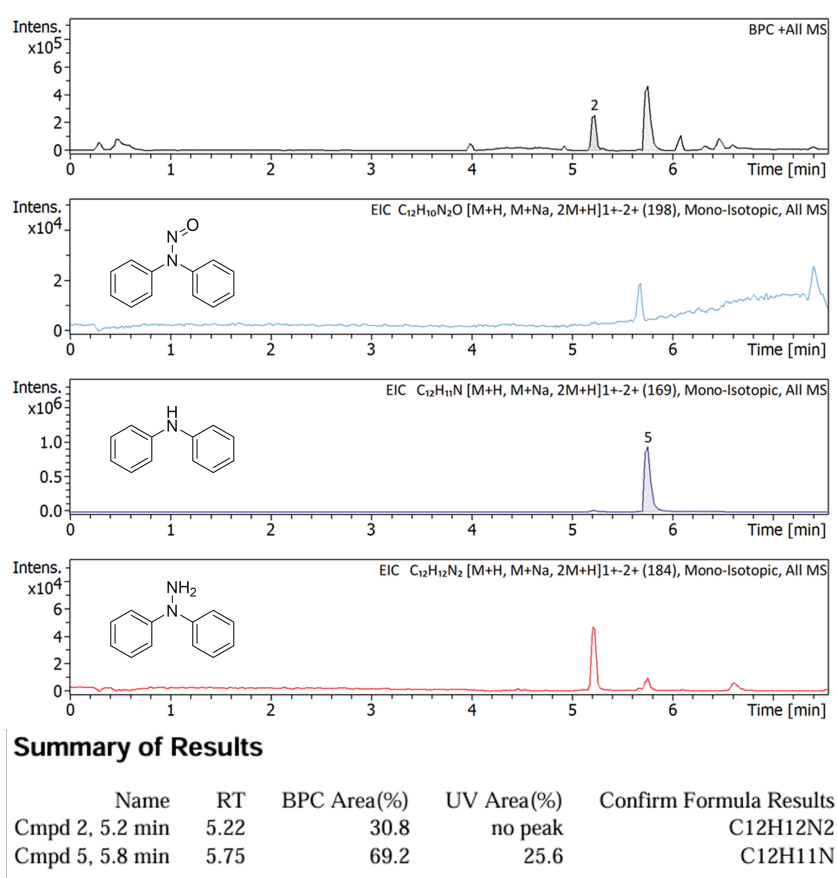


Figure 3.40: LC-MS/MS chromatogram for *N*-nitrosodiphenylamine (N4) in reaction condition 14.

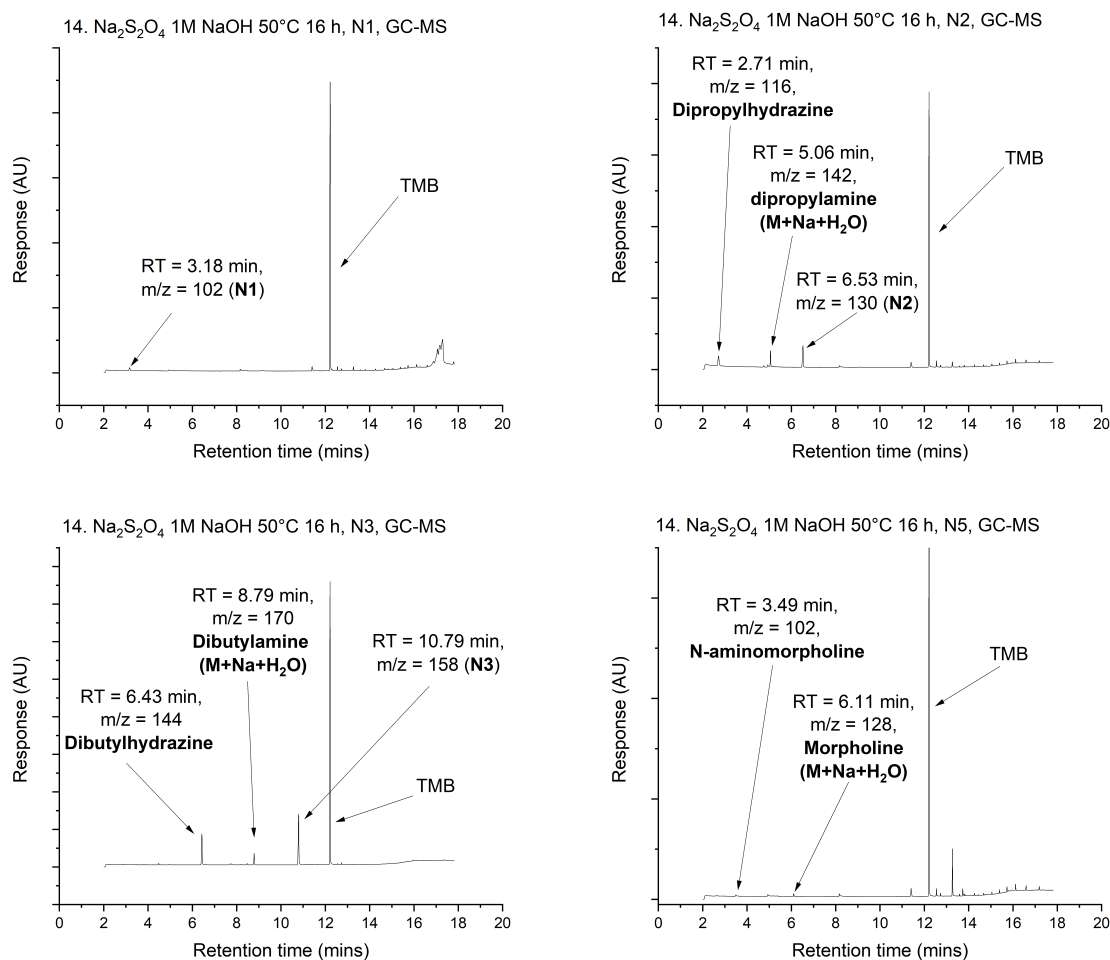


Figure 3.41: GC-MSMS plots for N1, N2, N3 and N5 condition 14. Jump back to experimental procedure 3.6

An attempt to use yet milder and cheaper conditions used sodium sulfite as the reductant. Which has a slightly lower reduction potential than sodium dithionite (Scheme 3.5). While low conversions with all nitrosamines but N6 were seen with a neutral solvent system (Condition 18), when the Na<sub>2</sub>SO<sub>3</sub> stock solution was prepared in NaOH (aq) N4 was converted to the amine product at 75% conversion of the starting material (Figure 3.43). This extremely mild reaction condition may be used if aryl nitrosamines are problematic during high-value chemical manufacture.

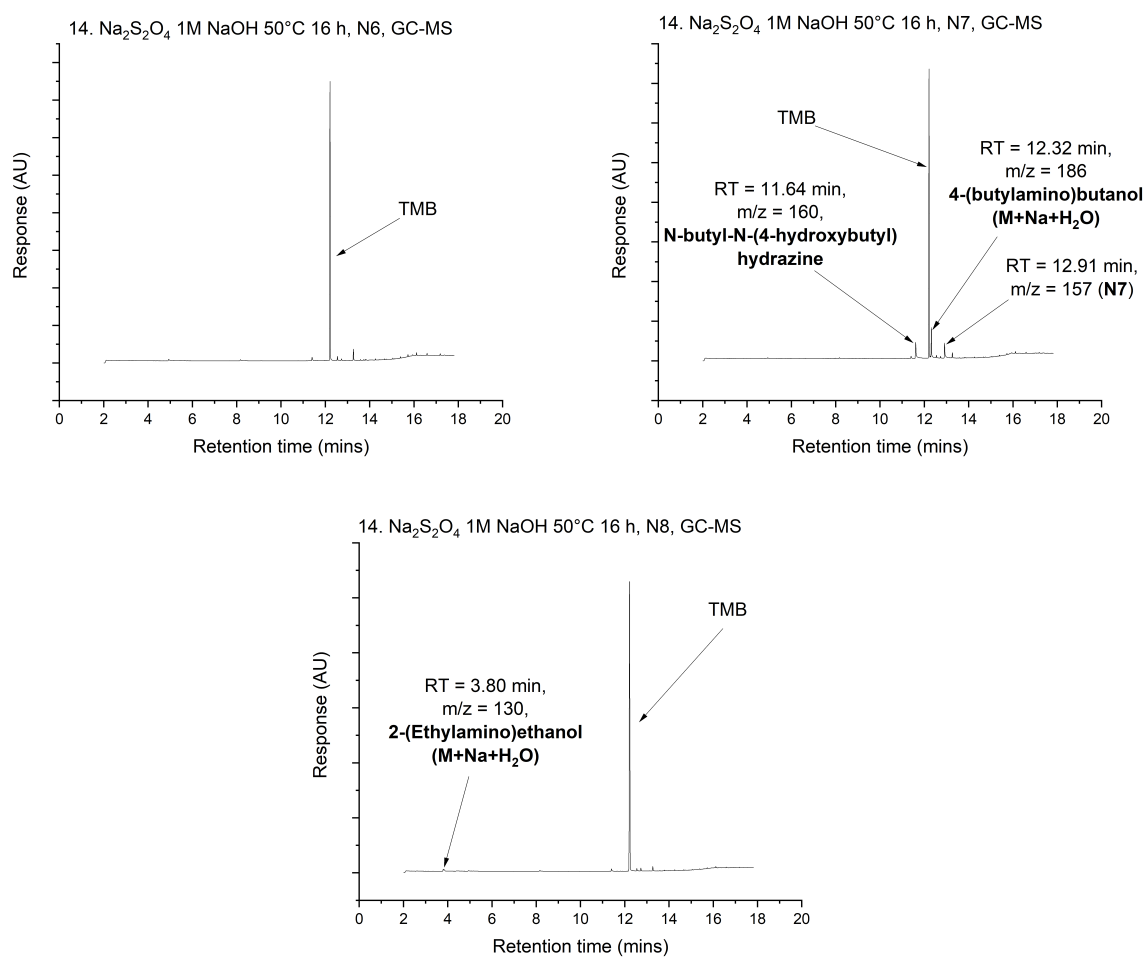


Figure 3.42: GC-MSMS plots for N6-N8 for condition 14.

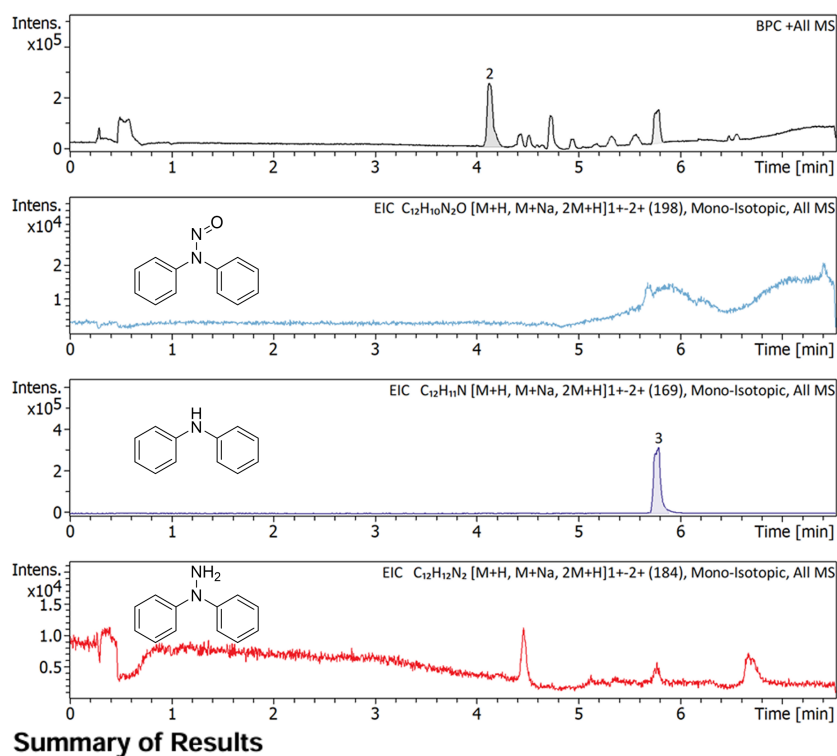


Figure 3.43: LC-MS/MS experiment chromatogram for *N*-nitrosodiphenylamine (N4) in reaction condition 19.

### 3.10 Conclusions

This chapter has expanded on the knowledge from Chapter two which highlighted that the general reactions of nitrosamines are reduction and denitrosation reactions. The set of conditions chosen was in response to the list provided by LHASA was filtered for reaction conditions that were too harsh, mild or already had literature data. This led to the construction of a tailored list of reaction conditions which sought to provide a broad spectrum method to destroy a wide range of structural classes of *N*-nitrosamine. This was achieved in four cases, with Condition 7 (ethanolic HCl (20 eq), 50°C, 16 h), Condition 10 (DiBAL-H (5 eq), THF, 22°C, 1 h), Condition 17 (Na<sub>2</sub>S<sub>2</sub>O<sub>4</sub> (20 eq), NaOH<sub>(aq)</sub> (20% w/v)/EtOH, 50°C, 16 h) and Condition 14 (Na<sub>2</sub>S<sub>2</sub>O<sub>4</sub> (20 eq), NaOH<sub>(aq)</sub> (1 M)/EtOH, 50°C, 16 h). It was found that although complete conversion was observed with the aryl nitrosamine (N4) in condition 7, the reaction produced multiple products amongst the expected rearrangement and denitrosation products. It is hence concluded that this condition is too harsh for aryl nitrosamines, and that alternatives should



be used if aryl nitrosamines are of concern in high-value chemical manufacture. Nevertheless, the dialkyl nitrosamines and alkyl; hydroxyalkyl nitrosamines showed good conversion to their amine products with no side reactions.

The many examples of reductions of *N*-nitrosamines in the data analysis in chapter two led to the selection of two hydride donor reductants in the reactivity screen, namely NaBH<sub>4</sub> and DiBAL-H. NaBH<sub>4</sub> was proven to be an excellent reductant for the *N*-nitrosocarbamate (N6) and the reaction conditions used in this study also led to reduction of the parent carbamate, though it is thought that these reaction conditions could be tuned to stop at the carbamate with fewer equivalents of the reductant. Low conversion (23%) was also seen with the aryl nitrosamine (N4), yielding the parent amine compound. DiBAL-H offered a much faster and effective method to reduce all the *N*-nitrosamines to their amine and hydrazine products, the current work expanded the substrate scope on literature which was performed on benzylic *N*-nitrosamines, and proved that dialkyl and alkyl; hydroxyalkyl nitrosamines are indeed reduced to their parent amines and hydrazines with high conversion after 1 h. N8 produced an unexpected product which was not verified in the timeframe of this project.

The success of DiBAL-H as a reductant is limited by its low functional group tolerance. As a result, milder alternatives were sought. Though recent work has found mild metal-free conditions for reducing aryl nitrosamines, the substrate scope is limited to this class.[32, 33] This led to the selection of Na<sub>2</sub>S<sub>2</sub>O<sub>4</sub> in basic media, as there was some evidence of reactivity with cyclic nitrosamines. [34] Though high conversions across all nitrosamines in the screen were seen under these conditions (condition 17), the limiting factor in the published method was the use of high concentrations (20% w/v) of sodium hydroxide used in the reaction to increase the redox potential of the reagent. This led to the refinement of the reaction conditions to use lower the concentration of sodium hydroxide. It was found that a concentration of 1 M was sufficient to provide reasonable conversion of the *N*-nitrosamines after 16 h at 50°C. This condition is acceptable for the aryl nitrosamine (N4) as the reaction is much cleaner and produces the amine and hydrazine products. Furthermore, yet milder conditions were attempted in conditions 18 and 19 which used Na<sub>2</sub>SO<sub>3</sub> as the reductant. These conditions were found to be sufficient for the reduction of N6 and N4, but better conversion was seen when the pH of the solution was decreased at elevated temperature in condition 19.

It is hoped that these results can aid reduce the risk of nitrosamine contamination in drug

products either by the application of the mild reaction conditions to remove nitrosamines with high tolerance for other functional groups, or through expanding the knowledge base of *in-silico* prediction tools such as Mirabilis to provide more confident predictions about nitrosamine purge during high-value chemical manufacture. [2]

## Chapter 4

# Final Conclusions and Future Work

This work has focussed on devising methods to control *N*-nitrosamine contamination in pharmaceutical products. Chapter 1 outlined the issues to human health posed by *N*-nitrosamines, and how the surrounding structural features can influence their toxicity and carcinogenicity. These slight structural changes can impact the stability of the nitrosamine both inside and outside of the human body, resulting in some *N*-nitrosamines being of less concern to the regulatory bodies than others. The new potency categories (set by the ICH) for *N*-nitrosamines were listed, and it was demonstrated that the number of important *N*-nitrosamines from a regulatory standpoint will likely increase in the near future. The current state-of-the-art method to circumvent the problem of large scale batch testing of potentially contaminated API's, ingredients and materials was outlined. Demonstrating the use of the *in-silico* tool Mirabilis, to successfully “de-risk” Candesartan of NDMA and NDEA contamination. Following this, the current knowledge base on *N*-nitrosamine reactivity was summarised from two leading reviews, discussing reactions with: reductants, oxidants, acids, bases, organolithium/Grignard reagents and photochemical reactions. It was noted that this knowledge base was focussed on the regulatorily important dialkyl nitrosamines, and is thus somewhat limited in scope. The aims of the project were two-fold: first, to expand on the current knowledge base of *N*-nitrosamine reactivity, including more structural classes of *N*-nitrosamine. The expanded knowledge base can then be fed into the *in-silico* prediction tools in order to improve risk assessment of *N*-nitrosamine contamination. Second, to find methods to destroy *N*-nitrosamines that are not specific to one structural class, with a focus on mild conditions with high functional group tolerance that can be applied in the later stages of API syntheses.

Chapter two was primarily focussed on addressing the first of the projects aims. Taking a cheminformatics approach, the available reactions on *N*-nitrosamines were downloaded from the Reaxys database. Python scripts were written to extract the relevant information, and clean up the data by removing entries with invalid SMILES codes and also reordering the reagents column to remove common solvents. These processes helped downstream removal of duplicates from the final dataset. Before this, the dataset needed to be pruned to leave only those reactions which transformed/destroyed the characteristic N-N=O group shared by all *N*-nitroso compounds. These reactions were found using a three stage process involving atom-atom mapping (AAM), reaction centre extraction and reaction centre parsing. For AAM, the reaction decoder tool was used, and the output file was passed directly to the ReactionCode software to generate machine readable text strings representative of the atoms and bonds that changed in the reaction (the reaction centre). SMARTS strings of the reaction centre were generated, which could then be parsed in python to reveal whether or not the N-N=O atoms were involved in the products i.e. whether or not the reaction occurred at N-N=O. The atom map numbers were used to find which atoms to search for. The resulting dataset after duplicate removal based on reagents and reaction centres contained 1080 reactions. The workflow itself is a significant contribution to the cheminformatics community, as it allows for extraction of useful data for reactions of a particular class which can support dataset generation for machine learning algorithms for applications such as reaction outcome prediction.

The resulting dataset of 1080 reactions that consumed *N*-nitrosamines in some way was then manually classified. Manual classification was selected mainly due to poor data quality of the reactions in the dataset. A two stage classification based on three subclasses was devised. The three subclasses were concerned with classifying the structural class of nitrosamine, the transformation occurring during the reaction, and the reagents used. The initial subclasses were then grouped together in the second stage of classification, leading to 7 structural classes of *N*-nitrosamine, 10 transformation classes and 21 reagent classes. The unique structure: transformation: reagent classes with count above 3 were considered for analysis to ensure confidence in the discussions, this left 651 reactions. Within the dataset of 651 reactions were many reactions which had already been covered, a large proportion of the *N*-nitrosamines were aryl nitrosamines of which the chemistry has been extensively studied. Where this work gains significance is highlighting examples of reactivity on more exotic structural classes of *N*-nitrosamine, and new examples of reactivity for the heavily studied classes of nitrosamine. The chemistry

of electrophilic nitrosamines, defined in the text as an *N*-nitrosamine with an electrophilic centre in the  $\alpha$  position were shown to primarily form diazonium ions upon reaction with base, a number of nucleophiles, and applied heat. This is problematic for API syntheses, as adverse modifications to the API could occur due to alkylation reactions between the API and the *in-situ* generated diazonium ions. *N*-nitrosamines with  $\beta$ -carboxylic acid and  $\beta$ -cyano groups showed different chemistry to the more common aryl and dialkyl nitrosamines. For these classes of *N*-nitrosamine, the reported reactions captured by the cheminformatics workflow involved ring formation reactions (to sydnones and sydnone imines) with acylating reagents (sydnones) and upon heating under basic conditions (sydnone imines). These reactions may serve as protecting reactions for the *N*-nitroso functional group, which may lead to  $\beta$ -carboxylic acid and  $\beta$ -cyano becoming important from a regulatory standpoint in the future. For the more well known aryl and dialkyl nitrosamines, the cheminformatics workflow uncovered reactions that were not discussed in the two reviews of *N*-nitrosamine reactivity. Firstly, azo-formation reactions on aryl nitrosamines can occur *via* a two step process which involves an initial Fischer-Hepp rearrangement of the aryl nitrosamine, to form the *p*-nitroso compound, which then reacts with an amine under acidic conditions to produce the azo compound. Note that azo formations can also occur with electrophilic nitrosamines under basic conditions in the presence of arenes. Furthermore, diazonium formation from  $\beta$ -unsaturated alkyl nitrosamines can occur via an E2 elimination mechanism under strongly basic conditions, this reaction is important from a regulatory standpoint as it is an overlooked method of purging alkyl nitrosamines. After discussion of the chemistry unveiled by the cheminformatics workflow, a summary was made on the various structural features which governed reactivity with various reagents. A few key features were highlighted, including the ortho-position of aryl nitrosamines for C-H activation by transition metal catalysts, the  $\alpha$ -hydrogen for denitrosation to oxoimines and the influence of electron withdrawing substituents on denitrosation reactions. Finally, promising reaction conditions for destroying multiple classes of nitrosamine were sought; and though none were found in the dataset, the conclusion was that most of the conditions that destroyed more than one class of nitrosamine were applicable to dialkyl nitrosamines, and any reactivity screen should consider dialkyl nitrosamines in the first instance.

Chapter 3 was focussed on the second aim of the project: to find methods to destroy *N*-nitrosamines that are not specific to one structural class, with a focus on mild conditions with high functional group tolerance that can be applied in the later stages of API syntheses. The re-

activity investigations began with the purchase of eight commercially available *N*-nitrosamines, six of which could be classified as dialkyl nitrosamines, with one electrophilic and one aryl nitrosamine. With safety in mind, the initial screening reactions were performed in flow at the ROAR facility at ICL. Unfortunately, the methods used in these initial investigations were limited to measure only short reaction times, as the comparison between a reference injection with no reagent vs a reaction injection with the reagent had to be made in the same run. This is due to slight modifications in the instrument setup upon resetting which had to be performed after roughly 8 hours, causing variations in peak intensity. This had a large impact on the weakly intense peak for N=O that was measured during the reactions. However, one significant result was obtained for the reaction of N6 (*N*-methyl-*N*-nitrosourethane) and sodium borohydride. After a 1 minute residence time, both the N=O and C=O bonds were consumed. This indicates that the electron withdrawing nitroso-group facilitates hydride addition to the carbamate C=O and subsequent decomposition, most likely *via* loss of an aldehyde, similar to the mechanism seen in the metabolic degradation pathway of dialkyl *N*-nitrosamines. This is a significant finding as BOC protected amines are not usually susceptible to cleavage *via* reductive amination.

Reactivity investigations then turned to a batch reaction campaign, with special measures in place to ensure safety and minimal handling of *N*-nitrosamines (spill tray, butyl rubber gloves, stock solutions, quenching of unreacted *N*-nitrosamines). In total 21 reaction conditions were tested. Reaction conditions were selected based on a list of common reaction/workup conditions used in process chemistry supplied by LHASA, and evidence from the classification of literature reactions performed in Chapter 2. The selected conditions included mild reductive, oxidative, acidic and basic conditions. Four broad spectrum methods of destroying *N*-nitrosamines were found, that are milder reaction conditions than previously reported. Namely, these reaction conditions are as follows: 1. Ethanolic hydrogenchloride (HCl) at 50°C for 16 hours at 20 molar equivalents of HCl, 2. Diisobutylaluminium hydride (DiBAL-H) (5 molar equivalents) in tetrahydrofuran (THF) at room temperature for 1 hour, 3. Sodium dithionite (20 molar equivalents) in 20% w/v sodium hydroxide (NaOH) at 50°C for 16 hours, 4. Sodium dithionite (20 molar equivalents) in 1 M NaOH at 50°C for 16 hours. The reaction conditions that were the most effective were DiBAL-H and sodium dithionite in 20% w/v NaOH<sub>(aq)</sub>. However, DiBAL-H has a low functional group tolerance and is therefore likely to interfere with the API if applied in the later stages of API synthesis, and the 20% w/v NaOH<sub>(aq)</sub> solution used with sodium dithionite has safety implications and causes the reaction to suffer from poor atom economy.

The tunable redox potential of sodium dithionite was leveraged, and it was found that using 1 M NaOH<sub>(aq)</sub> was sufficient to provide high conversion of the nitrosamines to their parent amines and hydrazines. Furthermore, heating *N*-nitrosamines in ethanolic HCl caused denitrosation with high conversions after 16 h. The existing knowledge on the mechanism of nitrosamine denitrosation was utilised to produce a reaction condition that affects more classes than just the reported aryl nitrosamines. Overall, the second aim of the project has been achieved, with multiple reaction conditions that can fit a variety of needs in a synthetic sense.

The cheminformatics guided classification of *N*-nitrosamine reactivity could be used in the future to create a web-based tool for initial estimations of *N*-nitrosamine reactivity, whereby the user inputs a structure, and the tool outputs the various reaction pathways that have been reported. This tool, and the data from the classification itself could also supplement purge based prediction tools such as Mirabilis, by improving the knowledge base of reactivity.

The reactivity screen discovered that sodium dithionite under mildly basic conditions was able to reduce *N*-nitrosamines with high conversion. Future investigations could delve into the minimum redox potential required to reduce each class of *N*-nitrosamine. This would allow for highly specific reaction conditions to be developed, that are capable of reducing *N*-nitrosamines to safer products, while leaving important functional groups in the API untouched. Finally, it would be beneficial to study the kinetics of the reactions which were successful in consuming *N*-nitrosamines. The reactivity screen was strict in keeping long reaction times for comparison between conditions, and to ensure reactivity was captured where feasible. The next step would be to calculate the rates of these reactions, to properly assess them as suitable conditions for removing *N*-nitrosamines on an industrial scale.

# References

- [1] U.S. Food and Drug Administration. *FDA Updates and Press Announcements - Angiotensin II Receptor Blocker (ARB) Recalls (Valsartan, Losartan)*. Accessed on: 2024-02-16. URL: <https://www.fda.gov/drugs/drug-safety-and-availability/fda-updates-and-press-announcements-angiotensin-ii-receptor-blocker-arb-recalls-valsartan-losartan#5cc3b83d3b22e%7D>.
- [2] Michael J Burns, Andrew Teasdale, Eric Elliott, and Chris G Barber. “Controlling a cohort: use of mirabilis-based purge calculations to understand nitrosamine-related risk and control strategy options”. In: *Organic Process Research & Development* 24.8 (2020), pp. 1531–1535.
- [3] Christopher J Borths, Michael Burns, Timothy Curran, and Nathan D Ide. “Nitrosamine reactivity: a survey of reactions and purge processes”. In: *Organic Process Research & Development* 25.8 (2021), pp. 1788–1801.
- [4] Jessica C Beard and Timothy M Swager. “An organic chemist’s guide to N-nitrosamines: their structure, reactivity, and role as contaminants”. In: *The Journal of Organic Chemistry* 86.3 (2021), pp. 2037–2057.
- [5] Bernt Krebs and Jürgen Mandt. “Kristallstruktur des N-Nitrosodimethylamins”. In: *Chemische Berichte* 108.4 (1975), pp. 1130–1137.
- [6] Kenneth B Wiberg, Paul R Rablen, Daniel J Rush, and Todd A Keith. “Amides. 3. Experimental and theoretical studies of the effect of the medium on the rotational barriers for N, N-dimethylformamide and N, N-dimethylacetamide”. In: *Journal of the American Chemical Society* 117.15 (1995), pp. 4261–4270.



- [7] Catharine E Looney, WD Phillips, and EL Reilly. “Nuclear magnetic resonance and infrared study of hindered rotation in nitrosamines”. In: *Journal of the American Chemical Society* 79.23 (1957), pp. 6136–6142.
- [8] Eswara Raju Kosuri, Mayank Bhanti, Mrunal A Jaywant, Mark Han, Xiaochun Wang, and Marcus Obeng. “A GC-MS/MS Method for Trace Level Quantification of Six Nitrosamine Impurities (NDMA, NDEA, NEIPA, NDIPA, NDPA, and NDBA) in Commercially Used Organic Solvents: Dichloromethane, Ethyl Acetate, Toluene, and O-xylene”. In: *Journal of Pharmaceutical Sciences* 112.5 (2023), pp. 1225–1230.
- [9] Farzad Malihi and Tao Wang. “An improved analytical method for quantitation of nitrosamine impurities in ophthalmic solutions using liquid chromatography with tandem mass spectrometry”. In: *Journal of Chromatography Open* 2 (2022), p. 100037.
- [10] Larry K Keefer, Joseph A Hrabie, Bruce D Hilton, and David Wilbur. “Nitrogen protonation of N-nitrosodimethylamine”. In: *Journal of the American Chemical Society* 110.22 (1988), pp. 7459–7462.
- [11] Peter N Magee and JM Barnes. “The production of malignant primary hepatic tumours in the rat by feeding dimethylnitrosamine”. In: *British journal of Cancer* 10.1 (1956), p. 114.
- [12] Larry K Keefer, Joseph A Hrabie, Bruce D Hilton, and David Wilbur. “Nitrogen protonation of N-nitrosodimethylamine”. In: *Journal of the American Chemical Society* 110.22 (1988), pp. 7459–7462.
- [13] William Lijinsky. “Structure-activity relations in carcinogenesis by N-nitroso compounds”. In: *Cancer and Metastasis Reviews* 6 (1987), pp. 301–356.
- [14] U.S. Food and Drug Administration. *FDA Updates and Press Announcements - Angiotensin II Receptor Blocker (ARB) Recalls*. Accessed on: 15/02/2024. 2024. URL: <https://www.fda.gov/drugs/drug-safety-and-availability/fda-updates-and-press-announcements-angiotensin-ii-receptor-blocker-arb-recalls-valsartan-losartan#5cc3b83d3b22e>.

- [15] S. Nianping, P. Wang, W. Zhang, and Z. Xiaoren. “Improved method for preparing tetrazole for valsartan”. Patent CN104045602A. Zhejiang Huahai Pharmaceutical Co Ltd. <https://patents.google.com/patent/CN104045602A/en>. Sept. 2014.
- [16] Joerg Schlingemann, Michael J Burns, David J Ponting, Carolina Martins Avila, Naiffer E Romero, Mrunal A Jaywant, Graham F Smith, Ian W Ashworth, Stephanie Simon, Christoph Saal, et al. “The landscape of potential small and drug substance related nitrosamines in pharmaceuticals”. In: *Journal of Pharmaceutical Sciences* 112.5 (2023), pp. 1287–1304.
- [17] Fiona J King, Andrew D Searle, and Michael W Urquhart. “Ranitidine—investigations into the root cause for the presence of N-nitroso-N, N-dimethylamine in ranitidine hydrochloride drug substances and associated drug products”. In: *Organic Process Research & Development* 24.12 (2020), pp. 2915–2926.
- [18] International Council for Harmonisation of Technical Requirements for Pharmaceuticals for Human Use. *ICH M7(R1) Guideline*. Accessed on: May 8, 2024. 2024. URL: [https://database.ich.org/sites/default/files/M7\\_R1\\_Guideline.pdf](https://database.ich.org/sites/default/files/M7_R1_Guideline.pdf).
- [19] Andrew Teasdale, Simon Fenner, Andrew Ray, Agnes Ford, and Andrew Phillips. “A tool for the semiquantitative assessment of potentially genotoxic impurity (PGI) carryover into API using physicochemical parameters and process conditions”. In: *Organic Process Research & Development* 14.4 (2010), pp. 943–945.
- [20] Emil Fischer. “Ueber die Hydrazinverbindungen der Fettreihe”. In: *Berichte der Deutschen Chemischen Gesellschaft* 9.1 (1876), pp. 111–116.
- [21] Akira Nakao, Hiroko Suzuki, Hiroaki Ueno, Hiroshi Iwasaki, Tomofumi Setsuta, Akiko Kashima, and Shinji Sunada. “Discovery and structural analyses of S-adenosyl-L-homocysteine hydrolase inhibitors based on non-adenosine analogs”. In: *Bioorganic & Medicinal Chemistry* 23.15 (2015), pp. 4952–4969.
- [22] Dan-Dan Li, Yi-Xuan Cao, and Guan-Wu Wang. “Palladium-catalyzed ortho-acyloxylation of N-nitrosoanilines via direct sp<sup>2</sup> C–H bond activation”. In: *Organic & Biomolecular Chemistry* 13.25 (2015), pp. 6958–6964.

- [23] Weiqing Yang, Xiang Lu, Tingting Zhou, Yongjing Cao, Yuanyuan Zhang, and Menglin Ma. “Selective reduction of N-nitroso aza-aliphatic cyclic compounds to the corresponding N-amino products using zinc dust in CO<sub>2</sub>-H<sub>2</sub>O medium”. In: *Chemistry of Heterocyclic Compounds* 54 (2018), pp. 780–783.
- [24] Ian D Entwistle, Robert AW Johnstone, and Anna H Wilby. “Metal-assisted reactions—Part 11: Rapid reduction of N-nitrosoamines to N, N-disubstituted hydrazines; the utility of some low-valent titanium reagents”. In: *Tetrahedron* 38.3 (1982), pp. 419–423.
- [25] Palle E. Iversen. “Organic Electrosyntheses. III. Reduction of N-Nitrosamines”. In: *Acta Chemica Scandinavica* 25 (1971), pp. 2337–2340. DOI: 10.3891/acta.chem.scand.25-2337.
- [26] PROMEGA CORP, CORONA, CESEAR, KLAUBERT, DIETER, and MCDUGALL, MARK. “Reactive Cyanine Compounds”. 2011026085A2. Published as EP2473563A2, EP2473563B1, JP2013503209A, JP5730311B2, US2011053162A1, US8309059B2, WO2011026085A2, WO2011026085A3. Mar. 2011.
- [27] Patricia Bataille, Michel Paterne, and Eric Brown. “Enantioselective syntheses of  $\alpha$ -phenylalkanamines via intermediate addition of Grignard reagents to chiral hydrazones derived from (R)-(-)-2-aminobutan-1-ol”. In: *Tetrahedron: Asymmetry* 9.12 (1998), pp. 2181–2192.
- [28] Huan Chen, Ting Li, Fang Jiang, and Zhe Wang. “Enhanced catalytic reduction of N-nitrosodimethylamine over bimetallic Pd-Ni catalysts”. In: *Journal of Molecular Catalysis A: Chemical* 421 (2016), pp. 167–177.
- [29] Xiangchen Huo, Jinyong Liu, and Timothy J Strathmann. “Ruthenium catalysts for the reduction of N-nitrosamine water contaminants”. In: *Environmental Science & Technology* 52.7 (2018), pp. 4235–4243.
- [30] Matthew G Davie, Kaimin Shih, Federico A Pacheco, James O Leckie, and Martin Reinhard. “Palladium- indium catalyzed reduction of N-nitrosodimethylamine: Indium as a promoter metal”. In: *Environmental Science & Technology* 42.8 (2008), pp. 3040–3046.

- [31] Andrew J Frierdich, John R Shapley, and Timothy J Strathmann. “Rapid reduction of N-nitrosamine disinfection byproducts in water with hydrogen and porous nickel catalysts”. In: *Environmental Science & Technology* 42.1 (2008), pp. 262–269.
- [32] Priyanka Chaudhary, Surabhi Gupta, Popuri Sureshbabu, Shahulhameed Sabiah, and Jeyakumar Kandasamy. “A metal free reduction of aryl-N-nitrosamines to the corresponding hydrazines using a sustainable reductant thiourea dioxide”. In: *Green Chemistry* 18.23 (2016), pp. 6215–6221.
- [33] Priyanka Chaudhary, Rishi Korde, Surabhi Gupta, Popuri Sureshbabu, Shahulhameed Sabiah, and Jeyakumar Kandasamy. “An efficient metal-free method for the denitrosation of aryl N-nitrosamines at room temperature”. In: *Advanced Synthesis & Catalysis* 360.3 (2018), pp. 556–561.
- [34] CG Overberger, Joseph G Lombardino, and Richard G Hiskey. “Novel reductions of N-nitrosodibenzylamines—a new reaction<sup>1</sup>”. In: *Journal of the American Chemical Society* 80.12 (1958), pp. 3009–3012.
- [35] Alfred Schmidpeter. “1Reaktionen von Nitrosaminen mit elektrophilen, I die Alkylierung von Nitrosaminen”. In: *Tetrahedron Letters* 4.21 (1963), pp. 1421–1424.
- [36] Siegfried Hünig, Gerhard Büttner, Jürgen Cramer, Lothar Geldern, Hanspeter Hansen, and Eberhard Lücke. “Alkoxy-diazenium-Salze, I. Synthese und allgemeine Eigenschaften”. In: *Chemische Berichte* 102.6 (1969), pp. 2093–2108.
- [37] Lena Ohannesian and Larry K Keefer. “Displacement of O-versus N-substituents from nitrosamine-derived diazenium ions by three divergent mechanisms”. In: *Tetrahedron Letters* 29.24 (1988), pp. 2903–2906.
- [38] Dieter Seebach and Dieter Enders. “Reaction of Metalated Nitrosamines with Nitriles. A New Method for Preparation of v-Triazoles”. In: *Angewandte Chemie International Edition in English* 11.12 (1972), pp. 1102–1103.
- [39] F. W. Bergstrom and W. Conard. Fernelius. “The Chemistry of the Alkali Amides. II.” In: *Chemical Reviews* 20.3 (1937), pp. 413–487. DOI: 10.1021/cr60067a003.

- [40] Heinrich Wieland and Hans Fressel. "Versuche zur Darstellung von Derivaten des Oxyhydrazins". In: *Berichte der Deutschen Chemischen Gesellschaft* 44.1 (1911), pp. 898–904.
- [41] Alvaro J Vazquez, Cristian Rodriguez, and N Sbarbati Nudelman. "Convenient methodology for the synthesis of trialkylhydrazines". In: *Synthetic Communications* 39.22 (2009), pp. 3958–3972.
- [42] Alvaro J Vazquez, Cristian Rodriguez, and N Sbarbati Nudelman. "The reaction of nitrosodicyclohexylamine with organolithiums". In: *Journal of Physical Organic Chemistry* 21.12 (2008), pp. 1098–1104.
- [43] Peter R Farina and Howard Tieckelmann. "Reactions of Grignard reagents with nitrosamines". In: *The Journal of Organic Chemistry* 40.8 (1975), pp. 1070–1074.
- [44] Peter R Farina and Howard Tieckelmann. "Reactions of organolithium compounds with nitrosamines". In: *The Journal of Organic Chemistry* 38.25 (1973), pp. 4259–4263.
- [45] Ian D. Biggs and D. Lyn H. Williams. "Kinetics and mechanism of the Fischer-Hepp rearrangement and denitrosation. Part V. The mechanism of denitrosation". In: *J. Chem. Soc., Perkin Trans. 2* (2 1975), pp. 107–111. DOI: 10.1039/P29750000107.
- [46] Leslie R. Dix, Shirlene M. N. Y. F. Oh, and D. Lyn H. Williams. "Denitrosation of nitrosamines—a quantitative study. Reactions of N-methyl-N-nitrosoaniline, N-nitrosoproline, dimethylnitrosamine and N-nitrososarcosine". In: *J. Chem. Soc., Perkin Trans. 2* (8 1991), pp. 1099–1104. DOI: 10.1039/P29910001099. URL: <http://dx.doi.org/10.1039/P29910001099>.
- [47] Shivraj S Johal, D Lyn H Williams, and Erwin Buncel. "Kinetics and mechanism of the denitrosation of nitrosamines in ethanol". In: *Journal of the Chemical Society, Perkin Transactions 2* 1 (1980), pp. 165–169.
- [48] D. Lyn H. Williams. "Kinetics and mechanism of the Fischer-Hepp rearrangement and denitrosation. Part 10. Reactions of 3-methoxy-N-methyl-N-nitrosoaniline". In: *J. Chem. Soc., Perkin Trans. 2* (7 1982), pp. 801–804. DOI: 10.1039/P29820000801.

- [49] William D. Emmons. “Peroxytrifluoroacetic Acid. I. The Oxidation of Nitrosamines to Nitramines1”. In: *Journal of the American Chemical Society* 76.13 (1954), pp. 3468–3470. DOI: 10.1021/ja01642a029. eprint: <https://doi.org/10.1021/ja01642a029>. URL: <https://doi.org/10.1021/ja01642a029>.
- [50] RG Gafurov, EM Sogomonyan, and LT Eremenko. “Conversion of nitrosamines to nitramines”. In: *Bulletin of the Academy of Sciences of the USSR, Division of Chemical Science* 22 (1973), pp. 2764–2764.
- [51] Megan H Plumlee and Martin Reinhard. “Photochemical attenuation of N-nitrosodimethylamine (NDMA) and other nitrosamines in surface water”. In: *Environmental Science & Technology* 41.17 (2007), pp. 6170–6176.
- [52] Mihaela I Stefan and James R Bolton. “UV direct photolysis of N-nitrosodimethylamine (NDMA): Kinetic and product study”. In: *Helvetica Chimica Acta* 85.5 (2002), pp. 1416–1426.
- [53] Yuan L. Chow. “Nitrosamine photochemistry. Reactions of aminium radicals”. In: *Accounts of Chemical Research* 6.10 (1973), pp. 354–360. DOI: 10.1021/ar50070a005. eprint: <https://doi.org/10.1021/ar50070a005>. URL: <https://doi.org/10.1021/ar50070a005>.
- [54] Michael J Burns, David J Ponting, Robert S Foster, Benjamin P Thornton, Naiffer E Romero, Graham F Smith, Ian W Ashworth, Andrew Teasdale, Stephanie Simon, and Joerg Schlingemann. “Revisiting the Landscape of Potential Small and Drug Substance Related Nitrosamines in Pharmaceuticals”. In: *Journal of Pharmaceutical Sciences* 112.12 (2023), pp. 3005–3011.
- [55] Daniel Probst, Philippe Schwaller, and Jean-Louis Reymond. “Reaction classification and yield prediction using the differential reaction fingerprint DRFP”. In: *Digital Discovery* 1 (2 2022), pp. 91–97. DOI: 10.1039/D1DD00006C. URL: <http://dx.doi.org/10.1039/D1DD00006C>.
- [56] Samuel Boobier, Yufeng Liu, Krishna Sharma, David RJ Hose, A John Blacker, Nikil Kapur, and Bao N Nguyen. “Predicting solvent-dependent nucleophilicity parameter

- with a causal structure property relationship”. In: *Journal of Chemical Information and Modeling* 61.10 (2021), pp. 4890–4899.
- [57] Connor W. Coley, Regina Barzilay, Tommi S. Jaakkola, William H. Green, and Klavs F. Jensen. “Prediction of Organic Reaction Outcomes Using Machine Learning”. In: *ACS Central Science* 3.5 (2017). PMID: 28573205, pp. 434–443. DOI: 10.1021/acscentsci.7b00064. eprint: <https://doi.org/10.1021/acscentsci.7b00064>. URL: <https://doi.org/10.1021/acscentsci.7b00064>.
- [58] *Reaxys: Chemistry Research Platform*. Accessed: 21/02/24. URL: <https://www.reaxys.com/#/search/quick>.
- [59] Daniel Mark Lowe. “Extraction of chemical structures and reactions from the literature”. PhD thesis. University of Cambridge, 2012.
- [60] David Weininger. “SMILES, a chemical language and information system. 1. Introduction to methodology and encoding rules”. In: *Journal of Chemical Information and Computer Sciences* 28.1 (1988), pp. 31–36. DOI: 10.1021/ci00057a005. eprint: <https://doi.org/10.1021/ci00057a005>. URL: <https://doi.org/10.1021/ci00057a005>.
- [61] Gian Marco Ghiandoni, Michael J Bodkin, Beining Chen, Dimitar Hristozov, James EA Wallace, James Webster, and Valerie J Gillet. “Development and application of a data-driven reaction classification model: comparison of an electronic lab notebook and medicinal chemistry literature”. In: *Journal of Chemical Information and Modeling* 59.10 (2019), pp. 4167–4187.
- [62] Nadine Schneider, Daniel M Lowe, Roger A Sayle, and Gregory A Landrum. “Development of a novel fingerprint for chemical reactions and its application to large-scale reaction classification and similarity”. In: *Journal of Chemical Information and Modeling* 55.1 (2015), pp. 39–53.
- [63] Philippe Schwaller, Daniel Probst, Alain C Vaucher, Vishnu H Nair, David Kreutter, Teodoro Laino, and Jean-Louis Reymond. “Mapping the space of chemical reactions using attention-based neural networks”. In: *Nature Machine Intelligence* 3.2 (2021), pp. 144–152.

- [64] Joseph L Durant, Burton A Leland, Douglas R Henry, and James G Nourse. “Reoptimization of MDL keys for use in drug discovery”. In: *Journal of Chemical Information and Computer Sciences* 42.6 (2002), pp. 1273–1280.
- [65] David Rogers and Mathew Hahn. “Extended-connectivity fingerprints”. In: *Journal of Chemical Information and Modeling* 50.5 (2010), pp. 742–754.
- [66] Wendy A Warr. “A short review of chemical reaction database systems, computer-aided synthesis design, reaction prediction and synthetic feasibility”. In: *Molecular Informatics* 33.6-7 (2014), pp. 469–476.
- [67] Philippe Schwaller, Benjamin Hoover, Jean-Louis Reymond, Hendrik Strobelt, and Teodoro Laino. “Extraction of organic chemistry grammar from unsupervised learning of chemical reactions”. In: *Science Advances* 7.15 (2021), eabe4166.
- [68] Michael F Lynch and Peter Willett. “The automatic detection of chemical reaction sites”. In: *Journal of Chemical Information and Computer Sciences* 18.3 (1978), pp. 154–159.
- [69] Joannis Apostolakis, Oliver Sacher, Robert Körner, and Johann Gasteiger. “Automatic determination of reaction mappings and reaction center information. 2. Validation on a biochemical reaction database”. In: *Journal of Chemical Information and Modeling* 48.6 (2008), pp. 1190–1198.
- [70] Syed Asad Rahman, Gilliean Torrance, Lorenzo Baldacci, Sergio Martínez Cuesta, Franz Fenninger, Nimish Gopal, Saket Choudhary, John W. May, Gemma L. Holliday, Christoph Steinbeck, and Janet M. Thornton. “Reaction Decoder Tool (RDT): extracting features from chemical reactions”. In: *Bioinformatics* 32.13 (Feb. 2016), pp. 2065–2066. ISSN: 1367-4803. DOI: 10.1093/bioinformatics/btw096. eprint: [https://academic.oup.com/bioinformatics/article-pdf/32/13/2065/49019364/bioinformatics\\\_32\\\_13\\\_2065.pdf](https://academic.oup.com/bioinformatics/article-pdf/32/13/2065/49019364/bioinformatics\_32\_13\_2065.pdf). URL: <https://doi.org/10.1093/bioinformatics/btw096>.
- [71] Arkadii Lin, Natalia Dyubankova, Timur I. Madzhidov, Ramil I. Nugmanov, Jonas Verhoeven, Timur R. Gimadiev, Valentina A. Afonina, Zarina Ibragimova, Assima Rakhimbekova, Pavel Sidorov, Andrei Gedich, Rail Suleymanov, Ravil Mukhametgaleev, Joerg Wegner, Hugo Ceulemans, and Alexandre Varnek. “Atom-to-atom Mapping: A Bench-



- marking Study of Popular Mapping Algorithms and Consensus Strategies”. In: *Molecular Informatics* 41.4 (2022), p. 2100138. DOI: <https://doi.org/10.1002/minf.202100138>. eprint: <https://onlinelibrary.wiley.com/doi/pdf/10.1002/minf.202100138>. URL: <https://onlinelibrary.wiley.com/doi/abs/10.1002/minf.202100138>.
- [72] Syed Asad Rahman, Sergio Martinez Cuesta, Nicholas Furnham, Gemma L Holliday, and Janet M Thornton. “EC-BLAST: a tool to automatically search and compare enzyme reactions”. In: *Nature Methods* 11.2 (2014), pp. 171–174.
- [73] Clara D. Christ, Matthias Zentgraf, and Jan M. Kriegl. “Mining Electronic Laboratory Notebooks: Analysis, Retrosynthesis, and Reaction Based Enumeration”. In: *Journal of Chemical Information and Modeling* 52.7 (2012). PMID: 22657734, pp. 1745–1756. DOI: 10.1021/ci300116p. eprint: <https://doi.org/10.1021/ci300116p>. URL: <https://doi.org/10.1021/ci300116p>.
- [74] Hans Kraut, Josef Eiblmaier, Guenter Grethe, Peter Löw, Heinz Matuszczyk, and Heinz Saller. “Algorithm for reaction classification”. In: *Journal of Chemical Information and Modeling* 53.11 (2013), pp. 2884–2895.
- [75] Marwin H. S. Segler and Mark P. Waller. “Neural-Symbolic Machine Learning for Retrosynthesis and Reaction Prediction”. In: *Chemistry - A European Journal* 23.25 (2017), pp. 5966–5971. DOI: <https://doi.org/10.1002/chem.201605499>. eprint: <https://chemistry-europe.onlinelibrary.wiley.com/doi/pdf/10.1002/chem.201605499>. URL: <https://chemistry-europe.onlinelibrary.wiley.com/doi/abs/10.1002/chem.201605499>.
- [76] Victorien Delannée and Marc C Nicklaus. “ReactionCode: format for reaction searching, analysis, classification, transform, and encoding/decoding”. In: *Journal of Cheminformatics* 12 (2020), pp. 1–13.
- [77] *NameRXN: Reaction Naming*. NextMove Software. 2024. URL: <https://www.nextmovesoftware.com/namerxn.html> (visited on 02/08/2024).

- [78] Leland McInnes, John Healy, and James Melville. “Umap: Uniform manifold approximation and projection for dimension reduction”. In: *arXiv preprint arXiv:1802.03426* (2018).
- [79] Janus Schreiber Larsen, Magnus Gustafsson, and Carsten Jessen. “A Phenyl Triazole Derivative and Its Use for Modulating the GABAA Receptor Complex”. Application EP2013063190W filed on June 25, 2013; Priority claimed from DKPA201270365A filed on June 26, 2012, and US201261664303P filed on June 26, 2012. Jan. 2014. URL: <https://patentscope.wipo.int/search/en/detail.jsf?docId=W02014001279>.
- [80] Dieter Seebach, Dieter Enders, Rolf Dach, and Reimund Pieter. “Reaktion metallierter Nitrosamine mit Nitrilen Eine neue Methode zur Darstellung von  $\nu$ -Triazolen”. In: *Chemische Berichte* 110.5 (1977), pp. 1879–1886.
- [81] YL Chow, NS Tam, and ACH Lee. “Photochemistry of nitroso compounds in solution. X. The reaction pattern of photo-excited nitrosamides”. In: *Canadian Journal of Chemistry* 47.13 (1969), pp. 2441–2448.
- [82] W Conard Fernelius and George W Watt. “Saponification of Diarylnitrosamines and Attempts to Prepare a Salt of Aquo-ammononitrous Acid”. In: *Journal of the American Chemical Society* 55.8 (1933), pp. 3482–3485.
- [83] Hai-Ming Guo, Li Cheng, Lin-Feng Cun, Liu-Zhu Gong, Ai-Qiao Mi, and Yao-Zhong Jiang. “L-Prolinamide-catalyzed direct nitroso aldol reactions of  $\alpha$ -branched aldehydes: a distinct regioselectivity from that with L-proline”. In: *Chemical Communications* 4 (2006), pp. 429–431.
- [84] Jun Luo, Zihao Lou, and Yu Zhang. “Ketoxime compound and synthesis method thereof”. CN109879774A. Published as CN109879774A. June 2019.
- [85] Luis Garcia-Rio, J Ramon Leis, M Elena Pena, and Emilia Iglesias. “Transfer of the nitroso group in water/AOT/isooctane microemulsions: intrinsic and apparent reactivity”. In: *The Journal of Physical Chemistry* 97.13 (1993), pp. 3437–3442.

- [86] Masayuki Tanno and SHOKO SUEYOSHI. “Preparation and properties of 3-alkyl-1-arylnitrosoureas and related compounds”. In: *Chemical and Pharmaceutical Bulletin* 35.4 (1987), pp. 1360–1371.
- [87] MICHIKO MIYAHARA, MAKOTO MIYAHARA, and SHOZO KAMIYA. “Action mechanism of anti-AH13 activity of 1, 3-diaryl-1-nitrosoureas and related compounds”. In: *Chemical and Pharmaceutical Bulletin* 32.2 (1984), pp. 564–570.
- [88] HU Daeniker. “Über eine neuartige Basen-katalysierte Umlagerung der Nitroso-Gruppe”. In: *Helvetica Chimica Acta* 47.1 (1964), pp. 33–46.
- [89] Karl Eiter, Klaus-Friedrich Hebenbrock, and Hans-Joachim Kabbe. “Neue offenkettige und cyclische  $\alpha$ -Nitrosaminoalkyl-äther”. In: *Justus Liebigs Annalen der Chemie* 765.1 (1973), pp. 55–77.
- [90] Xinwei Hu, Xun Chen, Youxiang Shao, Haisheng Xie, Yuanfu Deng, Zhuofeng Ke, Huanfeng Jiang, and Wei Zeng. “Co (III)-catalyzed coupling-cyclization of aryl C–H Bonds with  $\alpha$ -diazoketones involving wolff rearrangement”. In: *ACS Catalysis* 8.2 (2018), pp. 1308–1312.
- [91] J De Boer and HJ Backer. “Diazomethane: Methane, diazo-”. In: *Organic Syntheses* 36 (2003), pp. 16–16.
- [92] Ronald A Henry. “The Reaction of Amines with N-Methyl-N-nitroso-N'-nitroguanidine”. In: *Journal of the American Chemical Society* 72.7 (1950), pp. 3287–3289.
- [93] IP Klimenko, EV Shulishov, Yu V Tomilov, and OM Nefedov. “Generation and reactions of diazo-3, 3-dideuterio-2-methylidenecyclopropane and isomerization of 3”, 3"-dideuterio-2"-methylidenespiro [4, 5-dihydropyrazole-5, 1"-cyclopropanes] into isopropenylpyrazoles”. In: *Russian Chemical Bulletin* 52 (2003), pp. 659–664.
- [94] M Ye Xiacong, Andrei W Konradi, Jenifer Smith, Danielle L Aubele, Albert W Garofalo, Jennifer Marugg, Marty L Neitzel, Chris M Semko, Hing L Sham, Minghua Sun, et al. “Discovery of a novel sulfonamide-pyrazolopiperidine series as potent and efficacious  $\gamma$ -secretase inhibitors (Part II)”. In: *Bioorganic & Medicinal Chemistry Letters* 20.12 (2010), pp. 3502–3506.

- [95] Emil H White, Charles P Lewis, Max A Ribic, and Thomas J Ryan. "Deamination via nitrogen derivatives of sulfonic acids: N-alkyl-N-nitroso-4-toluenesulfonamides, N-alkyl-N-nitro-4-toluenesulfonamides, and N-alkyl-N'-(4-toluenesulfonyloxy) diimide N-oxides". In: *The Journal of Organic Chemistry* 46.3 (1981), pp. 552–558.
- [96] Tara E Agnew, Hyun-Joong Kim, and James C Fishbein. "Diazonium ion chemistry: replacement of H by alkyl at the central carbon accelerates an SN2 substitution reaction". In: *Journal of Physical Organic Chemistry* 17.6-7 (2004), pp. 483–488.
- [97] Hilmar Johannes Backer. "LXVIII.—Electro-reduction of alkylnitrosoamides". In: *Journal of the Chemical Society, Transactions* 101 (1912), pp. 592–599.
- [98] Peter J Giddings, D Ivor John, Eric J Thomas, and David J Williams. "Preparation of 6 $\alpha$ -monosubstituted and 6, 6-disubstituted penicillanates from 6-diazopenicillanates: reactions of 6-diazopenicillanates with alcohols, thiols, phenylseleninyl compounds, and allylic sulphides, and their analogues". In: *Journal of the Chemical Society, Perkin Transactions 1* (1982), pp. 2757–2766.
- [99] Daniel T. Glatzhofer, Raymond R. Roy, and Kimberly N. Cossey. "Conversion of N-Aromatic Amides to O-Aromatic Esters". In: *Organic Letters* 4.14 (2002). PMID: 12098244, pp. 2349–2352. DOI: 10.1021/ol1026051d. eprint: <https://doi.org/10.1021/ol1026051d>. URL: <https://doi.org/10.1021/ol1026051d>.
- [100] Núria Torra, Fèlix Urpí, and Jaume Vilarrasa. "N-nitrosation and N-nitration of lactams. From macrolactams to macrolactones". In: *Tetrahedron* 45.3 (1989), pp. 863–868.
- [101] Ingrid Mergelsberg, Heinz Langhals, and Christoph Rüchardt. "Nachweis von 4-Homocubyl-Carbenium-Ionen als reaktive Zwischenstufen". In: *Chemische Berichte* 116.1 (1983), pp. 360–366.
- [102] Lee Proctor. "A METHOD FOR THE PREPARATION OF DIAZOALKANES". WO2013110932A1. Published as CN104203907A; CN104203907B; DK2807145T3; EP2807145A1; EP2807145B1; ES2629100T3; HRP20170947T1; HUE033610T2; IN1703MUN2014A; LT2807145T; PL2807145T3; PT2807145T; RS56107B1; SI2807145T1; US2015038687A1; US9593073B2. Aug. 2013.

- [103] Shozo KAMIYA, Kentaro YAMAGUCHI, Makoto MIYAHARA, and Naoki MIYATA. “Cyclization of 1-Aryl-1-nitroso-3-(2-pyridymethyl) ureas to 2-Aryl-5-(2-pyridyl)-2, 4-dihydro-1, 2, 4-triazol-3-ones”. In: *Chemical and Pharmaceutical Bulletin* 38.12 (1990), pp. 3226–3229.
- [104] Xin-Feng Cui and Guo-Sheng Huang. “Rhodium-catalyzed tandem acylmethylation/annulation of N-nitrosoanilines with sulfoxonium ylides for the synthesis of substituted indazole N-oxides”. In: *Organic & Biomolecular Chemistry* 18.21 (2020), pp. 4014–4018.
- [105] Yury V Tomilov, Irina V Kostyuchenko, Evgeny V Shulishov, and Oleg M Nefedov. “Formation of cyclopropylazoarenes in the azo coupling reactions of the cyclopropane-diazonium ion with active aromatic compounds”. In: *Mendeleev Communications* 12.3 (2002), pp. 104–106.
- [106] MICHIKO MIYAHARA, MAKOTO MIYAHARA, and SHOZO KAMIYA. “Action mechanism of anti-AH13 activity of 1, 3-diaryl-1-nitrosoureas and related compounds”. In: *Chemical and Pharmaceutical Bulletin* 32.2 (1984), pp. 564–570.
- [107] JN Abrams. “Alternative method for the synthesis of triazenes from aryl diazonium salts”. In: *Tetrahedron* 89 (2021), p. 132185.
- [108] Oskar Nuyken, Jürgen Stebani, Alexander Wokaun, and Thomas Lippert. “Polymers with Triazene Units in the Main Chain: Application for Laser-Lithography”. In: *Macromolecular Engineering: Recent Advances* (1995), pp. 303–318.
- [109] Lienhard Hoesch. “1-Amino-2-phthalimido-diazen-1-oxide: Bildung, Eigenschaften und Fragmentierungen in Imido-und Amino-nitrene”. In: *Helvetica Chimica Acta* 64.3 (1981), pp. 890–904.
- [110] VG Yashunskii, VV Ogorodnikova, and LE Kholodov. “Preparation of sydnoneimines by basic cyclization of N-nitrosoaminoacetonitriles”. In: *Chemistry of Heterocyclic Compounds* 16.9 (1980), pp. 941–945.
- [111] Susana MM Lopes, Cátia FO Correia, Sandra CC Nunes, Nelson AM Pereira, Ana RF Ferreira, Emanuel P Sousa, Clara SB Gomes, Jorge AR Salvador, Alberto ACC Pais, and Teresa MVD Pinho e Melo. “Synthesis of chiral hexacyclic steroids via  $[8\pi + 2\pi]$

- cycloaddition of diazafulvenium methides”. In: *Organic & Biomolecular Chemistry* 13.34 (2015), pp. 9127–9139.
- [112] O Ao Litvinov, O No Kataeva, VA Naumov, GA Marchenko, and VI Kovalenko. “Molecular structure of the Z-isomer of N-methyl-N'-methoxy-diazene-N-oxide in the gas phase”. In: *Journal of Structural Chemistry* 29.3 (1988), pp. 469–471.
- [113] H Maskill, John T Thompson, and Alan A Wilson. “Solvolysis of secondary alkyl azoxytosylates. A new reaction related to solvolytic deamination and arenesulphonate solvolysis”. In: *Journal of the Chemical Society, Perkin Transactions 2* 10 (1984), pp. 1693–1703.
- [114] OA Luk'yanov, GA Smirnov, and PB Gordeev. “N'-tetrazolylmethoxyl derivatives of N-methyldiazene N-oxides”. In: *Russian Journal of Organic Chemistry* 43 (2007), pp. 1228–1231.
- [115] OA Luk'yanov and TI Zhiguleva. “Alkylation of silver salts of nitrosohydroxylamines by  $\alpha$ -halomethyl ethers and esters”. In: *Bulletin of the Academy of Sciences of the USSR, Division of chemical science* 31 (1982), pp. 1269–1270.
- [116] Tetsuji Itoh, Akira Takada, Katsuyuki Hirai, and Hideo Tomioka. “Preparation of sterically congested Di (4-pyridyl) diazomethanes and characterization of triplet carbenes from them”. In: *Organic Letters* 7.5 (2005), pp. 811–814.
- [117] Jordi Garcia and Jaume Vilarrasa. “New synthetic “tricks”. From aliphatic amines and amides to azides and/or how to convert RNHCOR' into RNHCOR avoiding drastic hydrolyses”. In: *Tetrahedron Letters* 28.3 (1987), pp. 341–342.
- [118] John E Wells, Donald E Babcock, and Wesley G France. “The Nature of Electrode Reactions. I. Factors Affecting the Electrochemical Reduction of N-Nitrosomethylaniline<sup>1</sup>”. In: *Journal of the American Chemical Society* 58.12 (1936), pp. 2630–2632.
- [119] Luis Garcia-Rio, J. Ramon Leis, M. Elena Pena, and Emilia Iglesias. “Transfer of the nitroso group in water/AOT/isooctane microemulsions: intrinsic and apparent reactivity”. In: *The Journal of Physical Chemistry* 97.13 (1993), pp. 3437–3442. DOI: 10 .

- 1021/j100115a057. eprint: <https://doi.org/10.1021/j100115a057>. URL: <https://doi.org/10.1021/j100115a057>.
- [120] Peter R Farina and Howard Tieckelmann. “Reactions of Grignard reagents with nitrosamines”. In: *The Journal of Organic Chemistry* 40.8 (1975), pp. 1070–1074.
- [121] Alvaro J Vazquez, Cristian Rodriguez, and N Sbarbati Nudelman. “Convenient methodology for the synthesis of trialkylhydrazines”. In: *Synthetic Communications*® 39.22 (2009), pp. 3958–3972.
- [122] G Hallett, SS Johal, TA Meyer, and DL Williams. “Reactions of nitrosamines with nucleophiles in acid solution.” In: *IARC Scientific Publications* 31 (1980), pp. 31–41.
- [123] Pavel Golubev and Mikhail Krasavin. “N-Isocyanodialkylamines generated in situ for the Joullié-Ugi reaction with indolenines”. In: *Tetrahedron Letters* 59.39 (2018), pp. 3532–3536. ISSN: 0040-4039. DOI: <https://doi.org/10.1016/j.tetlet.2018.08.025>. URL: <https://www.sciencedirect.com/science/article/pii/S0040403918310074>.
- [124] Uroš Grošelj, David Bevk, Renata Jakše, Anton Meden, Branko Stanovnik, and Jurij Svete. “Stereoselective additions to the exocyclic CC bond of some  $\alpha$ -alkylidene-(+)-camphor derivatives”. In: *Tetrahedron: Asymmetry* 17.8 (2006), pp. 1217–1237. ISSN: 0957-4166. DOI: <https://doi.org/10.1016/j.tetasy.2006.04.014>. URL: <https://www.sciencedirect.com/science/article/pii/S0957416606002722>.
- [125] Hideaki Kakeya, Masaya Imoto, Yoshikazu Takahashi, Hiroshi Naganawa, Tomio Takeuchi, and Kazuo Umezawa. “Dephostatins, a novel protein tyrosine phosphatase inhibitor produced by *Streptomyces* II. structure determination”. In: *The Journal of Antibiotics* 46.11 (1993), pp. 1716–1719.
- [126] Gerald F Grillot. “The Reduction of Diphenylnitrosamine in the Presence of Raney Nickel Catalyst and Platinum Catalyst<sup>1</sup>”. In: *Journal of the American Chemical Society* 66.12 (1944), pp. 2124–2124.
- [127] Joseph E Saavedra, Caroline T Temu, and David W Farnsworth. “Oxidation of  $\beta$ -Hydroxynitrosamines to  $\beta$ -Ketonitrosamines with  $\text{KMnO}_4$ -Metal.  $\text{SO}_4$ .  $\text{XH}_2\text{O}$  in Non-Aqueous Media”. In: *Synthetic Communications* 19.1-2 (1989), pp. 215–220.

- [128] Pradip K Gadekar, Maryann Hoermann, Faith Corbo, Rajiv Sharma, S Sarveswari, and Abhijit Roychowdhury. “Reductive removal of methoxyacetyl protective group using sodium borohydride”. In: *Tetrahedron Letters* 55.2 (2014), pp. 503–506.
- [129] Ling Wang, Sa-Sa Wang, Giang VO-Thanh, and Ye Liu. “The oxidative halogenations of arenes in water using hydrogen peroxide and halide salts over an ionic catalyst containing sulfo group and hexafluorotitanate”. In: *Journal of Molecular Catalysis A: Chemical* 371 (2013), pp. 56–62. ISSN: 1381-1169. DOI: <https://doi.org/10.1016/j.molcata.2013.01.023>. URL: <https://www.sciencedirect.com/science/article/pii/S1381116913000368>.
- [130] TS Sorensen. “THE pKa OF PROTONATED  $\alpha$ ,  $\beta$ -UNSATURATED CARBOXYLIC ACIDS”. In: *Canadian Journal of Chemistry* 42.4 (1964), pp. 724–730.
- [131] Organic Chemistry Data. *Organic Chemistry Data - Solvents*. <https://organicchemistrydata.org/solvents/>. Accessed: 30/04/2024.
- [132] Scott E Denmark, Wen-Tau T Chang, KN Houk, and Peng Liu. “Development of chiral bis-hydrazone ligands for the enantioselective cross-coupling reactions of aryldimethylsilylanolates”. In: *The Journal of Organic Chemistry* 80.1 (2015), pp. 313–366.
- [133] C. Sharpe. Housecroft. *Inorganic Chemistry*. Vol. 4. Pearson Education Ltd., 2012, p573–577.



# Appendix A

## Code listings

### A.1 XML parse

Listing A.1: Python script to extract and clean data from Reaxys.

```
import pandas as pd
import rdkit
from rdkit import Chem
from lxml import etree
import csv

def xml_parse(xmlfile, outfile, outfile2):

    '''Takes master xml file as input and parses it, retrieves reaction
    information in outfile
    and molfile data in outfile2 for later conversion into SMILES.'''

    # Remove any bold, italic, subscript, superscript, highlights from xml file
    with open(xmlfile) as f:
        xml_str = f.read()

    xml_str = xml_str.replace('<hi>', '')
    xml_str = xml_str.replace('</hi>', '')
    xml_str = xml_str.replace('<sub>', '')
    xml_str = xml_str.replace('</sub>', '')
    xml_str = xml_str.replace('<SUB>', '')
    xml_str = xml_str.replace('</SUB>', '')
    xml_str = xml_str.replace('<sup>', '')
    xml_str = xml_str.replace('</sup>', '')
    xml_str = xml_str.replace('<SUP>', '')
    xml_str = xml_str.replace('</SUP>', '')
    xml_str = xml_str.replace('<i>', '')
    xml_str = xml_str.replace('</i>', '')
    xml_str = xml_str.replace('<br/>', '')

    with open(xmlfile, 'w') as f:
        f.write(xml_str)

    # Assign lists for use as columns in resulting DataFrame
```

```
data = []
reactants = []
reagents = []
catalyst = []
all_reagents = []
products = []
prep = []
Yield = []
stage = []
steps = []
condition = []
solvent = []
time = []
temperature = []
year = []
ref = []
reaction = 0

# Column titles for csv file and DataFrame
Titles = ['Reaction Number',
          'Reaxys ID',
          'Reactant(s)',
          'Product(s)',
          'Procedure',
          'Yield (%)',
          'Stages',
          'Reagent(s)',
          'Condition',
          'Catalyst',
          'Solvent(s)',
          'Time (h)',
          'Temperature (C)',
          'All Reagents',
          'Publication Year',
          'Reference']

# Write column titles to outfile
with open(outfile, 'w+', newline='') as f:
    writer = csv.writer(f)
    writer.writerow(Titles)

# Parse master XML file
for event, element in etree.iterparse(xmlfile, events=("start", "end")):
    # Reaction index
    if element.tag == "reaction" and event == "start":
        reaction += 1

    # Reaction ID from Reaxys
    elif element.tag == 'RX.ID' and event == "start":
        reaction_ID = str(element.text)

    # Publication year
    elif element.tag == "CIT.PY" and event == "start":
        year = str(element.text)

    # Append reactants to list
    elif element.tag == "RX.RCT" and event == "start":
        reactant = str(element.text)
        # filter for non-nitrosamine reactants
        if any(keyword.lower() in reactant.lower() for keyword in ["nitroso", "nitrosamine"]):
```

```
        reactants.append(reactant)
    else:
        all_reagents.append(reactant)
        reagents.append(reactant)

# Assign reaction product
elif element.tag == "RX.PRO" and event == "start":
    product = element.text
    products.append(product)

# Assign reaction condition
elif element.tag == "RXD.COND" and event == "start":
    condition.append(element.text)

# Assign reaction procedure
elif element.tag == "RXD.TXT" and event == "start":
    prep = element.text

# Assign reaction yield
elif element.tag == "RXD.NYD" and event == "start":
    Yield = element.text

# Number of stages
elif element.tag == "RXD.STG" and event == "start":
    stage.append(element.text)

# Reagents
elif element.tag == "RXD.RGT" and event == "start":
    reagent = element.text
    all_reagents.append(reagent)
    reagents.append(reagent)

# Catalysts
elif element.tag == "RXD.CAT" and event == "start":
    cats = element.text
    all_reagents.append(cats)
    catalyst.append(cats)

# Append solvent to list
elif element.tag == "RXD.SOL" and event == "start":
    solv = element.text
    all_reagents.append(element.text)
    solvent.append(solv)

# Append reaction time to list
elif element.tag == "RXD.TIM" and event == "start":
    time.append(element.text)

# Append temperature to list
elif element.tag == "RXD.T" and event == "start":
    temperature.append(element.text)

# Append patent author to reference list
elif element.tag == "CIT.PA" and event == "start":
    ref.append(element.text)
# Append patent year to reference list
elif element.tag == "CIT.PREPY" and event == "start":
    ref.append(element.text)
# Append patent pages to reference list
elif element.tag == "CIT.PAGES" and event == "start":
    ref.append(element.text)
# Append page number to reference list
```

```
elif element.tag == "CIT.PN" and event == "start":
    ref.append(element.text)
# Append author to reference list
elif element.tag == "CIT.AU" and event == "start":
    ref.append(element.text)
# Append journal to reference list
elif element.tag == "CIT.JTS" and event == "start":
    ref.append(element.text)
# Append volume number to reference list
elif element.tag == "CIT.VL" and event == "start":
    ref.append(element.text)
# Append issue number to reference list
elif element.tag == "CIT.NB" and event == "start":
    ref.append(element.text)
# Append publication year to reference list
elif element.tag == "CIT.PY" and event == "start":
    ref.append(element.text)
# Append page number to reference list
elif element.tag == "CIT.PAG" and event == "start":
    ref.append(element.text)
# Append DOI to reference list
elif element.tag == "CIT.DOI" and event == "start":
    ref.append(element.text)

# End of <RXD> entry write to file
elif element.tag == "RXD" and event == "end":

    # Assign number of reaction steps
    if len(stage) == 0:
        steps = '1'
    else:
        steps = stage[-1]

    # Convert all lists to strings with , separator
    rcts = ", ".join([str(x) for x in reactants])
    prds = ", ".join([str(x) for x in products])
    cat = ", ".join([str(x) for x in catalyst])
    rgt = ", ".join([str(x) for x in reagents])
    all_rgts = ", ".join([str(x) for x in all_reagents])
    solvs = ", ".join([str(x) for x in solvent])
    times = ", ".join([str(x) for x in time])
    temperatures = ", ".join([str(x) for x in temperature])
    ref2 = ", ".join([str(x) for x in ref])
    conds = ", ".join([str(x) for x in condition])

    # Write variables to list
    data = [reaction,
            reaction_ID,
            rcts,
            prds,
            prep,
            Yield,
            steps,
            rgt,
            conds,
            cat,
            solvs,
            times,
            temperatures,
            all_rgts,
            year,
            ref2]
```

```
# If no value assign blank
data = ['None' if i == '' else i for i in data]

# Write data to file
with open(outfile, 'a+', encoding='utf-8', newline='') as f:
    writer = csv.writer(f, delimiter=',')
    writer.writerow(data)

# Clear all variables and lists in <RXD>
prep = ""
Yield = ""
steps = ""
rgt = ""
all_rgts = ""
year = ""
reagents.clear()
stage.clear()
all_reagents.clear()
solvent.clear()
time.clear()
temperature.clear()
condition.clear()
data.clear()
catalyst.clear()
ref.clear()

# At end of reaction clear reactants and products
elif element.tag == "reaction" and event == "end":
    reactants.clear()
    products.clear()
    rcts = ""
    prds = ""

# Else remove from memory
else:
    pass
    element.clear()

# Correct/Remove characters in output file
with open(outfile) as f:
    csv_str = f.read()

csv_str = csv_str.replace('(1)', '(I)')
csv_str = csv_str.replace(' ', "")
csv_str = csv_str.replace('[ ]', "None")
csv_str = csv_str.replace('; ', "")

with open(outfile, 'w') as f:
    f.write(csv_str)

# Molfile csv file generation

# Assign lists again
reactionind = 0
reactantmols = []
productmols = []
towrite = []

# column titles for csv file
headings = ['Reaction Number', 'Reactant molfiles', 'Product molfiles']

# Write column titles to file
with open(outfile2, 'w+', newline='') as f:
```

```

writer = csv.writer(f)
writer.writerow(headings)

# Parse XML file
for event, element in etree.iterparse(xmlfile, events=("start", "end")):
    # Reaction index
    if element.tag == "reaction" and event == "start":
        reactionind += 1

    # Append reactant molfile string to list
    elif element.tag == 'RY.RCT' and event == "start":
        rmol = element.text
        reactantmols.append(rmol)

    # Append product molfile string to list
    elif element.tag == 'RY.PRO' and event == "start":
        pmol = element.text
        productmols.append(pmol)

    # End of entry write data to csv file
    elif element.tag == 'reaction' and event == 'end':
        # create strings from lists
        rmols = ", ".join([str(x) for x in reactantmols])

        pmols = ", ".join([str(x) for x in productmols])

        # Write data to file
        towrite = [reactionind, rmols, pmols]

        # If no value assign blank
        towrite = ['None' if i == '' else i for i in towrite]

        with open(outfile2, 'a+', encoding='utf-8', newline='') as f:
            writer = csv.writer(f, delimiter=',')
            writer.writerow(towrite)

    # Clear entries
    pmols = ""
    rmols = ""
    reactantmols.clear()
    productmols.clear()
    towrite.clear()
    element.clear()

# Assign file names and run xml_parse
xmlfile = 'nitrosamine_master.xml'
outfile = 'nitrosamine_parsed_2.csv'
molfile_csv = 'nitrosamine_mfs_2.csv'
xml_parse(xmlfile, outfile, molfile_csv)

def getsmiles(outfile, molfile_csv):

    '''Takes the .csv output file from the parsed xml data and converts the
    molfile data into SMILES
    appends smiles to dataframe.'''

    # Read outfile and molfile into DataFrames
    mols = pd.read_csv(molfile_csv)
    main = pd.read_csv(outfile)

    # Convert molfile representation into SMILES and append to a list for
    reactants then products
    reactantsmiles = []

```

```

for i in range(len(mols)):
    reactantlist = []
    rcts = mols.loc[i][1].split(", ")
    for molfile in rcts:
        try:
            mol = Chem.MolFromMolBlock(molfile)
            reactantlist.append(Chem.MolToSmiles(mol))
        except:
            reactantlist.append('None')
    reactantsmiles.append(reactantlist)

productsmiles = []
for i in range(len(mols)):
    productlist = []
    prds = mols.loc[i][2].split(", ")
    for molfile in prds:
        try:
            mol = Chem.MolFromMolBlock(molfile)
            productlist.append(Chem.MolToSmiles(mol))
        except:
            productlist.append('None')
    productsmiles.append(productlist)

# Create a list containing the index number for each reaction in outfile
indexnum = []
for ind in main['Reaction Number']:
    indexnum.append(ind)

# Match the index's to the appropriate SMILES codes
rcolumn = []
pcolumn = []
for num in indexnum:
    rcolumn.append(".".join(reactantsmiles[num-1]))
    pcolumn.append(".".join(productsmiles[num-1]))

# Add the SMILES codes to the main DataFrame
main['Reactant Smiles'] = rcolumn
main['Product Smiles'] = pcolumn
main['Reaction'] = main['Reactant Smiles'].str.cat(main['Product Smiles'],
sep=">>")

return(main)

# Apply the function and return the Dataframe with SMILES
main = getsmiles(outfile, molfile_csv)

# Drop any entries in the 'Product Smiles' column with errors
producterrors = main[main['Product Smiles'].str.contains('None', regex=False)]
main.drop(producterrors.index, inplace=True)
main.reset_index(inplace=True, drop=True)

# Drop any entries in the 'Reactant Smiles' column with errors
reactanterrors = main[main['Reactant Smiles'].str.contains('None', regex=False)
]
main.drop(reactanterrors.index, inplace=True)
main.reset_index(inplace=True, drop=True)

# Remove multi-stage reactions from the dataset to make the classification less
  complicated
single_stage = main[main['Stages']==1]
single_stage.shape[0]

# How many multi-stage reactions do we have?

```

```

multi_stage = main[main['Stages']!=1]
multi_stage.shape[0]

# Finally, save the dataframe as a csv file for further processing
single_stage.to_csv("nitrosamine_master_with_smiles.csv")

```

## A.2 AAM and ReactionCodes

Listing A.2: Filtering the dataset to leave only reactions which consume nitrosamines.

```

import pandas as pd
import glob
import os
from rdkit import Chem
import csv
import matplotlib.pyplot as plt
from openbabel import pybel
import re
from collections import defaultdict
import numpy as np
import seaborn as sns

# Import the nitrosamine dataset from the XML parsed data
data = pd.read_csv("xml_parse/nitrosamine_master_with_smiles.csv")

# Pull out the unique reaction smiles and their index to iterate through and
# create mapping .bat file for RDT
reaction_smiles_Reaxys = data.drop_duplicates(subset="Reaction Number")["
Reaction"]
reaction_index = data.drop_duplicates(subset="Reaction Number")["Reaction
Number"]

# Construct the .bat file for the computation of AAM for the reaction SMILES
with open('rdt.bat', 'w') as outfile:

    # Assign the file path for reaction decoder tool
    # such that we can reference to it from a different directory
    # this requires that the rdt.jar file is located in the
    # same directory as the .bat file (it will be so no need to move anything.)
    outfile.write("set rdtpath=%~dp0\n")

    # loop through every reaction string
    # using the index in the data DataFrame
    # as reference for file names
    for index, reaction_string in zip(reaction_index, reaction_smiles_Reaxys):
        outfile.write('mkdir "%rdtpath%rdt_1\\"
            + str(index)
            + '" && cd "%rdtpath%rdt_1\\"
            + str(index)
            + r'" && java -jar "%rdtpath%rdt_2.5.0.jar" -Q SMI -q "'
            + reaction_string
            + '" -g -c -j AAM -f TEXT'
            + '\n')

    # Pull out the failed reactions from the AAM step and
save to csv
directory_path = 'rdt_1'

```



```

empty_folders = []

# Loop through all folders in the directory
for folder_name in os.listdir(directory_path):
    folder_path = os.path.join(directory_path,
folder_name)

    # Check if the path is a directory
    if os.path.isdir(folder_path):
        # Check if the directory is empty
        if not os.listdir(folder_path):
            # Append the empty folder name to the list
            empty_folders.append(int(folder_name))

# Pull out the failed reactions from the AAM step and
save to csv
unsuccessful_after_rdt = data[data["Reaction Number"].
isin(empty_folders)]
unsuccessful_after_rdt.shape

# Construct .bat file for ReactionCode generation

with open('ReactionCode.bat', 'w') as outfile:

    # Assign the file path for ReactionCode.jar
    # such that we can reference to it from a different
directory
    # this requires that the .jar file is located in the
    # same directory as the .bat file (it will be so no
need to move anything.)
    outfile.write("set reactioncodepath=%~dp0\n")

    # loop through every reaction string
    # using the index in the excel sheet
    # as reference for file names
    for index, reaction_string in zip(reaction_index,
reaction_smiles_Reaxys):
        outfile.write('mkdir "%reactioncodepath%
ReactionCode_1\\'
                    + str(index)
                    + '" && cd "%reactioncodepath%rdt_1
\\'
                    + str(index)
                    + r'" && java -jar "%
reactioncodepath%ReactionCode_1.2.2.jar" '
                    + ' -q ECBLAST_smiles_AAM.rxn -o '
                    + '"%reactioncodepath%
ReactionCode_1\\'
                    + str(index)
                    + '\n')

# RUN BAT FILE AND WAIT UNTIL IT IS COMPLETED

# Rename ReactionCodes to reflect their index in the dataset
with open ("rename_1.bat", 'w') as outfile:

    outfile.write("set reactioncodepath=%~dp0\n")

    for index, reaction_string in zip(reaction_index, reaction_smiles_Reaxys):
        outfile.write('rename "%reactioncodepath%ReactionCode_1\\'
                    +str(index)
                    +'\encoded_reactionsCode.csv" "')

```

```

        +str(index)
        +'.csv'
        +'\n')

# Then we need to move the ReactionCodes into a single directory
with open ("move_1.bat", 'w') as outfile:

    outfile.write("set reactioncodepath=%~dp0\n")
    outfile.write("mkdir moved_1\n")

    for index, reaction_string in zip(reaction_index, reaction_smiles_Reaxys):
        outfile.write(r'move "%reactioncodepath%ReactionCode_1\\"'
            + str(index)
            + '\\\
            + str(index)
            + '.csv'
            + r'"%reactioncodepath%moved_1\\"'+'\n')

# Next pull in all those ReactionCodes (.csv files) into a single dataframe
indexed by the index in the excel table

path = 'moved_1\\\'

all_files = glob.glob(os.path.join(path, "*.csv"))

all_df = []
for f in all_files:
    try:
        df = pd.read_csv(f, sep='\t')
        df['Index'] = f.split('\\')[1]
        df['Index'][0] = df['Index'][0][:-4]
        all_df.append(df)
    except:
        pass
merged_df = pd.concat(all_df, ignore_index=True, sort=True)

# We can now pull out the reaction codes at various depths, to zoom in on the
reaction centre and figure out which atoms change in the reaction

# Set the index of the excel file dataframe to be the reaxys index
data.set_index("Reaction Number", inplace=True)
# convert the index to integers
data.index = data.index.astype(int)
# set the index of merged_df to perform the join later
merged_df.set_index("Index", inplace=True)
# convert the index to integers
merged_df.index = merged_df.index.astype(int)
# Merge the dataframes on the index
RCs_added = pd.merge(data, merged_df, left_index=True, right_index=True, how='
    outer')
# Create a new column in the dataframe to pull out only the depth 0 and 1
reaction codes
RCs_added["RC_depth_1"] = RCs_added.reactionCode.str.split("|", 3, expand=True)
    .iloc[:,0:2].apply(lambda row: '|'.join(row.astype(str)), axis=1)
RCs_added["RC_depth_0"] = RCs_added.reactionCode.str.split("|", expand=True).
    iloc[:,0] + "|" #need the "|" character to make it work

# fill in the NaN values with "nan" for depth 1 cores
RCs_added["RC_depth_0"].fillna("nan", inplace=True)

```

```

# Decode the ReactionCodes into reaction SMARTS (Full length), can use these
  later if necessary. just doing this for completeness

# Create a bat file to loop through each reactioncode and output the reaction
  SMILES so we can compare to the original reaction SMILES from Reaxys

with open('decode_reactionCodes_full.bat', 'w') as outfile:

    # Some clever trickery to assign the file path for ReactionCode.jar
    # such that we can reference to it from a different directory
    # this requires that the .jar file is located in the
    # same directory as the .bat file (it will be so no need to move anything.)
    outfile.write("set reactioncodepath=%~dp0\n")

    # Make a directory to store all the individual decoded reactionCodes
    outfile.write("mkdir decoded_reactionCodes_full\n")

    # Start by looping through the indexes list of ReactionCodes
    for index, reactionCode in zip(RCs_added.index, RCs_added.reactionCode):
        outfile.write('mkdir "%reactioncodepath%decoded_reactionCodes_full\\'
            + str(index)
            + '" && cd "%reactioncodepath%decoded_reactionCodes_full
            '\\',
            + str(index)
            + r'" && java -jar "%reactioncodepath%ReactionCode_1.2.2.
            jar" -q "'
            + str(reactionCode)
            + '" -m -i -p "decode"'
            + '\n')

        # Pull in all the individual csv files and combine them
        into one indexed csv file

        base_path = "decoded_reactionCodes_full\\"
        csv_file = "reaction_SMARTS_full.csv"

        # Clear or create the CSV file
        with open(csv_file, "w", newline='') as file:
            writer = csv.writer(file)
            writer.writerow(["index", "Reaction SMARTS"])

        # Loop through each directory
        for dir_name in os.listdir(base_path):
            dir_path = os.path.join(base_path, dir_name)
            if os.path.isdir(dir_path):
                try:
                    text_file = os.path.join(dir_path, "
                    decode_SMIRKS.txt")

                    # Extract the first line from the text file
                    with open(text_file, "r") as file:
                        first_line = file.readline().strip()

                    # Append the first line and directory name to
                    the CSV file

                    with open(csv_file, "a", newline='') as file:
                        writer = csv.writer(file)
                        writer.writerow([dir_name, first_line
                        [2:]]

                except:
                    # Append failed
                    with open(csv_file, "a", newline='') as file:
                        writer = csv.writer(file)

```

```

writer.writerow([dir_name, "failed"])

# Decode Depth 0 reactioncodes

# Write a bat script to compute the reactions smarts of the depth 0 reaction
centres

# drop nan entries on RCs_added dataframes
depth_0_cores = RCs_added.drop(RCs_added[RCs_added['RC_depth_0'] == 'nan'].
index)

with open('decode_reactionCodes_depth_0.bat', 'w') as outfile:

    # Assign the file path for ReactionCode.jar
    # such that we can reference to it from a different directory
    # this requires that the .jar file is located in the
    # same directory as the .bat file (it will be so no need to move anything.)
    outfile.write("set reactioncodepath=%~dp0\n")

    # Make a directory to store all the individual decoded reactionCodes
    outfile.write("mkdir decoded_depth_0_reactionCodes\n")

    # Start by looping through the indexes list of ReactionCodes
    for index, reactionCode in zip(depth_0_cores.index, depth_0_cores.
RC_depth_0):
        outfile.write('mkdir "%reactioncodepath%decoded_depth_0_reactionCodes\\'
,
+ str(index)
+ '" && cd "%reactioncodepath%
decoded_depth_0_reactionCodes\\'
+ str(index)
+ r'" && java -jar "%reactioncodepath%ReactionCode_1.2.2.
jar" -q "'
+ str(reactionCode)
+ '" -m -i -p "decode"'
+ '\n')

    # pull all the decoded SMIRKS into a csv file

    base_path = "decoded_depth_0_reactionCodes\\"
    csv_file = "depth_0_reaction_SMARTS.csv"

    # Clear or create the CSV file
    with open(csv_file, "w", newline='') as file:
        writer = csv.writer(file)
        writer.writerow(["index", "Depth_0_Core"])

    # Loop through each directory
    for dir_name in os.listdir(base_path):
        dir_path = os.path.join(base_path, dir_name)
        if os.path.isdir(dir_path):
            try:
                text_file = os.path.join(dir_path, "
decode_SMIRKS.txt")

                # Extract the first line from the text file
                with open(text_file, "r") as file:
                    first_line = file.readline().strip()

                # Append the first line and directory name to
the CSV file

                with open(csv_file, "a", newline='') as file:
                    writer = csv.writer(file)

```

```

writer.writerow([dir_name, first_line
[2:]]
    except:
        # Append failed
        with open(csv_file, "a", newline='') as file:
            writer = csv.writer(file)
            writer.writerow([dir_name, "failed"])

# Decode Depth 1 reaction codes

# Write a batch script to compute the reactions smarts of the depth 1 reaction
centres

# drop nan entries on RCs_added dataframes
depth_1_cores = RCs_added.drop(RCs_added[RCs_added['RC_depth_1'] == 'nan|nan'].
index)

with open('decode_reactionCodes_depth_1.bat', 'w') as outfile:

    # Assign the file path for ReactionCode.jar
    # such that we can reference to it from a different directory
    # this requires that the .jar file is located in the
    # same directory as the .bat file (it will be so no need to move anything.)
    outfile.write("set reactioncodepath=%~dp0\n")

    # Make a directory to store all the individual decoded reactionCodes
    outfile.write("mkdir decoded_depth_1_reactionCodes\n")

    # Start by looping through the indexes list of ReactionCodes
    for index, reactionCode in zip(depth_1_cores.index, depth_1_cores.
RC_depth_1):
        outfile.write('mkdir "%reactioncodepath%decoded_depth_1_reactionCodes\\
,
            + str(index)
            + '" && cd "%reactioncodepath%
decoded_depth_1_reactionCodes\\'
            + str(index)
            + r'" && java -jar "%reactioncodepath%ReactionCode_1.2.2.
jar" -q "'
            + str(reactionCode)
            + '" -m -i -p "decode"'
            + '\n')

    # Pull all the decoded SMIRKS into a csv file

    base_path = "decoded_depth_1_reactionCodes"
    csv_file = "depth_1_reaction_SMARTS.csv"

    # Clear or create the CSV file
    with open(csv_file, "w", newline='') as file:
        writer = csv.writer(file)
        writer.writerow(["index", "Depth_1_Core"])

    # Loop through each directory
    for dir_name in os.listdir(base_path):
        dir_path = os.path.join(base_path, dir_name)
        if os.path.isdir(dir_path):
            try:
                text_file = os.path.join(dir_path, "
decode_SMIRKS.txt")

                # Extract the first line from the text file
                with open(text_file, "r") as file:

```

```

        first_line = file.readline().strip()

        # Append the first line and directory name to
the CSV file
        with open(csv_file, "a", newline='') as file:
            writer = csv.writer(file)
            writer.writerow([dir_name, first_line

[2:]])

        except:
            # Append failed
            with open(csv_file, "a", newline='') as file:
                writer = csv.writer(file)
                writer.writerow([dir_name, "failed"])

# Once all the cores at various depths have been computed, we can merge them
with the data we have from Reaxys

# Import the csv file containing depth 0,1 and full smarts
depth_0_reaction_SMARTs = pd.read_csv("depth_0_reaction_SMARTs.csv")
depth_0_reaction_SMARTs.set_index("index", inplace=True)
depth_1_reaction_SMARTs = pd.read_csv("depth_1_reaction_SMARTs.csv")
depth_1_reaction_SMARTs.set_index("index", inplace=True)
full_reaction_SMARTs = pd.read_csv("reaction_SMARTs_full.csv")
full_reaction_SMARTs.set_index("index", inplace=True)

# Convert the index to integers
depth_0_reaction_SMARTs.index = depth_0_reaction_SMARTs.index.astype(int)
depth_1_reaction_SMARTs.index = depth_1_reaction_SMARTs.index.astype(int)
full_reaction_SMARTs.index = full_reaction_SMARTs.index.astype(int)

# Perform merges with the original dataset to get a new dataframe with all the
reactioncodes at the various depths added
depth_0s_added = pd.merge(RCs_added, depth_0_reaction_SMARTs, left_index=True,
right_index=True,how='outer')
depth_1s_added = pd.merge(depth_0s_added, depth_1_reaction_SMARTs, left_index=
True, right_index=True,how='outer')
full_added = pd.merge(depth_1s_added, full_reaction_SMARTs, left_index=True,
right_index=True,how='outer')

# Now weve got the cores we can filter them to leave only those reactions which
consume the nitrosamines
full_added["Depth_1_reactants"] = full_added["Depth_1_Core"].str.split(">>",
expand=True)[0]
full_added["Depth_1_products"] = full_added["Depth_1_Core"].str.split(">>",
expand=True)[1]

# Need to get around the reactions which have the nitrosamine as part of the
leaving group
# I.e. need to make sure the nitrosamine N-N=O are accounted for in our
reactions products
# To do this we can track the atom map numbers of the N-N=O from the reactants
and see if they are present in the products
# Any reactions which no not meet this criteria will be discarded.

consumes_nitrosamine = []
# loop through the reactants and products of the depth 2 reaction cores
for reactants, products in zip(full_added["Depth_1_reactants"], full_added["
Depth_1_products"]):
    try:
        # Read molecule using Pybel
        reactant_mol = pybel.readstring("smi", reactants)
        # Convert the molecule to RDKit format
        rdkit_reactant_mol = Chem.MolFromSmarts(reactants)

```

```

# Get the product mols as SMARTS
product_mols = Chem.MolFromSmarts(products)

# Perform SMARTS matching on the reactants using Open Babel
smarts = pybel.Smarts("[#7]-[#7]=[#8]") # SMARTS Pattern for N-N=O
matching_atoms = smarts.findall(reactant_mol)

# If there is a match for the N-N=O
if matching_atoms != []:

    # Get the atom map numbers from the matched atoms using RDKit
    atom_map_nums = []
    for atom_indices in matching_atoms:
        for atom_index in atom_indices:
            atom = rdkit_reactant_mol.GetAtomWithIdx(atom_index - 1) #
RDKit atom indices start from 0
            atom_map_num = atom.GetAtomMapNum()
            if atom_map_num != 0:
                atom_map_nums.append(atom_map_num)

    # check if the nitrosamine atoms are present in the products
    if set(atom_map_nums).issubset([atom.GetAtomMapNum() for atom in
product_mols.GetAtoms()]) == True:
        consumes_nitrosamine.append(True)
    else:
        consumes_nitrosamine.append(False)

except:
    consumes_nitrosamine.append(False)

full_added["Consumes_Nitrosamine_depth_1"] = consumes_nitrosamine

# With the reactions that consume the nitrosamines in hand we can see how many
unique reaction cores there are
nitrosamines_consumed = full_added[full_added["Consumes_Nitrosamine_depth_1"]==
True]

# How many unique depth 0 transformations are there?
unique_depth_0_Cores = len(nitrosamines_consumed["Depth_0_Core"].unique())
print("Number of unique depth 0 transformations: " + str(unique_depth_0_Cores))

# result = 410

# Some of the cores will have the same atoms but different Atom-Atom-mapping
numbers. This can't be helped as there are multiple ways to map the
reactions. To try to find these codes, we can remove the atom mapping
numbers and re-run the cat-code generation to see how many unique cores we
have.

# lets start by accessing the depth 0 cores and removing their atom mapping
numbers

# Function to remove atom-atom mapping numbers
def remove_mapping_numbers(smarts_string):
    return re.sub(r":\d+", "", smarts_string)

# Remove the mapping numbers
nitrosamines_consumed["Depth_0_Core_unmapped"] = nitrosamines_consumed["
Depth_0_Core"].apply(remove_mapping_numbers)

# How many unique depth 0 transformations are there after removing AAM?
print("Number of unique depth 0 transformations after removing AAM: " + str(len
(nitrosamines_consumed["Depth_0_Core_unmapped"].unique())))

```

```

# result = 390

# PREPARE DATA FOR MANUAL CLASSIFICATION

# Define a list of common solvents to remove from All Reagents column
common_solvents = ["1,4-dioxane", "water", "methanol", "DMSO", "dichloromethane",
    "dichloromethane-d2", "tetrahydrofuran",
    "benzene", "tetrachloromethane", "diethyl ether", "ethanol",
    "xylene", "petroleum ether",
    "Acetone", "chloroform", "n-heptane", "acetonitrile", "
chloroform-d1", "neat (no solvent)",
    "1,2-dichloro-ethane", "toluene", "n-heptane", "N,N-dimethyl
-formamide", "cyclohexane",
    "ethoxyethoxyethanol", "butan-1-ol", "2-methoxy-ethanol", "
pentane", "Petroleum ether",
    "1,1-dichloroethane"]

# Extract the reagents column from the pre-parsed dataset
allreagents = []
allsolvents = []
for i in nitrosamines_consumed['All Reagents']:
    reagents = i.split(',')
    solvents = []
    # Remove solvents from the reagents
    for reagent in reagents[:]:
        if reagent in common_solvents:
            reagents.remove(reagent)
            solvents.append(reagent)
    allreagents.append(reagents)
    allsolvents.append(solvents)

# We need to homogenise the list of allreagents so that all similar sublists
are identical.
# This is done by reading in each sublist and reorder the terms with the
function set().
# Then we dump the reordered sublist into a new list.
allreagents_homogenised = []
allsolvents_homogenised = []
for sublist1, sublist2 in zip(allreagents, allsolvents):
    item1 = set(sublist1)
    item2 = set(sublist2)
    allreagents_homogenised.append(item1)
    allsolvents_homogenised.append(item2)

# Now we combine each sublist into a string and recreate the reagent list as a
simple list of strings
allreagents_list = []
allsolvents_list = []
separator = ', '
for sublist1, sublist2 in zip(allreagents_homogenised, allsolvents_homogenised):
    item1 = separator.join(sublist1)
    item2 = separator.join(sublist2)
    allreagents_list.append(item1)
    allsolvents_list.append(item2)

# Now we can add these as a new columns in our dataframe "Homogenised Reagents"
and "Homogenised Solvents"
nitrosamines_consumed["Homogenised Reagents"] = allreagents_list
nitrosamines_consumed["Homogenised Solvents"] = allsolvents_list

# Add a cat code column to make it easier to filter in excel

```



```
nitrosamines_consumed['Reagents_Cat_Codes'] = nitrosamines_consumed['
    Homogenised Reagents'].astype("category").cat.codes
nitrosamines_consumed['Depth_0_Cat_Codes_unmapped'] = nitrosamines_consumed['
    Depth_0_Core_unmapped'].astype("category").cat.codes

# Make a new code which combines the unique reagent combinations and the unique
# depth 1 transformations
nitrosamines_consumed["Reagent_Transformation_Code"] = nitrosamines_consumed["
    Reagents_Cat_Codes"].astype(str) + nitrosamines_consumed["
    Depth_0_Cat_Codes_unmapped"].astype(str)

nitrosamines_consumed.to_csv("nitrosamine_consumed_reagents_homogenised.csv")

# Drop duplicates to leave only unique reagent/transformation combinations to
# manually classify
unique_reagent_df = nitrosamines_consumed.drop_duplicates(subset=["
    Reagent_Transformation_Code", "Condition"])

# Reset the index and retain the Reaction Number from XML parsing
unique_reagent_df.reset_index(inplace=True)
unique_reagent_df.rename(columns={'index': 'Reaction Number'}, inplace=True)

# Save these reactions for manual classification
unique_reagent_df.to_csv("for_manual_classification.csv")
```



## Appendix B

# Classification hierarchies

Table B.1: Transformation classification class hierarchy.

Transformation Classification (Level 1)	Transformation Classification (Level 2)
Deprotonation-cyclisation with CN	-
denitrosation	De/Transnitrosation
denitrosation, alkene addition	De/Transnitrosation
denitrosation; 3+2	De/Transnitrosation
transnitrosation	De/Transnitrosation
transnitrosation to amine	De/Transnitrosation
C-NO formation	De/Transnitrosation
S-NO formation	De/Transnitrosation
fischer-hepp	Fischer-Hepp
fischer-hepp and oxidation	Fischer-Hepp
fischer-hepp and reduction	Fischer-Hepp
N1-X cleavage (Diazonium formation)	Dizonium formation
diazonium formation; 3+2	Dizonium formation
diazonium formation; C=N	Dizonium formation
diazotate formation	Dizonium formation
fischer-hepp and azo formation	azo formation
azo formation	azo formation
triazene formation	N3 formation with amine
reduction to amine	Reduction
reduction to hydrazine	Reduction
reduction to diazo	Reduction
reduction to hydrazine; azide formation	Reduction
reduction to ketone	Reduction
dimerisation to N-N=N-N	Reduction
dimerisation to N-NH-NH-N	Reduction
dimerization to C=N-N=C	Reduction
N-alkylation	-
intramolecular cyclisation	O-Si/C/S bond formation
O-S bond formation	O-Si/C/S bond formation
O-acylation	O-Si/C/S bond formation
O-alkylation	O-Si/C/S bond formation
O-silylation	O-Si/C/S bond formation
C-C bond formation via diazonium	O-Si/C/S bond formation
NO to NO <sub>2</sub>	

Table B.2: Reagent classification class hierarchy.

Reagent Classification (Level 1)	Reagent Classification (Level 2)
acid	Acid
acid + sulfur based reducing agent	Acid
acid + alkene + irradiation	Acid+hv
acid + irradiation	Acid+hv
acid + oxygen + irradiation	Acid+hv
alkene + acid + irradiation + hydrogenation with catalyst	Acid+hv
acid + anhydride	Acyating reagent
anhydride	Acyating reagent
anhydride + alkyne	Acyating reagent
anhydride + base	Acyating reagent
base + anhydride	Acyating reagent
R-C=O-X	Acyating reagent
diazomethane	Alkylating reagent
dimethyl sulfate	Alkylating reagent
epoxide	Alkylating reagent
MeOTf	Alkylating reagent
methyl oxonium	Alkylating reagent
R-X	Alkylating reagent
sulfonium bromide	Alkylating reagent
aromatic amine	Amine
primary amine	Amine
secondary amine	Amine
tertiary amine	Amine
acid + aromatic amine	Arene
base + e-rich aromatic compound	Arene
e-rich aromatic compound	Arene
e-rich aromatic compound + OH(-)	Arene
RO(-)	Base
base + alkene	Base

Table B.2 continued from previous page

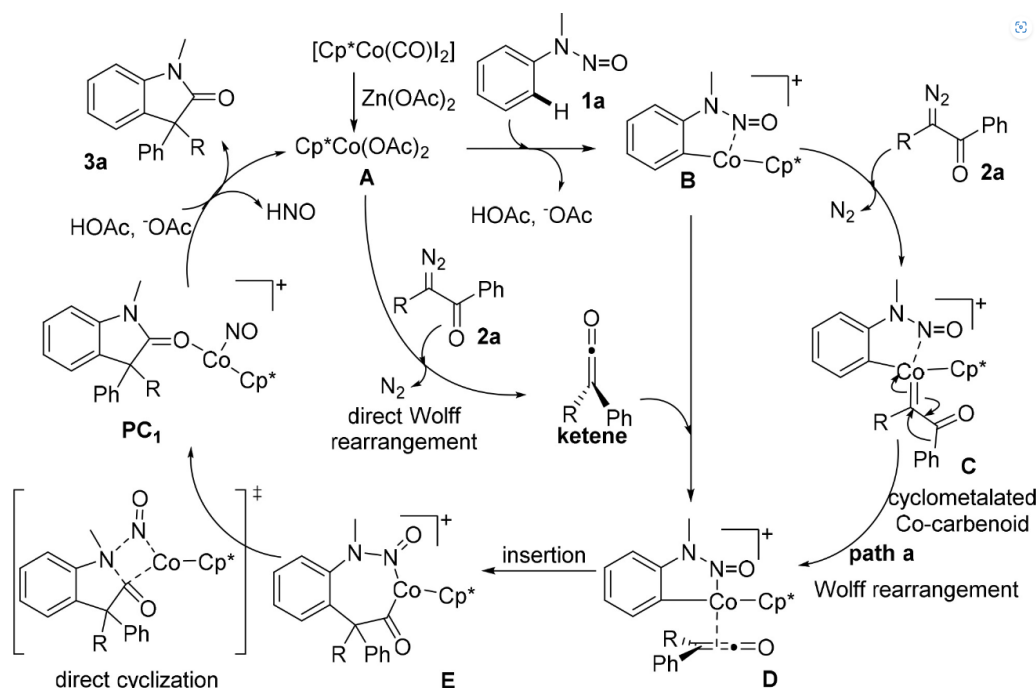
Reagent Classification (Level 1)	Reagent Classification (Level 2)
base + alkyne	Base
OH(-)	Base
base	Base
base + anhydride	Base
base + R-C=O-X	Base
base + R-X	Base
CO <sub>3</sub> (2-)	Base
CO <sub>3</sub> (2-) + alkene	Base
CO <sub>3</sub> (2-) + R-C=O-CH <sub>2</sub> -R <sub>2</sub>	Base
HCO <sub>3</sub> (-)	Base
nitrile + LDA	Base
OH(-) + alkene	Base
Pyrrolidine	Base
RO(-) + acid chloride	Base
RO(-) + alkene	Base
RO(-) + alkyne	Base
Grignard reagent	delete
Electrochemical reduction	Electrochemical reduction
Heating	Heating
HNO <sub>3</sub>	HNO <sub>3</sub>
hν	hν
hν + sulfur based reducing agent	hν
O <sub>2</sub> +hν	hν
Metal hydride	Hydride
Metal hydride + mercury	Hydride
Aluminium	Metal
Aluminium + base	Metal
Fe/H(+)	Metal
Na	Metal
Na/H(+)	Metal

Table B.2 continued from previous page

Reagent Classification (Level 1)	Reagent Classification (Level 2)
Na/NH <sub>3</sub>	Metal
Pd/H(+)	Metal
Sn/H(+)	Metal
Sn + Nitrous acid	Metal
Titanium reagent	Metal
Zn	Metal
Zn/H(+)	Metal
Zn/H(+), Nitrous acid	Metal
Zn/Hg	Metal
Zn/Hg/H(+)	Metal
Zn/OH(-)	Metal
ammonia	N-nucleophile
base + LiN <sub>3</sub>	N-nucleophile
functionalised hydrazine	N-nucleophile
functionalised urea	N-nucleophile
H <sub>2</sub> N(-)	N-nucleophile
LiN <sub>3</sub>	N-nucleophile
Pb(OAc) <sub>4</sub> /Amine/CO <sub>3</sub> ( <sup>2-</sup> )	Pb(OAc) <sub>4</sub> /Amine/base
Alkyl lithium	RMg/Li
Aryl lithium	RMg/Li
Grignard reagent	RMg/Li
sulfur based reducing agent	S-based reductant
sulfur based reducing agent + base	S-based reductant
carbon anion	Stabilised carbanion
O=C1CNC(N1)=S	Stabilised carbanion
R-C=C-CH <sub>2</sub> -R <sub>2</sub>	Stabilised carbanion
R-C=N-CH <sub>2</sub> -R <sub>2</sub>	Stabilised carbanion
R-C=O-CH <sub>2</sub> -R <sub>2</sub>	Stabilised carbanion
TM catalyst	TM catalyst
TM catalyst + diazoketone	TM catalyst

Table B.2 continued from previous page

Reagent Classification (Level 1)	Reagent Classification (Level 2)
TM catalyst + organic peroxide	TM catalyst
TM Catalyst + sulfanylidene	TM catalyst



Scheme B.1: Examples of denitrosation reactions under basic conditions.

The mechanism for denitrosation of alkyl; phenyl nitrosamines with Co(III) catalysts as described in chapter 2 proceeds *via* C-H activation at the ortho position on the nitrosamine substrate, followed by coordination of the coupling partner (in this case an  $\alpha$ -diazo- $\beta$ -ketoester) *via* loss of  $N_2$ . The Co-carbenoid then undergoes a Wolff-rearrangement to the ketene and then inserts into the C-Co bond. A cyclisation reaction then occurs between the amine nitrogen of the nitrosamine and the inserted carbonyl, the leaving group is the nitrosonium which forms a new Co-N bond, producing the oxindole product. (Scheme B.1).

## Appendix C

# Stock solution preparation

Table C.1: N-nitrosamine stock solution preparation as referenced in Chapter 3, general experimental procedure Section 3.5.

Nitrosamine	Date	Solvent	Mass (g)	Volume (mL)	MW (g/mol)	[Stock] (mM)
N1	09/05/2023	EtOH	1.0354	100	102.14	101.37
N2	09/05/2023	EtOH	1.3095	100	130.19	100.58
N3	09/05/2023	EtOH	1.5834	100	158.25	100.06
N4	09/05/2023	EtOH	1.9805	100	198.23	99.91
N5	09/05/2023	EtOH	1.1855	100	116.12	102.09
N6	09/05/2023	EtOH	1.3256	100	132.12	100.33
N7	09/05/2023	EtOH	1.753	100	174.24	100.61
N8	09/05/2023	EtOH	0.5134	50	118.14	86.91
TMB	09/05/2023	EtOH	0.5	100	168.18	29.73
TMB	05/07/2023	EtOH	0.5078	100	168.18	30.19
N6	08/08/2023	EtOH	1.3533	100	132.12	102.43
N8	08/08/2023	EtOH	0.6194	50	118.14	104.86
TMB	09/08/2023	EtOH	0.5041	100	168.18	29.97
N1	15/08/2023	EtOH	1.0218	100	102.14	100.04
N2	15/08/2023	EtOH	1.3098	100	130.19	100.61
N3	15/08/2023	EtOH	1.5944	100	158.25	100.75
N4	15/08/2023	EtOH	1.9989	100	198.23	100.84
N5	15/08/2023	EtOH	1.168	100	116.12	100.59
N7	15/08/2023	EtOH	1.7504	100	174.24	100.46
TMB	05/09/2023	EtOH	0.5078	100	168.18	30.19



Table C.1 continued from previous page

Nitrosamine	Date	Solvent	Mass (g)	Volume (mL)	MW (g/mol)	[Stock] (mM)
N1	25/09/2023	EtOH	0.1017	10	102.14	99.57
N2	25/09/2023	EtOH	0.1392	10	130.19	106.92
N3	25/09/2023	EtOH	0.1694	10	158.25	107.05
N4	25/09/2023	EtOH	0.203	10	198.23	102.41
N5	25/09/2023	EtOH	0.1301	10	116.12	112.04
N6	25/09/2023	EtOH	0.1352	10	132.12	102.33
N7	25/09/2023	EtOH	0.1851	10	174.24	106.23
N8	25/09/2023	EtOH	0.3122	25	118.14	105.71
TMB	26/09/2023	EtOH	0.5125	100	168.18	30.47
N1	05/10/2023	EtOH	0.115	10	102.14	112.59
N2	05/10/2023	EtOH	0.1378	10	130.19	105.85
N3	05/10/2023	EtOH	0.1679	10	158.25	106.10
N4	05/10/2023	EtOH	0.4958	25	198.23	100.05
N5	05/10/2023	EtOH	0.1168	10	116.12	100.59
N6	05/10/2023	EtOH	0.1473	10	132.12	111.49
N7	05/10/2023	EtOH	0.1887	10	174.24	108.30
N8	05/10/2023	EtOH	0.1269	10	118.14	107.41
TMB	05/10/2023	EtOH	0.5037	100	168.18	29.95
N1	23/10/2023	EtOH	0.105	10	102.14	102.80
N2	23/10/2023	EtOH	0.1423	10	130.19	109.30
N3	23/10/2023	EtOH	0.1694	10	158.25	107.05
N4	23/10/2023	EtOH	0.508	25	198.23	102.51
N5	23/10/2023	EtOH	0.1432	10	116.12	123.32
N6	23/10/2023	EtOH	0.1544	10	132.12	116.86
N7	23/10/2023	EtOH	0.206	10	174.24	118.23
N8	23/10/2023	EtOH	0.1265	10	118.14	107.08
TMB	24/10/2023	EtOH	0.508	100	168.18	30.21
N1	06/11/2023	EtOH	0.1055	10	102.14	103.29
N2	06/11/2023	EtOH	0.1409	10	130.19	108.23
N3	06/11/2023	EtOH	0.1694	10	158.25	107.05
N4	06/11/2023	EtOH	0.5095	25	198.23	102.81
N5	06/11/2023	EtOH	0.1425	10	116.12	122.72
N6	06/11/2023	EtOH	0.152	10	132.12	115.05
N7	06/11/2023	EtOH	0.2201	10	174.24	126.32

Table C.1 continued from previous page

Nitrosamine	Date	Solvent	Mass (g)	Volume (mL)	MW (g/mol)	[Stock] (mM)
N8	06/11/2023	EtOH	0.1229	10	118.14	104.03
TMB	06/11/2023	EtOH	0.5083	100	168.18	30.22
N1	28/11/2023	THF	0.1003	10	102.14	98.20
N2	28/11/2023	THF	0.1452	10	130.19	111.53
N3	28/11/2023	THF	0.162	10	158.25	102.37
N4	28/11/2023	THF	0.5028	25	198.23	101.46
N5	28/11/2023	THF	0.1165	10	116.12	100.33
N6	28/11/2023	THF	0.1361	10	132.12	103.01
N7	28/11/2023	THF	0.2	10	174.24	114.78
N8	28/11/2023	THF	0.1232	10	118.14	104.28
TMB	28/11/2023	THF	0.5098	100	168.18	30.31
N1	05/12/2023	EtOH	0.1201	10	102.14	117.58
N2	05/12/2023	EtOH	0.1496	10	130.19	114.91
N3	05/12/2023	EtOH	0.1658	10	158.25	104.77
N4	05/12/2023	EtOH	0.4995	25	198.23	100.79
N5	05/12/2023	EtOH	0.1345	10	116.12	115.83
N6	05/12/2023	EtOH	0.1783	10	132.12	134.95
N7	05/12/2023	EtOH	0.194	10	174.24	111.34
N8	05/12/2023	EtOH	0.1356	10	118.14	114.78
TMB	07/12/2023	EtOH	0.5036	100	168.18	29.94

## Appendix D

# HPLC Calibrations

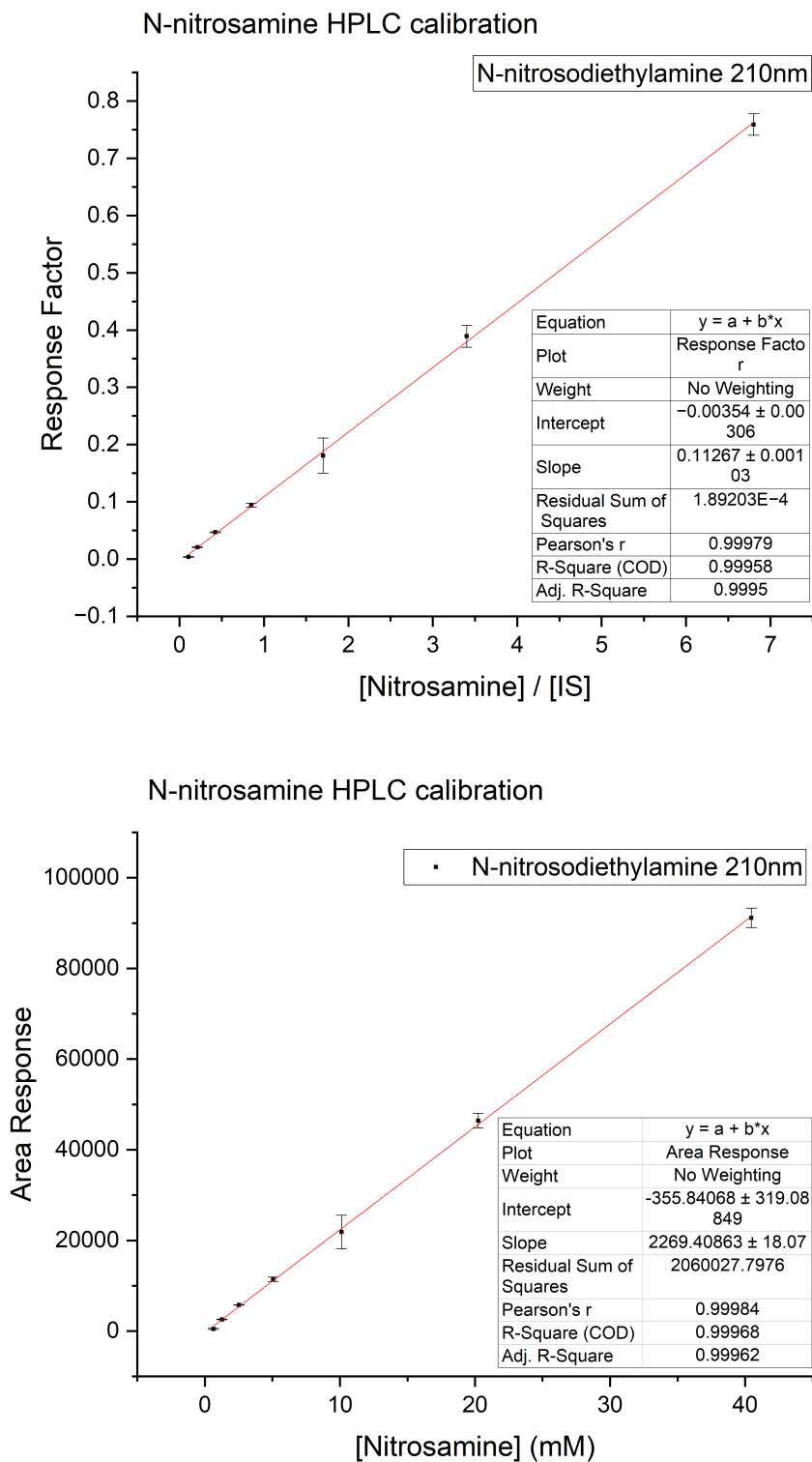


Figure D.1: HPLC Calibration curves for N-nitrosodiethylamine (N1) at 210nm. Referenced in Chapter 3, general experimental procedure Section 3.5 and in Table 3.5.

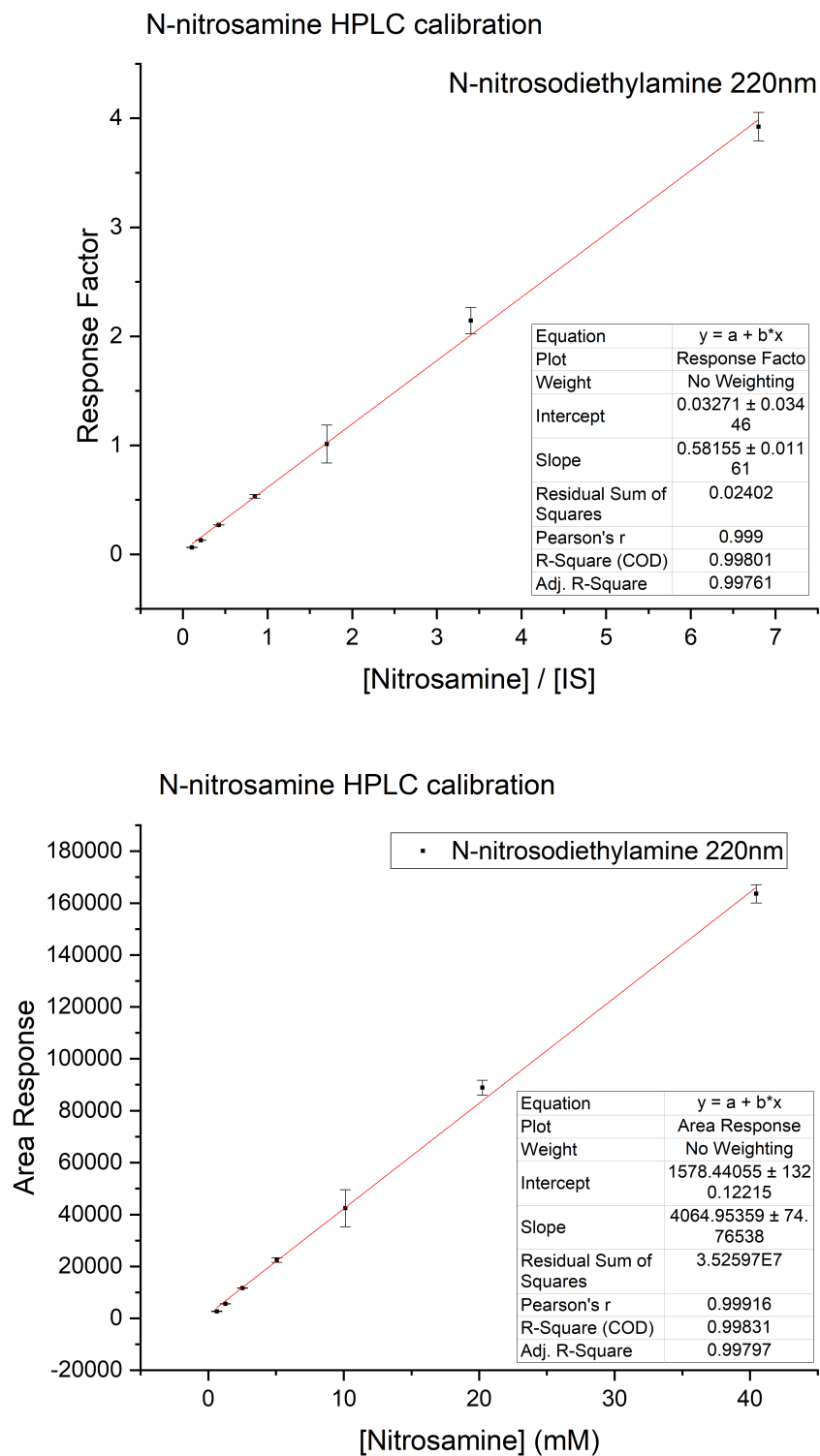


Figure D.2: HPLC Calibration curves for N-nitrosodiethylamine (N1) at 220nm. Referenced in Chapter 3, general experimental procedure Section 3.5 and in Table 3.5.

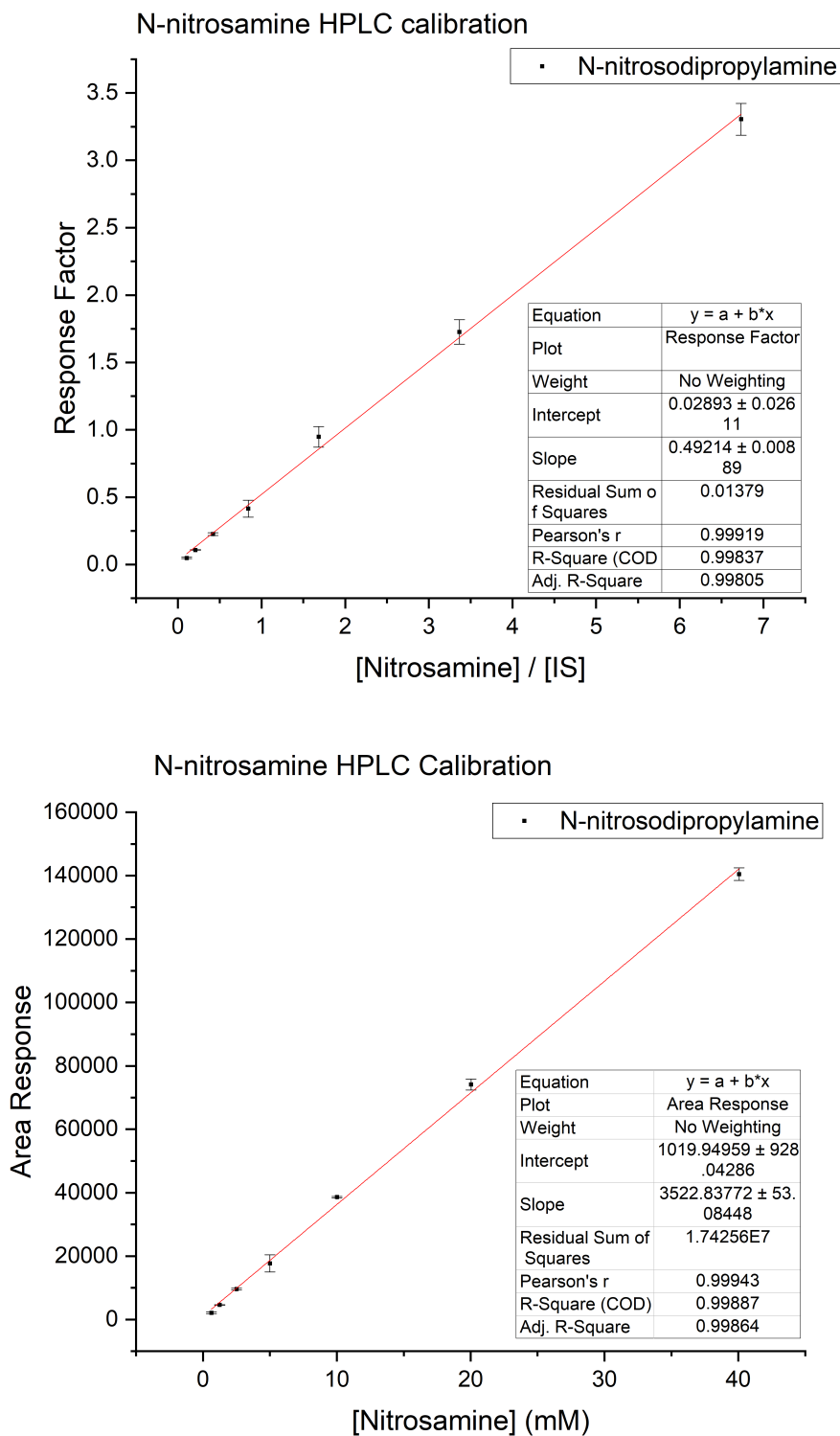


Figure D.3: HPLC Calibration curves for N-nitrosodipropylamine (N2). Referenced in Chapter 3, general experimental procedure Section 3.5 and in Table 3.5.

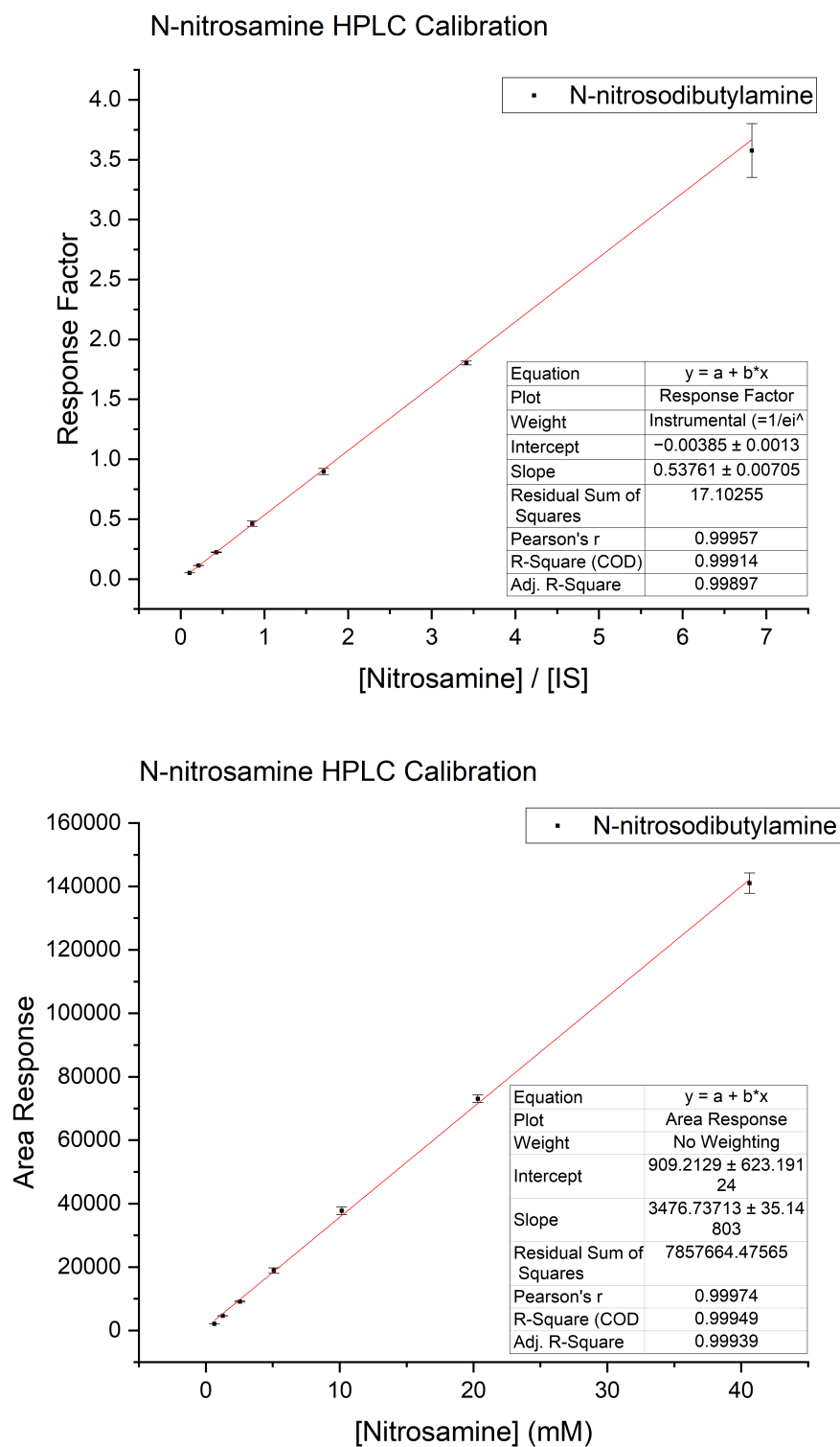


Figure D.4: HPLC Calibration curves for N-nitrosodibutylamine (N3). Referenced in Chapter 3, general experimental procedure Section 3.5 and in Table 3.5.

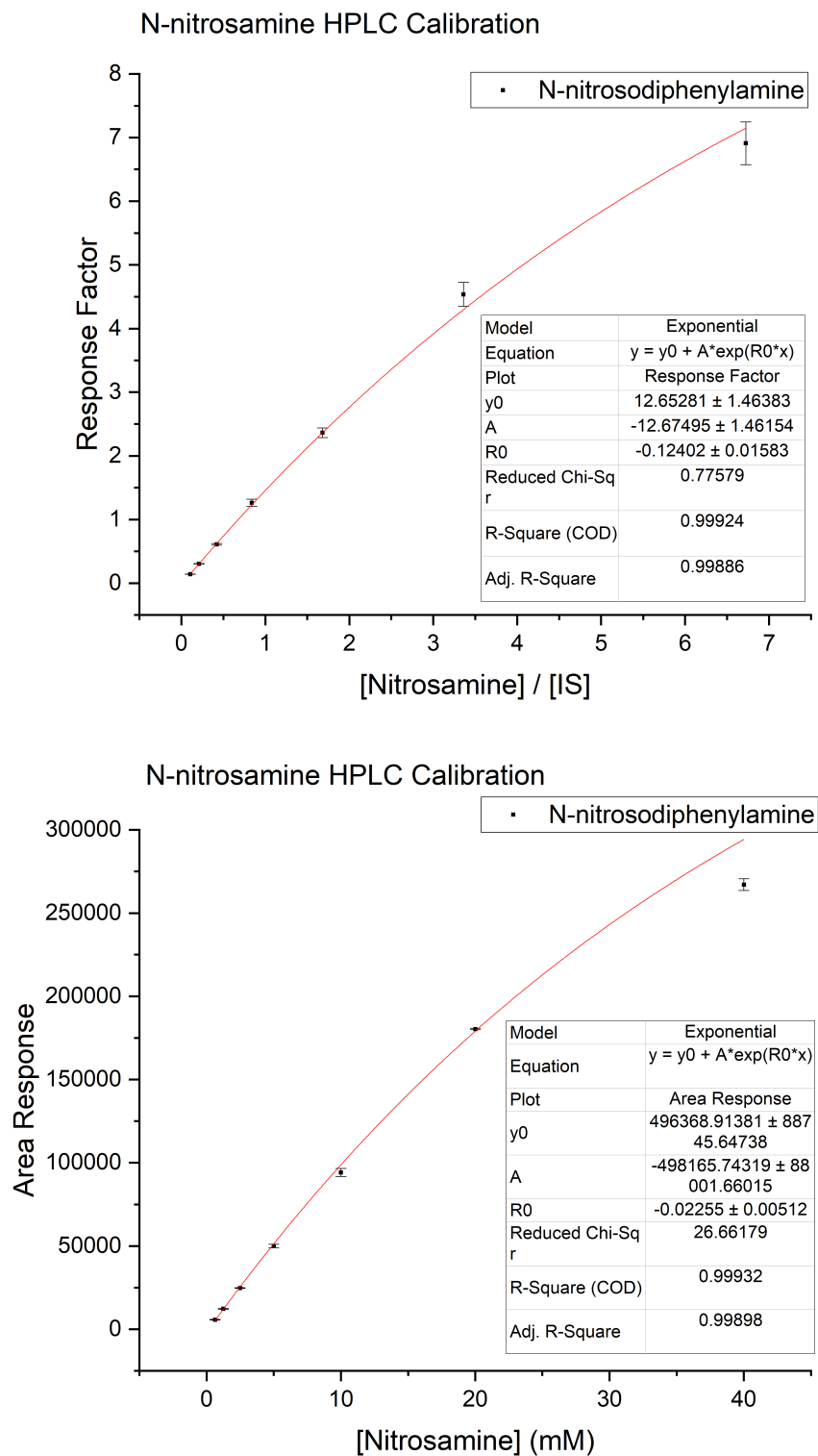


Figure D.5: HPLC Calibration curves for N-nitrosodiphenylamine (N4). Referenced in Chapter 3, general experimental procedure Section 3.5 and in Table 3.4.



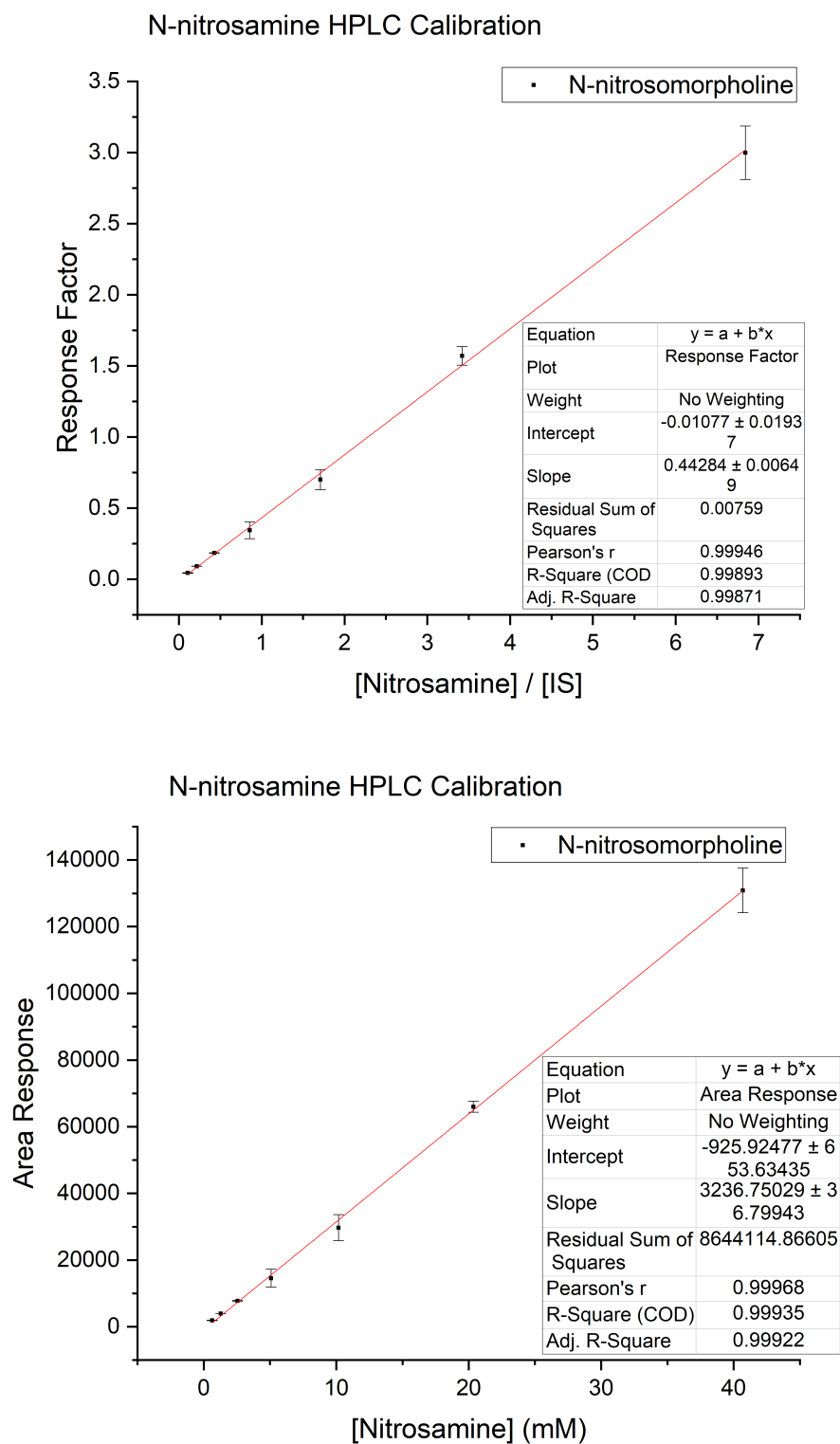


Figure D.6: HPLC Calibration curves for N-nitrosomorpholine (N5). Referenced in Chapter 3, general experimental procedure Section 3.5 and in Table 3.5.

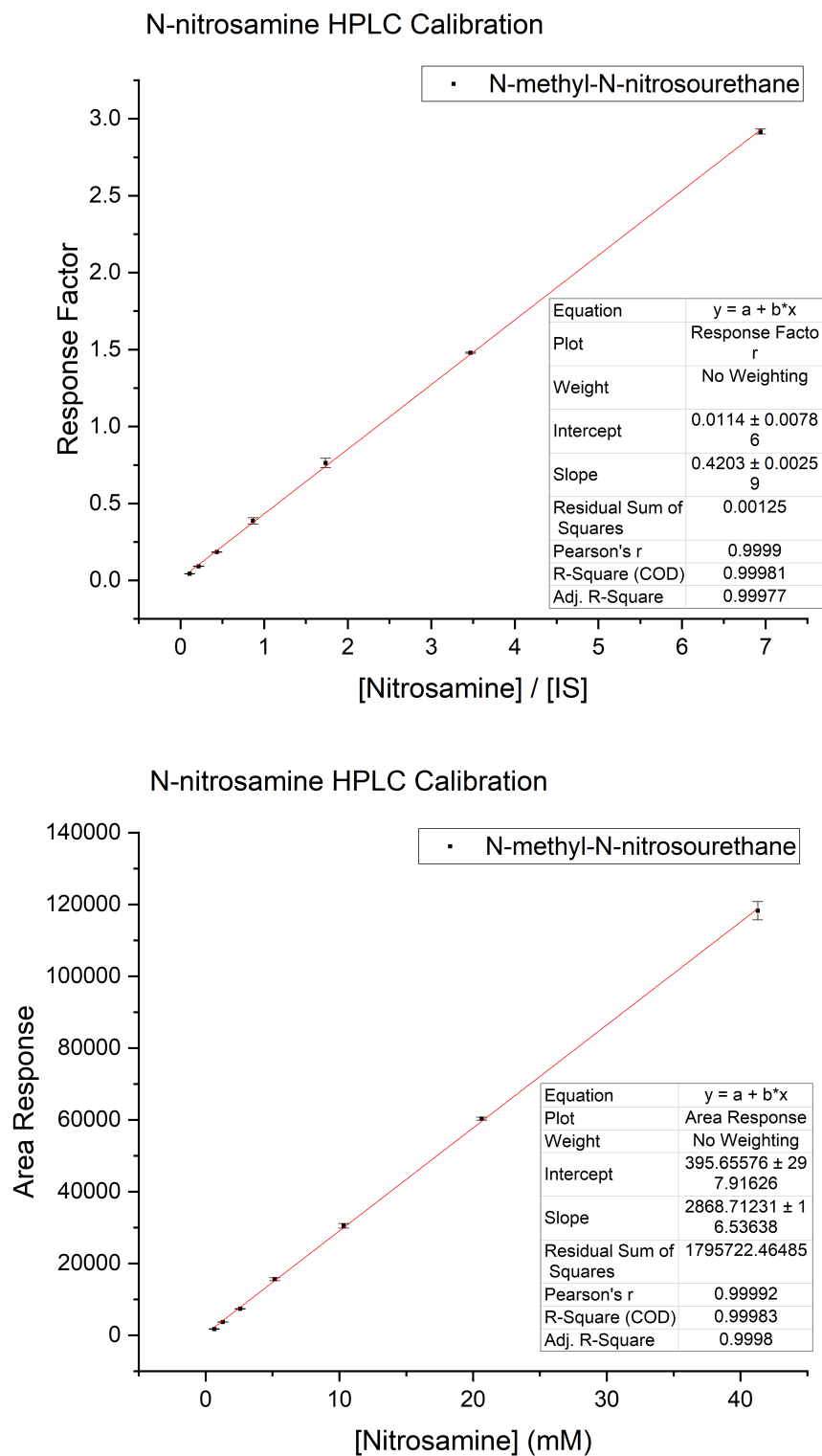


Figure D.7: HPLC Calibration curves for N-methyl-N-nitrosourethane (N6). Referenced in Chapter 3, general experimental procedure Section 3.5 and in Table 3.5.

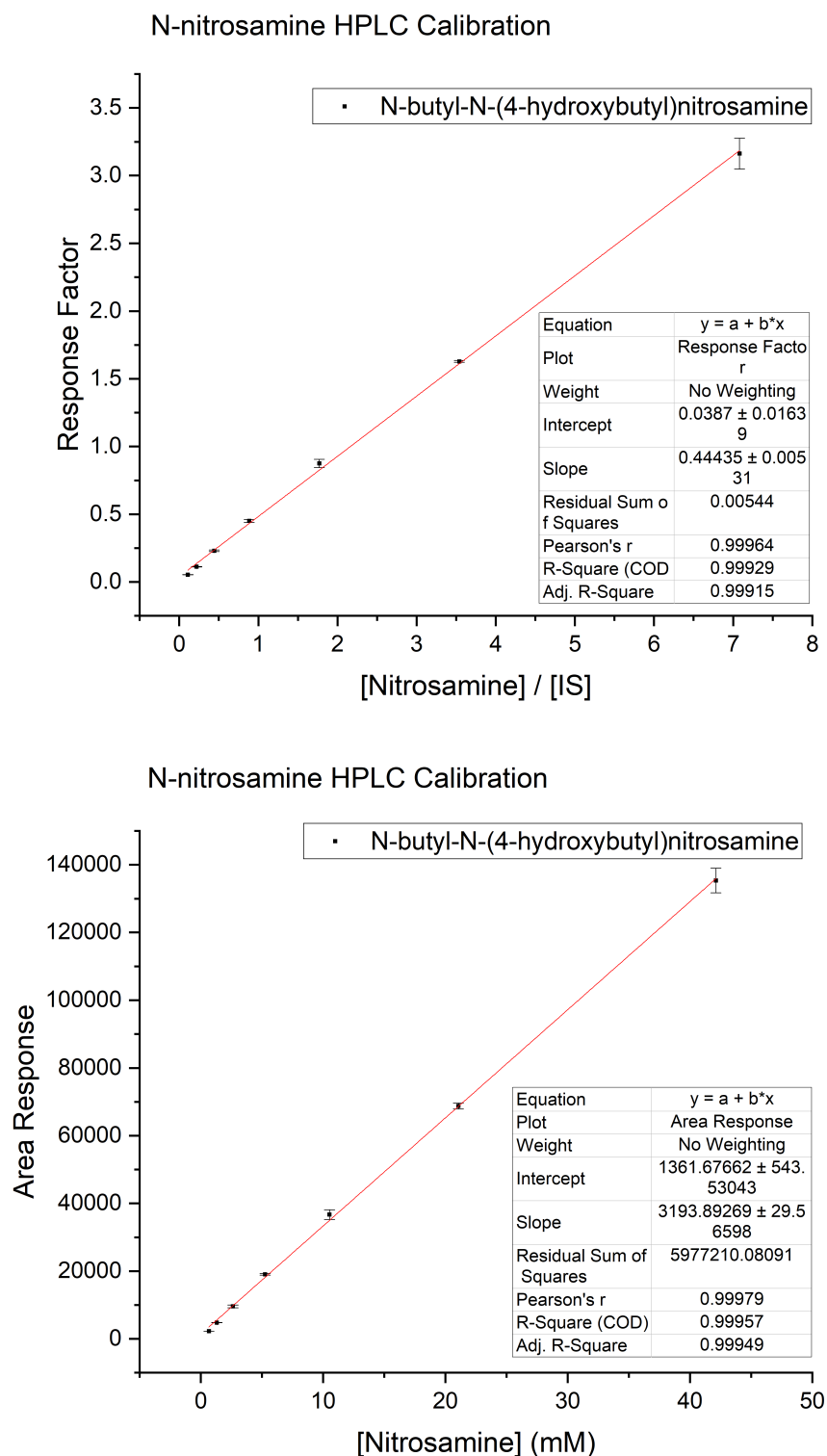


Figure D.8: HPLC Calibration curves for N-butyl-N-(4-hydroxybutyl)nitrosamine (N7). Referenced in Chapter 3, general experimental procedure Section 3.5 and in Table 3.5.

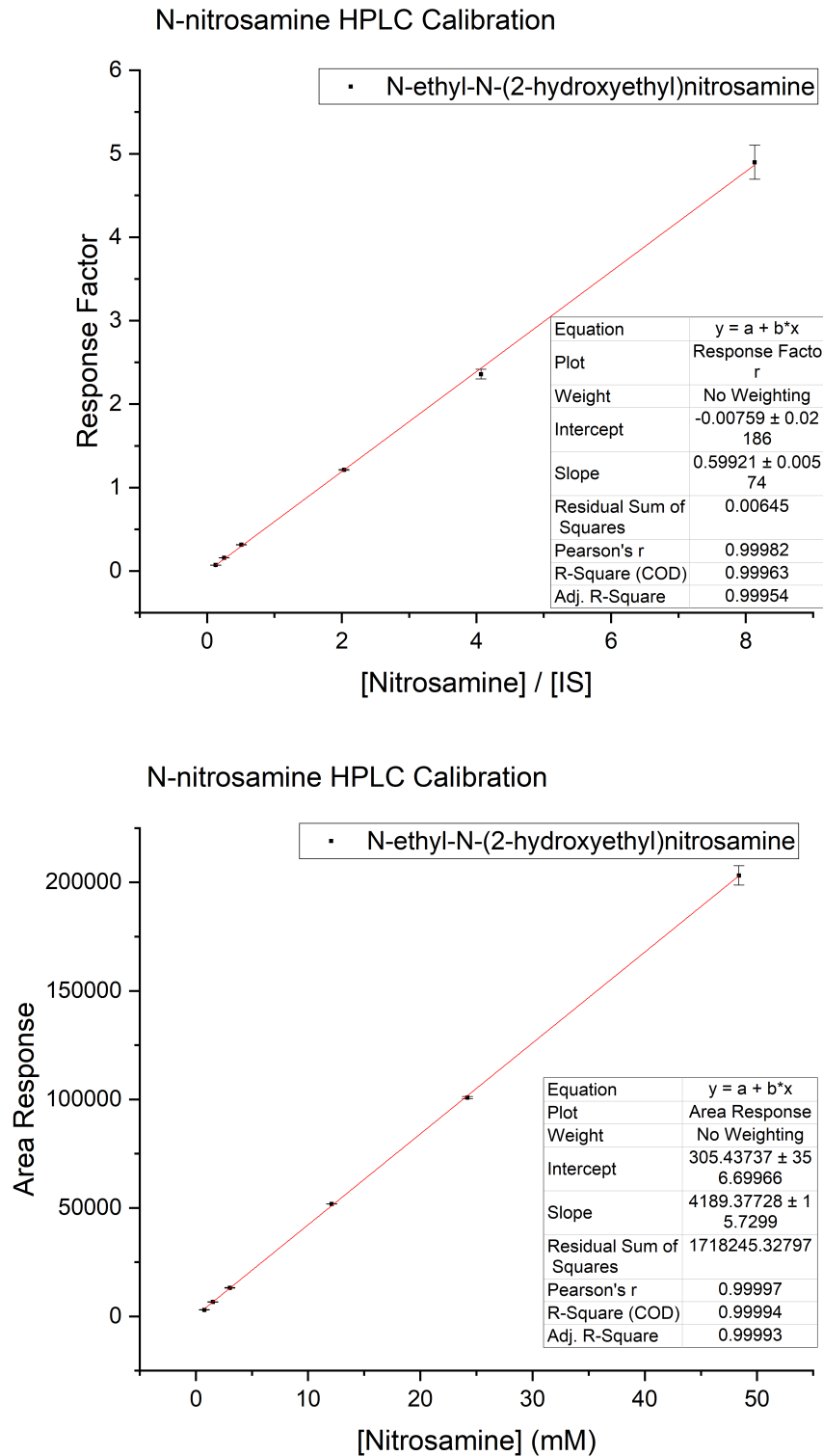


Figure D.9: HPLC Calibration curves for N-ethyl-N-(2-hydroxyethyl)nitrosamine (N8). Referenced in Chapter 3, general experimental procedure Section 3.5 and in Table 3.5.

## Appendix E

# GC-MS/MS Calibrations

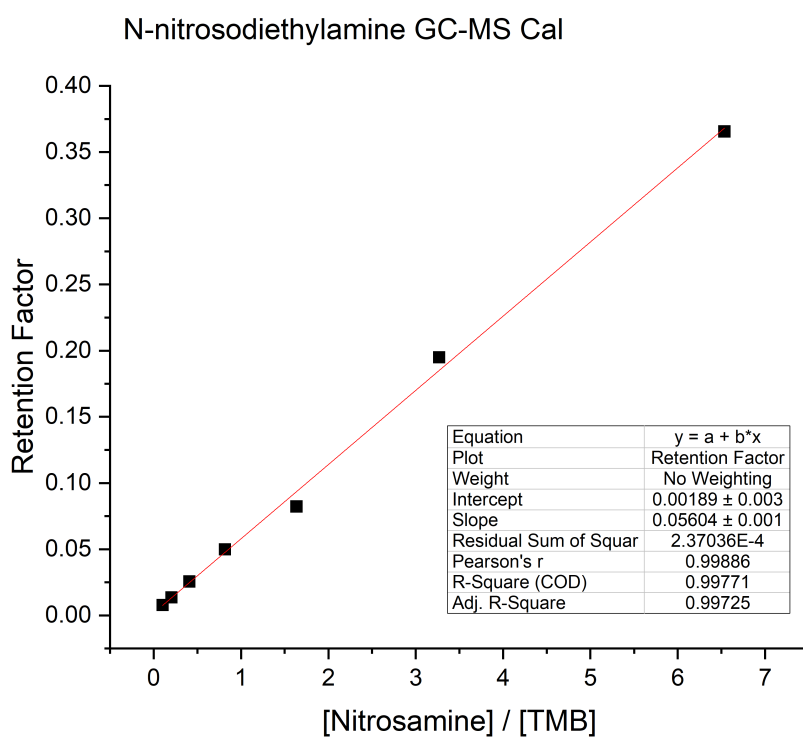


Figure E.1: GC-MSMS Calibration curve for N-nitrosodiethylamine (N1). Referenced in Chapter 3, general experimental procedure Section 3.5 and in Table 3.7.

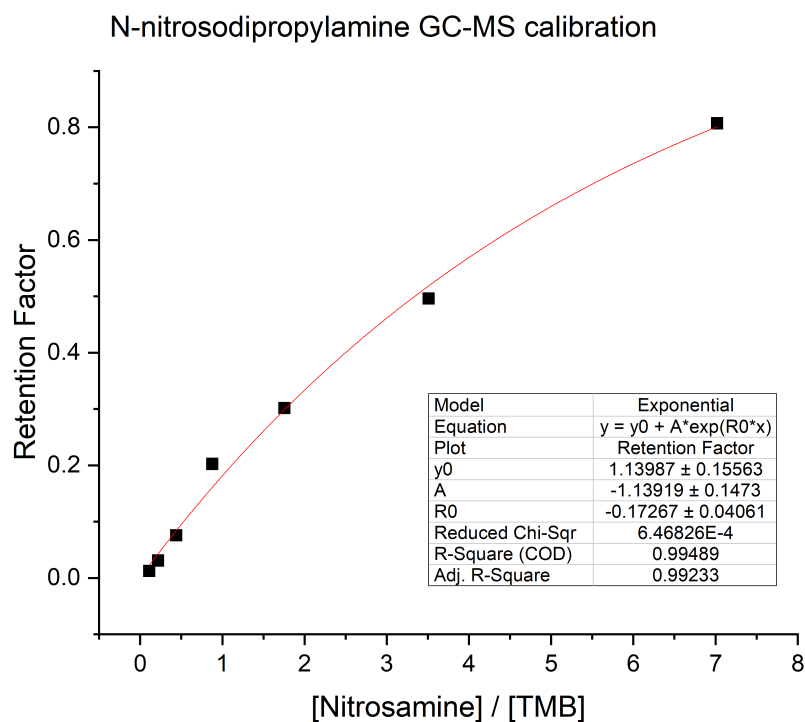


Figure E.2: GC-MSMS Calibration curve for N-nitrosodipropylamine (N2). Referenced in Chapter 3, general experimental procedure Section 3.5 and in Table 3.7.

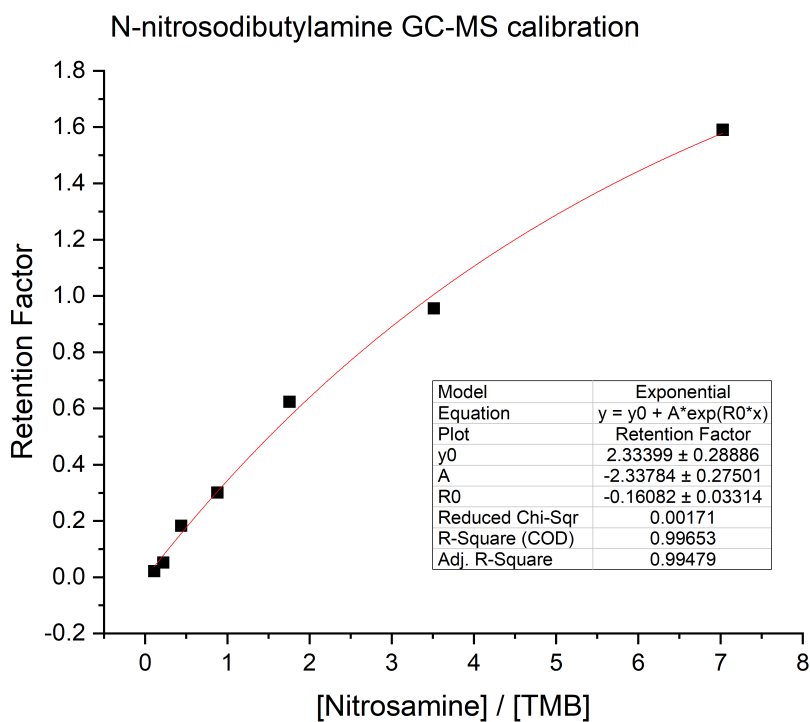


Figure E.3: GC-MSMS Calibration curve for N-nitrosodibutylamine (N3). Referenced in Chapter 3, general experimental procedure Section 3.5 and in Table 3.7.

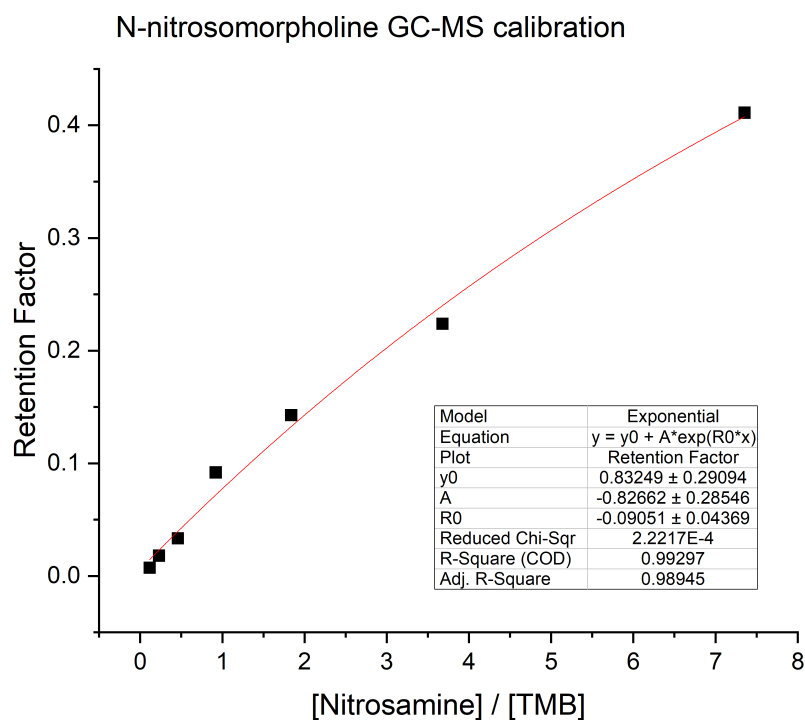


Figure E.4: GC-MSMS Calibration curve for N-nitrosomorpholine (N5). Referenced in Chapter 3, general experimental procedure Section 3.5 and in Table 3.7.

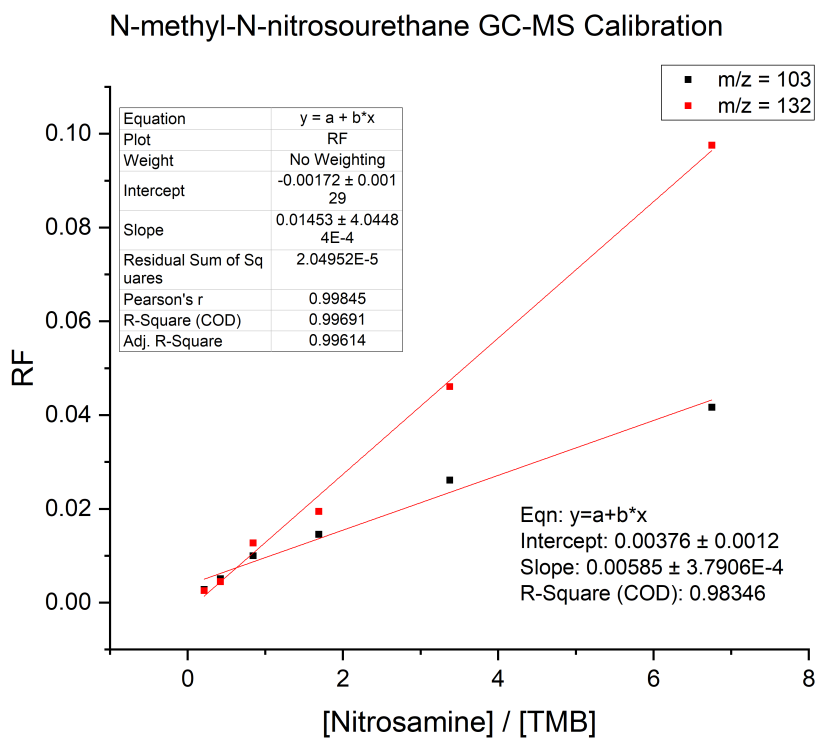


Figure E.5: GC-MSMS Calibration curve for N-methyl-N-nitrosourethane (N6). Referenced in Chapter 3, general experimental procedure Section 3.5 and in Table 3.7.

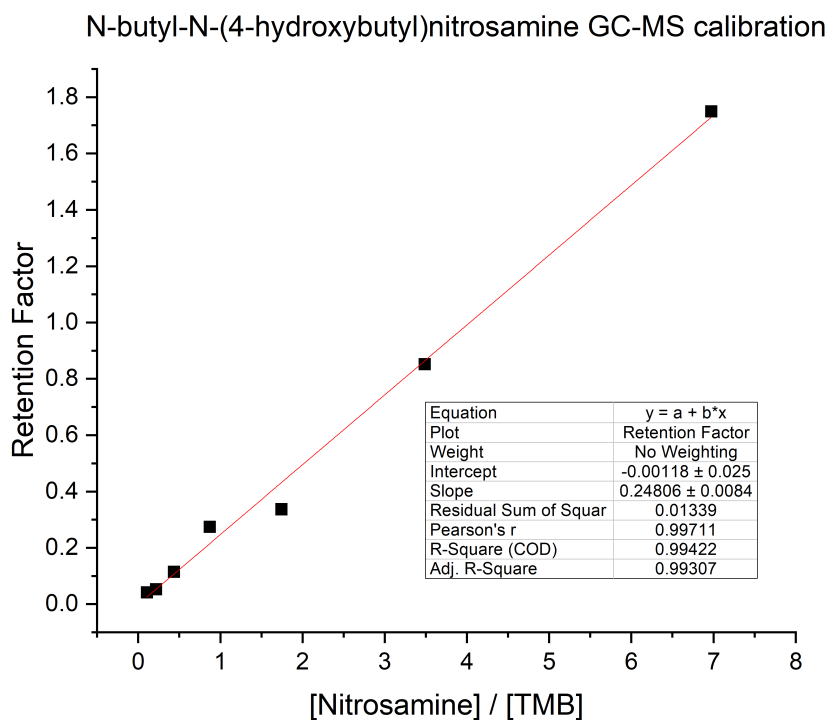


Figure E.6: GC-MSMS Calibration curve for N-butyl-N-(4-hydroxybutyl)nitrosamine (N7). Referenced in Chapter 3, general experimental procedure Section 3.5 and in Table 3.7.

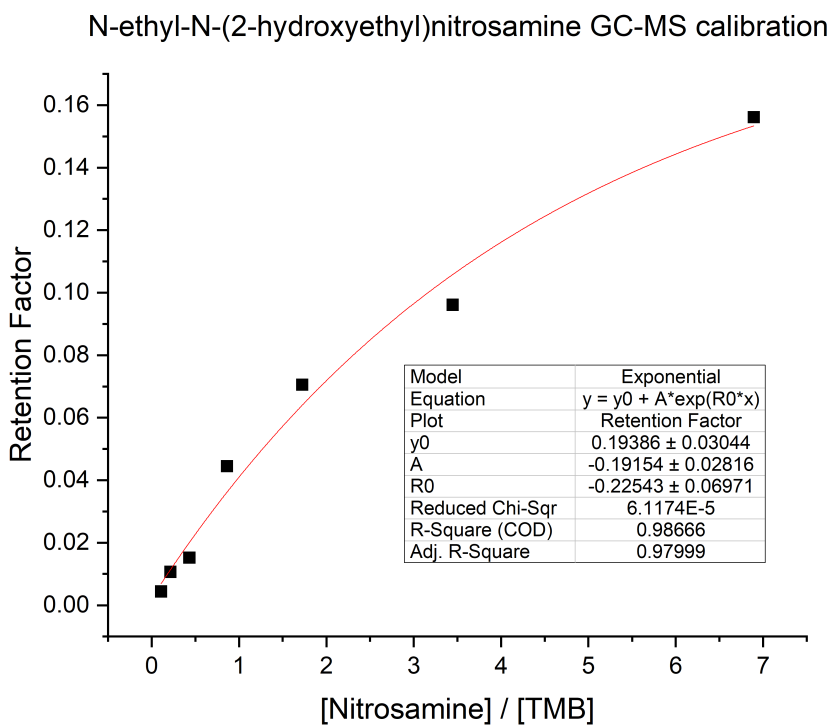


Figure E.7: GC-MSMS Calibration curve for N-ethyl-N-(2-hydroxyethyl)nitrosamine (N7). Referenced in Chapter 3, general experimental procedure Section 3.5 and in Table 3.7.



# Appendix F

## GC-MS/MS References

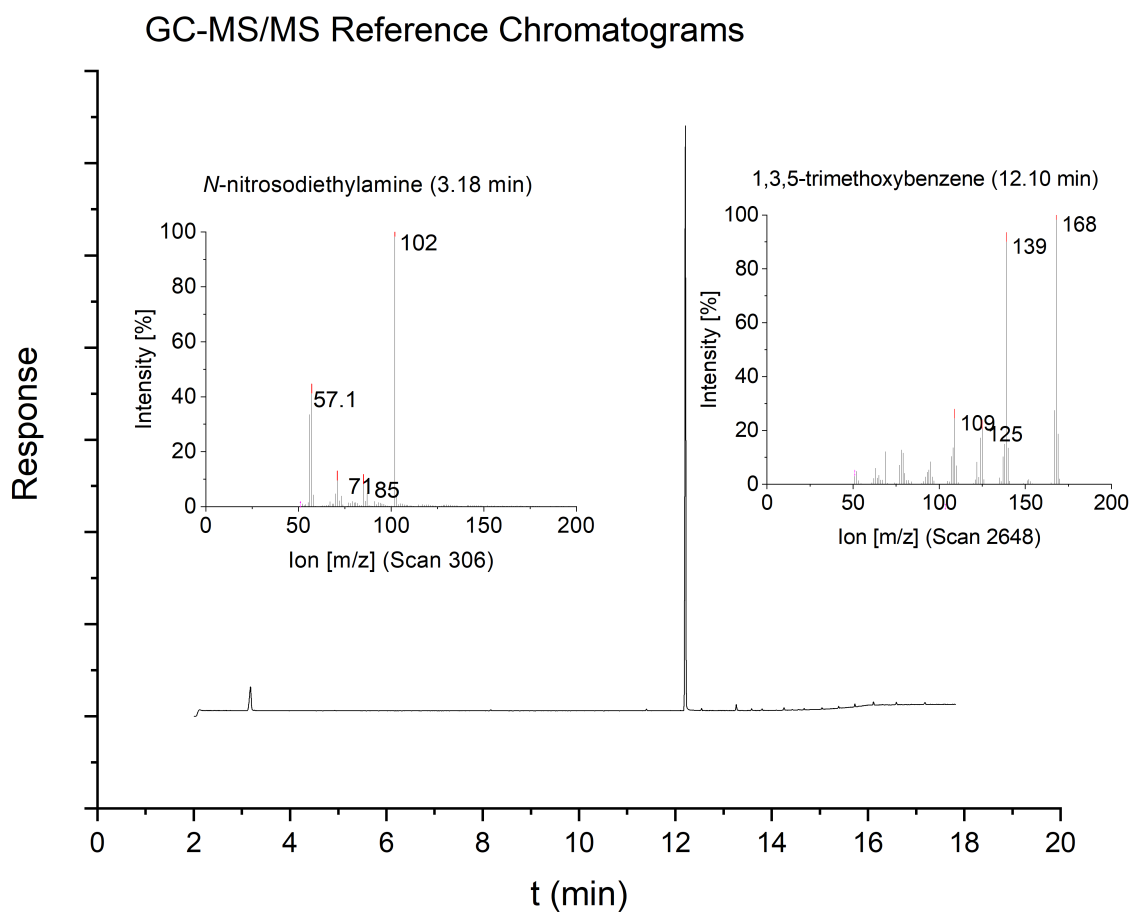


Figure F.1: GC-MSMS reference for N-nitrosodiethylamine. Referenced in Table 3.8

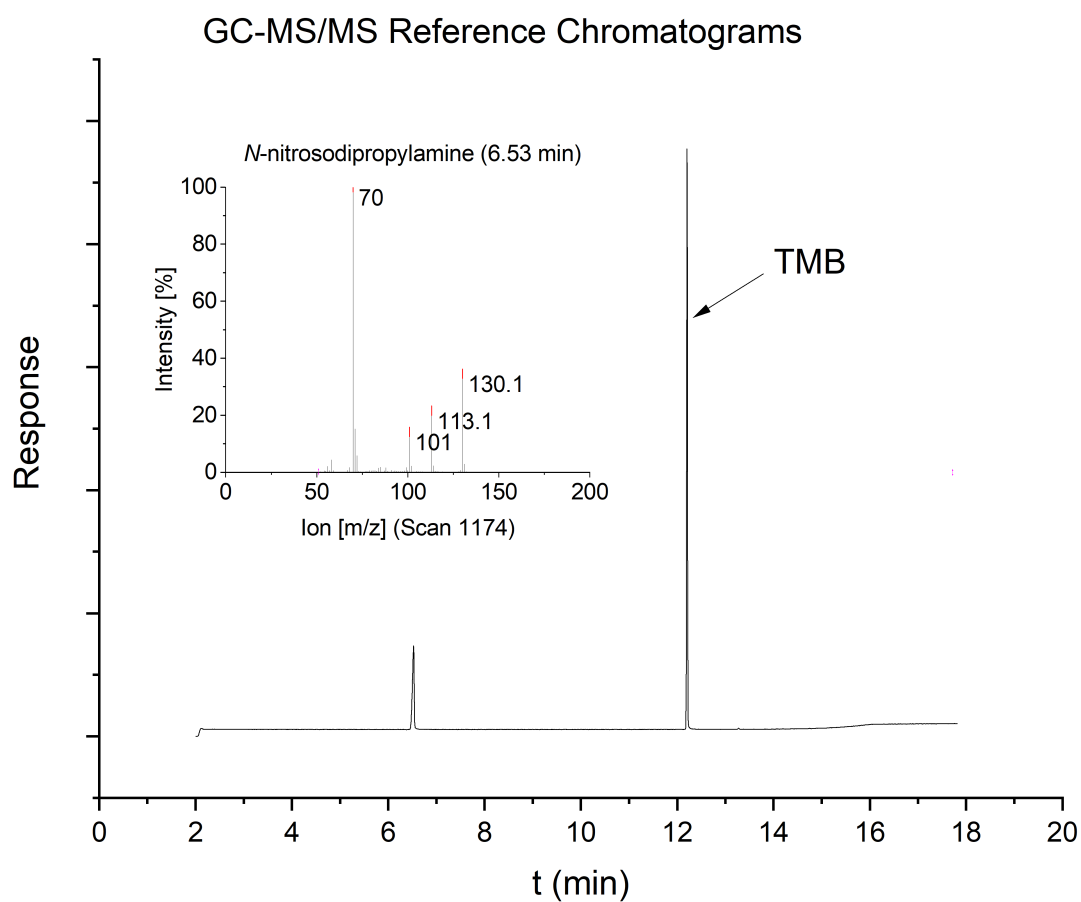


Figure F.2: GC-MSMS reference for N-nitrosodipropylamine. Referenced in Table 3.8

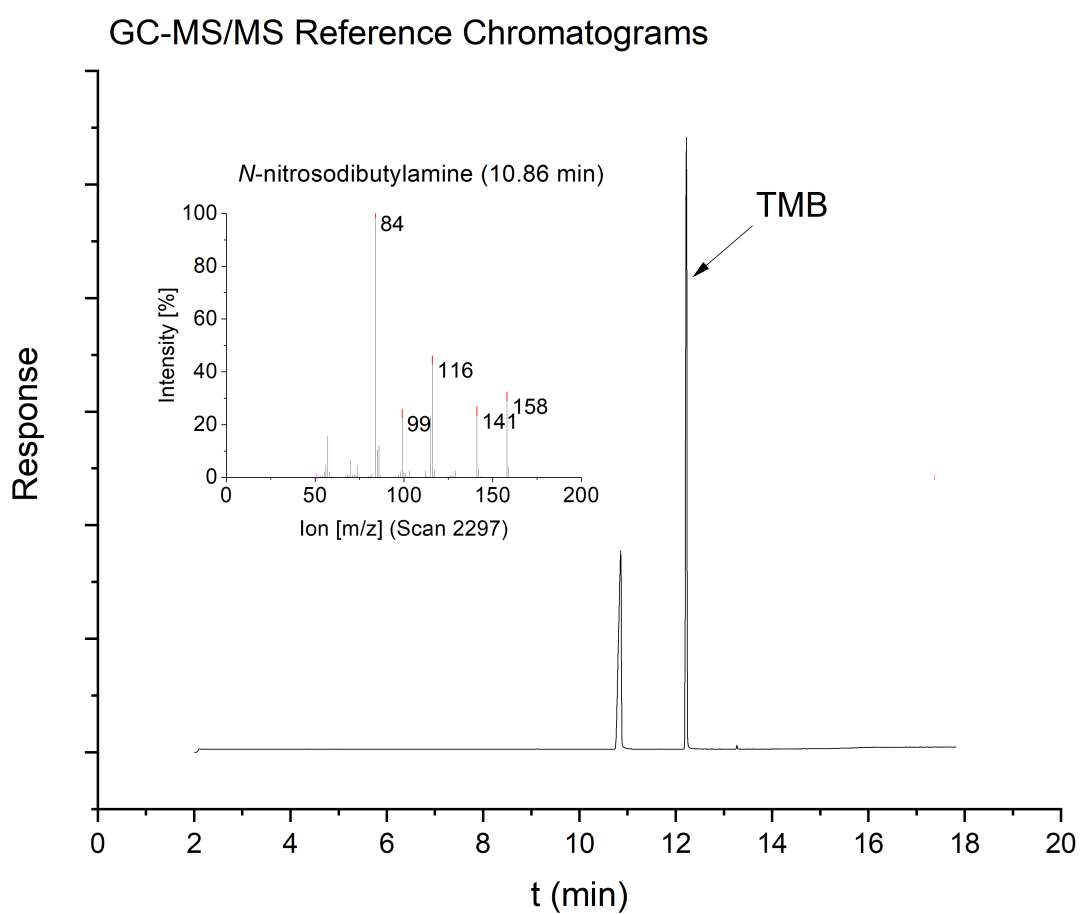


Figure F.3: GC-MSMS reference for N-nitrosodibutylamine. Referenced in Table 3.8

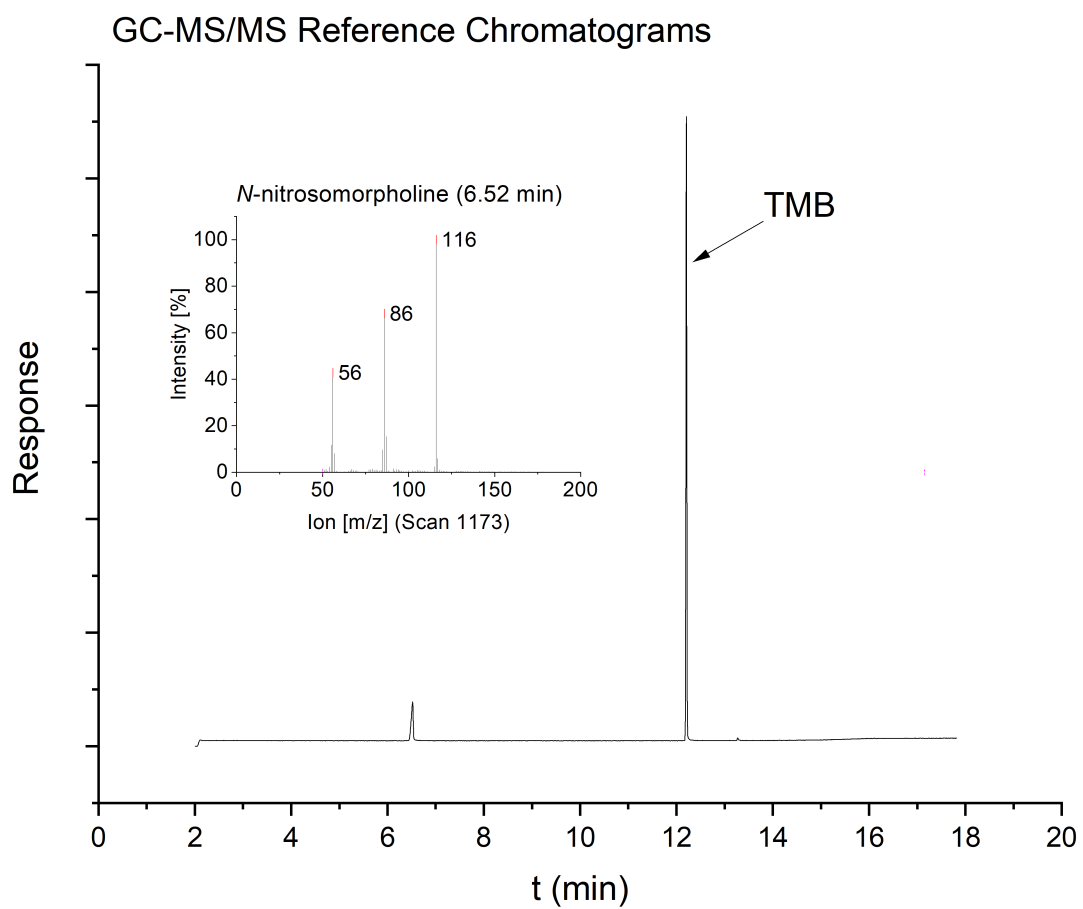
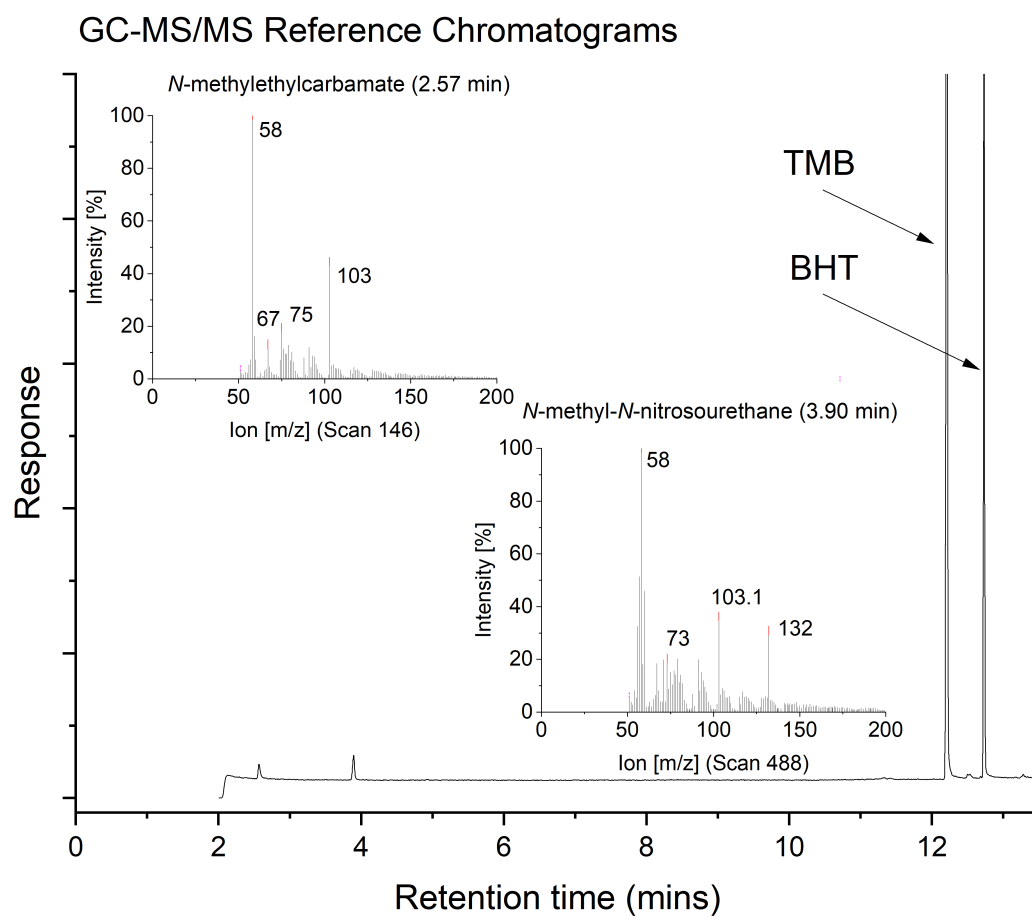


Figure F.4: GC-MSMS reference for N-nitrosomorpholine. Referenced in Table 3.8

Figure F.5: GC-MSMS reference for *N*-methyl-*N*-nitrosourethane. Referenced in Table 3.8

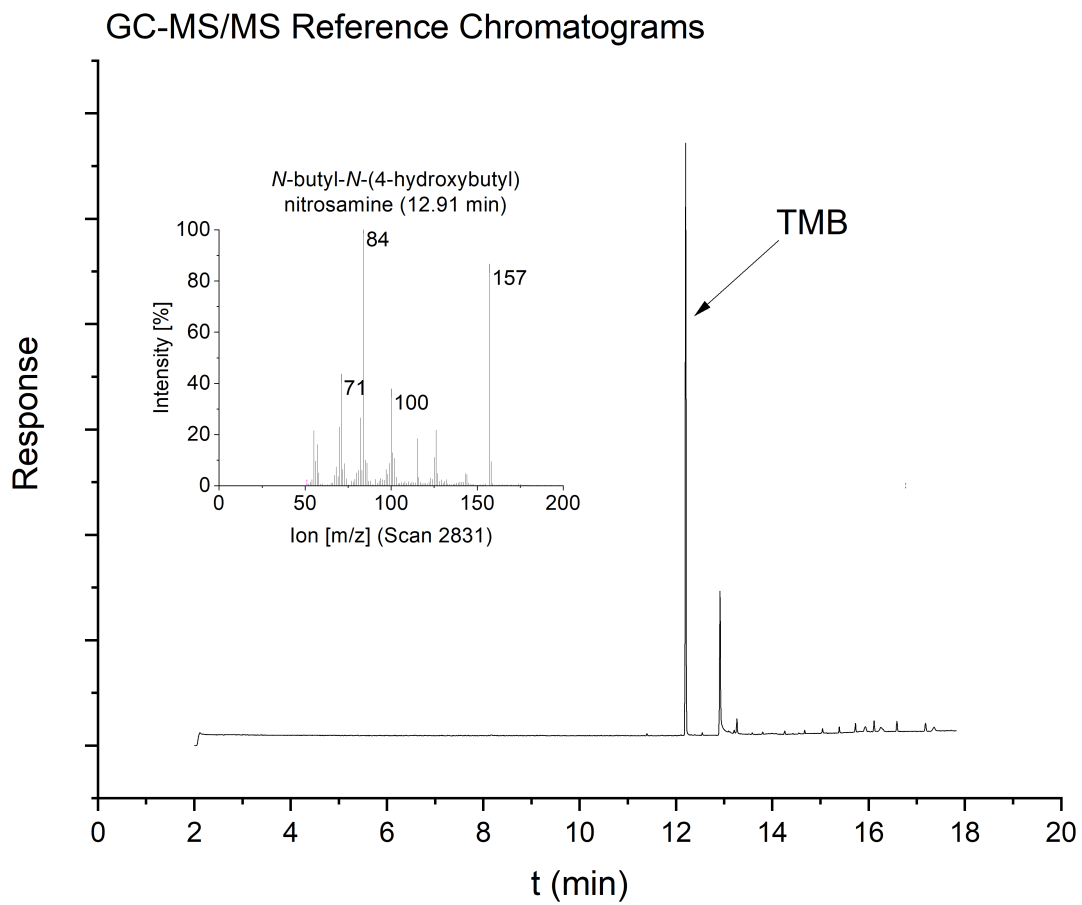


Figure F.6: GC-MSMS reference for *N*-butyl-*N*-(4-hydroxybutyl)-nitrosamine. Referenced in Table 3.8

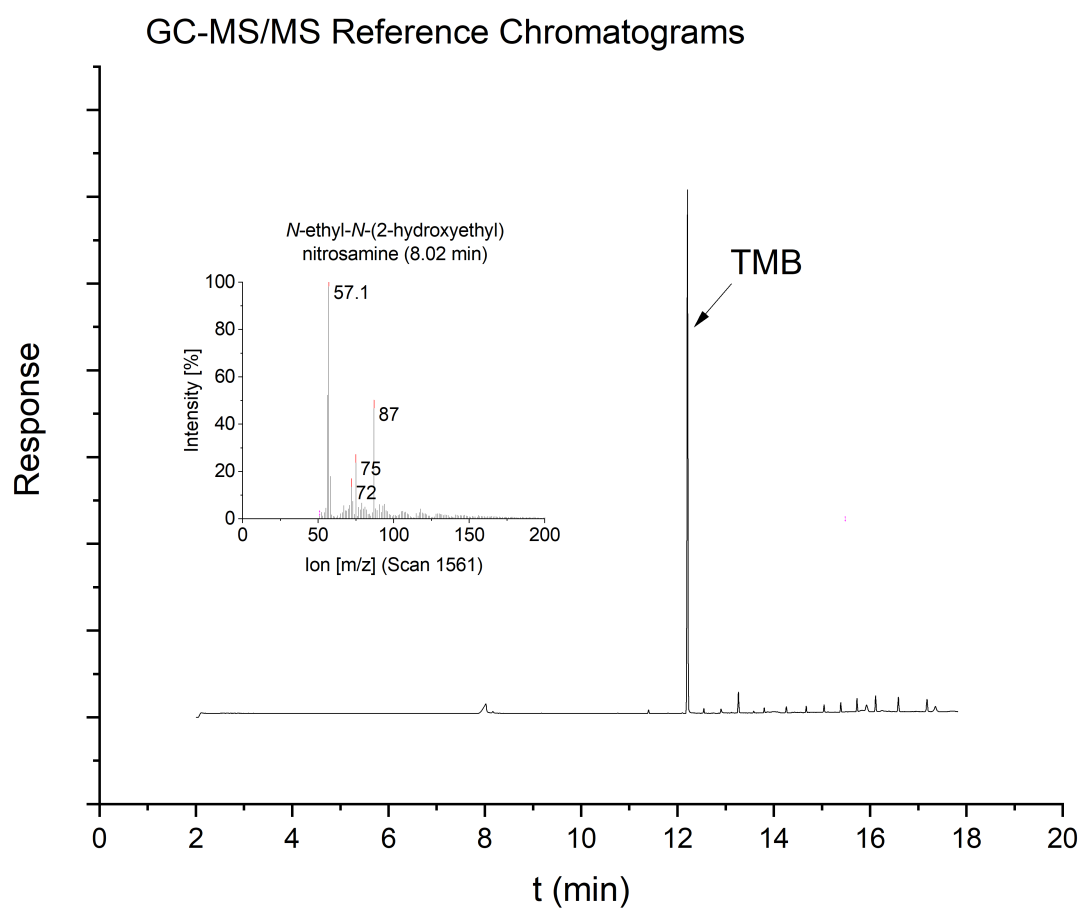


Figure F.7: GC-MSMS reference for N-ethyl-N-(2-hydroxyethyl)-nitrosamine. Referenced in Table 3.8

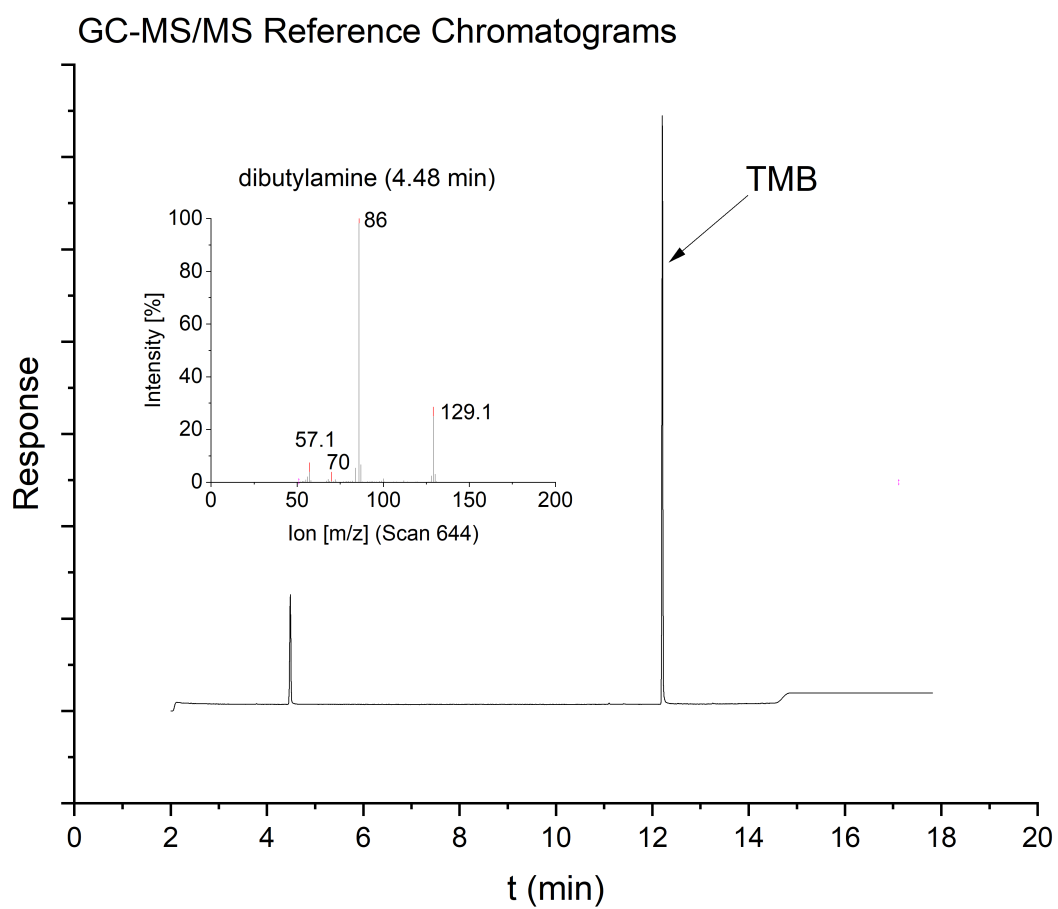


Figure F.8: GC-MSMS reference for dibutylamine. Referenced in Table 3.8



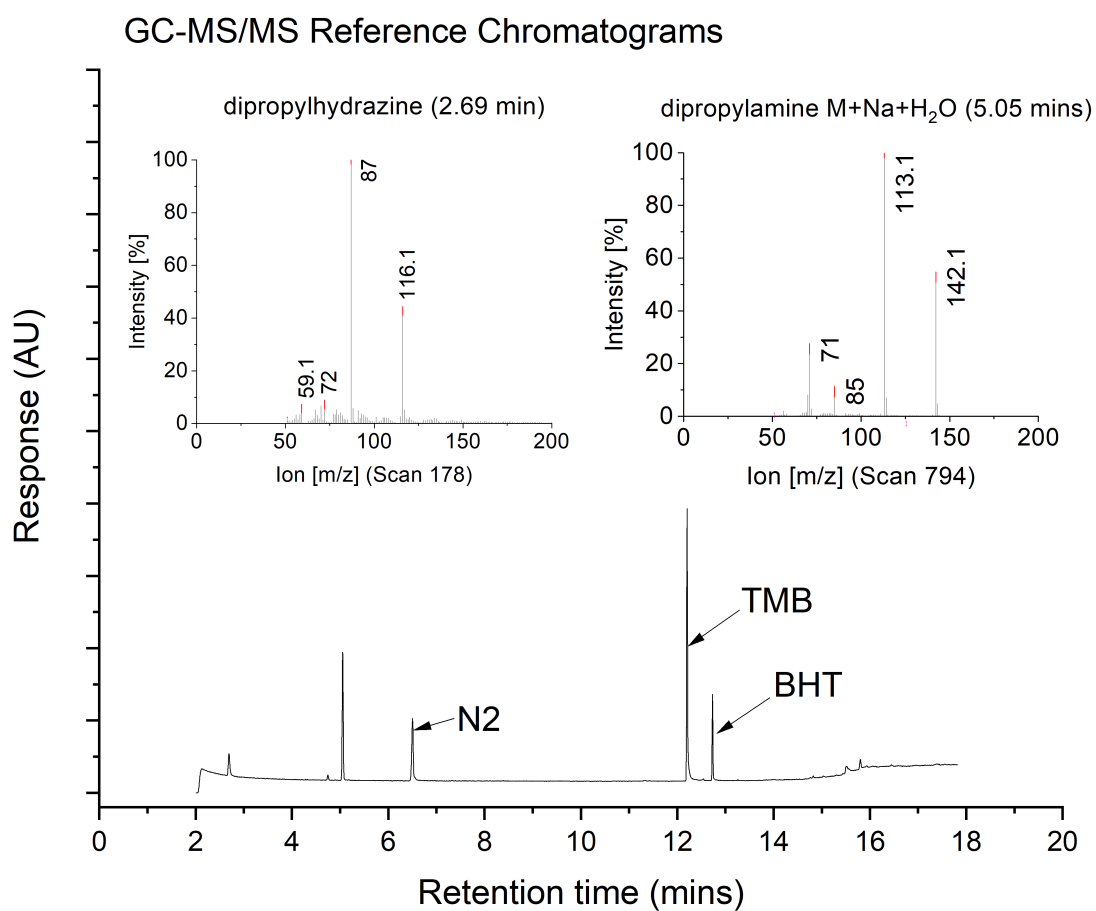


Figure F.9: GC-MSMS reference for dipropylamine and dipropylhydrazine, from reaction of N<sub>2</sub> with DiBAL-H. Referenced in Table 3.8

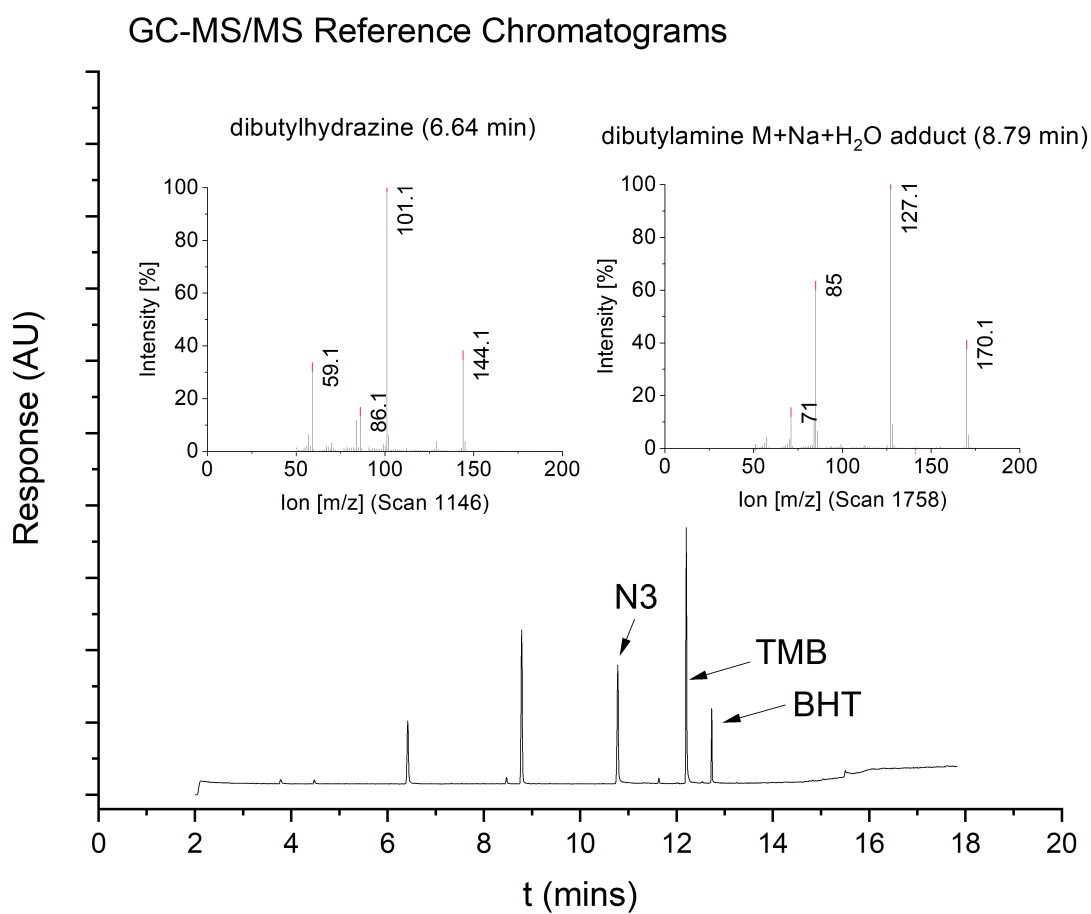


Figure F.10: GC-MSMS reference for dibutylamine and dibutylhydrazine, from reaction of N3 with DiBAL-H. Referenced in Table 3.8

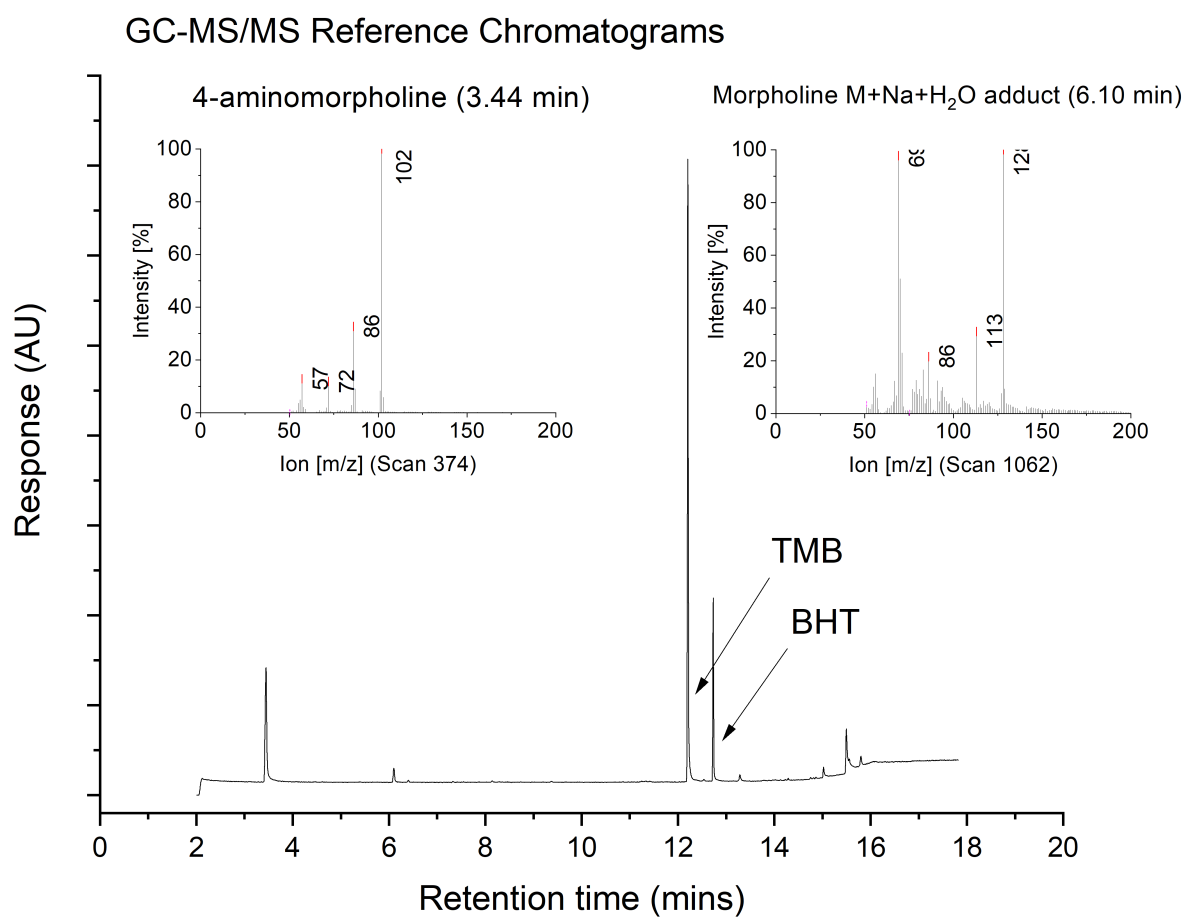


Figure F.11: GC-MS/MS reference for morpholine and 4-aminomorpholine, from reaction of N5 with DiBAL-H. Referenced in Table 3.8

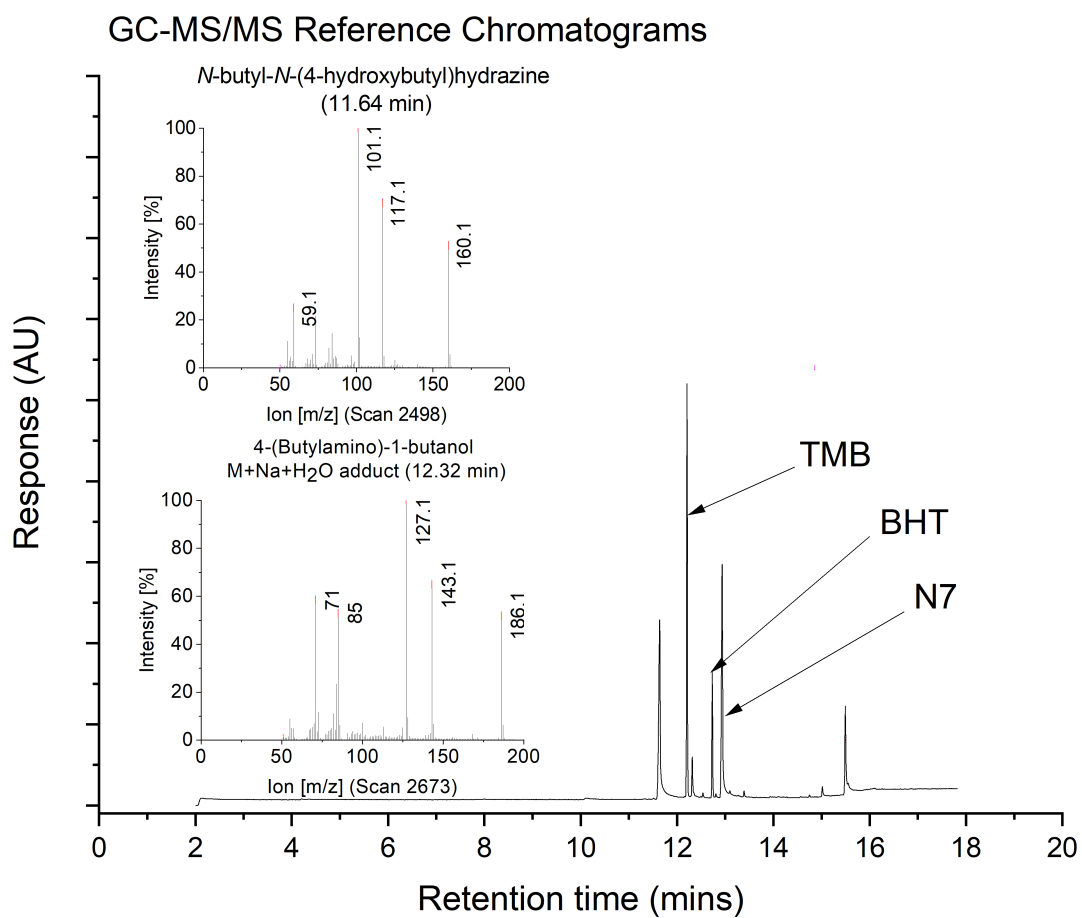


Figure F.12: GC-MS/MS reference for 4-(butylamino)-1-butanol and *N*-butyl-*N*-(4-hydroxybutyl)hydrazine, from reaction of N7 with DiBAL-H. Referenced in Table 3.8

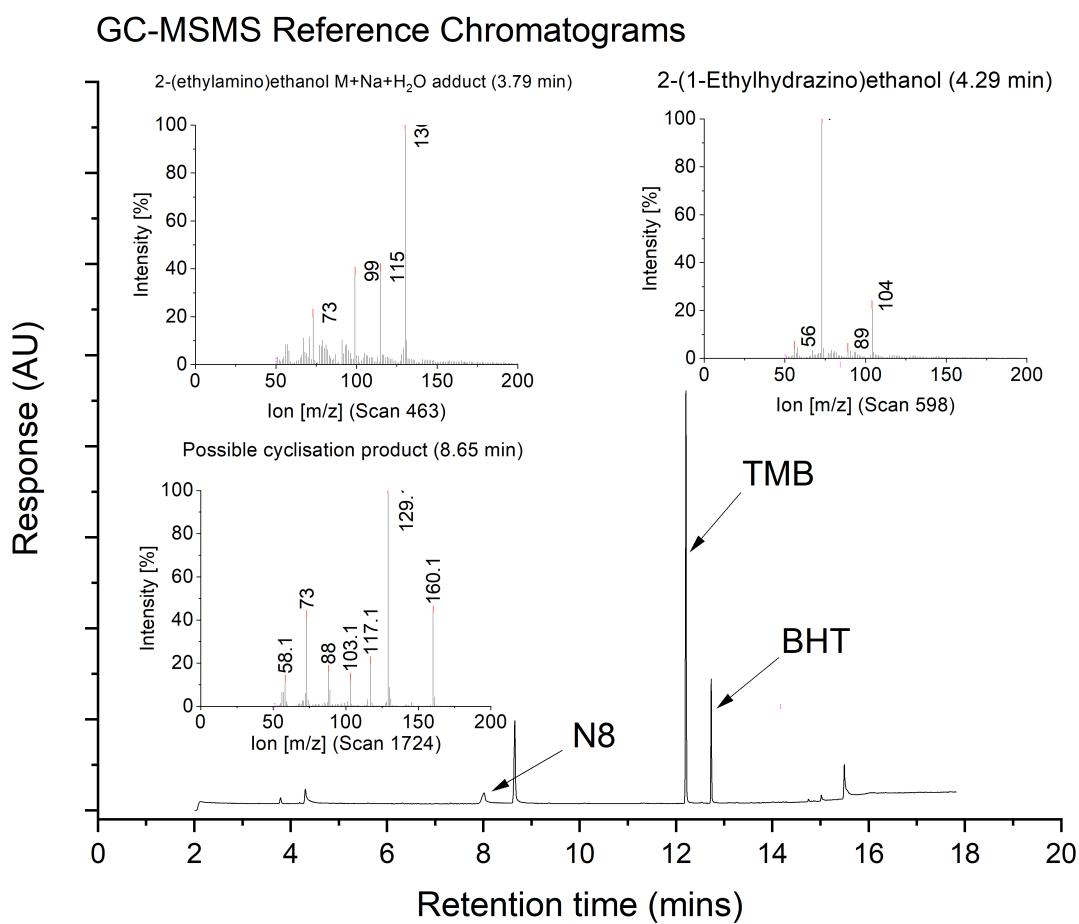


Figure F.13: GC-MSMS reference for 2-(ethylamino)ethanol and 2-(1-ethylhydrazino) ethanol, and possible cyclisation product from reaction of N8 with DiBAL-H. Referenced in Table 3.8

## GC-MS/MS Reference Chromatograms

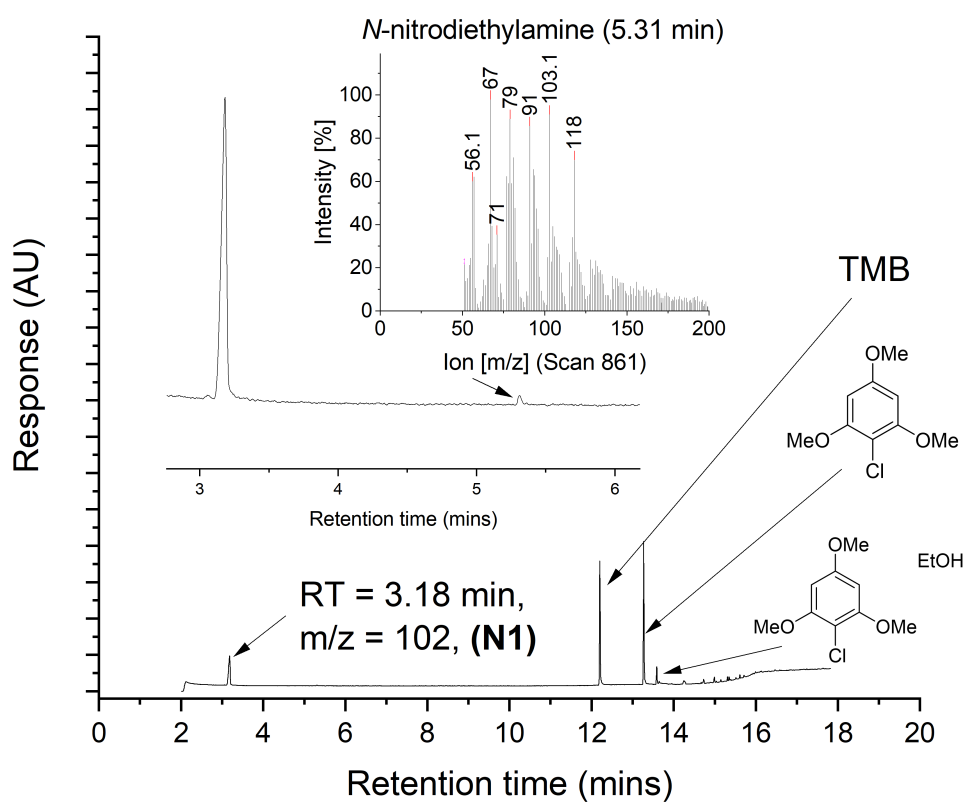


Figure F.14: GC-MSMS reference for N-nitrodiethylamine from reaction of N1 with  $\text{CH}_3\text{CO}_3\text{H}$ . Referenced in Table 3.8

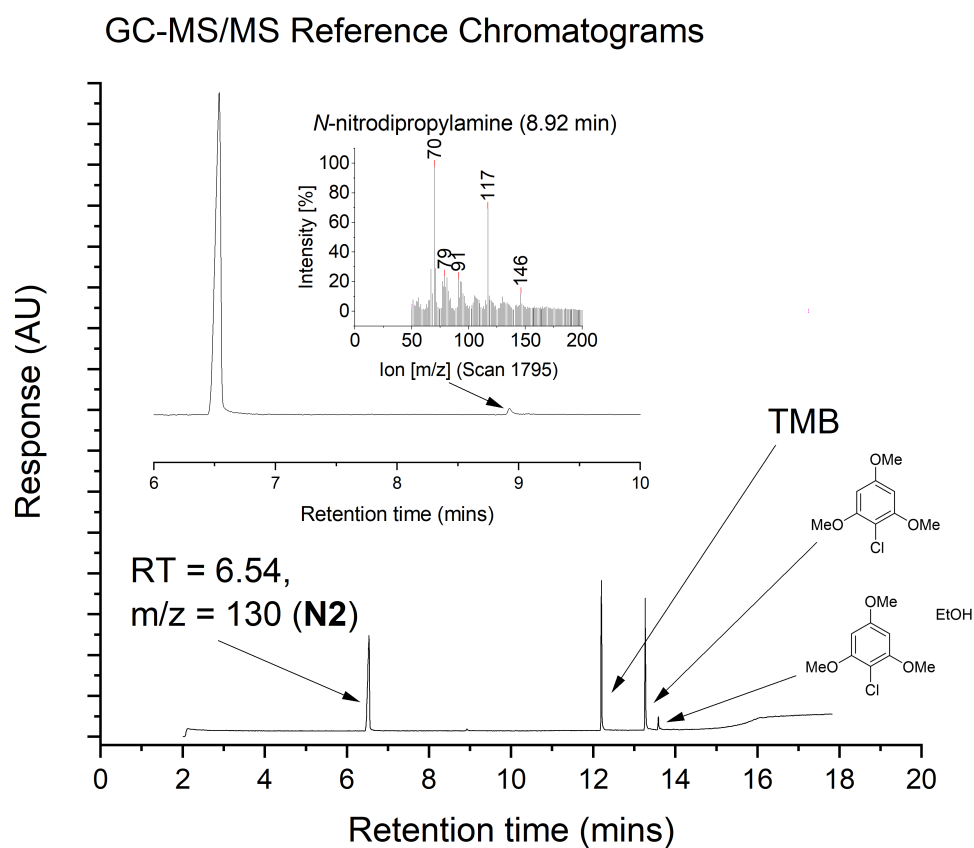


Figure F.15: GC-MSMS reference for N-nitrodipropylamine from reaction of N<sub>2</sub> with CH<sub>3</sub>CO<sub>3</sub>H. Referenced in Table 3.8

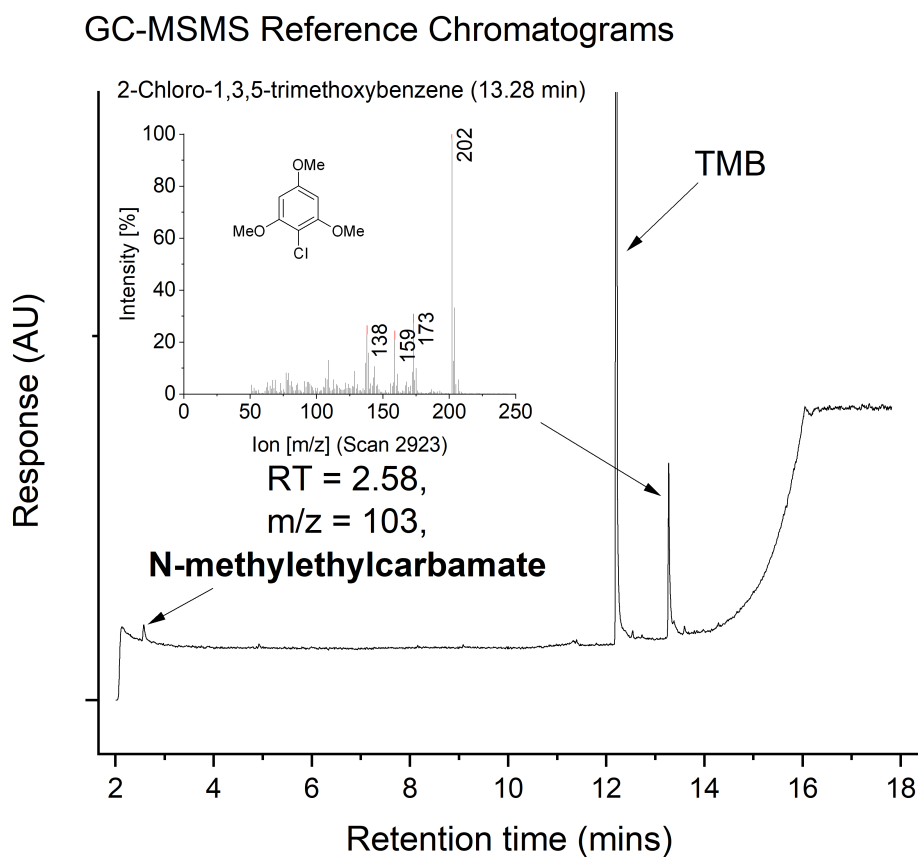


Figure F.16: GC-MSMS reference for 2-Chloro-1,3,5-trimethoxybenzene from reaction of N6 with  $\text{H}_2\text{O}_2$ . Referenced in Table 3.9



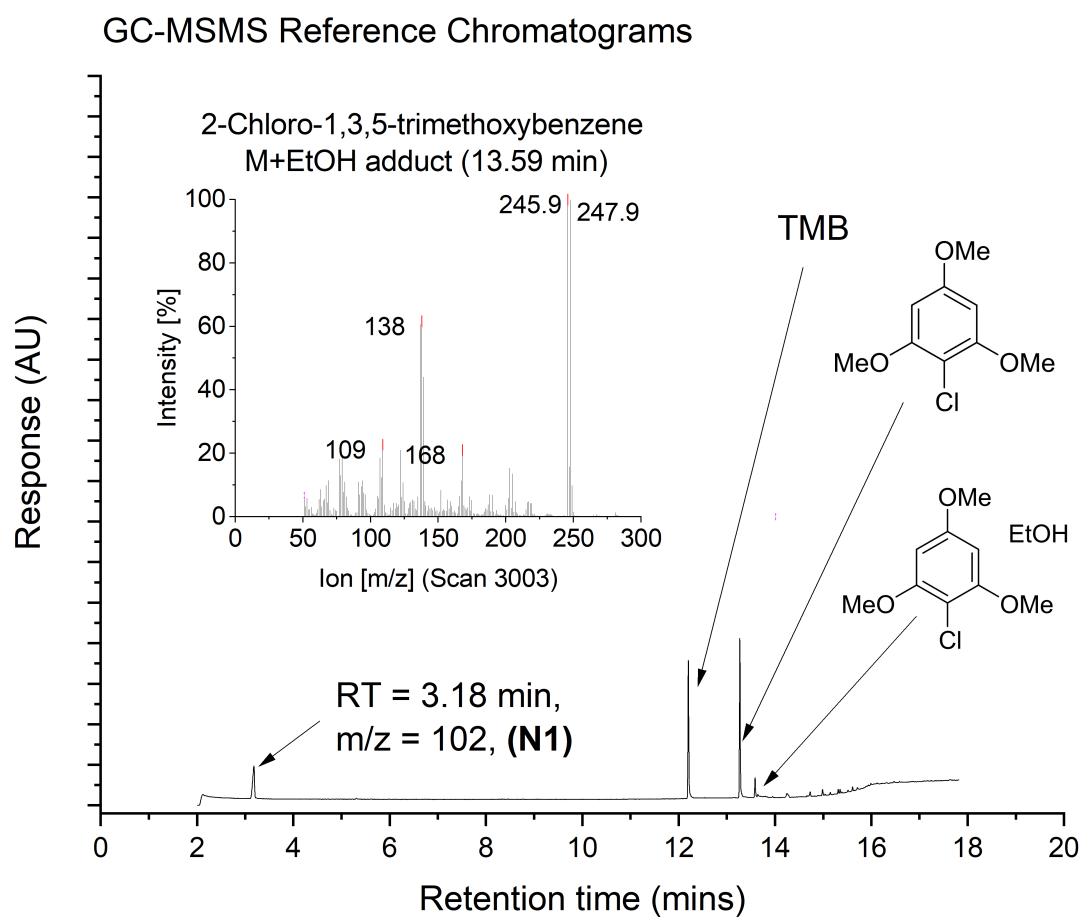


Figure F.17: GC-MSMS reference for 2-Chloro-1,3,5-trimethoxybenzene (M+EtOH adduct) from reaction of N1 with  $\text{CH}_3\text{CO}_3\text{H}$ . Referenced in Table 3.9

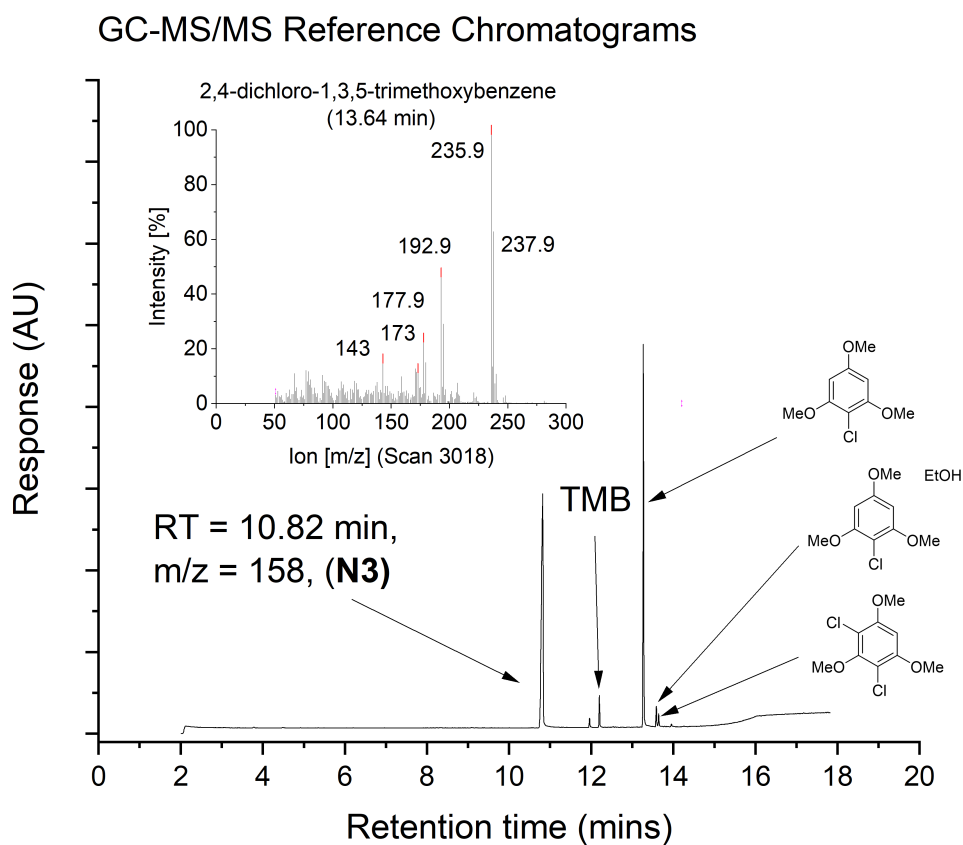


Figure F.18: GC-MSMS reference for 2,4-dichloro-1,3,5-trimethoxybenzene from reaction of N3 with  $\text{CH}_3\text{CO}_3\text{H}$ . Referenced in Table 3.9

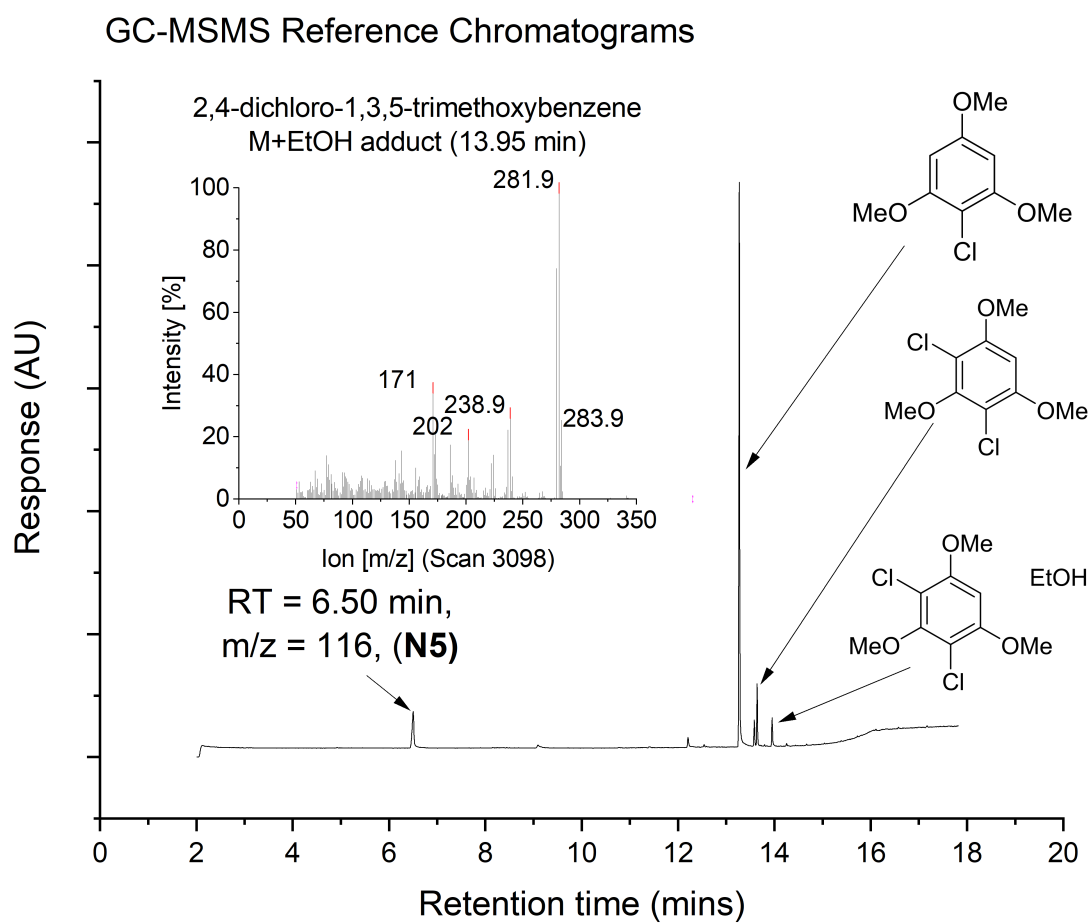


Figure F.19: GC-MSMS reference for 2,4-dichloro-1,3,5-trimethoxybenzene (M+EtOH adduct) from reaction of N5 with  $\text{CH}_3\text{CO}_3\text{H}$ . Referenced in Table 3.9

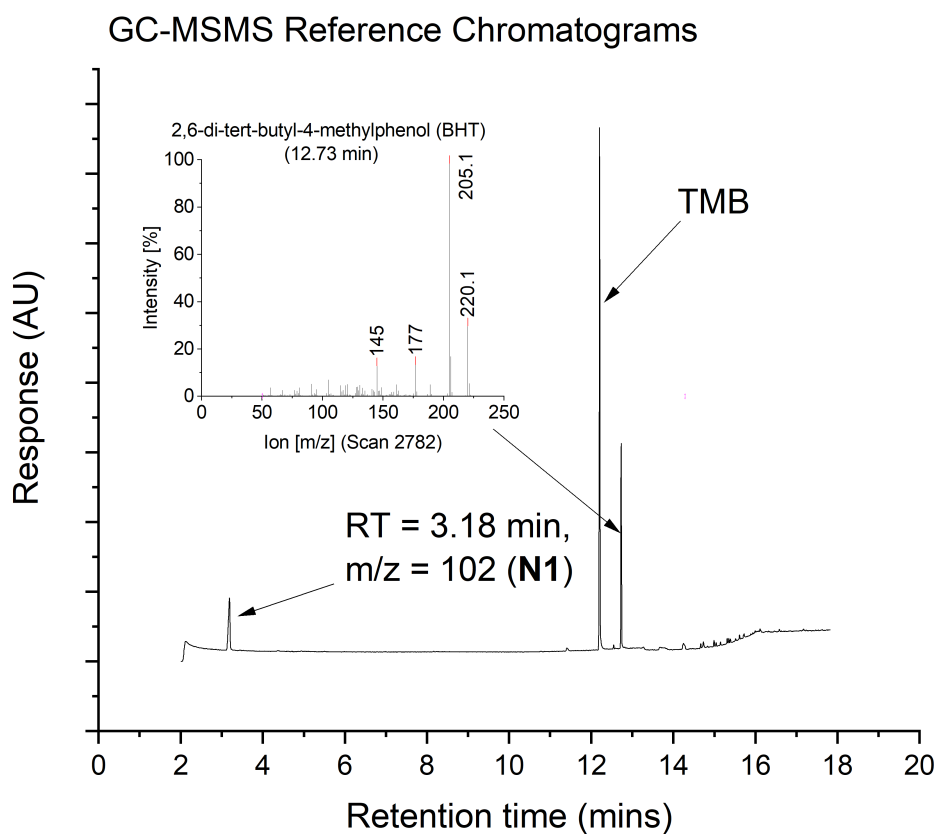


Figure F.20: GC-MSMS reference for 2,6-di-tert-butyl-4-methylphenol (BHT) from reaction of N1 with  $\text{NaBH}_4$ . Referenced in Table 3.8

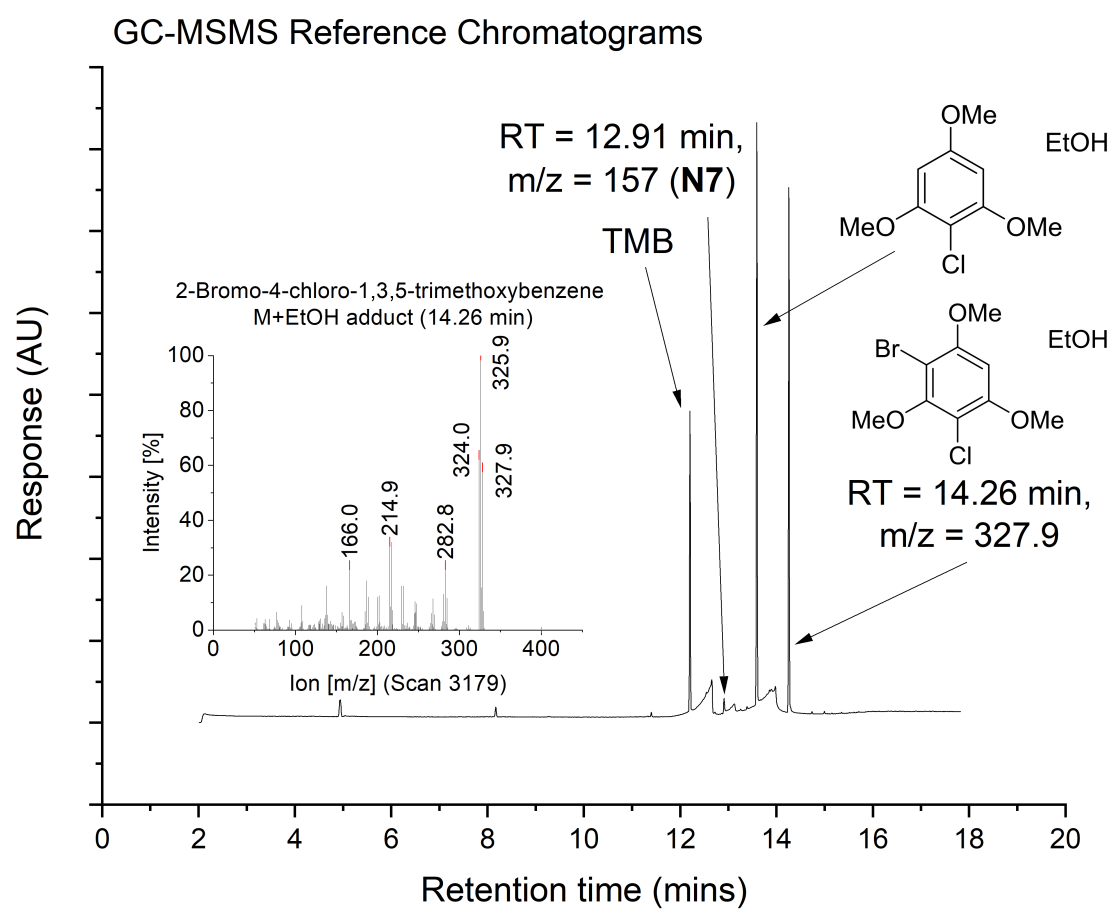


Figure F.21: GC-MSMS reference for 2-Bromo-4-chloro-1,3,5-trimethoxybenzene M+EtOH adduct from reaction of N7 with HBr. Referenced in Table 3.9

## Appendix G

### GC-MS/MS Experiment plots

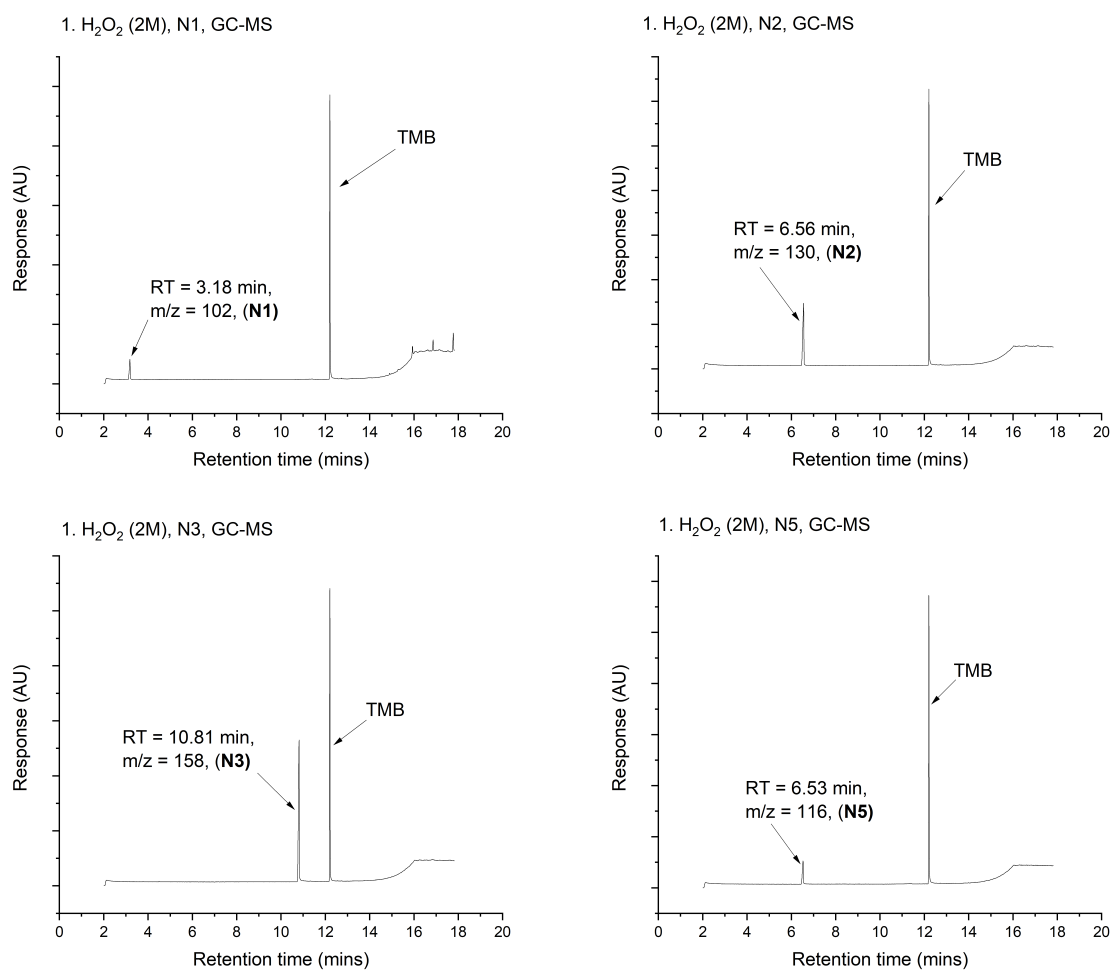


Figure G.1: GC-MSMS plots for N1, N2, N3 and N5 condition 1. As referenced in Section 3.6

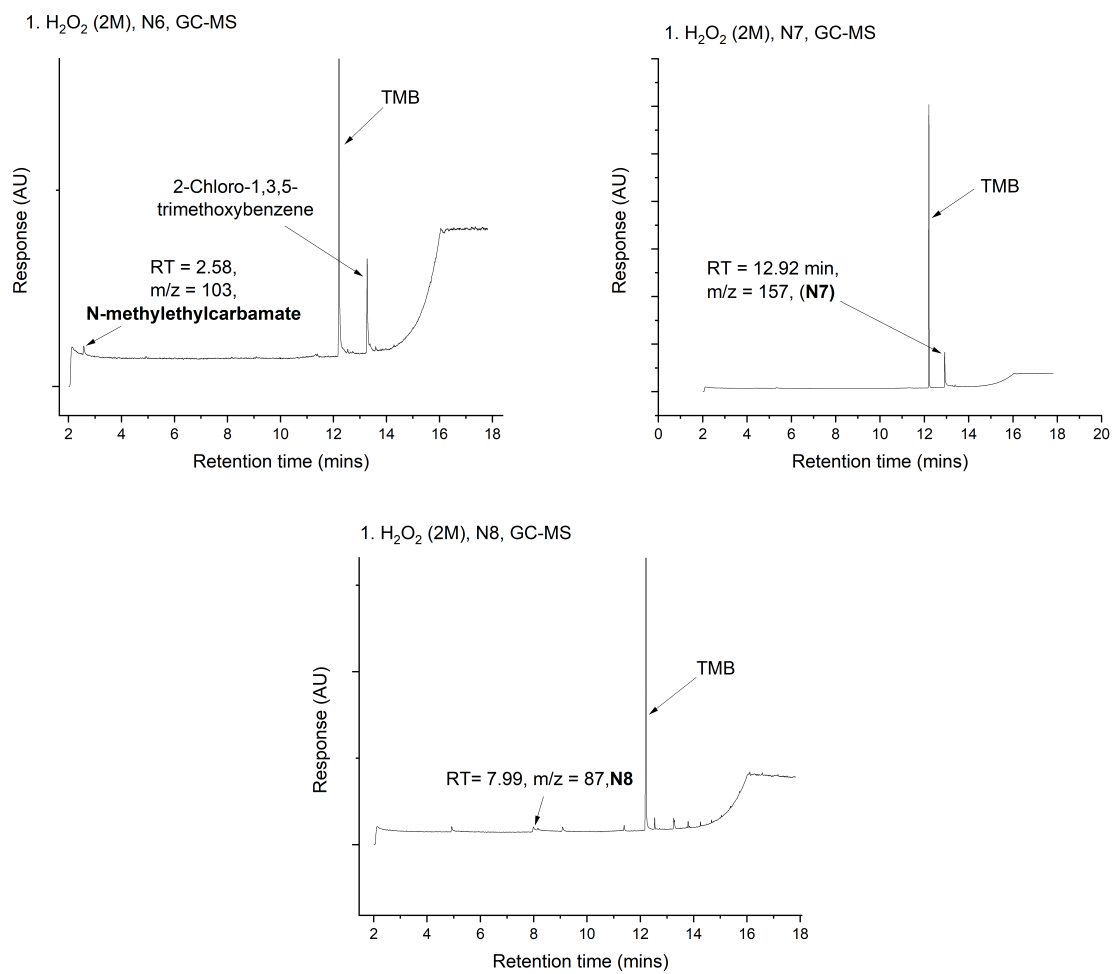


Figure G.2: GC-MSMS plots for N6-8 for condition 1. As referenced in Section 3.6



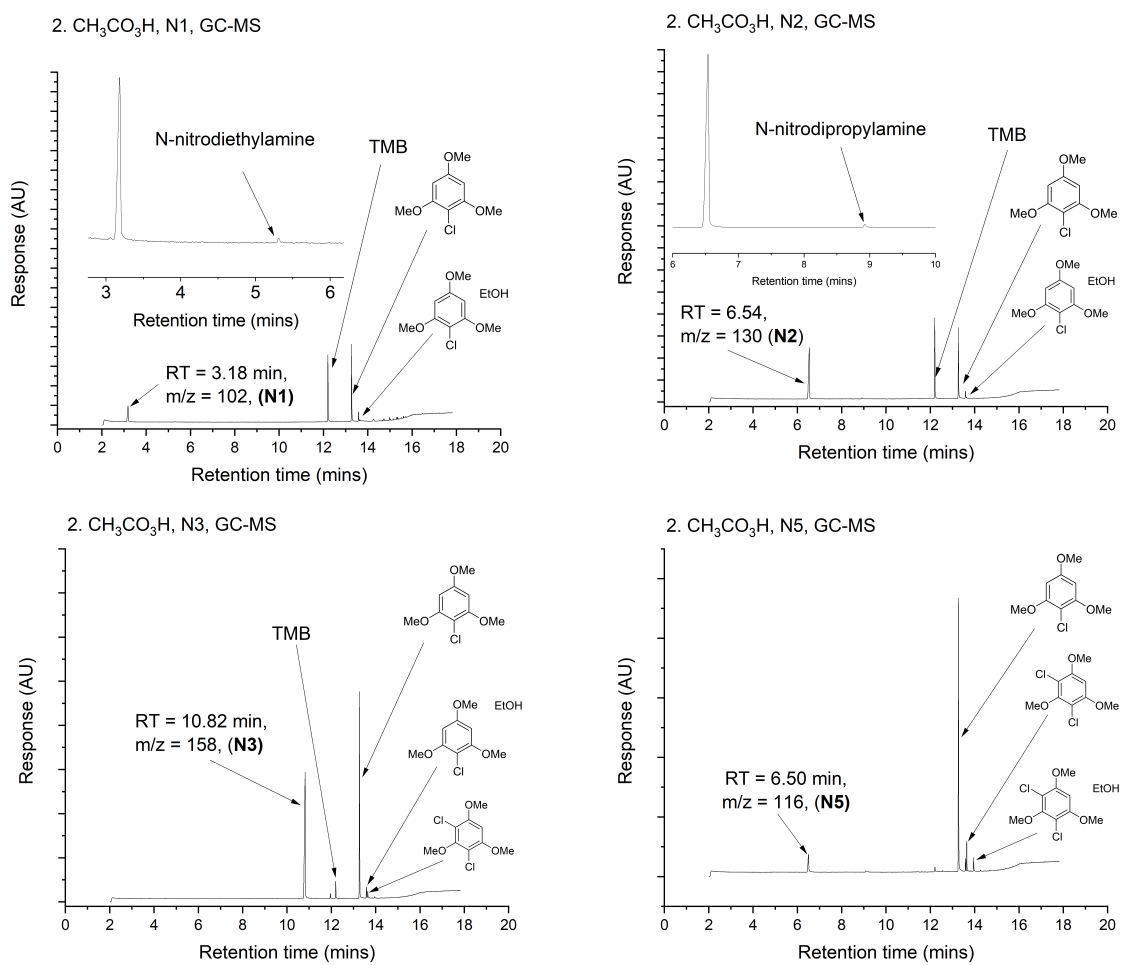


Figure G.3: GC-MSMS plots for N1, N2, N3 and N5 condition 2. As referenced in Section 3.6

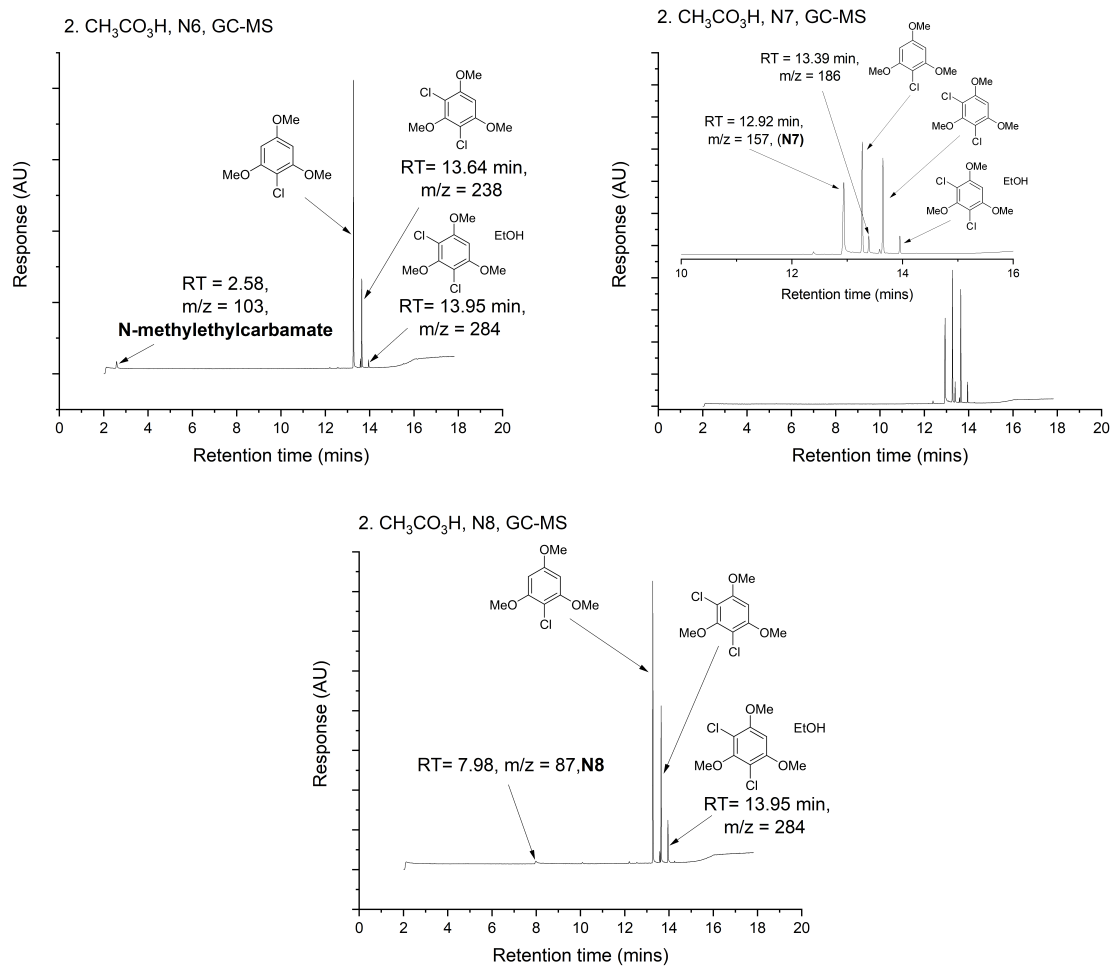


Figure G.4: GC-MSMS plots for N6-8 for condition 2. As referenced in Section 3.6

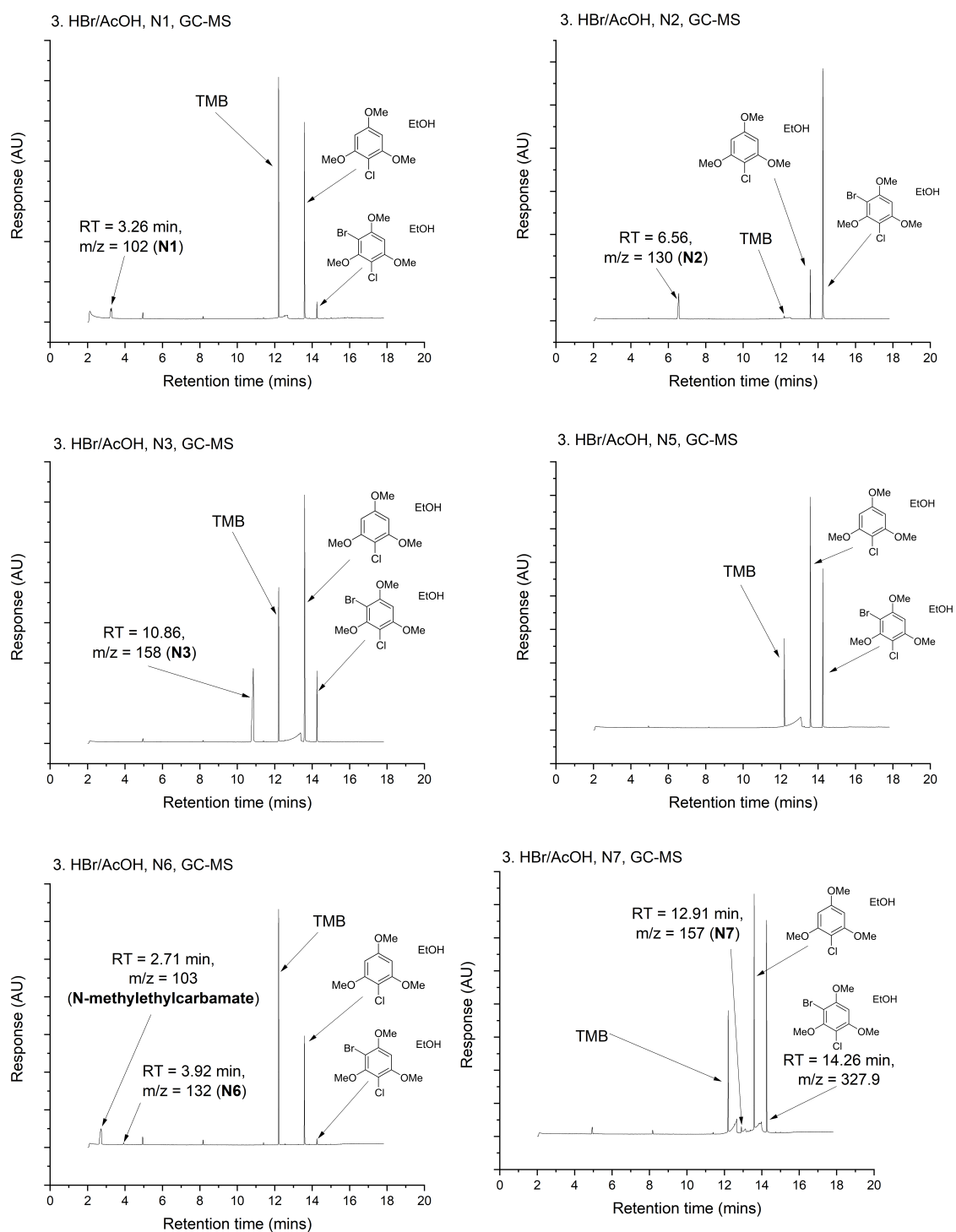


Figure G.5: GC-MSMS plots for N1, N2, N3, and N5-7 for condition 3. As referenced in Section 3.6

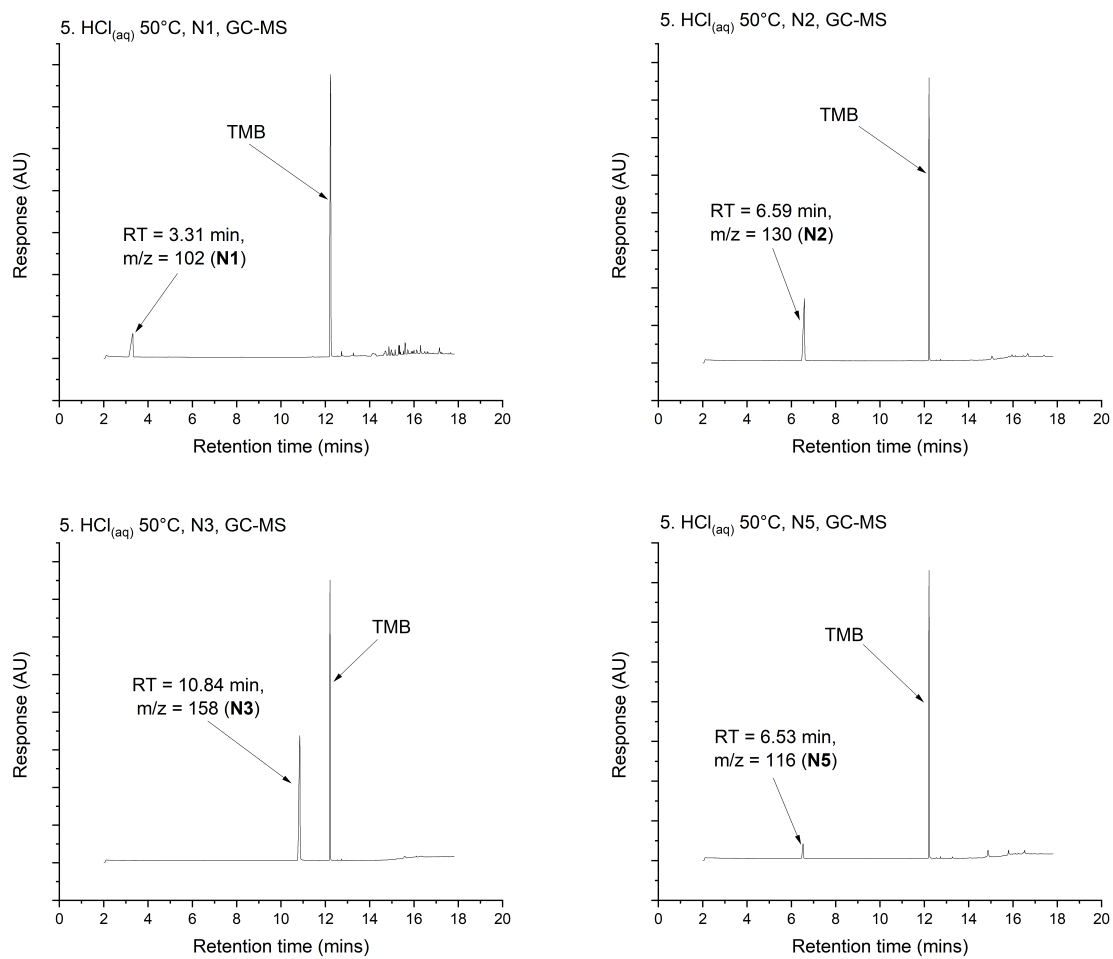


Figure G.6: GC-MSMS plots for N1, N2, N3 and N5 condition 5. As referenced in Section 3.6

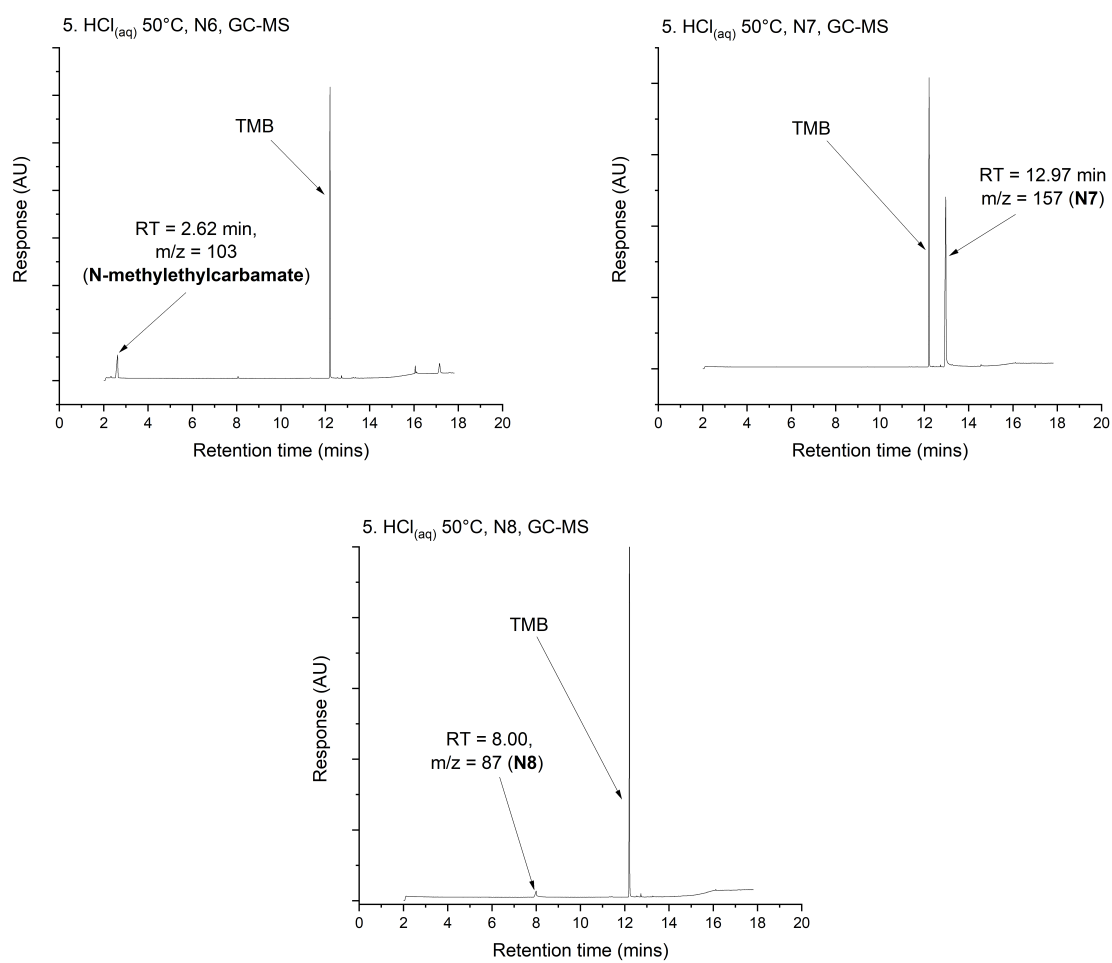


Figure G.7: GC-MSMS plots for N6-8 for condition 5. As referenced in Section 3.6

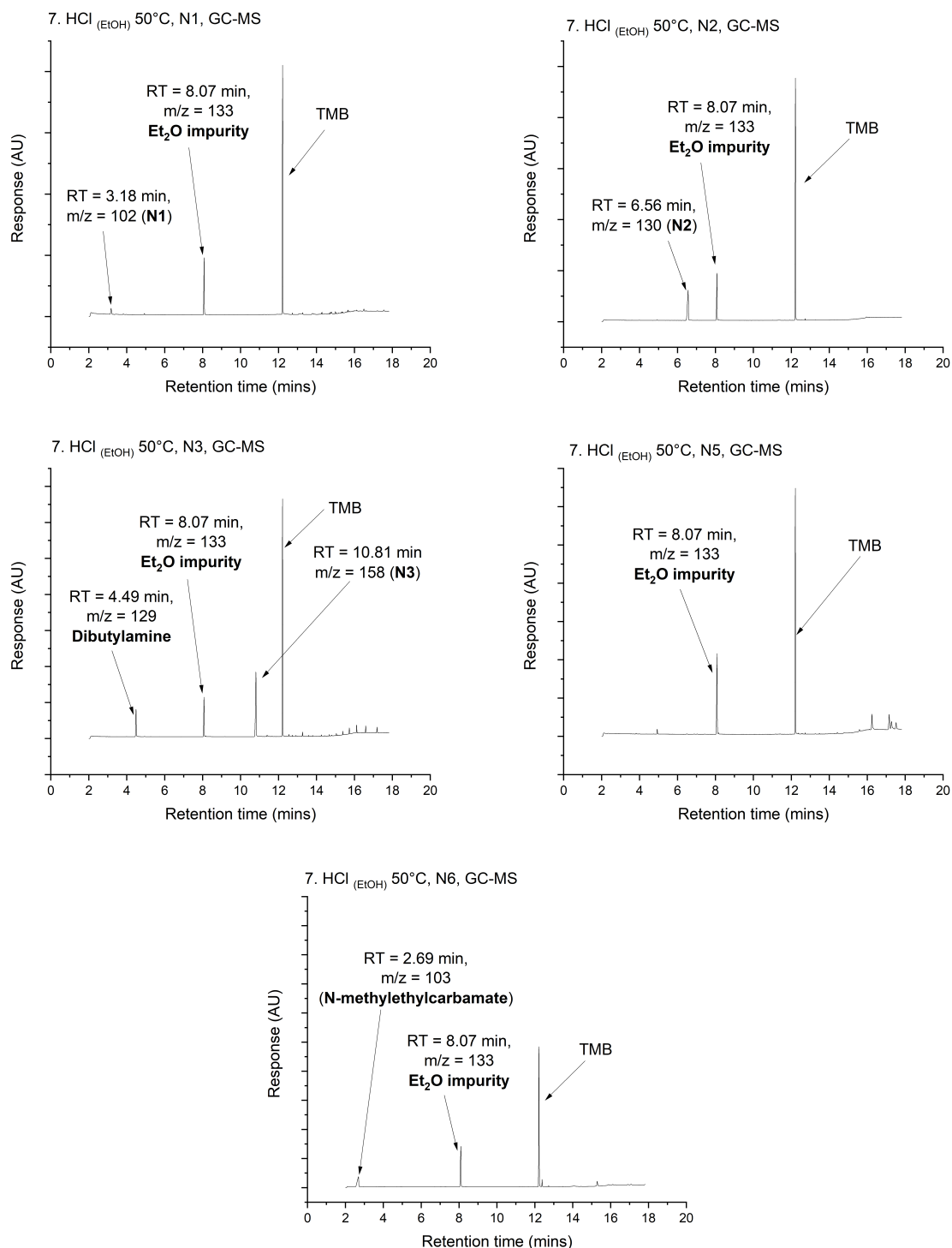


Figure G.8: GC-MS/MS plots for N1, N2, N3, N5 and N6 for condition 7. As referenced in Section 3.6

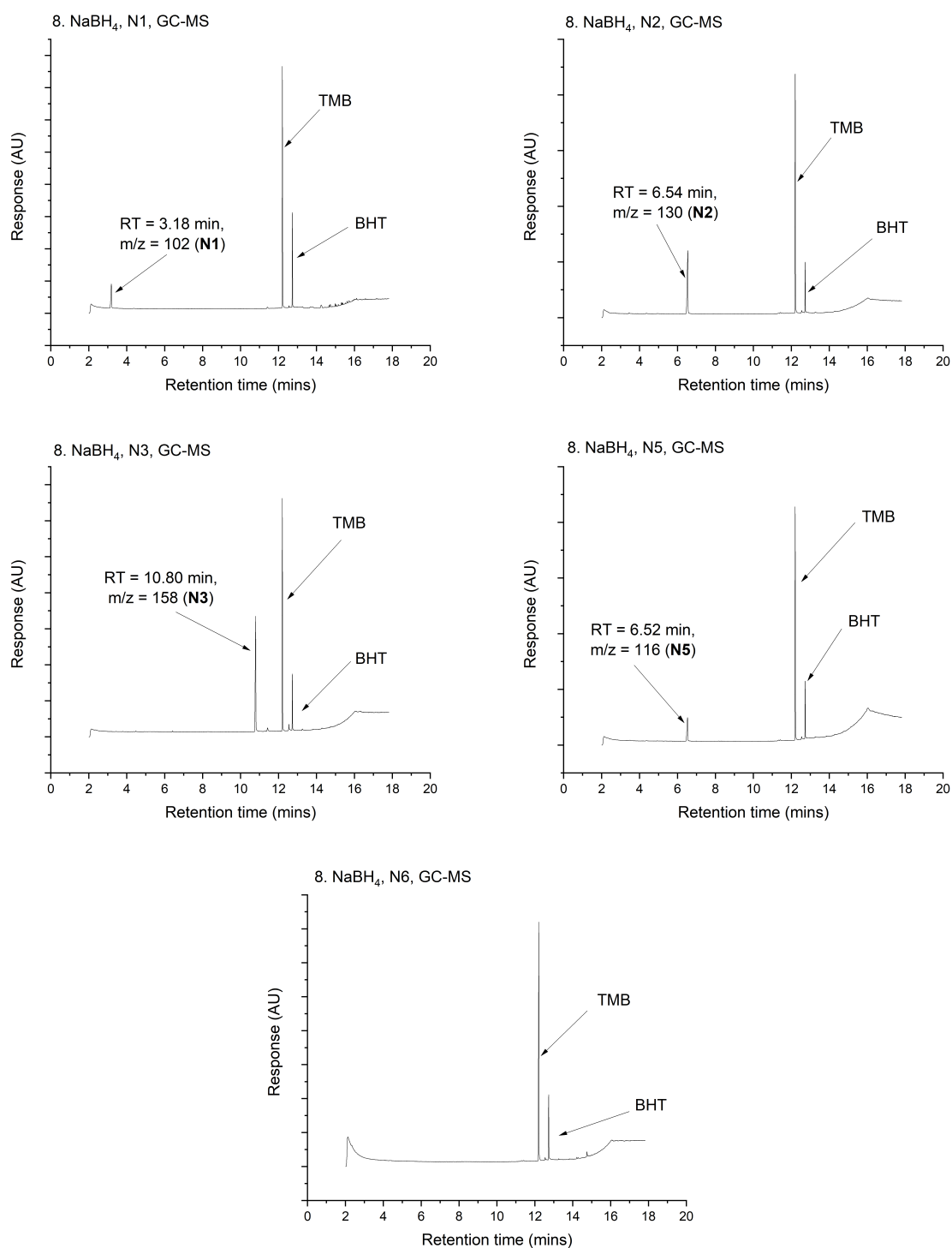


Figure G.9: GC-MSMS plots for N1, N2, N3, N5 and N6 for condition 8. As referenced in Section 3.6

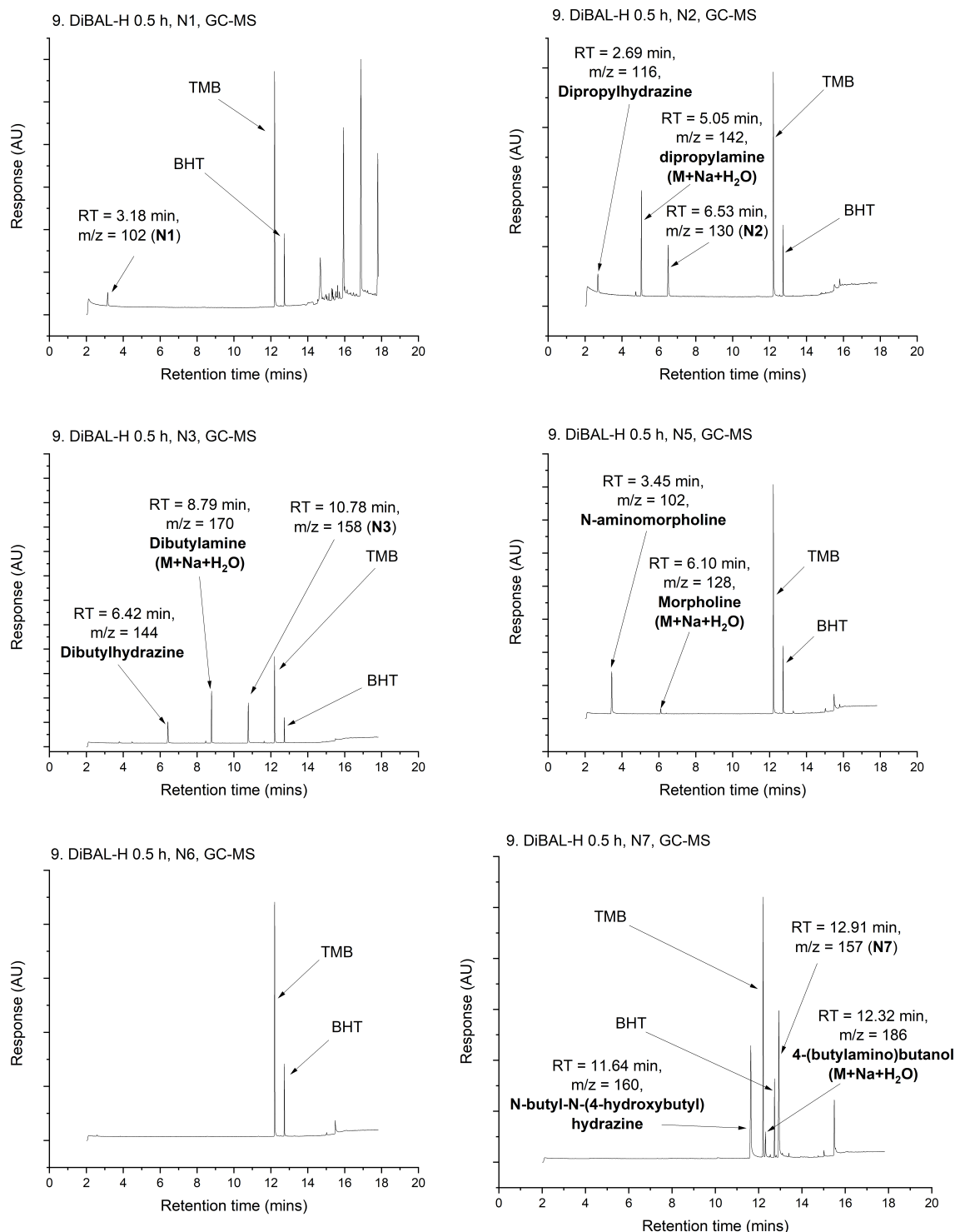


Figure G.10: GC-MS/MS plots for N1, N2, N3 and N5-7 for condition 9. As referenced in Section 3.6



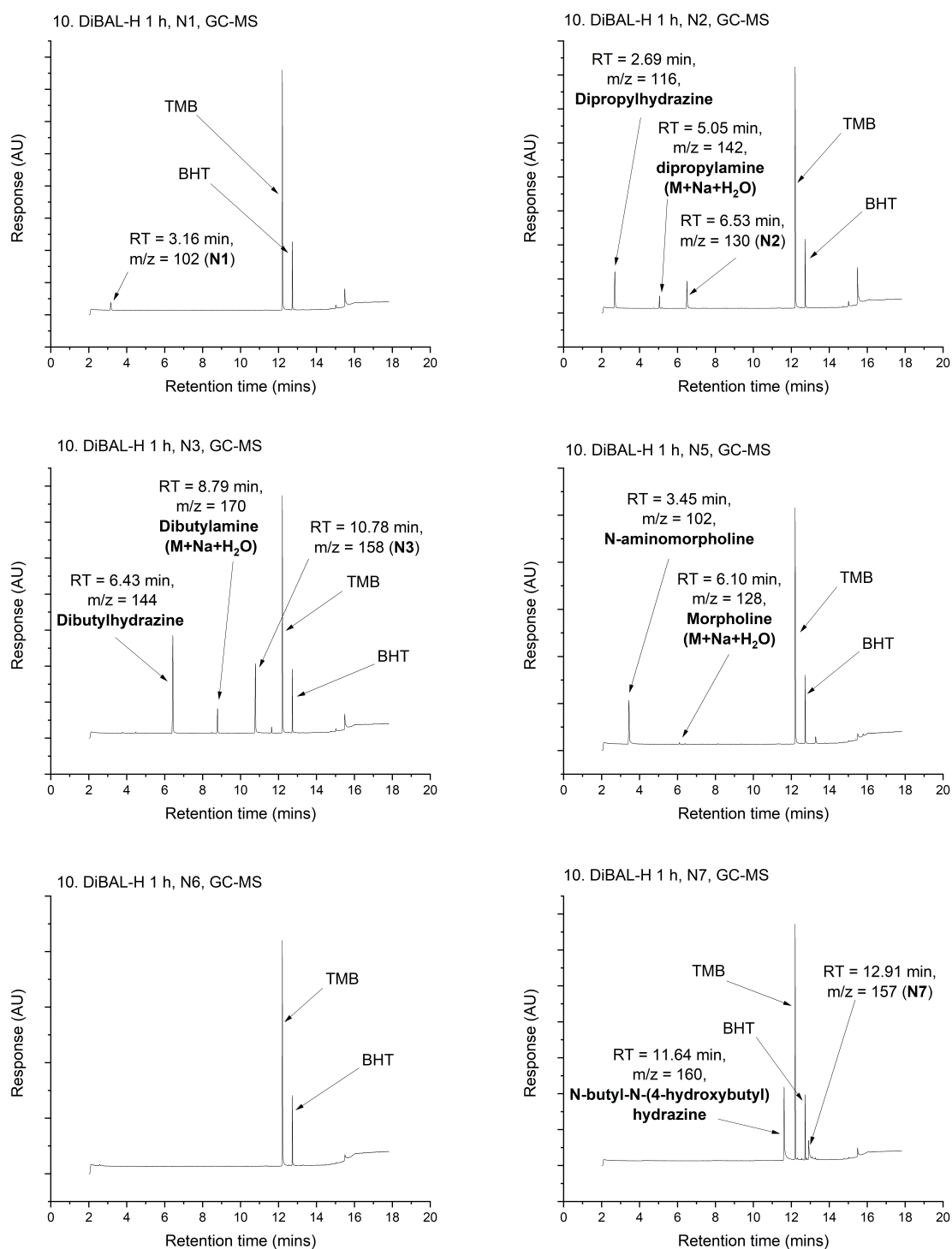


Figure G.11: GC-MSMS plots for N1, N2, N3 and N5-7 for condition 10. As referenced in Section 3.6

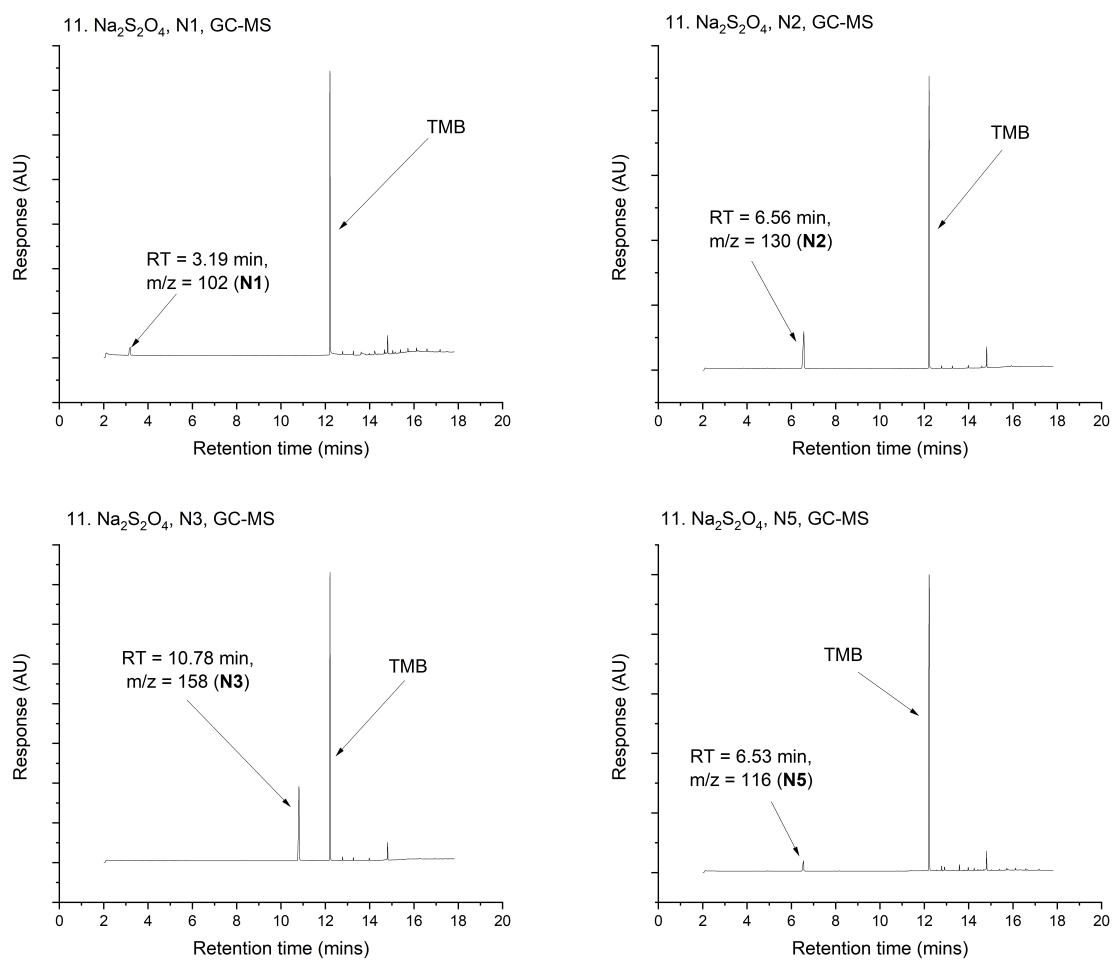


Figure G.12: GC-MSMS plots for N1, N2, N3 and N5 condition 11. As referenced in Section 3.6

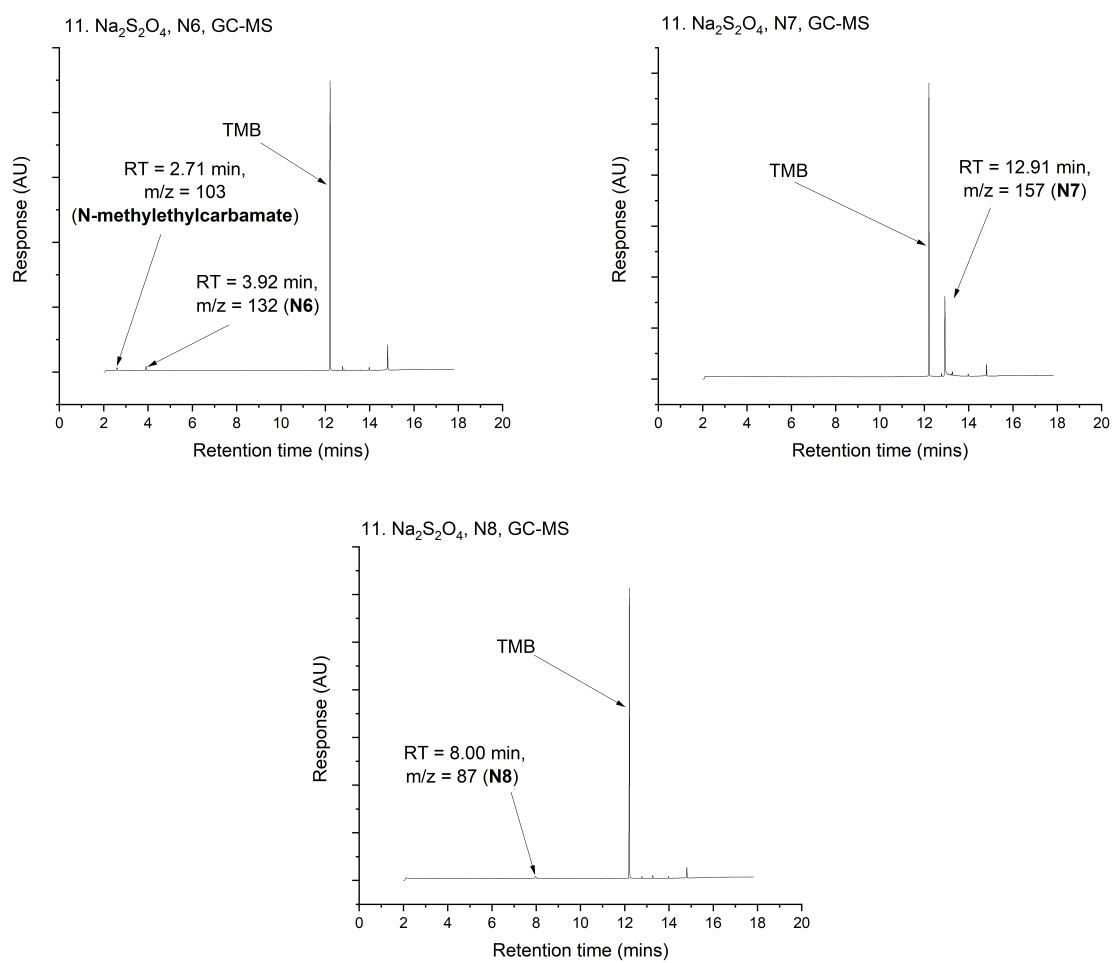


Figure G.13: GC-MSMS plots for N6-8 for condition 11. As referenced in Section 3.6

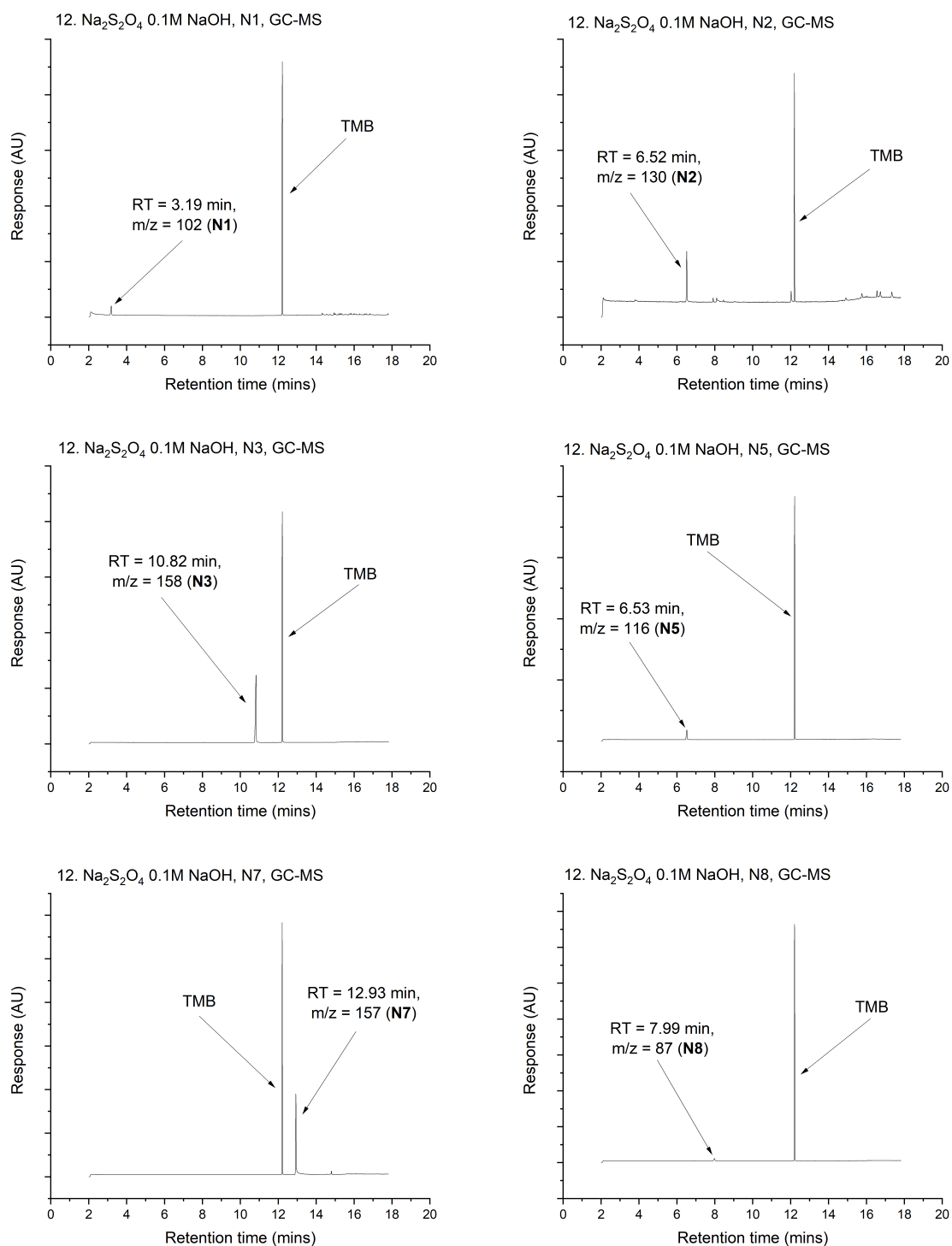


Figure G.14: GC-MSMS plots for N1-3, N5, N7 and N8 for condition 12. As referenced in Section 3.6

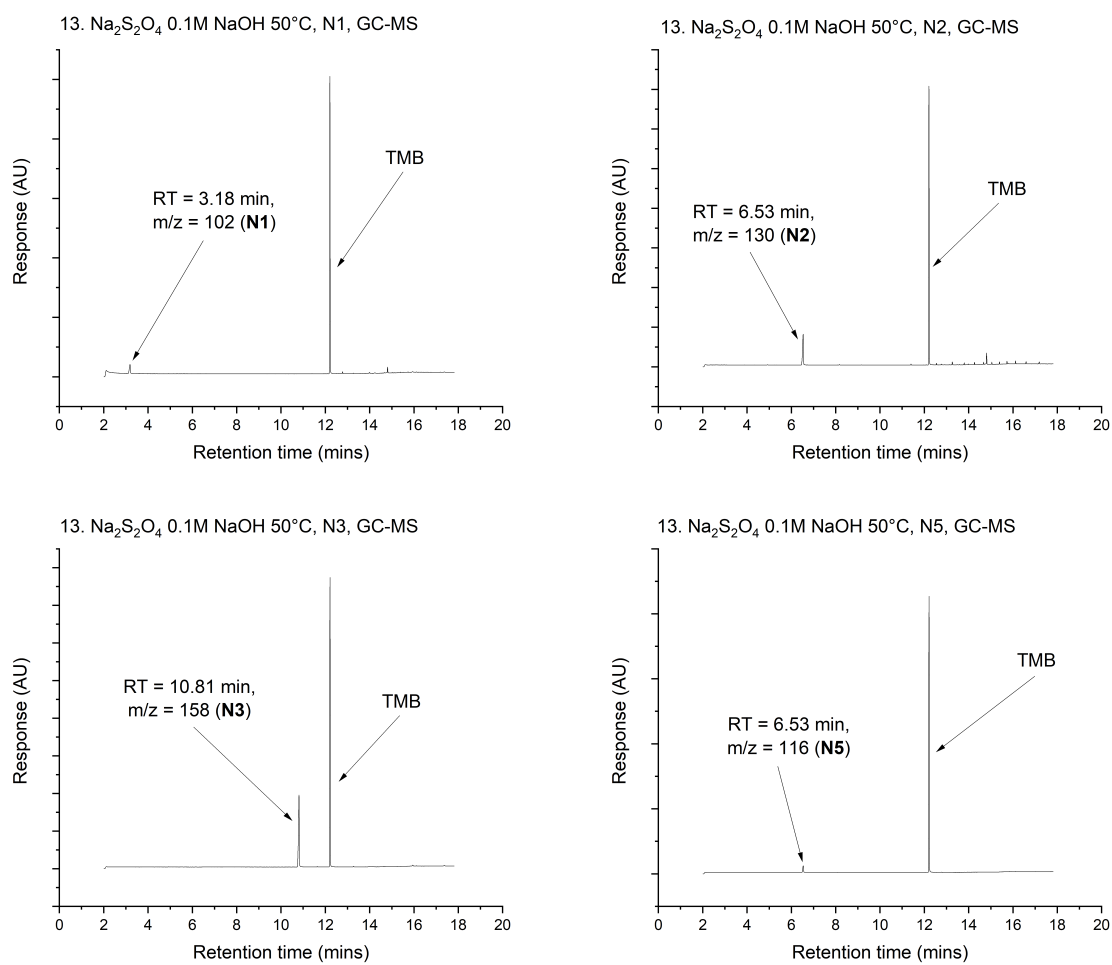


Figure G.15: GC-MSMS plots for N1, N2, N3 and N5 condition 13. As referenced in Section 3.6

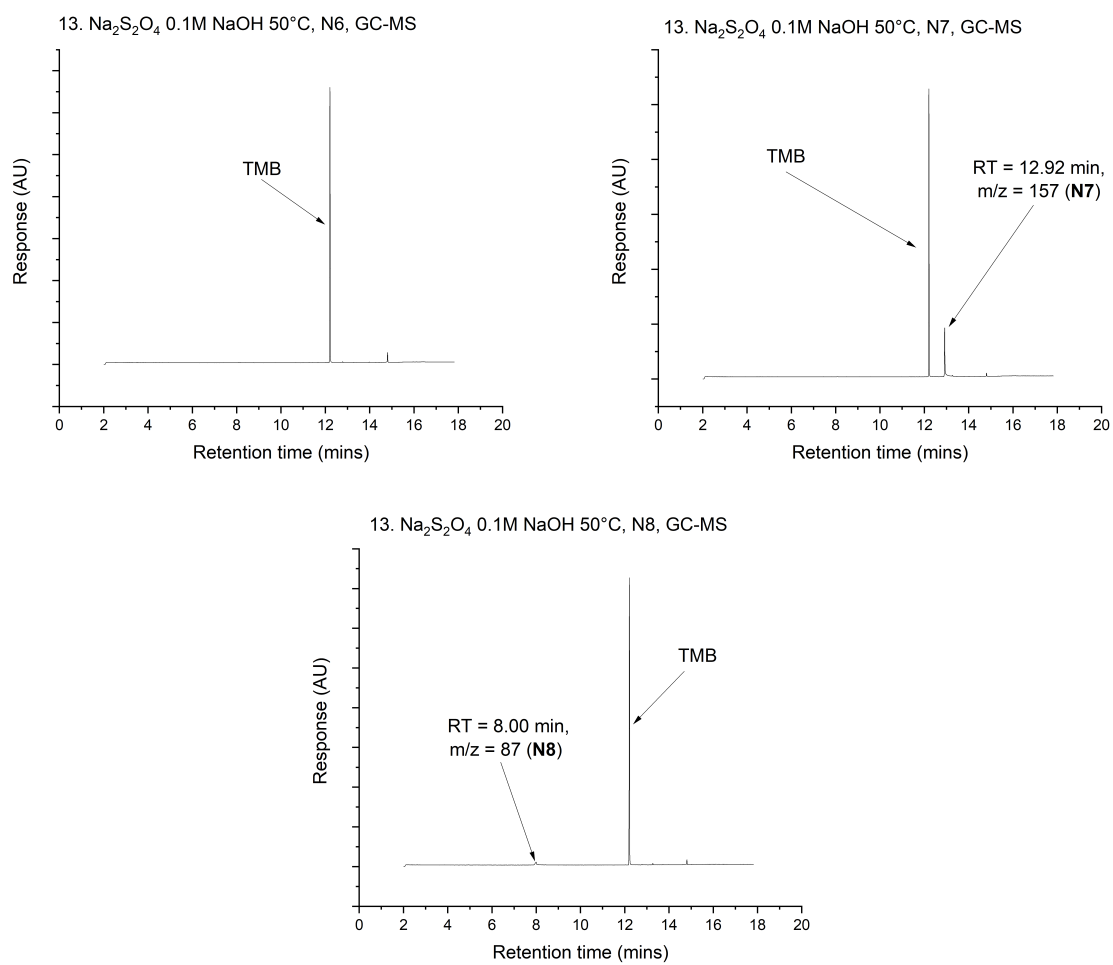


Figure G.16: GC-MSMS plots for N6-N8 for condition 13. As referenced in Section 3.6

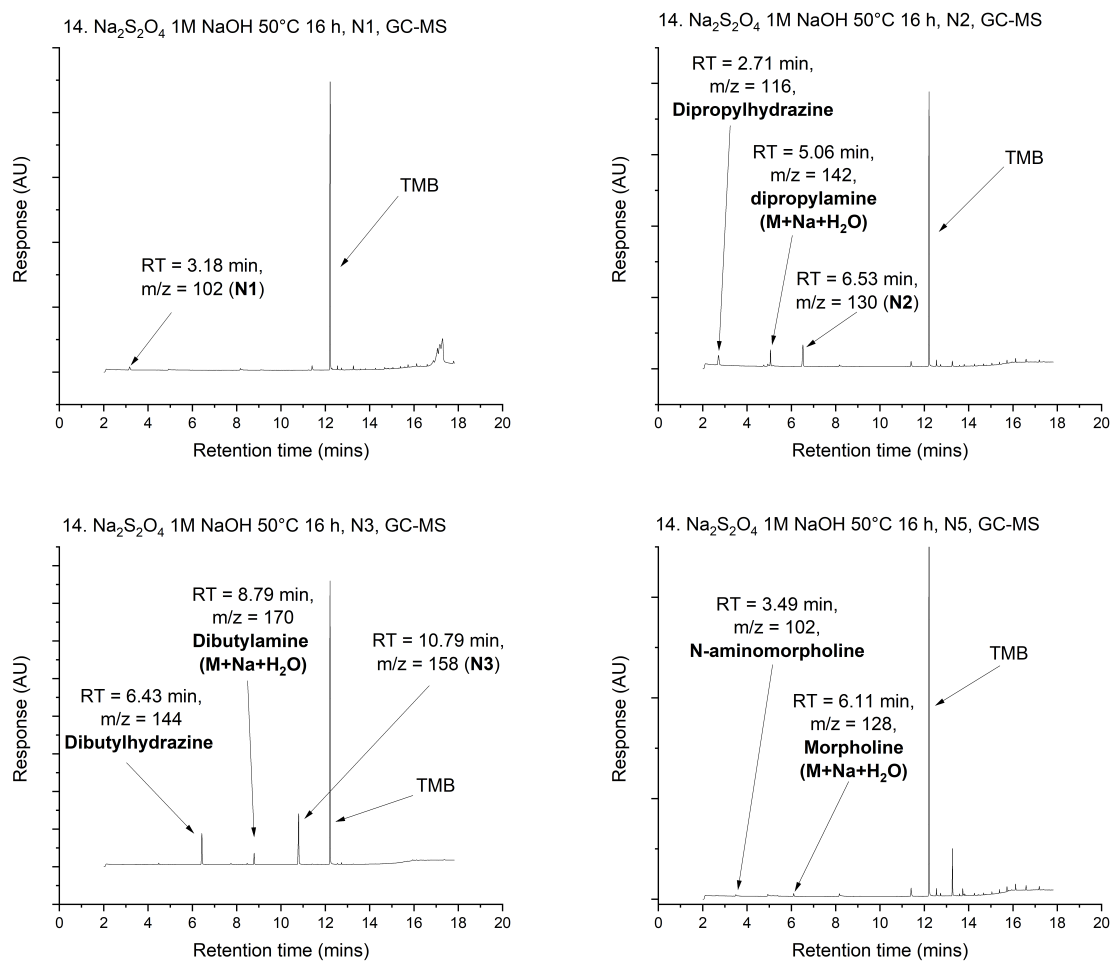


Figure G.17: GC-MSMS plots for N1, N2, N3 and N5 condition 14. As referenced in Section 3.6

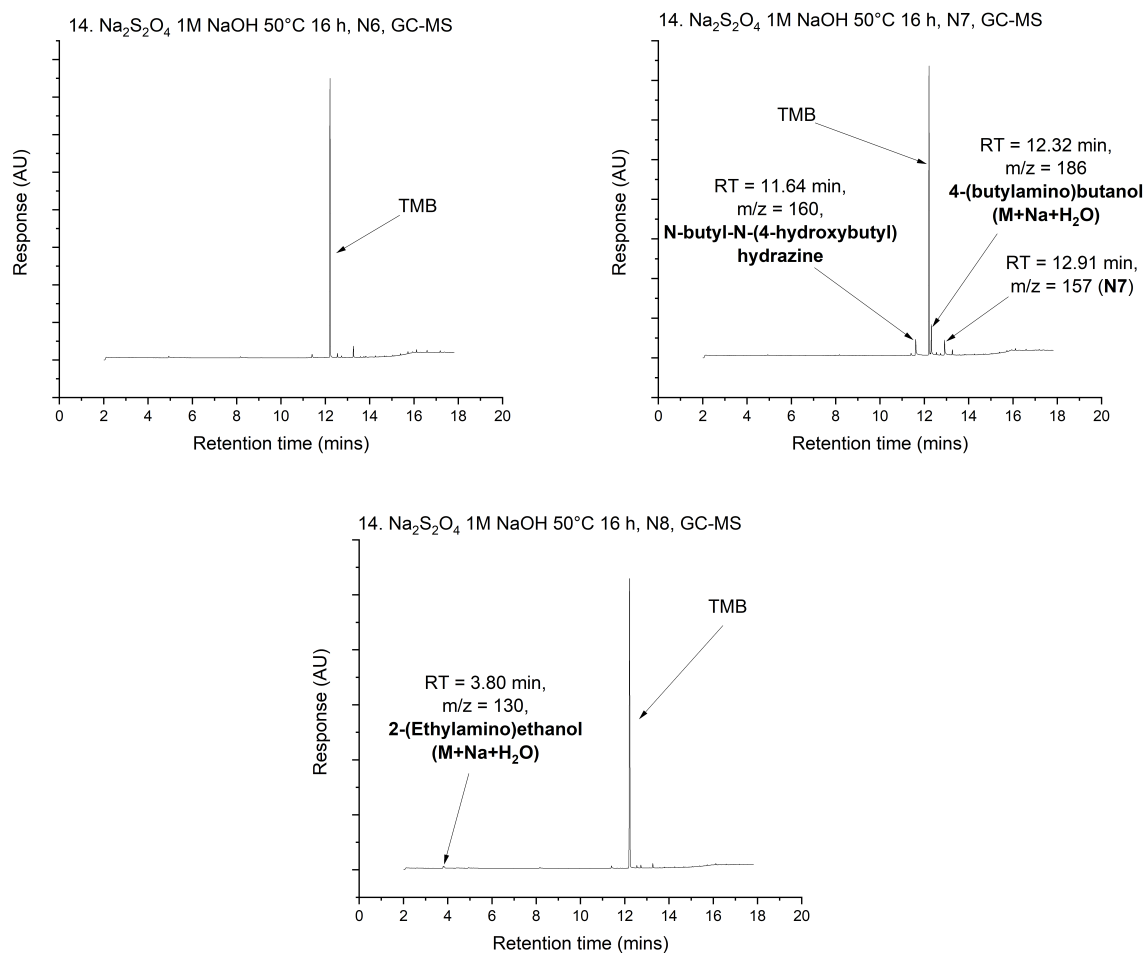


Figure G.18: GC-MSMS plots for N6-N8 for condition 14. As referenced in Section 3.6



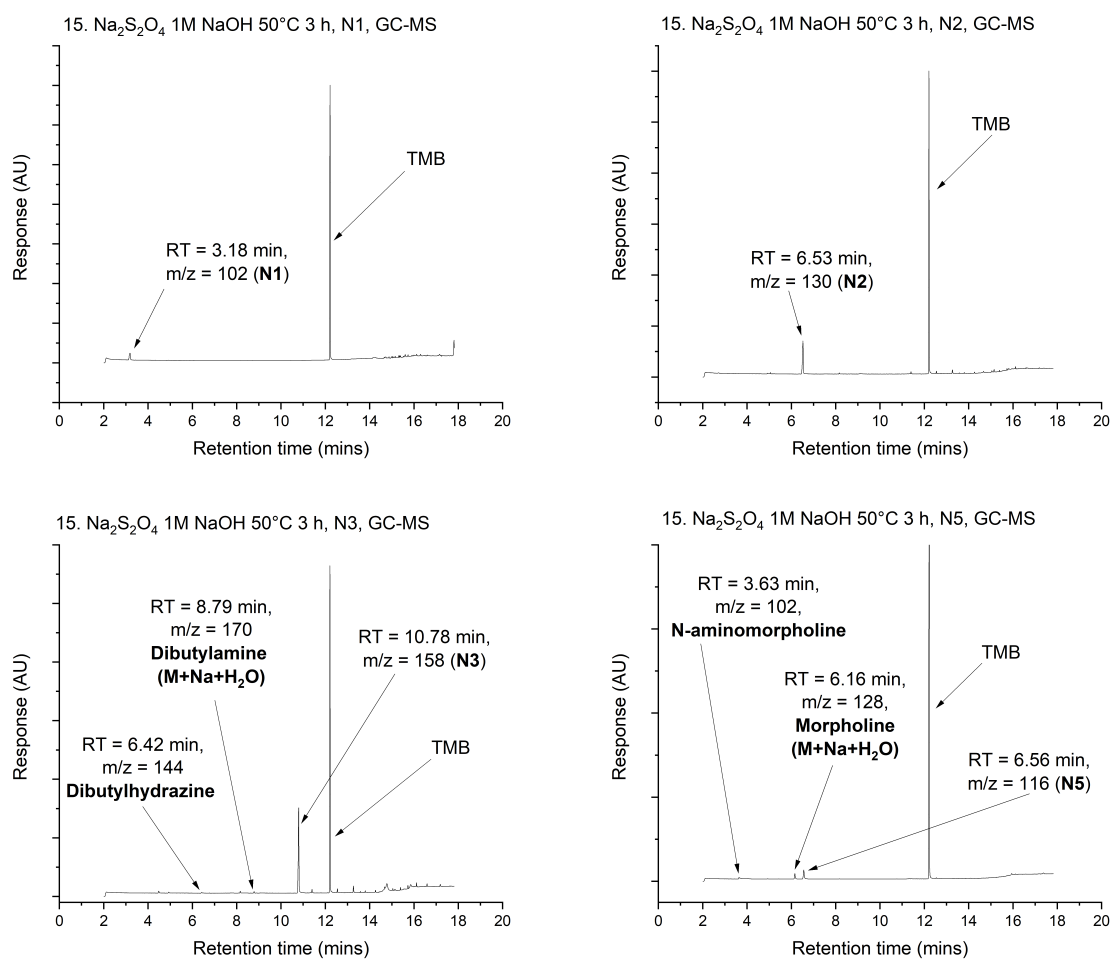


Figure G.19: GC-MSMS plots for N1, N2, N3 and N5 condition 15. As referenced in Section 3.6

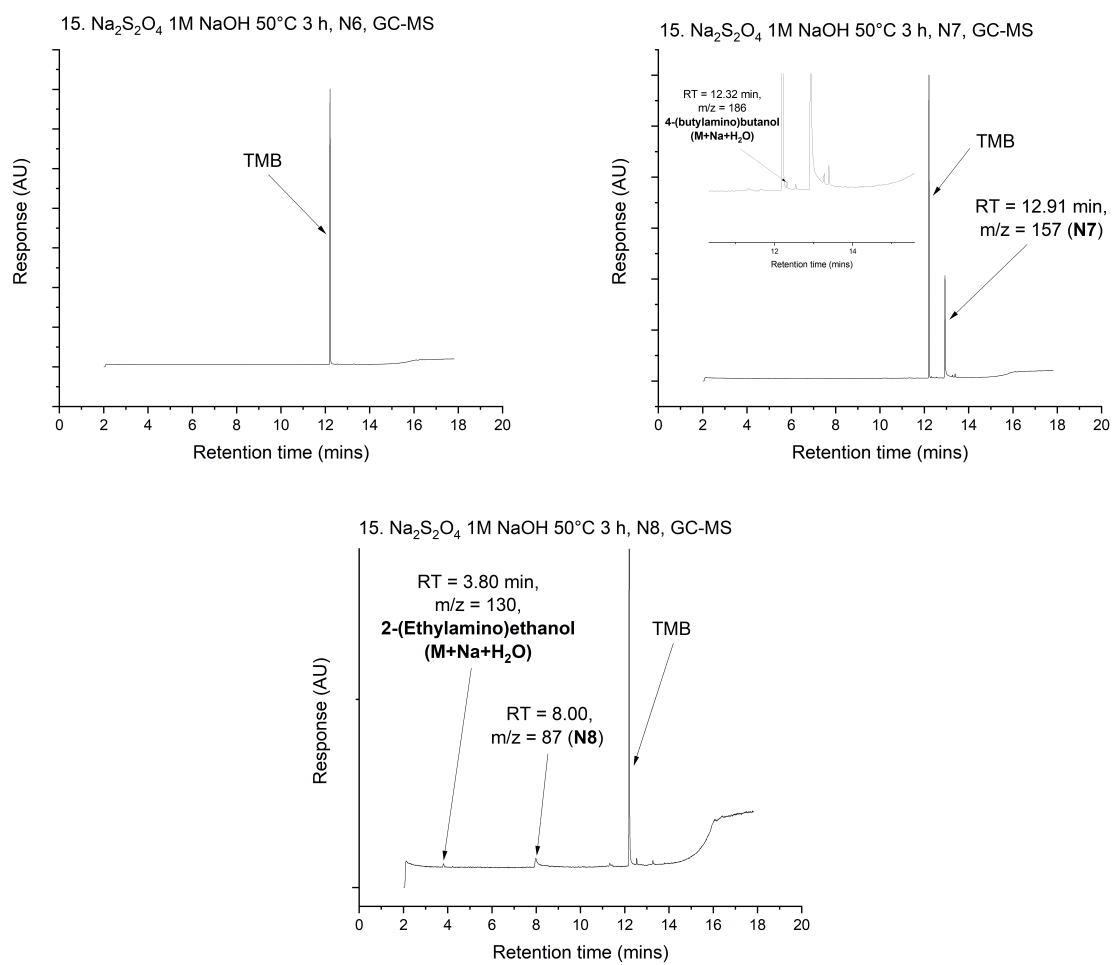


Figure G.20: GC-MSMS plots for N6-N8 for condition 15. As referenced in Section 3.6

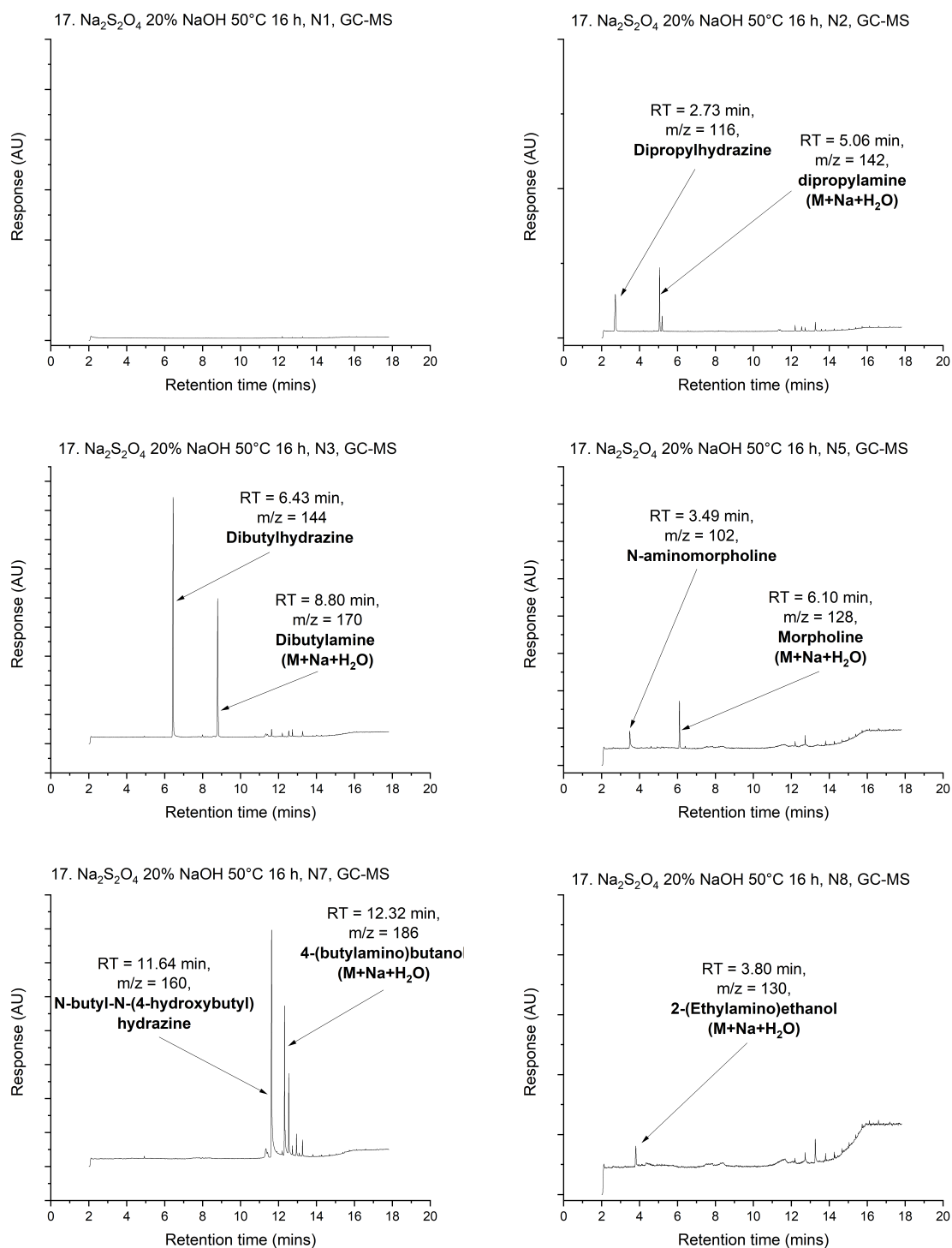


Figure G.21: GC-MSMS plots for N1-3, N5, N7 and N8 for condition 17. As referenced in Section 3.6

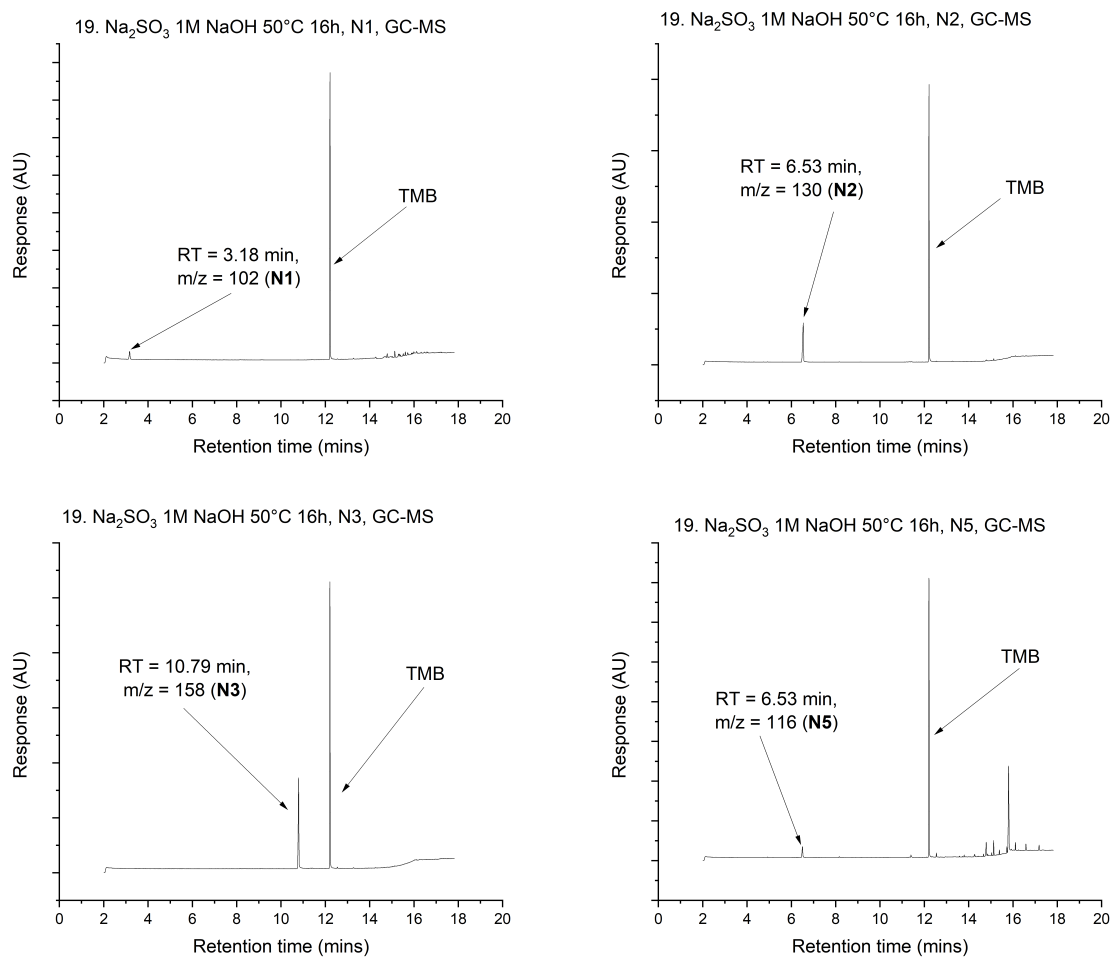


Figure G.22: GC-MSMS plots for N1, N2, N3 and N5 condition 19. As referenced in Section 3.6

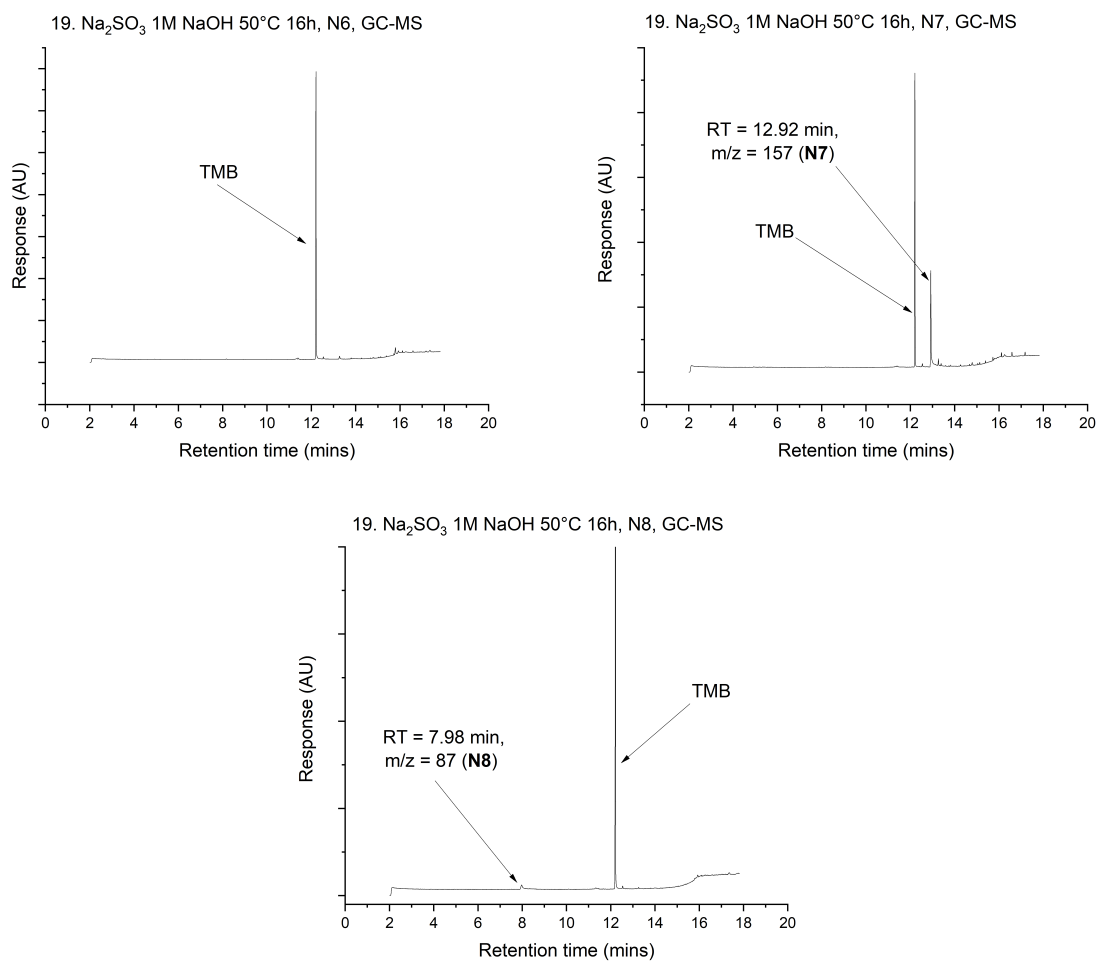


Figure G.23: GC-MSMS plots for N6-N8 for condition 19. As referenced in Section 3.6

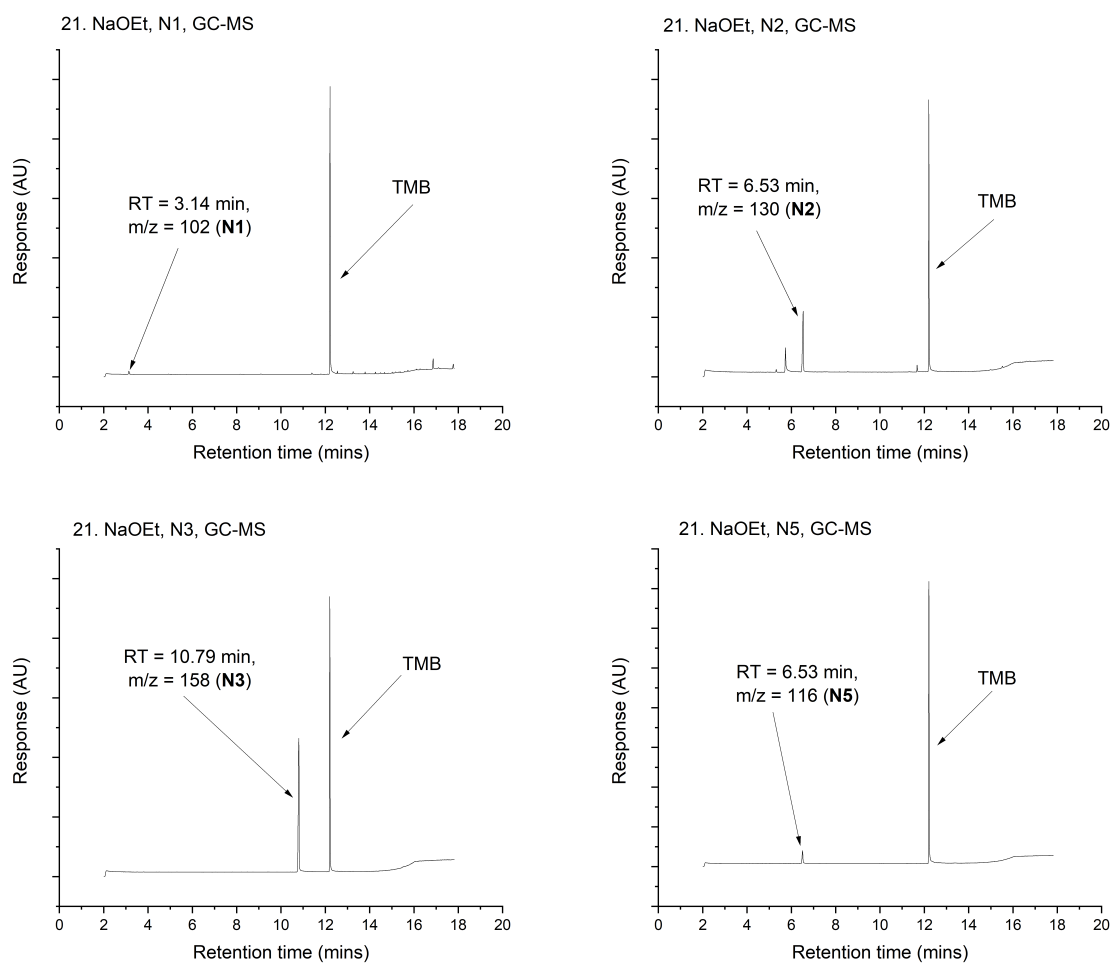


Figure G.24: GC-MSMS plots for N1, N2, N3 and N5 condition 21. As referenced in Section 3.6

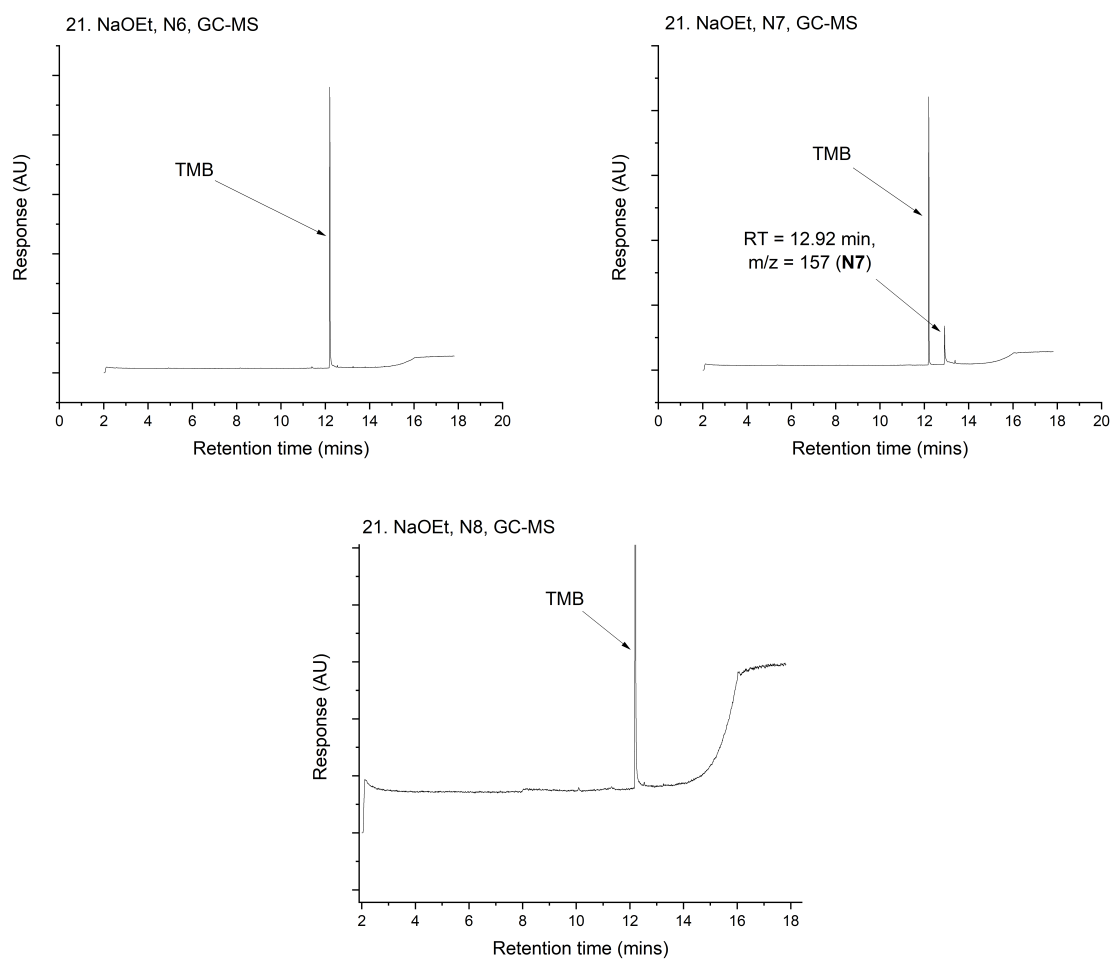
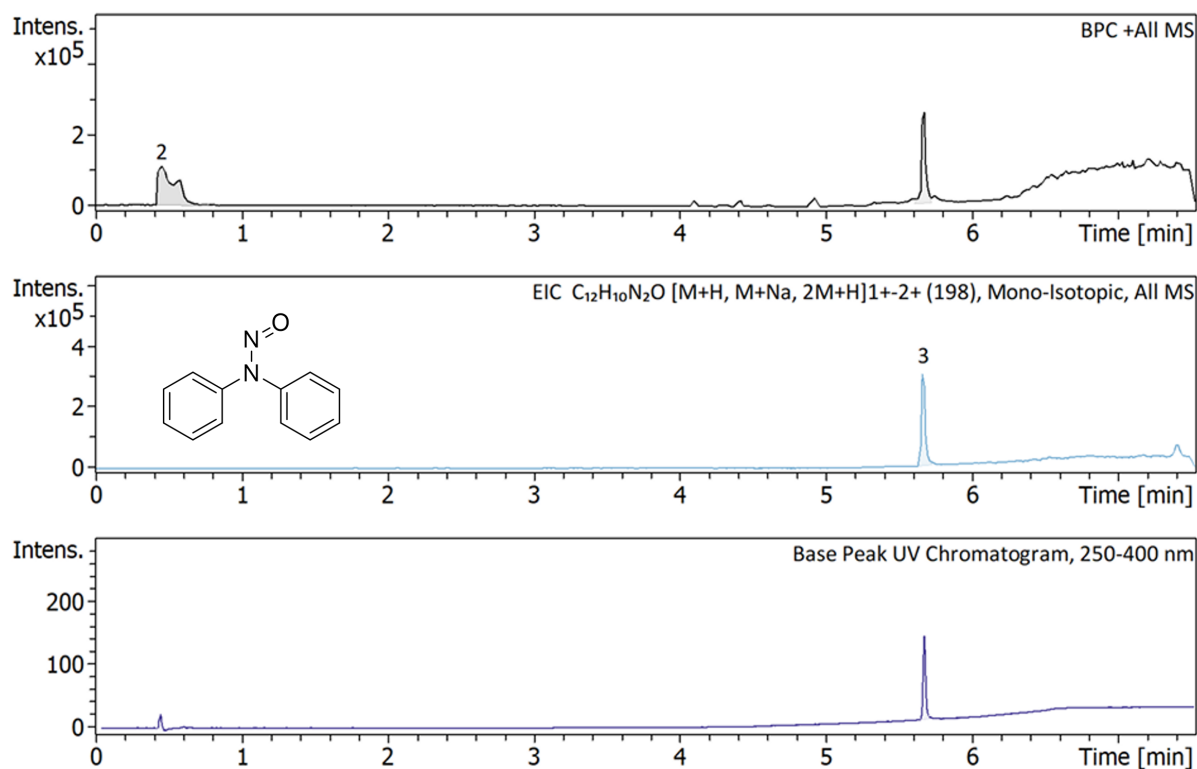


Figure G.25: GC-MSMS plots for N6-N8 for condition 21. As referenced in Section 3.6

## Appendix H

### LC-MS/MS References



#### Summary of Results

Name	RT	BPC Area(%)	UV Area(%)	Confirm Formula Results
Cmpd 2, 0.5 min	0.45	62.0	14.1	
Cmpd 3, 5.7 min	5.66	38.0	85.9	$C_{12}H_{10}N_2O$

Figure H.1: LC-MSMS reference chromatogram for N-nitrosodiphenylamine (N4). As referenced in Table 3.11.



NDPA\_LCMSMS\_3-1-13\_1\_5561.swx

1: MS +c SM0 AM2 RT: 5.6600 minutes, Scan 1541, NL 1.00e+2

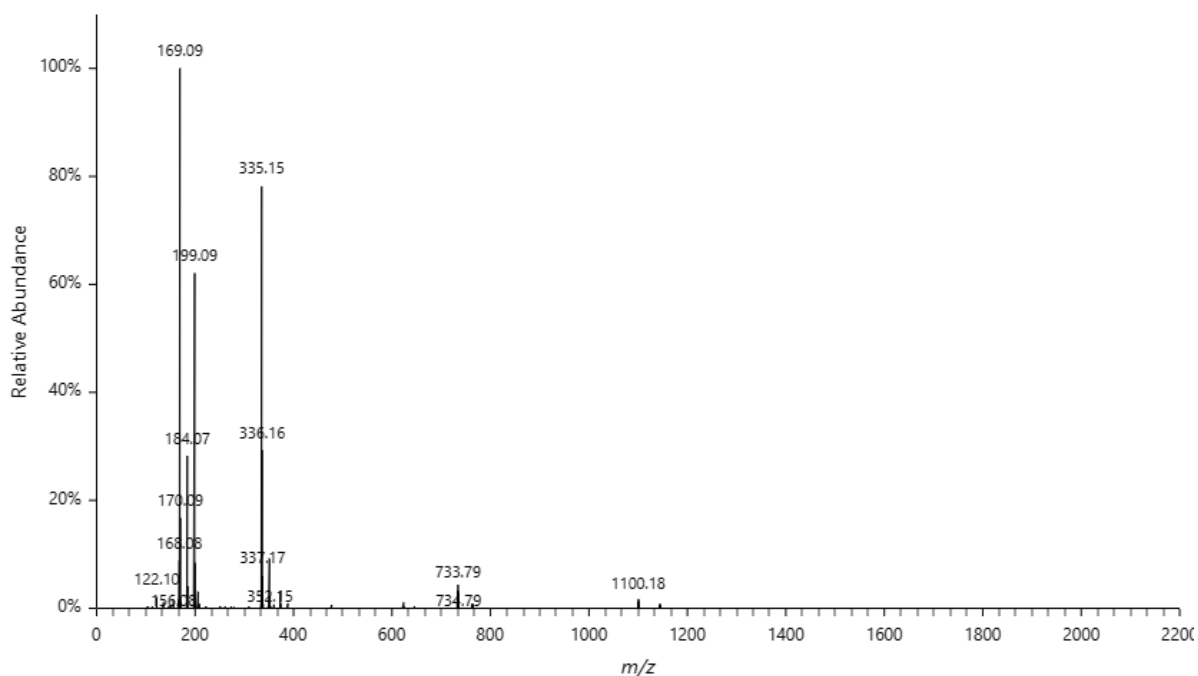
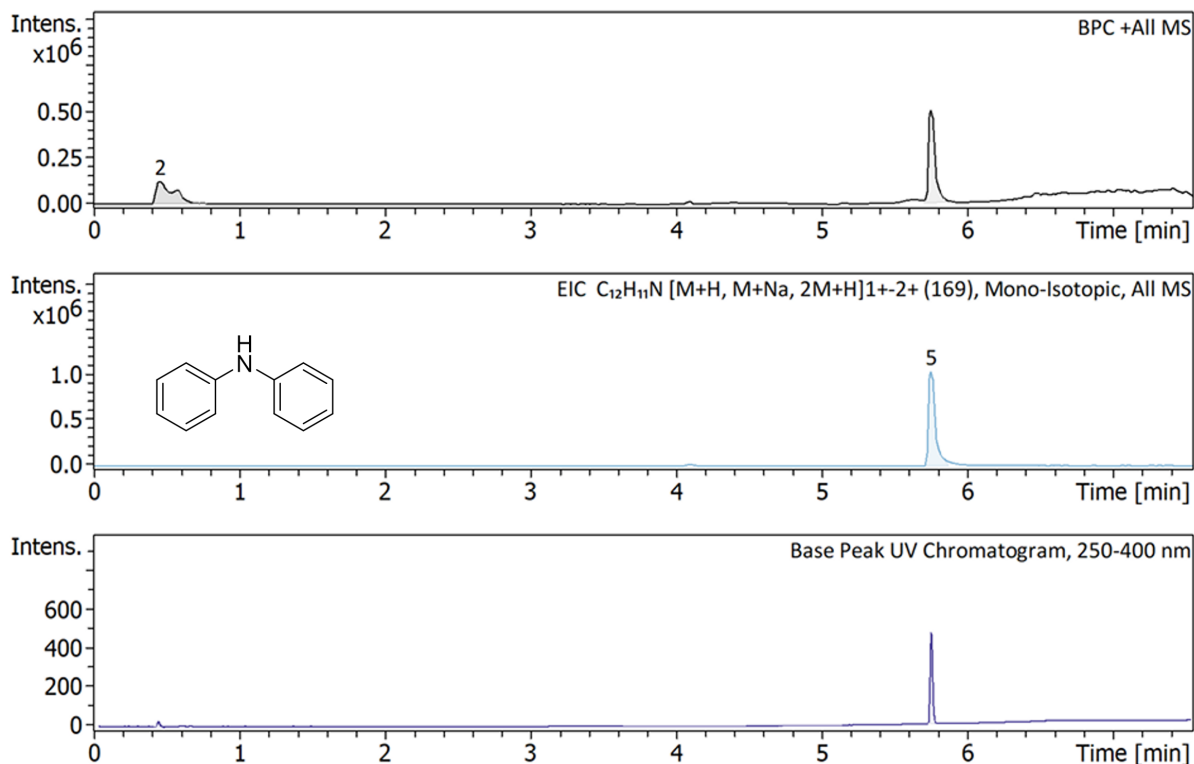


Figure H.2: LC-MSMS reference mass peaks for N-nitrosodiphenylamine (N4). As referenced in Table 3.11.



### Summary of Results

Name	RT	BPC Area(%)	UV Area(%)	Confirm Formula Results
Cmpd 2, 0.5 min	0.46	38.5	4.5	
Cmpd 5, 5.7 min	5.75	61.5	78.2	C <sub>12</sub> H <sub>11</sub> N

Figure H.3: LC-MSMS reference chromatogram for diphenylamine. As referenced in Table 3.11.

DPA\_LCMSMS\_3-1-14\_1\_5562.swx

1: MS +c SM0 AM2 RT: 5.7503 minutes, Scan 1612, NL 1.00e+2

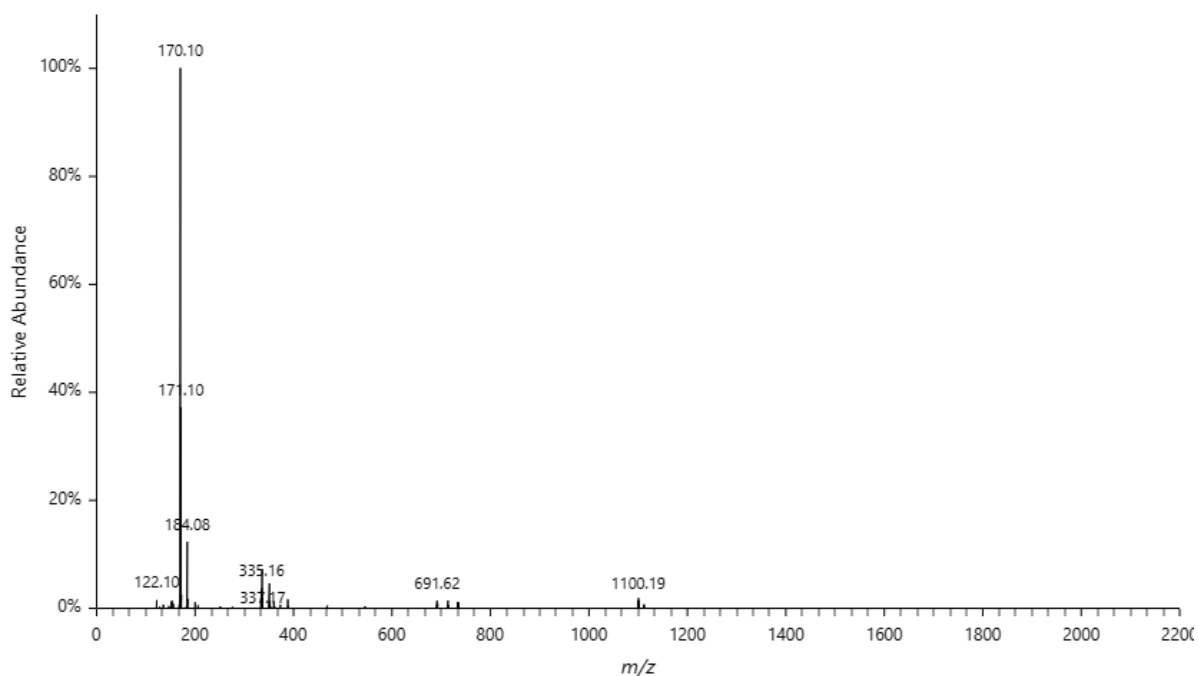
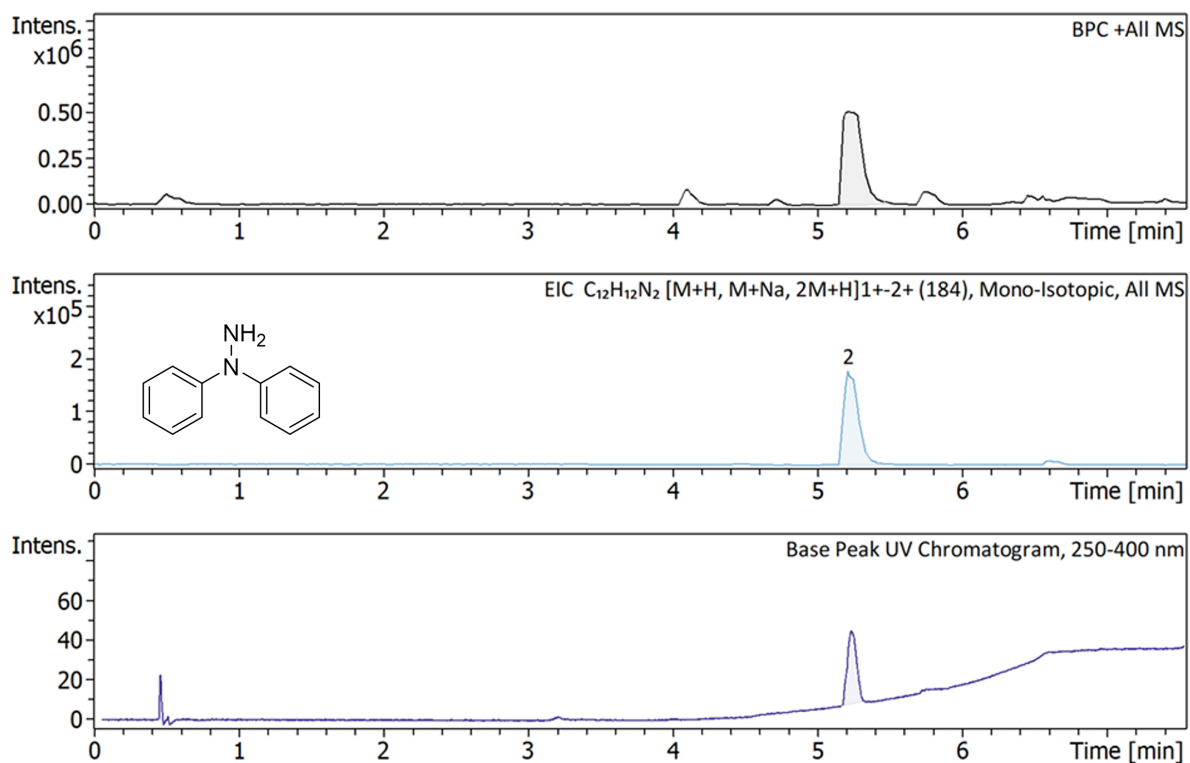


Figure H.4: LC-MSMS reference reference mass peaks for diphenylamine. As referenced in Table 3.11.



### Summary of Results

Name	RT	BPC Area(%)	UV Area(%)	Confirm Formula Results
Cmpd 2, 5.2 min	5.21	100.0	88.4	C <sub>12</sub> H <sub>12</sub> N <sub>2</sub>

Figure H.5: LC-MSMS reference chromatogram for N,N'-diphenylhydrazine. As referenced in Table 3.11.

DPH\_LCMSMS\_ref\_1-1-48\_1\_6905.swx

1: MS +c SM0 AM2 RT: 5.2081 minutes, Scan 1510, NL 1.00e+2

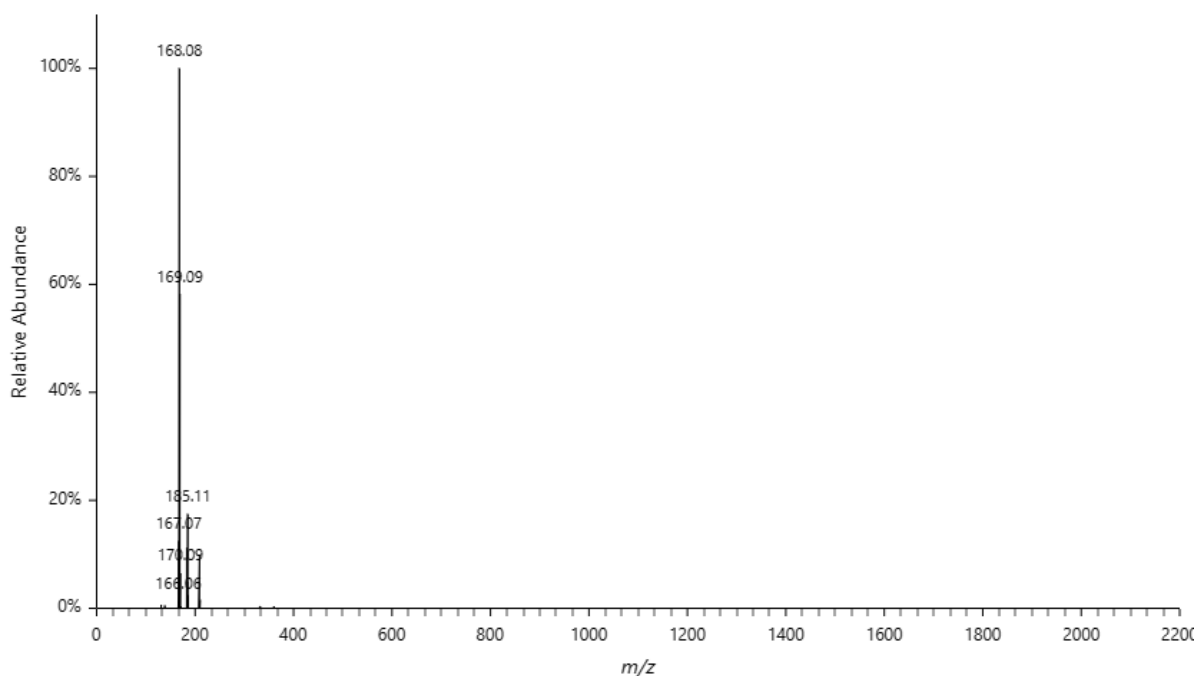
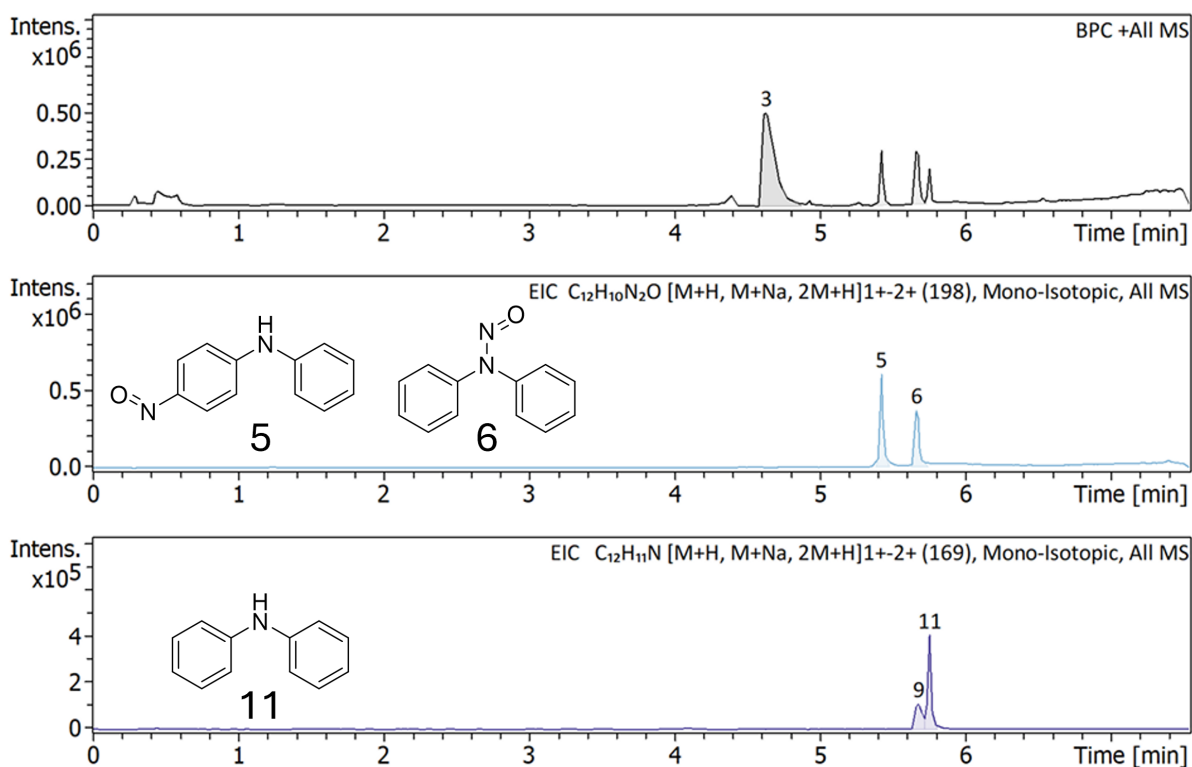


Figure H.6: LC-MSMS reference mass peaks for N,N'-diphenylhydrazine. As referenced in Table 3.11.



### Summary of Results

Name	RT	BPC Area(%)	UV Area(%)	Confirm Formula Results
Cmpd 3, 4.6 min	4.63	72.8	no peak	
Cmpd 5, 5.4 min	5.42	10.9	no peak	C <sub>12</sub> H <sub>10</sub> N <sub>2</sub> O
Cmpd 6, 5.7 min	5.66	16.3	78.2	C <sub>12</sub> H <sub>10</sub> N <sub>2</sub> O
Cmpd 9, 5.7 min	5.67	16.3	78.2	C <sub>12</sub> H <sub>10</sub> N <sub>2</sub> O
Cmpd 11, 5.8 min	5.75	no peak	4.3	C <sub>12</sub> H <sub>11</sub> N

Figure H.7: LC-MSMS reference chromatogram for *p*-nitrosodiphenylamine from reaction condition 4. As referenced in Table 3.11.

GH104\_Ph\_1-1-43\_1\_5517.swx

1: MS +c 5M0 AM2 RT: 5.4221 minutes, Scan 1528, NL 1.00e+2

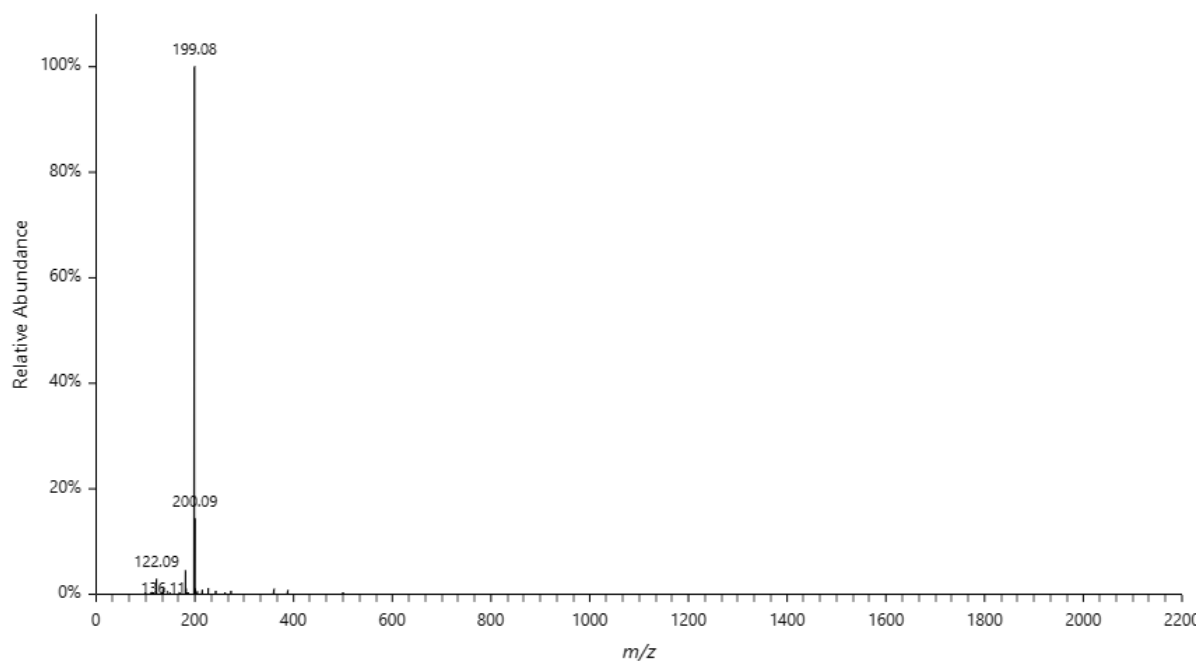
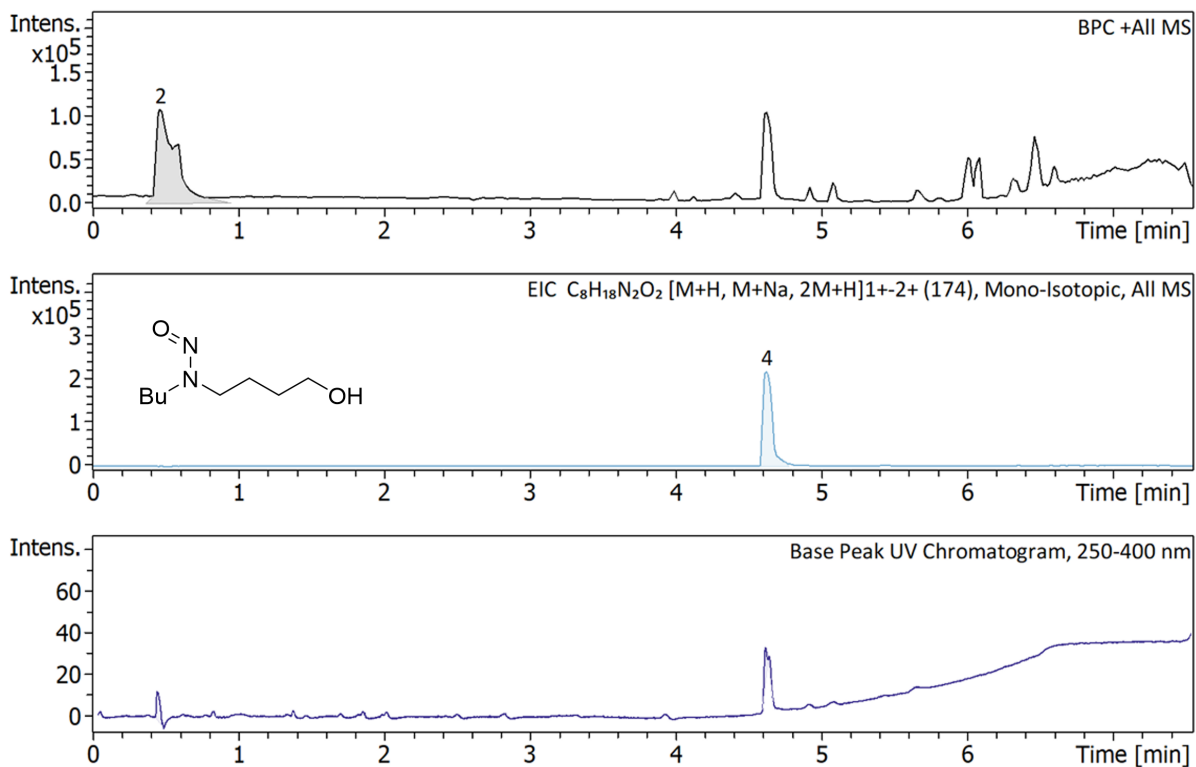


Figure H.8: LC-MSMS reference mass peaks for *p*-nitrosodiphenylamine from reaction condition 4. As referenced in Table 3.11.



### Summary of Results

Name	RT	BPC Area(%)	UV Area(%)	Confirm Formula Results
Cmpd 2, 0.5 min	0.47	100.0	47.0	
Cmpd 4, 4.6 min	4.62	no peak	36.4	C8H18N2O2

Figure H.9: LC-MSMS reference chromatogram for N-butyl-N(4-hydroxybutyl)nitrosamine N7. As referenced in Table 3.11.



4OHBu\_reference\_3-2-12\_1\_6271.swx

1: MS +c SM0 AM2 RT: 4.6353 minutes, Scan 1064, NL 1.00e+2

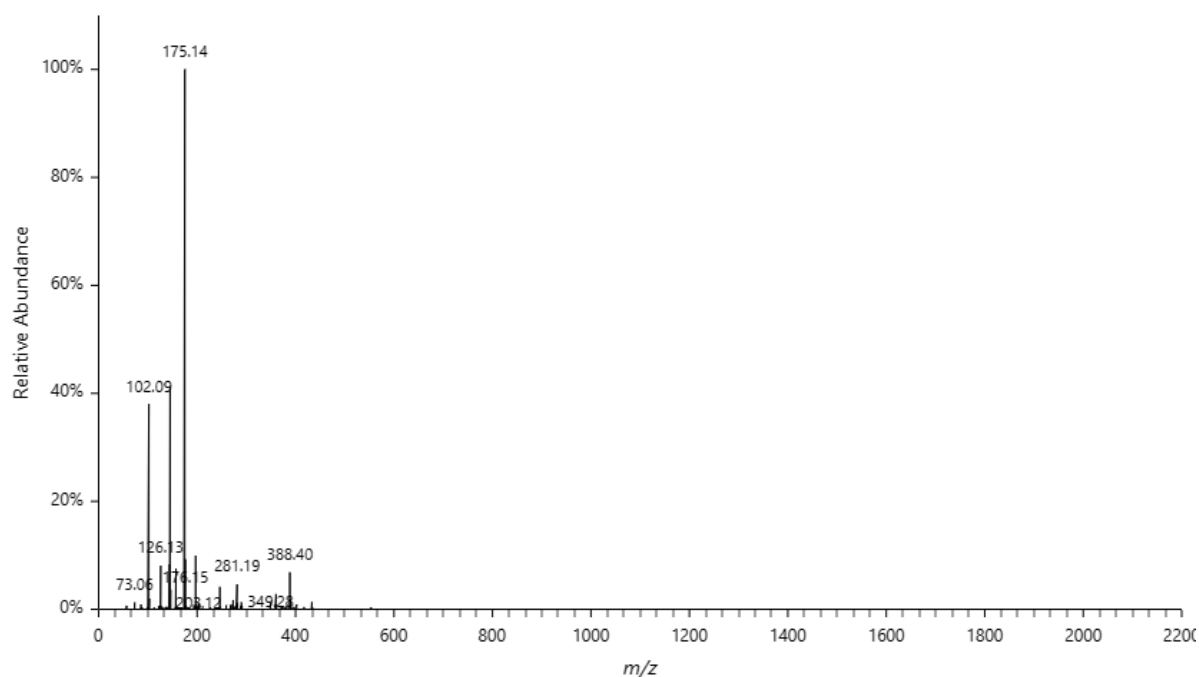


Figure H.10: LC-MSMS reference mass peaks for N-butyl-N(4-hydroxybutyl)nitrosamine N7. As referenced in Table 3.11.

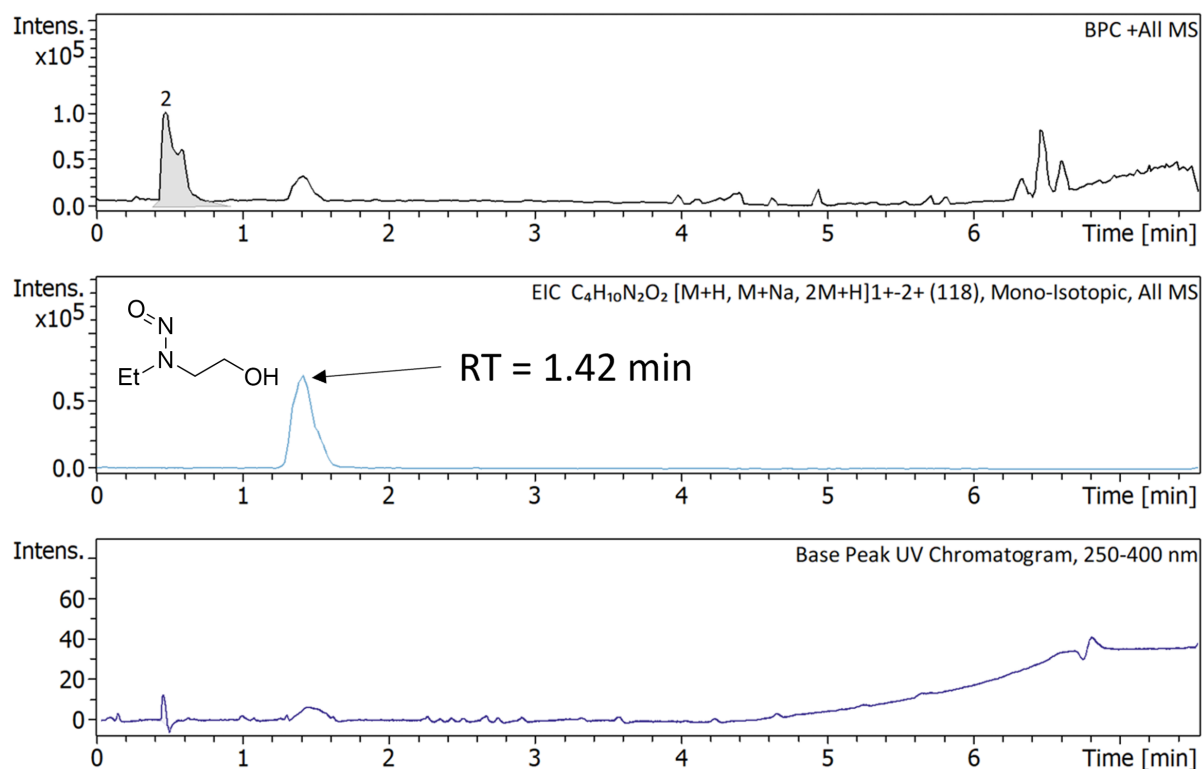


Figure H.11: LC-MSMS reference chromatogram for N-ethyl-N(2-hydroxyethyl)nitrosamine N8. As referenced in Table 3.11.

2OHEt\_reference\_1-1-36\_1\_6270.swx

1: MS +c 5M0 AM2 RT: 1.4174 minutes, Scan 436, NL 1.00e+2

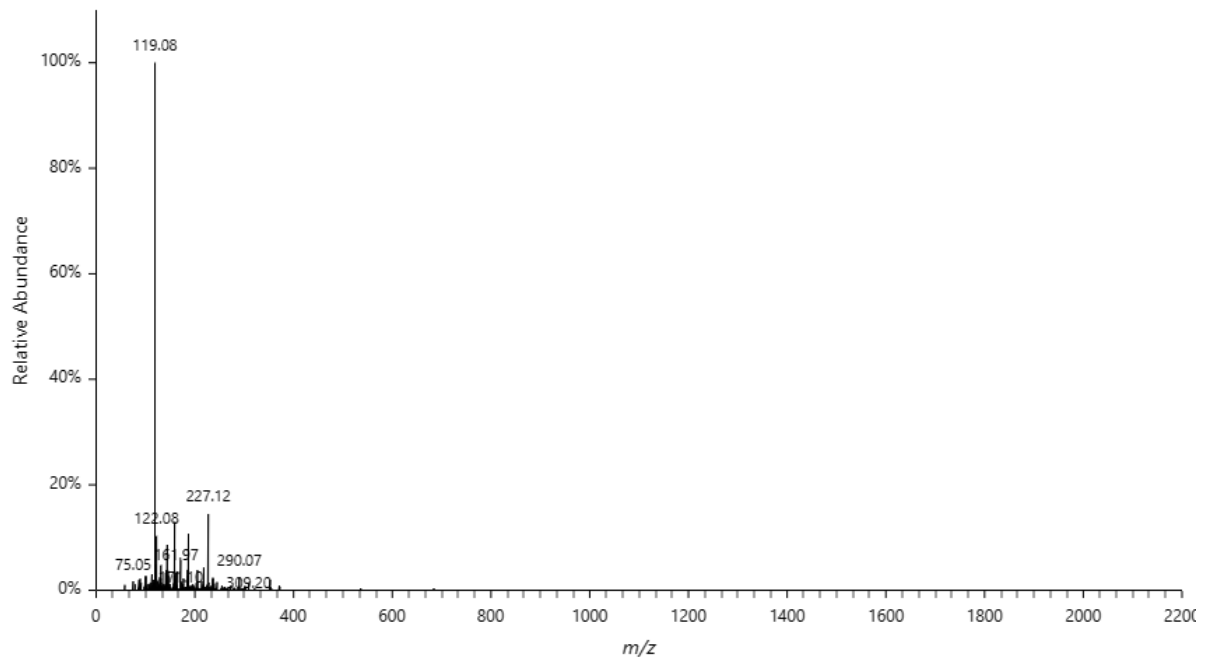
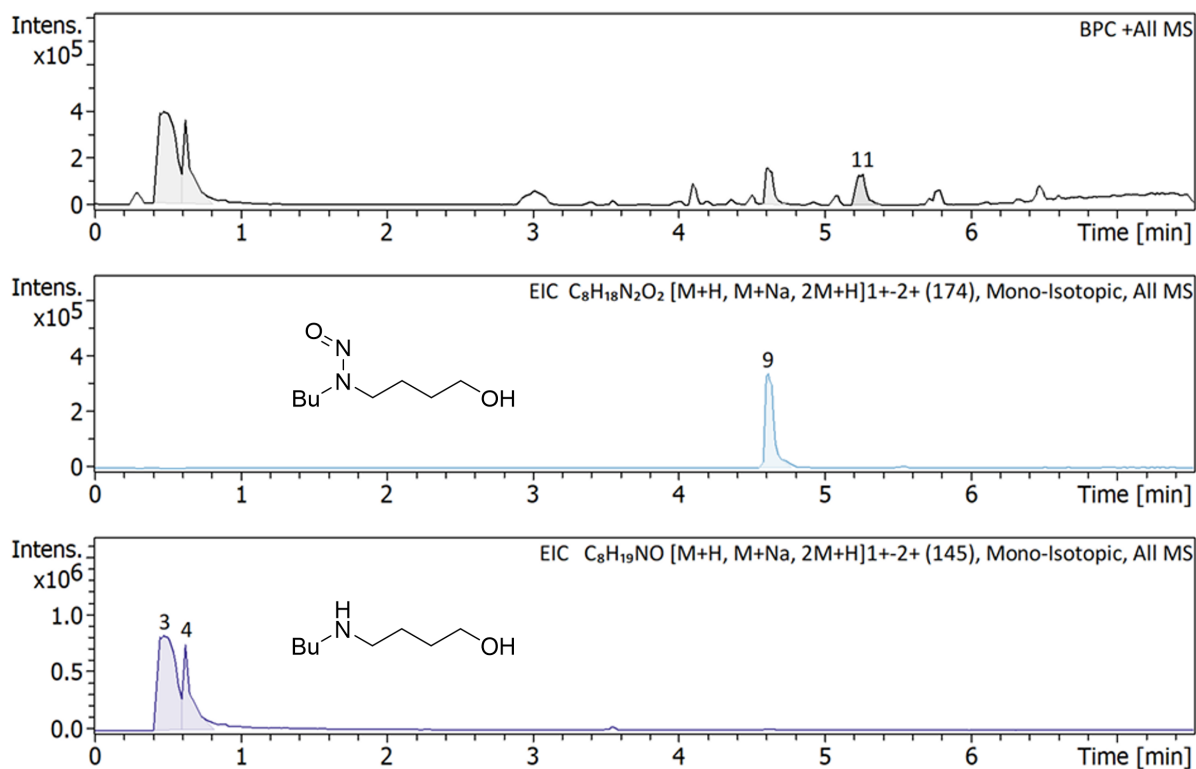


Figure H.12: LC-MSMS reference mass peaks for N-ethyl-N(2-hydroxyethyl)nitrosamine N8. As referenced in Table 3.11.



### Summary of Results

Name	RT	BPC Area(%)	UV Area(%)	Confirm Formula Results
Cmpd 3, 0.5 min	0.48	59.0	30.6	C <sub>8</sub> H <sub>19</sub> NO
Cmpd 4, 0.6 min	0.63	22.3	no peak	C <sub>8</sub> H <sub>19</sub> NO
Cmpd 9, 4.6 min	4.61	9.1	35.9	C <sub>8</sub> H <sub>18</sub> N <sub>2</sub> O <sub>2</sub>
Cmpd 11, 5.3 min	5.26	9.6	no peak	

Figure H.13: LC-MSMS reference chromatogram for 4-(butylamino)-1-butanol from condition 7. As referenced in Table 3.11.

GH141\_4OHBu\_3-2-16\_1\_6272.swx

1: MS +c 5M0 AM2 RT: 0.4869 minutes, Scan 128, NL 1.00e+2

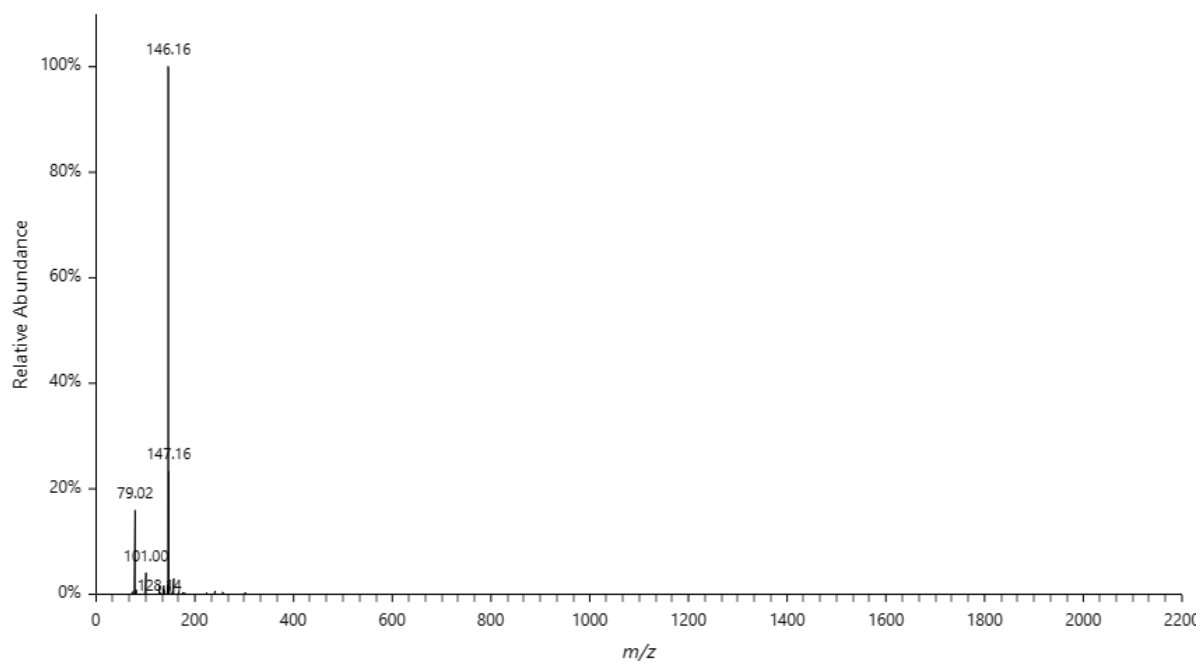
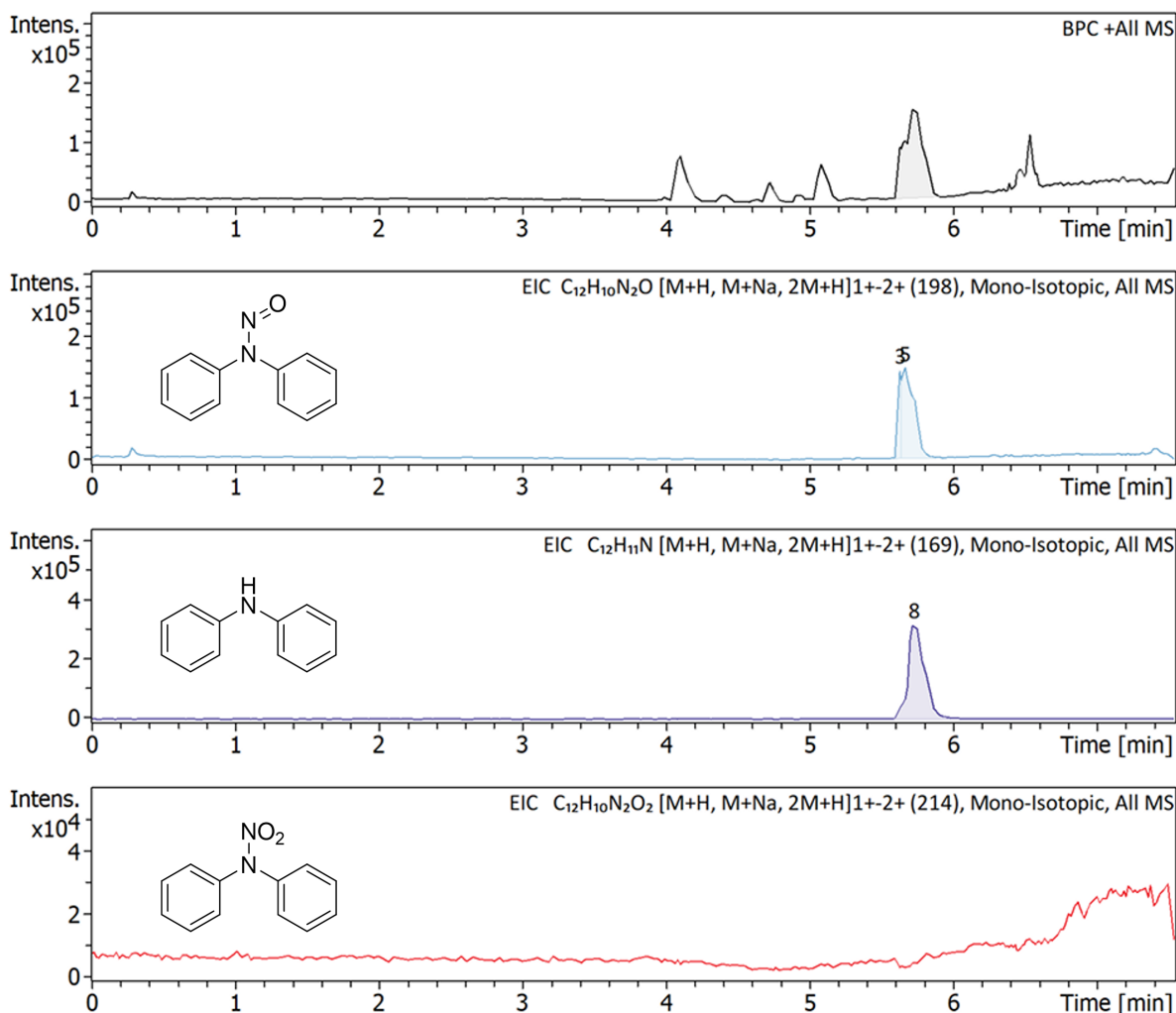


Figure H.14: LC-MSMS reference mass peaks for 4-(butylamino)-1-butanol from condition 7. As referenced in Table 3.11.

## Appendix I

# LC-MS/MS Experiment

## chromatograms



### Summary of Results

Name	RT	BPC Area(%)	UV Area(%)	Confirm Formula Results
Cmpd 3, 5.6 min	5.63	no peak	27.9	C12H10N2O
Cmpd 5, 5.7 min	5.66	100.0	27.9	C12H10N2O,C12H11N
Cmpd 8, 5.7 min	5.72	100.0	15.9	C12H10N2O,C12H11N

Figure I.1: LC-MSMS experiment chromatogram for N-nitrosodiphenylamine (N4) in reaction condition 1. Referenced in Section 3.6.

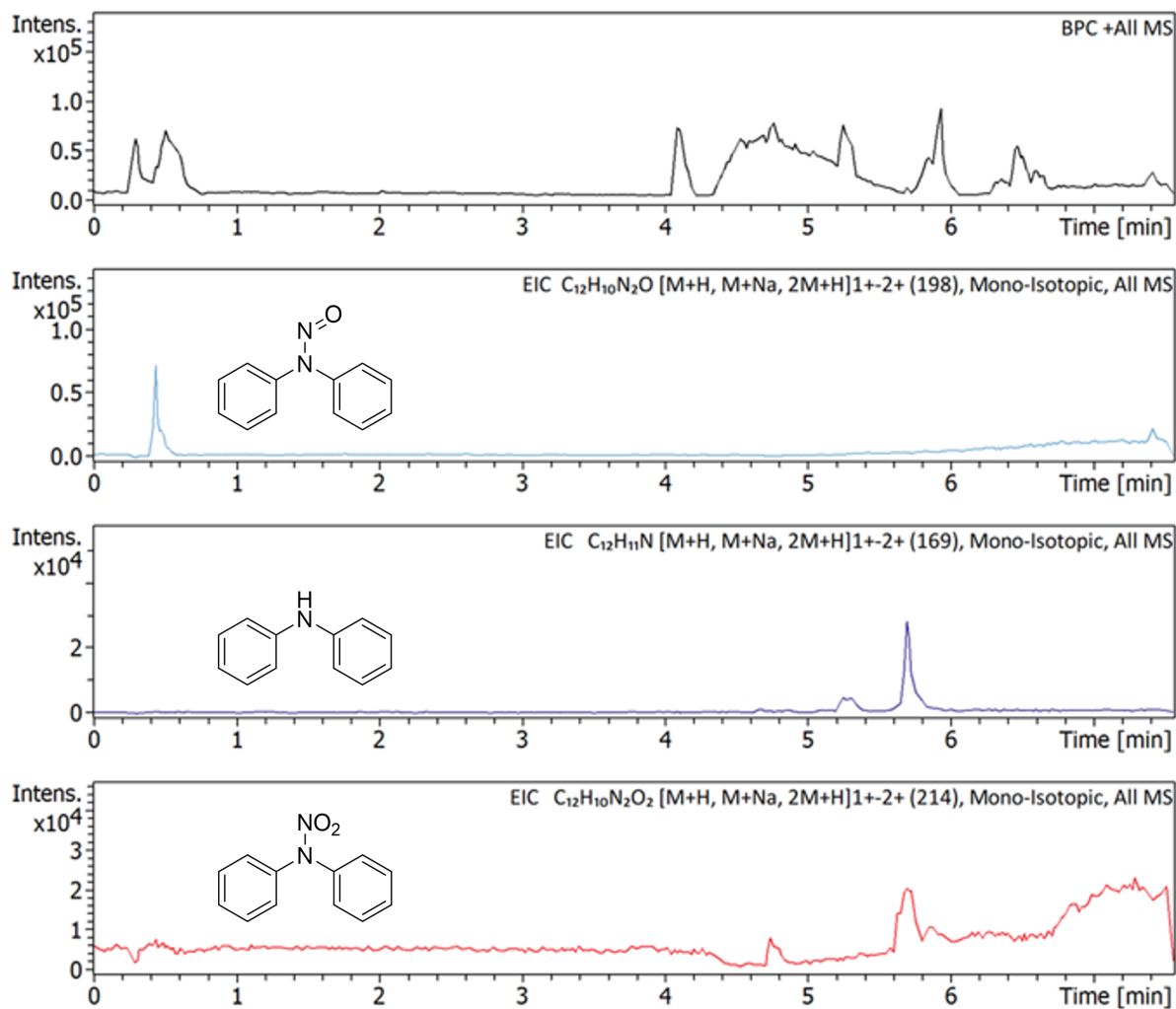
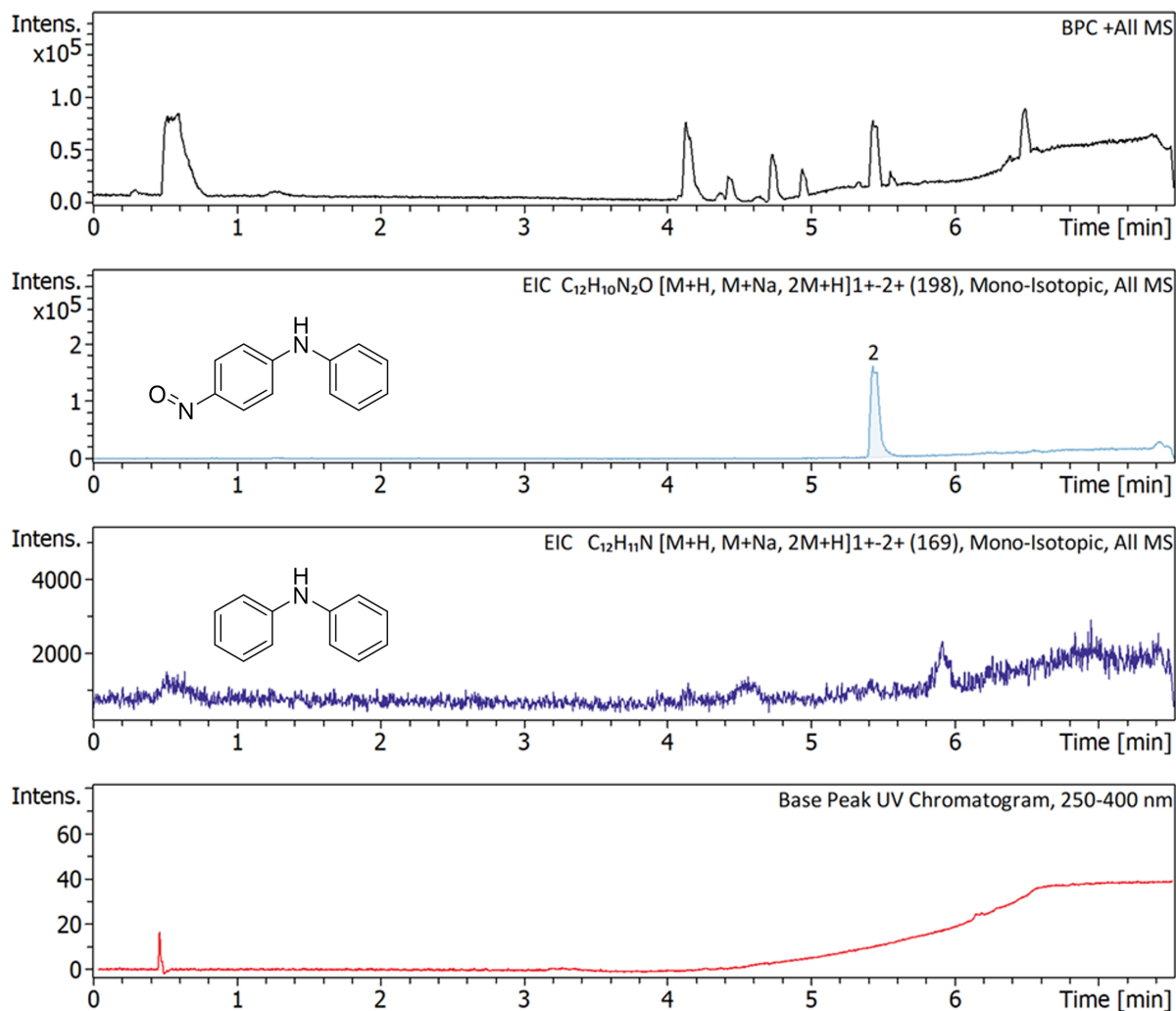


Figure I.2: LC-MSMS experiment chromatogram for N-nitrosodiphenylamine (N4) in reaction condition 2. Referenced in Section 3.6.

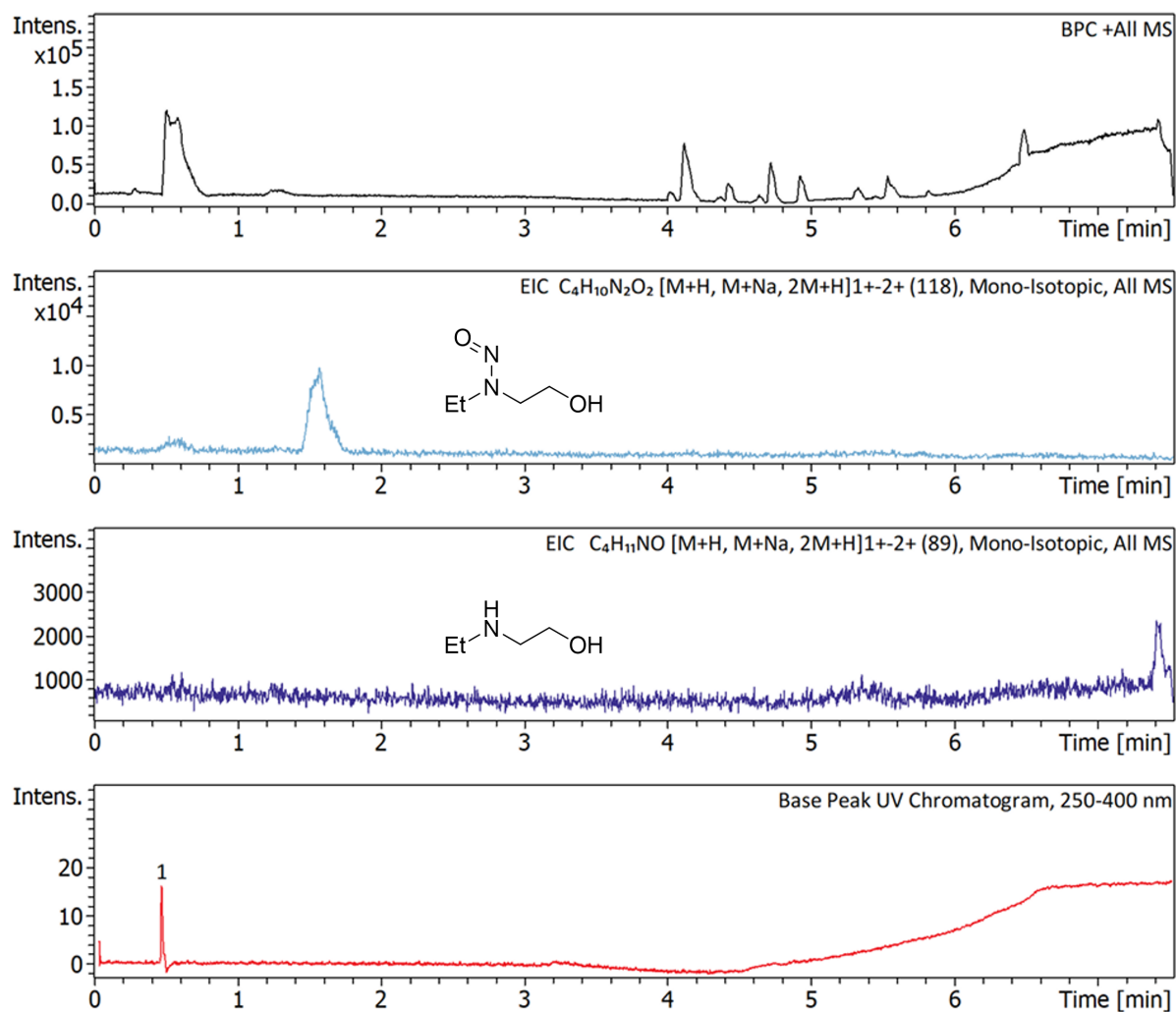


### Summary of Results

Name	RT	BPC Area(%)	UV Area(%)	Confirm Formula Results
Cmpd 2, 5.4 min	5.43	no peak	no peak	$C_{12}H_{10}N_2O$

Figure I.3: LC-MSMS experiment chromatogram for N-nitrosodiphenylamine (N4) in reaction condition 3. Referenced in Section 3.6.

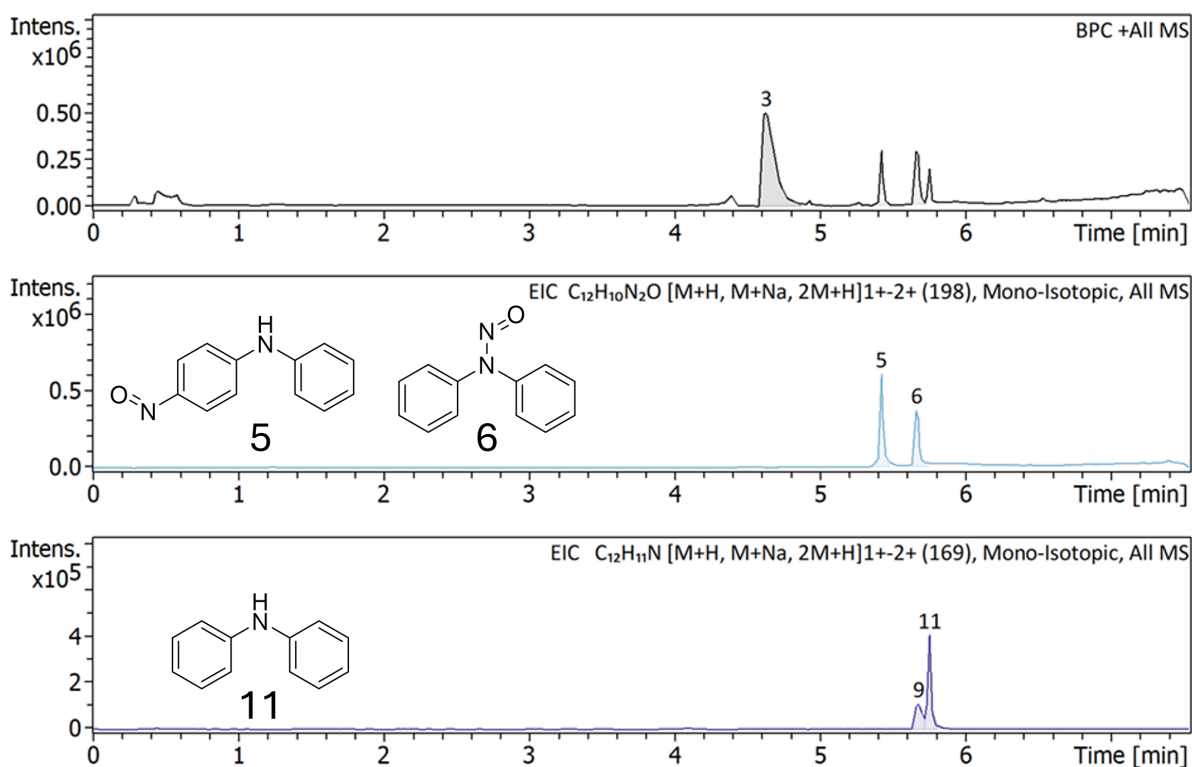




### Summary of Results

Name	RT	BPC Area(%)	UV Area(%)	Confirm Formula Results
Cmpd 1, 0.5 min	0.47	no peak	no uv	

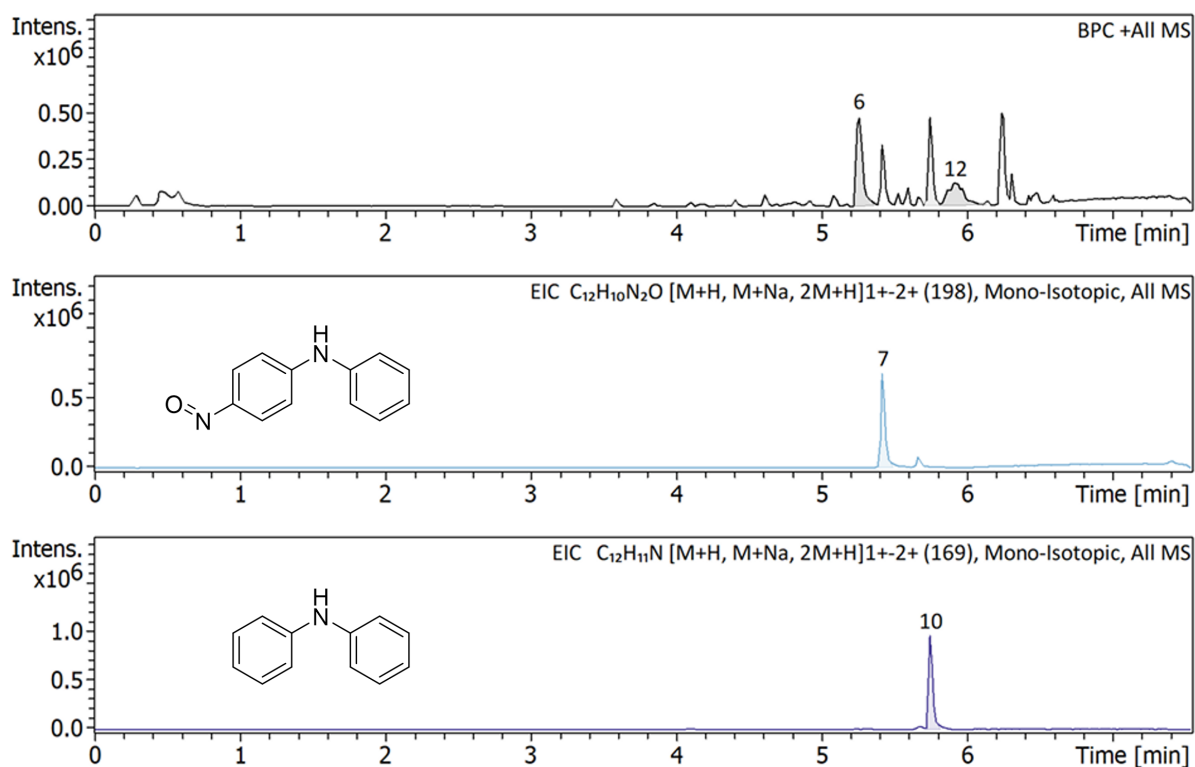
Figure I.4: LC-MSMS experiment chromatogram for N-ethyl-N-(2-hydroxyethyl)nitrosamine (N8) in reaction condition 3. Referenced in Section 3.6.



### Summary of Results

Name	RT	BPC Area(%)	UV Area(%)	Confirm Formula Results
Cmpd 3, 4.6 min	4.63	72.8	no peak	
Cmpd 5, 5.4 min	5.42	10.9	no peak	C12H10N2O
Cmpd 6, 5.7 min	5.66	16.3	78.2	C12H10N2O
Cmpd 9, 5.7 min	5.67	16.3	78.2	C12H10N2O
Cmpd 11, 5.8 min	5.75	no peak	4.3	C12H11N

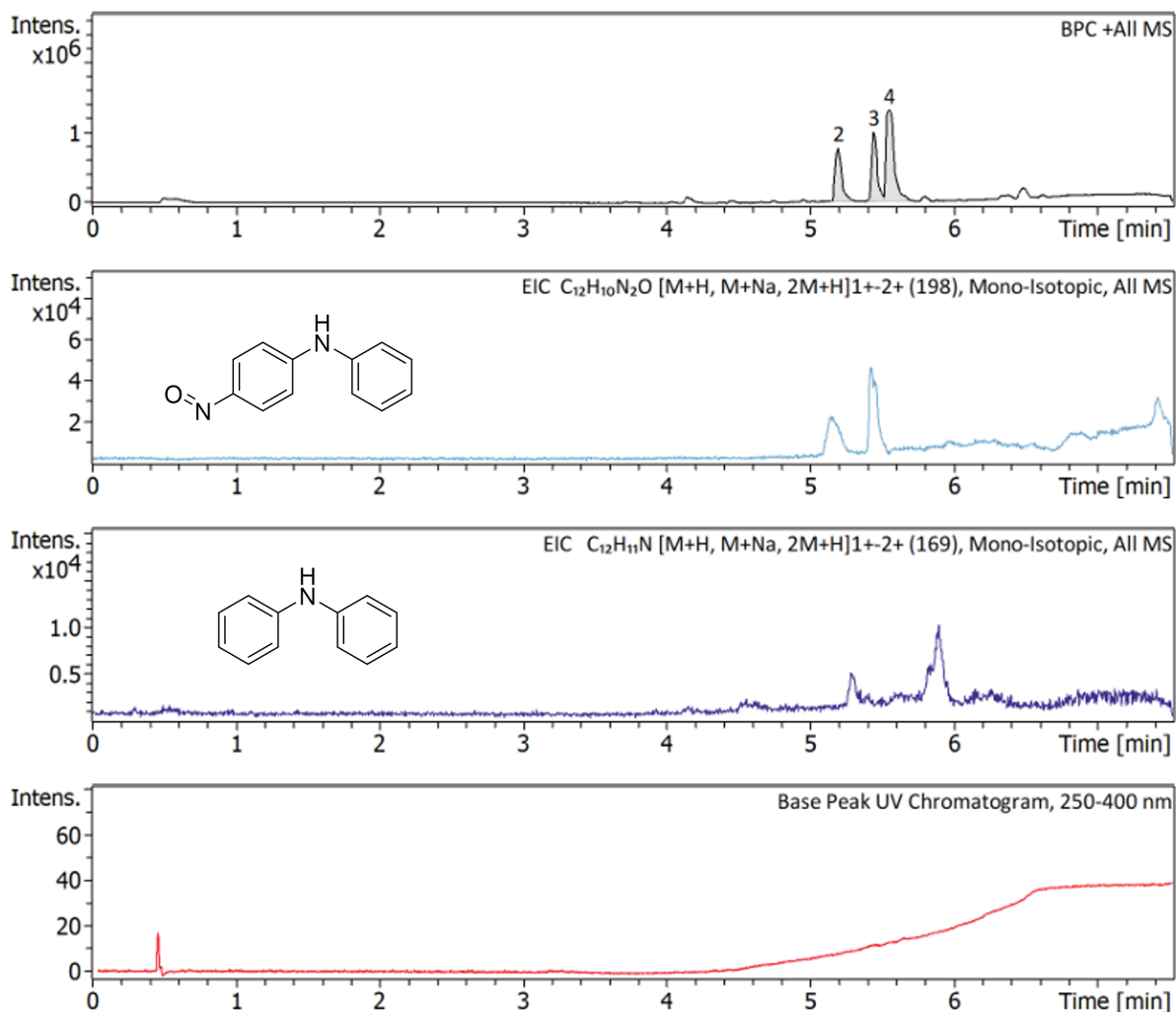
Figure I.5: LC-MSMS experiment chromatogram for N-nitrosodiphenylamine (N4) in reaction condition 4. Referenced in Section 3.6.



### Summary of Results

Name	RT	BPC Area(%)	UV Area(%)	Confirm Formula Results
Cmpd 6, 5.3 min	5.26	44.2	no peak	
Cmpd 7, 5.4 min	5.42	no peak	no peak	C <sub>12</sub> H <sub>10</sub> N <sub>2</sub> O
Cmpd 10, 5.7 min	5.75	28.6	34.5	C <sub>12</sub> H <sub>11</sub> N
Cmpd 12, 5.9 min	5.92	27.2	no peak	

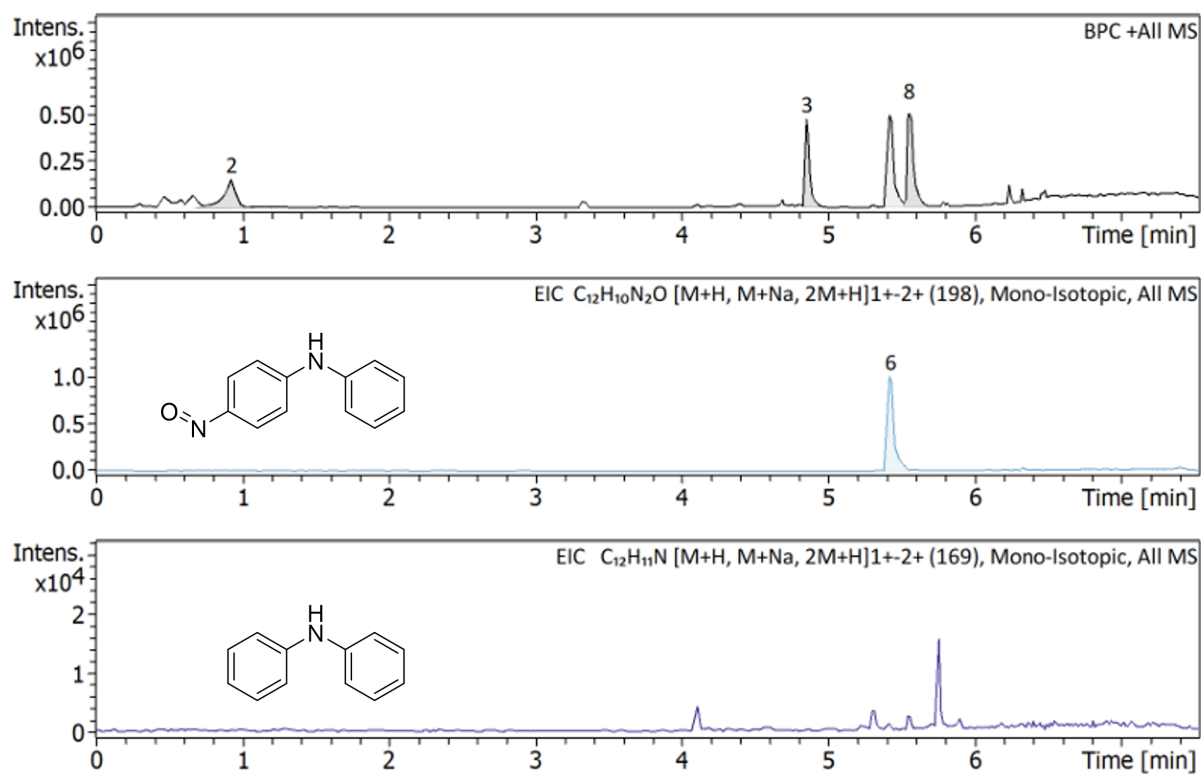
Figure I.6: LC-MSMS experiment chromatogram for N-nitrosodiphenylamine (N4) in reaction condition 5. Referenced in Section 3.6.



### Summary of Results

Name	RT	BPC Area(%)	UV Area(%)	Confirm Formula Results
Cmpd 2, 5.2 min	5.19	23.2	no peak	
Cmpd 3, 5.4 min	5.44	25.9	no peak	C <sub>12</sub> H <sub>10</sub> N <sub>2</sub> O
Cmpd 4, 5.5 min	5.55	50.8	no peak	

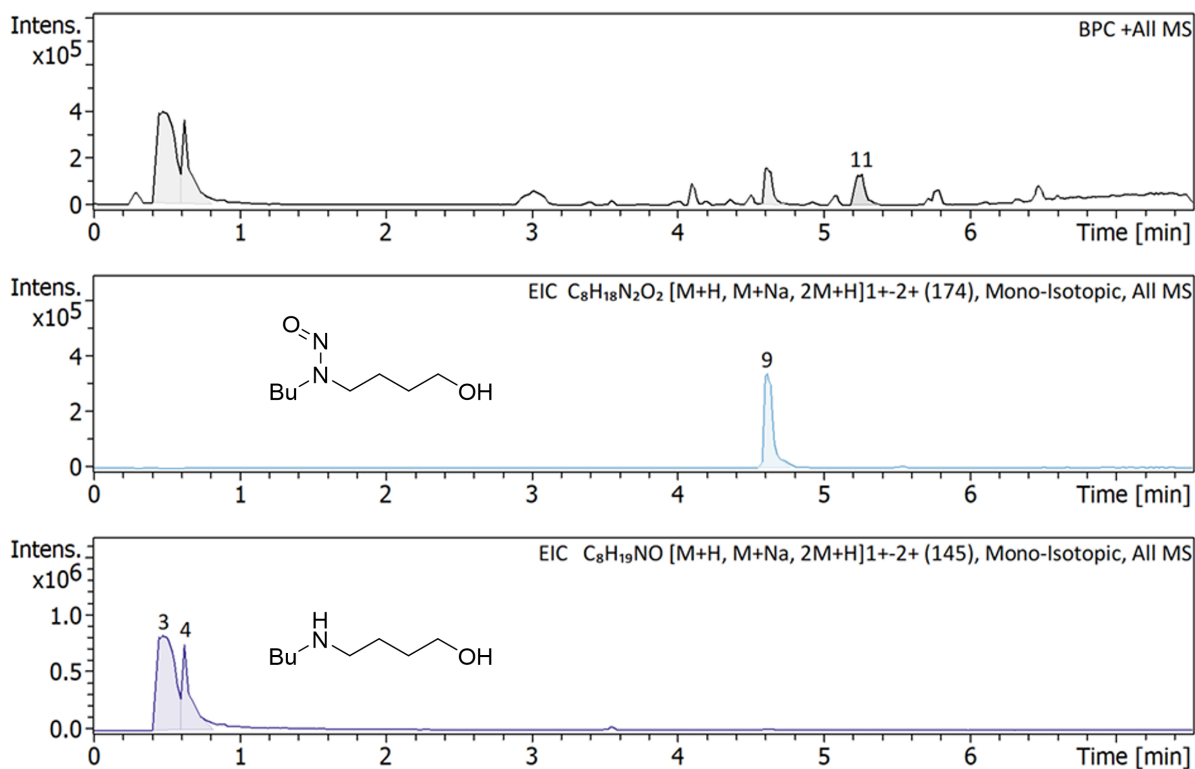
Figure I.7: LC-MSMS experiment chromatogram for N-nitrosodiphenylamine (N4) in reaction condition 6. Referenced in Section 3.6.



### Summary of Results

Name	RT	BPC Area(%)	UV Area(%)	Confirm Formula Results
Cmpd 2, 0.9 min	0.93	18.4	no peak	
Cmpd 3, 4.9 min	4.85	21.4	18.0	
Cmpd 6, 5.4 min	5.42	29.2	14.0	C <sub>12</sub> H <sub>10</sub> N <sub>2</sub> O
Cmpd 8, 5.5 min	5.55	30.9	30.6	

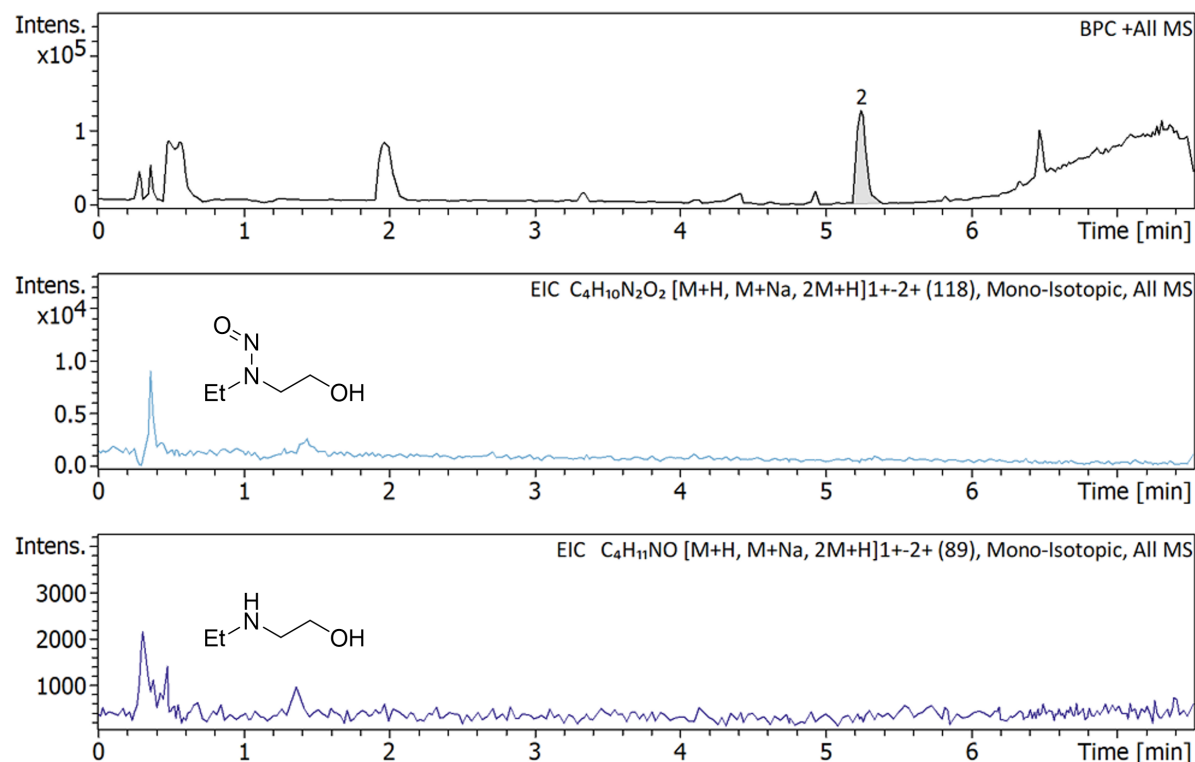
Figure I.8: LC-MSMS experiment chromatogram for N-nitrosodiphenylamine (N4) in reaction condition 7. Referenced in Section 3.6.



### Summary of Results

Name	RT	BPC Area(%)	UV Area(%)	Confirm Formula Results
Cmpd 3, 0.5 min	0.48	59.0	30.6	C <sub>8</sub> H <sub>19</sub> NO
Cmpd 4, 0.6 min	0.63	22.3	no peak	C <sub>8</sub> H <sub>19</sub> NO
Cmpd 9, 4.6 min	4.61	9.1	35.9	C <sub>8</sub> H <sub>18</sub> N <sub>2</sub> O <sub>2</sub>
Cmpd 11, 5.3 min	5.26	9.6	no peak	

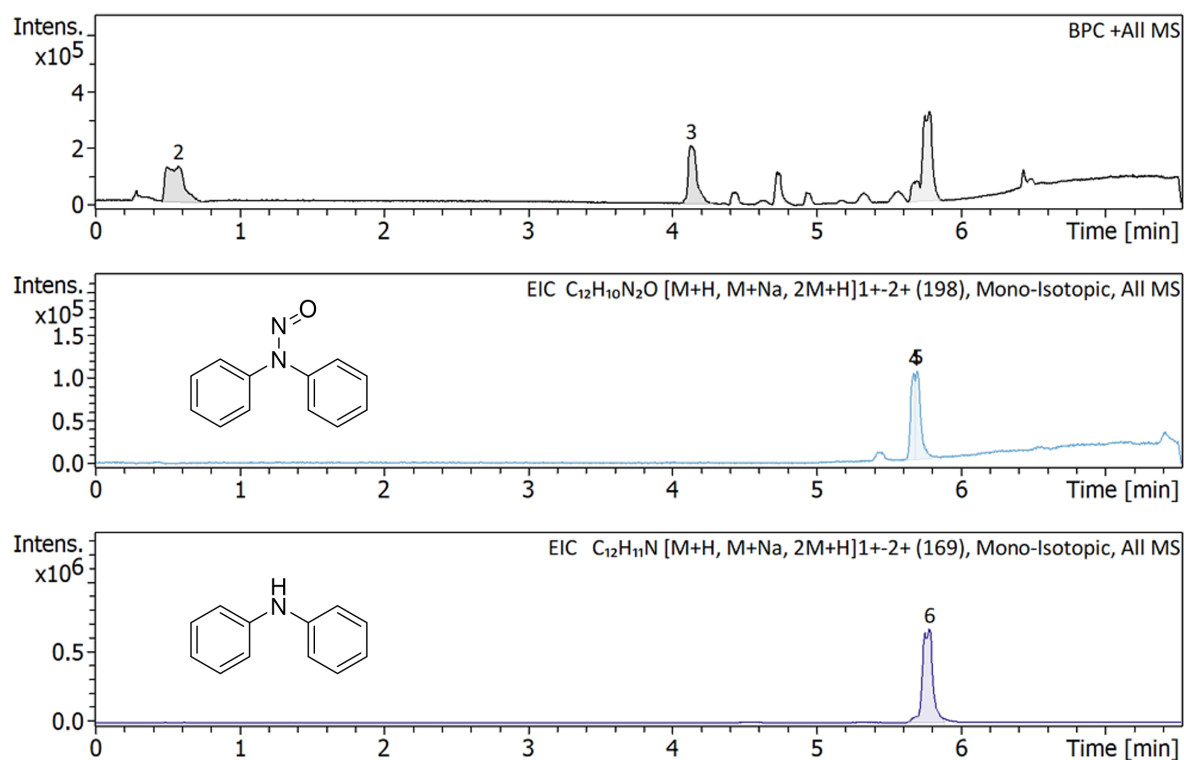
Figure I.9: LC-MSMS experiment chromatogram for N-butyl-N-(4-hydroxybutyl)nitrosamine (N7) in reaction condition 7. Referenced in Section 3.6.



### Summary of Results

Name	RT	BPC Area(%)	UV Area(%)	Confirm Formula Results
Cmpd 2, 5.2 min	5.24	no peak	no peak	

Figure I.10: LC-MSMS experiment chromatogram for N-ethyl-N-(2-hydroxyethyl)nitrosamine (N8) in reaction condition 7. Referenced in Section 3.6.

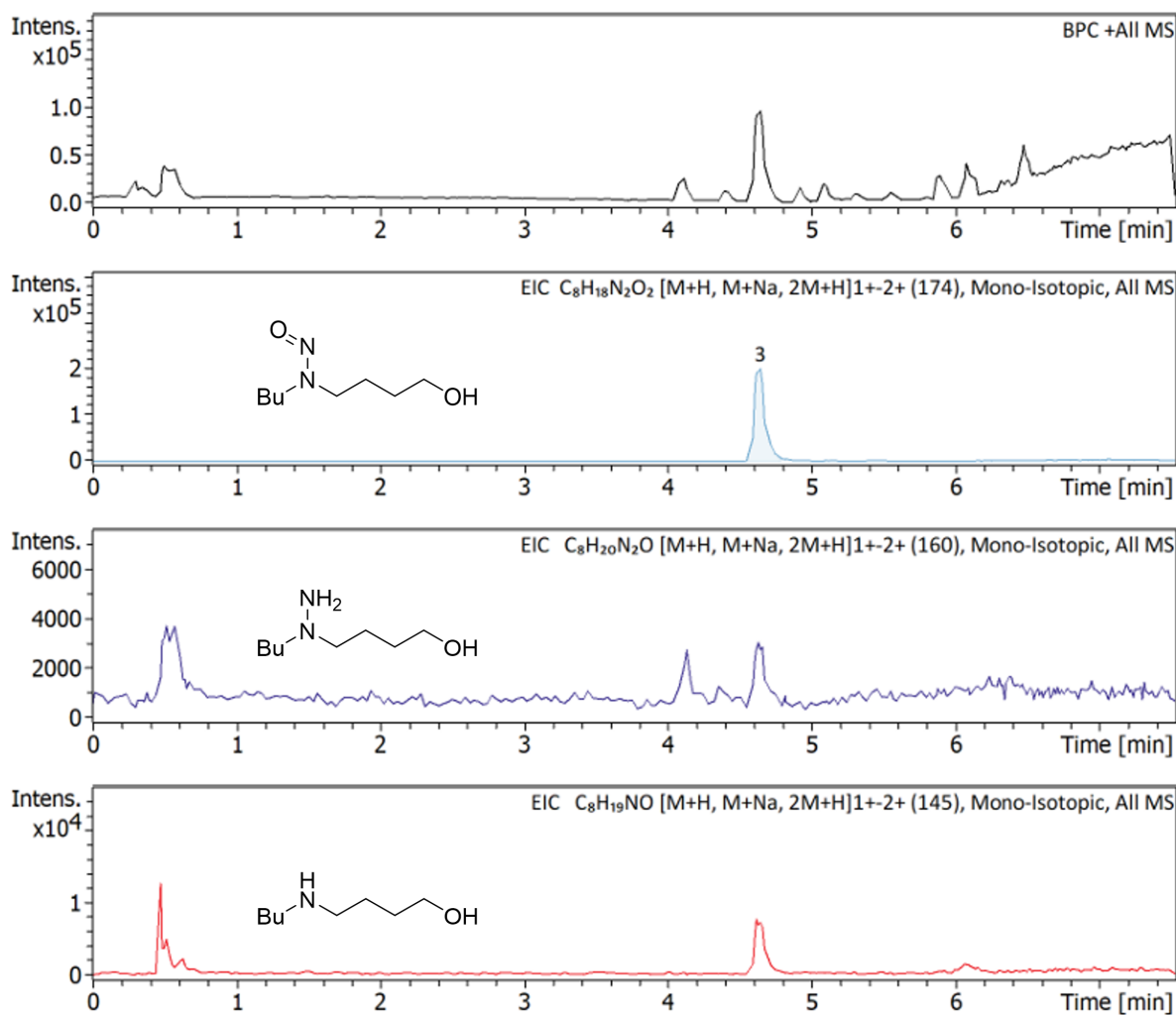


### Summary of Results

Name	RT	BPC Area(%)	UV Area(%)	Confirm Formula Results
Cmpd 2, 0.6 min	0.58	30.7	no peak	
Cmpd 3, 4.1 min	4.13	24.5	no peak	
Cmpd 4, 5.7 min	5.67	no peak	no peak	C <sub>12</sub> H <sub>10</sub> N <sub>2</sub> O
Cmpd 5, 5.7 min	5.70	no peak	no peak	C <sub>12</sub> H <sub>10</sub> N <sub>2</sub> O
Cmpd 6, 5.8 min	5.78	44.8	no peak	C <sub>12</sub> H <sub>11</sub> N

Figure I.11: LC-MSMS experiment chromatogram for N-nitrosodiphenylamine (N4) in reaction condition 8. Referenced in Section 3.6.

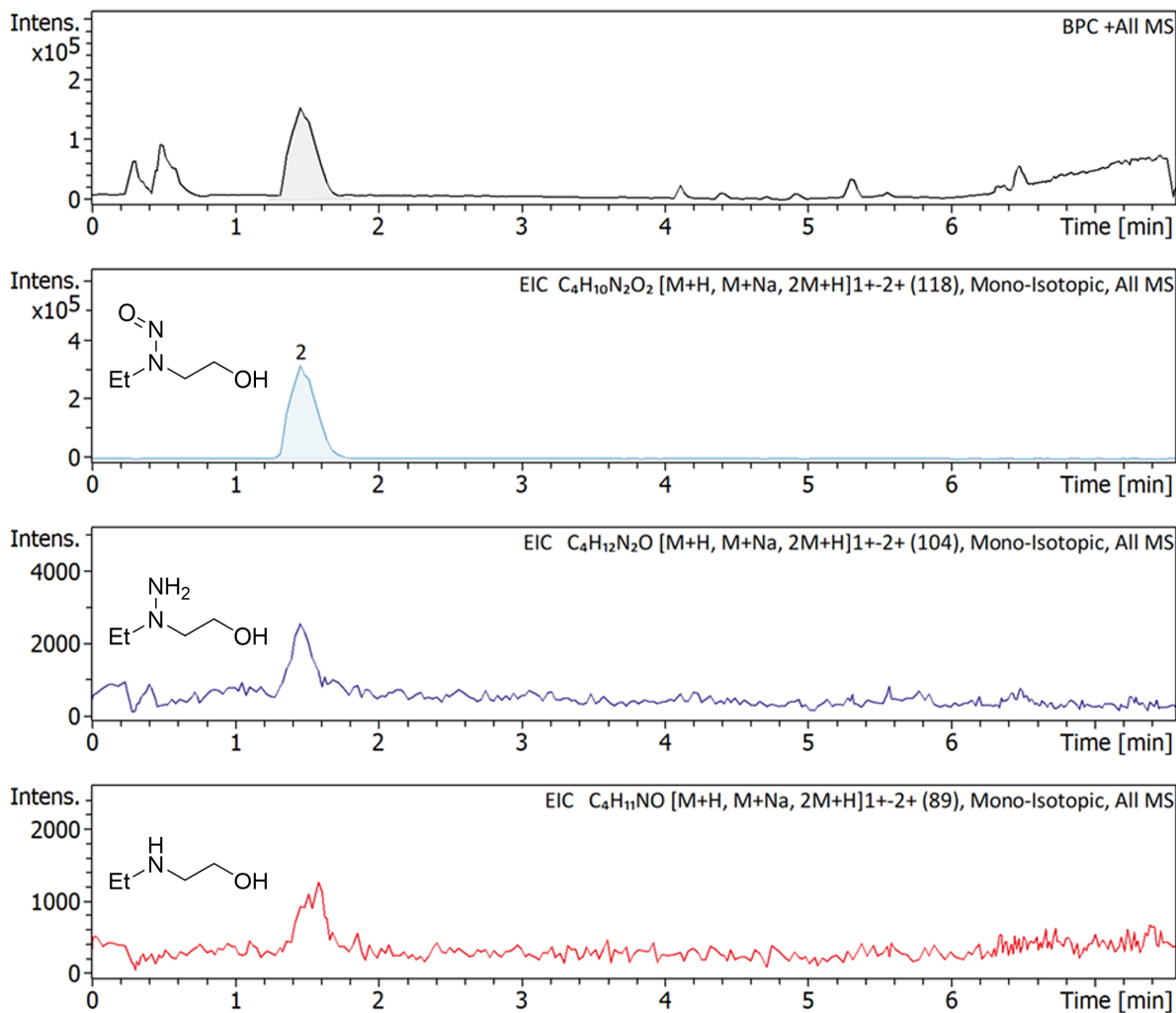




### Summary of Results

Name	RT	BPC Area(%)	UV Area(%)	Confirm Formula Results
Cmpd 3, 4.6 min	4.64	no peak	88.0	C8H18N2O2

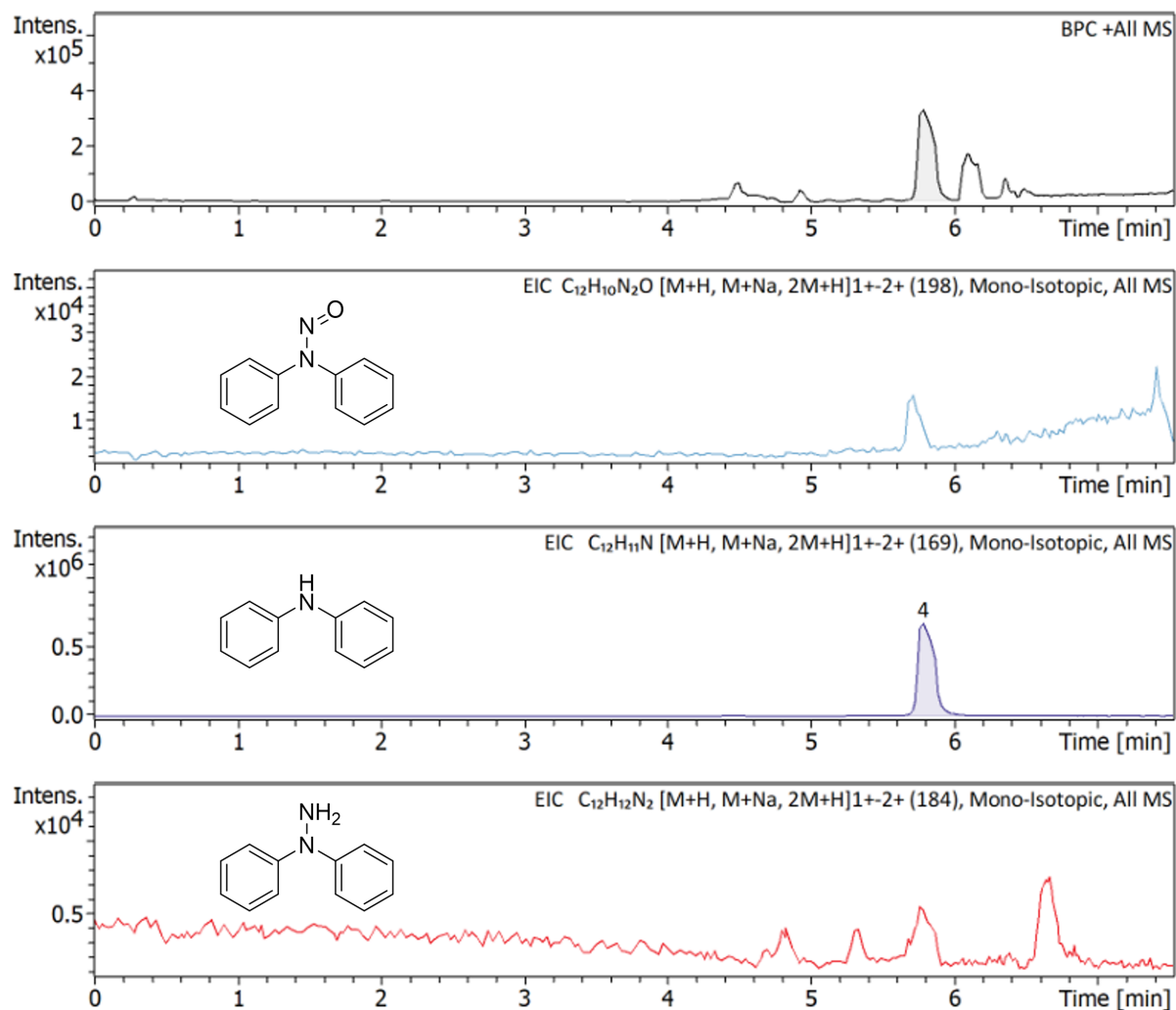
Figure I.12: LC-MSMS experiment chromatogram for N-butyl-N-(4-hydroxybutyl)nitrosamine (N7) in reaction condition 8. Referenced in Section 3.6.



### Summary of Results

Name	RT	BPC Area(%)	UV Area(%)	Confirm Formula Results
Cmpd 2, 1.5 min	1.46	100.0	63.3	$C_4H_{10}N_2O_2, C_4H_{10.5}N_2O_2$

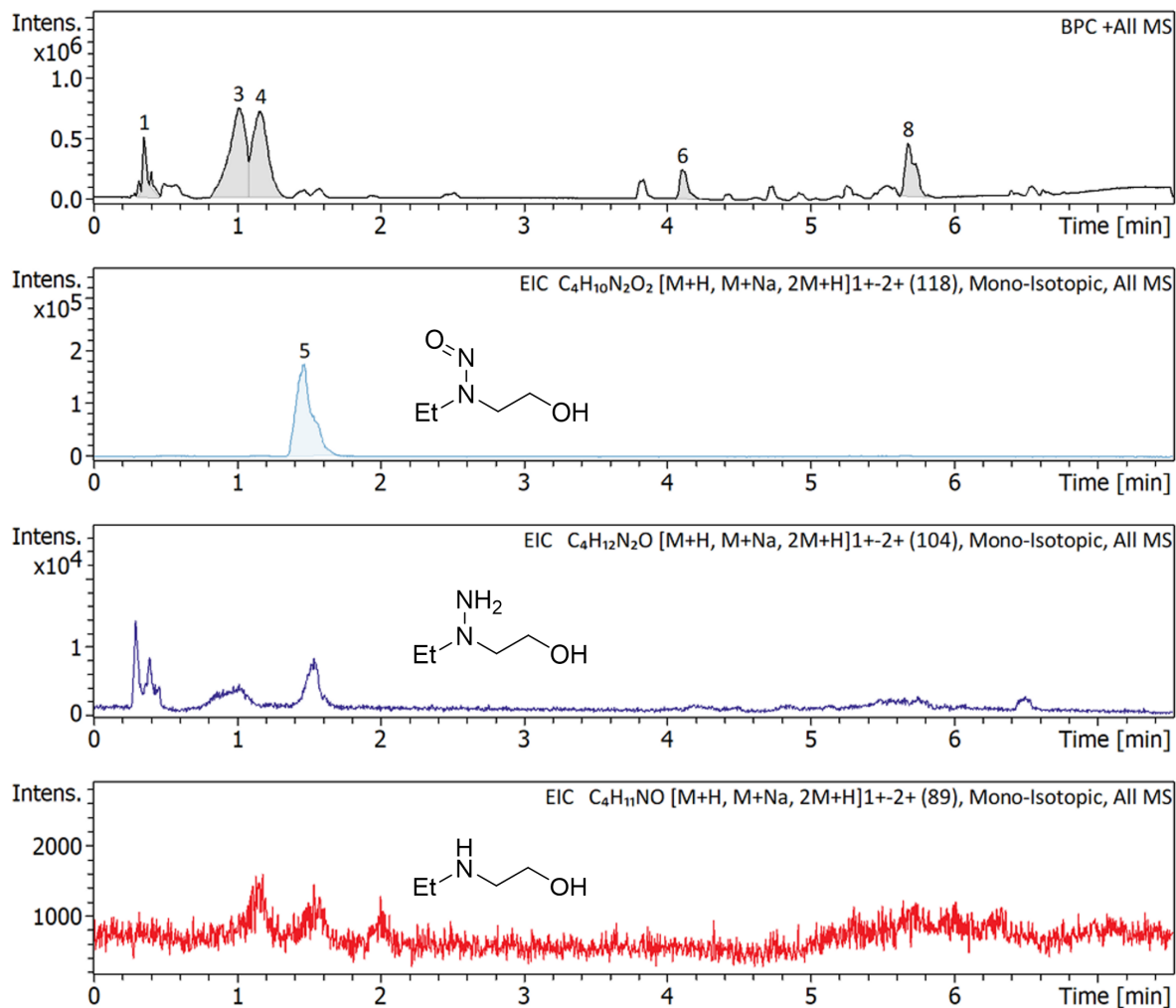
Figure I.13: LC-MSMS experiment chromatogram for N-ethyl-N-(2-hydroxyethyl)nitrosamine (N8) in reaction condition 8. Referenced in Section 3.6.



### Summary of Results

Name	RT	BPC Area(%)	UV Area(%)	Confirm Formula Results
Cmpd 4, 5.8 min	5.78	100.0	28.5	C12H11N

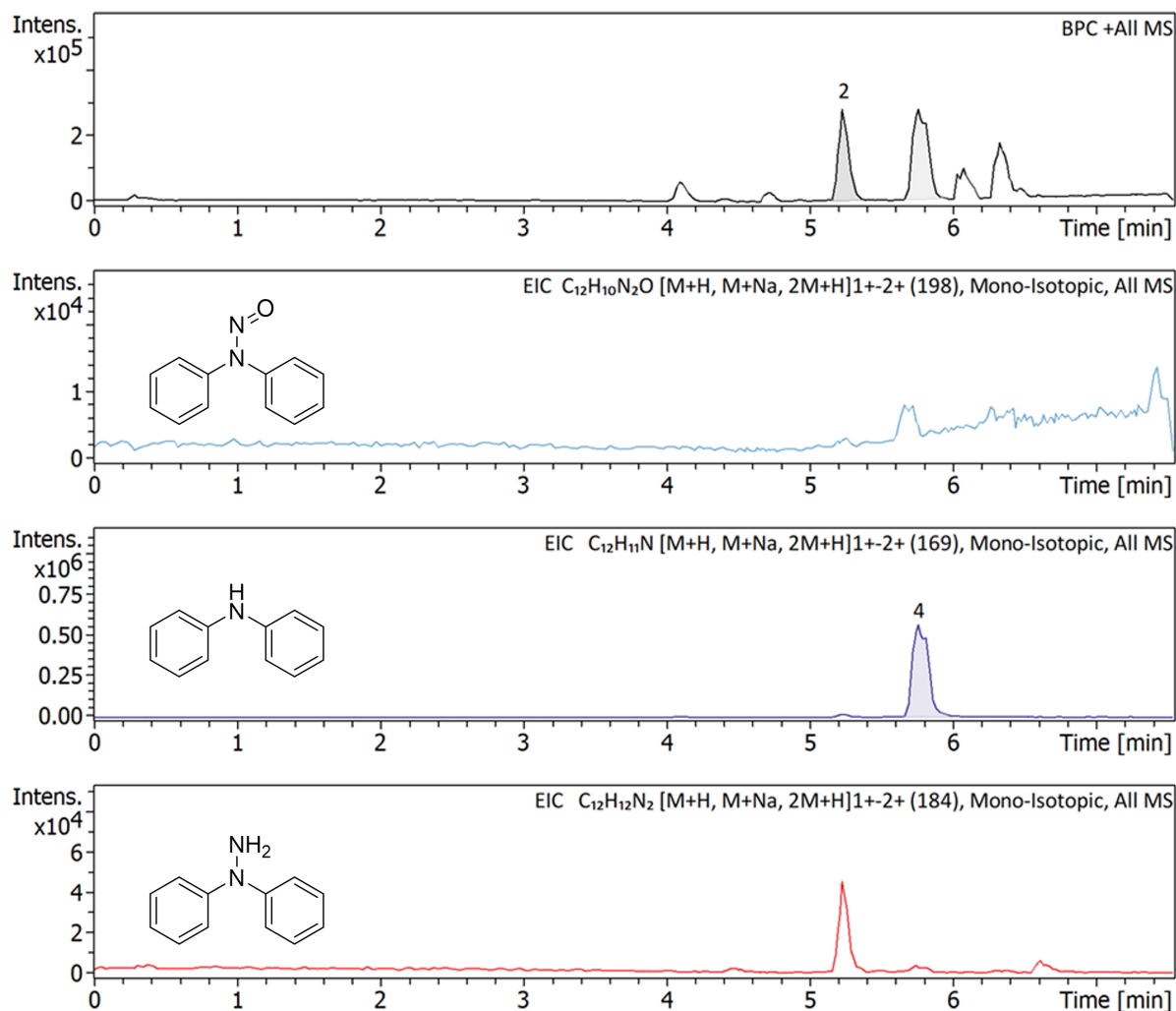
Figure I.14: LC-MSMS experiment chromatogram for N-nitrosodiphenylamine (N4) in reaction condition 9. Referenced in Section 3.6.



### Summary of Results

Name	RT	BPC Area(%)	UV Area(%)	Confirm Formula Results
Cmpd 1, 0.4 min	0.36	7.9	no peak	
Cmpd 3, 1.0 min	1.01	37.9	no peak	
Cmpd 4, 1.2 min	1.17	34.3	no peak	
Cmpd 5, 1.5 min	1.47	no peak	no peak	C4H10N2O2, C4H10.5N2O2
Cmpd 6, 4.1 min	4.11	6.0	no peak	
Cmpd 8, 5.7 min	5.68	13.9	48.8	

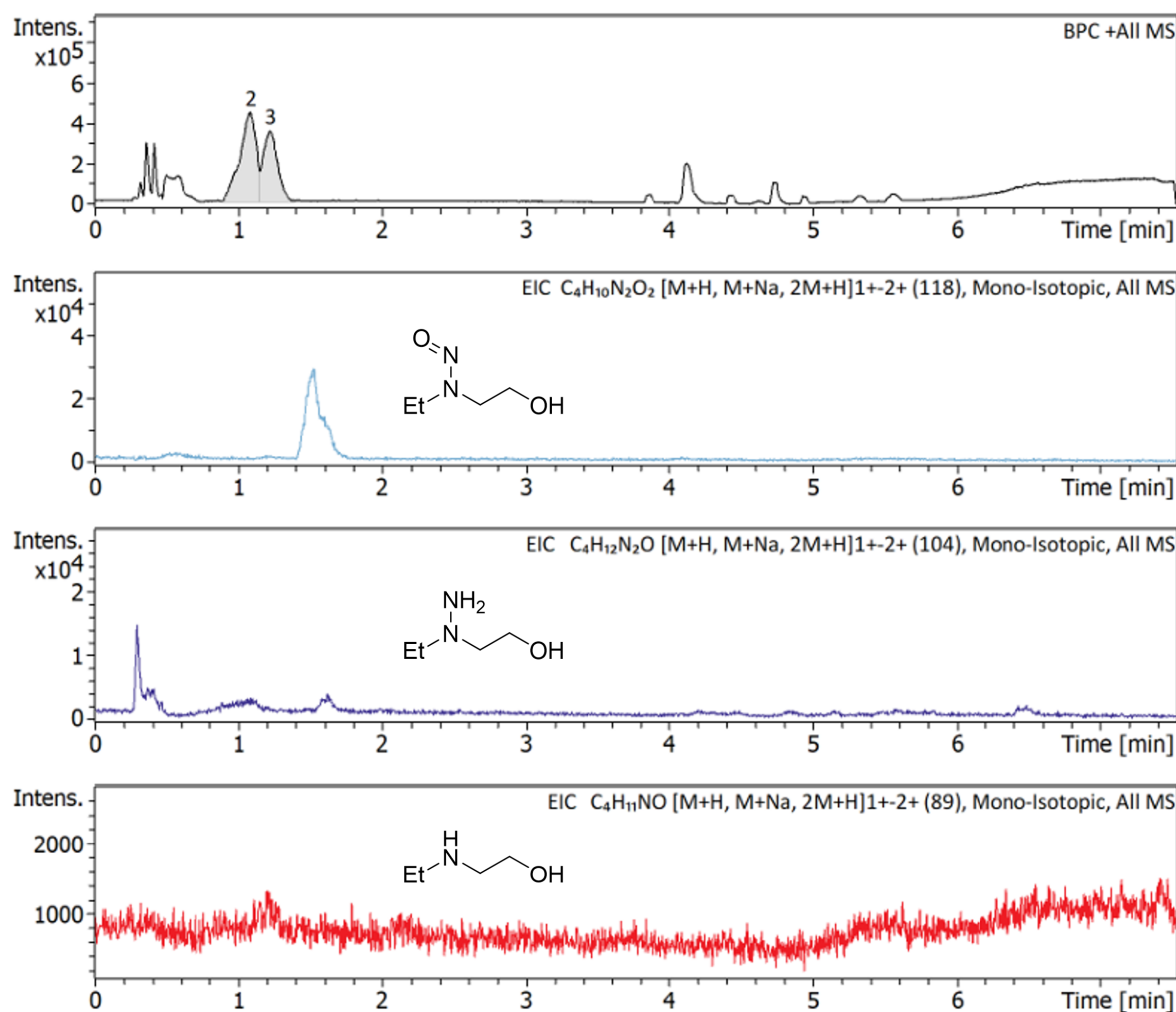
Figure I.15: LC-MSMS experiment chromatogram for ethyl-N-(2-hydroxyethyl)nitrosamine (N8) in reaction condition 9. Referenced in Section 3.6.



### Summary of Results

Name	RT	BPC Area(%)	UV Area(%)	Confirm Formula Results
Cmpd 2, 5.2 min	5.23	39.9	no peak	$C_{12}H_{12}N_2$
Cmpd 4, 5.8 min	5.76	60.1	32.6	$C_{12}H_{11}N$

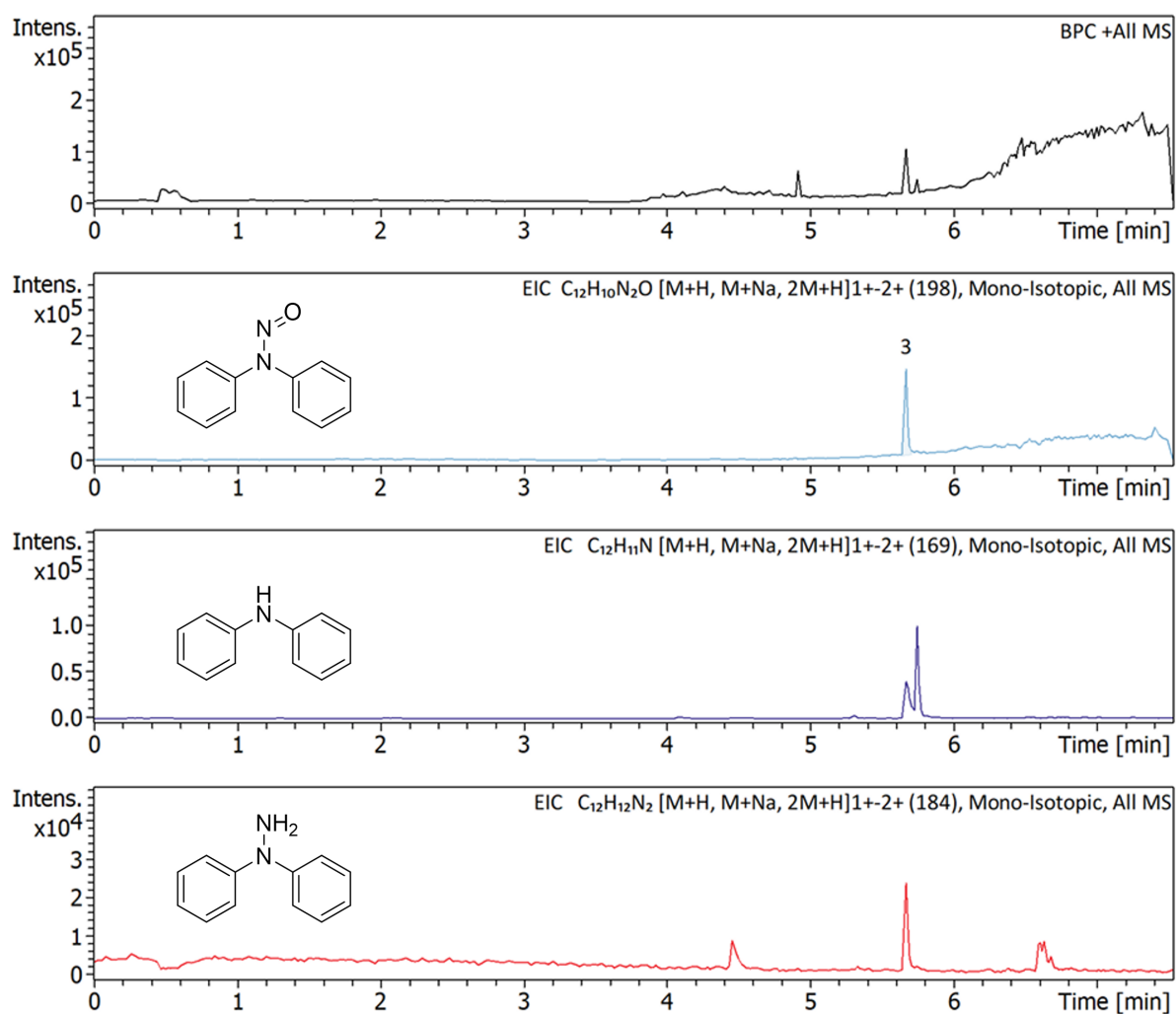
Figure I.16: LC-MSMS experiment chromatogram for N-nitrosodiphenylamine (N4) in reaction condition 10. Referenced in Section 3.6.



### Summary of Results

Name	RT	BPC Area(%)	UV Area(%)	Confirm Formula Results
Cmpd 2, 1.1 min	1.09	58.3	no peak	
Cmpd 3, 1.2 min	1.22	41.7	no peak	

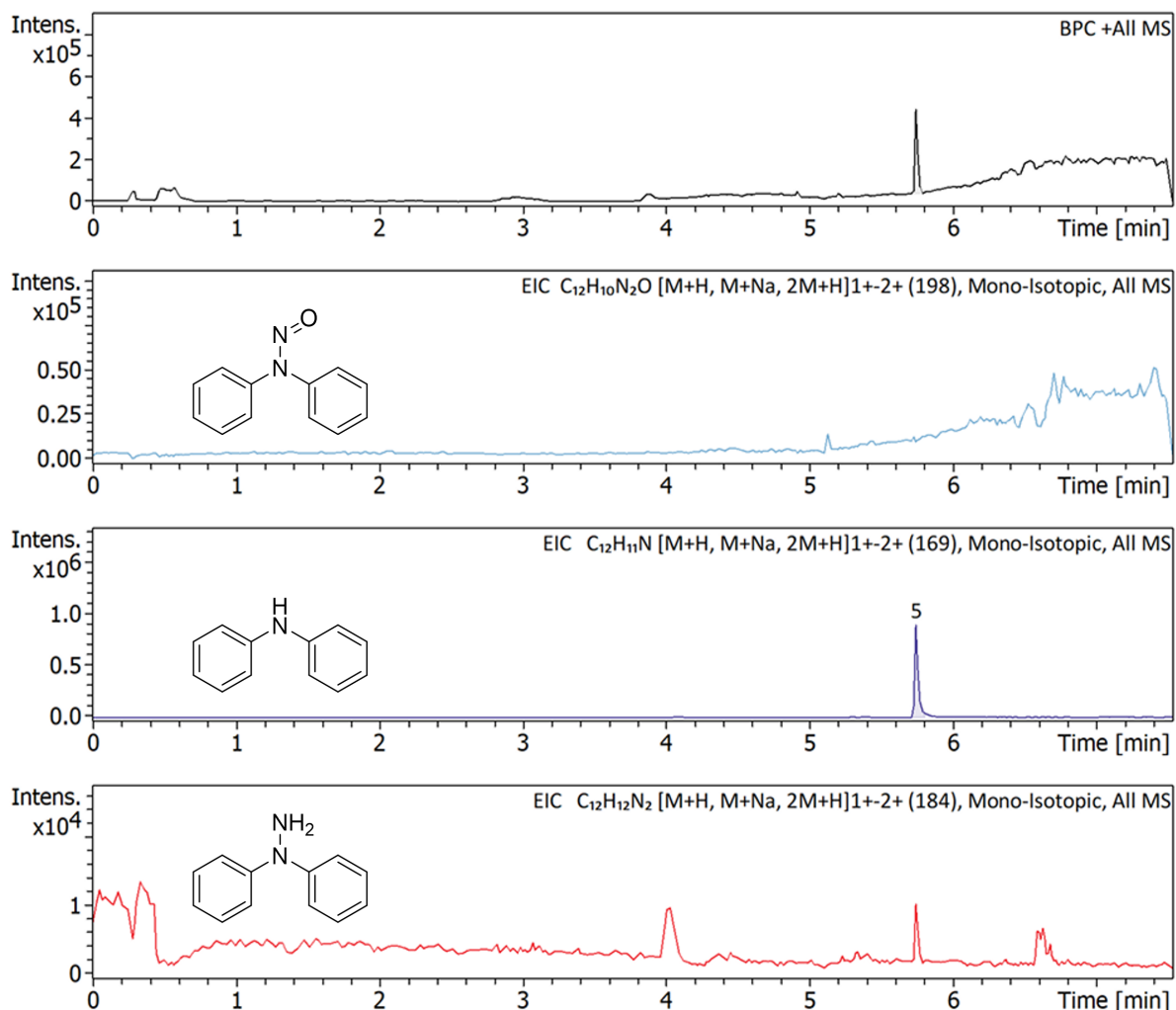
Figure I.17: LC-MSMS experiment chromatogram for ethyl-N-(2-hydroxyethyl)nitrosamine (N8) in reaction condition 10. Referenced in Section 3.6.



### Summary of Results

Name	RT	BPC Area(%)	UV Area(%)	Confirm Formula Results
Cmpd 3, 5.7 min	5.66	no peak	62.4	C <sub>12</sub> H <sub>10</sub> N <sub>2</sub> O

Figure I.18: LC-MSMS experiment chromatogram for N-nitrosodiphenylamine (N4) in reaction condition 11. Referenced in Section 3.6.

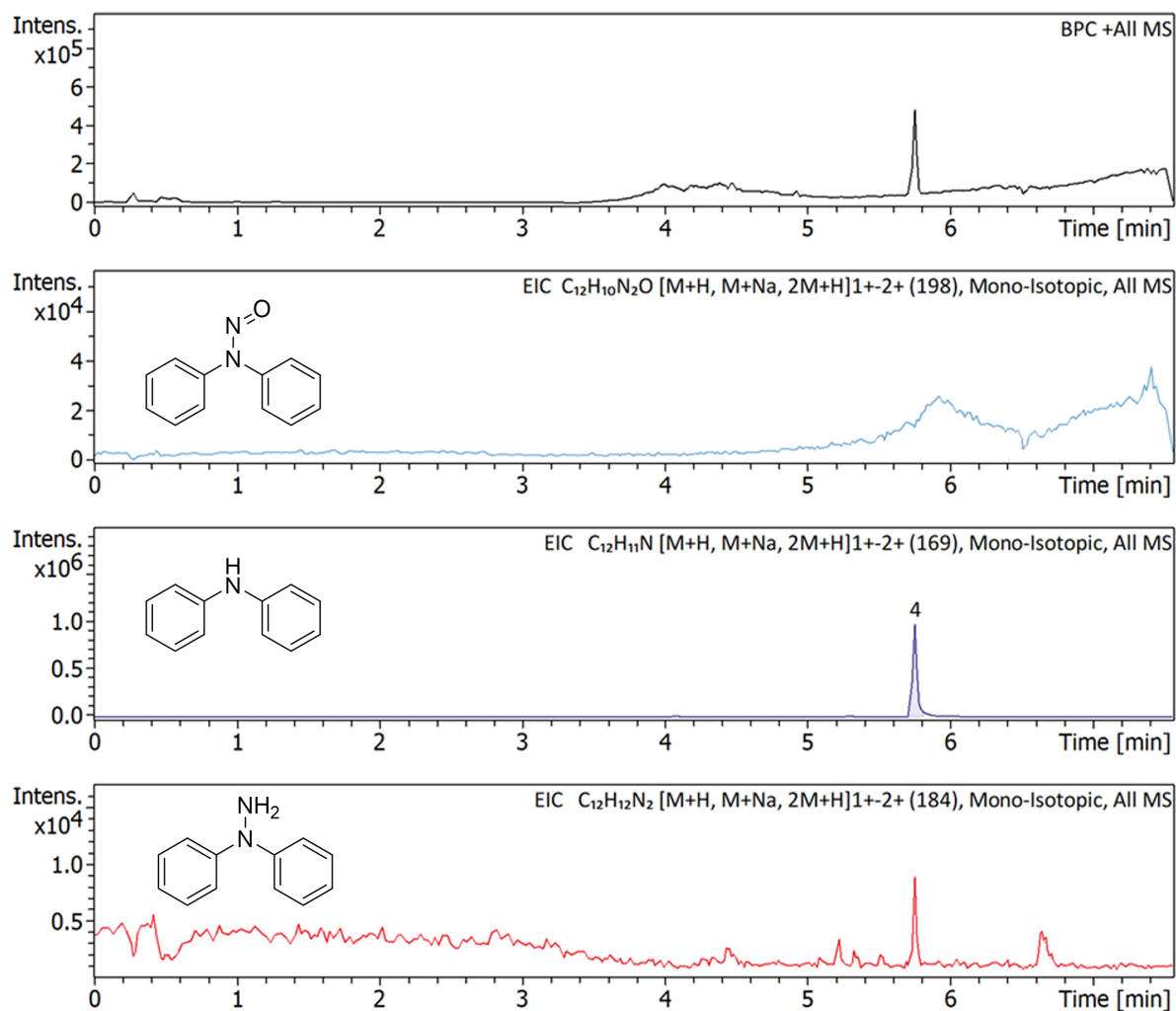


### Summary of Results

Name	RT	BPC Area(%)	UV Area(%)	Confirm Formula Results
Cmpd 5, 5.7 min	5.74	100.0	70.0	C12H11N

Figure I.19: LC-MSMS experiment chromatogram for N-nitrosodiphenylamine (N4) in reaction condition 12. Referenced in Section 3.6.

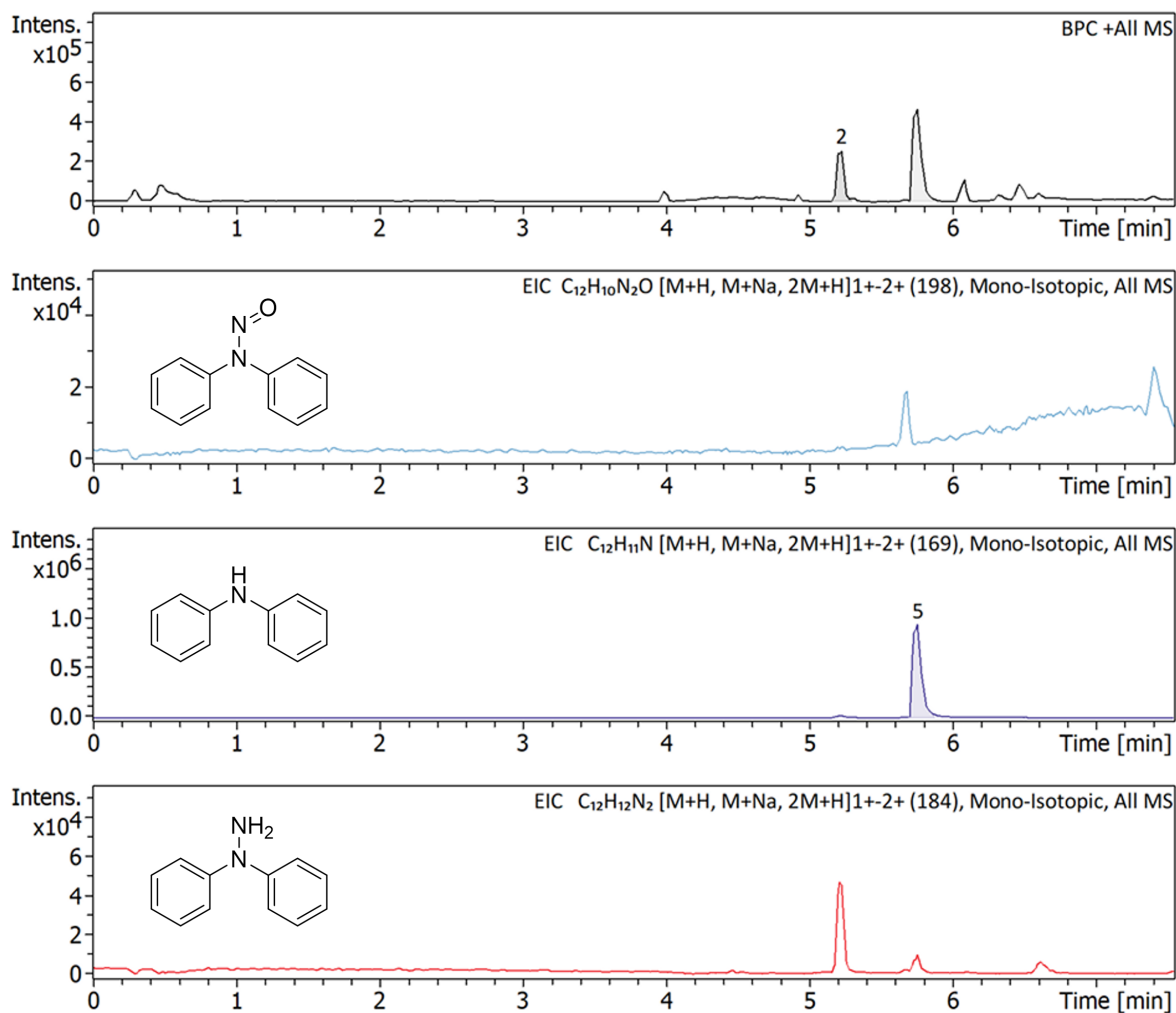




### Summary of Results

Name	RT	BPC Area(%)	UV Area(%)	Confirm Formula Results
Cmpd 4, 5.7 min	5.75	no peak	80.9	C12H11N

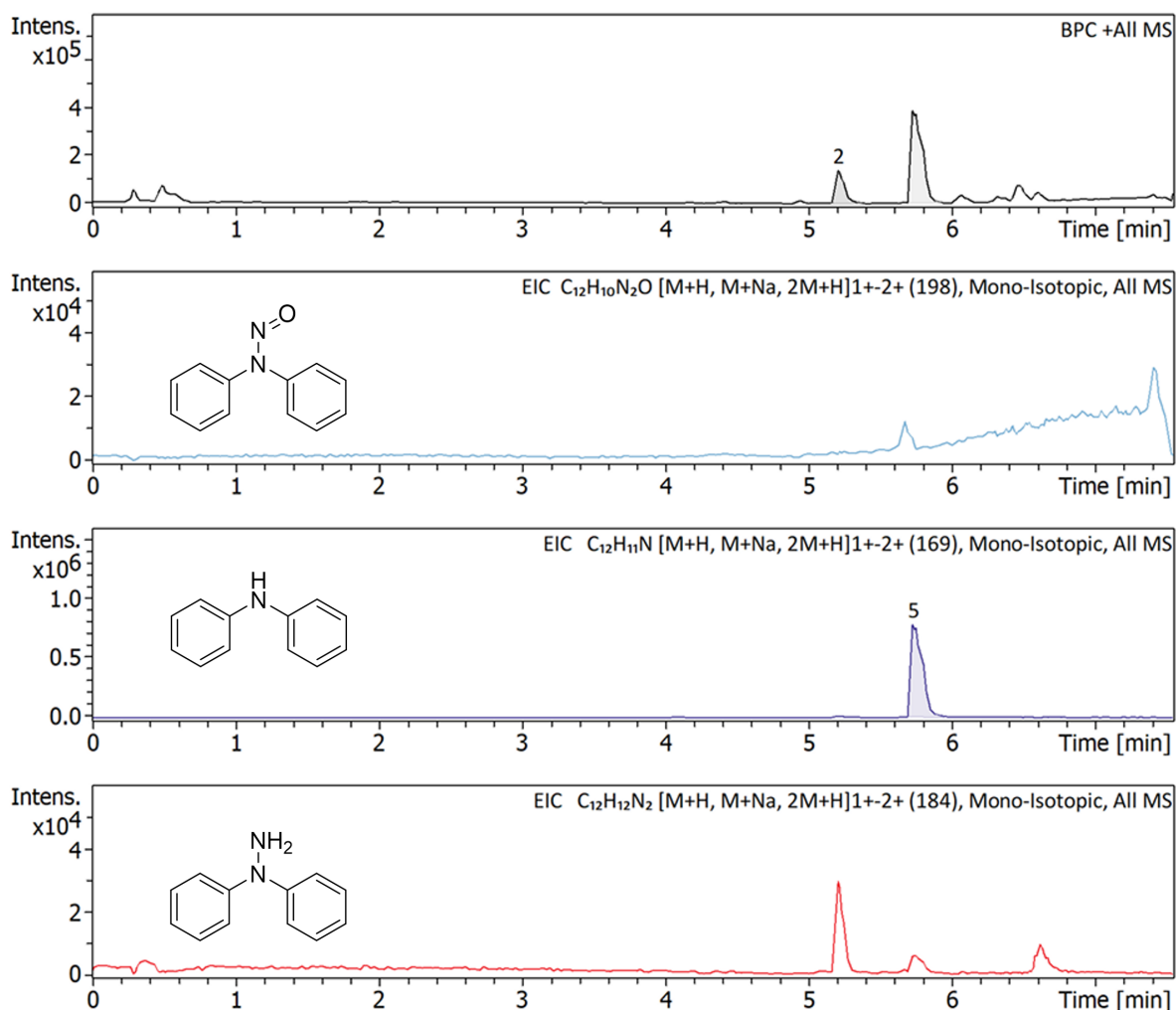
Figure I.20: LC-MSMS experiment chromatogram for N-nitrosodiphenylamine (N4) in reaction condition 13. Referenced in Section 3.6.



### Summary of Results

Name	RT	BPC Area(%)	UV Area(%)	Confirm Formula Results
Cmpd 2, 5.2 min	5.22	30.8	no peak	C <sub>12</sub> H <sub>12</sub> N <sub>2</sub>
Cmpd 5, 5.8 min	5.75	69.2	25.6	C <sub>12</sub> H <sub>11</sub> N

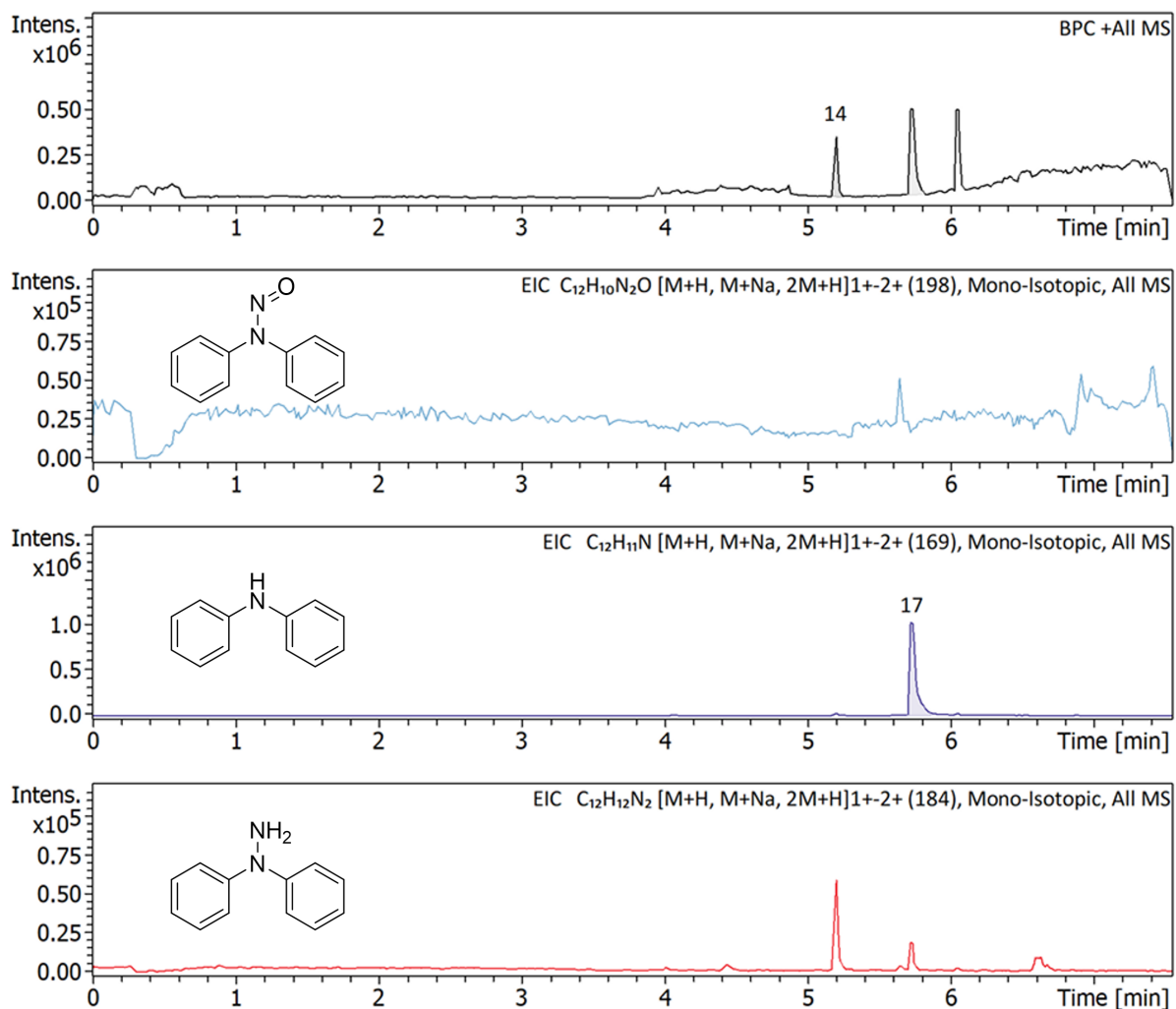
Figure I.21: LC-MSMS experiment chromatogram for N-nitrosodiphenylamine (N4) in reaction condition 14. Referenced in Section 3.6



### Summary of Results

Name	RT	BPC Area(%)	UV Area(%)	Confirm Formula Results
Cmpd 2, 5.2 min	5.21	19.1	no peak	$C_{12}H_{12}N_2$
Cmpd 5, 5.7 min	5.73	80.9	89.1	$C_{12}H_{11}N$

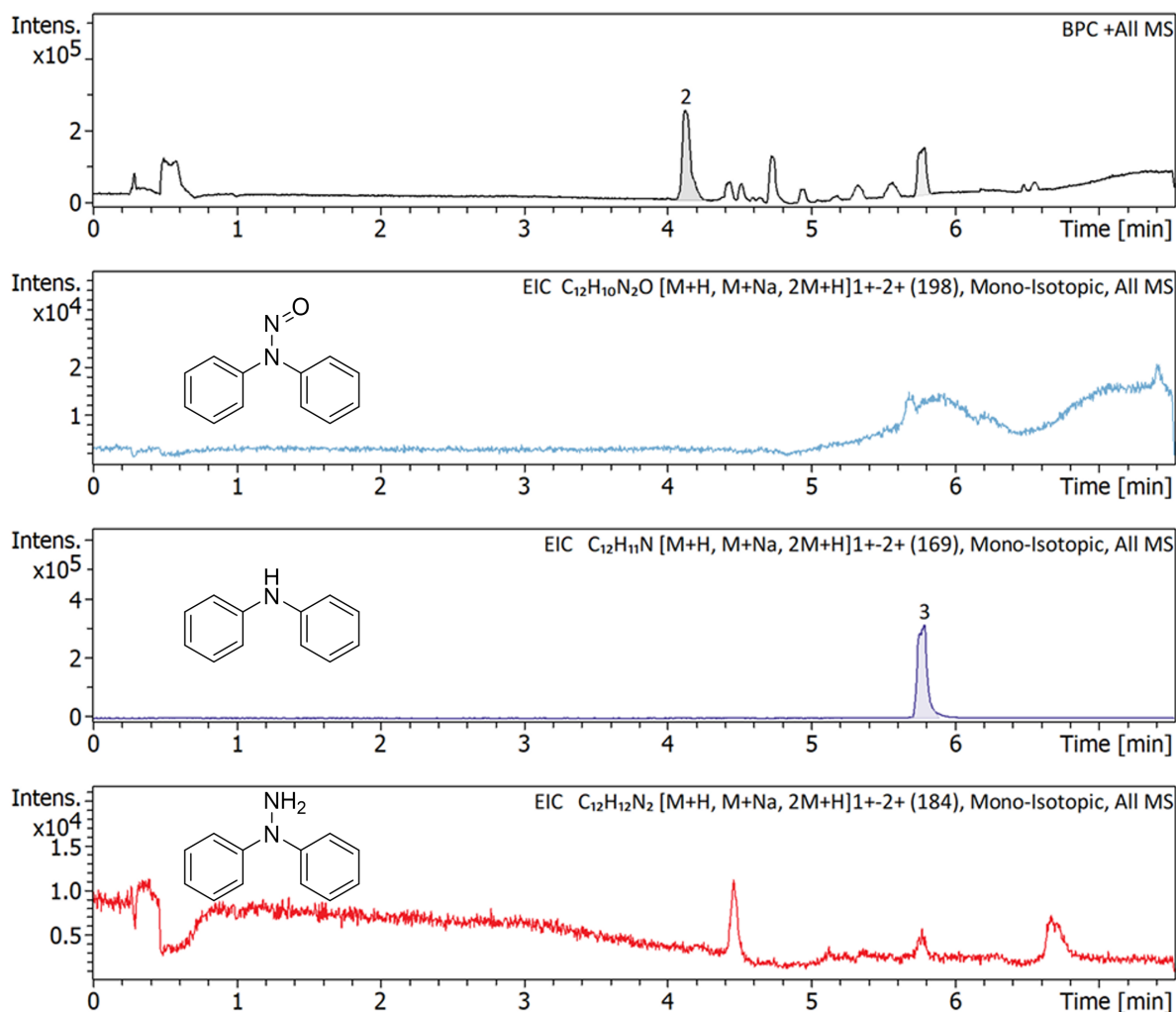
Figure I.22: LC-MSMS experiment chromatogram for N-nitrosodiphenylamine (N4) in reaction condition 15. Referenced in Section 3.6



### Summary of Results

Name	RT	BPC Area(%)	UV Area(%)	Confirm Formula Results
Cmpd 14, 5.2 min	5.19	40.5	1.8	C <sub>12</sub> H <sub>12</sub> N <sub>2</sub>
Cmpd 17, 5.7 min	5.73	59.5	78.0	C <sub>12</sub> H <sub>11</sub> N

Figure I.23: LC-MSMS experiment chromatogram for N-nitrosodiphenylamine (N4) in reaction condition 17. Referenced in Section 3.6



### Summary of Results

Name	RT	BPC Area(%)	UV Area(%)	Confirm Formula Results
Cmpd 2, 4.1 min	4.13	66.7	no peak	
Cmpd 3, 5.8 min	5.79	33.3	no peak	$C_{12}H_{11}N$

Figure I.24: LC-MSMS experiment chromatogram for N-nitrosodiphenylamine (N4) in reaction condition 19. Referenced in Section 3.6

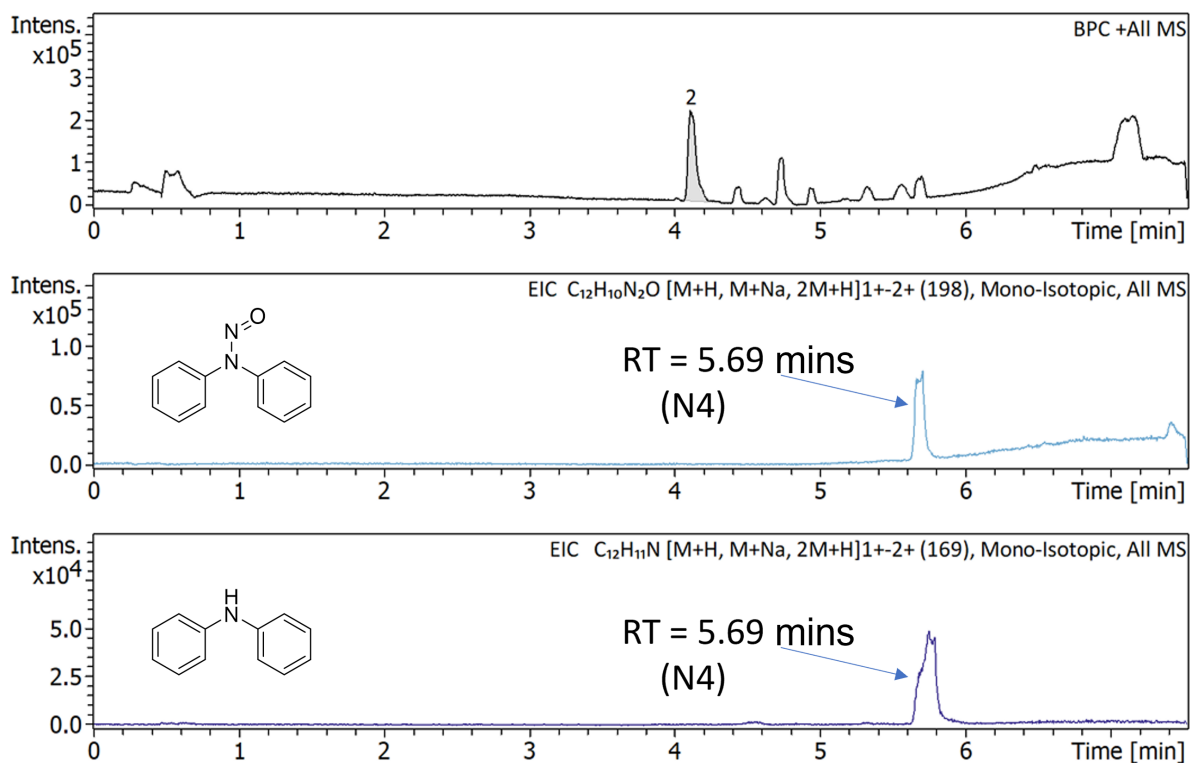
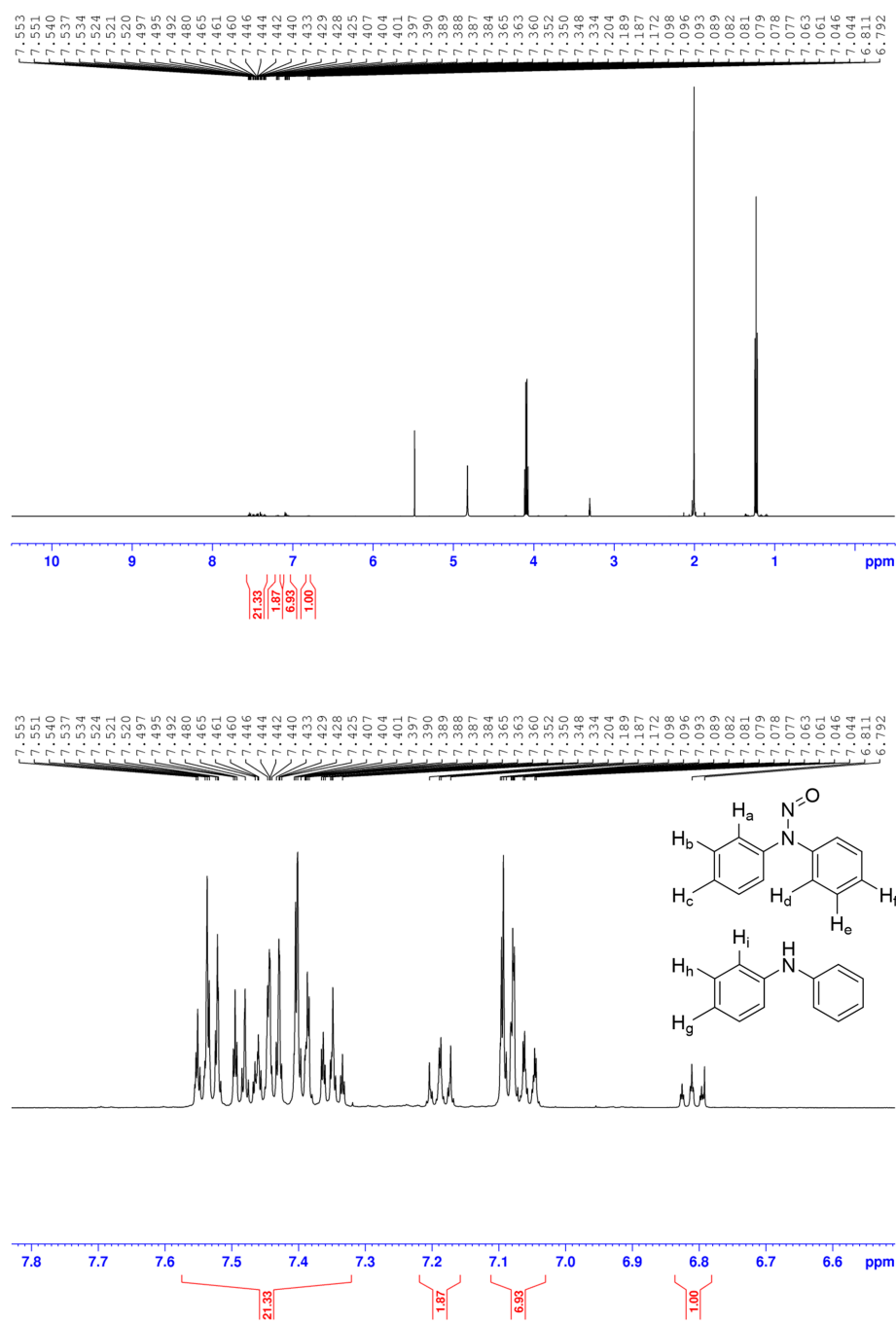


Figure I.25: LC-MSMS experiment chromatogram for N-nitrosodiphenylamine (N4) in reaction condition 21. Referenced in Section 3.6

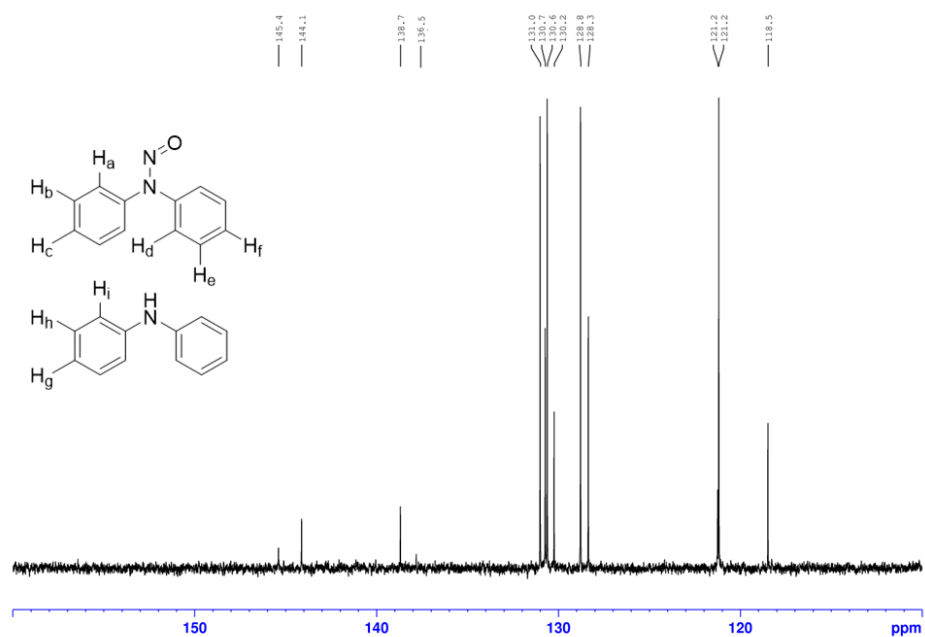
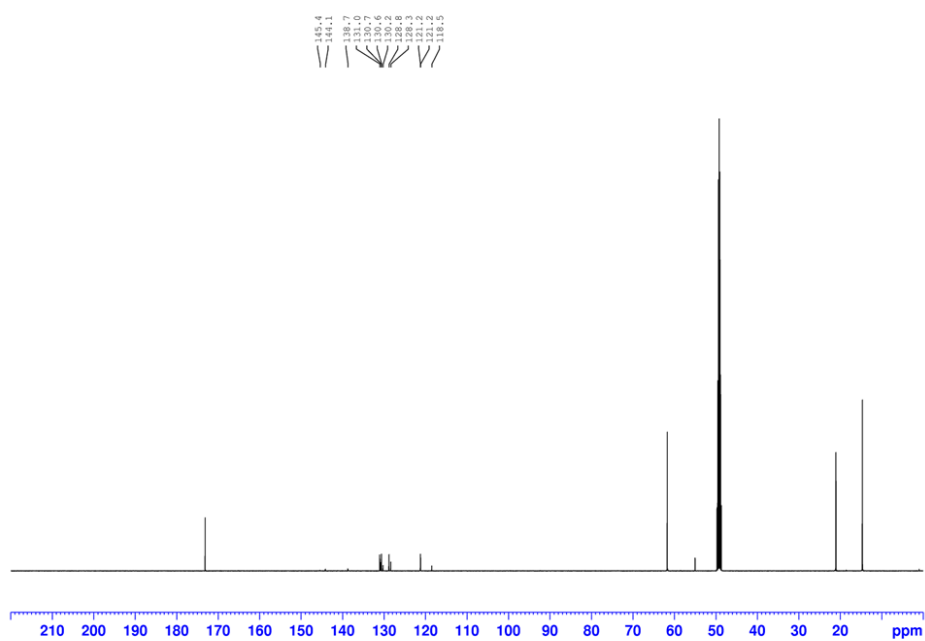
## Appendix J

# NMR Analysis

### J.1 N4 Condition 1

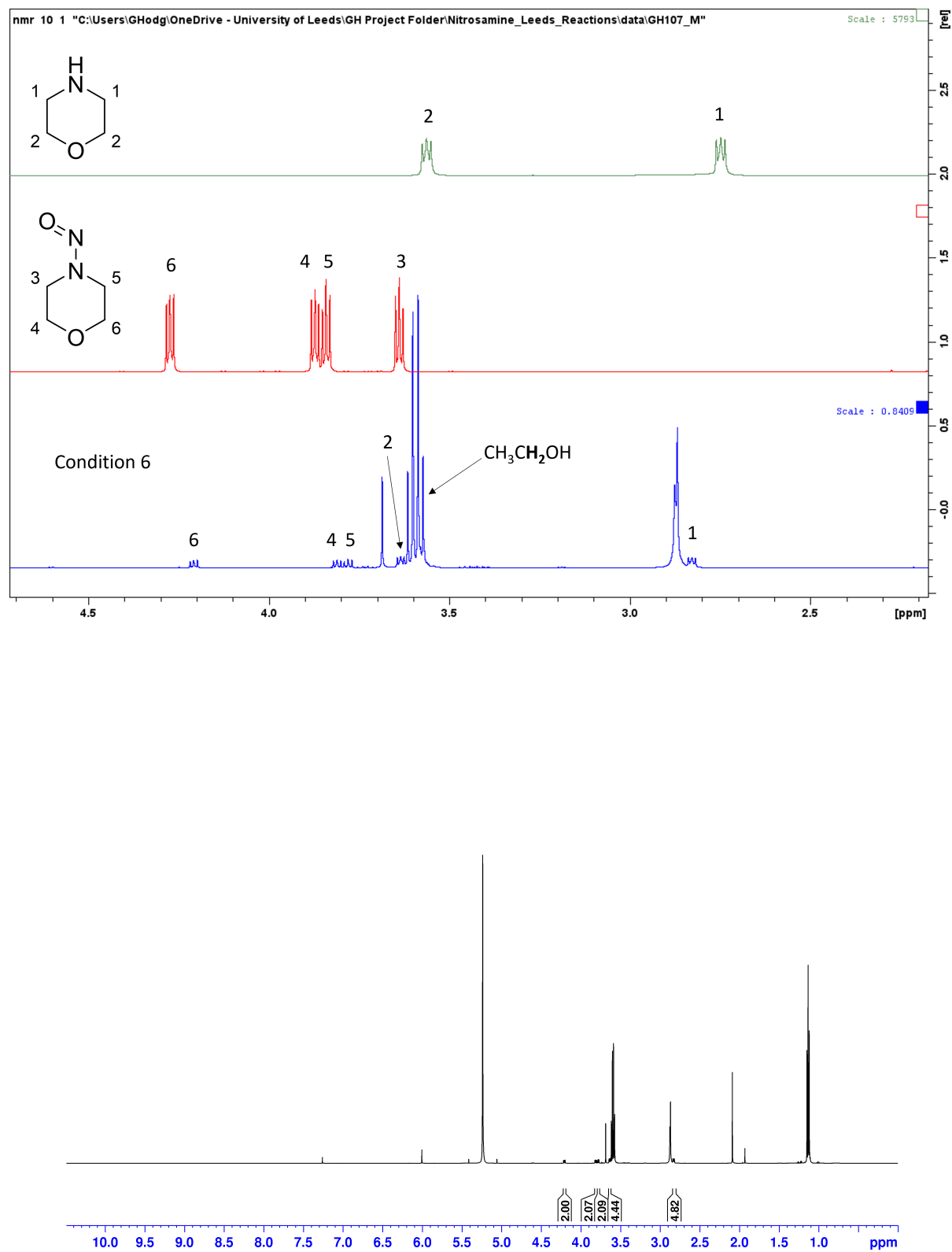
Figure J.1:  $^1\text{H}$  NMR analysis of crude reaction mixture for N4 in condition 1.



Figure J.2:  $^{13}\text{C}$  NMR analysis of crude reaction mixture for N4 in condition 1.

$^1\text{H}$  NMR  $\delta$ (MeOD, 500 MHz): 7.56-7.33 (8H, m, Ha, b, d, e), 7.21-7.17 (2H, m, Hh/i), 7.09-7.07 (2H, m, Hc) 7.06-7.04 (2H, m, Hh/i), 6.82-6.79 (2H, m, Hg).  $^{13}\text{C}$  NMR,  $\delta$  (MeOD, 125 MHz): 131.99 (**NDPA**), 130.75 (**NDPA**), 130.65 (**NDPA**), 130.23 (**DPA**), 128.80 (**NDPA**), 128.39 (**NDPA**), 121.25 (**DPA**), 121.20 (**NDPA**), 118.48 (**DPA**).

## J.2 N5 Condition 5

Figure J.3: <sup>1</sup>H NMR analysis of crude reaction mixture for N5 in condition 6.

$^1\text{H}$  NMR  $\delta(\text{CDCl}_3, 500 \text{ MHz})$ : 4.21 (2H, t,  $J = 5.1 \text{ Hz}$ , H6), 3.81 (2H, t,  $J = 5.1 \text{ Hz}$ , H4), 3.81 (2H, t,  $J = 5.1 \text{ Hz}$ , H5), 3.63 (4H, t,  $J = 4.7 \text{ Hz}$ , H2), 2.28 (4H, t,  $J = 4.7 \text{ Hz}$ , H1)